Groundwater flow, heat and mass transport in geothermal systems of a Central Alpine Massif.

The cases of Lavey-les-Bains, Saint-Gervais-les-Bains and Val d'Illiez.

by

Romain Sonney

PhD thesis to the faculty of Sciences of the University of Neuchâtel
to satisfy the requirements of the degree of Doctor of Philosophy in Science

PhD thesis evaluation committee

Prof. Pierre Perrochet	Thesis director (Center for Hydrogeology and Geothermics, Neuchâtel, Switzerland)
Dr. François-David Vuataz	Thesis co-director (Swiss Laboratory for Geothermics - CREGE, Neuchâtel, Switzerland)
Prof. Eva Schill	Examiner (Swiss Laboratory for Geothermics - CREGE, Neuchâtel, Switzerland)
Gabriele Bianchetti	Examiner (Alpgeo Sàrl, Sierre, Switzerland)
Dr. Werner Balderer	Examiner (Swiss Federal Institute of Technology, Zurich, Switzerland)
Dr. Bruce Mountain	Examiner (Institute of Geological and Nuclear Sciences, New Zealand)

Thesis jury defence date: 11 March 2010
Public presentation date: 28 May 2010

IMPRIMATUR POUR LA THESE

Groundwater flow, heat and mass transport in
geothermal systems of a Central Alpine Massif.
The cases of Lavey-les-Bains, Saint-Gervais-les-Bains
and Val d'Illiez

Romain SONNEY

UNIVERSITE DE NEUCHATEL

FACULTE DES SCIENCES

La Faculté des sciences de l'Université de Neuchâtel,
sur le rapport des membres du jury

Mme E. Schill , MM. P. Perrochet (directeur de thèse), F.-D. Vuataz (co-directeur de thèse),
W. Balderer (ETH Zürich), B. Mountain (Wairakei, Nlle Zélande) et
G. Bianchetti (Alpgeo, Sierre CH)

autorise l'impression de la présente thèse.

Neuchâtel, le 22 avril 2010

Le doyen :
F. Kessler

◇

*Je
dédicace
cette thèse à
mes parents Jean
et Mauricette, mes
mentors et mes héros. Je
n'oublierai jamais les
sacrifices qu'ils ont
fait pour sub-
venir à mes
besoins.*

◇

Table of Contents

III Lavey-les-Bains   63

3 General description of the study area   65

4 Geological investigations at Lavey-les-Bains   73

5 Hydrogeological and geochemical investigations at Lavey-les-Bains   85

VI Concluding comments

VII Bibliography

Bibliography

VIII Appendixes: Chemical and isotopic analyses of waters

A Description of analysed and measured parameters

B Lavey-les-Bains, Switzerland

C Saint-Gervais-les-Bains, France

D Val d'Illiez, Switzerland

E CD-R

List of Figures

List of Tables

Acknowledgments

A long work always comes with a long list of people to thank. Firstly, I would like to thank sincerely Dr. François-David Vuataz, co-director of this PhD thesis with whom I shared pleasant and unforgettable moments during three years. Through these many discussions, François transmitted to me his knowledge about scientific techniques to understand the Alpine deep flow systems and to investigate the hydrothermal reservoir using the chemical-mineral processes. We also shared political and economic discussions on the situation of the geothermics in Switzerland, and I learned a lot. Moreover, François involved me in current geothermal projects in Switzerland such as BDFGeotherm, AGEPP, Geothermie-Brig and Triemli, and I delighted to work with him. I especially thank him for the time he dedicated to proofreading and correcting my manuscript and various articles we have published in international journals and congress. One last word to thank him for his kindness and availability.

I also address my sincere gratitude to Prof. Dr. Pierre Perrochet, thesis director, who gave me his full confidence to realize this thesis although a significant part of the research that I undertook is not directly related to its research domain, especially for the domains of the structural geology and the chemical-mineral processes. Pierre helped me to perform and improve the numerical models and through his guidance I improved my knowledge in the modelling of groundwater flow, heat and mass transport. I also have enjoyed working with him, and I thank him again for his cheerfulness.

I would like to thank particularly Gabriele Bianchetti who has contributed significantly to the achievement of this thesis, with whom I had the opportunity to exchange knowledge about the Alpine deep flow systems. He also kindly hosted me in the Alpgeo consulting office at Sierre (Wallis, Switzerland) where we exchanged and discussed the data for the Lavey-les-Bains and Val d'Illiez study sites.

I particularly appreciated the fact that he was willing to accompany me on the field.

Financial aid for the analyses in tritium of this thesis was provided by the Swiss Laboratory in Geothermics, managed by Prof. Dr. Eva Schill. I would like to thank also Eva who agreed to be part of this thesis. In the same way, I would like to address my gratitude to Dr. Werner Balderer from Zurich and to Dr. Bruce Mountain from GNS Science, New Zealand, who also agreed to be part of this thesis.

Then, I would like to thank the people who helped me to solve some of the problems that presented themselves: Dr. Sandrine Portier for the geochemical modelling, Dr. Ellen Milnes for the use of the Feflow software, Dr. Heinz Surbeck for the radio-isotope analyses in waters of Saint-Gervais-les-Bains, Dr. François Negro for the geological structure of the Champéry window, Dr. Julien Straubhaar and Dr. Grégoire Mariethoz for their logistical advice, and finally Chantal Crisinel who kindly corrected this manuscript.

This thesis has been possible through the cooperation of owners, directors, managers and technicians of the studied spas. In detail, I would like to address my gratitude to Mr. Aymon (technician at Lavey-les-Bains) for the pumping tests carried out in 2007, to Thierry Coffinet and Maud Durant respectively director and manager for the Hygiene Service of the Saint-Gervais-les-Bains spa for their agreement to collect and use the existing data and to sample all the boreholes and springs, and to Cédric Rodriguez and Mr. Rielle respectively director and technician of the spa in the Val d'Illiez who permitted me to sample all the boreholes and springs.

Finally, thanks to my family especially my parents Jean and Mauricette, my brother Damien, my lovely girlfriend Noémie, and my friends including all the staff for their moral support and patience.

Abstract

Groundwater flow, heat and mass transport in geothermal or hydrothermal systems locally occurs in the Alps Range where a series of precise conditions are met such as active downflow, permeability at depth, concentrated and fast upflow and favorable geomorphological surface patterns. Advanced studies of the regional and local geology, thermal water chemistry, mixing processes, infiltration area, water-rock interactions, circulation depth, uprising conditions, groundwater residence time, mineral-chemical fingerprint, etc. allow the deep flow system to be understood. To carry out these studies, different methods can be employed and combined together such as geological, hydrogeological, geophysical, geochemical, isotopic and numerical investigations. Moreover, these investigations represent a scientific basis providing information required to better manage the short and long term exploitation of the discharged thermal water, qualitatively and quantitatively. They also provide crucial knowledge to prepare future geothermal projects with boreholes and to limit failures that may occur in subsurface and deep geothermal prospection. Due to the high costs for the implementation of a deep borehole, the risk of failure needs to be lowered as much as possible, i.e. it requires a good knowledge of the explored site. This is important for long term sustainable development of geothermal projects.

The three selected hydrothermal sites are Lavey-les-Bains and Val d'Illiez in Switzerland and Saint-Gervais-les-Bains in France, where the uprising thermal waters are continuously exploited for various uses such as spa, heating buildings, medical care and cosmetics. Lavey-les-Bains and Saint-Gervais-les-Bains were selected due to several criteria: 1) deep flow systems in the basement, 2) similar chemical and isotopic properties, 3) presence of several end-members with mixing processes, 4) interesting properties of the geothermal reservoirs, 5) many data available and 6) on-going geothermal projects or planned. On the contrary, Val d'Illiez was selected for orther criteria: 1) deep flow system in the autochthonous sedimentary cover of the basement where the hydrothermal systems of Lavey-les-Bains and Saint-Gervais-les-Bains occur, 2) comparison of the chemical and isotopic properties of thermal waters from the cover with those of thermal waters flowing in the basement, 3) history of the site related to the Salanfe Lake and 4) many data available. These three studied sites are located around the Aiguilles Rouges Massif, one of the external crystalline massifs of the Western Alps. Lavey-les-Bains and Saint-Gervais-les-Bains represent the two low-elevation points of the Aiguilles Rouges basement, respectively on the north-eastern and south-western sides. In contrast, Val d'Illiez is located out of the Aiguilles Rouges basement in a sedimentary domain belonging to the autochthonous cover which outcrops along the north-western edge of the basement.

Firstly, the investigations the selected hydrothermal systems were used to study the geological setting and the fracturing conditions for each site. Then, a new sampling campaign was carried out with pumping tests aiming to define the chemical-mineral processes leading to the composition of groundwaters. Finally, two and three-dimensional numerical models were established to validate the assumptions formulated from the geochemical investigations, and to represent the deep flow system, the geothermal anomalies and the mixing processes.

Groundwater analyses since 1973 at Lavey-les-Bains have revealed a mixing process between a deep $Na-SO_4$ and high-Cl thermal component circulating in the basement (68°C and TDS 1.4 g/L) and cold shallow water from the mountain slope and the Quaternary filling. The production rate of the new deep well P600, installed in 1997, has amplified this mixing process in the well P201, for which a decline in temperature and total dissolved

solids has been observed. Numerical hydrogeological two and three-dimensional models of flow, heat and mass transport reproduced the deep flow system and forecasted the long-term exploitation potential of the geothermal resource. Computed temperature of the deep inferred reservoir (100-130°C) is in agreement with the geothermometers, whereas the simulated thermal water flux (5400-9000 m^3/d) is probably underestimated. Different fluid production scenarios have been documenting the decline and stabilization phases of temperatures in the hydrothermal field since 1997. For P201, the mixing ratio calculated before and during the exploitation of P600 is comparable with observed data; the computed temperature tends towards stabilization in P201 at 56°C after 10 to 15 years of production at P600. Another planned new well is likely to reduce the thermal output of the existing wells.

The crystalline rocks are not directly outcropping at the Saint-Gervais-les-Bains spa but certainly exist beyond 300 m depth. Uprising waters are pumped from two different aquifers below the Quaternary deposits of the Bon Nant Valley. In the lower Trias-Permian aquifer crossed by De Mey boreholes (27-36°C), the ascending Na-SO$_4$ and high-Cl thermal water from the basement (4.8 g/L) is mostly mixed by a Ca-SO$_4$ and low-Cl cold water circulating in the autochthonous cover of the Aiguilles Rouges basement. The origin of the saline thermal water probably results from infiltration and circulation in the basement until it reaches deep thrust faults where there is leaching of residual brines or there are fluid inclusions at depth. The dissolution of Triassic halite is not possible at Saint-Gervais-les-Bains because the Triassic cold waters have a very low-Cl concentration ($<$ 20 mg/L). For the De Mey Est borehole, gypsum dissolution is occurring with cationic exchanges involving Na, as well as low-temperature Mg dissolution from dolomite in the Triassic formations. The aquifer made of imbricated structures (upper-middle Trias) and crossed by the Lépinay well (39°C) contains thermal waters which are strongly mixed with a low-Cl water, where gypsum dissolution also occurs. The infiltration area for the thermal end-member is in the range of 1700-2100 meters, close to the Lavey-les-Bains hydrothermal system, and corresponds to the average elevation of the Aiguilles Rouges Massif. For the Ca-SO$_4$ and low-Cl end-member, the infiltration area is lower (1100-1300 m), showing circulation from the Mont Joly Massif. The geother-

mometry method indicates a reservoir temperature of probably up to 65°C but not exceeding 100°C.

The deep flow system leading to the thermal springs in the Val d'Illiez occurs at the bottom of the autochthonous cover of the Aiguilles Rouges basement, mainly inside the Triassic formations. The structure of the cover is a great recumbent anticline with an axial plane plunging towards the south-east which would be limited by a basal thrust fault related to the thrust system between the Aiguilles Rouges and Infa-Aiguilles Rouges basements. Mixing processes occur between a Ca-HCO$_3$ cold groundwater and a Ca-SO$_4$ and low-Cl thermal end-member, having a temperature and a total dissolved solids roughly of 30-31°C and 1.8 g/L respectively. The thermal component acquires its mineral composition from the dissolution of gypsum and dolomite occurring in the Triassic formations, in a different way compared to Lavey-les-Bains and Saint-Gervais-les-Bains. The thermal component has an infiltration area close to the elevation of the Salanfe Lake ($\approx$ 1900 m) and the reservoir temperature of the deep flow system should probably not exceed 35-40°C at a depth of around 1 kilometre below the Val d'Illiez spring zone. Using the tritium data, the piston-flow model calculated an average residence time for the thermal end-member of around 5 years. A two-dimensional model of groundwater flow and heat transport was carried out to study the relation between the Salanfe Lake and the thermal springs. Four scenarios were tested with different values of water losses from the lake and a long-term cooling of the host rocks was simulated. The natural variations of parameters in the springs indicate that the lake probably does not act on the thermal regime as a single intake. It appears that temperature and chemistry of the thermal waters in the Val d'Illiez have a current steady evolution, while the flow rate seems to vary with the natural variation of the water level of the lake with a time lag of around 140 days. This should indicate that an upper aquifer is situated on the thermal aquifer, without mixing processes, adding a pressure which raises the flow rate of the thermal spring without changing its temperature and chemistry.

The understanding gained through this study on groundwater flow, heat and mass transport in the Aiguilles Rouges Massif improves the knowledge for the other external crystalline massifs where hydrothermal sites are present at the front of them. The Mont Blanc Massif is also an area where a large

amount of thermal water can discharge from its low-elevation points. The hydrothermal site of Saxon along the Rhone Valley in Switzerland is an interesting site to investigate for this reason. Generally, the density of hydrothermal sites is often higher in the Western Alps where the basement outcrops. Indeed, vertical faults in the basement facilitate the deep infiltration of water leading to deep flow systems, whereas in sedimentary domain the superposition of nappes tends to generate shallower flow systems. Consequently, it would be interesting to investigate other low-elevation zones bordering the external crystalline massifs where the Quaternary filling could mask areas of uprising thermal waters.

Résumé

Les processus de transport de chaleur et de masse vers la surface associé aux systèmes hydrothermaux alpins se produisent locallement lorsque des conditions bien particulières sont réunies : infiltration profonde via des formations perméables et remontée rapide des fluides vers la surface. Des études détaillées sur la géologie régionale et locale, la chimie des eaux thermales, les processus de mélange, la zone de recharge, les interactions eau-roche, les circulations profondes, les conditions de remontée du fluide, le temps de transit souterrain, l'origine des éléments dissous, etc. permettent de comprendre le fonctionnement des systèmes hydrothermaux. Elles sont réalisées à partir d'investigations géologiques, hydrogéologiques, géophysiques, géochimiques et isotopiques couplées ensemble. Ces investigations représentent une base scientifique donnant des informations nécessaires pour mieux gérer qualitativement et quantitativement l'exploitation à court et long terme des eaux thermales. Ces investigations fournissent également des connaissances primordiales pour préparer des futurs projets de géothermie avec la réalisation et l'exploitation de nouveaux forages, et pour limiter les risques d'échec. Comme les coûts sont élevés pour réaliser un forage profond, il est indispensable de bien connaître le site exploré. Ceci est important pour le développement à long terme de projets de géothermie.

Les trois sites choisis sont Lavey-les-Bains et Val d'Illiez en Suisse et Saint-Gervais-les-Bains en France, où les eaux thermales sont continuellement exploitées à des usages variés : bains thermaux, chauffage des bâtiments, soins médicaux et cosmétiques. Lavey-les-Bains et Saint-Gervais-les-Bains ont été sélectionés selon plusieurs critéres : 1) système d'écoulement profond dans le socle cristallin, 2) propriétés chimiques et isotopiques similaires, 3) présence de plusieurs types d'eau avec des processus de mélange, 4) propriétés intéressantes des réservoirs géothermiques 5) nombreuses données à

disposition et 6) projets de géothermie en cours de réalisation ou planifiés. Au contraire, le site de Val d'Illiez a été choisi pour d'autres raisons : 1) système d'écoulement profond dans la couverture sédimentaire autochtone du socle cristallin où les systèmes hydrothermaux de Lavey-les-Bains et Saint-Gervais-les-Bains ont lieu, 2) comparaison des propriétés chimiques et isotopiques des eaux thermales de la couverture autochtone avec celles des eaux thermales circulant dans le socle cristallin, 3) historique du site avec la mise en charge du lac de Salanfe et 4) nombreuses données à disposition. Les trois sites sont localisés autour du massif cristallin des Aiguilles Rouges, un des massifs cristallins externes des Alpes occidentales. Lavey-les-Bains et Saint-Gervais-les-Bains représentent les deux "points-bas" du socle des Aiguilles Rouges, respectivement au nord-est et au sud-ouest. Contrairement, le site de Val d'Illiez est localisé en dehors du domaine cristallin, dans un environnement sédimentaire appartenant à la couverture autochtone du socle des Aiguilles Rouges et qui affleure le long de celui-ci sur sa bordure nord-ouest.

Dans un premier temps, les méthodes utilisées pour investiguer ces systèmes étaient de comprendre le contexte géologique et d'étudier la fracturation régionale et locale. Ensuite, une nouvelle campagne de prélèvements de d'analyses a été réalisée pour chaque site sur toutes les eaux à disposition. Des essais de pompage ont également été entrepris pour mettre en avant les processus de mélange se produisant entre les différents pôles de mélange. Finalement, des modèles numériques en deux et trois dimensions ont été construits pout valider les résultats obtenus avec les méthodes géochimiques, et pour représenter le système d'écoulement profond, l'anomalie géothermique dans la zone de remontée et les processus de mélange.

A Lavey-les-Bains, les analyses chimiques ont montré l'existence d'un mélange entre une eau thermale Na-SO$_4$, riche en chlorure et circulant dans le

socle cristallin (68°C et 1.4 g/L), et des eaux froides peu profondes circulant dans le versant et dans le remplissage Quaternaire. L'exploitation du forage P600, réalisé en 1997, a amplifié ces mélanges. En effet, depuis 1997, la température et la minéralisation des eaux du forage P201 ont diminué. Des modèles numériques en deux et trois dimensions ont reproduit le système d'écoulement profond et ont permis de visualiser les effets à long terme de l'exploitation sur la ressource géothermale. Les températures simulées du réservoir profond sont en accord avec celles estimées par les géothermomètres (100-130°C) alors que le flux calculé d'eau thermale ascendante semble être sous-estimé (5400-9000 m^3/j). Plusieurs simulations ont été réalisées en changeant les conditions d'exploitation de la ressource géothermale dans le but de reproduire la baisse des paramètres physico-chimiques observée depuis 1997, et pour visualiser une éventuelle stabilisation des paramètres à long terme. Pour le forage P201, les taux de mélange calculés avant et après l'exploitation du P600 sont comparables avec les taux de mélange observés. Les températures simulées au P201 montrent une stabilisation vers 56°C après 10-15 ans d'exploitation du P600. La réalisation et l'exploitation de futurs forages profonds sur ce site pourrait également avoir une incidence sur le potentiel géothermique des forages actuellement exploités.

Le socle cristallin n'affleure pas directement sur le site des bains de Saint-Gervais-les-Bains mais il est certainement présent au-delà de 300 mètres de profondeur. Les eaux thermales sont pompées dans deux aquifères différents sous les dépôts du torrent Bon Nant. Dans l'aquifère du Permien-Trias inférieur percé par les forages De Mey Est et De Mey Ouest (27-36°C), les eaux thermales Na-SO$_4$, riches en chlorure et circulant dans le socle (4.8 g/L), sont mélangées par une eau Ca-SO$_4$ et pauvre en chlorure circulant dans la couverture autochtone du socle. L'origine de l'eau thermale saline vient certainement de l'infiltration et de la circulation d'eau météorique dans le massif cristallin des Aiguilles Rouges. Cette eau atteindrait en profondeur des plans de chevauchement où elle lessiverait des résidus d'eau saumâtre. Pour expliquer les fortes teneurs en chlorure (1.1 g/L) dans les eaux thermales, la dissolution d'halite Triasique n'est pas possible car les eaux froides du Trias auraient également des fortes teneurs en chlorures, ce qui n'est pas le cas (< 20 mg/L). Pour le forage De Mey Est, la dissolution de gypse et dolomie se produit avec des échanges cationiques. L'aquifère des écailles du Trias moyen et supérieur, recoupé par Lépinay (39°C), contient une eau thermale mélangée avec une eau pauvre en chlorure. La dissolution du gypse est plus important pour cet aquifère car les teneurs en sulphate y sont plus élevées. Pour la composant thermale, l'altitude d'infiltration a été évaluée vers 1700-2100 mètres. C'est proche de l'estimation faite pour le système de Lavey-les-Bains, et ça correspondrait bien à l'altitude moyenne des Aiguilles Rouges. Pour la composante froide Triasique circulant dans le massif du Mont Joly, l'altitude d'infiltration calculée est plus basse (1100-1300 m). Enfin, l'utilisation des géothermomètres indique une température du réservoir profond entre 65 et 100°C.

Le système d'écoulement profond aboutissant aux sources de Val d'Illiez se produit à la base de la couverture autochtone des Aiguilles Rouges, dans les formations du Trias. Cette couverture forme un anticlinal avec un plan axial plongeant vers le sud-est qui serait délimité par un plan de chevauchement au nord-ouest. Ce chevauchement rejoindrait en profondeur la limite entre les Aiguilles-Rouges et l'Infra-Aiguilles Rouges. A Val d'Illiez, l'eau thermale Ca-SO$_4$ et pauvre en chlorure est mélangée avec une eau froide Ca-HCO$_3$ et peu profonde. L'eau thermale pure a une température d'environ 30-31°C et une minéralisation vers 1.8 g/L. Cette composante thermale acquière sa composition en dissolvant le gypse et la dolomie du Trias et s'infiltrerait à une altitude moyenne proche de celle du lac de Salanfe ($\approx$ 1900 m). La température du réservoir ne devrait pas excéder 35-40°C vers une profondeur d'environ 1 kilomètre sous Val d'Illiez. En utilisant toutes les analyses existantes en tritium et le modèle "piston-flow", le temps de transit souterrain a été évalué à environ 5 ans. Un modèle numérique en deux dimensions a été construit pour étudier la relation entre la lac de Salanfe et les sources thermales. Quatre scénarios ont été testés avec différentes valeurs de perte du lac ce qui a permis de montrer un refroidissement à long terme de la couverture sédimentaire où l'eau circule. D'après les variations naturelles des paramètres des sources thermales, il semblerait que les eaux du lac infiltrées exercent une pression sur l'aquifère thermale, sans mélange important. En effet, la température et la conductivité des sources sont stables alors que les débits varient significativement avec un décalage dans le temps par rapport à la hauteur d'eau du lac.

Les connaissances apportées par cette étude sur les systèmes hydrothermaux localisés en bordure des Aiguilles Rouges peuvent être utiles pour d'autres systèmes à proximité des autres massifs cristallins externes. Le massif cristallin du Mont-Blanc est aussi une région où des eaux thermales peuvent émerger vers ses "points-bas". Le site hydrothermal de Saxon dans la vallée du Rhône en Suisse est un endroit à prospecter plus en profondeur pour cette raison. D'une manière générale, la densité des sites hydrothermaux est plus élevée dans les Alpes occidentale où le socle affleure. En effet, les massifs cristallins sont caractérisés par la présence de nombreuses failles verticales permettant ainsi une infiltration importante des eaux météoriques en profondeur, et donc la naissance de systèmes hydrothermaux. Au contraire, le domaine sédimentaire est caractérisé par une succession de nappes ce qui va plutôt favoriser les écoulements de plus faible profondeur. Il serait donc intéressant de prospecter les endroits en bordure des massifs cristallins externes où les remontées d'eau thermale seraient masquées par les remplissages Quaternaires.

Résumé étendu

1. Introduction (partie I)

En Suisse, des systèmes d'écoulement profond dans des couches géologiques perméables peuvent donner naissance à des systèmes géothermaux dits de basse enthalpie. Pour voir ces systèmes géothermaux se manifester en surface, il faut des conditions bien spécifiques. Par exemple, la présence d'une faille permettra la remontée rapide de fluides profonds naturellement réchauffés par le gradient géothermique. Cet exemple est souvent rencontré dans des zones où les structures géologiques et tectoniques sont complexes, comme dans les chaînes de montagne. Les Alpes sont une région d'Europe où de nombreuses sources thermales sont recensées et sont continuellement exploitées pour divers usages : spa, chauffage, soin médicaux, cosmétique, etc.

Les études géologiques, hydrogéologiques, géochimiques, isotopiques, géophysiques et numériques réalisées sur un nombre limité de sites permettent de comprendre les processus d'écoulement profond à l'origine des émergences thermales. Ces études représentent une base scientifique indispensable pour une gestion durable à court et long terme des ressources géothermales exploitées, d'un point de vue qualitatif et quantitatif. Elles sont également cruciales pour le développement de projets de géothermie désirant réaliser des forages profonds. En effet, les coûts élevés liés à la réalisation d'un forage nécessitent une diminution des risques géologiques.

Initialement et dans le cadre du projet Alpine Geothermal Power Production (AGEPP), des études complémentaires sont menées sur le système hydrothermal de Lavey-les-Bains (Vaud, Suisse), avec comme objectif de décrire et quantifier les caractéristiques du réservoir profond. Le projet AGEPP a pour but d'exploiter ce réservoir à partir d'un ou deux forages dépassant 1.5 kilomètres de profondeur (probablement jusqu'à 3 kilomètres de profondeur). Ensuite, le système hydrothermal de Saint-Gervais-les-Bains (France) est étudié car les eaux thermales de ce site ont des propriétés chimiques et isotopiques proches de celles des eaux de Lavey-les-Bains. De plus, leurs contextes géologiques sont également analogues puisque ces deux sites se trouvent aux deux extrémités du massif cristallin des Aiguilles Rouges (point bas du système hydrogéologique régional). Pour cette raison, il est intéressant de les comparer d'autant plus que certains doutes subsistaient sur l'origine des fluides profonds de Saint-Gervais-les-Bains. Enfin, des recherches complémentaires sont menées sur le système hydrothermal de Val d'Illiez. Val d'Illiez est localisé en bordure du massif hercynien des Aiguilles Rouges et ses eaux thermales proviennent d'écoulements profonds dans la couverture autochtone. Là aussi il est intéressant de comparer le fonctionnement de ce système en milieu purement sédimentaire avec celui exposé pour les deux précédents cas en milieu cristallin.

2. Description des méthodes (partie II, chapitre 2)

Les investigations géologiques, hydrogéologiques, géochimiques et numériques réalisées sur les trois sites hydrothermaux sont menées en parallèle pour mieux comprendre les processus à l'origine des émergences thermales. Dans un premier temps et pour chaque site, le contexte géologique régional est décrit avec l'élaboration de coupes géologiques expliquant les différentes unités présentes, leurs structures profondes et leurs relations. Une étude de la fracturation des massifs concernés est en-

suite réalisée dans le but de mettre en évidence les différentes familles de fractures et failles favorisant l'infiltration profonde des eaux météoriques, et donc de visualiser les directions potentielles d'écoulement souterrain. Un inventaire des roches rencontrées est également proposé en vue d'élaborer des modèles numériques en couplant les processus de transport et les interactions eau-roche.

La deuxième étape consiste à étudier le contexte géologique autour de la zone de remontée des eaux thermales. Là aussi des coupes géologiques sont proposées pour mettre en évidence les structures géologiques permettant la remontée des fluides profonds vers la surface (unités, fractures, failles, etc.). Ces coupes sont élaborées grâce aux différents relevés géologiques des forages présents sur le site.

Pour comprendre les processus chimiques eau-roche, tous les points d'eau dans la zone thermale sont prélevés et analysés dans la mesure du possible. Ces points d'eau sont les ouvrages exploitant les eaux thermales, les anciens ouvrages non utilisés, les sources subthermales, les sources froides, les eaux froides de la nappe phréatique et les cours d'eau. De plus, les paramètres physico-chimiques sont mesurés pour chaque point d'eau au moment du prélèvement ou bien lors d'un contrôle : température, conductivité électrique, pH, oxygène dissous et débit. Pour chaque échantillon prélevé, les ions majeurs, les éléments traces, les radio-isotopes et les isotopes stables de l'eau sont mesurés au laboratoire d'analyse du Centre d'hydrogéologie de Neuchâtel (CHYN). Toutes les données sont contrôlées et validées, et avec les données historiques compilées, une série de graphiques est élaborée pour l'interprétation des résultats.

Dans un premier temps, les différents types géochimiques des eaux sont définis à l'aide des diagrammes de Piper et Schoeller. Ensuite les processus de mélange entre les différents pôles sont déterminés, et pour chaque pôle de mélange, une composition chimique et isotopique est évaluée. Pour confirmer ces processus de mélange, des essais de pompage sont réalisés dont l'objectif est de faire varier les paramètres physico-chimiques des eaux des forages exploités en modifiant drastiquement les débits.

La modélisation géochimique avec le code PHREEQC permet de calculer pour chaque pôle de mélange et pour les eaux exploitées les plus chaudes les indices de saturation des minéraux constituant les roches rencontrées. Cette méthode permet de connaître l'état de saturation de l'eau vis-à-vis d'un ensemble de minéraux. En imposant une augmentation de la température dans la modélisation géochimique, il est possible de visualiser la variation des indices de saturation et donc d'estimer la température du réservoir profond et la composition chimique du fluide dans son réservoir. En utilisant les résultats de la modélisation géochimique, l'origine des éléments dissous dans l'eau est évaluée. D'autres méthodes complètent cette évaluation comme l'utilisation de certains isotopes, notamment pour les sulfates, et le calcul des rapports ioniques Cl/Br pour connaître l'origine des chlorures.

En utilisant différentes équations et les valeurs obtenues pour les isotopes stables de l'eau, l'altitude moyenne de la zone d'infiltration des eaux est calculée. Ensuite, la température du réservoir profond est également calculée sur la base d'une sélection de géothermomètres, et enfin le temps de transit souterrain est évalué à partir des données isotopiques. Tous les résultats obtenus provenant des investigations géologiques, hydrogéologiques, géochimiques et isotopiques sont finalement intégrés dans un modèle conceptuel d'écoulement régional.

Le modèle conceptuel d'écoulement régional ainsi élaboré est ensuite vérifié grâce à la construction d'un modèle numérique en deux ou trois dimensions. A partir d'une coupe géologique ou d'un bloc diagramme, une grille de calcul est conçue mettant en évidence les différentes unités géologiques. Cette étape de discrétisation permet ensuite d'imposer des paramètres au modèle comme par exemple le flux d'eau entrant, la perméabilité des roches, le flux thermique, etc. Les équations du transport de masse et de chaleur permettent de calculer, en régime permanent dans un premier temps, les valeurs de température et de charge hydraulique pour chaque nœud de la grille de calcul. Les résultats obtenus par la simulation sont comparés aux données observées afin de calibrer le modèle. Après avoir représenté l'état initial du système hydrothermal en régime permanent, une condition particulière est ajoutée au modèle pour certains cas montrant par exemple les effets à long terme d'un puits de production ou encore de la mise en charge d'un lac dans une région donnée.

3. Lavey-les-Bains (partie III)

3.1 Géologie (chapitre 4)

Le site hydrothermal de Lavey-les-Bains en Suisse est localisé dans la vallée du Rhône sur sa rive droite entre les villes de Martigny et de Saint-Maurice (Figure 1). Géologiquement, le site est localisé à l'extrémité nord-est du massif cristallin des Aiguilles Rouges qui représente un des massifs cristallins externes des Alpes occidentales. En survolant l'ensemble des Aiguilles Rouges, on peut s'apercevoir que la zone de remontée des eaux thermales se situe au niveau du point altitudinal (ou topographique) le plus bas atteint par cette unité géologique dans la région. Dans la zone des forages, les gneiss hercyniens sont présents sous le recouvrement Quaternaire qui s'épaissit fortement en direction du centre de la vallée (environ 500 mètres de dépôts). En revanche, à proximité de l'établissement thermal situé quelques hectomètres en aval des forages, la couverture sédimentaire autochtone affleure et forme d'imposantes falaises dont il est possible d'apercevoir de nombreux plis couchés.

Le massif cristallin des Aiguilles Rouges est composé de plusieurs types de roche dont les plus fréquents sont les paragneiss et les orthogneiss. Ces roches ont été fortement déformées par les contraintes hercyniennes et alpines et les différentes directions de fractures observées témoignent de ces deux épisodes. Néanmoins, la direction NE-SO à NNE-SSO est clairement la plus visible en surface, c'est-à-dire plus ou moins parallèle à l'allongement du massif. L'infiltration des eaux météoriques se réaliserait en grande partie grâce à cette famille de fractures, dans la zone décomprimée d'une part puis plus en profondeur lorsque les failles sont suffisamment profondes et perméables.

Les structures géologiques mettant en contact le massif cristallin des Aiguilles Rouges avec les autres massifs voisins sont complexes. En effet, le socle des Aiguilles Rouges est chevauché sur sa bordure sud-est par celui du Mont-Blanc, et entre les deux unités il existe une zone étroite de roches sédimentaires appartenant à la base de la nappe de Morcles. Vers le nord-ouest, le socle des Aiguilles Rouges chevauche un autre socle appelé Infra-Aiguilles Rouges. Ce dernier n'affleure pas car il est recouvert par de nombreuses nappes sédimentaires, mais il est probablement présent à 2-3 kilomètres de profondeur sous la vallée du Rhône à la hauteur de Lavey-les-Bains. Ce plan de chevauchement collecterait les eaux infiltrées depuis les reliefs des Aiguilles Rouges et permettrait la remontée du fluide géothermal vers la surface.

3.2 Hydrogéologie et géochimie (chapitre 5)

L'eau thermale à Lavey-les-Bains est exploitée grâce à deux forages recoupant les fractures des gneiss du massif des Aiguilles Rouges. Il s'agit du puits P201 à 201 mètres de profondeur réalisé en 1972, et du puits P600 à 517 mètres de profondeur réalisé en 1997, dont les débits maximaux d'exploitation sont respectivement d'environ 480 L/min et 1280 L/min. Depuis la mise en production du forage P600 en 1997, des baisses significatives de température et de conductivité ont été observées. Au P201, ces paramètres ont diminué de 63 à 57°C et de 1700 à 1400 μS/cm ; au P600 de 68 à 65°C et de 2200 à 1700 μS/cm.

Une accentuation du mélange a pu être mise en évidence entre une eau bicarbonatée calcique froide issue de la nappe du Rhône sus-jacente et/ou des gneiss au pied des Dents de Morcles et l'eau thermale chaude sulfatée sodique et chlorurée. L'augmentation du taux de mélange est matérialisée par une diminution de la température, de la minéralisation totale et des teneurs en Li, Na, K, Cl, SO_4, F et SiO_2 alors que les concentrations en Ca, Mg, HCO_3 et tritium augmentent. Le taux de mélange entre ces eaux s'est accentué entre 1997, année de mise en service du P600, et 2001. La composante froide a pris plus d'importance durant cette période. Depuis 2001, la conductivité s'est stabilisée alors que la température a continué de décroitre, mais depuis 2004, il semblerait que cette baisse s'atténue. Cependant, d'après les mesures effectuées en 2009 sur le puits P201, la température semble de nouveau baisser (communication du bureau Alpgeo). Les données chimiques depuis 1972 au P201 montrent une légère augmentation de

l'alcalinité et du magnésium et une diminution des autres éléments majeurs et surtout de la teneur en silice, l'un des marqueurs de l'eau la plus chaude dans les gneiss. Dans le détail, et depuis 1997 cette diminution est accompagnée par des variations saisonnières cycliques dues aux changements de débit de pompage en fonction des besoins de l'établissement thermal. La période hivernale engendre une augmentation des débits au P600 et donc une baisse de la température et de la conductivité au P201. En été, c'est le contraire qui est observé.

Dans le cadre du projet Alpine Geothermal Power Production, une estimation de la composition chimique de l'eau thermale présumée à 2-3 kilomètres de profondeur et 100-110°C a été réalisée, en prenant comme hypothèse que l'aquifère est géologiquement homogène. Autrement dit, la composante thermale pure de l'eau captée au P600 (soit environ 95%) est représentative de l'eau thermale profonde non mélangée et refroidie par conduction lors de sa remontée. Sa composition chimique évolue donc peu. En tenant compte de l'équilibre chimique de l'eau thermale pure avec les minéraux constitutifs de la roche dans le réservoir simulée à l'aide du logiciel PHREEQC, la minéralisation totale de l'eau thermale pure est légèrement plus élevée que celle de l'eau du P600 (TSD: environ 1750 mg/L contre 1400). De plus, l'extrapolation des données des analyses chimiques et isotopiques des différents forages du site de Lavey-les-Bains, basée sur le caractère conservatif du chlorure, montre également une minéralisation totale de l'eau thermale pure un peu plus élevée que celle du P600.

3.3 Modélisation numérique (chapitres 6 et 7)

L'exploitation du forage P600 depuis 1997 a engendré des baisses significatives de température et de conductivité électrique sur le forage P201, qui est moins profond que le P600, par augmentation des processus de mélange. Pour une gestion optimale à long terme de la ressource géothermale, il est important de connaître ces processus et de prévoir leurs évolutions dans le futur. Pour cette raison, des modèles numériques en deux et trois dimensions ont été construits et ont reproduit le système d'écoulement profond. Ces modèles ont également permis de visualiser les effets à long terme de l'exploitation des puits sur la ressource géothermale.

Dans un premier temps, un modèle numérique en deux dimensions, à partir d'une coupe géologique dans le massif des Aiguilles Rouges, a reconstitué un champ de température depuis la zone d'infiltration au niveau des reliefs des Aiguilles Rouges jusqu'à la zone de remontée du fluide profond. Les températures simulées sont très proches de celles supposées avant l'exploitation des puits de pompage. De plus, les températures modélisées du réservoir profond sont en accord avec celles estimées par les géothermomètres (100-130°C). Cependant, le flux simulé d'eau thermale ascendante semble être sous-estimé

(5400-9000 m^3/j) car il correspond à environ 2-4 fois le débit maximal exploité (2380 m^3/j). Pour cette raison, il est possible que la zone de recharge de l'aquifère thermal soit plus étendue que celle utilisée par le modèle. Autrement dit, la zone de recharge pourrait s'étendre un peu plus en direction du sud-ouest, proche de la limite hydrographique entre les bassins versants du Rhône et de l'Arve (vers la frontière entre la France et la Suisse).

Plusieurs simulations ont été réalisées depuis un modèle en trois dimensions construit dans la zone des forages. En changeant les conditions d'exploitation de la ressource géothermale, la baisse des paramètres physico-chimiques observée depuis 1997 a été reproduite, et une éventuelle stabilisation des paramètres à long terme a été modélisée. Pour le forage P201, les taux de mélange calculés avant et après l'exploitation du P600 sont comparables avec les taux de mélange observés. Les températures simulées au P201 montrent une stabilisation vers 56°C après 10-15 ans d'exploitation du P600. La réalisation et l'exploitation de futurs forages profonds sur ce site, tels que ceux prévus dans le cadre du projet AGEPP, pourrait également avoir une incidence sur le potentiel géothermique des forages actuellement exploités.
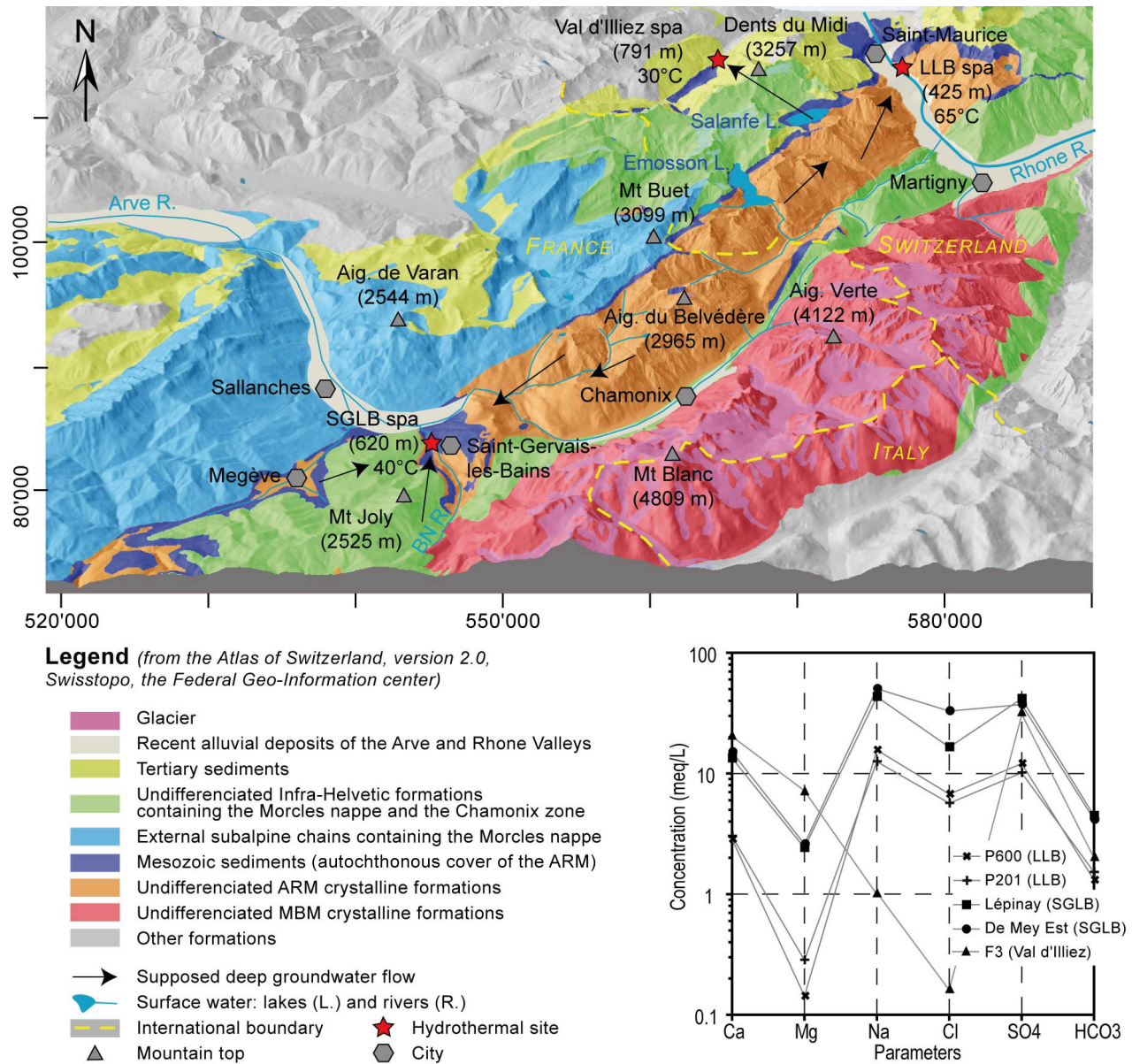
Figure 1: Modèle conceptuel régional des systèmes hydrothermaux de Lavey-les-Bains, Saint-Gervais-les-Bains et Val d'Illiez. Le diagramme de Shoeller montre le type géochimique des eaux thermales de ces trois sites.

4. Saint-Gervais-les-Bains (partie IV)

4.1 Géologie (chapitre 9)

Le site hydrothermal de Saint-Gervais-les-Bains est localisé après les gorges étroites du Bon Nant, affluent de l'Arve, au pied du massif du Mont Blanc en France (Figure 1). Le site est reconnu pour les soins thérapeutiques pratiqués, des eaux thermales y sont exploitées par trois puits de production. Saint-Gervais-les-Bains est également positionné au niveau topographique le plus bas atteint par le socle des Aiguilles Rouges dans cette région. Le socle hercynien n'affleure pas directement sur le site thermal mais est probablement présent à quelques centaines de mètres de profondeur sous la couverture sédimentaire autochtone le recouvrant (Trias-Permien). Les structures profondes du massif des Aiguilles Rouges, mises en évidence sous le site de Lavey-les-Bains, sont certainement aussi présentes en profondeur dans la région de Saint-Gervais-les-Bains, à savoir l'existence d'un contact chevauchant entre les Aiguilles Rouges et l'Infra-Aiguilles Rouges.

A proximité de la zone des bains, la couverture autochtone est chevauchée par la nappe de Morcles qui forme les massifs du Mont d'Arbois et du Mont Joly. Cette nappe est composée de formations sédimentaires mésozoïques (calcaires et marnes) dessinant des plis couchés facilement observable. Dans la région de Megève, cette nappe est érodée ce qui permet au socle et à sa couverture autochtone

d'affleurer. Ce secteur était auparavant considérée comme zone de recharge de l'aquifère thermal.

Dans la région de Saint-Gervais-les-Bains, des failles verticales de direction N-S à NNO-SSE empruntent la vallée du Bon Nant et recoupent toutes les formations géologiques. Ce système complexe de failles permet vraisemblablement la remontée du fluide profond vers la surface car une de ces failles passe sous la zone des forages (faille des sources).

La couverture autochtone a été intensément déformée par les contraintes tectoniques alpines. Les investigations géologiques menées dans les années 1980 et les analyses des cuttings des forages De Mey Est, De Mey Ouest, Lépinay et F99 montrent qu'il existe au sein de cette couverture un plan de chevauchement majeur. Ce plan de chevauchement délimite deux unités géologiques bien distinctes : les formations détritiques du Permien-Trias inférieur recoupées par les forages De Mey Est et De Mey Ouest, les formations dolomitiques et gypseuses du Trias moyen et supérieur traversées par le forage Lépinay. La base de cette dernière unité, aussi appelée zone des écailles, est représentée par une couche peu épaisse (10 mètres environ) de schistes noir et vert. Le forage F99 est le seul qui aurait apparemment recoupé les deux unités. Les sources Sulfureuse et Gontard émergeraient le long de ce chevauchement.

4.2 Hydrogéologie et géochimie (chapitre 10)

Les eaux thermales sont continuellement exploitées grâce à trois forages : Lépinay, De Mey Est et de Mey Ouest. Les forages Lépinay (101.5 m de profondeur avec un débit d'exploitation de 13 m^3/h) et De Mey Est (196 m et 5.5 m^3/h) sont utilisés pour les soins médicaux et la fabrication des produits cosmétiques alors que le forage De Mey Ouest (207 m et 3.5 m^3/h) n'est pas directement utilisé mais garantit une exploitation stable du forage De Mey Est. Le maintien d'une pression artésienne dans le vieux puits Gontard (7.5 m) permet de ne pas surexploiter la ressource géothermale et évite d'avoir des processus de mélange trop importants. A quelques dizaines de mètres en aval de la

zone des forages, deux sources froides nommées Ferrugineuse et Magnésienne émergent dans le lit du torrent Bon Nant au pied des formations dolomitiques et gypseuses du Trias moyen et supérieur. Des dépôts d'oxyde de fer sont visibles sur ces deux sources.

Plusieurs essais de pompage ont pu mettre en évidence les différentes connectivités hydrauliques entre les sources et les forages. Les deux forages De Mey, recoupant les formations détritiques du Permien-Trias inférieur, sont hydrauliquement connectés. En revanche, ils ne le sont pas avec les forages Lépinay et F99, le puits Gontard et la source Sulfureuse, et vice-versa. Par conséquent,

deux aquifères seraient présents sous les dépôts du Bon Nant et contiendraient des eaux thermales. Ces deux aquifères seraient séparés par le plan de chevauchement mettant en contact le Trias moyen et supérieur sur le Permien-Trias inférieur.

Sur le site des bains, trois types d'eau sont présents:

- une eau thermale ascendante Na-SO_4, riche en chlorure ($\approx$ 1.1 g/L) et qui proviendrait du socle des Aiguilles Rouges, avec une conductivité électrique proche de 5 mS/cm et une température d'environ 35°C. Ce type d'eau est caractéristique des eaux thermales jaillissant des forages De Mey Est et De Mey Ouest. En revanche, les eaux provenant du forage Lépinay, qui sont un peu plus chaudes (39°C), sont plus pauvres en chlorure ($\approx$ 0.6 g/L) et sont légèrement enrichies en sulfate.

- une eau froide Ca-SO_4 pauvre en chlorure ($<$ 20 mg/L) avec une conductivité d'environ 2.5 mS/cm et une température entre 8 et 12°C. Ce type d'eau est représenté par les sources Ferrugineuse et Magnésienne en aval des bains qui émergent dans les formations dolomitiques et gypseuses de la couverture autochtone triasique.

- une eau froide circulant à faible profondeur dans les dépôts Quaternaires de la vallée du Bon Nant. La température de cette eau varie entre 4 et 12°C environ en fonction des saisons avec une conductivité toujours inférieure à 0.5 mS/cm.

Les processus de mélange entre ces trois pôles différents dans les deux aquifères de part et d'autre du plan de chevauchement. Ainsi dans l'aquifère du Permien-Trias inférieur, les eaux thermales jaillissant des forages De Mey Est et De Mey Ouest sont mélangées avec une eau Ca-SO_4, riche en magnésium et pauvre en chlorure, qui ressemble fortement à l'eau des sources Ferrugineuse et Magnésienne. Ce processus de mélange est accompagné par une baisse de la température, de la minéralisation, des ions alcalins et des chlorures. En revanche, le calcium et le magnésium augmentent considérablement, alors que les sulfates restent plus ou moins stables car les deux pôles sont riches en sulfate.

Dans l'aquifère des écailles du Trias moyen et supérieur, les processus chimiques semblent être plus compliqués. Les eaux thermales du forage Lépinay sont moins riches en chlorure et plus chaudes, ce qui laisse à penser que ces eaux sont également mélangées avec une eau de type triasique à 35-40°C, riche en sulfate et pauvre en chlorure. Cette mixture serait ensuite mélangée avec les eaux froides des dépôts Quaternaires. Actuellement, l'exploitation de Lépinay engendre une baisse considérable des paramètres physico-chimiques des eaux du vieux puits Gontard (20°C et 1.6 g/L au lieu de 41°C et 5.1 g/L auparavant).

L'origine des fortes teneurs en chlorure dans les eaux thermales ($\approx$ 1.1 g/L) ne peut pas être expliquée par la dissolution de l'halite (NaCl) dans les roches triasiques car:

- les eaux froides des sources Ferrugineuse et Magnésienne circulant uniquement dans les roches triasiques contiennent peu de chlorure ($<$ 20 mg/L). De ce fait, les roches triasiques ne renferment pas d'halite dans cette région.

- les rapports Cl/Br calculés pour les eaux de Saint-Gervais-les-Bains, et comparés avec toutes les eaux thermales des Alpes et des régions limitrophes, montrent que les chlorures proviendraient du lessivage de saumure d'origine marine ou d'inclusion fluide par les eaux infiltrées depuis les roches cristallines fracturées des Aiguilles Rouges. Plus en détail, ce processus se produirait au niveau des plans de chevauchement des massifs cristallins externes vers 2-3 kilomètres de profondeur où ces saumures pourraient être piégées. De plus, la dissolution de la biotite contenue dans les roches cristallines pourrait être également à l'origine des fortes teneurs en chlorure dans les eaux thermales.

Dans les eaux thermales de Saint-Gervais-les-Bains, le sodium est en excès par rapport au chlorure. Des échanges cationiques entre le calcium et le sodium pourraient expliquer cet excès d'autant plus que les sulfates sont aussi en excès par rapport au calcium. De plus, la dissolution des plagioclases contenus dans les roches cristallines des Aiguilles Rouges apporte du sodium mais pas de chlorure, donc cet excès en sodium peut aussi être expliqué de cette manière.

La comparaison des données des isotopes stables des sulfates entre les eaux thermales de Saint-Gervais-les-Bains et les eaux thermales d'autres sites alpins montrent qu'à Saint-Gervais-les-Bains les sulfates auraient une origine mixte. Une partie

des sulfates dans les eaux thermales proviendrait directement des roches cristallines (dissolution de veines de gypse et d'anhydrite, oxydation des sulfures, lessivage des saumures), et une autre partie proviendrait de la dissolution du gypse contenu dans les roches triasiques de la couverture autochtone lors de la remontée du fluide profond depuis le socle.

L'eau thermale Na-SO$_4$ est en équilibre chimique avec la calcite. Elle est sous-saturée en dolomite et en gypse, ce qui n'est pas le cas pour les eaux froides des sources Ferrugineuse et Magnésienne où il y a équilibre. Enfin, l'eau thermale est légèrement sursaturée en quartz et en calcédoine pouvant aboutir à des précipitations de ces minéraux lors de la remontée du fluide profond. Par conséquent, le calcul de la température du réservoir géothermal peut être sous-estimé en utilisant le géothermomètre de la calcédoine.

Le système d'écoulement régional aboutissant aux émergences thermales de Saint-Gervais-les-Bains peut être résumé de la manière suivante:

- la zone d'infiltration doit probablement se situer au niveau du massif des Aiguilles Rouges vers 1700-2100 mètres d'altitude comme pour le système hydrothermal de Lavey-les-Bains. Pour les eaux froides des sources Ferrugineuse et Magnésienne, la zone d'infiltration se situe probablement au niveau du Mont d'Arbois et du Mont Joly, à des altitudes plus basses que pour l'eau thermale (1100-1300 m).

- l'infiltration des eaux en profondeur se ferait principalement grâce aux nombreuses fractures et failles orientées N-S à ENE-OSO dans le massif des Aiguilles Rouges.

- les eaux infiltrées attendraient le réservoir profond au niveau du plan de chevauchement des Aiguilles Rouges sur l'Infra-Aiguilles Rouges où elles acquerraient en partie leur minéralisation en lessivant les saumures piégées ou les inclusions fluides. En utilisant les géothermomètres et les équilibres chimiques, la température du réservoir a été estimée entre 65 et 100°C.

- la remontée du fluide depuis le réservoir profond se ferait dans une zone fracturée et perméable qui pourrait correspondre au système faillé N-S de la vallée du Bon Nant, affectant toutes les formations géologiques présentes.

- avant d'émerger, les eaux thermales traversent les couches sédimentaires de la couverture autochtone en empruntant les zones les plus fracturées et perméables dont le plan de chevauchement mettant en contact le Permien-Trias inférieur et le Trias moyen et supérieur. Dans cette zone, de nombreux processus chimiques comme les mélanges entre les différents pôles, la dissolution des roches triasiques et les échanges cationiques se produisent et sont à l'origine de la diversité chimique des eaux rencontrées.

4.3 Modélisation numérique (chapitre 11)

A partir d'une coupe géologique dans la partie occidentale du massif des Aiguilles Rouges, un modèle numérique en deux dimensions a reconstitué le système hydrothermal de Saint-Gervais-les-Bains. Ce modèle en mode permanent représente donc le champ de température simulé depuis la zone d'infiltration sur les reliefs des Aiguilles Rouges jusqu'à la zone de remontée du fluide profond. De plus, ce modèle intègre le secteur du Mont d'Arbois et du Mont Joly jusqu'au soubassement cristallin de Belledonne et met en évidence les écoulements dans la couverture autochtone triasique à l'origine des sources froides Ferrugineuse et Magnésienne.

Les températures simulées à la base du système hydrothermal sont comprises entre 60 et 75°C,

légèrement inférieures à l'estimation faite à partir des équilibres chimiques et des géothermomètres (65-100°C). En réalité, la température du réservoir dépend de la profondeur où se trouverait le plan de chevauchement des Aiguilles Rouges sur l'Infra-Aiguilles Rouges ; cette profondeur est difficile à évaluer dans la région de Saint-Gervais-les-Bains. Dans le secteur du Mont d'Arbois et du Mont Joly, les écoulements simulés dans la couverture autochtone donnent une température des sources Ferrugineuse et Magnésienne d'environ 10°C, ce qui correspond bien à ce qui est observé sur le terrain. Pour ce secteur dans le modèle, il y a très peu d'écoulement dans le socle cristallin de Belledonne localisé sous la couverture autochtone (faible per-

méabilité), et donc le gradient géothermique simulé est relativement fort.

Le flux d'eau thermale ascendant simulé est compris entre 90 et 160 m^3/h, selon la largeur sélectionnée du bassin d'alimentation. Ce flux calculé représente 4 à 7 fois le débit maximal des trois forages d'exploitation (22.5 m^3/h). Cela semble peu si on suppose qu'une grande partie des eaux thermales ascendantes (facteur 10 ou plus par rapport à ce qui est actuellement exploité) se diffuse dans la couverture autochtone et dans les formations Qua-

ternaires. Les dimensions de la zone d'infiltration sont difficiles à juger pour ce site et donc les résultats donnés par la modélisation numérique sont à considérer avec précaution. Enfin, les structures géologiques complexes dans la zone des bains, notamment dans la couverture autochtone, sont un obstacle à l'élaboration d'un modèle numérique en trois dimensions. Il faudrait des études complémentaires, notamment géophysiques, pour mieux discerner les relations entre les différentes unités géologiques.

5. Val d'Illiez (partie V)

5.1 Géologie (chapitre 13)

Le site hydrothermal de Val d'Illiez est localisé dans le canton du Valais en Suisse à une altitude d'environ 790 mètres dans la vallée de la Vièze au lieu dit Buchelieule. La Vièze est un affluent du Rhône et se jette dans ce dernier à la hauteur de Monthey. Respectivement à 1 kilomètre en amont et en aval de Buchelieule, des eaux subthermales ont été détectées dans un puits peu profond à Play et dans une source au lieu dit Le Fayot.

La zone hydrothermale de Val d'Illiez est située à la limite entre les Préalpes au nord-ouest et le domaine helvétique au sud-est. Le domaine helvétique où est positionné le site thermal est composé du massif cristallin des Aiguilles Rouges, des formations sédimentaires autochtones et parautochtones et enfin de la nappe de Morcles. Les Dents du Midi forment les plus hauts sommets de la région (3257 m) et mettent en valeur les plis couchés de la nappe de Morcles. Cette nappe chevauche les flyschs parautochtones qui chevauchent les formations sédimentaires de la couverture autochtone du socle des Aiguilles Rouges. C'est à la base de la couverture autochtone que le système d'écoulement des eaux thermales de Val d'Illiez se produit, autrement dit dans les formations dolomitiques et gypseuses du Trias. Ces formations affleurent sur la bordure nord-ouest du massif cristallin et forment une bande de quelques hectomètres de largeur sur plus de 20 kilomètres de longueur. L'épaisseur de la couverture autochtone semble augmenter considérablement en allant vers le nord-ouest. Elle a une épaisseur de quelques dizaines de mètres là où elle af-

fleure en bordure du socle et aurait une épaisseur supérieure à 1000 mètres sous la vallée de la Vièze. La fenêtre de Champéry le long de la Vièze laisse dévoiler d'imposantes falaises de plusieurs dizaines de mètres de hauteur avec des calcaires massifs du Jurassique supérieur-Crétacé. Ces formations reposent sur une épaisse couche de marne et de calcaire du Jurassique inférieur et moyen qui reposent sur le Trias. Les formations détritiques du Tertiaire (flysch, grès, etc.) complètent cette série.

Le contexte géologique régional de la couverture autochtone sous les Dents du Midi est complexe. En effet, il est supposé que la couverture forme un vaste anticlinal avec, au front de celui-ci, un plan de chevauchement majeur de pendage vers le sud-est qui se rattacherait profondément au plan de chevauchement du massif des Aiguilles Rouges sur l'Infra-Aiguilles Rouges.

Sur le site des bains, les structures géologiques semblent également complexes. En effet, la limite chevauchante entre le flysch parautochtone et le toit de l'anticlinal de la couverture autochtone recoupe la vallée de la Vièze à la hauteur des sources thermales. A cet endroit, la couverture autochtone est composée de formations Tertiaires, autrement dit des flyschs et des grès. D'après les observations des cuttings des forages, les grès des Carrières présents sur la rive gauche de la vallée, sous les dépôts Quaternaires, permettraient la remontée des eaux thermales vers la surface en raison de leur fracturation intense.

5.2 Hydrogéologie et géochimie (chapitre 14)

C'est en 1953 que les sources thermales de Val d'Illiez ont apparu après une série de secousses sismiques. Peu de temps avant l'apparition des secousses, un lac artificiel créé à partir d'un barrage hydroélectrique, le lac de Salanfe, a été implanté dans la zone d'infiltration du système hydrothermal, sur les formations triasiques de la couverture autochtone en bordure de socle des Aiguilles Rouges. Des fluites par le fond du lac ont été rapidement constatées au niveau des formations triasiques perméables et ont généré une augmentation des pressions sur l'aquifère thermal et certainement l'ouverture de fractures. Ceci a vraisemblablement causé les secousses ressenties et l'activation accrue du système hydrothermal. Cependant, des récits datant d'avant 1953 mentionnaient déjà la présence d'une zone marécageuse avec des eaux vers 18°C au niveau de l'emplacement actuel des sources thermales à Buchelieule, ce qui laisse à penser que le système hydrothermal existait réellement avant la construction du barrage hydroélectrique.

Pour empêcher de trop grosses pertes du lac quand le niveau était au dessus de 1910 mètres, des travaux d'étanchéification ont été réalisés. Grâce à ces travaux, le niveau du lac a pu atteindre la cote d'environ 1925 mètres en 1994, et peu de temps après, suite à une nouvelle crise sismique, les débits des sources thermales ont considérablement augmenté avec l'apparition de nouvelles sources. Le débit des résurgences thermales varie de façon saisonnière, de la même manière que le niveau d'eau du lac de Salanfe mais avec un décalage d'environ 140 jours.

Trois forages F1 (26 m), F2 (42.5 m) et F3 (113 m) ont été réalisés en 1994 suite à l'augmentation des débits des sources thermales. Les trois forages sont jaillissants et l'eau thermale qui sort de ces forages à une température entre 28 et 30°C et une minéralisation proche de 1.8 g/L. Actuellement, le forage F3 qui a le débit le plus important est exploité pour le remplissage des piscines. Le forage F1 alimente plusieurs conduites pour réchauffer les dalles au sol vers la cascade thermale et alimente l'étang, alors que les eaux du forage F2 sont directement déversées au pied de la cascade thermale avant de rejoindre le torrent Vièze.

La cascade thermale, la petite cascade de la grotte et la douche sont alimentées par la dite "chambre de captage" construite en 1980. Actuellement, 6 drains horizontaux implantés dans le versant alimentent la chambre de captage avec des débits, des températures et des minéralisations variant entre 7 et 300 L/min, 22.1 et 23.9°C, et 1250 et 1470 mg/L (valeurs mesurées en juin 2009). Dans la chambre de captage, les eaux thermales des ces 6 drains se mélangent et sont ensuite évacuées vers la cascade, la grotte et la douche avec la possibilité de réguler les débits pour chaque point. Les eaux mélangées de la chambre de captage se dirigeant vers la cascade empruntent un conduit aussi nommé "cascade centre". A coté de celui-ci, un autre conduit appelé "cascade droite" alimente également la cascade et est indépendant de la chambre de captage.

Sur le site des bains, deux types d'eau sont présents:

- une eau thermale Ca-SO$_4$ émergeant des forages F1, F2 et F3. Cette eau a une température entre 28 et 30°C et une minéralisation proche de 1.8 g/L. Elle a la particularité d'être pauvre en chlorure (< 5 mg/L) et en éléments alcalins (≈ 20 mg/L), et d'être riche en magnésium (≈ 75 mg/L), ce qui laisse à penser que cette eau s'est minéralisée au contact des roches triasiques gypseuses et dolomitiques de la couverture autochtone des Aiguilles Rouges sans influence des roches cristallines.

- une eau Ca-HCO$_3$ émergeant des sources froides autour des bains dont les températures ne dépassent pas 10°C et dont les minéralisations sont inférieures à 500 mg/L. Cette eau circule dans les formations Quaternaires et Tertiaires de la vallée de la Vièze et le long des versants.

Des processus de mélange entre ces deux pôles sont observables en analysant les différents points d'eau. En supposant que l'eau thermale non mélangée a une température d'environ 30-31°C et une minéralisation proche de 2 g/L, il est possible d'en conclure que les eaux jaillissant des forages F1, F2 et F3 sont relativement peu influencées par les processus de mélange. En revanche, les eaux thermales provenant de la chambre de captage sont mélangées : environ 60% d'eau thermale pure et 40% d'eau froide. La composante thermale

non mélangée est en équilibre avec les carbonates et légèrement sous-saturée en gypse et anhydrite. Cette eau a également un léger excès en sulfate par rapport au calcium (21 meq/L contre 26.7) ce qui laisse à penser que des précipitations de calcite sont possibles en profondeur.

La signature chimique de la composante thermale montre que l'eau s'est minéralisée au contact des roches triasiques perméables à la base de la couverture autochtone. Cependant, les calcaires fracturés et probablement karstifiés du Malm et le Crétacé de la couverture autochtone, au dessus du Trias, peuvent aussi contenir des quantités d'eau importantes (circulations karstiques). Pour cette raison, il n'est pas exclu que les eaux de ces formations aient une influence sur la composante thermale non mélangée pendant la remontée du fluide vers la surface.

La composante thermale non mélangée a des valeurs en isotopes stables de l'eau très proches des valeurs mesurées pour les eaux thermales du système de Lavey-les-Bains. Il est donc supposé qu'une zone de recharge se situe à une altitude entre 1700 et 2100 mètres dans la région du lac de Salanfe dont l'altitude est d'environ 1900 mètres. D'après les équilibres chimiques, la température du réservoir profond serait entre 35 et 40°C, et celui-ci serait situé à environ 1 kilomètre sous la zone des bains. A partir des données existantes en tritium et en utilisant le modèle piston-flow, le temps transit souterrain moyen du système hydrothermal serait proche de 5 ans.

5.3 Modélisation numérique (chapitre 15)

Dans un premier temps un modèle thermohydraulique en deux dimensions, à partir d'une coupe géologique passant par la zone des bains, les Dents du Midi et la région du lac de Salanfe, a permis de reconstituer l'état naturel du système hydrothermal avant l'implantation du lac de Salanfe. Ce modèle prend en compte le fait que la couverture forme un vaste anticlinal délimité au nord-ouest par un plan de chevauchement majeur. En mode permanent, un champ de température a été simulé depuis la zone d'infiltration sur l'autochtone affleurant en bordure des Aiguilles Rouges jusqu'à la zone de remontée du fluide profond, avec les résultats suivants : 31°C à 200 mètres de profondeur sous la zone des bains, 36-40°C au niveau du réservoir à 1 kilomètre de profondeur environ. En considérant que l'infiltration des eaux se produit sur toute la bordure des Aiguilles Rouges, soit une vingtaine de kilomètres environ, la recharge totale obtenue est de 4800 m^3/j ou 3330 L/min. Cette approximation peut tout-à-fait représenter le flux d'eau thermale ascendant avant l'implantation du lac de Salanfe.

Après avoir représenté le système dans son état naturel, le lac de Salanfe a été ajouté dans le modèle numérique. L'objectif est de savoir si les pertes d'eau du lac observées dans les formations triasiques à Salanfe alimentent directement les sources thermales comme si l'on faisait couler de l'eau dans un simple tuyau depuis le lac vers les sources. Il est évident qu'un tel processus doit engendrer des modifications du régime thermal c'est-à-dire un changement des paramètres physico-chimiques des sources et un refroidissement des roches où l'eau circule. Pour répondre à cette question, trois scénarios ont été testés avec différentes valeurs de perte du lac (1, 2 et 5 mm/j) représentant la baisse du niveau d'eau du lac en millimètre par jour. Enfin, un quatrième scénario a été testé en fixant une charge imposée égale à l'altitude du lac, mais cette hypothèse ne semble pas correspondre à la situation réelle car il existe certainement une zone non saturée assez épaisse (d'où le décalage entre l'évolution des niveaux du lac et l'évolution du débit des sources).

Pour chaque scénario en mode permanent, un refroidissement à l'exutoire du modèle et dans les roches est simulé. Plus les apports depuis le lac sont importants et plus le refroidissement à long terme est marqué. En mode permanent, pour une perte équivalente à 2 mm/j, la température à l'exutoire du modèle est de 11.6°C avec une température à 1 kilomètre de profondeur de 15°C.

En visualisant les résultats en fonction du temps, en régime transitoire, on s'aperçoit dans un premier temps que l'augmentation du débit à l'exutoire est accompagnée par une hausse de la température. Pour chaque scénario, cette hausse est d'environ 5°C et se produit durant les premières années après l'implantation du lac. Ceci est dû à la poussée accrue de l'eau chaude du réservoir vers la surface par une plume d'eau froide. Après quelques années, les simulations montrent une baisse progressive des températures sans modification des débits. Ceci est

dû à l'arrivée de la plume froide vers la surface après l'évacuation des eaux chaudes du réservoir. Enfin, les températures simulées tendent progressivement vers les valeurs calculées en régime permanent.

La variation des paramètres physico-chimiques simulés à l'exutoire du modèle ne correspond pas aux variations naturelles observées des sources thermales. Pour rappel, l'augmentation des débits des sources thermales a été brutale suite à plusieurs secousses sismiques, quelques mois après l'implantation du lac de Salanfe en 1953. Plus tard dans les années nonante, il a été démontré que le débit des sources thermales varie de la même manière que le niveau d'eau du lac, avec un décalage d'environ 140 jours. Seuls les travaux d'étanchéification du lac en 1994 ont perturbé les débits des sources. En effet, ces travaux avaient permis au lac d'atteindre sa cote la plus haute (1925 m), et quelques mois après, les débits des sources avaient considérablement augmenté. Ajouté à cela, les températures des sources les plus chaudes n'ont pratiquement pas évolué en 56 ans, entre 1953 et 2009. Les nombreuses mesures depuis les années

quatre-vingt indiquent que la température est restée pratiquement stable autour de 30°C.

En comparant les résultats de la simulation avec les observations sur les sources, il s'avère que la relation entre le lac de Salanfe et les sources thermales semble plus compliquée qu'il n'y paraît. En effet, l'eau s'écoulant depuis les pertes du lac ne communiquerait pas directement avec les sources thermales. Cette eau exercerait en profondeur une pression sur l'aquifère thermal provoquant ainsi une augmentation des débits à l'exutoire du système hydrothermal, sans processus de mélange et donc sans modification sensible de la température et des paramètres chimiques des sources. Dans le canton des Grisons en Suisse, le système hydrothermal de Bad Ragaz ressemble à celui de Val d'Illiez, où des pressions sont exercées sur l'aquifère thermal, dans des formations sédimentaires, par un autre aquifère sus-jacent. Les pressions les plus fortes sont exercées au moment de la fonte des neiges et après des évènements pluvieux importants, augmentant fortement le débit de la source thermale de Bad Ragaz sans modification sensible des autres paramètres.

6. Conclusion et perspectives (partie VI)

Les sites hydrothermaux de Lavey-les-Bains et de Saint-Gervais-les-Bains sont localisés au niveau des deux "points-bas" du massif cristallin des Aiguilles Rouges, au nord-est et au sud-ouest respectivement. Les eaux thermales issues de ces deux sites ont des caractéristiques chimiques et isotopiques semblables. Le massif cristallin des Aiguilles Rouges, qui forme une bande orientée NE-SO, est délimité au nord-ouest et au sud-est par les plans de chevauchement des massifs cristallins externes. Le massif des Aiguilles Rouges est pincé entre le massif du Mont Blanc et le massif nommé Infra-Aiguilles Rouges qui n'affleure pas. Sur les côtés, les vallées du Rhône et du Bon Nant, orientées NNO-SSE recoupent perpendiculairement les Aiguilles Rouges où des failles sont présentes. Cette morphologie particulière est favorable aux systèmes d'écoulement profond avec l'émergence d'eau thermale au niveau des points-bas.

Dans les Alpes occidentales, il existe d'autres massifs cristallins externes : Aar, Mont Blanc, Belledonne, Pelvoux et Argentera du nord au sud. En bordure de ces massifs, excepté pour Pelvoux, des sites hydrothermaux sont présents dont les

eaux thermales ont des caractéristiques chimiques et isotopiques semblables. Lavey-les-Bains et Saint-Gervais-les-Bains ne sont donc pas des cas isolés. Pour quelques sites, le recouvrement Quaternaire peut localement masquer la remontée des eaux thermales car celles-ci se diffusent dans le Quaternaire et se mélangent avec les eaux froides. D'autre part, les processus de mélange avec des eaux plus froides, circulant dans les formations sédimentaires le long des massifs cristallins, peuvent induire en erreur sur le potentiel géothermique réel d'un secteur. Par exemple à Saxon, le long de la vallée du Rhône en Suisse, une eau thermale à 24°C émerge à la limite entre le massif cristallin du Mont Blanc et sa couverture autochtone. Des forages peu profonds dans le socle à proximité de la source de Saxon ont capté des eaux à 26°C avec une signature chimique différente. Saxon est situé au niveau topographique le plus bas atteint par le massif cristallin du Mont Blanc dans la région, ce qui laisse à penser que ce site est localisé sur une zone dont le potentiel géothermique serait plus important qu'il n'y paraît. Le site de Brigerbad est également très intéressant car il se situe au niveau topographique le plus bas atteint par le

massif cristallin de l'Aar. Une source à 50°C est exploitée dont la signature chimique Na-SO$_4$ montre un écoulement profond dans les roches cristalline, et des forages entre 100 et 600 mètres de profondeur ont été récemment réalisés. Pour détecter d'autres zones de remontée de fluides profonds vers la surface, des investigations géophysiques tels que la tomographie seraient utiles. Comme les eaux thermales sont très souvent plus minéralisées que les eaux froides de plus faible profondeur, la tomographie pourrait donner des informations intéressantes car cet outil permet la détection d'anomalies électriques à quelques dizaines de mètres de profondeur.

Part I

Introduction

1. Foreword and objectives

Deep groundwater systems in normal heat flow conditions are considered as low-enthalpy geothermal systems and are widespread compared to high-enthalpy geothermal systems in the world. This is because their occurrence only requires the presence of either a deep flow, or a shallow flow at a close proximity a geothermal resource, which is then heated by the local heat flux (Albu et al. 1997). In Switzerland, there is no volcanic or magmatic activity at depth and thus the presence of low-enthalpy systems in Switzerland is related to natural deep flow systems of meteoric water origin whose occurrence is determined by a series of precise conditions: infiltration area, active downflow, permeability at depth, concentrated and fast upflow, favorable geomorphological surface patterns, etc. These hydrogeological conditions often occur in areas where the geological setting is complex with dipping sedimentary formations, fault intersections, thrust faults, etc., putting in contact various types of rocks. The Alps range is one of the areas in Europe where many deep circulation systems can occur as thermal springs. According to Bowen (1989), deep flow systems are convective geothermal systems characterized by both high porosity and high permeability, and by deep natural circulation of the working fluid (meteoric water), with the majority of the heat being transferred by circulating fluids and not by conduction. The convective process induces increased temperatures in the upper part of the circulation system and a corresponding lowering of temperature occurs in the lower part.

In the Swiss and French parts of the Alps Mountain, some of the discharged thermal springs are directly used or pumped via boreholes at different depths, mainly for spa and various medical treatments and sometimes for heating buildings and drinking water: Acquarossa, Andeer, Bad Ragaz, Brigerbad, Lavey-les-Bains, Leukerbad, Ovronnaz (Leytron spring), Saillon, Sankt-Moritz, Saxon, Vals and Val d'Illiez in Switzerland; Aix-les-Bains, Allevard, Berthemont-les-Bains, Brides-les-Bains, Challes-les-Eaux, Digne-les-Bains, Gréoux-les-Bains, La Léchère, Le Monêtier-les-Bains, Montbrun-les-Bains, Saint-Gervais-les-Bains, Salins-les-Bains and Uriage-les-Bains in France. For these thermal waters under exploitation, global geological and hydrogeological studies were often carried out with the aim to understand the deep flow systems.

The raised questions for the Alpine deep flow systems often revolve around the same subjects: regional and local geology, water chemistry, mixing processes, infiltration area, water-rock interaction, circulation depth, upflow conditions, residence time, fluid origin, etc. To reply to these quoted questions, different methods can be employed and combined together such as geological, hydrogeological, geophysical, geochemical, isotopic and numerical investigations. The time spent studying a hydrothermal system and the financial resources available are two factors limiting quality and quantity of investigations required to decipher the characteristics of the studied deep flow system. In this thesis, geophysical investigations could not be achieved. However, geophysical measurements would have certainly provided interesting results to compare with the other methods, and would have probably brought additional knowledge, in particular for the deep geological structure of the hydrothermal reservoir. Concerning the chemical and isotopic investigations, the financial resources available were limited to the analysis of chemical species dissolved in water, especially for the major ions. Some selected waters were analysed for their trace elements and water stable isotopes, also carried out at the Center for Hydrogeology in Neuchâtel. Expensive analyses for more sophisticated isotopes and dissolved gas could not be carried out. For each studied hydrothermal site, a single large sampling campaign was conducted including the thermal, subthermal and cold waters. Finally, the representation of the deep flow systems using a coupled flow and heat numerical model was useful to validate assumptions formulated from other methods. These investigations bring a scientific basis providing information required to better manage the short and long term exploitation of the discharged thermal water, qualitatively and quantitatively. They also bring crucial knowledge to prepare future geothermal projects with boreholes and to limit failures that may occur for sub-surface and deep geothermal prospection. High costs for the implementation of a deep borehole are necessary to lower the risk of failure as much as possible, i.e. it requires a good knowledge of the explored site. This is important for the long term sustainable development of geothermal projects.

2. Selected sites

The three selected hydrothermal sites are represented in Figure 2 on the tectonic map of the Western Alps. They are located in the northern Alpine foreland and Helvetic nappes domain according to Schmid et al. (2004). Two of them are located in Switzerland (Lavey-les-Bains and Val d'Illiez) and the third is in France (Saint-Gervais-les-Bains). The first selected hydrothermal system is Lavey-les-Bains to the north-east end of the Aiguilles Rouges crystalline Massif, studied during my Master-thesis with the aim of highlighting the physico-chemical changes with the exploitation of the thermal aquifer (Sonney 2007). The Master-thesis ended in February 2007 and much important knowledge had already been acquired before the beginning of this study, especially concerning mixing processes between deep geothermal fluids and shallow groundwater. Additional investigations, including some modelling investigatins, were made for Lavey-les-Bains in 2007 within the framework of the Alpine Geothermal Power Production (AGEPP) project. The main objective of this project is to exploit the deep fluid in its reservoir from one or two boreholes which are expected to exceed 1.5 kilometres depth. The AGEPP project is ongoing and drilling works may occur as soon as 2010.

The second selected site is Saint-Gervais-les-Bains in France and was studied in 2008. The choice of this site was based on the fact that its location is very similar to the south-western end of the Aiguilles Rouges crystalline Massif, on the sedimentary cover of this massif. Moreover, several investigations at Saint-Gervais-les-Bains during the 1980's showed that the thermal water has high complicated chemical fingerprints, an association of Ca-SO$_4$ and Na-Cl waters with some chemical and isotopic similarities to the thermal water

at Lavey-les-Bains, discharging from a highly deformed geological setting putting in contact various rock types. Therefore, it was interesting to investigate this largely unknown complicated hydrothermal system. One of the main objectives is to highlight the relation existing between the Lavey-les-Bains and Saint-Gervais-les-Bains deep flow systems as weel as the deep geological structure at the bottom of the Aiguilles Rouges Massif. There is no ongoing geothermal project at Saint-Gervais-les-Bains supporting more advanced investigations, but for all the reasons mentioned above, the section of this hydrothermal site was well in the logical continuity of this study.

Val d'Illiez in Switzerland represents the third investigated hydrothermal site. Its location in a sedimentary domain of the Aiguilles Rouges basement shows at first sight a lack of relation with respect to the two other sites. In detail, the Val d'Illiez deep flow system occurs in sedimentary formations related to the Aiguilles Rouges crystalline Massif, in particular in the Triassic rocks covering the basement and outcropping along its northwestern edge. The chemical and isotopic fingerprint of the thermal waters in the Val d'Illiez is quite different compared to Lavey-les-Bains and Saint-Gervais-les-Bains due to low concentrations of Na-Cl ions. Investigations conducted in the Val d'Illiez are therefore a good way to compare thermal regimes occurring inside the basement and its sedimentary cover, hence the chosen title of this study: groundwater flow, heat and mass transport in geothermal systems of a Central Alpine Massif. One of the main objectives allowed the groundwater residence time to be evaluated based on a new tritium sampling campaign in 2009 and using previous tritium data during the 1990's.

3. Structure of this study

The research study is structured as follows: the first part describes the methods applied for interpreting the results, and to explain the generalities about thermal waters and natural flows in the Alpine domain. The other parts are describing the obtained results for the three selected hydrothermal sites. In detail, the chapter 1 speaks about definition, use and properties of mineral and

thermal waters. A section highlights the use and properties of geothermal fluids in Switzerland, related to the BDFGeotherm database (Sonney and Vuataz 2008, Sonney and Vuataz 2010c) built in 2007 under contract for the Swiss Federal Office of Energy (SFOE). This section shows the majority of geothermal-hydrothermal sites of Switzerland, whether in use or not. This chapter concludes by

describing the natural flows in the Alpine domain leading to thermal springs. Based on previous studies within the crystalline and Triassic environments of interest, the flow patterns are grouped into three types (surface, sub-surface and depth).

The chapter 2 is fully devoted to the methods used to investigate each site. Firstly, the geological investigations, and then the hydrochemical and numerical methods are described. In-situ measurements, sampling and laboratory analyses for each type of dissolved species are explained. Then the interpretation of the methods are described. A longer section is devoted to studying the applicability of geothermometers, also being sent for the Proceedings of the World Geothermal Congress in 2010 (Sonney and Vuataz 2010b). This study was realized from chemical and isotopic data in deep boreholes in the Molasse Basin and the Tabular Jura where there were temperature measurements representative of the aquifer conditions. The comparison between the measured and calculated temperatures showed which geothermometers were more reliable and thus would be employed in this study. An introduction of the numerical modelling of groundwater flow, heat and mass transport is presented with the solved equations and the overall procedure to follow in order to make the model operational.

The second, third and fourth parts deal with the results obtained from investigations on each site, starting with Lavey-les-Bains, then Saint-Gervais-les-Bains and lastly Val d'Illiez. Each part begins with a chapter covering the geographical setting, and then the geological setting, the hydrogeological setting, and finally the two dimensional vertical modelling of groundwater flow and heat transport. The geographical setting chapter discusses the history of the site, the characteristics of used springs and wells, and the transport and exploitation of thermal waters. The geological setting chapter is divided into two sections: the regional and the local geological settings. In this chapter, rock types are described, as well as the geological events, the fracturing and the deep structure. The chapter describing the hydrogeological setting and the interpretation of the results is also separated into the local and regional setting. The local hydrogeological setting is as follows: Studies that have previously been done on the site, water chemistry, mixing processes, composition of the end-members, variations of physical and chemical parameters, water-rock interactions. For the regional hydrogeological setting, the section firstly discusses the nature of the regional deep flow system, then the mean elevation of the recharge zone, the reservoir temperature, the depth evaluation of the reservoir and finally the groundwater residence time. The chapter about two-dimensional vertical modelling of groundwater flow and heat transport aims to represent the deep flow system and to validate assumptions formulated from the geological and hydrogeological investigations. In this chapter, the overall procedure to build a model is described, starting from the geological cross section, its discretization, the assigned parameters and finally the comparison between computed values and field measurements. For Lavey-les-Bains, another chapter was added concerning the three-dimensional local modelling of groundwater flow, heat and mass transport, published in 2009 in Hydrogeology Journal (Sonney and Vuataz 2009) with the aim to discuss the long-term consequences of exploiting the thermal aquifer.

Finally, the chemical and isotopic data collected during this study are illustrated in appendixes, and are divided into three sections for each site. The historical data for all sampling points are present in a CD-ROM accompanying this manuscript (Sitename_data.xls).
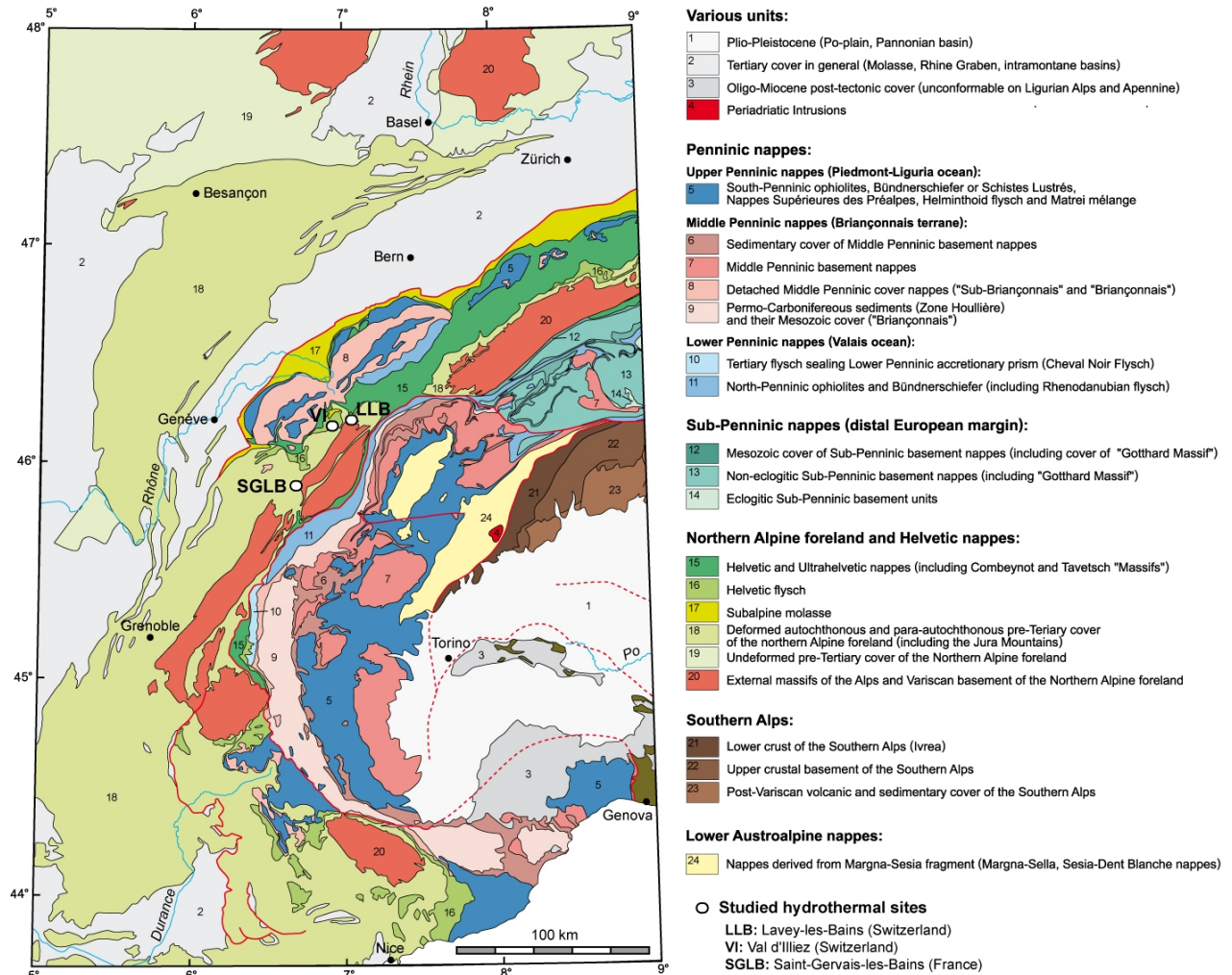
Figure 2: Location of the three studied hydrothermal sites on the tectonic map of the Alps (modified from Schimd et al. 2004).

Part II

Generalities about thermal waters and natural flows in the Alpine domain. Description of methods

1

Definition, use and properties of mineral and thermal waters

1.1 What is a mineral and a thermal water ?

THERE certainly exist several ways of characterizing natural mineral and thermal waters. Emerging with the favour of a hydrogeological and a geomorphological exception (fault, fold, etc., Vuataz 1997), mineral and thermal waters show a great variety in their chemical composition and are endowed with certain beneficial properties for health (Collin 2004, Pomerol and Ricour 1992, BRGM 2006). Actually, the only valid definition of mineral water is of legal order (Féneyrou 1989). According to some dictionaries, the mineral water is *a water which contains minerals in solution and which one employs for drinking or therapeutic baths*. But according to Féneyrou (1989), this definition is not satisfactory because he mentions that all natural waters, including rainwaters, are more or less mineralized and many waters classified such as "mineral" have a total mineralization lower than various public distribution waters. He proposes a more concise definition as *a mineral water is a water which can be exploited in its initial state from a ministerial authorization.*

Pomerol and Ricour (1992) mention the hydrogeological and legislative character for the nomination of a mineral water. In France for example, a mineral water is a *naturally pure groundwater,* *of constant physico-chemical composition and which contains elements (salts, gases and muds) acting effectively on health.* For the British, this concept is rather quantitative because the mineral water must have a total mineralization superior than 1 g/L. From a hydrogeological point of view, a mineral water is according to (Pomerol and Ricour 1992) *a water which is distinguished from another water of a given area by its physico-chemical composition, and often by its temperature.* Consequently a mineral water can also be a thermal water.

There is no official definition of a thermal water (Gilli et al. 2004). A thermal water corresponds to a *naturally hot water at the emergence which can be exploited as a mineral water* (Castany and Margat 1977, Féneyrou 1989), with a temperature superior than the temperature of the phreatic groundwater of a given area (Pomerol and Ricour 1992). In France, a water is described as thermal when its emergence temperature is higher than 4°C compared to the annual average air temperature of the site, whereas in Germany, water must have a temperature above 20°C to be described as thermal (BRGM 2006). According to Castany (1963), thermal water can be gathered in four families : cold springs (< 20°C), hypo-thermal springs (20°C

< T(°C) < 35°C), meso-thermal springs (35°C < T(°C) < 50°C) and hyper-thermal springs (> 50°C). But, this classification has no interest for the hydrogeologist because all the thermal waters come from depth and have the same general descending then uprising circulation (Pomerol and Ricour 1992).

Mineral and thermal groundwaters have always occupied a central position in the history of civilization, and the value of such waters was known to many ancient civilizations. They usually had a social and religious function as well as being of economic importance (Albu et al. 1997). From the earliest times humanity has associated certain springs with divine power of healing and the presence of hot springs was explained by religious beliefs. During the first millennium BC, the Greeks believed and built many temples to divinities associated with thermal and mineral waters and their curative properties (Albu et al. 1997). Until the 19 [th] century, the texts only describe the value of thermal springs and their therapeutic effects (Thiébaud

2008). In the middle of the 19 [th] century, the origin of thermal springs was evoked as *volcano reduced on its aqueous phase* or *gas emanations, which [...] arrive condensed to the surface in mineral and thermal water* (Durand-Fardel 1857 in Thiébaud 2008). The debate on the juvenile or meteoric origin of thermal springs became extensive in the middle of last century (Moret 1946, Castany 1963, Blavoux 1978, Blavoux and Berthier 1985), and one has started to be interested in geochemistry of thermal waters and their relationships with the geological context (Carlé 1975, Högl 1980, Vuataz 1982, Dubois 1991, Calmbach 1995, Muralt 1999, Pastorelli 1999, Duriez 2006). More recently, studies have been taking into account together geology, hydrogeology, hydrodynamics, geochemistry as well as thermo-hydraulic modelling (Le Fanic 2005, Gallino 2008, Thiébaud 2008), geochemical modelling (Clauser 2003, Kühn 2004), and simulation of coupled thermo-hydro-chemical processes (André et al. 2006, Portier et al. 2007).

1.2 Use of thermal waters and geothermal energy in the world

Geothermal energy represents the heat of the earth emitted at the surface of the crust. Rocks contain various amount of radiogenic isotopes, whose natural radioactive decay produces heat (Lüttig 1985, Pruess 2002). Ascending hot magmatic rocks, the local thinning of the crust and natural deep flow systems are at the origin of geothermal anomalies, which in certain cases can lead to geothermal fluids.

Archeology proves that prehistoric humans used geothermal water from natural pools and hot springs for cooking and bathing and keeping themselves warm, for more than 10000 years (Cataldi 1999 in Kühn 2004). After the Second World War, some countries were attracted by geothermal energy, considering it to be economically competitive with other forms of energy. Electricity generation is the most important form of utilization of high-temperature geothermal resources today (Kühn 2004). Bertani (2005) reviews the geothermal fields in the world which are currently under exploitation to generate electricity. He presents the geothermal capacities for each country in early 2005, the annual energy production, the number of

geothermal units installed and the percentage of energy produced nationally from geothermal resources (Table 1.1). Countries having the greatest running capacities as USA, Philippines, Mexico, Italy, Indonesia, Japan, New Zealand, Iceland and countries of the Central America are linked to volcanic phenomena. The first unit ever producing electricity energy is located in Italy (Larderello, Tuscany): the industrial power plant went into operation in 1913, with a 250 kW turbo alternator unit (Allegrini et al. 1992). Finally, electricity production is also possible without a volcanic environment and it consists to stimulate a deep geothermal reservoir with an increase of fracturing (Enhanced Geothermal Systems). In Europe, several sites produce electricity from geothermal energy such as Landau in Germany (Bächler et al. 2003), and Soultz-sous-Forêts in France which is related to an European research program (Baria et al. 1999, Gérard et al. 2006). Geothermal waters is not only used for electricity production. Medium to low temperature resources are suitable for many types of application. Lindal (1973) published a diagram, listed in Table 1.2, which shows various use of geothermal energy.

Table 1.1: Worldwide geothermal power generation in early 2005 (Bertani 2005). n/a means no available data.

Country	Installed capacity (MW$_e$)	Running capacity (MW$_e$)	Annual energy produced (GWh/year)	Number of units	Percent of national energy
Australia	0.2	0.1	0.5	1	Negligible
Austria	1.2	1.1	3.2	2	Negligible
China	28	19	96	13	30% of Tibet
Costa Rica	163	163	1145	5	15
El Salvador	151	119	967	5	22
Ethiopia	7.3	7.3	0	2	n/a
France (Guadeloupe)	15	15	102	2	9
Germany	0.2	0.2	1.5	1	Negligible
Guatemala	33	29	212	8	3
Iceland	202	202	1483	19	17.2
Indonesia	797	838	6085	15	6.7
Italy	791	699	5340	32	1.9
Japan	535	530	3467	19	0.3
Kenya	129	129	1088	9	19.2
Mexico	953	953	6282	36	3.1
New Zeland	435	403	2774	33	7.1
Nicaragua	77	38	271	3	9.8
Papua New Guinea (Lihir island)	6	6	17	1	n/a
Philippines	1930	1838	9253	57	19.1
Portugal (Sao Miguel island)	16	13	90	5	n/a
Russia	79	79	85	11	Negligible
Thailand	0.3	0.3	1.8	1	Negligible
Turkey	20	18	105	1	Negligible
USA	2564	1935	17'917	209	0.5
Total	**8933**	**8035**	**56'786**	**490**	
In 2009	> 10'000				

1.3 Use and properties of geothermal fluids in Switzerland

In Switzerland, geothermal direct use in 2008 is estimated to have reached an installed capacity of about 1022 MWth, with 2040 GW/h of heat production, mostly in installations coupled to geothermal heat pumps (GHP). This corresponds to an annual saving of 150,000 tons of fossil fuel, and reduces the emission of CO_2 by about 485,000 tons per year (GEOWATT 2009). These data are different compared to the situation in 2006 (Rybach and Minder 2007).

There is also some use of Alpine deep aquifers and hot spring resources, respectively in small district heating networks and for the heating of several spas. So far there is no electricity generation using geothermal fluids in Switzerland. In the Alps range, geothermal resources concern the low-temperature application (20-100ºC) and are primarily used for baths, bottled water as in Vals (Hartmann 1998) or sometimes for the heating production as in Lavey-les-Bains (Bianchetti 2002) or at Oberwald where the used fluid comes from springs in the Furka tunnel (Vuataz et al. 1993). Recently, the thermal waters flowing from several springs in the Loetschberg basis tunnel in the Swiss Alps are continuously used at Frutigen for breeding sturgeon. In 2011, a new geothermal deep borehole will be drilled in the Lavey-les-Bains area (AGEPP project) aiming to exploit the geothermal resource in its reservoir roughly at 2-3 kilometres depth.

Table 1.2: The Lindal classification of low to high temperature geothermal energy use (from Lindal 1973 in Albu et al. 1997). EG: Electricity Generation.

T (^{o}C)	Geothermal energy application	Steam	Water	EG
≥180	Power, evaporation of highly, concentrated solutions, refrigeration by ammonia absorption, digestion in paper pulp	○		○
170	Heavy water via hydrogen sulphide process, drying of diatomaceous earth	○		○
160	Drying of fish meal, drying of timber	○		○
150	Alumina via Bayer's process	○		○
140	Drying farm products	○		○
130	Evaporation in sugar refining, extraction of salts	○		○
120	Fresh water by distillation, multiple effect evaporation	○	○	○
110	Drying and curing of light aggregate cement labs	○	○	○
100	Drying of organic material (vegetables, etc.), washing of wool	○	○	○
90	Drying of stock fish, intense de-icing operations		○	
80	Space heating, greenhouses by space heating		○	
70	Refrigeration (lower temperature limit)		○	
60	Animal husbandry, greenhouses by space or hotbed heating		○	
50	Mushroom growing, balneological baths		○	
40	Soil warming, baths		○	
30	Swimming pools, biodegradation, fermentation, warm water		○	
20	Hatching of fish, fish warming, bottled water		○	

A database on geothermal fluids in Switzerland, called BDFGeotherm, has been compiled in 2007 (Sonney and Vuataz 2007 and 2008). It consists of nine related tables with fields describing the geographical, geological, hydrogeological and geothermal conditions of each sampling location. In total, 212 springs and boreholes from 84 geothermal sites in Switzerland and neighbouring regions are listed in this new interactive Microsoft Access database. BDFGeotherm can be useful to all geothermal projects dealing with the exploration, production, and injection of geothermal fluids. The projects may involve permeable geological reservoirs or may be based on the technology of enhanced geothermal systems (EGS). The tool may also be used to estimate and forecast the chemical composition of geothermal fluids. The database is also of interest for studies related to the risks of mineral deposition or corrosion in boreholes and in surface installations, and also for studies on interactions between rocks and thermal waters (Sonney and Vuataz 2008). In 2008, the database BDFGeotherm on ACCESS code was modified to improve its availability and attractivity by using Google Earth free software and the website of Centre for Geothermal Research, CREGE <www.crege.ch>. Google Earth is used to visualize general information about sites in Switzerland and neighbouring areas, whereas the CREGE website is used to compile all data in a SQL format.

Data in BDFGeotherm were obtained from deep boreholes drilled for geological evaluations, oil exploration, geothermal prospecting, thermal spas, thermal springs and fluid outflows from tunnel-drainage systems. All these data are contained in a variety of reports and papers, often unpublished and not easily accessible to potential users of the information (Sonney and Vuataz 2007).

Geographically, all Switzerland is covered by geothermal sites, although the distribution of data is quite heterogeneous (Fig. 1.1). Their location on the Swiss tectonic map shows a concentration of sites in the northeastern part of the Jura range, which is characterized by a high geothermal gradient and a significant heat flow anomaly (> 150 mW/m2) (Rybach et al. 1987), and to a lesser extent in the upper Rhone Valley. The Alpine sites are primarily thermal springs, discharging from deep vertical flow systems in the presence of vertical fractures. On the Plateau (Molasse Basin), extending NE-SW and containing the largest lakes of Switzerland, the number of sites is much smaller because of the thick Tertiary Molasse cover. Finally, a number of sites in Germany (5), France (3) and Italy (6) were selected either because they are located near Swiss hot springs or deep boreholes, have similar geological features or represent a significant geothermal potential.
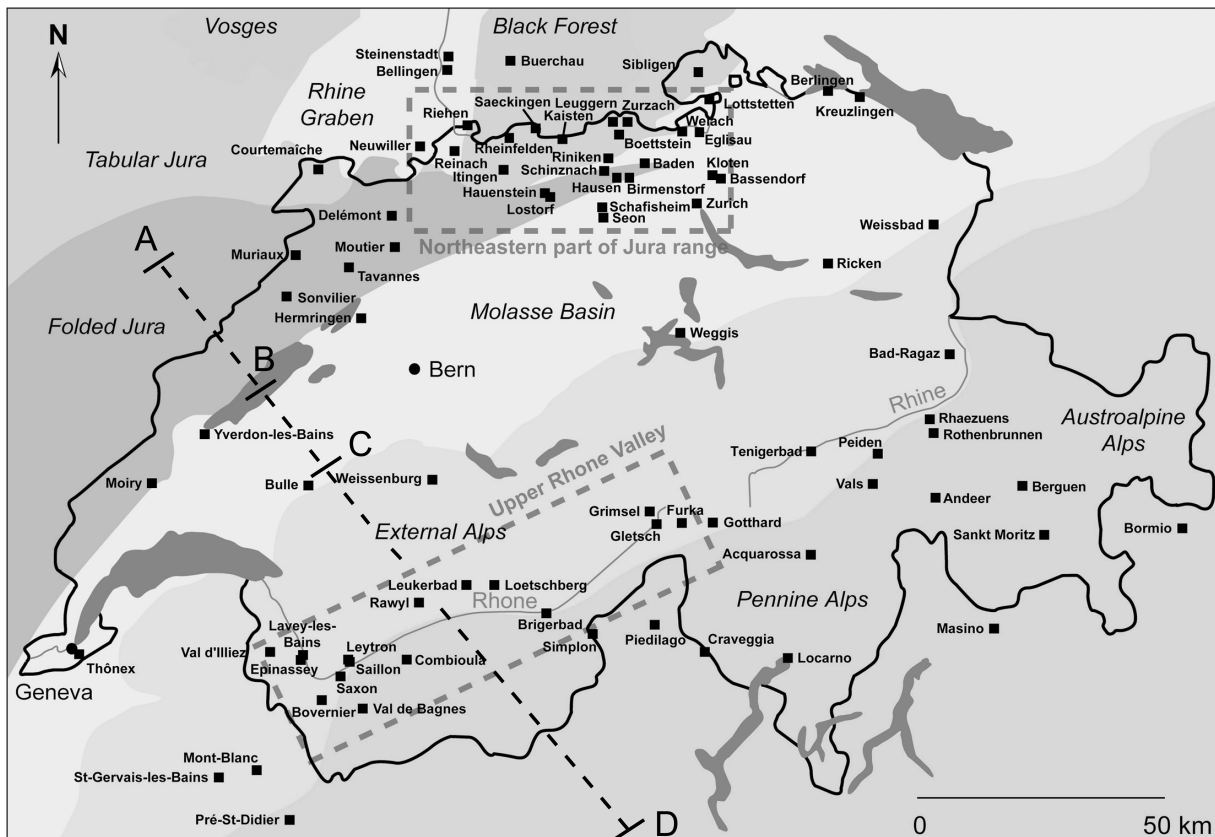
Figure 1.1: Locations of geothermal sites included in BDFGeotherm. The shaded areas correspond to the main tectonic units of Switzerland (Sonney and Vuataz 2008).

Based on the publication by Trümpy (1980), the geological description of potential geothermal reservoirs can be summarized. Geologically, Switzerland can be divided into three parts: 12.5% of its surface lies in the Jura, 30.5% in the Molasse Basin and 57% in the External and Pennine Alps (Fig. 1.1). The term "External Alps" refers to a pre-Triassic basement complex, affected by the Variscan (Hercynian) and older orogenies, with Triassic to Lower Oligocene sediments that were deformed only by the Alpine movements (middle-Cretaceous to Pliocene). The Pennine Alps consists of a nappe series with recumbent folds in which the basement and its sedimentary cover have the same tectonic behaviour.

The Jura range is not very high (lower than 1700 m in Switzerland). The range extends from Geneva to Basel and consists of a succession of SW-NE folded chains with valleys about 700-1000 metres of elevation. The altitude and breadth of the Jura decrease towards the northeast. The Folded Jura becomes the Tabular Jura in the northwestern part of Switzerland. The Tabular Jura consists of subhorizontal Mesozoic cover rocks affected by Oligocene faulting south of the Rhine Graben. The Jura Mesozoic and Cenozoic reservoirs correspond to karstified limestones of the Dogger and Malm formations (Fig. 1.2), with a variable thickness in the range of 200-500 metres.
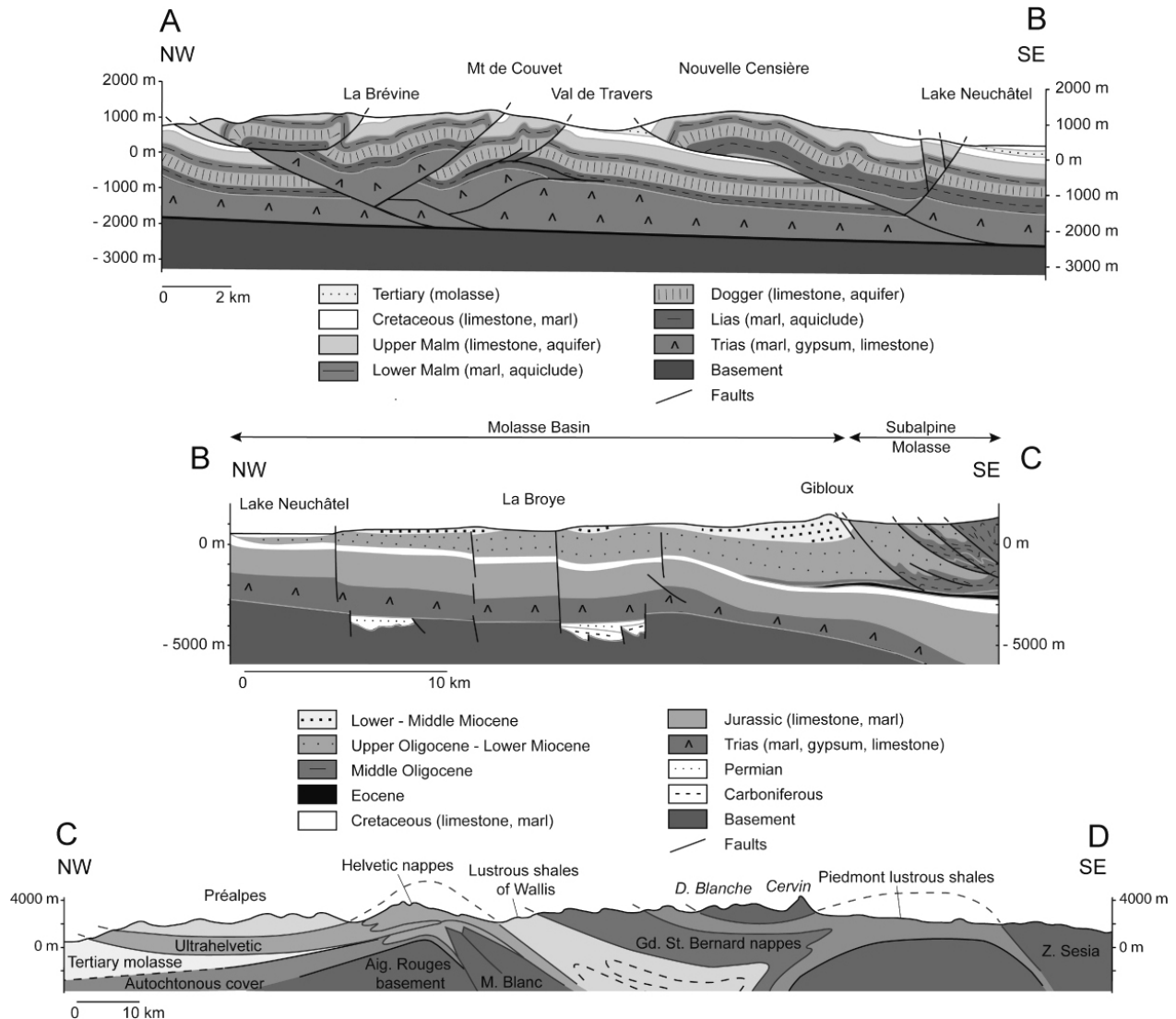
Figure 1.2: Geological cross sections through Switzerland (see the line section in Figure 1.1). AB represents the Folded Jura structures with two major deep aquifers in the Dogger and Upper Malm limestones (modified after Sommaruga 1997). BC is a section across the Molasse Basin; CD is a simplified view of the great Alpine structures (modified after Debelmas and Kerkhove 1980). Elevations in metre above sea level are given on the vertical axes (Sonney and Vuataz 2008).

The Plateau or Molasse Basin has a hilly landscape, studded with lakes and with a few large plains. Valley bottoms lie at 350-600 metres, the intervening hills a few hundred metres higher, except towards the southern margin, where the morphological transition to the Alps is gradual. The Tertiary deposits, which stratigraphically overlie the Cenozoic and Mesozoic formations that are found in the Jura, consist of three units: Lower Marine Molasse, Lower Fresh-water Molasse and Upper Marine Molasse (Trümpy 1980) (Fig. 1.2). Groundwater flow is often absent in the Lower Fresh-water Molasse; it is therefore regarded as an aquiclude. Groundwater flow through the Upper Marine Molasse sandstone is common but dependent on local conditions. The geological formations of the Muschelkalk, Dogger and Malm beneath the Tertiary deposits represent the aquifers, and can contain great quantities of hot water in permeable fractures (Balderer 1990).

The Alps are divided into two parts by the large longitudinal valleys of the Rhone and Rhine Rivers. The northern mountains comprise a high chain to the south and lower ranges to the north. South of the Rhone-Rhine depression, the high Pennine Alps occupy the southernmost part of eastern Switzerland. In general, Alpine rocks fall into two categories: a pre-Triassic basement complex affected by the Variscan and older orogenies, and Triassic to Lower Oligocene sediments which were deformed only by the Alpine movements. Reservoirs in the Alps can be encountered in all the major geological units. These aquifers may be fractured (granite, gneiss), karstified (limestone) or porous (sandstone, fluvio-alluvial deposits). The locations and limits of the aquifers are not easily definable at this scale, however, and are highly dependent on local tectonic features.

The 212 sample points recorded in BDF-Geotherm have temperatures ranging from 10°C in the Malm limestone of the Jura (Tavannes borehole; Ziegler 1992) to 112°C in the deep crystalline basement below the Molasse Basin (Weiach borehole, Pearson et al. 1989). Measured temperatures in thermal springs, boreholes and thermal outflows in tunnels are illustrated on the simplified Swiss tectonic map in Figure 1.3 and show that the warmer waters (> 60°C) are found in deeper boreholes (> 1 km), the exception being Lavey-les-Bains in the External Alps where water at 68°C inflows at a depth of 200-400 metres (Bianchetti 1994). This relatively high temperature is not due to the existence of a heat flow anomaly (Rybach et al. 1987) but results from deep flow systems through permeable faults or subvertical formations in the Alps (Vuataz 1982, Vuataz et al. 1993). This process also gives rise to many thermal springs present in the Alps. The warmest springs exceed 40°C, examples being Brigerbad (52°C) and Leukerbad (51°C) in Switzerland (Muralt and Vuataz 1993), Saint-Gervais-les-Bains (41°C) in France and Bormio (42°C) in Italy (Vuataz 1982). The measured temperatures of thermal outflows in tunnels do not exceed 40°C. The maximum values are associated with water from the Mont Blanc (34°C in Lebdioui 1985 and Dubois 1991) and Simplon tunnels in the Alps (38.6°C in Bianchetti et al. 1993 and Vuataz et al. 1993). Nevertheless, these tunnels drain large quantities of water (> 10 L/s), which enables them to be considered as geothermal resources, and currently waters from 8 tunnels are used. In the Eastern Swiss Alps, in the Upper Rhine watershed, thermal springs have low temperatures and discharge rates are often rich in carbon dioxide (Bissig 2004, Hartmann 1998).

In the Molasse Basin, measured water temperatures in the Tertiary deposits do not exceed 30°C (29°C in the Zürich borehole, Högl 1980), although temperatures are higher in the Muschelkalk, Dogger and Malm formations because of their depth (Pearson et al. 1989, Gorhan and Griesser 1998). When developing a geothermal project, temperature forecasting is rather easy; however, it is a difficult task is to estimate borehole production rate. For example, the Thônex deep borehole near Geneva (88°C in the Malm) was not sufficiently productive (3.1 L/s at 39°C) and is still unused (Jenny et al. 1995, Muralt 1999). In the Tabular Jura, in northern Switzerland, thermal waters (> 40°C) occur at relatively shallow depth due to the presence of high heat flow (> 150 mW/m^2; Chapman and Rybach 1985, Rybach et al. 1987). For example, the Riniken borehole presents warm (50°C) water inflows at a depth of 800 metres in subhorizontal Triassic sandstones (Pearson et al. 1989).

In the Folded Jura, the warmest waters are located at the north-eastern end of the Jura Massif in Baden (47°C in Högl 1980 and Vuataz 1982). As in the Alps, this is due to the upflowing of deep hot water into the Muschelkalk. Elsewhere, thermal waters are found in shallow boreholes (< 650 m) in the fractured and karstified limestones of the Dogger and Malm, but the measured temperatures do not exceed 25°C (Muralt 1999).
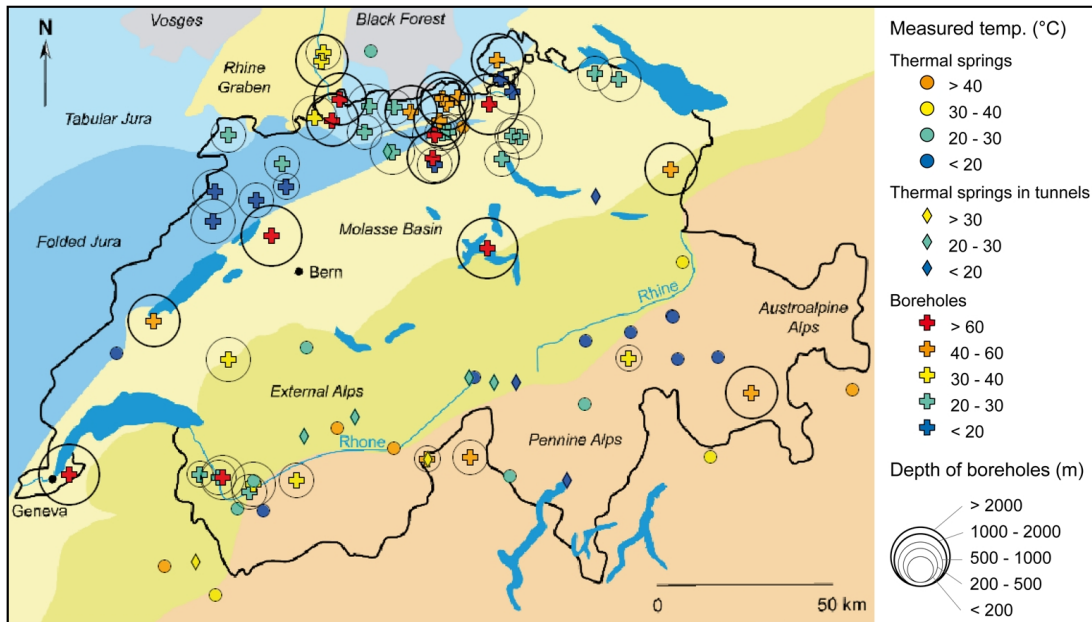
Figure 1.3: Location and temperature of the thermal sample points after data included in BDFGeotherm (Sonney and Vuataz 2008).
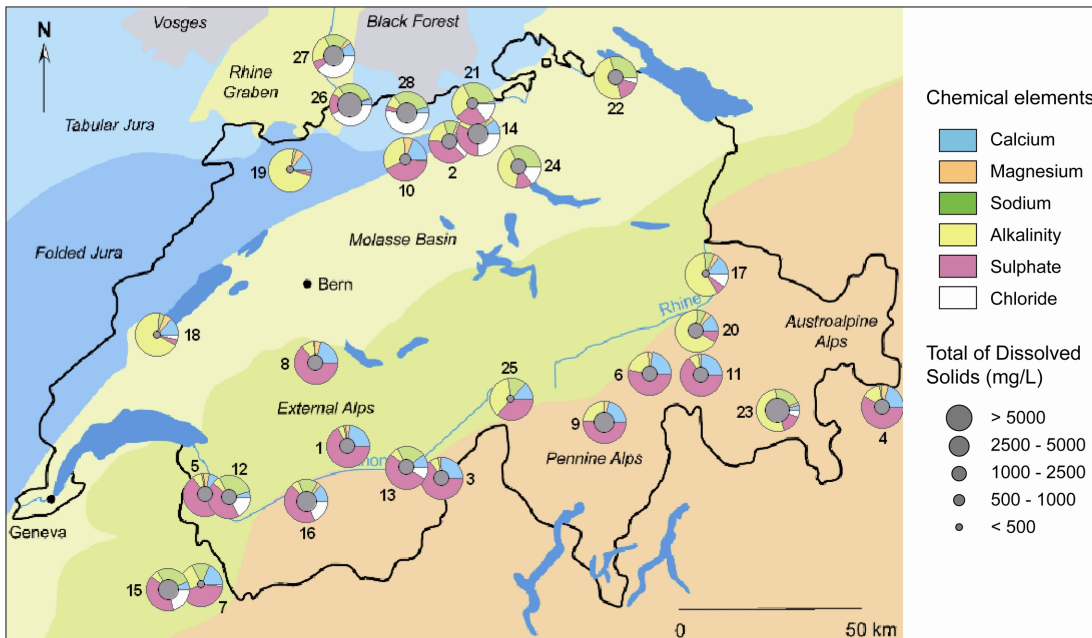
Figure 1.4: Location and geochemical type of selected thermal water samples from data included in BDFGeotherm. The colours in the pie-charts represent the major chemical elements, and the size of the gray circles illustrates the amount of Total Dissolved Solids (TDS). The numbers near the pie-charts relate to the site number of which data are illustrated in Sonney and Vuataz 2008.

Concerning water chemistry of the selected sites, different types of geothermal fluids can be described (Fig. 1.4). For Ca-SO_4 waters, the selected thermal sites have Total Dissolved Solids (TDS) ranging between 800 and 2700 mg/L, an exception being the lightly mineralized water of Mont-Blanc. These waters are influenced by the dissolution of sulphate minerals (mainly gypsum and anhydrite) contained in the Triassic sediments. Gypsum and anhydrite are much more soluble and dissolve faster than Al-silicates; the Ca-SO_4 fingerprint is easily acquired by shallow or deep groundwaters upon interaction with these rocks (Pastorelli et al. 2001). This lithotype is found in the Alps due to the occurrence of Triassic rocks, which played a central role in the position of the Alpine nappes. They are often found in the thrust faults and in the north-eastern part of the Jura where these formations are at shallow depth. Acquarossa thermal waters in the Pennine Alps are a good example of circulation in the contact zone between the crystalline basement and pinched Triassic layers (Vuataz 1982). The water circulation starts with infiltrated rain water descending progressively, being heated at depth and locally rising to surface, preserving the physical and chemical Triassic characteristics (TDS = 2663 mg/L, with SO_4 = 1300 mg/L) (Pastorelli et al. 1999).

Some Ca-SO_4 waters do not contact the Triassic rocks. These waters generally have a low TDS ($<$ 300 mg/L) and come from interactions with granitic or gneissic rocks. An example is the thermal springs in the Mont Blanc tunnel with the chemical type Ca-Na-SO_4-HCO_3. In this case, the sulphate comes from dissolution and oxidation of sulphide minerals from hydrothermal veins in crystalline rocks (Bianchetti 1994).

As regards Na-SO_4 and Na-HCO_3 waters, selected thermal waters rich in sodium often have a TDS over 1000 mg/L except for the lightly mineralized waters of the Furka tunnel (TDS = 153 mg/l). These waters mainly circulate in crystalline rocks. Their sulphate concentration is due to the dissolution of sulphide minerals. Sodium comes mainly from reactions with feldspars in crystalline rocks (Pastorelli et al. 2001). These geochemical types are found in the Alps and, more precisely, at the peripheral regions of the external crystalline massifs (Brigerbad, Lavey-les-Bains and Saint-Gervais-les-Bains). Na-HCO_3 waters are those that penetrated

the basement under the Tabular Jura (Zurzach-Bad). In the Molasse Basin, there are also Na-HCO_3 waters in the Lower Marine Molasse with TDS close to 1000 mg/L (Berlingen and Zürich).

Some waters rather rich in calcium (Na-Ca-SO_4) have an intermediate composition type between those from crystalline rocks and those in contact with Triassic gypsum and anhydrite. For example, the thermal springs of Combioula emerge from Triassic formations but circulate partly in crystalline rocks found below these sediments. The deep borehole of St-Moritz contains strongly mineralized thermal water (TDS $>$ 13 g/L), which is believed to be due to high levels of CO_2 favouring acidic rock dissolution (Aemissegger 1993, Bissig et al. 2006, Wexsteen 1988, Wexsteen et al. 1988).

Thermal Ca-HCO_3 waters are generally lightly mineralized, with a TDS often below 500 mg/L, except for the Rothenbrunnen thermal spring (TDS = 1213 mg/l) in the Pennine Alps which belongs to the family of "carbogaseous" springs (Hartmann 1998). This fingerprint is typical of a calcareous environment as observed for the Malm thermal waters in the Jura (Yverdon-les-Bains and Delémont) and for the waters of Bad-Ragaz in the External Alps (Fig. 1.4).

Thermal Na-Cl waters have generally a high mineralization (TDS $>$ 3 g/L) with concentrations sometimes exceeding 10 g/L, as in Riehen (17 g/L). The origin of this fingerprint is twofold: it could be due either to the mixing of old, deep, strongly mineralized seawater and fresh water at shallow depth, or to the dissolution of halite deposits. Na-Cl water is found throughout the geological column, from the Tertiary deposits to the crystalline basement. For example, the boreholes of Riehen and Steinenstadt contain saltwater that originates in the Muschelkalk and Jurassic limestones, while the saltwater thermal springs of Saeckingen arise from the Hercynian granites of the Black Forest. Stober and Bucher (2007 and 1999) studied deep groundwaters in the crystalline basement of the Black Forest. They concluded that the saline thermal water used in spas has its origin in crystalline reservoirs at 3-4 kilometres depth. Moreover, the saline thermal water has developed its composition by a mixing of surface freshwater with saltwater (of ultimately marine origin), and water-rock reactions with an increasing mineral dissolution due to the presence of CO_2.

The geothermal deep and shallow resources in Switzerland are found in most parts of the country (Fig. 1.5). Well-known deep resources are located in the northern part of Switzerland and the upper Rhone valley. Deep fluids are used in small district heating networks and for the heating of spas. Some areas are not endowed with obvious geothermal resources, for example the southern part of the Folded Jura and the high Alpine relief, but Alpine valleys drain large amounts of water coming from the mountain slopes and may contain thermal waters at depth. However, the identification of hidden deep sources remains difficult because of the fluvio-glacial sedimentary cover. In some cases, it is possible to observe temperature anomalies in the shallow groundwater.

The estimated thermal energy potential of the springs and wells shown in Figure 1.5 varies because of the differences in temperatures and discharges. Potential geothermal energy (P in kWth) was calculated from the discharge (Q in L/s), the initial temperature (T in °C) and a final temperature after cooling (t in °C) arbitrarily fixed at 10°C (modified from Signorelli 2004):

$$P = 1000(Q \times (T - t))/239 \qquad (1.1)$$
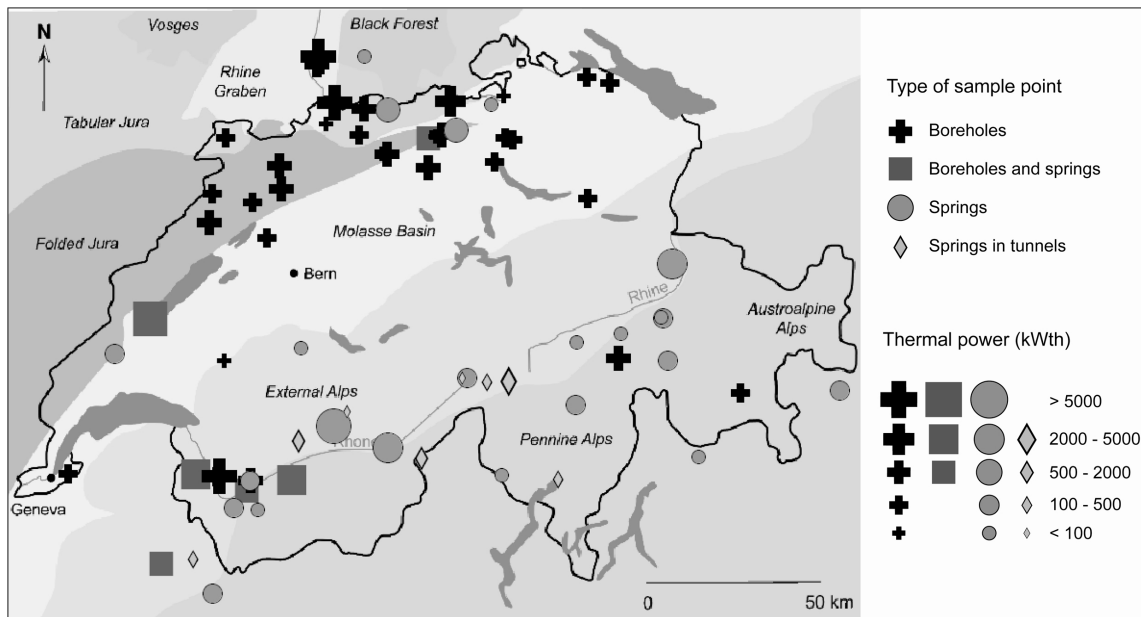
Figure 1.5: Location and thermal power of geothermal resources included in BDFGeotherm. The thermal power of a given site corresponds to the sum of all the sample points. Some sites are not represented due to lack of discharge data (Sonney and Vuataz 2008).

1.4 Description of natural flows in Alpine domain

1.4.1 Alpine deep flow systems leading to thermal springs

Chemical and isotopic composition of thermal waters at the emergence results from several stages during which the physico-chemical parameters are acquired (Fig. 1.6) (Castany 1963, Vuataz 1982). The first stage is linked with the rainwater becoming surface or soil water. These meteoric waters are labeled by their isotopic signature in oxygen-18 and deuterium corresponding to the Global Mete-

oric Water Line (Blavoux 1978, Fontes 1976, Fritz and Fontes 1986, Nicholson 1993, Pearson et al. 1991), which could be modified due to continental effects and during the next stages. The $\delta^{18}O$ values of geothermal waters can be higher (less negative) than those of local meteoric waters. This has been interpreted as a result of isotopic exchange at high temperature ($\geq 150^{\circ}$C) between the water and the rock minerals which are richer in $\delta^{18}O$. The values of δ^2H are often constant (Arnórsson 2000). In the Alpine range, calculated reservoir temperatures of different geothermal systems (≤ 100-110°C after Vuataz 1982) are not sufficiently high to generate this isotopic exchange.

The second stage refers to the infiltration of water which begins inside the superficial soil before continuing until the saturated zone. This infiltration is composed from rainwater which is removed by the effective evapotranspiration, the surface runoff and the variation of storage:

$$Inf = P - SR - ETR - \Delta S \qquad (1.2)$$

Inf = Infiltration, P = Precipitation, SR = Surface runoff, ETR = Effective evapotranspiration and ΔS = Variation of storage.
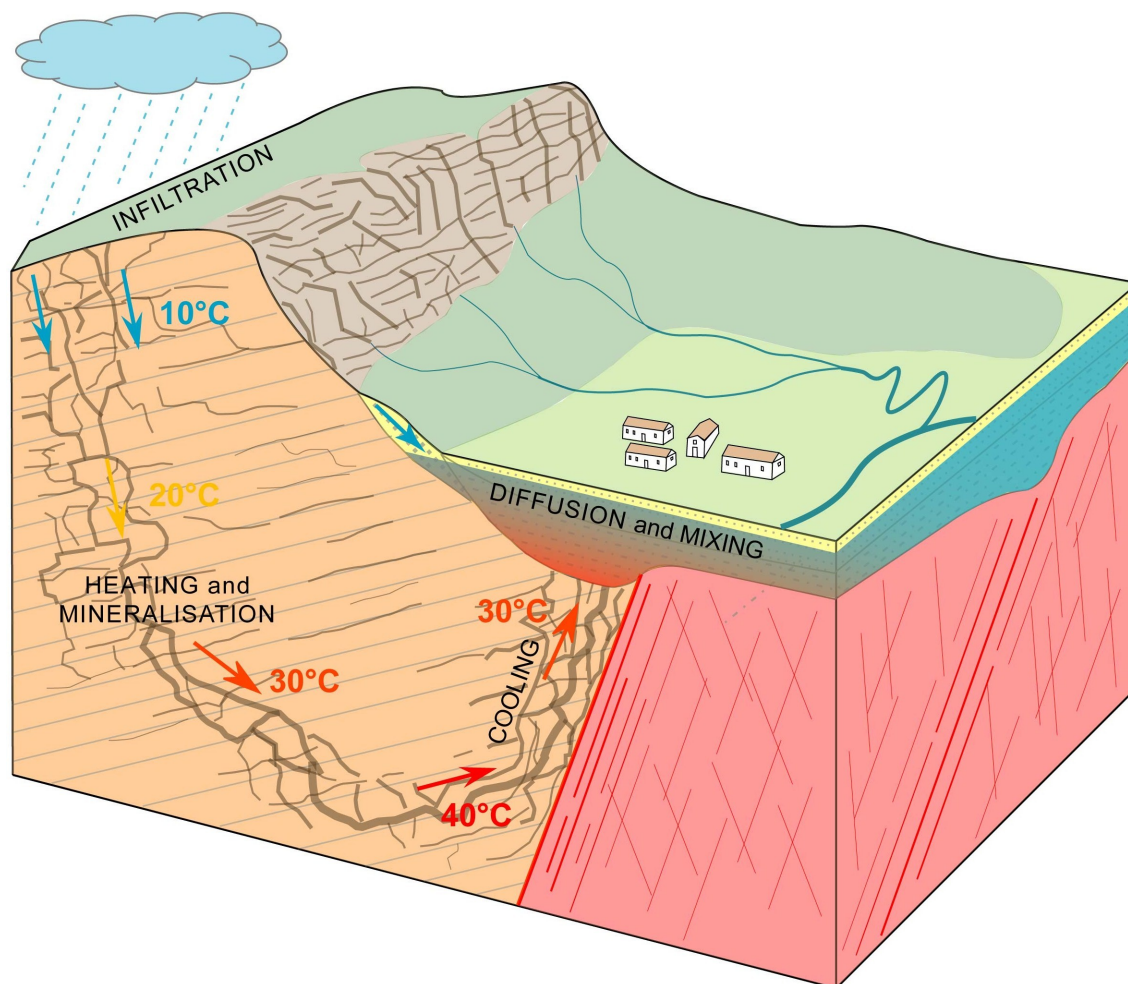
Figure 1.6: Conceptual model showing an example of a deep flow system in a karstified aquifer with mixing processes occurring in the Quaternary deposits. In this example, the the rise of thermal water is supplied by the presence of a fault involving a permeability contrast (modified from Collin 2004).

During the infiltration inside the subsurface fractured or porous rocks, the initial reactions of dissolution of minerals take place leading to the chemical composition of local cold waters. These waters become in particular enriched in calcium and bicarbonate due to the presence of calcite inside the fractures for example.

In high mountains areas, infiltration in fractured massif is heterogeneous according to the depth. Infiltration is more important in the decompressed zone than in the deep fractured rocks because of contrast of permeability due to the existence of open fractures in the decompressed zone (Cruchet 1985, Dzikowski and Lhomme 2004, Lhomme et al. 1996), and the increase of pressure at depth (Maréchal 1998, 1999a and 1999b). Groundwater recharge in high mountains also depends on the climatic conditions. The winter marks the lowest infiltration because of snow storage, whereas in summer the groundwater recharge is favoured by snow melt.

The third stage begins when waters circulate below the decompressed zone towards deep and hot zones. These circulations are possible through permeable and vertical layers or major faults and thrusts. This stage can lead to two types of geothermal systems: one dynamic with more or less continuous slow circulations in a hot aquifer or another one with a storage of thermal water at depth forming a geothermal reservoir. In the two cases, chemical reactions between rocks and fluid are taking place and are increasing with temperature and pressure at depth. Thus, the geothermal fluid tends to be at equilibrium with minerals of host rocks in the reservoir. If equilibrium conditions are reached, the chemical and isotopic composition of the geothermal fluid will give important indications to decipher the nature of the host rocks and the maximum reservoir temperature.

The fourth stage is the uprising of the deep and hot fluid from its reservoir to the surface. The deep fluid can keep part of its natural heat if the uprising velocity is sufficient. This condition is dependent on the variation of hydraulic conductivities such as the presence of faults, fractured vertical layers, thrusts faults, etc. It is important, for the estimation of the reservoir temperature with geothermometers and saturation indices, that a minimum of interactions occurs between uprising fluid and host rocks. If interactions take place at this stage, the fluid chemical composition is modified and chemical equilibrium reached in the reservoir can be strongly modified.

Finally, the last stage takes place in the final uprising circuit and refers to possible mixing processes between the deep thermal component and cold shallow groundwaters. Two cases are possible:

- Mixing with cold waters from the **decompressed fractured zone**. In the Alps for example, natural thermal springs of Brigerbad (Wallis) are diluted by cold and weakly mineralized waters coming from the mountainous slope of the Aar Massif and circulating in the decompressed zone.

- Mixing with cold waters from a **porous shallow aquifer**. The Quaternary filling of the major valleys (Rhone, Rhine, etc.) can hide the thermal outflows. The deep fluid infiltrates inside the porous deposits, forming a thermal plume in the Quaternary filling which is mostly invisible without boreholes.

To summary this subsection concerning thermal waters in the Alpine environment, more than 70 emergence zones are known and present various physical and chemical characteristics depending on geological, tectonic and climatic conditions. The important points for the comprehension of these processes are summarized in Vuataz (1997). He specifies that the existence of deep faulting tectonics allows the infiltrating groundwaters to reach 1-4 kilometres depth, the strong hydraulic gradients induce thermal water rise along the glacial and alluvial valleys. Close to the surface, temperature of thermal upflows is probably limited to a maximum of 80°C.

As regards the quality of thermal waters, Vuataz (1997) evokes the different possibilities of hydrochemical types assemblage and the problem of complex mixing processes at shallow depth. Time variations of thermal waters can be divided into short- middle- and long-term changes. Vuataz (1997) explains that natural causes of these variations are obviously linked to the hydrologic cycle, but also to other phenomena such as earth tides, seismic events, climatic cycles, etc. He also treats impact of human activities on Alpine thermal systems which are progressively increasing due to the density of population in the vicinity of emergence sites and the renewed interest of thermal water uses. Constructions such as buildings, roads, galleries, dams can profoundly alter the thermal water properties on a temporary or perennial basis. On the contrary, new deeper boreholes often guarantee the sustainability or the improvement of the thermal water resource.

1.4.2 Generalities about surface, subsurface and deep flow systems in an Alpine crystalline massif: the case of the Aiguilles Rouges Massif

Alpine crystalline massifs mainly consist of rocks named *crystalline*. According to Foucault and Raoult (2001), a crystalline rock is made of visible crystals (grained rock). Therefore, it generally refers to magmatic or metamorphic Hercynian rocks which appear as separate massifs, resulting from distinct Alpine basement fold structure (Von Raumer and Bussy 2004). In the Alps, all basement rocks and older than their Mesozoic cover and consist of metamorphosed sedimentary or lithologies, such as granites, metagraywackes, micaschists, marbles, orthogneisses, amphibolites, metabasites, etc. Different units can be distinguished, on the basis of their metamorphic evolution. Lithologies of the polymetamorphic basement, presumed ages and petrography of crystalline rocks are illustrated in the Table 1.3 according to a study on the Aiguilles Rouges and Mont Blanc Massifs (Von Raumer and Bussy 2004, Fig. 1.7).

Hydrogeological characteristics of crystalline formations are not known in detail, although they represent an important part of Alpine massifs. The properties of the aquifers within these mountainous regions are currently poorly constrained, although they are of great importance for engineers and hydrogeologists working in Alpine areas (Maréchal 1999a). Data collected during the realization of tunnels for road, railway and hydro-electric purposes have been used to characterize the hydraulic conductivities of these crystalline rocks from the discharge rates. Results presented by Maréchal

The flow system of the decompressed zone is illustrated by the block diagram No 2 and physico-chemical data of the Tines spring. This spring is located in the Arve Valley near the city of Chamonix, at the bottom of the slope of the Aiguilles Rouges Massif (Fig. 1.7). This cold spring (6°C) drains waters circulating in the decompressed zone of the Eastern mountain slope of the Aiguilles Rouges Massif. Circulations in the decompressed zone start in the subsurface superficial zone (conducting function) before connecting itself to the mylonitized zones (capacitive function) (Lhomme et al. 1996). Tines spring is an example of this process because it is located at the southwestern end of the Vallorcine mylonitic zone. Waters of the Tines spring have a weak mineralization of around 85 μS/cm. Effects of snow melt exist because the

(1999a) show that hydraulic conductivities are variable (from 1.4×10^{-5} to 6×10^{-12} m/s) due to the difference of crystalline lithology, the local tectonic context and the depth. These observations brought an extensive knowledge about the hydraulic role of the decompression zone of fissured mountainous massifs (Maréchal 1999b), which has a considerable water storage capacity (Lhomme et al. 1996).

Active water circulations through an Alpine crystalline massif can be divided in three specific systems (Fig. 1.8). Each system is differentiated by their hydraulic and physico-chemical properties (infiltration, natural circulation, temperature, electrical conductivity, etc.) in relation to the climate and the structure of the geological formations (Lhomme et al. 1996). The surface flow system is represented as an example by the block diagram No 1 of the Figure 1.8 and the evolution of physico-chemical parameters of the Arve River according to data of Payraud (1991). The Arve River drains the Eastern mountain slope of the Aiguilles Rouges Massif and is supplied by many subglacial torrents of the Mont-Blanc Massif. Its rising outline is less pronounced than that mountain streams and is controlled by hydro-electrical constructions (Lhomme et al. 1996). Water of Arve River has a weak mineralization which varies between winter and summer (240 to 80 μS/cm). In summer, low electrical conductivities are due to snow melt. Consequently, water temperature is influenced by surface climatic conditions.

flow rate is higher and the electrical conductivity is lower during summer. The temperature is stable all over the year, above the temperature of the Arve River in winter and below the temperature of precipitation in summer, due to a buffer effect between waters and host rocks of the aquifer (Lhomme et al. 1996).

Other examples of groundwaters are presented by Dubois (1991) within the framework of the study about the typology of crystalline aquifers, and in particular those of the Aiguilles Rouges and Mont-Blanc Massifs. This hydrogeological study was part of the AQUITYP project, which has been carried out at the Geology Laboratory of the Swiss Federal Institute of Technology, Lausanne (GEOLEP) (Dubois 1991). Observation, sampling and chemical analyses of more than 40 surface and groundwaters

Table 1.3: Lithologies of the polymetamorphic basement in the Aiguilles Rouges and Mont Blanc Massifs (Von Raumer and Bussy 2004).

Interpretation	Presumed age	Observed petrography
Magmatic origin		
Granites	Ordovician	Coarse grained Kf-augengneisses - Orthogneiss
Granodiorites	Cambro-Ordovician	Gneiss with plagioclase, biotite $\pm$ amphibolite
Acidic volcanites	Lower Palaeozoic	Amphibolites, eclogites
Ultramafic rocks	Lower Palaeozoic	Serpentinites
Sedimentary origin		
Al-rich argillaceous sediments	Neoproterozoic to Lower Palaeozoic	Garnet-sillimanite schists $\pm$ staurolite
Carbonates	Lower Palaeozoic	Diopside-garnet marbles
Layered units of graywackes and Al-rich units	Neoproterozoic to Lower Palaeozoic	Gneiss with biotite-plagioclase-quartz and micashists $\pm$ staurolite $\pm$ sillimanite
Sandstones	Lower Palaeozoic	Garnet-kyanite quartzite

in galleries were realized for the Aiguilles Rouges and Arpille Massifs. For the Arpille area, springs have temperature and Total Dissolved Solids (TDS) lower than 7°C and 100 mg/L respectively.

Concerning the Aiguilles Rouges and more precisely in the sector of the Emosson lake (see location in Figure 4.1), natural springs and springs in galleries are also cold (< 7°C) and less mineralized (< 150 mg/L). These waters are Ca-$HCO_3 > SO_4$ chemical type and contain high arsenic concentrations which can reach 150 μg/L, in particular in the west gallery from the Emosson Lake. Aqueous arsenic in groundwater exists primarily as arsenate (As^{5+}) and arsenite (As^{3+}). Arsenate predominates in waters polluted, whereas arsenite is present in sulfidic and methanic waters (Welch et al. 2000). In this case, arsenic associated with sulfide miner-als in veins of gneissic rocks such as arsenopyrite (FeAsS) can be released by the weathering effects of oxygen-rich environments.

Finally, the deep flow system is highlighted by the block diagram No 3 and the example of the well P201 for the Lavey-les-Bains hydrothermal system. Deep circulations are supplied by the presence of subvertical fractures allowing the deepening of the fluid. The presence of a regional geothermal gradient at depth, the long residence time in the aquifer and the rapid uprising of waters to the surface allow having temperatures up to 4°C compared to the annual average temperature and moderate mineralization. If these waters are not subjected to mixing processes with shallow groundwaters, physico-chemical parameters have a great stability with time.
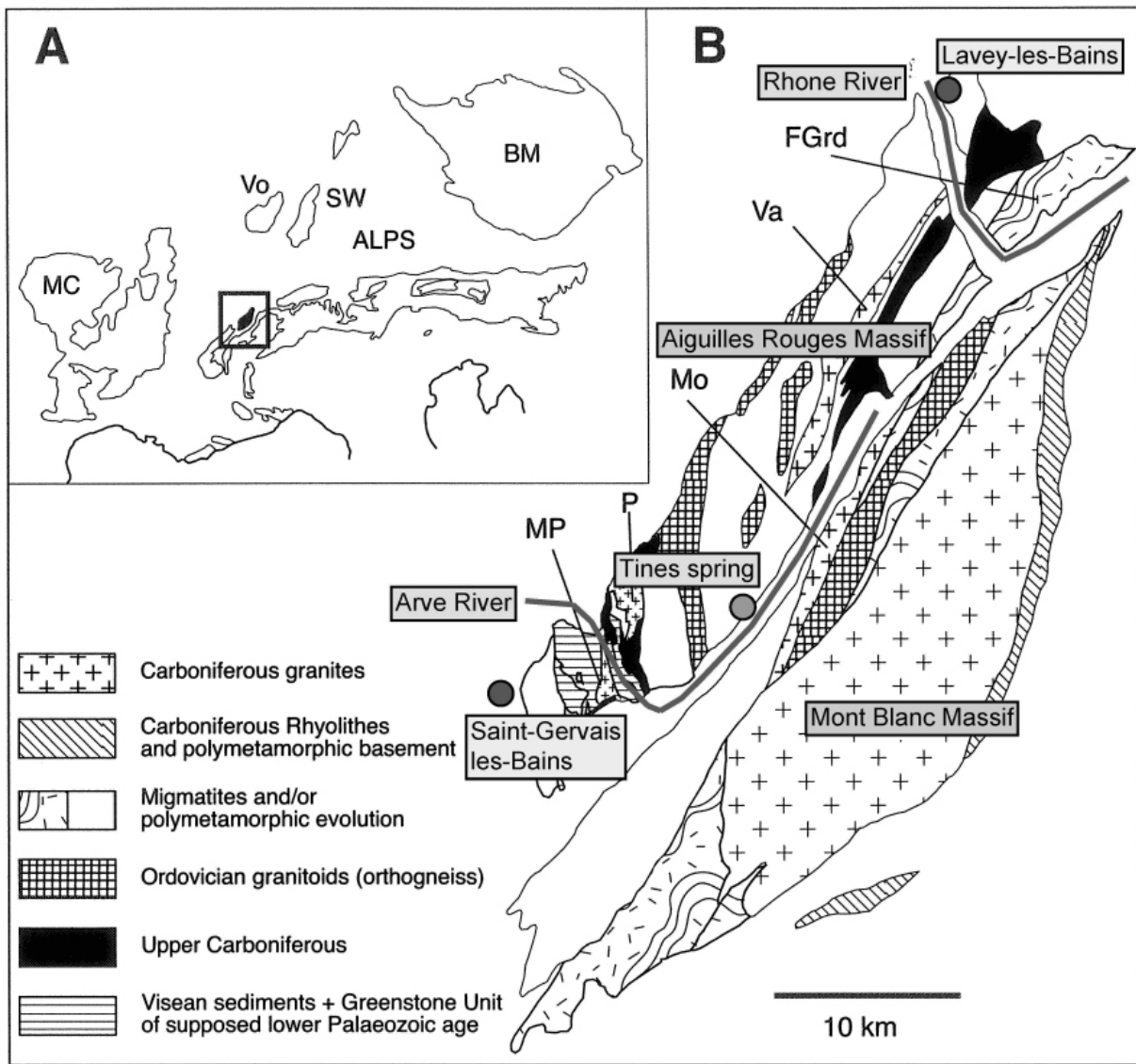
Figure 1.7: Geological map of the Aiguilles Rouges and Mont Blanc areas (from Von Raumer and Bussy 2004).

A: Location of Aiguilles Rouges and Mont Blanc areas (frame) in the Alpine mountain chain, and its Variscan framework: BM - Bohemian Massif; MC - French Massif Central; Vo - Vosges; SW - Black Forest (Schwarzwald). B: Schematic geological map of Aiguilles Rouges and Mont Blanc areas with indication of the main Variscan granite bodies: FGrd - Fully Granodiorite; MB - Mont Blanc granite; Mo - Montenvers granite; MP - Montées Pélissier granite; P - Pormenaz granite; Va - Vallorcine granite (modified after Von Raumer and Bussy 2004).
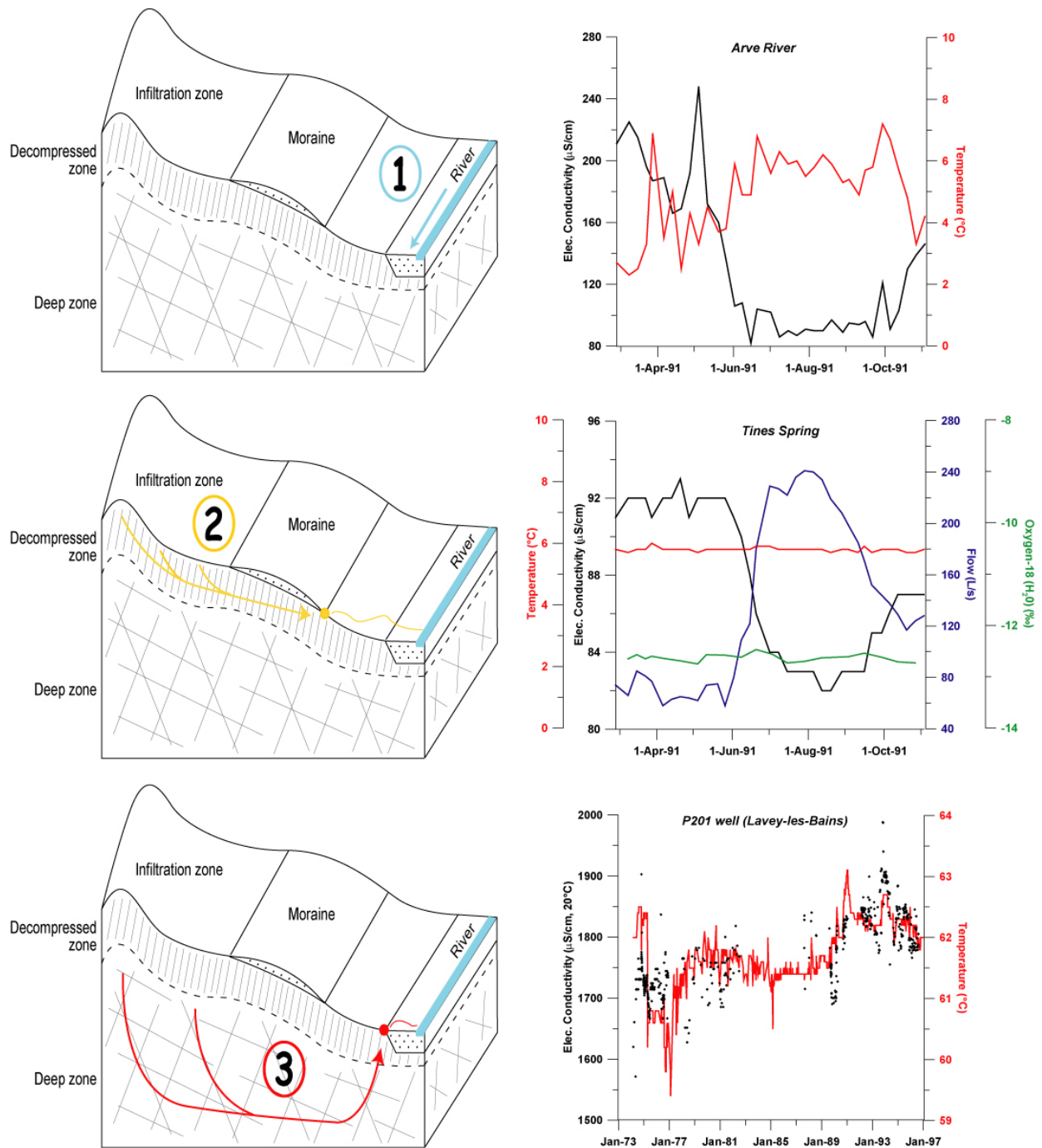
Figure 1.8: Active water circulations through an Alpine crystalline massif. Data of Arve River and Tines spring come from Payraud (1991) and data of P201 well were provided by the Alpgeo consulting office. The case number one represents a surface water system, the number two a shallow groundwater system in the decompressed zone and the number three a hydrothermal system.

1.4.3 Generalities about groundwaters in Alpine sedimentary domains: the case of Triassic aquifers

Typology of groundwaters in Triassic domain is presented by Mandia (1991) within the framework of the AQUITYP project. This study has been carried out at the Geology Laboratory of the Swiss Federal Institute of Technology, Lausanne (GEOLEP), in the same way as Dubois (1991) did for aquifers in crystalline rocks. It was decided to highlight investigation results from Mandia because he also sampled and analysed the main thermal spring in the Val d'Illiez which has similarities in hydrochemistry compared to other studied sites. Sampling and chemical analyses of more than one hundred sources including Val d'Illiez were realized for vast observation network laid out in the Rhone Basin, above Lake Geneva in Switzerland, and are linked to the evaporitic aquifers of Trias. Mandia specifies that studied areas concern the tectonic units of the Western Alps such as Median Prealps, Helvetic, Ultrahelvetic and Penninic.

Before Mandia, no general hydrogeological study of waters of Triassic evaporites of this region had ever been carried out. Mandia focused on sources whose annual average temperature is less than 12°C in addition to three selected hydrothermal sites (Combioula, Leytron, Val d'Illiez). The distribution map of water facies in Triassic domain is illustrated in Fig. 1.9. Globally, the dominating facies is Ca-SO$_4$ with sometime an enrichment in magnesium and alkalinity. These waters are poor with respect to chloride showing the virtual absence of halite in evaporites. This observation is quite interesting and important for understanding the hydrothermal systems studied in this study.
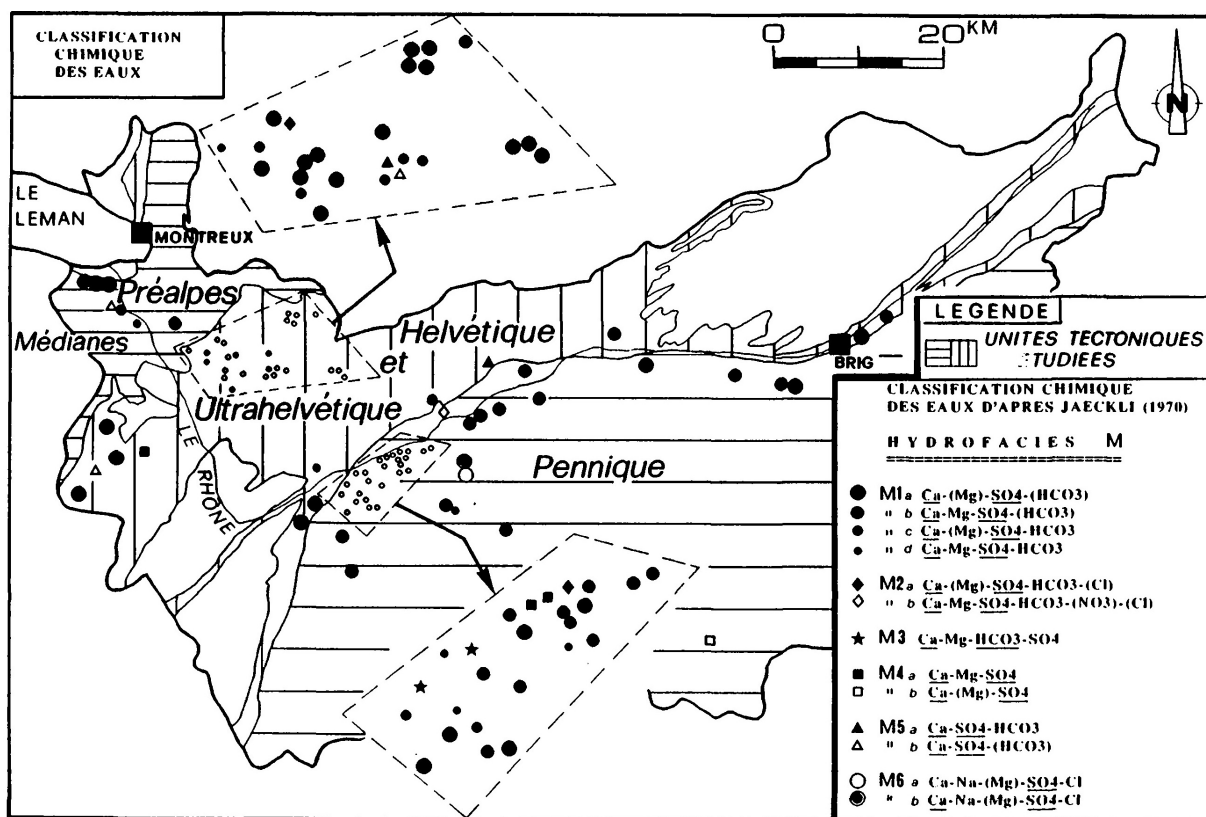
Figure 1.9: Distribution map of geochemical types of groundwaters in Triassic domain (Mandia 1991). The Jaeckli classification (1970) represents ions in meq/L in the range 10-20% (brackets), 20-50% and up to 50% (underlined).

Inside Triassic formations, Mandia precises that gypseous rocks constitute the principal rock aquifer of Triassic according to various degrees of karstification. The gypsum leaves a strong chemical imprint on the waters. This is characterized by a total average mineralization of 1.8 g/L with 50 to 90% of sulphate and calcium. other karstic rocks mineralize more or less strongly in these waters. They are calcareous dolomitic rocks (dolomite, dolomitic limestone, cellular dolomite). Levels of alcalinity and magnesium were observed, each which may represent 10 to 20% of the total chemical composition. The carbonated rocks make up the secondary aquifer associated with the gypseous karst.

In order to better characterize the chemical composition of these waters, Mandia focused on the minor and trace elements detected in waters. The ion strontium found in waters showed itself to be another marker of the gypseous aquifers. Indeed, it is related to the presence of celestine in gypseous rocks. Analysed contents of strontium in waters were often higher than those of potassium and sodium. Concerning trace elements, the significant markers on the water according to analyses from Mandia are rubidium, nickel, copper, scandium and yttrium.

The approach based on hydrogeological flow patterns and time variations in the physico-chemical parameters of the water showed that, in spite of variable flows related to snow melt, the temperature and mineralization remain stable for sources from Triassic aquifers (Mandia 1991). This observation implies that waters remained a sufficient amount of time in the aquifer for thermal and geochemical equilibrium. Globally in the Western Alps from Switzerland, the evaporitic aquifers have a chemical composition which is very different from those which characterize other aquifer types. Most are more mineralized, and the minimum levels of sulphate, calcium, magnesium, strontium and rubidium observed in the Triassic waters are superior to the former one in many cases.

<div align="right">**2**</div>

Description of methods

2.1 Geological investigations

2.1.1 Description of the regional geological setting

THE first approach for the description of the regional geological setting consists of a mapping study from collected geological and tectonic maps on a given area. For this regional geological view, all formations are gathered in different geological units in function of their lithology and their presumed age. For example, the sedimentary cover of the Morcles nappe was subdivided into two units gathering each one the formations of Dogger-Malm and Cretaceous-Oligocene (Fig. 4.1). The objective is to identify these units on a regional tectonic map and to describe their structure at depth from several cross sections parallel to the Alpine compressive stress. These cross sections are sufficiently deep to highlight the major thrust faults of external crystalline massifs which certainly have an important role on Alpine deep flow systems (Arthaud and Dazy 1989).

The second stage is an inventory of the rocks found on the studied area. The mineralogical composition of rocks are described from data in bibliography with the aim of being able to use these data for coupled flow and geochemical models. In this study, regional numerical modelling of flow and chemical transport was not carried out due to the number of cases but it can realized other investigations with adapted codes such as in SHEMAT (Clauser 2003). However, the description of the mineralogical composition of rocks was taken into account for the study of the saturation indices and the calibration of geochemical simulations with the PHREEQC code (Parkhurst and Appelo 1999).

The ultimate stage of the description of the regional geological setting is the study of directions of fractures planes. The representation of these fractures and faults on a map is important to gain a global view of preferential directions of regional flow and to choice the orientation of the cross section for the 2-dimensional vertical model of flow and heat transport. This study is realized from searches in the literature, in-situ fracture measurements and analysis of aerial views (maps and diagrams).

2.1.2   Description of the local geological setting

The local geological setting is also investigated from a geological map study and the realization of local cross sections near the geothermal zone. The objective is to show the uprising condition of the deep fluid from its reservoir to the surface, often related to vertical fractures or thrust faults. Exploration and exploitation boreholes realized on the geothermal zone bring additional details about the local geological setting and the upflowing condition.

The second and ultimate stage is the study of local fracture planes. The objective is to identify major fracture orientations observed in several outcrops near the hydrothermal zone. The type of fracture is defined such as mylonites, extension cracks, compressed faults, brecciated faults, etc. and illustrated on a 3-dimensional diagram. The abundance and the nature of these fractures give decisive information on the local flow direction.

2.2   Hydrochemical investigations

This section describes the methods used on the hydrothermal fields to measure the in-situ physico-chemical parameters and to sample in-situ the thermal and cold waters. It also describes methods employed at the CHYN laboratory to analyse major ions, trace elements and water stable isotopes.

From results of the chemical and isotopic analyses, it will be discussed about techniques used to highlight the characteristics of the deep flow system such as the study of mixing processes, water-rock interaction, mean elevation of the recharge zone, reservoir temperature, groundwater residence time, etc.

2.2.1   In-situ measurements

Sampling campaigns took place between May 2007 and June 2009, and they followed recommendations from the Federal Office for the Environment (FOEN, Switzerland, Thierrin et al. 2003). Samplings on the hydrothermal field for the chemical and isotopic analyses were always accompanied by physico-chemical in-situ measurements. Measured parameters are temperature, conductivity, pH, dissolved oxygen and flow rate, their units and the employed devices are illustrated in the Table 2.2. These values require to be employed with caution in

the data interpretation. Devices were regularly calibrated before field measurements with the aim to have workable and reproducible data. After calibration on the field, pH measurements were directly realized on waters and always represent a delicate operation due to potential problems with the probes, the natural wear of the device, problems encountered during the calibration, and the variability of all these parameters which depend on external factors not easily controllable.

Lavey-les-Bains (May and August 2009)

On the first investigated hydrothermal site, the temperature and the electrical conductivity measurements were carried out with the device *WTW Cond 340i with probe TetraCon*® used by F Gainon for his PhD thesis (Gainon 2008) and used for the AGEPP project (Sonney et al. 2007). During measurements, a device from the Alpgeo consulting office was also used because it has been employed in Lavey-les-Bains since more than 15 years for the long-term follow-up of parameters. In this device, one probe is connected and gives an electrical conductivity in μS/cm corrected at 20°C instead of

25°C occurring for the other device. Values of temperature depend on the used device and the hydrogeological condition at the surface. Indeed, for some sampling points, it was supposed slight heat losses because some measurements cannot be realized directly in the resurgence for springs and in the well head for boreholes. Moreover, heat losses can also occur in the upflowing zone for sampling points having a low discharge.

With the *WTW Cond 340i with probe TetraCon*® device, the electrical conductivity and the temperature were sometime measured with a

data logger reaching 500 recordings of which the frequency vary between 30 minutes to 10 seconds. The data logger has been very useful during pumping tests to follow the evolution of the parameters in P201 and P600 wells and also in sampled piezometers. The pH was measured with the device *Metrohm 826 pH mobile with a combined glass electrode (reference electrode KCl) and with a combined annular electrode Pt*, also employed by F Gainon for its PhD thesis, as the device *Hach Lange HQ10*

with probe Luminescent Dissolved Oxygen for the dissolved oxygen measurements in the same way. For the P201 and P600 well, values of flow rates are recorded by a data logger installed in the two well heads. On the contrary, it was necessary to use a graduated container and a chronometer for piezometers to estimate the discharges upflowing from a submersible Grundfos pump with a 2-inch diameter.

Saint-Gervais-les-Bains (July 2008) and Val d'Illiez (June 2009)

Between the sampling campaigns of Lavey-les-Bains (August 2007) and Saint-Gervais-les-Bains (July 2008), new devices were bought by the Center for Geothermal Research (CREGE). They have been used to measure the parameters at Saint-Gervais-les-Bains and Val d'Illiez, and are two *Hach Lange HQ40d* with a *probe CD401* for the temperature and the electrical conductivity, a *probe pHC301* for the pH, and finally a *probe LDO101* for the dissolved oxygen (Table 2.2). As enumerated for Lavey-les-Bains, values of temperature can be modified by the local hydrogeological conditions occurring and the distance from the discharged zone.

With the *Hach Lange HQ40d* devices, the electrical conductivity and the temperature were sometime registered with a data logger reaching 500 recordings of which the frequency vary between 30

minutes to 10 seconds. The data logger has been useful during pumping tests to follow the evolution of the parameters in Lépinay and De Mey Est wells at Saint-Gervais-les-Bains. In the Val d'Illiez, there is no submersible pump in the three wells (F1, F2 and F3) due to the natural artesian discharge occurring, and thus data logger were not used because it was not possible to undertake pumping tests.

For the Lépinay, De Mey Est and De Mey Ouest wells at Saint-Gervais-les-Bains and for the F3 well in the Val d'Illiez, values of flow rates were given by a data logger installed in the well heads. On the contrary, it was necessary to use a graduated container and a chronometer for springs and drains to estimate the discharge rates. The Grundfos submersible pump was employed to sample water in the F99 well at Saint-Gervais-les-Bains.

Table 2.1: Bottles used for the sampling of waters in the field.

Analysed parameters	Type of bottle	Volume of sampled water (mL)
Cations	Polyethylene	20, with one drop of HNO_3 10 %
Anions	"	20
Alkalinity and dissolved silica	"	250
Trace elements	"	50, with two drops of HNO_3 65 %
Water stable isotopes	Glass	8
Tritium	Polyethylene	500
Radon	Glass	20
Uranium and Radium	Polyethylene	250

2.2. HYDROCHEMICAL INVESTIGATIONS

Table 2.2: In situ measurement methods and analytical methods in laboratory for the studied groundwaters. Water temperature, electrical conductivity, pH, and Dissolved oxygen were measured in waters at Lavey-les-Bains with methods and apparatus described in Gainon (2008).

PARAMETERS	UNITS	METHODS AND DEVICES	ACCURACY	ERROR
IN SITU MEASUREMENT				
Water Temp.	°C	Hach Lange HQ40d with probe CD401	± 0.1°C	± 1 %
Elec. Cond. 25°C	μS/cm	"	± 1 μS/cm	± 1 %
Flow Rate	L/min	Containers and chronometers - Electronic metre	± 1 L/min	± 10 %
pH	no unit	Hach Lange HQ40d with probe pHC301	± 0.01	± 5 %
Oxygen at saturation	%	Hach Lange HQ40d with probe LDO101	± 0.1 %	± 5 %
Oxygen	mg/L	"	± 0.01 mg/L	± 5 %
Final Drawdown in wells	m	Electronic or manual measurement	Depends on the used method	
LABORATORY ANALYSES			DETECTION LIMIT	
CATIONS				
Li	mg/L	Ionic chromatography - Dionex Corporation DX120	0.25 mg/L	± 5 %
Na	"	"	"	"
K	"	"	"	"
Mg	"	"	"	"
Ca	"	"	"	"
Sr	"	"	"	"
ANIONS				
F	mg/L	Ionic chromatography - Dionex Corporation DX120	0.3 mg/L	± 5 %
Cl	"	"	"	"
Br	"	"	0.5 mg/L	"
SO$_4$	"	"	0.3 mg/L	"
HCO$_3$	"	Alkalimetric titration	1 mg/L	"
UNDISSOCIATED				
SiO$_2$	mg/L	Spectrometry PerkinElmer Lambda 10	0.1 mg/L	± 5 %
B	"	ICP-MS PerkinElmer Elan 6100	0.1 μg/L	± 10 %
TRACE ELEMENTS				
Rb	μg/L	ICP-MS PerkinElmer Elan 6100	0.1 μg/L	± 10 %
Ba	"	"	"	"
Al	"	"	"	"
Cr	"	"	"	"
Co	"	"	"	"
Ni	"	"	"	"
Cd	"	"	"	"
U	"	"	"	"
Pb	"	"	"	"
Ti	"	"	"	"
As	"	"	"	"
Mn	"	"	"	"
Fe	"	"	"	"
Mo	"	"	"	"
Cu	"	"	"	"
Zn	"	"	"	"
I	"	"	"	"
IONIC BALANCE				
Cations	meq/L	Sum of the dissolved cations	1 meq/L	± 5 %
Anions	"	Sum of the dissolved anions	"	"
Difference	%	$(\sum cations - \sum anions)/(\sum cations + \sum anions)$	± 0.1 %	
ISOTOPES				
Deuterium (H$_2$O)	‰	High-Precision Laser Spectrometry	4000 ppmv	± 0.8 ‰
Oxygen-18 (H$_2$O)	"	"		± 0.1 ‰
Tritium	TU	Scintillation spectrometry (Hydroisotop, Germany)	0.6 TU	± 5 %
Radon-222	Bq/L	Liquid Scintillation Counting TRI-CARB® 2250A	0.5 Bq/L	Specified
Radium-226	mBq/L	Spectrometry-α with silicon barrier	5 mBq/L	Specified
Uranium-238	"	"	"	"
Uranium-234	"	"	"	"

2.2.2 Sampling

Bottles used for the sampling of waters in the field are mentioned in the Table 2.1. Samples were stored in a closed container at air temperature to avoid abrupt changes in temperature especially for thermal waters and to protect from light. To minimize gas exchanges of oxygen, carbon dioxide and radon, samplings were carried out closest to the outlet source. Concerning boreholes, a small pipe was connected to the sample-tap and the end was plunged into a container. With this method, measurements and samplings could well be done while avoiding contact with the atmosphere. For the radon, it is imperative that the sample contains no air bubble, the recommended method is to fill the 20 mL bottle glass and to close directly the bottle in the container containing the sampled water.

With a manual pump and an adapted small container, sampled waters were filtrated (0.45 μm) to remove impurities. This is imperative for analyses of major ions, trace elements and water stable isotopes, and should not be done as far as possible for tritium, and radio-isotopes. In addition to the filtration, acidification of samples for cationic and trace elements analyses requires to be undertaken directly in the field to avoid precipitation of the carbonates and co-precipitation with iron and manganese hydroxides. Finally, quantities of sampled waters showed in the Table 2.1 could appear large compared to the volumes needed for analyses. This surplus of water is a safety margin if analyses must be redone due to handling errors, specifically related to the dilution of the samples.

2.2.3 Analyses in laboratory

Major ions

For all sampled waters from the three hydrothermal sites, major ions excepted the alkalinity and the dissolved silica were analysed by ionic chromatography with the device *Dionex Corporation DX120*. For each element, the accuracy, the detection limit and the error are given in the table 2.1. The method consists to measure the inferred electrical conductivity for each ion. Cations and anions are not analysed in the same time. The device requires to have waters with electrical conductivity lower than 400 mg/L. Therefore, for samples with higher conductivities, a dilution process with an almost pure water ($<$ 20 μS/cm) is required. The dilution factor depends on the total mineralization of the sample, and in the study of these three hydrothermal sites especially for Saint-Gervais-les-Bains, the dilution factor reached 10. The dilution process is a delicate handling and can be undertaken in two ways: using a graduated micro-pipette or weighing accurately the quantities of water. The first quoted method was employed in this study because it is faster, but the uncertainties on the collected quantities are greater. To verify the obtained results, the ionic balance is calculated for each sample, and if it exceeds $\pm$5% the analysis is redone. For all undiluted samples from the three sites, the ionic balance has always been lower than $\pm$5%. Sometimes, the balance was up to $\pm$5% for diluted waters, and

it was assumed that errors came from the dilution process.

Waters of which concentrations for each major element are known, also called standard, are placed every 12 samples in the series. This method is relatively effective for detecting analytical errors but it does not directly apply to samples taken on the field. To remedy this, it was decided to select one water by site (often the most mineralized) and to analyse it 3 times in the series: beginning, middle and end. For each analysed element, the results showed concentration differences lower than $\pm$1%.

The alkalinity or the bicarbonate content was measured using the alkalimetric titration method. The chemical equilibrium between HCO_3^- and H_2CO_3 is attained with a pH in the range 4.3-4.5. A hydrochloric acid (0.1M) is added into the sample to reach this equilibrium. The volume of added hydrochloric acid can be calculated and finally the alkalinity in mg/L (122 $*$ mL HCl (0.1M)). After the calibration of the device, 12 samples of 50 mL can be analysed following. Three samples from the same bottle are analysed in three different series to validate the obtained results, and the observed variations never exceed $\pm$1%. The imprecision of measurements may be caused by the dosage of 50 mL.

The analyses for the silica content were carried out by the spectrophotometric method proposed by the manual "Standards Methods for Examination of Water and Wastewater" (Eaton et al. 1995), and especially, the Molybdo-silicate method was employed. The spectrophotometer compares the colouring between the sample without reagent and the same sample with reagent, the precipitation of the molybdo-silicate generates a greenish yellow colouring of the water. As enumerated before, one sample has been selected and analysed three times with the aim to validate the obtained results. Results for the other samples were compared with respect to the previous measurements available in the literature.

Trace elements

The Inductively Coupled Plasma Mass Spectrometry (ICP-MS) allowed trace elements in sampled waters from the three hydrothermal sites to be measured. For each trace element, the detection limit is 0.1 μg/L (Table 2.1) and the analyses were carried out at the Center for Hydrogeology (CHYN, Neuchâtel). Due to local and particular hydrogeological conditions on certain sampling points, some trace elements were deposited in the host rocks before the sampling, especially for iron and manganese (hydroxide deposits formed by reaction with the oxygen). The list of analysed trace elements is given in appendix A, and values have to be considered with caution because they correspond to emergence conditions depending on mixing processes and oxygen concentrations of the end-members. The data of the trace elements are documented in appendixes for each selected site, but they are not interpreted because trace elements are not one of the main objectives of this study even if they often give interesting results about the origin of the thermal waters. The data could be useful for additional geochemical investigations.

Water stable isotopes

Water stable isotopes were analysed at the Center for Hydrogeology with the High-Precison Laser Spectrometry device implemented at the beginning of 2008. Therefore, waters from Lavey-les-Bains sampled in 2007 were not analysed for deuterium and 18-oxygen. The D/H and $^{18}O/^{16}O$ measurements of microliter natural water samples (Lis et al. 2007) was employed to analyse the water stable isotopes. This technique requires 1.5 mL of water and during the measurement, the device automatically converts the obtained result with respect to the Standard Mean Ocean Water (SMOW). It was necessary to collect the samples in glass bottles.

Radio-isotopes

Analytical methods used to measure the radio-isotopes, are described below in Gainon (2008), who studied four isotopes of the series ^{222}Rn, ^{226}Ra, ^{238}U and ^{234}U in thermal groundwaters from Switzerland. The analyses were carried out by Dr. H Surbeck at the Center for Hydrogeology. Since 2009, the radio-isotope laboratory was closed and therefore, analyses could not be realized for the hydrothermal site in the Val d'Illiez, where waters were sampled in June 2009. The obtained results for Lavey-les-Bains and Saint-Gervais-les-Bains are integrated in appendixes B and C but not interpreted because the radio-isotopes are not one of the main objectives of this study. For the hydrothermal sites of Lavey-les-Bains and Val d'Illiez, Gainon (2008) had already given relevant explanations on the values obtained in thermal and cold waters. In the same way as the trace elements, data illustrated in appendixes B and C could be however useful for additional geochemical investigations.

The alpha spectrometry method allows measuring ^{226}Ra, ^{238}U and ^{234}U in groundwaters. Sample preparation followed a procedure developed by Surbeck (1995, 2000), based on a selective adsorption of isotopes. The detection limit with this method is 5 mBq/L for each isotope.

The photoluminescence method (Liquid Scintillation Counting - LSC) was employed to analyse

^{222}Rn in groundwaters. The sample procedure described in Gainon (2008) is based on the mixing with an organic solvent increasing the solubility of the radon. With this technique, the detection limit is 0.5 Bq/L. Due to its relative short half-life period (3.8 days), the time between sampling and measurement should be lower than one week.

2.2.4 Water chemistry

Hydrochemical investigations are often an integral part of groundwater and surface water studies. Often hydrochemical investigations are carried out in the framework of water quality studies to decipher water pollution. Another important field of water chemistry is the use of hydrochemical data to gain insight into the flow patterns of water and interactions between groundwater and surface water (Appelo and Postma 2005, Drever 1997, Hem 1985, Hunkeler 2006, Langmuir 1997, Mazor 2004).

The chemical composition of a water highlights the chemical-mineral processes occurring: dissolution of the host rock and gas, clay exchange, redox reactions, bacterial decomposition, mixing processes, etc. Moreover, other factors are crucial for the chemical evolution of waters such as aquifer temperature, pollution, biological activity, velocity of groundwater, etc. (Muralt 1999).

The presence or absence of dissolved species in waters and their concentration allows deciphering the geological origin of the host rock during the underground circulation. In this context, hydrochemical parameters can serve as natural tracer to gain insight into the origin of water and the pathways along which is has migrated. For example, a water circulating inside the Triassic evaporites will be enriched with respect to the calcium and sulphate from the dissolution of gypsum, and sometimes with magnesium when dolomitic rocks are present.

The studied waters from the three hydrothermal sites are firstly represented in a Piper trilinear plot with the aim to highlight their geochemical type. The Schoeller diagram is then used to show the proportional difference occurring for waters having a similar geochemical type but different salinities which is not put into evidence on the Piper plot. It was decided to represent the geochemical type of the studied waters from plots instead of using the conventional classifications such as those used by Jaeckli (1970) or Schmassmann (1980).

An example of a Piper plot was realized with a set of data from subthermal and thermal waters in Switzerland and neighbouring areas gathered in the BDFGeotherm database (Sonney and Vuataz 2008). The selected waters come from deep boreholes or natural springs in the Alps range, including the eastern French Alps and the northern Italian Alps, and also the Molasse Basin, the Jura range, the Black Forest and finally the southern part of the Rhine Graben. For each water, the geological setting of the deep reservoir was highlighted (Fig. 2.1). The figure shows a series of geochemical types occurring in the various geological domains, with conspicuous dominance in particular for the Triassic (Ca-SO$_4$) and Jurassic (Ca-HCO$_3$) groundwaters.

2.2.5 Mixing processes and composition of the end-members

Significant variations in space and time of the chemistry of groundwaters in a studied area provide information about mixing processes occurring between different types of waters, or about variations of the flow patterns. The deep thermal water may mix with shallow groundwater before being discharged in a spring or well. Cold waters are usually less mineralized than the thermal fluid, and the interpretation of spring and well water chemistry is important to recognize mixed fluids from 2-3 end-members, as well as criteria which indicate that dilution occurs (Nicholson 1993). These mixing processes are often best illustrated by the use of mixing models (binary diagrams) and by geochemical modelling (PHREEQC code).

Mixing models are an effective tool in all stages of hydrothermal investigations. The discharged of thermal waters from Alpine deep flow systems are often mixed with shallow groundwaters, even the warmest waters. Consequently, the geothermal re-
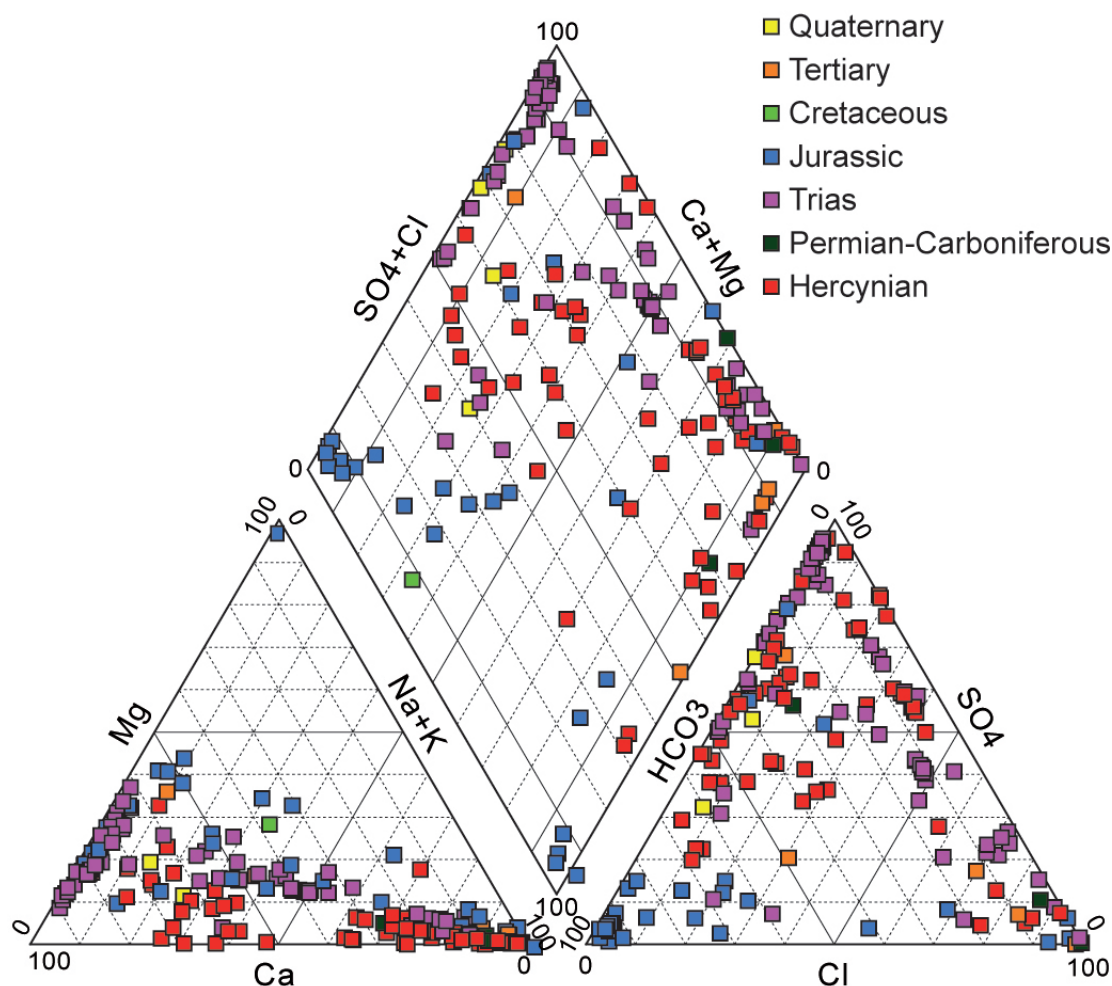
Figure 2.1: Piper diagram for subthermal and thermal waters from Switzerland and neighbouring areas related to their geological setting. Used data were documented in BDFGeotherm database (Sonney and Vuataz 2008).

source of a given site can be improved, by collecting unmixed fluids at depth with boreholes. To decipher the chemical composition of the pure thermal water, mixing diagrams have to be established with chemical and isotopic data for all sampling points. From these diagrams and assuming particularities about the origin of the deep fluid, such as low tritium (infiltration before the beginning of atmospheric nuclear tests) or low magnesium content (example in crystalline environment), it is possible to extend the mixing lines towards the different end-members. Then, the chemical and isotopic composition of the end-members can be evaluated using equations of linear correlation. In this study, correlations between all parameters with respect to

temperature, total dissolved solids (TDS) or electrical conductivity, chloride, sulphate and calcium concentrations were employed. The hydrothermal system of La Léchère (Savoie, France) is illustrated as an example of a deep flow system with three end-members (Fig. 2.2). A Na-Cl upflowing thermal water from the basement (Belledonne Massif, external crystalline massif) is mixed with two shallow groundwaters circulating in the Triassic formations and in the Quaternary filling. When the thermal water penetrates in the Triassic formations containing dolomite, cellular dolomite, gypsum and anhydrite, $Ca-SO_4$ and $Ca-Mg-HCO_3$ dissolution occurs, modifying the chemical composition of groundwaters and increasing the total mineralization.
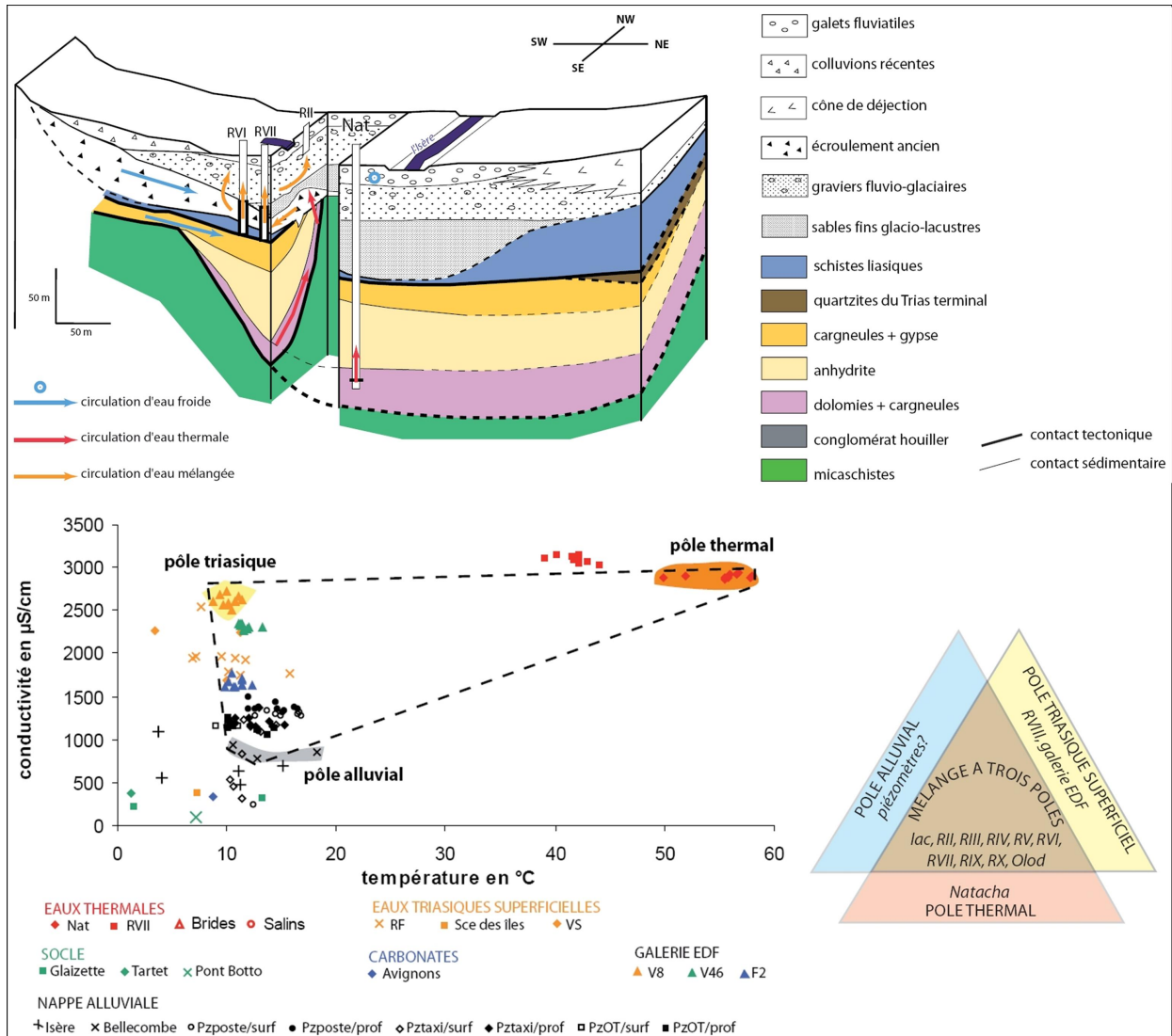
Figure 2.2: Geological and hydrochemical settings of the hydrothermal system of La Léchère (Savoie, France) showing complex mixing and dissolution processes (Thiébaud 2008).

2.2.6 Variation of physico-chemical parameters

Short-term and long-term variations of physico-chemical parameters in waters from the discharged springs and wells are important to study, as they contribute to the understanding of the thermal and chemical processes in the exploited zone, often subjected to mixing processes. The reasons are multiple and mainly concern the aspects of the resource management and the long-term optimization of production rates. Moreover, short and long-term changes in parameters also provide us information about mixing process. They also give us information about the physical changes in the exploited zone, such as heat exchange by advection-diffusion due to modification of exfiltration velocities from the deep reservoir, effects caused by the variation of recharge in the infiltration area (melt of glaciers),

etc. Finally, the static and dynamic water levels in the production wells allow knowing if the thermal aquifer is exploited in a sustainable way or not.

In the Alps range, many spas exploit the upflowing thermal waters for decades and even centuries, but continuous or discrete measurements of the physico-chemical parameters are not systematically undertaken. Typically, measurements are carried out during the implementation of boreholes, pumping tests, or rehabilitation of old springs and wells. Thus, there may be a lot of data concentrated on short periods and no data on longer periods sometimes exceeding 10 years. The long-term variation of parameters from the Alun and Soufre springs, belonging to the hydrothermal system of Aix-les-Bains (Haute-Savoie, France) in a sedimentary domain, is illustrated as an example. In this case, data were collected between 1975 and 1995 with a high density of measurements after 1986 (Fig. 2.3). Two events modified the system after 1986: the implementation of two deep boreholes Reine-Hortense (1989/1990) and Chevalley (1991/1992), and a very important

flooding of the springs in February 1990. The data show a great influence of the flooding on the parameters, with a decrease of temperature and mineralization. The implementation of the two boreholes generated a significant decrease of parameters in the springs.

Concerning short-term evolution of parameters, the chosen strategy was to impose a disruption on the hydrological functioning of the thermal aquifer by a sudden change of the production rates. This strategy was a success to highlight mixing processes in the exploited zone because mixing rates were modified. Before modifying the production rate in the studied sampling point (increase then decrease), parameters were measured and a sample was taken to define the initial background. During the short pumping tests (roughly 1-2 hours), a data logger allows following the evolution of temperature, electrical conductivity, pH and dissolved oxygen with a frequency measurement previously selected. Several samples were taken in the modified fluid when parameters changed.

2.2.7 Water-rock interaction

Depending on conditions such as temperature, pH, dissolved CO_2, etc., each mineral can be dissolved in water with various degrees. All minerals have a maximum solubility, and compared with the effective concentrations in water, the degree of saturation of water with respect to minerals can be evaluated. It is often of interest to evaluate the saturation state of a solution with respect to certain minerals. This provides information about likely sources/sinks of ions or indirect information on how long water was in contact with a mineral. The longer the contact time, the closer to saturation should the solution be (Appelo and Postma 2005, Drever 1997, Hem 1985, Hunkeler 2006, Langmuir 1997, Mazor 2004). The saturation state can be evaluated and the degree of under-or over-saturation quantified by comparing the solubility product K_{SO} with the product of the activities of ions, which is usually denoted as ion activity product (IAP). For example for gypsum, the solubility and ion activity products are given by:

$$K_{SO} = \{Ca^{2+}\}\{SO_4{}^{2-}\} \qquad (2.1)$$

activities at equilibrium (maximal value)

$$IAP = \{Ca^{2+}\}\{SO_4{}^{2-}\} \qquad (2.2)$$

actual activities in water sample

The saturation state can be characterized by the ratio between IAP and K_{SO}:

$$\Omega = IAP/K_{SO} \qquad (2.3)$$

Thus, for $\Omega = 1$ the solution is at equilibrium with respect to gypsum. For $\Omega < 1$ the activities in the IAP are smaller than the activities at equilibrium and thus the solution is under-saturated with respect to gypsum. $\Omega > 1$ represents over-saturation. Often the ratio is given on a logarithmic scale and denoted as saturation index SI:

$$SI = log(IAP/K_{SO}) \qquad (2.4)$$

For $SI = 0$ the solution is at equilibrium, $SI < 0$ indicates under-saturation and $SI > 0$ over-saturation. Often it is illustrative to represent the saturation state graphically, especially if data from a number of sampling locations are discussed. This can be done by plotting the saturation index for example as a function of space or as a function of the concentration of some ions (Appelo and Postma 2005, Drever 1997, Hem 1985, Hunkeler 2006, Langmuir 1997, Mazor 2004). Alternatively,

and in this study, the saturation indices of selected sampling points of the studied hydrothermal sites (often warmest water) were illustrated as values for each selected mineral.

For calculating the saturation index and for other calculations, the activities of ions in solution require to be known. The calculation has to be carried out in a recursive way because the activity coefficient depends on the proportions of free ions and complexes, which depends on the activity of these compounds. There are several computer codes that calculates activity coefficients and proportions of free ions and complexes. One of the most complete programs is PHREEQC (version 2.12.04) developed by Parkhurst and Appelo (1999), and this was employed to calculate saturation indices for the three studied hydrothermal sites. In this study, saturation indices of aluminosilicates were calculated using three aluminum con-

centrations (1,5 and 10 μg/L) according to data documented in literature for the three studied hydrothermal sites (Bianchetti 1993b, Gainon 2008). In Bianchetti (1993b) and Gainon (2008), the aluminum concentrations were analysed several times in stable thermal waters having constant physicochemical parameters, respectively with quantitative and semiquantitative methods. However, the results showed large variations caused by several factors: pollution of samples, problems during the dilution of samples, analytical interference, memory effect, low atomic weight of aluminum. But, while comparing all the documented data with the values measured in this study (not all shown in the appendices), it is possible to assume that the concentrations of aluminum for thermal waters of Lavey-les-bains and Saint-Gervais-les-Bains are in the range of 1-10 μg/L, and those in the Val d'Illiez have contents close to 1 μg/L.
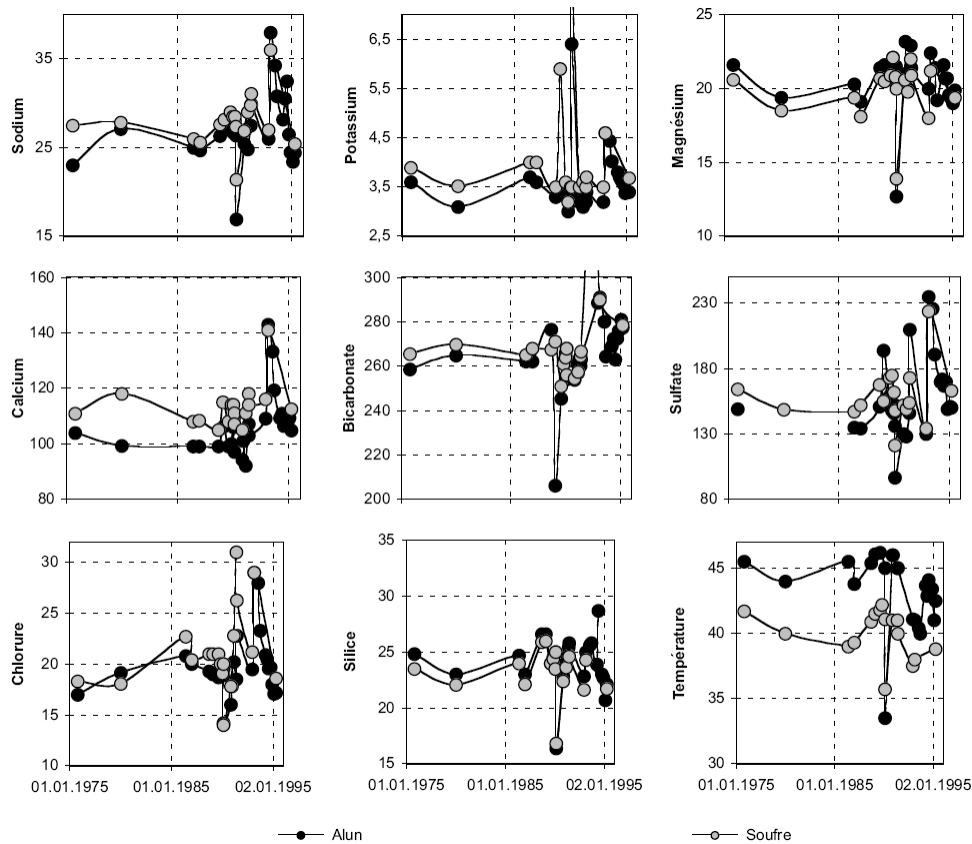
Figure 2.3: Temporal evolution of the parameters in Alun and Soufre springs between 1975 and 1995 (Aix-les-Bains hydrothermal system, Haute-Savoie, France). Temperature in °C and concentration in mg/L (Muralt 1999).

2.2.8 Regional deep flow system

Interpretation based on geological, hydrogeological and hydrochemical methods allows undertaking a regional conceptual model of the different flow patterns. The developed conceptual model of a hydrothermal system can be summarized into four main parts:

1. The recognition of the infiltration area where rainwater leading to surface or soil water occurs. These meteoric waters are labeled by their isotopic signature in oxygen-18 and deuterium.

2. The highlight of geological formations and their associated fractures where the infiltration occurs until the hydrothermal reservoir. In crystalline domain, groundwaters circulate below the decompressed zone throughout permeable and vertical layers or major faults and thrusts. In sedimentary context, the flow pattern tends to follow the direction of the permeable formations.

3. The characterization of the uprising zone of the deep and hot fluid from its reservoir towards the surface. The upflowing occurrences are often related to the presence of faults, fractured vertical layers, thrusts faults, etc., generating a great contrast of permeabilities.

4. The summing-up of mixing processes between the deep thermal component and the cold shallow groundwaters taking place in the final uprising circuit.

The hydrothermal system of Acquarossa (Ticino, Switzerland) is illustrated as an example of a deep flow system of which the infiltration area, geological formations supplying the flow pattern, the uprising zone and mixing processes have been quite well defined (Fig. 2.4). For Acquarossa, meteoric waters infiltrate roughly at 1700 metres of elevation inside the Triassic formations in the area of Acquacalda. The deep flow system follows these rocks pinched between two crystalline domains, the Lucomagno-Leventina and Simano massifs. Then, the thermal water upflows towards the surface due to the outcropping of the Triassic formations before mixes with a cold groundwater from the Quaternary filling (alluvial deposits and rock falls).

2.2.9 Mean elevation of the recharge zone

Selected groundwater samples from the three studied hydrothermal sites in the Aiguilles Rouges area were analysed for their δ^2H and δ^{18}O values with the aim to calculate the mean elevation of the recharge zone. The results of these analyses are given in appendixes and are interpreted in terms of the conditions under which the groundwaters infiltrated. To interpret groundwater isotope data requires knowledge of the δ^2H and δ^{18}O content, which are given relative to the Standard Mean Ocean Water (SMOW), that explained in several books such as Clark and Fritz (1997), Cook and Herczeg (2000), Fritz and Fontes (1986), Mazor (1991); and Etcheverry (2002) and Kullin and Schmassmann (in Pearson et al. 1991) for the Swiss groundwaters.

The isotopic composition of thermal waters in Switzerland from deep flow systems depend slightly on physical processes such as condensation, evaporation, exchange between phases, etc. There is no enrichment in oxygen-18 in spite of the relative high temperature of the hydrothermal reservoirs reaching 100-120°C in the Alps Mountain (Vuataz 1982). These processes often occur for high enthalpy geothermal systems (Arnórsson 2000, Fournier 1981, Nicholson 1993). In Switzerland, water stable isotopes in thermal fluids are close to the SMOW line showing that thermal fluids are meteoric waters (Fig. 2.5). The δ^2H and δ^{18}O values are determined by the isotopic fractionation which depends on the air temperature, latitude, geographical location, elevation, seasonal period, origin and intensity of precipitation, location of precipitation, etc. On the global level, these processes generate variation between δ^2H and δ^{18}O values according to the world meteoric water line (Yurtsever and Gat 1981 in Kullin and Schmassmann 1991):

$$\delta^2 H(\%_{\text{o}}) = 8.2 * \delta^{18}O(\%_{\text{o}}) + 10.8 \quad (2.5)$$

1. Infiltration:

- altitude de recharge à environ 1730 m.s.m.
- Trias affleurant
- eau froide, non minéralisée et oxygénée (pluies, pertes)

2. Ecoulement profond:

- réseau karstique dans les évaporites du Trias, au contact avec la nappe du Lucomagno
- acquisition du caractère "thermominérale". Température maximale du réservoir: ~60°C pour une profondeur d'environ 2-3 km. Minéralisation par dissolution des minéraux triasiques, notamment du gypse
- consommation de l'oxygène dissous et acquisition du caractère réduit. Mise en solution du fer.

3. Remontée et mélange:

- depuis l'Est, par la culmination du pli Molare.
- avant d'atteindre le cône d'éboulis il y a ramification de l'écoulement en 2 branches principales, l'une donne la source Sciarina, l'autre donne les 3 sources Satro.
- une partie de l'écoulement se disperse dans le cône d'éboulis et se mélange avec la nappe locale.
- Refroidissement de la composante thermale par conduction lors de la remontée, et par dilution lors du mélange avec la nappe. Ce phénomène atteint surtout la source Satro Gauche.
- Dès que l'eau est au contact avec l'oxygène atmosphérique, il y a précipitation du "Fango".

Figure 2.4: Conceptual model of the Acquarossa hydrothermal system (Ticino, Switzerland). The deep flow system occurs in the Triassic formations pinched between two crystalline massifs (modified from Preisig 2009).

In the northern and eastern part of Switzerland, Kullin and Schmassmann (1991) have been established a Swiss meteoric water line from 64 samples of precipitation, surface and groundwater, which differs slightly:

$$\delta^2 H(\text{‰}) \quad = \quad 7.55 * \delta^{18} O(\text{‰}) + 4.8 \quad (2.6)$$

Other equations were developed for different regions of Switzerland and neighbouring areas. The study of the elevation of the recharge zone is based on data of water stable isotopes, because δ^2H and δ^{18}O values are function of the elevation. These relations vary according to geographical regions and are illustrated in Table 2.3. They mainly concern areas in the Molasse Basin in the northern and eastern part of Switzerland, the northern part of the Jura range including the region of Yverdon-les-Bains (canton of Vaud) and the Bernese Alps.

For the southern part of the Jura range and Molasse Basin and the Western Alps, there is almost no information on the relationship elevation/isotopes, except the Lemanic Prealps in the region of Thonon-Evian (Haute-Savoie, France) studied by Blavoux (1978) for his PhD thesis.

Concerning the Alps Mountain including the western part of Switzerland and France, it is more appropriate to use relations of Kullin and Schmassmann (1991) for the Bernese Alps, Blavoux (1978) and Vuataz (1982). The other relations were developed in regions more distant from the study area and thus were not employed in this study, especially for the relation of Bortolami et al. (1979) which was defined under a Mediterranean climate having a different isotopic signature in precipitation.

Table 2.3: Relation between the mean elevation of the recharge zone and water stable isotopes in groundwaters.

Domain	Equation	Reference
Western Vosges and Alsace	$\delta^{18}O$ = -0.0021±0.0007 x Elev. - 7.8±0.3 δ^2H = -0.0238±0.0043 x Elev. - 47.8±1.6	Kullin and Schmassmann 1991
Central Jura Mountain	$\delta^{18}O$ = -0.002±0.0001 x Elev. - 8.2±0.1 δ^2H = -0.0164 x Elev. - 56.4	"
NE-Jura and Black Forest	$\delta^{18}O$ = -0.0019±0.0002 x Elev. - 8.6±0.3 δ^2H = -0.0107±0.0018 x Elev. - 63.1±1.9	"
Mittelland	$\delta^{18}O$ = -0.0028±0.0004 x Elev. - 8.7±0.3 δ^2H = -0.0186±0.0043 x Elev. - 63.2±1.6	"
Bernese Alps	$\delta^{18}O$ = -0.0017±0.0005 x Elev. - 10.1±0.4 δ^2H = -0.013 x Elev. - 72.0	"
Hasli Valley	$\delta^{18}O$ = -0.0021±0.0006 x Elev. - 10.6±0.7 δ^2H = -0.0172 x Elev. - 76.1	"
Lake Uri area	$\delta^{18}O$ = -0.0014±0.0004 x Elev. - 9.1±0.3 δ^2H = -0.0092±0.0049 x Elev. - 64.7±3.0	"
Central Graubünden and Engadine	$\delta^{18}O$ = -0.0028±0.0007 x Elev. - 8.1±0.2 δ^2H = -0.0265 x Elev. - 45.4	"
Mesolcina Valley	$\delta^{18}O$ = -0.0022 x Elev. - 5.7 δ^2H = -0.0146 x Elev. - 40.3	"
Jura, Northern Alps	$\delta^{18}O$ = (3110 + Elev.) / -367 δ^2H = (2650 + Elev.) / -45.9	Vuataz 1982
French Jura and Central Swiss Jura	$\delta^{18}O$ = -0.0018 x Elev. - 8.62 δ^2H = -0.015 x Elev. - 59.9[a]	Blavoux et al. 1979
Yverdon-les-Bains area	$\delta^{18}O$ = -0.0033 x Elev. - 7.57 δ^2H = -0.027 x Elev. - 51.3[a]	Kern 1982
Lemanic Prealps Thonon-Evian area	$\delta^{18}O$ = -0.003 x Elev. - 8.1[b] δ^2H = -0.025 x Elev. - 55.1[a]	Blavoux 1978
Maritime Alps	$\delta^{18}O$ = -0.00312 x Elev. - 8.03 δ^2H = -0.0249 x Elev. - 51.1	Bortolami et al. 1978

a) For these regions, deuterium was not analysed. Equations were defined from oxygen-18 data and the world meteoric water line of Yurtsever and Gat (1981).

b) This relation was defined from data in groundwaters at Thonon and neighbouring zones with the a gradient of 0.3‰ indicated by Blavoux (1978).
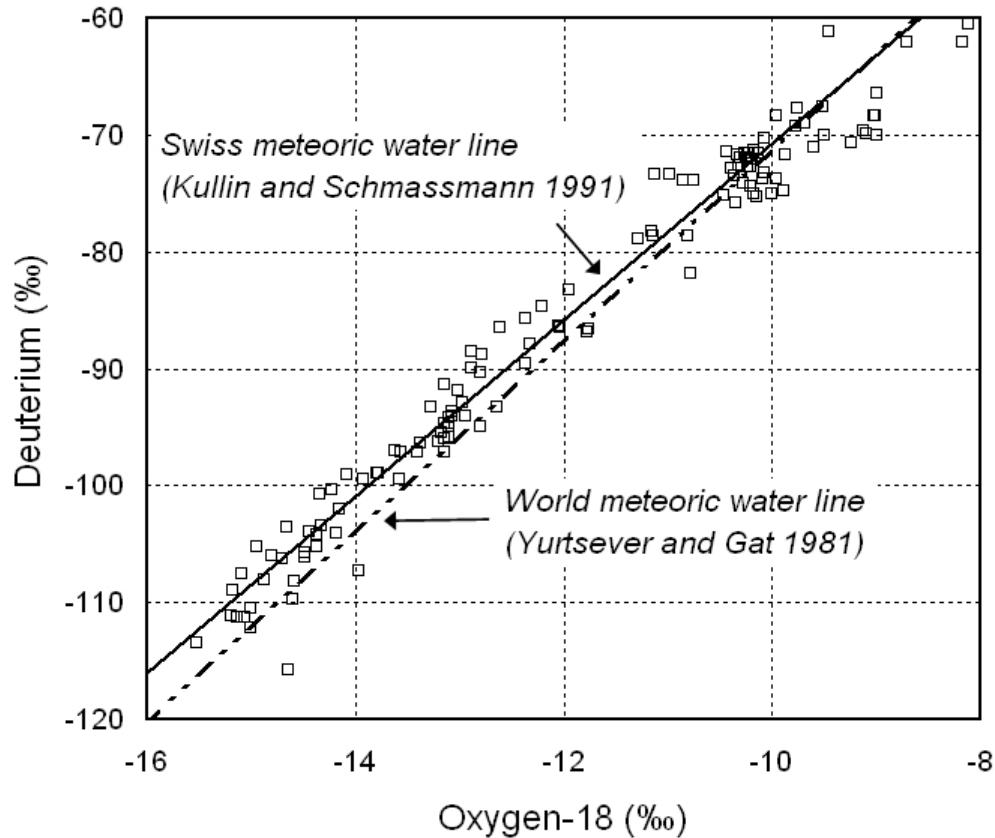
Figure 2.5: Relation between oxygen-18 and deuterium in thermal waters from Switzerland and neighbouring areas (according to BDFGeotherm data, Sonney and Vuataz 2008).

2.2.10 Reservoir temperature

Geothermometers (from Sonney and Vuataz 2010b)

Many different chemical and isotopic reactions might be used as geochemical thermometers or geothermometers to estimate reservoir temperature (Fournier 1981). Geothermometers constitute one of the most important geochemical tool for the exploration and development of geothermal resources, and also during exploitation when monitoring the response of geothermal reservoirs to the production load (D'Amore and Arnórsson 2000). They were developed from the mid-1960's to the mid-1980's and the most important ones are the silica (quartz, chalcedony and amorphous silica), Na/K, Na-K-Ca. Others that have been developed are based on Na/Li, Li/Mg, K/Mg, Ca/Mg, Na/Ca, K/Ca

ratios and Na-K-Mg relationships. Moreover, the geothermometer using the fractionation of oxygen isotopes between water and dissolved sulphate is also discussed in this section. Gas and other isotope geothermometers were not employed in this study, and therefore were not discussed. To discuss about the applicability of the geothermometers in the case of hydrothermal systems in the Alps considered as low-enthalpy geothermal systems (< 150°C), it was decided to highlight a study based on this applicability for thermal waters from the Molasse Basin and Tabular Jura. Based on discussions brought by this study, certain geothermometers will be selected with the aim to estimate depth temperature

for the three studied hydrothermal sites. Interpretation of results of these computations requires consideration of the geological and hydrogeological settings, and petrographical properties as well as complete chemical analyses of the sampled deep fluid (Fournier 1981). Solute geothermometers are based on temperature-dependent mineral-fluid equilibria and their successful application relies on five basic assumptions (Fournier 1977, Nicholson 1993):

1) The concentration of the elements or species to be used in the geothermometer is controlled only by a temperature-dependent mineral-fluid reaction.

2) There is an abundance of the minerals and/or dissolved species in the rock-fluid system for the reaction to occur readily.

3) The reaction attains equilibrium in the reservoir or aquifer.

4) There is a fast flow towards the surface with no re-equilibration after the fluid leaves the reservoir, ie. no near-surface reactions. In this paper, this condition does not occur because the studied deep fluids are subjected to lateral flows or are trapped in sub-horizontal formations. Moreover, the deep fluids come from boreholes and not springs.

5) There is no mixing or dilution of the deep fluid (this assumption can be circumvented if the extent of dilution/mixing ratio can be evaluated).

Sonney and Vuataz (2010b) studied the applicability of geothermometers in low temperature deep aquifers (200-2000 m) from Northern Switzerland with known reservoir temperature from borehole measurements (12-112°C).Measured temperature refers to the aquifer temperature from which the sample was taken, directly measured during the sampling campaign or estimated from the geothermal gradient in the borehole. Temperatures illustrated in this study are as representative as possible of the average temperature of the sampled aquifer. The approach based on the comparison on measured/calculated temperature is useful to evaluate the applicability of geothermometers for low-enthalpy geothermal systems. This study emphasizes that different geothermometers can be applied in different geological setting and temperature ranges.

Geological setting of the northern Switzerland (Sonney and Vuataz 2010b). In total, 62 water analyses from deep boreholes in 16 geothermal sites were used. Their position on the simplified Swiss tectonic map can be subdivided into two areas (Fig. 2.6). Some sites are located in the tectonic unit named Molasse Basin or Plateau whereas others are situated close to the Rhine River between the northeastern part of the Jura range in Switzerland and the Black Forest in Germany. This large area is characterized by a high geothermal gradient and a significant heat flow anomaly which can exceed 150 mW/m^2 (Rybach et al. 1987). For this reason, this area was regarded since decades as a zone of geothermal interest, and other boreholes exist but were not selected due to the absence of water analyses. Moreover, sites with ascending thermal springs located in the folded Jura between the Tabular Jura and the Molasse Basin were not taken into account. Indeed, the study of the application of geothermometers requires selecting sites where reservoir depth is known, what is often difficult to identify for sites with ascending thermal fluids.

Geologically, Switzerland can be divided into three main parts: 12.5% of its surface lies in the Jura, 30.5% in the Molasse Basin and 57% in the External and Pennine Alps (Fig. 2.6). The Jura can be also subdivided into two domains: the folded and the tabular Jura. The folded Jura extends from Geneva to Basel and consists of a succession of SW-NE folded chains, whereas the tabular Jura located at the south of the Rhine Valley contains subhorizontal formations which are slightly affected by tectonic events. In detail, the Tabular Jura consists of subhorizontal Mesozoic and Cenozoic cover rocks affected by Oligocene faulting overlapping a complex Hercynian basement (granite, gneiss) which outcrops in Germany (Back Forest). This sedimentary cover consists of an alternation of karstified limestones considered as aquifers and marls. At the bottom of the sedimentary cover, sandstones, quartzite and conglomerates are also present and can contain groundwater. Borehole investigations for geothermal prospection highlighted potential geothermal reservoirs from the Cretaceous to the Carboniferous. For the Jurassic formations, the Malm (upper) and Dogger (middle) karstified limestones with a variable thickness in the range of 200-500 metres are separated by the Oxfordian marl.
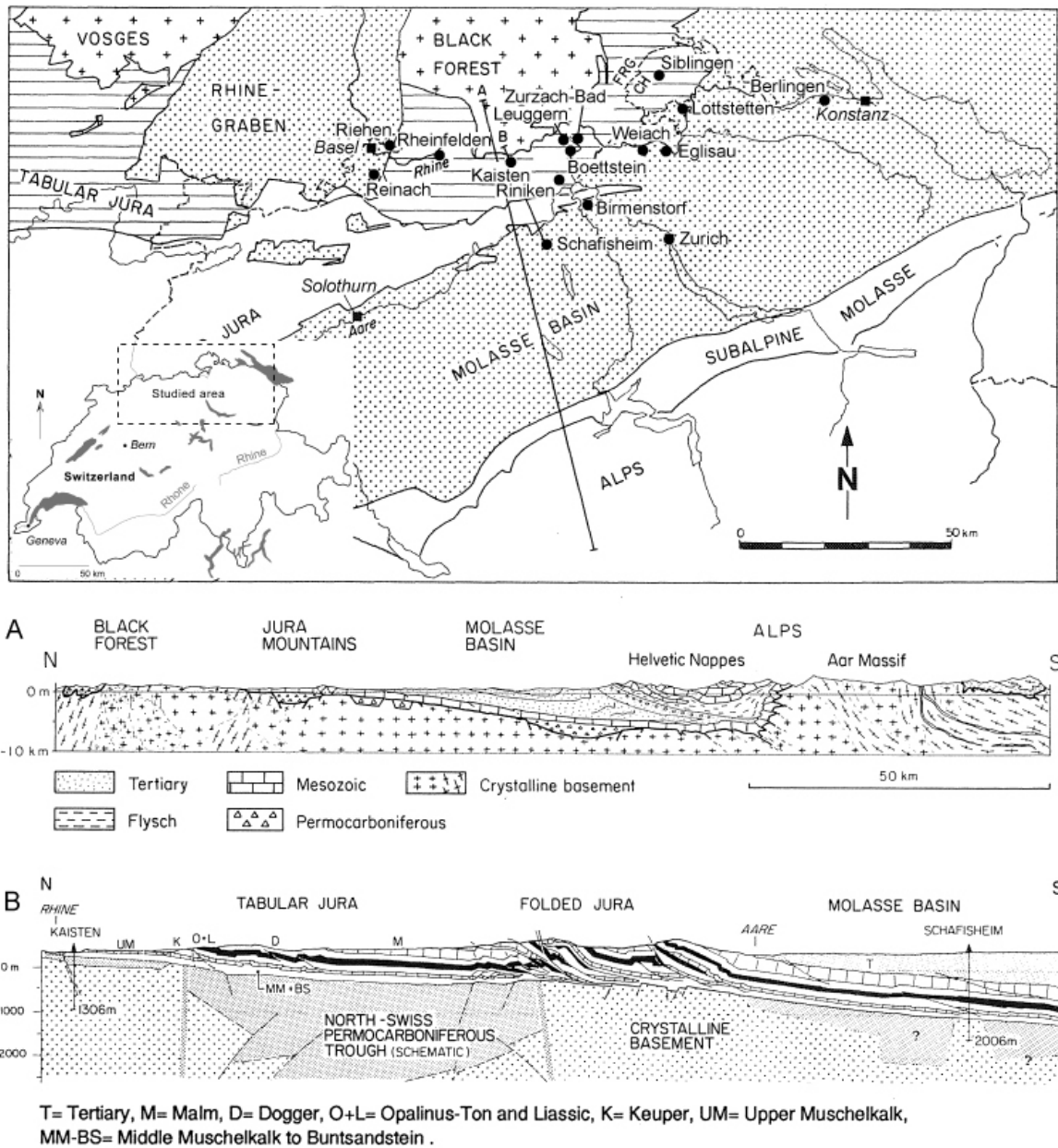
Figure 2.6: Map showing major structural units of Northern Switzerland and location of selected deep boreholes. Geological cross sections through Central and Northern Switzerland (A) and through Tabular and Folded Jura (B) (modified from Pearson et al. 1991 in Sonney and Vuataz 2010b).

The Triassic formations are unconformable with respect to the Permian and Carboniferous layers. They contain a greater variety of rocks than the Jurassic such as evaporite in the Keuper and Muschelkalk (Upper and Middle Triassic respectively), dolomite in the Muschelkalk and sandstone in the Buntsandstein (Lower Triassic). These rocks are considered as aquifers in addition to limestones which are also present, in particular in the Muschelkalk. Concerning the Permian and Carboniferous

sediments, they are detrital deposits in old grabens inside the Hercynian basement. They are locally present in particular in a WSW-ENE band going through Riniken and Weiach boreholes. In these two sites, boreholes crossed an alternation of sandstone, quartzite and silt with a thickness exceeding 1000 metres. More in the south (Schafisheim), the Buntsandstein sandstone of limited thickness directly overlies the Hercynian basement.
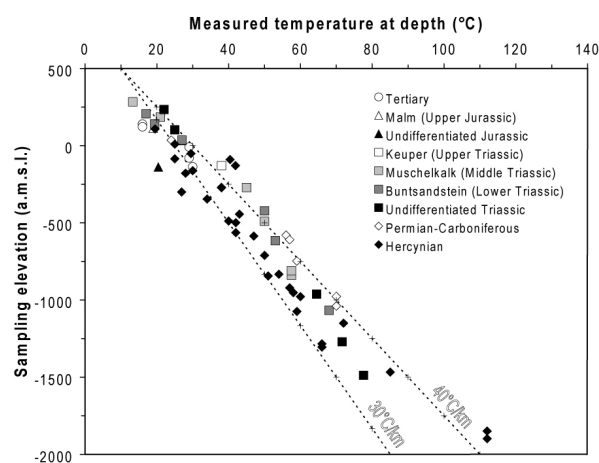
Figure 2.7: Plot of sampling elevation vs. measured temperature at depth for the studied deep fluids in boreholes. Deep fluids were subdivided into different symbols showing their geological setting. Two temperature gradient lines were added from an annual average air temperature of around 10°C at the surface (Sonney and Vuataz 2010b).

On the southern part of the extremity of the Jura range, Cenozoic and Mesozoic formations are covered by Tertiary sediments of which the thickness increases towards the south and the Alps Mountains (Fig. 2.6). This zone named Molasse Basin or Plateau has a hilly landscape, studded with lakes and with a few large plains. The Tertiary deposits, which stratigraphically overlie the Cenozoic and Mesozoic formations that are found in the tabular Jura, consist of three units: Lower Marine Molasse, Lower Fresh-water Molasse and Upper Marine Molasse (Trümpy 1980). Groundwater flow is often absent in the Lower Fresh-water Molasse; it is therefore regarded as an aquiclude. Groundwater flow through the Upper Marine Molasse sandstone is common but dependent on local conditions.

The geological formations of the Muschelkalk, Dogger and Malm beneath the Tertiary deposits represent the most important aquifers, and can contain great quantities of hot water in permeable fractures (Balderer 1990).

Selected boreholes crossed the described aquifers at different depths due to the weak dip of layers towards the south. Some of boreholes reached the basement and samples and measurements were carried out on water inflows. The measured temperatures at depth at different sampling elevations highlight a geothermal gradient in the range 30-40°C/km from an average temperature at the surface fixed at 10°C (Fig. 2.7). This result was already highlighted by Rybach (1992) in the study of the geothermal potential of the Swiss Molasse Basin. Some samples can be locally subjected to the rise of deep fluids from fractures or to mixing process with shallow groundwater due to their position beyond the gradient 30-40°C/km. The highest temperature at depth was measured at 112°C in the crystalline basement for the 2.3 kilometres deep borehole at Weiach.

Water chemistry (Sonney and Vuataz 2010b). Many reports and publications concern the chemistry of geothermal fluids in formations of the sedimentary cover and its crystalline basement below. Chemical data of selected sites are given in Table 1 and are interesting from a geothermal point of view, because their temperature, mineralization and geological setting give information on potential geothermal reservoir. Their position on the Piper diagram (Fig. 2.8) in relation to their geological formations indicates that different geochemical types of geothermal fluids occur. The geochemical type is defined by the most important cations and anions. Moreover, the Total Dissolved Solids (TDS) of waters tends to increase with depth, and a difference of TDS is visible between waters in the crystalline basement and waters from sedimentary formations which have higher TDS (Fig. 2.9). In the following subsections, the different types of geothermal fluids are described in terms of geochemistry.

Two selected sites at Leuggern and Weiach have a Ca-SO_4 type water with a TDS of 1.1 and 3.3 g/L respectively. Measured temperatures for this type are 13 and 50°C. This water was met in the fractured Muschelkalk limestone and is influenced by the dissolution of sulphate minerals (mainly gypsum and anhydrite) contained in the Triassic sediments.

Gypsum and anhydrite are quickly dissolved and therefore, the Ca-SO$_4$ fingerprint is easily acquired by shallow or deep groundwaters upon interaction with these rocks. This lithotype is also found in the Jura range and the Alps due to the occurrence of Triassic rocks, which are often found in thrust faults and are locally present at shallow depth.

circulate in crystalline rocks, their sulphate concentration is due to the dissolution of sulphide minerals or anhydrite veins and their sodium comes mainly from reactions with feldspars. Four Na-SO$_4$ waters were analysed in the Muschelkalk, Buntsandstein and Permian-Carboniferous formations with higher mineralization reaching 15 g/L, strongly influenced by the dissolution of Triassic evaporite.

Figure 2.8: Piper diagram of deep fluids in Northern Switzerland (Sonney and Vuataz 2010b).
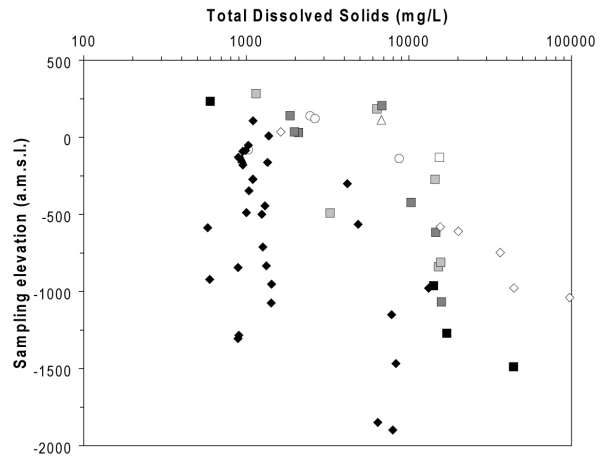
Figure 2.9: Sampling elevation vs. Total Dissolved Solids (see legend of symbols in Fig. 2.7, from Sonney and Vuataz 2010b).

Sampled Na-HCO$_3$ waters were often met in the selected boreholes and have a TDS lower than 1.4 g/L except for the mineralized waters of the Rheinfelden well (TDS = 4.2 g/L). Measured temperatures for this type are in the range 20-66°C, and this water mainly circulates in crystalline rocks. Their mineralization is relatively weak compared to other water types which are up to 1 g/L (Fig. 2.9). The sodium concentration of Na-HCO$_3$ waters is related to reactions with feldspars in crystalline rocks. In the Tertiary deposits of the Molasse Basin, Na-HCO$_3$ waters were pumped in the Lower Marine Molasse with temperature and TDS close to 29°C and 1 g/L respectively (Berlingen and Zürich). Two other Na-HCO$_3$ waters were respectively sampled in the Jurassic (20°C, 0.9 g/L) and Triassic (22°C, 0.6 g/L) formations of the tabular Jura at Lottstetten and Siblingen.

Five selected waters in the basement at Kaisten, Leuggern and Weiach have a Na-SO$_4$ type water and a TDS in the range 1-1.4 g/L except for one mineralized water (TDS = 4.9 g/L). These waters

Thermal Na-Cl waters have generally a high mineralization (TDS > 1 g/L) with concentrations sometimes exceeding 10 g/L, as in Weiach (97 g/L) or Reinach (44 g/L). Measured temperatures at depth for 29 sampled Na-Cl waters from 10 sites are in the range 16-112°C for any geological formations and any depth. The origin of this fingerprint is twofold. It could be due to the mixing of old, deep, strongly mineralized seawater and fresh water at different depths as observed in the crystalline basement and the Tertiary deposits (Chloride/Bromide molar ratio lower than the ocean line in Fig. 2.10). Stober and Bucher (1999) studied deep groundwaters in the crystalline basement of the Black Forest region which is directly located in the north of the tabular Jura. They concluded that saline thermal water used in spas has its origin in crystalline reservoirs at 3-4 kilometres depth. Moreover, the saline thermal water has developed their composition by mixing of surface freshwater with saltwater (of ultimately marine origin), and by water-rock reactions with an increasing mineral dissolution due to the

presence of CO_2. Concerning thermal waters in the sedimentary cover below the Tertiary rocks, dissolution of halite deposits, locally present in the Triassic formations, generates high Na-Cl contents in water with Chloride/Bromide molar ratio up to the ocean line (Fig. 2.10).
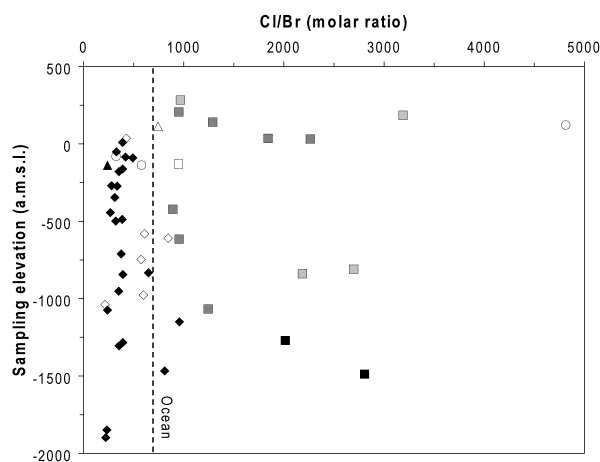
Figure 2.10: Sampling elevation vs. Chloride/Bromide molar ratio (see legend of symbols in Fig. 2.7, from Sonney and Vuataz 2010b).

Water geothermometers (Sonney and Vuataz 2010b). A series of geothermometers based on a temperature-dependent fluid-mineral equilibrium and an assemblage of minerals has been applied to deep groundwaters contained in sub-horizontal formations of Northern Switzerland. Equations of geothermometers were represented on plots by curves and their variations with temperature could be compared to the measured temperature at depth for sampled waters. The approach based on the comparison on measured/calculated temperature is useful to evaluate the applicability of geothermometers for low temperature. To clarify the discussion about the applicability of the geothermometers, this part highlights individually each specific geothermometer.

The silica phases present in geothermal fluids are quartz, chalcedony and amorphous silica (D'Amore and Arnórsson, 2000). The total dissolved silica in selected waters and measured temperature at depth were plotted and curves representing equations of geothermometers were added (Fig. 2.11). The dispersion of points indicates that geothermal fluids

are often strongly affected by mixing processes with either shallow groundwaters containing low silica concentrations or trapped seawater. Therefore, the silica content of the discharged mixed water is usually below the reservoir concentration, and silica temperatures are therefore underestimated. Various petrographical properties of rocks met at depth are also at the origin of under-balanced dissolved silica concentrations analysed in geothermal fluids.
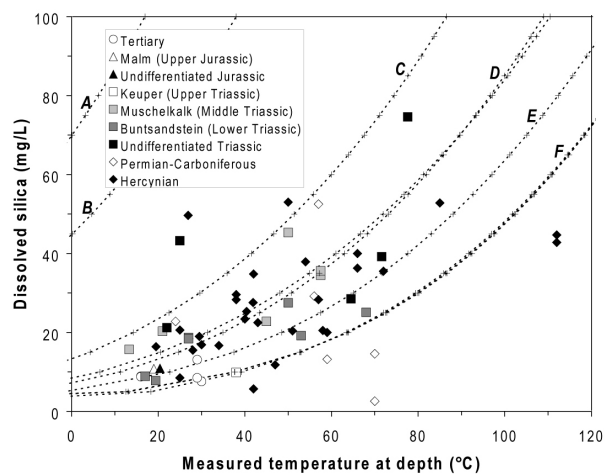
Figure 2.11: Dissolved silica vs. measured temperature at depth of deep fluids in Northern Switzerland. Curves correspond to selected silica geothermometers. A: amorphous silica; B: cristobalite ; C: cristobalite (A to C: Fournier 1977); D: chalcedony (Fournier 1977 and Arnórsson et al. 1983); E: quartz (Arnórsson et al. 1983); F: quartz (Fournier 1977, Truesdell 1976, Fournier and Potter 1982 and Verma and Santoyo 1997, from Sonney and Vuataz 2010b).

A general tendency to the increase of dissolved silica with temperature is observed, which follows the curves D of the two geothermometers using chalcedony (Fournier 1977 and Arnórsson et al. 1983). For reservoir temperatures lower than 120-160°C, conditions present in the studied region, chalcedony has a higher solubility than quartz and controls silica concentrations in solutions (Arnórsson 1975, Nicholson 1993). Fournier (1981 and 1977) specifies that below 100°C, geothermal fluids may remain supersaturated with respect to quartz for years, and therefore the quartz geothermometer works best in the temperature range 150-225°C.

The Na-K geothermometer was initially developed to locate the major upflow in high enthalpy

geothermal systems, because a general decrease in Na/K ratios of geothermal fluids with increasing temperatures was observed (D'Amore and Arnórsson 2000). This geothermometer is related to the variation of sodium and potassium in thermal waters due to ion exchange of these elements between co-existing alkali feldspars (Nicholson 1993). Na-K equations are adapted for reservoir temperatures in the range 180-350°C (Ellis 1979), but are limited at lower temperatures, notably less than 120°C (Nicholson 1993) as illustrated in Figure 2.12.
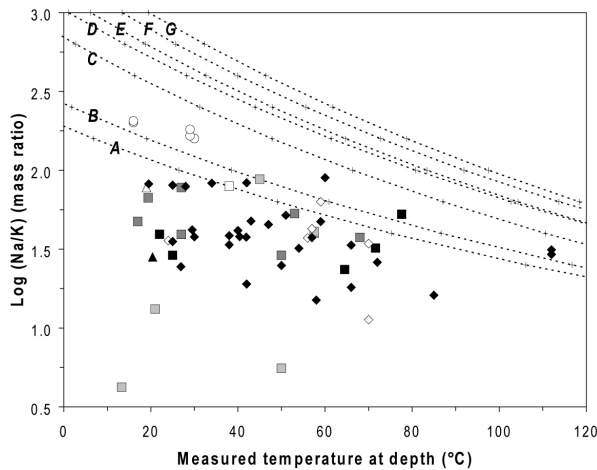
Figure 2.12: Log (Na/K) vs. measured temperature at depth of deep fluids in Northern Switzerland (see legend of symbols in Fig. 2.10). Curves correspond to Na-K geothermometers. A: Truesdell 1976; B: Arnórsson et al. 1983; C: Nieva and Nieva 1987; D: Fournier 1979; E: Verma and Santoyo 1997; F: Arnórsson et al. 1998; G: Giggenbach 1988 (Sonney and Vuataz 2010b).

Ion exchange between feldspars is limited for groundwaters of the sedimentary formations covering the basement because rocks are carbonates, evaporites or detrital deposits. The source of sodium and potassium comes from other minerals such as clays, seawater and precipitated minerals from seawater evaporation. Consequently, these two elements are not controlled by the feldspar ion-exchange reaction, and associated points on the plot in Figure 2.12 representing Na/K vs. measured temperature at depth are widely dispersed. Concerning selected data in the crystalline basement, values of Na/K ratios are better correlated with a general tendency to the decrease of Na/K ratios with temperature and thus depth.

The Na-K-Ca geothermometer, developed by Fournier and Truesdell (1973), does not give high and misleading results for cold and slightly thermal, non-equilibrated waters (D'Amore and Arnórsson 2000), compared to the Na/K geothermometer which generally gives very high calculated temperatures for low enthalpy systems when geothermal fluids have high calcium contents (Nicholson 1993). The Na-K-Ca geothermometer is also based on ion-exchange reactions between feldspars. As discussed above, the source of sodium, potassium and calcium in studied groundwaters comes from other geochemical processes, and they are not controlled by the feldspar ion-exchange reaction, and as observed for the Na/K geothermometer, estimated temperatures systematically over-estimate measured temperatures at depth (Fig. 2.13).
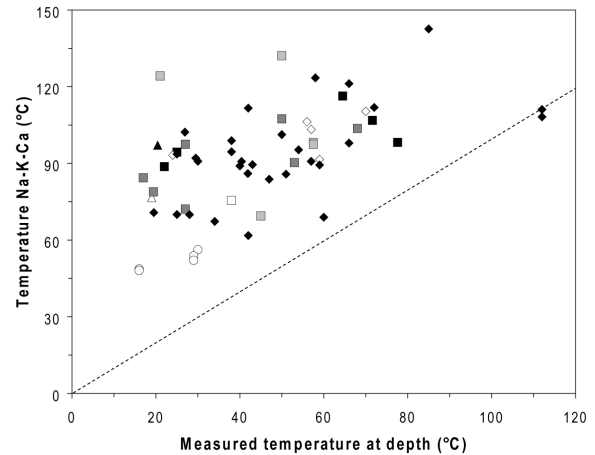
Figure 2.13: Computed temperature with Na-K-Ca geothermometer of Fournier and Truesdell (1973) vs. measured temperature at depth of deep fluids in Northern Switzerland (see legend of symbols in Fig. 2.10, from Sonney and Vuataz 2010b).

Falsely high temperatures were estimated by the Na-K-Ca geothermometer, as shown in Figure 2.13, when applied to low-temperature reservoirs (< 120°C) relatively rich in magnesium. The geothermometer using magnesium correction developed by Fournier and Potter (1979) was applied to the studied groundwaters. Due to specific conditions described in the formulas of Fournier and Potter (1979), only some fluids were subjected to the magnesium correction (Fig. 2.14). The reason is related to various magnesium concentrations in geothermal fluids, lower than 1 mg/L generally for waters in the crystalline basement and mostly

up to 10 mg/L for carbonated aquifers containing dolomite (especially for the Triassic formations).
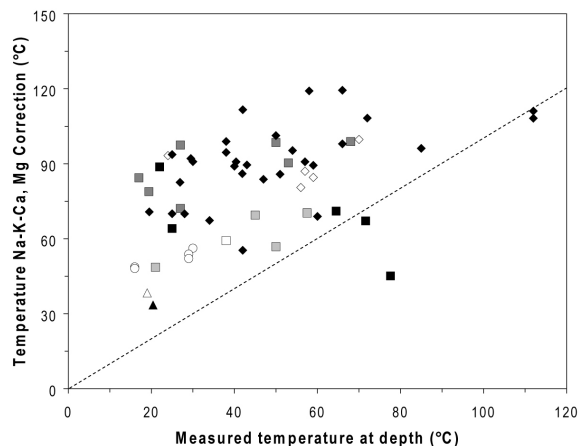
Figure 2.14: Computed temperature with Na-K-Ca geothermometer using magnesium correction of Fournier and Potter (1979) vs. measured temperature at depth of deep fluids in Northern Switzerland (see legend of symbols in Fig. 2.10, from Sonney and Vuataz 2010b).
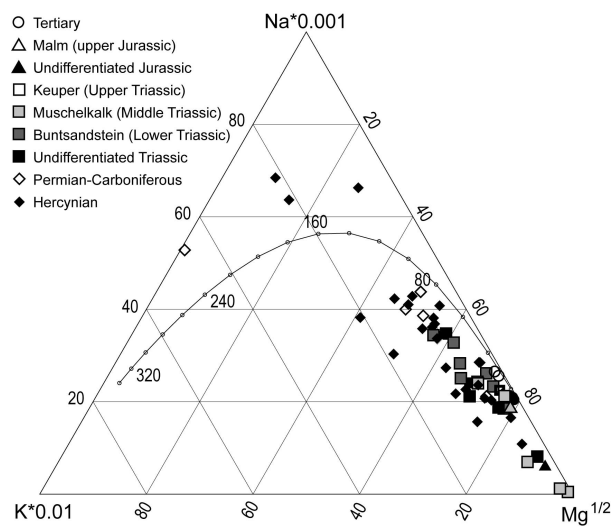
Figure 2.15: Giggenbach diagram of deep fluids in Northern Switzerland. The line on the ternary plot represents the full equilibrated line determined by variations of the Na/K geothermometry equation of Giggenbach (1988) (Sonney and Vuataz 2010b).

Selected data of geothermal fluids in Northern Switzerland were plotted in the ternary diagram of Giggenbach (1988) to estimate reservoir temperature and to recognize groundwaters which have attained equilibrium with the host lithologies (Fig. 2.15). Corresponding groundwaters plot below the full equilibrium curve which determines variations of the Na/K geothermometry equation of Giggenbach (1988). Therefore, these groundwaters are not suitable for Na/K geothermometry as shown previously. Points representing groundwaters are shifted towards the magnesium vertex indicating that waters are partially equilibrated or mixed. Dilution and mixing coupled to water-rock interactions in studied heterogeneous geological formations are processes limiting the application of these types of ionic solute geothermometers.

Two K-Mg geothermometers of Giggenbach (1988) and Fournier (1991) were applied to studied geothermal fluids to test their applicability. Data plotted in Figure 2.16 illustrate a trend to the increase of the K/Mg ratios with measured temperature at depth, but separated from curves which over-estimate temperature. Initially, the K-Mg geothermometer was developed in the same way as the Na-K geothermometer. D'Amore and Arnórsson (2000) explain that progressive interaction between water and rock towards equilibrium changes Na/K ratios towards equilibrium with feldspars, and similarly, magnesium concentrations decrease because magnesium is incorporated into precipitating minerals such as smectite and chlorite. These processes cause K/Mg ratios to increase strongly. The K-Mg geothermometer was first applied to waters from a low-enthalpy reservoir which had not attained equilibrium with alkali feldspars (Nicholson 1993), as for the studied geothermal fluids which are partially equilibrated or mixed waters (Fig 2.15). However, data plotted in Figure 2.16 indicate that the K-Mg geothermometer is not appropriate because it over-estimates temperature. By considering only geothermal fluids in formations of the sedimentary cover which consist of carbonate, evaporite and detrital deposits, the K-Mg geothermometers cannot be applied. Indeed, these formations are poor in feldspars implying another origin for these elements such as dolomite dissolution, leaching of seawater brines, etc. Data plotted for sedimentary groundwaters are widely dispersed in Figure 2.16.
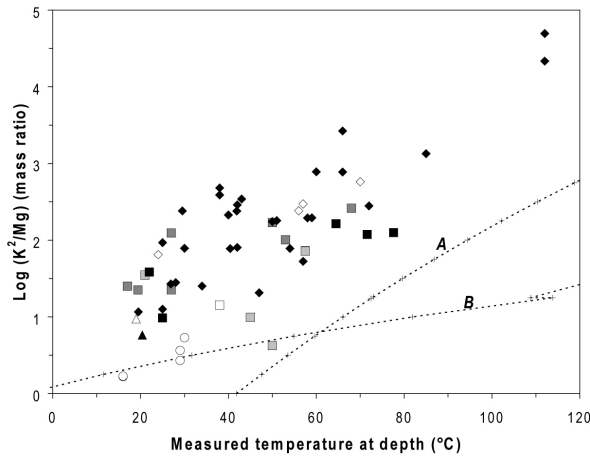
Figure 2.16: Log (K^2/Mg) vs. measured temperature at depth of deep fluids in Northern Switzerland (see legend of symbols in Fig. 2.15). Curves correspond to K-Mg geothermometers. A: Giggenbach 1988; B: Fournier 1991 (Sonney and Vuataz 2010b).
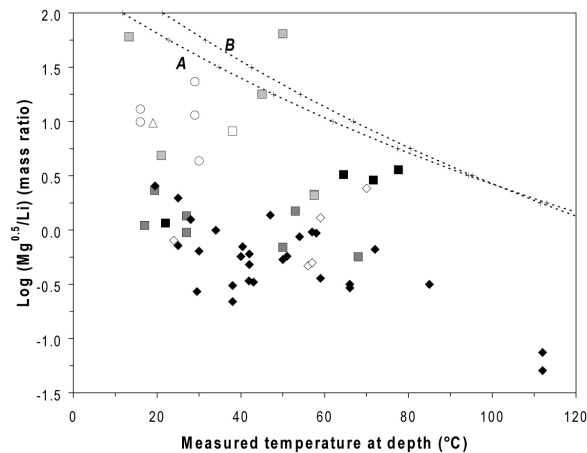
Figure 2.17: Log ($Mg^{0.5}$/Li) vs. measured temperature at depth of deep fluids in Northern Switzerland (see legend of symbols in Fig. 2.15). Curves correspond to Mg-Li geothermometers. A: Kharaka et al. 1985; B: Kharaka and Mariner 1989 (Sonney and Vuataz 2010b).

The Mg-Li geothermometer was developed in the same way as the K-Mg geothermometer, resting on exchange reactions with magnesium, for waters from a low-enthalpy reservoir which had not attained equilibrium with alkali feldspars (Nicholson

1993). Thereby, these processes cause Mg/Li ratios to decrease strongly, and conversely for K/Mg. The two equations of Kharaka et al. (1985) and Kharaka and Mariner (1989) were tested on the studied geothermal fluids but they strongly overestimate temperature, especially for waters in the crystalline basement (Fig. 2.17). Data plotted in Figure 12 show a general trend to the decrease of the Mg/Li ratios with measured temperature at depth. This tendency is better organized for crystalline thermal waters. Data plotted for sedimentary groundwaters are widely dispersed due to the occurrences of dilution and mixing processes and water-rock interactions which are more pronounced in sedimentary formations.
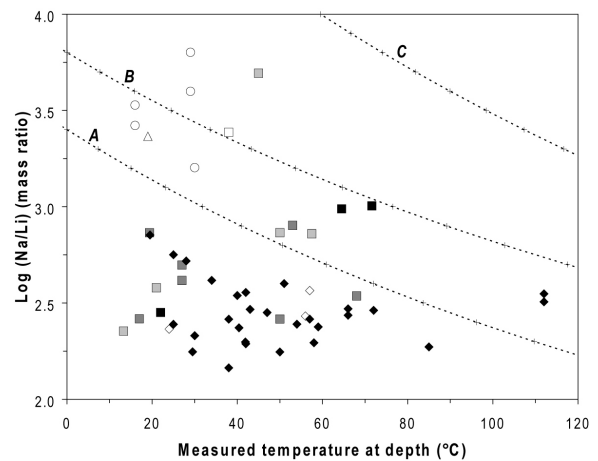
Figure 2.18: Log (Na/Li) vs. measured temperature at depth of deep fluids in Northern Switzerland (see legend of symbols in Fig. 2.15). Curves correspond to Na-Li geothermometers. A: Verma and Santoyo 1997, B: Fouillac and Michard 1981, C: Kharaka et al. 1982 (Sonney and Vuataz 2010b).

The Na-Li geothermometer was initially developed by Fouillac and Michard (1981) from a statistic study about groundwaters in granitic and volcanic domains. Two other Na-Li geothermometers are documented in Kharaka et al. (1982) and Verma and Santoyo (1997) and were tested on the studied waters. These two other equations are relatively distant because they results from empirical calibration, based on data in selected geothermal fields. Data plotted in Figure 2.18 highlight two distinct features. The first relates to geothermal fluids in sedimentary formations where data are widely dispersed. Some geothermal fluids have high Na/Li ratios because sodium is enriched by the dissolution

49

of halite and the leaching of trapped seawater. Frequently, waters in deep carbonate aquifers have low lithium contents (< 1 mg/L) what can also explain the strong ratios. The second concerns groundwaters in crystalline rocks which have generally lower Na/Li ratios due to higher lithium concentrations (> 1 mg/L). Moreover, Na/Li ratios remain relatively stable around 2.5 whatever the measured temperature at depth. The Na/Li geothermometer appears to be sensitive to the total dissolved solids of the water at depth, locally controlled by contributions of Na-Cl, and the rock type.

on the studied waters. According to D'Amore and Arńorsson (2000), they have not been employed much for geothermal exploration, and they seem to be affected by CO_2 partial pressure. These geothermometers are also related to ion-exchange reactions between feldspars and, therefore, are suitable for equilibrated waters. Concerning the studied groundwaters, they give strongly over-estimated results (Fig. 2.19). In this case, the mineral assemblages involved are different from those used for the calibration of these geothermometers, as it was already mentioned by Marini et al. (1986) for carbonate-evaporite geothermal reservoirs.

The Ca-Mg geothermometer of Marini et al. (1986) was also taken into account and is specific for carbonate-evaporite geothermal reservoirs. Thereby, it was interesting to test this geothermometer for geothermal fluids in carbonate-evaporite aquifers of the Mesozoic sedimentary cover. The presence of dolomite in the sedimentary cover allows having thermal waters with magnesium concentrations up to 1 mg/L, and thus, Ca/Mg ratios tend to decrease compared to crystalline waters poor in magnesium (<1 mg/L). Data plotted of selected waters in Figure 2.20 show differences due to their geological setting. Points for the sedimentary cover are clearly closer to the Ca-Mg geothermometer than points representing crystalline waters.

Figure 2.19: Log ($Na/Ca^{0.5}$) and log ($K/Ca^{0.5}$) vs. measured temperature at depth of deep fluids in Northern Switzerland (see legend of symbols in Fig. 2.15). Curves A correspond to Na-Ca and K-Ca geothermometers of Tonani (1980) (Sonney and Vuataz 2010b).

The two Na-Ca and K-Ca geothermometers developed by Tonani (1980) were selected and tested
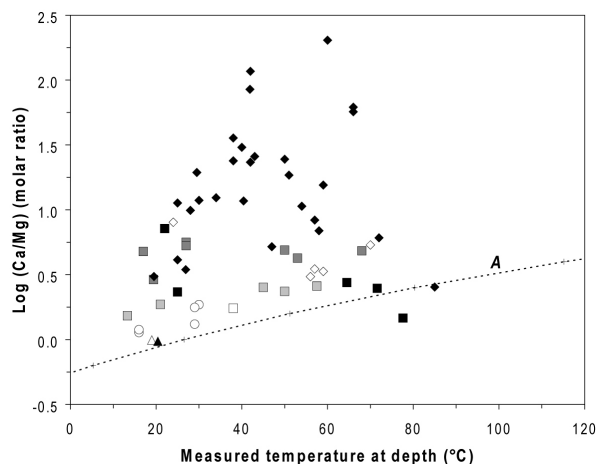
Figure 2.20: Log (Ca/Mg) vs. measured temperature at depth of deep fluids in Northern Switzerland (see legend of symbols in Fig. 2.15). Curve A corresponds to Ca-Mg geothermometer of Marini et al. (1986) (Sonney and Vuataz 2010b).

The sulphate oxygen isotope geothermometer is based upon the experimental work of Lloyd (1968),

who measured the fractionation of oxygen-16 and oxygen-18 between $SO_4{}^{2-}$ and water at 350°C, as well as the work of Mizutani and Rafter (1969) who measured the oxygen-16 and oxygen-18 between water and $HSO_4{}^-$ at 100 to 200°C (Fournier 1981). Only the geothermometer of Mizutani and Rafter was applied to studied geothermal fluids (Fig. 2.21).
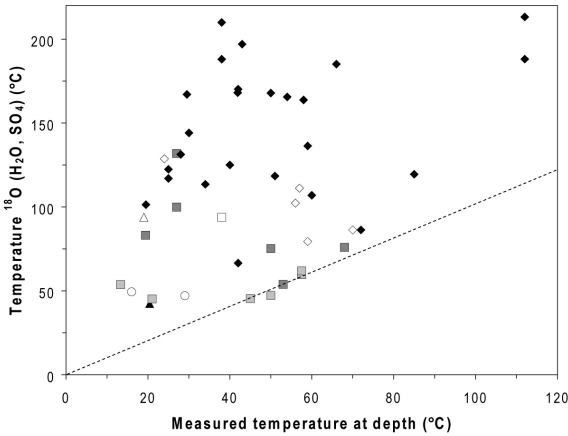
Figure 2.21: Computed temperature with oxygen isotope geothermometer of Mizutani and Rafter (1969) vs. measured temperature at depth of deep fluids in Northern Switzerland (see legend of symbols in Fig. 2.15, from Sonney and Vuataz 2010b).

In the case of geothermal fluids of northern Switzerland, various isotopic signatures of oxygen-18 in water and sulphate are observed due to water-rock interactions and chemical processes in different geological domains. As observed for the Paris Basin in France (Fouillac et al. 1990), the sulphate in studied groundwaters has different origins: dissolution of evaporite (gypsum and anhydrite), oxidation of sedimentary sulphides in rocks and leaching of trapped seawater. For each case, isotopic values of oxygen-18 in sulphate can be strongly different. Moreover, oxygen-18 values of marine evaporite sulphate minerals vary with their geologic age due to changes in the isotopic composition of oceanic sulphate with time (Pearson et al. 1991). Concerning oxygen-18 in water, a great difference in values can be caused by mixing processes with shallow groundwater or trapped seawater. All these processes in studied geothermal fluids induce that the oxygen isotope geothermometer is often not suitable. Data plotted in Figure 2.21 indicate that this

geothermometer has the tendency to over-estimate temperature, especially for crystalline waters.

Chemical and isotopic geothermometers were applied on chemical data and measured temperature at depth of geothermal fluids in boreholes from northern Switzerland, in the range of 12-112°C and considered as low-temperature geothermal systems. For each type of geothermometer, the method used was to plot measured temperature at depth with the corresponding geotemperature curves. Thereby, the accuracy and applicability of various geothermometers can be evaluated in these low-temperature geothermal systems.

For instance, there is some uncertainty in the interpretation of dissolved silica concentration in geothermal fluids because the solid phase controlling dissolved silica is often unknown (quartz or chalcedony in general), mixing processes with shallow groundwaters and trapped seawater occur and water-rock interactions are difficult to identify. Consequently, the application of silica geothermometers often gives underestimated values even if the chalcedony geothermometer was shown to be the most accurate of these.

Cationic geothermometers using ratios between lithium, sodium, potassium, magnesium and calcium were also tested and obtained results largely overestimate the measured temperature at depth. Application of these geothermometers is more suitable for high-enthalpy systems ($>$ 150°C), containing groundwaters reaching equilibrium with feldspars and clay minerals. This assumption is fundamental for the use of the majority of cationic geothermometers, what is not verified for studied geothermal fluids, subjected to various chemical processes. Finally, the oxygen isotope geothermometer based on the oxygen-18 of water and sulphate did not give useful results, especially for crystalline thermal waters. The isotopic signature of the oxygen-18 in particular in sulphate depends of a lot on different origins from various geological domains. In conclusion, chemical and isotopic geothermometers can be applied in low temperature geothermal systems ($<$ 100°C) with a much greater cautiousness than in high temperature systems ($>$ 150°C). Indeed, chemical reactions or isotopic fractionation may not reach equilibrium in low temperature reservoirs during the underground transit time of the deep fluids. Mixing of various types of fluids in heterogeneous rocks composition does not favour a complete equilibrium. However, detailed

rock and fluid geochemistry in a given geothermal exploration zone can alleviate the uncertainties in the use of geothermometers.

Geothermometers used in the case of the Alpine deep flow systems. In terms of geochemistry, different types of hydrothermal fluids from various geological settings also occur in the Alps range compared to aquifers from the Molasse Basin and the Tabular Jura as highlighted previously. Proximity between the Alps range and the Molasse Basin - Tabular Jura implies that the same physico-chemical processes occur leading to these different types of hydrothermal fluids. In the absence of deep drilling within the Alpine deep flow systems with a few exceptions however, it is not possible to measure the temperature of the hydrother-

mal reservoir, and thus to test the applicability of the geothermometers. Given that all hydrothermal fluids in Switzerland have a similar hydrogeochemical behaviour, it can be assumed that the study of the geothermometers in the Molasse Basin - Tabular Jura region can be more or less implemented to the Alpine domain. Consequently, it is not feasible to use all geothermometers quoted previously to calculate the reservoir temperatures for the Apline deep flow systems. We therefore advocate the use of a limited number of geothermometers and represent those which should give plausible results. For the studied hydrothermal systems in this study, used geothermometers are mostly chalcedony, Na-K-Ca with Mg correction, K^2/Mg, and oxygen-18 isotopes. Equations referring to these geothermometers are illustrated in Table 2.4.

Table 2.4: Selection of geothermometers to calculate the reservoir temperature for Alpine deep flow systems. Other geothermometers and their use are also given in Arnórsson 2000. All concentrations are in mg/kg. $\delta^{18}O$ is expressed in ‰.

Reference	Equation
Fournier (1977)	Chalcedony: $T_{SiO2} = 1032/(4.69 - logSiO2) - 273.15$
Arnórsson et al. (1983)	Chalcedony: $T_{SiO2} = 1112/(4.91 - logSiO2) - 273.15$
	Mg correction to the Na-K-Ca geothermometer $T_{Mg-corrNa-K-Ca} = T_{Na-K-Ca} - \Delta T_{Mg}$
Fournier and Truesdell (1973)	With: $T_{Na-K-Ca} = 1647/log(Na/K) + b \left[log\left((\sqrt{Ca}/Na) + 2.06\right) + 2.47\right]$ -273.15 and $b = 1/3$ because $T_{Na-K-Ca} > 100$
Fournier and Potter (1979)	$\Delta T_{Mg} = 10.664 - (4.7415 \times logR) + \left(325.87 \times (logR)^2\right)$ $- \left(1.032.10^5 \times (logR)^2/T_{Na-K-Ca}\right) - \left(1.968.10^7 \times (logR)^2/T^2_{Na-K-Ca}\right)$ $+ \left(1.605.10^7 \times (logR)^3/T^2_{Na-K-Ca}\right)$ because R = 5 to 50 $R = (Mg/(Mg + 0.61Ca + 0.31K)) \times 100$
Fournier (1977)	$T_{K^2/Mg} = 1000/\left(3.66 - 0.542 \times log(K/\sqrt{Mg})\right) + 0.0575 \times log(K/\sqrt{Mg})^2$ $-0.00275 \times log(K/\sqrt{Mg})^3 - 273.15$
Giggenbach (1988)	$T_{K^2/Mg} = 4410/(log(K/\sqrt{Mg}) + 14.00) - 273.15$
Lloyd (1968)	$T_{\Delta^{18}O} = \sqrt{3'251'000/(1000 \times ln\alpha + 5.6)} - 273.15$ With: $\alpha = \left(1000 + \delta^{18}O(SO_4{}^{2-})\right)/\left(1000 + \delta^{18}O(H_2O)\right)$
Mizutani and Rafter (1969)	$T_{\Delta^{18}O} = \sqrt{2'880'000/(1000 \times ln\alpha + 4.1)} - 273.15$ With: $\alpha = \left(1000 + \delta^{18}O(SO_4{}^{2-})\right)/\left(1000 + \delta^{18}O(H_2O)\right)$

Saturation indices

The behaviour of saturation indices (SI) of major minerals was simulated using the PHREEQC code (Parkhurst and Appelo 1999), imposing an increase of temperature from the emergence temperature to a selected temperature widely upper than the supposed reservoir temperature given by the geothermometer method. This method requires to compute the evolution of SIs from the warmest water or the thermal end-member. For simulation, it was formulated that the deep hydrothermal reservoir is in equilibrium with respect to some of the host minerals.

An example of a SIs simulation was carried out for the hydrothermal system of Combioula (Wallis, Switzerland) aiming to estimate the reservoir temperature (Ladner 2005, Suski et al. 2008). Recent sampling by means of pumping tests and corresponding analyses of the water of borehole C2 yields an average pH of 6.8 and an average fluid electrical conductivity of 2990 μS/cm (Ladner 2005). The dominant ions are calcium and sulphate and the chemical type of the fluid is Ca>Mg-SO$_4$. The observed water chemistry of the Combioula thermal springs is thought to principally originate from dissolution within the local carbonate and evaporite series consisting predominantly of dolomitic limestone containing gypsum and anhydrite layers (Suski et al. 2008).

The calculation of SI of the sampled water in well C2 has shown that the water is (1) oversaturated for quartz, (2) close to saturation with respect to gypsum and (3) under-saturated for dolomite and calcite (Fig. 2.22). This in turn indicates that primarily hydrated forms of silica and, to a more limited extend, gypsum can be expected to precipitate along the borehole walls and inside the hydraulically active fractures (Suski et al. 2008). Concerning the reservoir temperature, the SI lines cross them for upper temperature compared to the discharged temperature, between 40 and 60°C. SI lines are close to the value equal to zero in this temperature range indicating that the fluid is in equilibrium with respect to these selected minerals. This is the assumption formulated for the chemical-mineral conditions in the assumed hydrothermal reservoir.
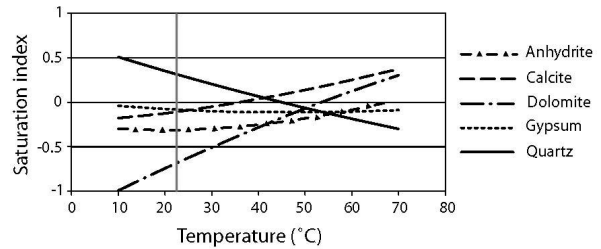
Figure 2.22: Calculations of the saturation index as a function of the temperature for water in borehole C2 (Combioula, Switzerland) with regard to anhydrite, calcite, dolomite, gypsum and quartz. The vertical line represents the water sample temperature inside the borehole (Suski et al. 2008).

2.2.11 Groundwater residence time

Tritium method

Tritium is a hydrogen isotope and the only one radioactive isotope forming the water molecule, of which the conventional symbol is ^{3}H. The tritium atoms are unstable and disintegrate in a half-life period of 12.43 years, forming stable atoms of helium-3 and a β^- radiation. The β^- radiation allows measuring the tritium quantity in a sample. A mass concentration is deduced from the measurement of the β^- emission. One tritium unit (TU) represents one tritium atom for 10^{18} hydrogen atoms, or equivalent to an activity of 0.119 Bq/L. Tritium is probably one of the important environmental isotopes for the study of groundwater. It is produced naturally by the interaction of cosmic rays with nitrogen and oxygen, mainly in the upper atmosphere, and takes part in the hydrological cycle. Before significant amounts of tritium were injected into the atmosphere through man's nuclear activities, precipitation had a natural background lower than 5 TU (Kaufman and Libby 1954, Rozanski et al. 1991). During the early sixties, when the effects of atmospheric testing of nuclear weapons peaked, tritium concentrations in the precipitation of over 2000 TU were measured in the world (Fig.

2.23) and in Switzerland (Fig. 2.24). In Switzerland, the present tritium concentration in precipitation range between 10 and 20 TU. Since most of the nuclear weapons tests were performed in the northern hemisphere, even today the tritium distribution is strongly asymmetric between the northern and southern hemisphere. Today atmospheric background levels in the northern hemisphere are between about 5 and 30 TU, and in the southern hemisphere between 2 -10 TU (IAEA/WMO 2006).

Concerning a thermal aquifer of which the thermal end-member is older than the first atmospheric weapon testing in 1954, tritium is a good indicator of the presence of mixing processes with "young water" infiltrated during the weapon tests or later. We will see that this process occurs for the hydrothermal systems of Lavey-les-Bains and Saint-Gervais-les-Bains in crystalline domain. For young thermal waters containing tritium from anthropogenic source such as Val d'Illiez (Triassic domain), several methods exist to estimate the groundwater residence time. Methods depend on the half-life period of the considered isotope and on the selected flow patterns, they are described after. Moreover, other isotopes such as argon, krypton or radon having various half-life period can also be used to evaluate the residence times of the groundwater.

The **piston-flow model** represents the simplest case study, and assumes that water infiltrates in a well defined area and flows like in a pipe towards the spring without mixing process. The tritium activity in the infiltrated area is thus modified only by radioactive decay:

$$C_{out}(t) = C_{in}(t - t_m)e^{-\lambda t_m} \qquad (2.7)$$

This model implies the same velocity and flow path for each water molecule, that seems to be limited to very special cases for homogeneous media (Etcheverry 2002).

The **exponential model** is based on the mixing processes in an exponential way between water having different residence times. The infiltrated area is greater than assumed for the piston-flow model and younger waters are more weighted than older waters in the calculation. The **linear model** is used for aquifers where linear mixing processes occur towards the spring, and each water has the same weight in the calculation.

In the case study of Val d'Illiez, the piston-flow model was selected to calculate the average residence time for the most mineralized thermal water of which mixing processes with cold and recent water are lower than 10% (see chapter 14).
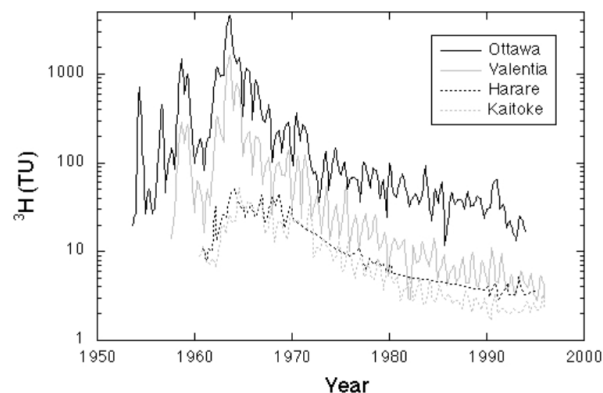
Figure 2.23: Tritium concentration in precipitation since 1950 at four IAEA stations (IAEA/WMO 2006): Ottawa, Canada (northern hemisphere, continental); Valentia, Ireland (northern hemisphere, marine); Harare, Zimbabwe (southern hemisphere, continental); Kaitoke, New Zealand (southern hemisphere, marine).
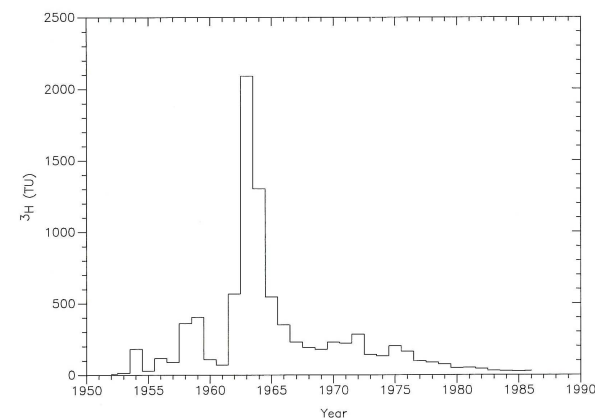
Figure 2.24: Measured tritium activity in precipitation of Switzerland (Pearson et al. 1991).

Carbon-14 method

Due to the inability to investigate deeply the carbon-14, the carbon-14 method was only employed for thermal water at Lavey-les-Bains with the aim to estimate the mean residence time. Thermal water from P600 and P201 wells were sampled in the framework of the study conducted by Sonney (2007). Results are discussed in chapter 5, but one of the sample (P600) was accidentally polluted during sampling and thus the measured value cannot be taken into consideration.

The carbon-14 has a half-life period of 5730 years. Its dating domain theoretically extends between 1000 and 50'000 years, but practically, it can be reduced until 25'000 years due to different processes which decrease the values of carbon-14 in groundwater independently from the decay. These processes can be dissolution, precipitation, adsorption, desorption, decomposition of organic compound, etc. Therefore, the residence time can be often over-estimated. The isotopic composition of dissolved carbonate in groundwater is determined by the sources of carbonate and by water-rock interactions (Pearson et al. 1991). It is rarely possible to describe carbonate chemistry so completely during the flow path, that an unambiguous calculation of carbon isotopic composition can be made. The source of dissolved carbonate in a groundwater

can be deciphered by the carbon-13 content. The carbon-13 measurement provides a basis for adjusting the initial carbon-14 content of a water for the effects of water-rock reactions.

The measurement unit of the carbon-14 is pmc (percent modern carbon). A value of 100 pmc corresponds to 13.56 disintegrations per minute per gram of carbon (0.226 Bq ^{14}C/gC) and represents the natural carbon activity before atmospheric weapon testing during the fifties. In the late sixties, this activity slightly increased and is today around 110-120 pmc (Muralt, 1999).

The method used is based on the carbon-13 correction from the following relation (Ingerson and Pearson 1964):

$$Ao \approx (\delta^{13}C_{measured}/\delta^{13}C_{gas}) \times 100 \qquad (2.8)$$

with $\delta^{13}C_{gas}$ in the range of -20 and -25 ‰.

The calculation of the average residence time is given by this equation (Geyh 2000):

$$At = Ao \times e^{-\lambda t_m} \qquad (2.9)$$
$$t_m = \ln(Ao/At) \times (t_{1/2}/\ln 2) \qquad (2.10)$$

with At being the measured 14-carbon in pmc, and with $1/\lambda = t_{1/2}/\ln 2$.

2.3 Numerical modelling of groundwater flow, heat and mass transport

2.3.1 Introduction

Long-term data of geothermal fields under production are a precious source of information for numerical modelling and a better understanding of the heat, mass and chemical transfer processes in geothermal reservoirs as well as for estimating the resource. With the development of computer simulation tools since the 1990's, numerous studies including numerical models applied to geothermal systems have proliferated. Applications generated by diverse functionalities of these models are varied: two or three-dimensional imaging of a geothermal system using stochastic methods (Teng and Koike 2007), fluid production and re-injection scenarios (Kühn and Stöfen 2004, Porras et al. 2007),

water-rock interactions (Dobson et al. 2004, Gevrek 2000), hydraulic connection with a deeper geothermal reservoir (Flores-Márquez et al. 2006), variation of local effective thermal stress (McDermott et al. 2006), and finally other applications concerning Enhanced Geothermal Systems (André et al. 2006, Kohl et al. 1995, Kolditz and Clauser 1998, Pruess 2006).

Alpine deep flow systems were not subject to numerical modelling even if the majority of them have been thoroughly studied. The first approaches of modelling related to the tunnels because it was observed a cooling of the massifs due to infiltrations

from the summits. Maréchal et al. (1999) studied thermal and hydraulic characteristics in the Mont Blanc Massif via observation on springs in the tunnel and long-term simulations. In this study, results indicated that this massif had not reached thermal equilibrium, and the continuous cooling of Alpine massifs occurs due to infiltration of waters from the surface since 12'000 years (end of the Quaternary glaciations).

Uprising thermal waters are partially exploited in the Alpine range. Emergence temperatures of thermal water, which correspond either to springs or boreholes, vary between 15 and 65°C for the warmest thermal water in the Swiss Alps (Lavey-les-Bains) with discharges lower than 35 L/s (Sonney and Vuataz 2008). Over-exploitation of thermal water usually generates important decreases of temperature and mineralization due to mixing processes with shallower cold water inflowing, and

creates problems for a sustainable long-term exploitation of the geothermal resource. In the studied hydrothermal systems (Lavey-les-Bains, Saint-Gervais-les-Bains and Val d'Illiez), spas have encountered this inconvenient from the exploitation of their geothermal resource with pumping rates. A loss of a few degrees of temperature questions about the exploitation rate and it was considered important to quantify cold groundwater inflows and visualize the long-term evolution of temperature with numerical methods.

Numerical simulation using the groundwater finite-element simulator FEFLOW$^©$ (Diersch 1996) handles the groundwater flow combined with heat transport for the two-dimensional models, and the groundwater flow combined with species and heat transport for the local three-dimensional models. Desired aims were to represent the hydrogeological deep flow system and to manage the long-term exploitation of the geothermal resource.

2.3.2 Solved equations

Groundwater flow

Fundamental equations concerning hydrodynamic aspects are described in several books and publications such as Bear (1972), Castany (1963), De Marsily (1986) and Zienkiewicz (1979). Table 2.5 lists the quantities and their abbreviations used in the text. Fluids move in response to forces, the most important of which are pressure and gravity. Capillary pressure may also be important. The fundamental law relating fluid flow to the forces causing the flow was established by Henri Darcy (1856), based on a series of experiments he did to observe water flowing through a sand pack (Pruess 2002).

In a column of section A, when water infiltrates through a length L of sand (Fig. 2.25), Darcy observed that there exists a proportionality between the flow rate Q crossing the sand and the value $\Delta H/L$ which is called hydraulic gradient i. The filtration coefficient K represents the proportionality factor between i and the flow rate, so that:

$$Q = KA\Delta H/L \qquad (2.11)$$
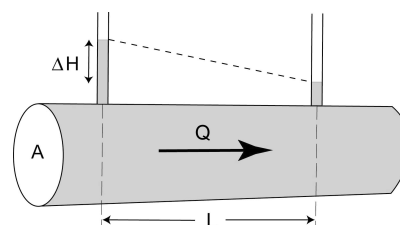
Figure 2.25: Darcy experiment.

If the Darcy law is divided by the area, the Darcy flux q is obtained:

$$q = K\Delta H/L \qquad (2.12)$$

with:

$$K = \frac{k\rho g}{\mu}$$

In three dimensions, the Darcy flux vector is:

$$\mathbf{q} = -\mathbf{K}\nabla H \qquad (2.13)$$

with:

$$H = \frac{p}{\rho g} + z$$

The conservation of mass is expressed by the continuity equation:

$$\nabla \cdot \mathbf{q} = -S_s \frac{\partial H}{\partial t} \qquad (2.14)$$

The Darcy law associated to the continuity equation allow defining the general equation of movement in a saturated environment:

$$\nabla \cdot (\mathbf{K}\nabla H) = S_s \frac{\partial H}{\partial t} \qquad (2.15)$$

Heat transport

Rocks contain various amounts of radiogenic isotopes of which the natural radioactive decay produces heat (Pruess 2002). In typical continental crust, temperatures increase roughly of 3°C for each 100 metres depth. The geothermal gradient is thus the ratio of temperature ΔT which increases with a vertical depth range Δz. When this average gradient prevails, we need to go down at about 6 kilometres depth to reach a temperature of 200°C. Geothermal gradients can be enhanced locally or regionally due to special geologic conditions, for example, where the earth's crust is unusually thin, or where hot molten rock has risen to shallower depths, forming igneous dikes or magma chambers (Pruess 2002).

In regions where Alpine deep flow systems occur, the average or moderately enhanced geothermal gradient can be sufficient to generate practically useful geothermal manifestations. Tectonic events had been generated fractures, faults, thrust faults and folds allowing fluid to be circulated at great depth.

Fundamental equations defining heat fluxes are detailed in this paragraph. Heat transfer is defined by the Fourier law, equivalent to the Darcy law in three dimensions:

$$\mathbf{f}_{dis} = -\Lambda \nabla T \qquad (2.16)$$

As for groundwater flow, the continuity equation is:

$$\nabla \cdot \mathbf{f} = -c\frac{\partial T}{\partial t} \qquad (2.17)$$

with:

$$c = \phi c_f + (1-\phi)c_s$$

Repartition of calculated hydraulic heads depends on boundary conditions assigned in the model and hydraulic conductivity imposed to the geological formations. In this study, we proceeded to the resolution of the problem in a direct way: boundary conditions are known and hydraulic heads are calibrated fixing the hydraulic conductivity field with several stages.

Table 2.5: List of quantities and their abbreviations used in the text. "-" means no unit.

Symbol	Quantity	Unit
A	area	m^2
C	concentration	mol/m^3
c_f, c_s	fluid and solid thermal capacity	$J/m^3/K$
D	dispersion tensor	m^2/s
f	heat flux vector	$J/m^2/s$
g	gravitation	m/s^{-2}
H	hydraulic head	m
$\Delta H/L$	hydraulic gradient	-
K	hydraulic conductivity	m/s
k	intrinsic permeability	m^2
m	diffusion flux vector	$Kg/m^2/s$
p	pressure	N/m^2
Q	flow rate	m^3/s
q	Darcy flux vector	m/s
S_s	Specific storage coefficient	m^{-1}
T	temperature	K
t	time	s
z	elevation	m
Λ	thermal dispersion tensor	J/m/s/K
μ	viscosity	Kg/m/s
ϕ	porosity	-
ρ	density	kg/m^3

Advection is the process of heat transfer by water moving. When the water moving is only due to the difference in density of fluids, it corresponds to the free advection, whereas the forced advection consists of water moving caused by the hydraulic gradient. Advection flux is described by:

$$\mathbf{f}_{adv} = c_f \mathbf{q} T \qquad (2.18)$$

When conduction and advection are implied in the heat transfer, the continuity equation applied to the total heat flux results in:

$$\underbrace{\nabla \cdot (\Lambda \nabla T)}_{conduction} - \underbrace{c_f \mathbf{q} \nabla T}_{advection} = \underbrace{c \frac{\partial T}{\partial t}}_{storage} \qquad (2.19)$$

For Alpine geothermal systems, heat transfers by free advection are negligible in comparison with transfers by conduction and forced advection.

Species transport

The general transport equation for dissolved species is derived from the combination of the Darcy velocity and the mass conservation. As for the heat transfer, the diffusive and dispersive solute flux in three dimensions is given in analogy to the Fick's first law:

$$\mathbf{m}_{dis} = -\mathbf{D}\nabla C \qquad (2.20)$$
$$\mathbf{m}_{adv} = \mathbf{q}C \qquad (2.21)$$
$$\mathbf{m} = \mathbf{q}C - \mathbf{D}\nabla C \qquad (2.22)$$

The continuity law for the transport of species becomes in this case:

$$\nabla \cdot \mathbf{m} = -\phi \frac{\partial C}{\partial t} \qquad (2.23)$$

Finally, the general transport equation is:

$$\nabla \cdot (\mathbf{D}\nabla C) - \mathbf{q}\nabla C = \phi \frac{\partial C}{\partial t} \qquad (2.24)$$

2.3.3 Construction of a numerical model

Introduction

Mostly, a two or three-dimensional numerical model is created aiming to represent a simplified version of groundwater flow, heat and mass transport in reality. Appropriate sets of differential equations which are illustrated in the previous section, and submitted to specific conditions, are solved by the FEFLOW© software. Sometimes, difficult issues of simulation can be met if specific boundary conditions were not appropriate, and therefore, it is important to adequately define these boundaries conditioning the mathematical modelling.

The finite-element method (FEM) and the finite difference method (FDM) are both families of numeric representations. According to Zienkiewicz (1979), FEM method is defined as a *general process of discretization of continuous problems described by mathematical relations.* So, the FEM method is adapted to the resolution of differential equations and applies to stationary (or not), linear (or not) problems, and applies to cases with one or more independent variables. This discretization method allow solving differential equations of groundwater flow, heat and mass transport in a more flexible way than the FDM method (Le Fanic 2005). FEM also allow describing in a better manner the form of limits of the model. Therefore, FEM is more adapted to the high complicated geological geometry of Alpine hydrothermal systems.

The followed procedure for the construction of the numerical model is detailed in Figure 2.26 and was respected in this study. The first stage consists to define the structure and the geometry of the flow domain and the hydrodynamical characteristics. Then, the flow domain is discretized and boundary conditions are assigned according to geological, hydrogeological and geothermal data. Finally, obtained simulations results were compared with observation data documented in literature or measured in the field such as temperature, discharge rate, etc. If the model allows field observation to be reproduced, the model is calibrated and operational for prediction.

Discretization and boundary conditions

The construction of a numerical model requires to know the properties of geological horizons where the deep flow system occurs, and the hydrodynamical and chemical properties these horizons (aquifer/aquitard). From a two-dimensional cross section or a three-dimensional local conceptual model, different geological formations can be discretized to finite elements. In this study, geological formations and fractured zones were individualized to several sub-domains, and in each sub-domain a selected number of triangular meshes was assigned instead of quadrangular meshes. Fractured zones and the subsurface hydrothermal area were refined aiming to have more precision in calculations. An example of discretization of the Dax geothermal system in France is illustrated in Figure 2.27.
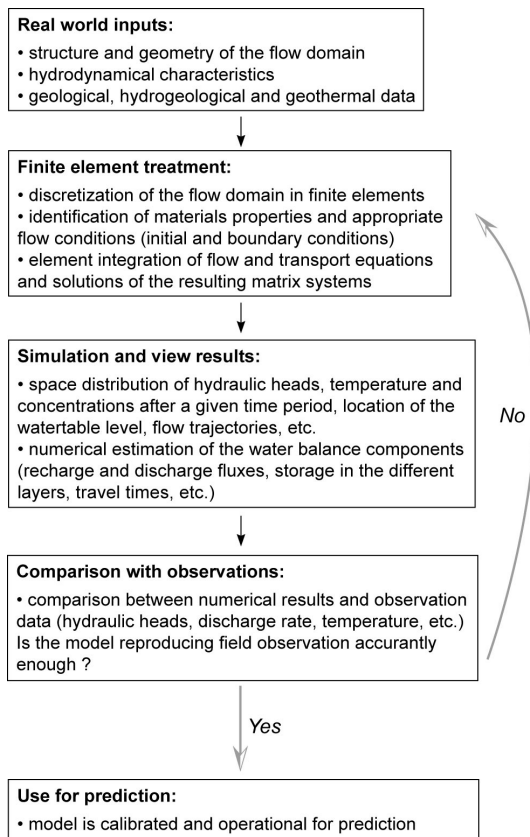
and mass conditions (initial boundary conditions) are imposed to the model. Firstly, flow boundaries are assigned to the model. In the case study of Alpine deep flow systems, imposed hydraulic heads correspond to the elevation of rivers crossed by the model and only contribute to water outflows. Water fluxes were imposed to summits of the domain for the two-dimensional model, laterally for the three-dimensional model, and correspond to precipitations removing from the surface runoff and the evapotranspiration. Precipitation values were extrapolated from data documented in the Swiss Meteorology and Climatology Federal Office on stations in the studied area including neighbouring regions.

Finally for flow boundaries, wells were added to transient models with the aim to represent their impact on temperature field. To add wells in the model, a local refining was made until to have a size mesh close to the diameter of wells. A rate was then assigned on each node (1/3 of total rate due to the mesh triangulation). For the two-dimensional models, the imposed values of rates were corrected from the evaluated width of the cone of influence of each well, because it is not appropriate to impose the real exploitation rates in a two-dimensional numerical model due to the radial flow components out of the cross section. On the contrary, for three-dimensional models, problems of radial flow components do not exist and thus total rates can be assigned.

Real world inputs:

• structure and geometry of the flow domain
• hydrodynamical characteristics
• geological, hydrogeological and geothermal data

Finite element treatment:

• discretization of the flow domain in finite elements
• identification of materials properties and appropriate flow conditions (initial and boundary conditions)
• element integration of flow and transport equations and solutions of the resulting matrix systems

Simulation and view results:

• space distribution of hydraulic heads, temperature and concentrations after a given time period, location of the watertable level, flow trajectories, etc.
• numerical estimation of the water balance components (recharge and discharge fluxes, storage in the different layers, travel times, etc.)

No

Comparison with observations:

• comparison between numerical results and observation data (hydraulic heads, discharge rate, temperature, etc.) Is the model reproducing field observation accurantly enough ?

Yes

Use for prediction:

• model is calibrated and operational for prediction

Figure 2.26: Overall procedure to follow in order to make a model operational (Perrochet 2006, modified).

After the discretization of the geological horizons, material properties and appropriate flow, heat

Mesh size: 120 m

Refinement: 40 m

Geothermal zone

Refinement: 8 m

Figure 2.27: Refining zone of the three-dimensional model of the Dax geothermal system in France (Le Fanic 2005, modified).

The second important stage consists to assign flow material properties on each element or geological layer. According to data in literature and obtained results of pumping tests, appropriate hydraulic conductivities can be assigned. For the two-dimensional models, conductivity is imposed on X-Y directions with a selected anisotropy factor representing the local geological properties such as fracture planes, lineations, stratigraphy, etc., whereas for the three-dimensional models, values of conductivities have to be considered in the third Z direction.

Finally, other parameters of flow materials which are the expansion coefficient, the storativity and the storage compressibility were not modified for the simulation. It can be assumed that the proposed standard values in the used software are appropriate in our case studies and do not have a significant incidence on the simulated results.

These enumerated boundary conditions are sufficient if the type of simulation is only groundwater flow. But for the modelling of Alpine deep flow systems, the flow transport was combined with the heat or mass transport, and consequently, properties of heat and mass conditions have to be defined (Table 2.6). The parameters were defined from existing data such as the surface temperature (data coming from the Swiss Meteorology and Climatology Federal Office), the heat conductivity of solid (from Clark and Niblett 1956), the porosity, etc. Whereas others parameters preserved their initial standard values because it can be assumed that they did not have significant influences in simulated results. Concerning the sorption process in three-dimensional models, we also assume that interactions between species and rocks don't occur and therefore the standard coefficient value (zero by default) in the software was preserved.

Table 2.6: Type of transport data required by the model. The listed variable are as those of the used software.

Type of transport data		Assigned value source
Heat data		
Heat transport boundaries	Temperature (°C)	Extrapolated data
	Heat flux $(J/m^2/d)$	Bibliography
Heat transport materials	Porosity	"
	Volum. heat capacity of fluid $(J/m^3/K)$	Standard value of Feflow
	Volum. heat capacity of solid $(J/m^3/K)$	"
	Heat conductivity of fluid $(J/m/s/K)$	"
	Heat conductivity of solid $(J/m/s/K)$	"
	Longitudinal dispersivity (m)	Depends on the size mesh
	Transverse dispersivity (m)	"
Mass data		
Mass transport boundaries	Mass concentration(mg/L)	Geochemical study
Mass transport materials	Porosity	Bibliography
	Molecular diffusion (m^2/s)	Standard value of Feflow
	Longitudinal dispersivity (m)	Depends on the size mesh
	Transverse dispersivity (m)	"
	Reaction decay (/s)	

Simulation results and calibration

The simulation can be started once boundary conditions and the type of problem were defined (steady or transient state, coupled flow and heat/mass transport, etc.). Obtained results are directly given under the form of numbers and thus options of the simulator run menu allow computed results to be visualized. Concerning the head, heat, mass and pressure, the range of values in space is given with isolines and fringes in the view option. The particle tracking is also present in this option and was used to estimate the flow patterns and the residence time. For the residence time, a value of porosity has to be selected.

The water balance option was employed to control the fluid, heat and mass balancing on the totality of the model or locally. Outfluxes in the model were quantified on imposed hydraulic heads

(rivers) while specifying local conditions of calculation (nodal, border, box, etc.). Moreover, the direction and value of a given Darcy flux was looked with the fluid flux analyser to control the flow direction through a selected section, primarily in the zone of uprising fluid. Finally, the representation of results via figures was carried out with an exportation of data (.dac) towards the FEFLOW© Explorer software.

Obtained simulations results were compared with observation data such as temperature, discharge rate, etc. If the model allows field observation to be reproduced and if the results are sufficiently acceptable to answer objectives, the model is calibrated and operational for prediction. The model calibration remains the major stage of work, which can be difficult in some cases (multilayered, heterogeneous systems, transient flow, etc.).

Part III

Lavey-les-Bains

3

General description of the study area

3.1 Geographical setting of Lavey-les-Bains

THE hydrothermal area of Lavey-les-Bains, canton of Vaud, is located in the Rhone Valley on the right bank of the Rhone River. More precisely, this site is in the Western External Alps of Switzerland, 15 kilometres upstream from Lake Geneva and 2 kilometres from the village of Saint-Maurice (canton of Wallis, Fig. 3.1). Geomorphologically, the studied zone is located on the Rhone alluvial deposits forming a large plain, compressed between the front of a fan delta, on one side of the valley, and the rock-falls from the mountain slope of the Grande Dent de Morcles on the other.

The old well "P201" (201 m depth) and the new well "P600" (595 m long, inclined borehole) are used by the spa for heating buildings and swimming pools. The uprising thermal waters come from the fractured gneiss of the Aiguilles Rouges Massif and are continuously pumped. On this site, one old exploitation well named "Ancien Puits", and several exploratory boreholes and piezometers are present with depths varying between 10 and 250 metres (Fig. 3.2). A detour tunnel going towards the Lavey hydro power plant drains part of the Rhone River. Several cold springs circulating in the slope discharge into this tunnel.
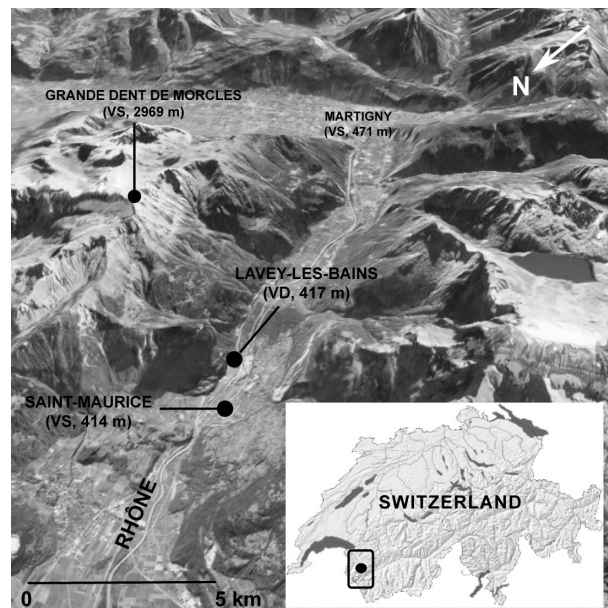
Figure 3.1: Geographical location of Lavey-les-Bains in Switzerland.

3.2   History of Lavey-les-Bains thermal baths

The thermal water of Lavey-les-Bains was discovered in 1831 emerging in the on the right bank of the Rhone bed. J de Charpentier, director of the salt mines of Bex (Wallis), was charged by the Swiss Confederation to carry out the first works with the aim to collect the uprising thermal water from a well currently named "Ancien Puits" (old well). In 1832, patients coming to be treated by the waters curing properties had makeshift baths to swim in. Later, the continued exploitation of the thermal spring via the deep boreholes allowed the development of the well-known Lavey-les-Bains spa, located 300 metres downstream from the area where the thermal water is discharging (Zahner et al. 1974).

Shortly after the discovery, the temperature and the flow rate of the spring started to drop. Successive deepening of the old well, carried out by J de Charpentier (1833) and then by his successors F Collomb (1856-1857), J François (1861), E Renevier, FA Forel and A Heim (1883-1884), had not yielded expected results. The physico-chemical character of the water varied with the exploitation because the uprising thermal water was mixed with a shallower groundwater circulating in the alluvial deposits. Consequently, it was necessary to decrease the cold water inflows while drilling more deeply (Zahner et al. 1974).

In 1943, final works on deepening the old well were carried out by Prof. E Gagnebin and the spring reached a better stability. Until 1973, its production rate, its temperature and its chemical properties were sufficient for the requirements of the spa (Zahner et al. 1974).

Since 1963, the interior and public health department of the canton of Vaud has again planned to develop the Lavey-les-Bains spa. Larger quantities of thermal water being necessary. Prof. A Bersier, H Badoux and A Falconnier were charged with investigating the geothermal potential, and to determine the possibility to undertake new deepening works. The conclusions were negative (Zahner et al. 1974). It was necessary to wait the beginning of the 1970's with Prof. K Sauer to implement a 201 metres deep borehole called P201, located roughly 50 metres upstream from the old well. Since 1972, this well has been pumping thermal water at 62°C flowing in the fractured gneiss of the Aiguilles Rouges Massif with a maximum production rate of 450 L/min (Bianchetti 1994, Vuataz 1982).

This resource promoted the development of the spa, property of the canton of Vaud (Jaffé et al. 1976). The P201 well also enabled the spa resort to be run solely on thermal water, thus attaining full thermal energy autonomy and guaranteeing the running of the swimming pools, building heating and warm water production without using fuels (Bianchetti 2002). Only an auxiliary oil-fired boiler was necessary for the greatest cold periods in winter.

After 1987, new prospection works via a series of deep boreholes were managed by the canton of Vaud and G. Bianchetti (Bianchetti 1990 and 1993a). Moreover, a regional hydrogeological study was undertaken by the Research Center Scientists Fundamental and Applied of Sion (in Wallis), within the framework of the geothermal prospecting program named GEOTHERMOVAL (CRSFA 1992a, Vuataz et al. 1993). In parallel, a detailed study about the deep flow systems in the Western External Alps was realized between 1989 and 1992, from a funding given by the National Funds of the Scientific Research (Bianchetti 1993a and 1994).

Although having a geothermal resource with a high temperature (62°C) and a high flow rate (maximum of 450 L/min), the heating of the buildings was sometimes ensured with a heat pump. The use of this heat pump generated an annual cost of around CHF 150'000 in the electricity consumption. For financial profitability reasons, the heat pump was replaced in 1996 by a large oil-fired boiler, with an annual payment about CHF 120'000. A deeper geothermal borehole was thus necessary to decrease these costs.

In 1992, a research project to study the energy optimization of the spa was funded by the Federal Office of Energy (SFOE). This project, carried out by the Industrial Energy Systems Laboratory (LENI) of the Federal Polytechnic School of Lausanne (EPFL), included the domains of energy and hydrogeology. It concluded that there is a possibility of guaranteeing energy autonomy by increasing the flow rate and the temperature of the thermal resource through the use of heat exchangers, without the use of heat pumps (Krummenacher and Bianchetti 1995).

The main condition leading to the success of this project consisted of collecting thermal water with a

flow rate around 800 L/min with a minimal temperature close to 63ºC, or a similar geothermal potential (for example 650 L/min at 70ºC). The implementation of a new deeper borehole seemed to be the obvious solution to increase the geothermal potential of the resource.

In July 1996, a request to obtain a geological risk assessment was given to the SFOE and it was accepted (Bianchetti and Hadorn 1996). In March 1997, the council of the canton of Vaud decided to fund the drilling of a new borehole called P600 (Bianchetti 2002). Since 1999, the Lavey-les-Bains spa was managed by Eurothermes and the exploitation of the P600 well started in March 2000. This geothermal project was an undeniable success due to its maximum production rate reaching 1300 L/min at 65ºC. Currently, the P600 well has the greatest geothermal potential of Switzerland.

A seismic event was identified in January 2006 in the area of Lavey-les-Bains, with a magnitude of 3.1 and a depth of around 3 kilometres. This earthquake did not induce significant variations of the physico-chemical parameters in thermal water.

The AGEPP project, Alpine Geothermal Power Production, started in 2006 and is managed by a group of experts including G Bianchetti and FD Vuataz. The goal of this project consists of producing electricity and geothermal heat while exploiting the geothermal reservoir at 2-3 kilometres depth at the bottom of the Aiguilles Rouges Massif. Indeed, the group of experts particularly studied the hydrothermal site of Lavey-les-Bains because it has geological, hydrogeological and geothermal properties more interesting compared to other sites in the Rhone Valley (Bianchetti et al. 2006).

The same group of experts supposes the existence of a deep aquifer pinched between the crystalline rocks of the Aiguilles Rouges and Infra-Aiguilles Rouges Massif. They assume that this aquifer could have hydrogeological characteristics economically interesting: good hydraulic conductivity, high fluid temperature (100 to 110ºC), good production rate (50 to 75 L/s) and low mineralization of water (< 2 g/L). After studying the possibilities to produce electricity and to distribute the heat, the geothermal project AGEPP project is currently looking for private and public investors to plan the installations and to realize the new deep borehole (Bianchetti et al. 2006).

3.3 Boreholes realized at Lavey-les-Bains

Nine vertical boreholes from 70 to 250 metres depth, and another 595 metres length borehole, met thermal waters below the Quaternary filling. Seven of them are not equipped because they were only put in place to explore the thermal aquifer. On the contrary, the P201 and P600 wells are continuously exploited and are equipped with a submersible pump. All the boreholes cross the Quaternary filling and penetrate more or less deeply into the fissured gneiss of the Aiguilles Rouges Massif. Their geographical coordinates are given in the location map of the wells and piezometers in the hydrothermal area (Fig. 3.2).

3.3.1 Production well P201

The P201 well was realized between July 1972 and January 1973, roughly 50 metres downstream from the old well (Fig. 3.2 and 3.3). At the beginning of drilling, a hole of 15 metres was dug and cemented with a casing of 14" diameter. After, drilling continued until 199.10 metres with a diameter of 5.5" in the fractured gneiss of the Aiguilles Rouges Massif (Zahner et al. 1974).

The daily controls during drilling, including the first measurements in temperature, gave expected results. Consequently, it was decided to widen the borehole (12 1/4") until 201 metres depth (Fig. 3.5). Since 1972 and before the implementation of the P600 well in 1997, the P201 well made possible the pumping of a thermal water at 62ºC with a maximum production rate of 450 L/min. This resource promoted the development of the thermal spa and allowed guarantying a full thermal energy autonomy without using heat pumps or fuels (Bianchetti 2002).

The geothermal potential of the used P201 well decreased since 1997 due to the exploitation of the deeper P600 well. In 2008, the annual average temperature of water in the P201 well is close to 57ºC, corresponding to a decrease of 5ºC over 10 years.
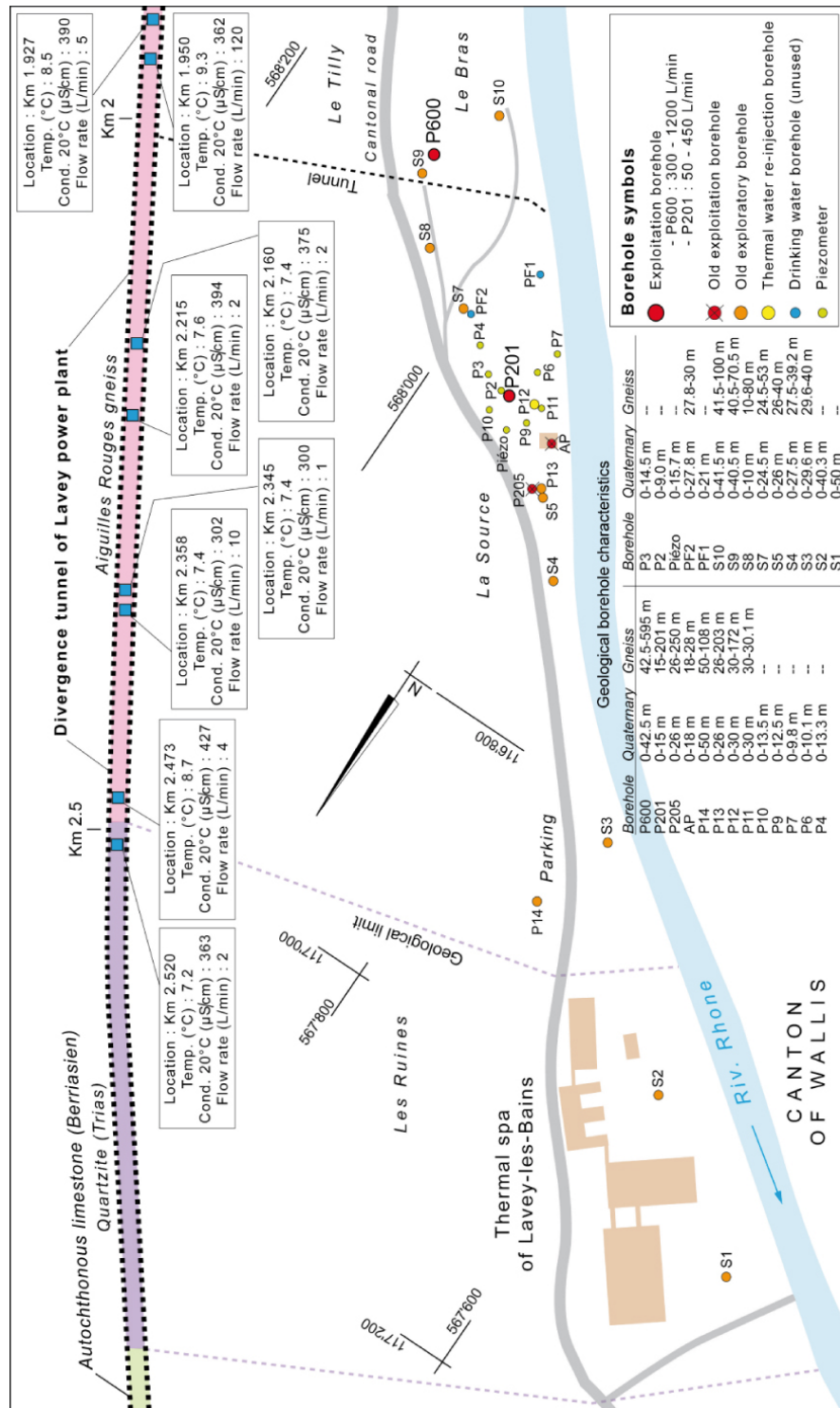
Figure 3.2: Location map and characteristics of the wells and piezometers in the spa area and of the springs in the divergence tunnel of Lavey hydro power plant. Location refers to the Swiss kilometric coordinates in projection, in standard CH1903.

Figure 3.3: View of the P201 well head (photos taken by the Alpgeo consulting office).

3.3.2 Production well P600

The P600 well was drilled between June and September 1997 and was supervised by the Alpgeo consulting office. This well is located 200 metres upstream from the P201 well on a gravel pit easily accessible (Fig. 3.2 and 3.4). Before the implementation of the borehole, four exploratory boreholes (S7 to S10) were drilled to explore thermal aquifer in the fissured gneiss (Bianchetti 2002).

At the beginning of drilling, a deviated hole of 50 metres depth below the surface with a dip of 8° was dug in the Quaternary filling till the top of the basement. Several full tubes of 16" and 13 3/8" diameter and a cement grout were successively set (Fig. 3.5). Then, the deep gneiss was perforated with a rotary drill until 105 metres depth. A first logging test (air-lift number 1) was realized, and after a full tube and a cement grout were installed (10 3/4"). Different phases of drilling, logging and pumping were successively carried out till 517 metres depth below the surface. The dip at the bottom of the well is about 48° and the total length of the well reached 595 metres.

The bottom of the well has an elevation of 85 metres below the sea level and the hole is open in the fissured gneiss between 254 and 595 metres allowing the thermal water to flow in. Different fractures produce thermal waters with various flow rates, temperatures and electrical conductivities. They were highlighted during the drilling (Fig. 3.5).

After drilling, several pumping tests with different flow rates were carried out between September and October 1997 with the aim to study the productivity of the well. The expected results were reached allowing the installation of the final equipment in the well in March 1998. Currently, the annual average temperature is about 65°C with a maximum production rate close to 1280 L/min.

Figure 3.4: View of the P600 well head (photos taken during the water sampling for this study).

69

3.4 Transport and exploitation of thermal waters

The Lavey-les-Bains spa exploits thermal water contained in the crystalline aquifer via two deep wells. The borehole P201 enables the exploitation of the thermal water of 57°C at about 450 L/min, whereas P600 is able to provide 1280 L/min water at 65°C. When the two boreholes pump at their maximum production rate, the volume of pumped water can reach four to five times the volume exploited before 1997.

The pumped thermal water is drained towards a large storage reservoir via three separate pipes. In this reservoir, the geothermal fluid circulates in heat exchangers used to heat the buildings and to produce warm waters, and the temperature decreases to 37°C. Then, the water is supplied to the swimming pools.

The spa exploits thermal waters with period alternations depending on the seasonal climatic conditions. In winter, during the coldest periods, moments of maximum production rate in the P600 well are more frequent (Fig. 3.6). On the contrary, moments of maximum production rate are less frequent in summer. The maximum production rates are about 1200 L/min and have time spans mostly ranging between 20 minutes and roughly 1 hour. During the warmest periods in summer, the P600 well mostly pumps the water with a rate of 300 L/min because water requirements are less important (no heating of buildings). Simultaneously, the P201 well exploits the water under a regular mode all year round with pumping rates ranging between 200-450 L/min.

The surplus of the pumped thermal water cannot be directly pumped into the Rhone River because of their high temperature. The temperature of Rhone River water should not increase more than 3°C and the rejected waters should not exceed 30°C (Ordinance on the protection of waters, 1998, Ch 7, Art 44). The excess of thermal water is temporarily stored in reservoirs but their volume capacity to control the water coming out is limited during the coldest periods due to the frequent moments of maximum production rates. For this reason, periods with maximum production rates cannot exceed 6-8 hours.
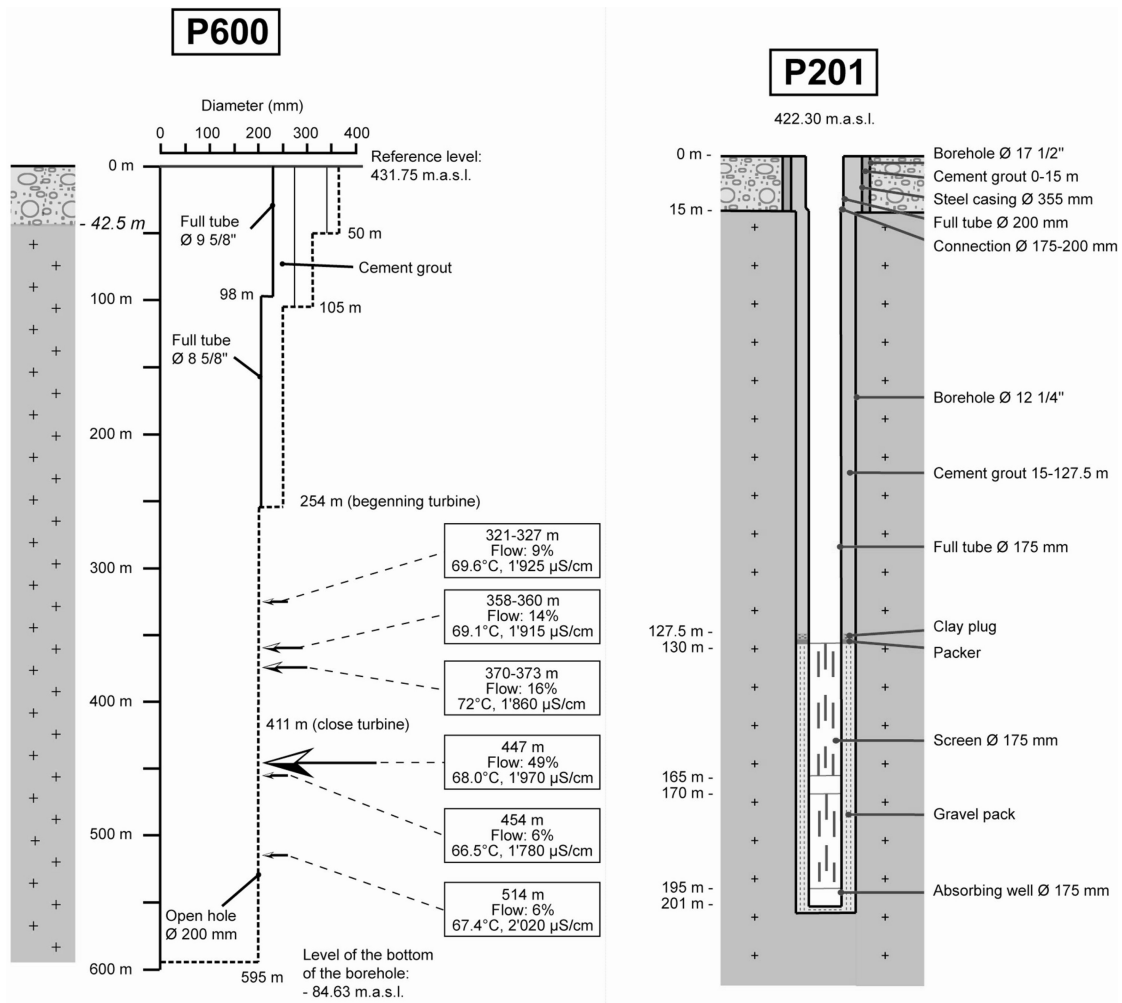
Figure 3.5: Geological logs of the P600 and P201 wells (modified from Bianchetti 2002 and Zahner et al. 1974).
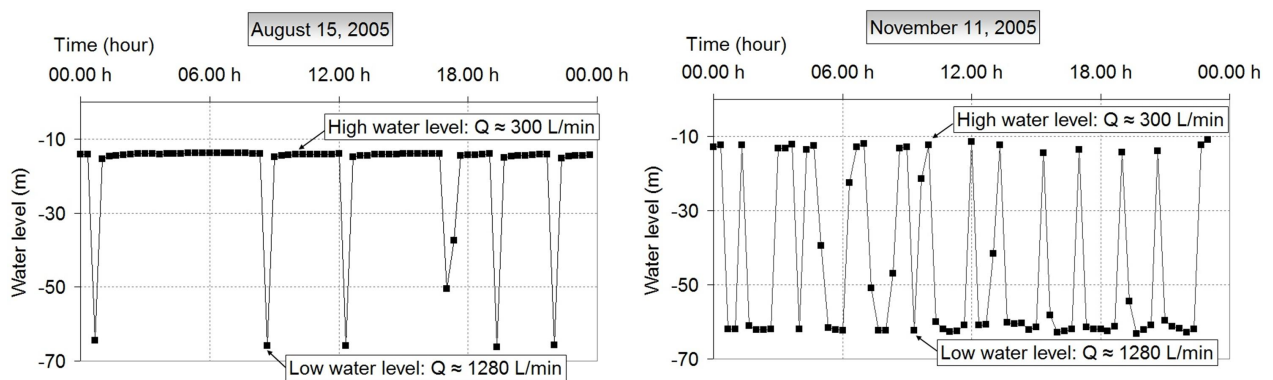
Figure 3.6: Production rates in the P600 well during a hot day in summer and another one colder in November (from Alpgeo data).

<div style="text-align: right; font-size: 3em; font-weight: bold; color: gray;">4</div>

Geological investigations at Lavey-les-Bains

4.1 Regional geological investigations

THE geological setting of the studied area is composed of two major tectonic units: the Hercynian crystalline basement and the Helvetic (Fig. 4.1).

The Hercynian crystalline basement forms to the Aiguilles Rouges, Arpille and Mont Blanc Massifs. The Aiguilles Rouges basement consists of various metamorphic rocks (old sedimentary and crystalline formations) and other units such as the granite Vallorcine and the Salvan Dorénaz syncline. A series of Carboniferous and Permian folded layers forms this syncline oriented NNE-SSW which overlies the Hercynian basement (Gagnebin 1934). This tectonic unit is largely described in section 4.2.

The Helvetic represents the Mesozoic to Tertiary sedimentary formations, highly deformed, which cover the Hercynian basement. The Helvetic was only affected by the Alpine events, as opposed to the basement which underwent the successive Hercynian and Alpine deformation phases (Badoux 1971, Collet et al. 1952, Gagnebin 1934, Jamier 1975, Steck et al. 2001, Von Raumer 1987). The basis of the Morcles nappe is pinched between the Aiguilles Rouges and Mont Blanc Massifs and forms a complex syncline named Chamonix-Martigny zone. It represents the lowest unit of the Helvetic and consists of a great recumbent fold with Jurassic to Cretaceous limestones and marls (Badoux 1971). This unit also forms the summits of the Dents du Midi and Dent de Morcles Massifs. Locally, tectonic slices are intercalated due to the movement of the Morcles nappe during the Alpine events (Gagnebin 1934).The autochthonous sedimentary cover of the Aiguilles Rouges Massif covers unconformably the Hercynian basement and is thrusted by the Morcles nappe. This cover which outcrops along the basement has a small thickness (Steck et al. 2001) and consists of quartzite and dolomites (Permian to Trias), limestones (Dogger, Malm and lower Cretaceous), breccia and marls (upper Eocene) and finally marls and sandstones (Oligocenous flysch, Val d'Illiez formation). Some great stratigraphic gaps due to erosion and absence of sedimentation occur during the upper Lias to lower Dogger and during the Tertiary (Steck et al. 2001). On the contrary, sedimentary formations of the Morcles nappe are thicker, in particular the Lias - Dogger series which is continuous.

Legend

- ● Surface water: lakes (L.) and rivers (R.)
- ▲ Mountain top
- ★ Hydrothermal site
- ⬡ City/Village
- — International boundary
- ▭ Geol. cross section

N

Monthey

Rhone R.

Vièze R.

Bex

Avançon R.

Tine R.

Troistorrents

St.Maurice

Lavey

Mauvoisin R.

Lavey-les-Bains

Dent de Morcles (2969 m)

Val-d'Illiez

Champéry

Dents du Midi Cime de l'Est (3178 m)

Epinassey

St. Barthélemy R.

Evionnaz

Switzerland

Dents du Midi Haute Cime (3257 m)

Vièze R.

Salanfe L.

Dent de Salantin (2485 m)

Miéville

Dorénaz

Tour Salière (3220 m)

Salanfe R.

Le Luisin (2785 m)

Salvan

Rhone R.

Vogealle L.

Mont Ruan (3053 m)

Triège R

Trient R.

Martigny

Emosson L

Dent d'Emaney (2568 m)

Giffre R.

Pte de la Finive (2838 m)

Bel Oiseau (2643 m)

Finhaut

Mont de l'Arpille (2085 m)

Dranse R.

Vieux Emosson L.

Trient R.

Les Perrons (2651 m)

Durand R.

Le Buet (3096 m)

Vallorcine

Croix de Fer (2343 m)

Eau Noire R.

Pte D'Orny (3270 m)

Aiguille du Belvédère (2965 m)

Blanc L.

Argentière

Aiguille du Chardonnet (3824 m)

Noirs L.

Cornu L.

Diosaz R.

France

Arve R.

Le Brévent (2525 m)

Aiguille Verte (4122 m)

Mont Dolent (3823 m)

Chamonix

0   5 km

74

LEGEND OF GEOLOGICAL MAP OF LAVEY-LES-BAINS AREA

Quaternary

- Not differentiated quaternary deposits

Subalpine molasse

- *Lower Freshwater Molasse*: Sandstone and conglomerate (red molasse, Mont Pelerin pudding stone, coal molasse): Chattien.
- *Lower Marine Molasse*: Marl and sandstone (Vaulruz sandstone): Lower Oligocene.

Aiguilles Rouges massif

- Marl and sandstone (parautochthonous Flysch): Lower Oligocene.
- Marl and sandstone (autochthonous Flysch): Lower Oligocene.
- Quartzite, dolomite, limestone and marl: Trias - Eocene.
- Conglomerate (Vallorcine pudding stone), sandstone, pelite and rhyolite: Carboniferous - Permian.
- Vallorcine granite: Upper Carboniferous (307 ± 2 Ma, Bussy and Hernandez 1997).
- Gneiss and migmatite: Proterozoic - Paleozoic.

Morcles nappe

- Limestone, marl and sandstone (including flysch): Cretaceous - Lower Oligocene.
- Limestone and marl: Dogger - Malm.

Chamonix zone *(root of reversed limb of the Morcles nappe)*

- Limestone, dolomite, marl and sandstone: Trias - Eocene.

Mont Blanc external crystalline massif

- Montenvers granitic gneiss: Carboniferous (307 ± 3 Ma, Bussy and Von Raumer 1993).
- Gneiss: Proterozoic - Paleozoic, lenticular banded gneiss (453 ± 3 Ma, Bussy and Von Raumer 1993).

Mont Blanc internal crystalline massif

- Leucogranite: Carboniferous - Permian.
- Mont Blanc granite: Upper Carboniferous (304 ± 3 Ma, Bussy and Von Raumer 1993).
- Rhyolite: Upper Carboniferous (307 ± 2 Ma, Bussy and Von Raumer 1993).
- Gneiss: Proterozoic - Paleozoic.

Ultrahelvetic nappes

- Sandstone: Eocene (Dent de Valère Flysch).
- Limestone and marl: Malm - Cretaceous (Anzeinde nappe).
- Wildflysch: Oligocene (Plaine Morte nappe).

Penninic nappe

- *Submedian zone*: Dolomite, evaporite, limestone, marl and sandstone (including flysch): Trias - Eocene.

Figure 4.1: Geological map and cross section of the Lavey-les-Bains regional area according to the tectonic map of the Western Switzerland Alps (modified after Steck et al. 2001).

4.2 Geological investigations of the north-eastern part of the Aiguilles Rouges basement

4.2.1 Overview of the geological history

The Aiguilles Rouges Massif is separated from the Mont Blanc Massif by the Chamonix-Martigny complex syncline (Collet et al. 1952). They extend in a NNE-SSW direction and form a strip up to 40 kilometres in length and 4-5 kilometres in width between Arve and Rhone Valleys. The southern half of Aiguilles Rouges is located on the French territory whereas the northern part belongs to Switzerland.

The Aiguilles Rouges Massif belongs to the pre-Mesozoic basement areas of the Alpine external crystalline massifs, unconformably overlied by its autochthonous sedimentary cover (Von Raumer et al. 2003). Before its involvement into the Alpine building, the Aiguilles Rouges Massif registered a multiple geological evolutions. Firstly, Neoproterozoic to Cambrian sediments were deposited with the emplacement of granitoid and metabasic to ultramafic magmatic rocks of Early Palaeozoic age (Von Raumer and Bussy 2004). After rifting and drifting (formation of Paleotethys) all rocks underwent polyphase metamorphic and structural transformations during the Variscan orogeny, and were intruded by late Variscan granitoids. The resulting polymetamorphic basement was eroded during formation of Upper Carboniferous sedimentary troughs (Von Raumer and Bussy 2004) receiving molasse-type detrital sediments. The deformation of the Aiguilles Rouges Massif continued during Alpine orogenic cycles but less extremely. Indeed, the Alpine metamorphism reached only the lowermost greenschist facies in the Aiguilles Rouges Massif (Von Raumer et al. 2003).

4.2.2 Description of the Aiguilles Rouges crystalline rocks

The description of the Aiguilles Rouges Massif crystalline rocks is illustrated in explanatory leaflets of the geological maps of Saint-Maurice (Gagnebin 1934), Saxon-Morcles (Lugeon and Argand 1937), Finhaut (Collet et al. 1952), Dent de Morcles (Badoux 1971), and in the note accompanying the tectonic map of the western Switzerland Alps (Steck et al. 2001). Moreover, several publications and reports discuss about these rocks and give details in their composition (Brändlein et al. 1994, Capuzzo and Bussy 2000, Jamier 1975, Kerrich et al. 1980, Marquer et al. 1994, Steyrer and Sturm 2002, Von Raumer 1984 and 1987, Von Raumer and Bussy 2004, and Von Raumer et al. 1990).

According to structural and petrographic properties, it is possible to subdivide the Aiguilles Rouges Massif into 6 zones forming narrow strips of NNE-SSW direction. These 6 zones are: the orthogneiss injection zone, the paragneiss area, the Vallorcine granite, the Salvan-Dorénaz syncline, the Shear Zone of Miéville and the paragneiss of the Arpille Massif.

The orthogneiss injection zone reaches 1-2 kilometres width in the northern half of the Aiguilles Rouges Massif. In the southern part, it narrows and divides into several lenses. The rocks have orthogneiss appearance but are extremely varied. They contain lenticular or spherical inclusions of hornfels and schistous paragneiss (Collet et al. 1952, Von Raumer and Bussy 2004).

The paragneiss and their injected veins are represented by two varieties of rocks (hornfels and schistous gneiss) having similar mineralogical composition but being different in their structure. The difference in the structure comes from the initial sedimentary material: argilloarenaceous sediments with fine grains for hornfels and with coarse grains for the schistous gneiss. The two formations are mostly injected of quartz seams. Marble lenses can be found resulting from the metamorphism of limestones and marly intercalations (Collet et al. 1952, Von Raumer and Bussy 2004) as well as amphibolites which result from the metamorphism of subvolcanic sills or dikes (Steck et al. 2001, Von Raumer et al. 1990).

The Vallorcine granite unit, a narrow strip about 15 kilometres in length and 1 kilometre width, extends from the village of Miéville in the Rhone Valley, upstream from Lavey-les-Bains and close to Dorénaz (Fig. 4.1), to the village of Vallorcine in France. It represents an important late Variscan

magmatic tectonic event in the Alpine basement which may be comparable to those observed outside the Alps (Brändlein et al. 1994). The Vallorcine granite intruded along a fractured mylonite-zone at 306 ± 1.5 My (Bussy et al. 2001). The rocks can be comparable to a granite rich in biotite, with fine grains being more widespread than the coarse grains (Collet et al. 1952).

The Salvan-Dorénaz syncline is a late Carboniferous continental basin exposed with a NNE-SSW direction along the eastern margin of the Aiguilles Rouges Massif. This syncline contains various types of continental facies such as volcanic rocks and detrital sedimentary rocks, deposited in a subsiding basin during the strike-slip tectonic events (Capuzzo and Bussy 2000). In details, formations are alternations of slates, sandstones and conglomerates. All the formations are folded in a complex syn-

cline during the Permian inside a crystalline basement folded before the Carboniferous period (Collet et al. 1952, Gagnebin 1934).

The Shear Zone of Miéville is a subvertical deformed zone which is about 50-200 metres in width and several kilometres length in a NNE-SSW direction (Steyrer and Sturm 2002). The crystalline rocks were highly deformed in dark mylonites forming a large shear zone (Kerrich et al. 1980, Marquer et al. 1994). It borders the Vallorcine granite towards the north-west and the Salvan-Dorénaz syncline in the south-east. Finally the Arpille crystalline rocks mainly consist of paragneiss with heterogeneous old sediments, and are located on the other side of the Salvan-Dorénaz syncline before the Chamonix-Martigny syncline (Fig. 4.1, Collet et al. 1952).

4.2.3 Description of the Hercynian and Alpine structures

The description of the Hercynian and Alpine structures in the Aiguilles Rouges Massif is considered in this study to highlight the potential direction of flow paths of infiltrated waters. Indeed, it can be assumed that the structures allow the occurrences of hydraulic connectivity between the aquifer in the decompressed zone and the geothermal reservoir. The structures are faults, open fractures and fold axes initially described by Von Raumer and Bussy (2004) and showed in Figure 4.3. The description of the structures is also present in explanatory leaflets of the geological maps, in the note of the tectonic map of the western Switzerland Alps, and in several publications such as Jamier (1975), Marquer et al. (1994), Von Raumer (1984 and

1987), Von Raumer and Bussy (2004), and Von Raumer et al. (2003).

The Aiguilles Rouges Massif basement underwent the Variscan and Alpine tectonic events which are responsible for the visible NNE to NE major faults, open fractures, lineation and fold axes. Collet (1952) highlighted the strong apparent dip of the structures seldom lower than 60° plunging towards the ESE direction. Finally, apart from great zones of mylonitisation, subvertical strike-slip faults with NW-SE direction are also met in the basement which is characteristic of the movements of great rock masses during the Alpine tectonic events (Collet et al. 1952, Von Raumer and Bussy 2004).

4.2.4 Description of the deep structures at the bottom of the Aiguilles Rouges Massif

The geological investigation until 517 metres depth at Lavey-les-Bains does not allow visualizing the deep structures at the bottom of the Aiguilles Rouges Massif. The use of a geophysical method with the aim of realizing a seismic profile is useful to have an idea of the deep structures. Within the framework of a research national plan NRP 20 (Pfiffner et al. 1997, Sartori et al. 2001) and of the

GEOTHERMOVAL project (Lehner 1990, Besson et al. 1992 and 1993), a seismic profile was carried out in the Western Alps going through Saint-Maurice and Martigny. The interpretation of this profile made possible the establishment of a tectonic cross section till the lower crust, through the Alps range from the Prealps to the Dent Blanche nappe which represents the border between Switzer-

Orthogneiss (coord CH: 560'650/102'210)

Chemical data: major elements (wt %)

SiO_2	67.25	MnO	0.05
TiO_2	0.6	MgO	1.23
Al_2O_3	15.93	CaO	1.93
Fe_2O_3	1.01	Na_2O	3.02
FeO	2.68	K_2O	4.15

Minerals association

Qz, Felds, Biot-Musc, Apat.

Ref: Wirsing, 1997 in Von Raumer & Bussy, 2004

Paragneiss (coord CH: 559'210/101'770)

Chemical data: major elements (wt %)

SiO_2	63.47	MnO	0.11
TiO_2	0.88	MgO	3.47
Al_2O_3	16.48	CaO	1.24
Fe_2O_3	1.37	Na_2O	1.31
FeO	6.1	K_2O	2.71

Minerals association

Qz, Felds, Biot-Musc, Cord, Anda, Sill, Garn, Tour, Amph, Pyro, Diop.

Ref: Von Raumer & Bussy, 2004

Granite (coord CH: 562'560/102'400)

Chemical data: major elements (wt %)

SiO_2	74.75	MnO	0.03
TiO_2	0.28	MgO	0.56
Al_2O_3	13.65	CaO	0.52
Fe_2O_3	1.71	Na_2O	3.22
FeO	1.1	K_2O	4.82

Minerals association

Qz, K-felds, Ano-Alb, Biot-Musc, Cord, Anda, Sill, Apat.

Ref: Von Raumer & Bussy, 2004

Paragneiss (Map 1305 Dent de Morcles)

Minerals association

Qz, Ano-Alb, K-felds, Biot-Musc, Amph.

Ref: Badoux, 1971

Figure 4.2: Photos of rocks met in the Aiguilles Rouges Massif (12/07/2007) and their mineral properties.

A represents an example of varied orthogneiss with subvertical quartz veins oriented NNE (coord CH: 560'700/101'900/1930). B illustrates schistous paragneiss (coord CH: 559'200/101'700/1940) and subvertical beds in gneissic hornfels (parking in the Emosson restaurant, coord CH: 560'900/102'000/1950). C represents a fractured outcrop of the Vallorcine granite in La Lechère (road between Finhaut and Emosson Lake, coord CH: 563'100/102'700/1450). D shows a outcrop of paragneiss in the Arpille Massif (road between Martigny and Salvan when the road winds steeply up, coord CH: 569'000/108'600/600). E illustrates a stratified outcrop of Carboniferous sediments in the Salvan-Dorénaz syncline (road between Trient and Le Châtelard, coord CH: 564'600/102'200/1300) with alternation of slates, sandstones and conglomerates (road, hammer and coin as scale).
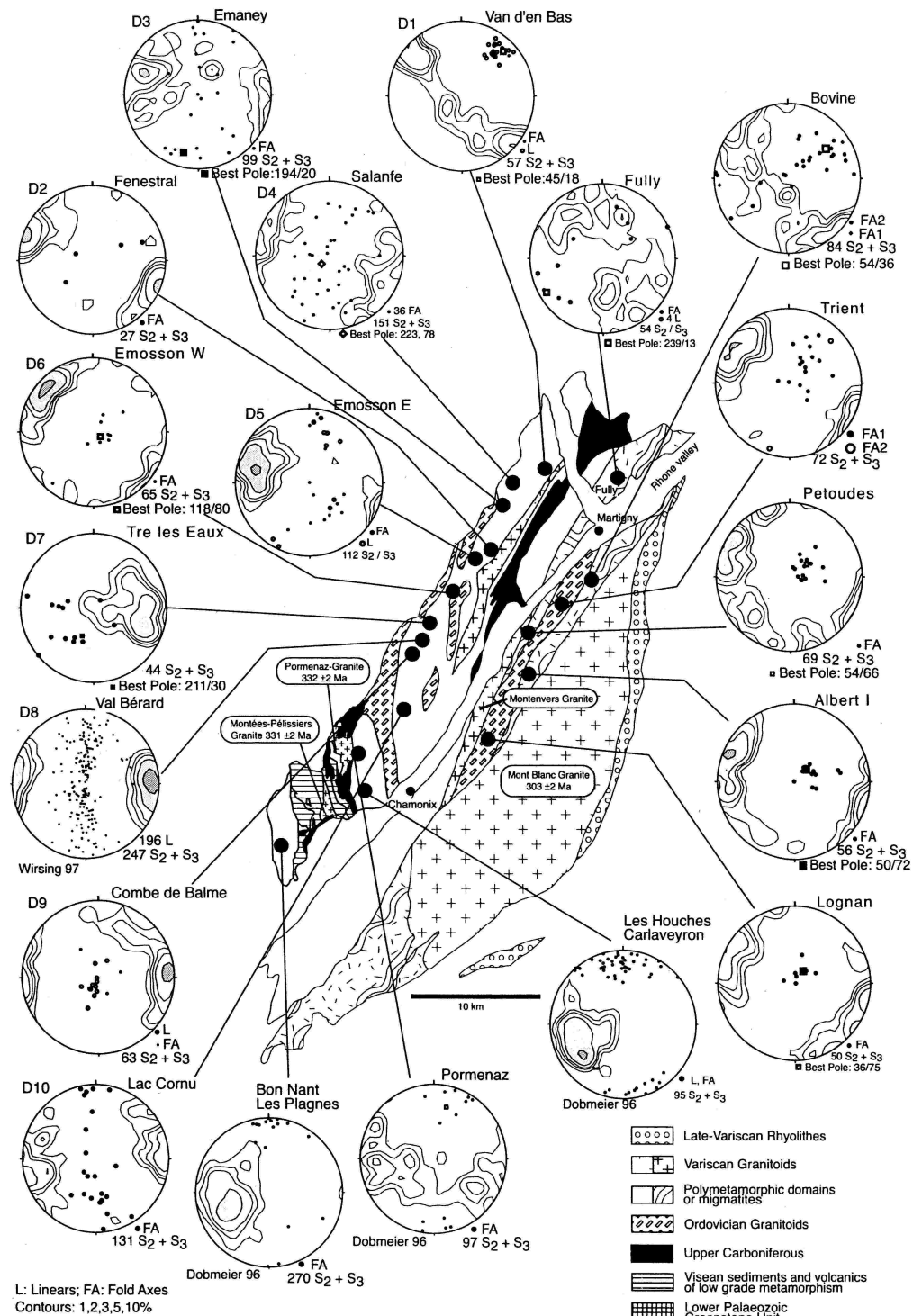
Figure 4.3: Distribution of Late Variscan structures in the polymetamorphic Aiguilles Rouges and Mont Blanc basements. Statistic of dominant orientations of composite surfaces S2/S3, lineations and fold axes (from Von Raumer and Bussy 2004).

land and Italy (Fig. 4.4). The seismic reflectors are mostly related to the stratification of the sedimentary formations, whereas the crystalline basement does not behave as reflectors: it generally appears transparent in seismic profiles (Bianchetti et al. 2006). Below Lavey-les-Bains, the interpretation of reflectors highlighted an anomaly roughly at 3 kilometres depth. This anomaly should be a synclinal structure with sedimentary rocks belonging to the autochthonous cover of the Aiguilles Rouges Massif. In detail, geologists assume that there is a syncline pinched inside the thrust fault between the Aiguilles Rouges Massif and another crystalline massif called Infra-Aiguilles Rouges. The thrust fault deepens towards the south-east below another one thrust fault putting in contact the Mont Blanc Massif on the Aiguilles Rouges Massif. The profile shows successive thrusts within the external crystalline massifs with movements in the north-west direction.

The assumption of a complex sedimentary syncline below Lavey-les-Bains however requires caution because there is no direct investigation via boreholes to prove its presence. Assuming its presence and assuming that the formations have a good hydraulic conductivity, this structure could drain the deep fluid towards high fractured areas in the Aiguilles Rouges Massif. If the formations have a low hydraulic conductivity, this structure can represent an impermeable screen for waters circulating in the Aiguilles Rouges Massif. In this case, the pressure of trapped waters can generate a natural hydraulic fracturing in the basement just above the thrust fault, and therefore can increase the hydraulic conductivity of the crystalline rocks which will allow the uprising of the deep fluid.

4.3 Local geological investigations

4.3.1 Local geological setting

The hydrothermal area of Lavey-les-Bains is located close to the geological limit between the Aiguilles Rouges basement and its autochthonous cover. Near the swimming pools, the Mesozoic cover outcrops and reveals successive folds in the dolomitic limestones. From establishments leaning on the steep valley side, cliffs of Triassic formation can be seen whereas in the zone of boreholes, few hectometres upstream from the buildings, the basement outcrops and is crossed by deep boreholes below the Quaternary deposits.

In the hydrothermal area, the thickness of the Quaternary filling varies between 0-100 metres from the slope to the Rhone River (Bianchetti 1993a). The limit between gneiss and the filling appears undulating with variable thickness over short distances (Cavalli 1993). The Quaternary filling consists of recent coarse alluvial deposits, and fine moraine deposits with lenses of rock falls (Badoux 1971, CRSFA 1992b, Lugeon and Argand 1937). Moreover, the deposits are crossed by several fan deltas. Geomorphologically, the front of a fan delta mostly represents the limit of the floodplain. The most important fan delta close to Lavey-les-Bains is located at the end of the Saint-Barthelemy torrent

where are implemented the Epinassey boreholes E1 and E2 (CRSFA 1992c).

In the area of Saint-Maurice, 1 kilometre downstream from Lavey-les-Bains, the glacier strongly dug the bedrock and the thickness of the Quaternary filling reaches 600 metres (CRSFA 1992b). The interpretation of a seismic-reflection profile showed the different horizons of the filling (Fig. 4.5). In the upper part, it consists of coarse gravels and river sands considered as an aquifer (30 to 100 m). Then, several hundred metres of laminated glaciolacustrine silts are present and are assumed to be an aquiclude (CRSFA 1989, Pugin et al. 1992). The bottom of the filling is probably composed of glacial coarse deposits which could have a large amount of water (Besson et al. 1993, Fischer et al. 1987).

Downstream from Saint-Maurice, the Triassic formations would have been eroded by the successive Quaternary glaciations (Nold 1991), but the calcareous bedrock outcrops abruptly, obstructing the Rhone Valley. It remains difficult to explain it. Several geologists think that there is a relationship between this and the presence of thermal waters at Lavey-les-Bains which would locally have melted the base of the glacier.
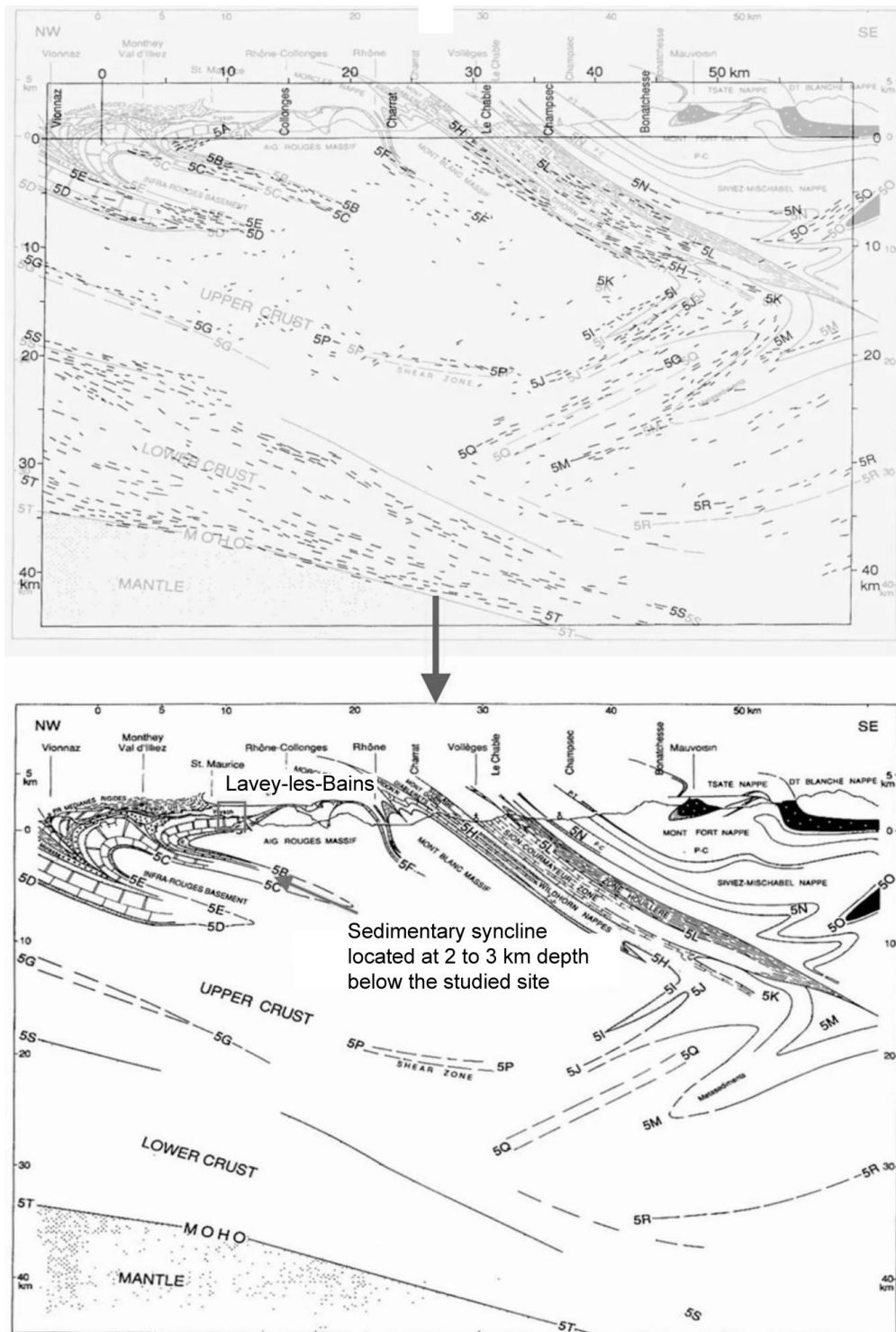
Figure 4.4: Deep geological structures of the Aiguilles Rouges Massif below Lavey-les-Bains according to the interpretation of the seismic profile NRP 20 (modified from Pfiffner et al. 1997).
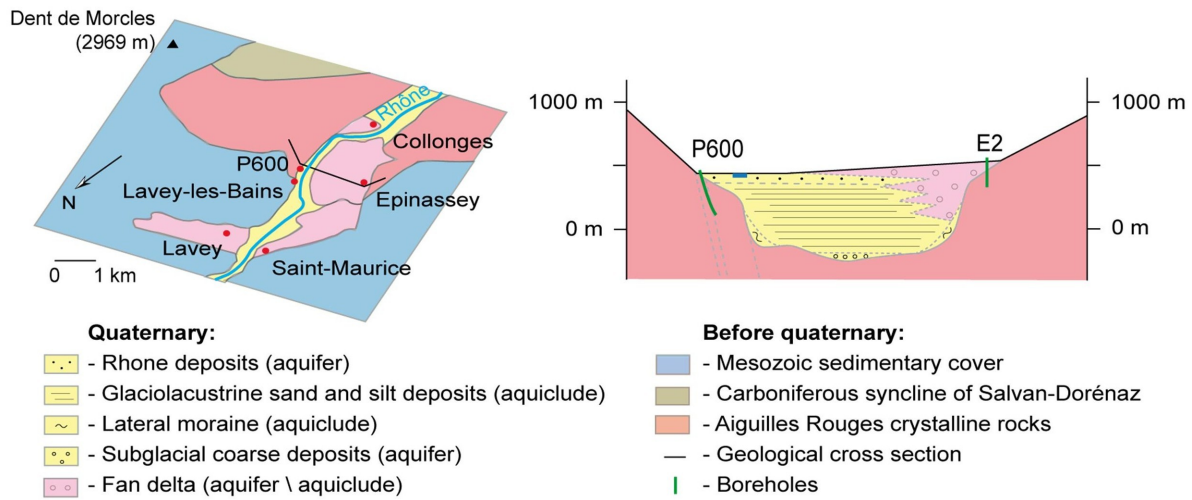
Figure 4.5: Geological setting of Lavey-les-Bains area and the Quaternary filling in the Rhone Valley.

4.3.2 Fracturing of the crystalline rocks close to Lavey-les-Bains

A study about the fracturing of the Aiguilles Rouges crystalline rocks in the area of Saint-Maurice was carried out by Flamm (1993) for the GEOTHERMOVAL project. The objective was to highlight the directions and the nature of fractures allowing the uprising of the thermal water. Moreover, the description of the fractures was considered for the implementation of the P600 well later aiming to cross fractures as much as possible.

Results from 530 measurements in 68 outcrops of gneiss grouped around Lavey-les-Bains showed the existence of six major families of fractures (Flamm 1993, Fig. 4.6):

1. a family of mylonite. Chronologically, this is the oldest family. Fractures are closed involving low hydraulic conductivity.

2. a NNW-SSE family of extension cracks, subvertical and parallel to the Rhone Valley. These are open and regular fractures without filling, except sometimes from calcite or quartz precipitation. They are perpendicular to the minimal stress during the Alpine tectonic events.

3. a NE-SW family of subvertical compression fault, perpendicular to the Rhone Valley.

They are often filled with chlorite and quartz minerals.

4. a NE-SW family of fault breccias associated to the previous family. These fractures are clearly visible in the observed area. They are brecciated and form large zones reaching 5 metres width, probably ensuring high hydraulic conductivity.

5. a SE-NW family of fault breccias. This family of brecciated fractures is less visible but could have high hydraulic conductivity at depth. Indeed, a zone of fractures of 15 metres width with ESE-WNW direction was observed.

6. a family of reverse fractures with low dip and brecciated. They are cataclasites representing micro-thrust faults. They are older than families 2 and 3 and they can extend towards more important thrust faults at depth.

These measurements make it possible to assume that the uprising of the deep fluid occurs in fractures belonging to the families 2, 4 and 6, which certainly have high hydraulic conductivity. In the area of Lavey-les-Bains, fractures of the family 2 were mostly crossed by boreholes and drain the thermal waters (Bianchetti 2002).
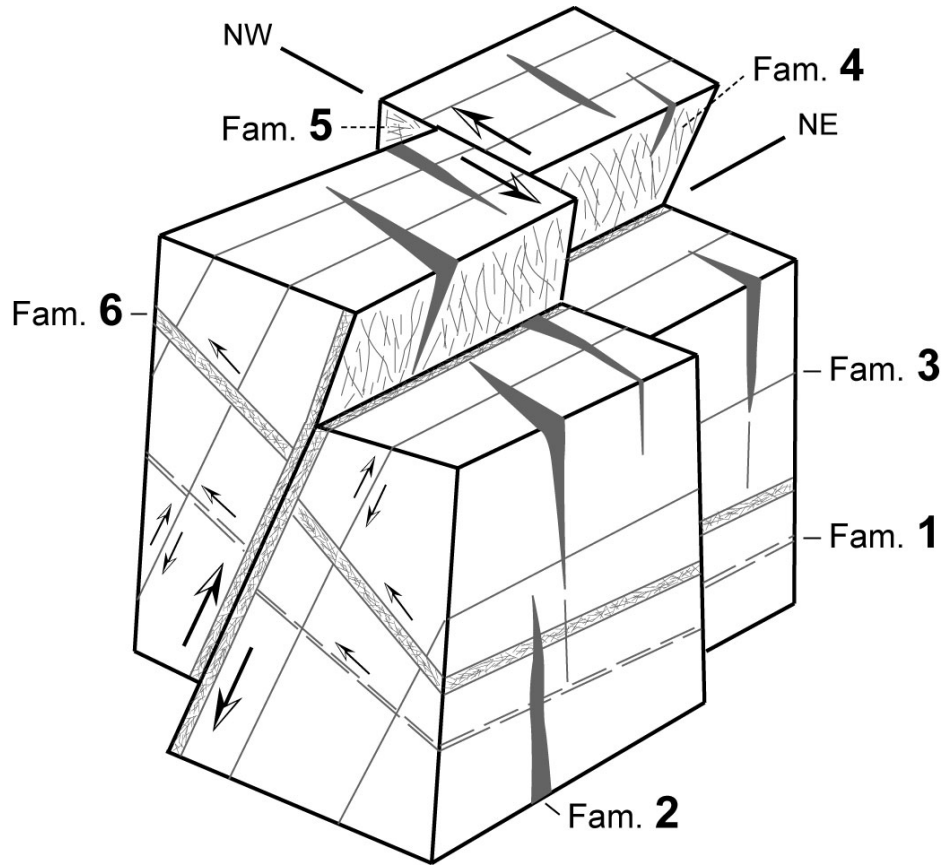
Figure 4.6: Six major families of fractures observed in 68 gneissic exposures around Lavey-les-Bains for the GEOTHERMOVAL project (modified from Flamm 1993). Family fractures 2 and 4 are supposed draining the deep fluid.

5

Hydrogeological and geochemical investigations at Lavey-les-Bains

5.1 Local hydrogeological and geochemical investigations

5.1.1 Overview before the implementation of the wells P201 and P600

THE available hydrogeological information before 1972 is limited to observations made in the old well during several pumping tests. Tests showed a fluctuating piezometric level of around 5 metres in the unconfined aquifer, and prolongation of thermal inflows in interstices of the Quaternary deposits at shallow depth and in fractures in the basement.

In the old well, mixing processes between thermal water and cold shallower water were observed. Mixing processes are governed by the relationship between the hydrostatic pressures of the two aquifers. Beneath natural hydraulic conditions, the static water level of the confined thermal aquifer is higher than the level of the phreatic groundwater. The natural water level in the old well varies between 1-2 metres above the level of the phreatic groundwater. Consequently, the thermal water is locally diffused in the porous Quaternary deposits. During pumping tests, the balance is disturbed and the thermal pressure decreases allowing the infiltration of cold waters in fractures in the basement. The interface between the thermal aquifer and the phreatic groundwater is not considered as a distinct limit, but a progressive mixing zone with depth (Bianchetti 1993a). A simple conceptual model

was built through observations (Fig. 5.1). In fractures of the basement, thermal inflows are probably mixed with other cold waters circulating in the decompressed zone.

The continuous thermal pressure in the old well ensures a good regularity in time of the physico-chemical parameters. Several thermal plumes certainly exist under the Quaternary filling out of the old well because temperature anomalies were mentioned in piezometers around. The natural water levels observed in piezometers also varies due to the effect of the thermal pressure where the uprising of thermal water occurs below the filling (Zahner et al. 1974).

Finally, the presence of thick moraine deposits in the middle of the valley, considered as aquiclude, should prevent the rise of thermal water in the middle of the valley. Consequently, the rise of thermal water takes place on the edges of the Quaternary filling where the basement is directly covered by the recent alluvial deposits. However, some thermal circulations could also exist in fan deltas and in subglacial coarse deposits, which can be considered as aquifers in the most permeable zones.
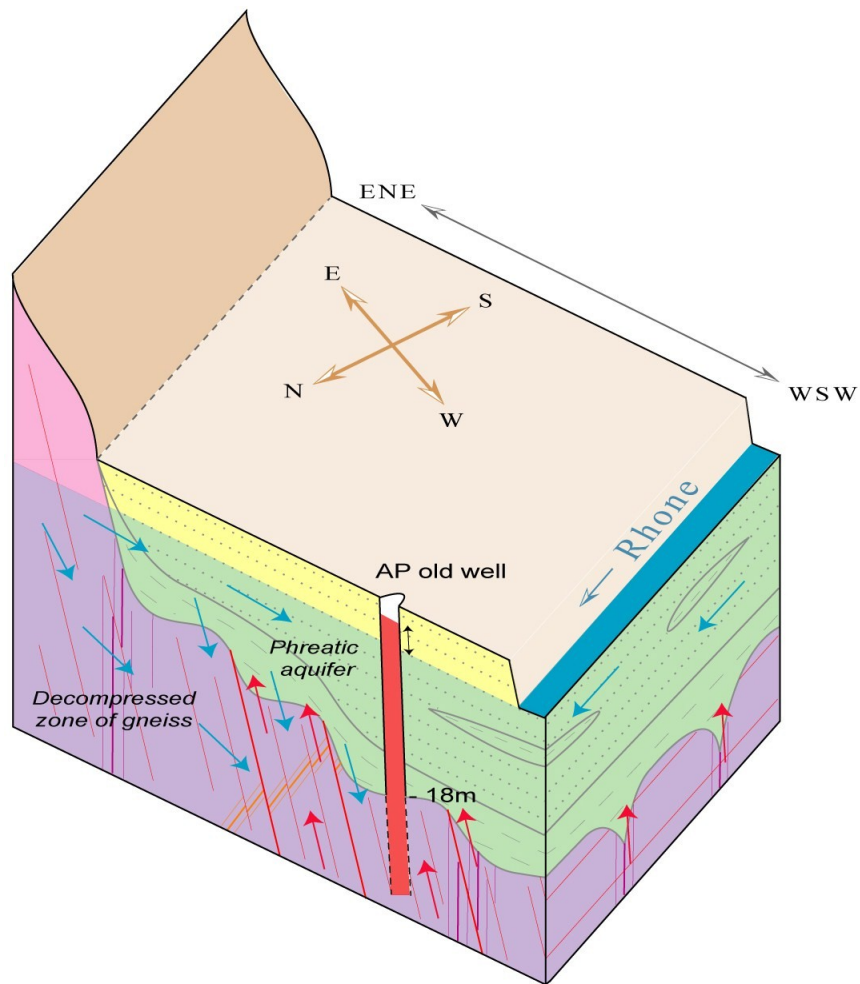
Figure 5.1: Diffusion of thermal and cold waters in the limit between the Quaternary deposits and the fractured gneiss. Situation before the deep wells.

5.1.2 Water chemistry

Waters in the Lavey-les-Bains hydrothermal area can be subdivided into three geochemical groups, defining the different end-members. The chemical composition of waters used to build the Piper and Schoeller diagrams in Figure 5.2 is given in the appendix B.

The Na-SO$_4$ thermal water rich in chloride is the first group of water. Waters in the P600 and P201 wells are characteristic of this geochemical type and are slightly mixed with shallower groundwater. This group represents the deep thermal component circulating in the crystalline rocks. The total mineralization ranges around 1.3-1.5 g/L and

the main chemical compounds, considered as natural markers of the thermal component, are Li, Na, K, Cl, SO$_4$, F and SiO$_2$. On the contrary, this water is relatively poor with respect to Ca, Mg and HCO$_3$ and does not contain tritium.

The Ca-HCO$_3$ cold water from the Rhone River and flowing in alluvial groundwater represents the second group. This group of water is less mineralized (TDS 100-300 mg/L) compared to the thermal component. Ca, Mg, HCO$_3$ and tritium are elements defining this group.

Lastly, the Ca-HCO$_3$ cold water flowing in the gallery of the Lavey power plant via several springs

represents the third group. This type of water comes from circulation at shallow depth in the decompressed zone in the gneiss of the Grande Dent de Morcles slope (Fig. 5.3). This water is also found in the S8 and S9 exploratory boreholes where mix-

ing processes occur with the thermal water. The geochemical type is similar to the Rhone alluvial groundwater with the same representative elements but with a stronger mineralization (TDS 300-400 mg/L).
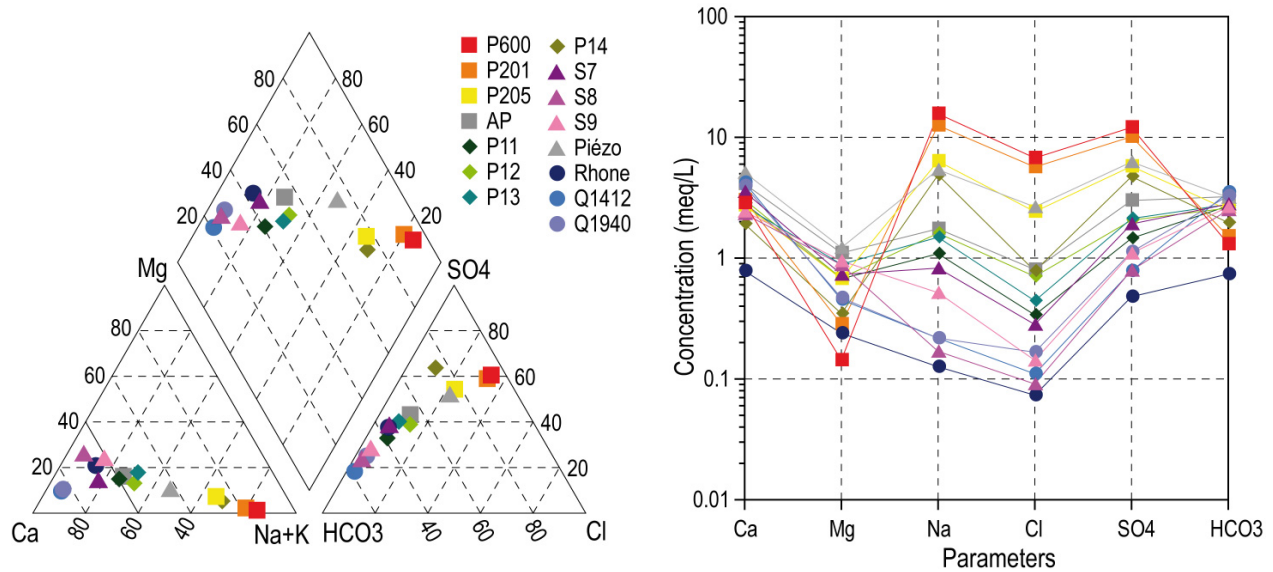
Figure 5.2: Piper and modified Schoeller diagrams of the waters of Lavey-les-Bains area. Locations of the samples are shown in Figure 3.2; Q1412 and Q1940 are springs in the divergence tunnel of Lavey power plant which were sampled (numbers 1412 and 1940 represent their location in metres). Data used for these diagrams come from the one-off sampling rounds described in appendix B, not averages of values.

5.1.3 Mixing processes

In the hydrothermal area, various mixing processes were observed between the three groups of water (Figs. 5.3 and 5.4). The evolution from the thermal end-member to the cold end-member is marked by a reduction in Li, Na, K, Cl, SO_4, F and SiO_2, compensated by an increase in Ca, Mg, HCO_3 and tritium. This evolution is also accompanied by a decrease of the total mineralization and of the temperature. Cold waters are slightly mineralized and tritiated, circulate in the alluvial aquifer and into the fissured gneissic massif, and are represented by the springs of the gallery of Lavey power plant and boreholes S8 and S9 at the proximity of the gallery (see location in Figure 3.2).

Chemical analyses of the deeper P600, P201, P205, P13, S8 and S9 boreholes including data

collected in August 2007 and the previous analyses show good correlations between temperature, conductivity, Na, Mg, Cl, SO_4, HCO_3 and SiO_2 (Fig. 5.4). These deeper boreholes, which are only screened into the fractured gneiss, are not diluted by the Rhone groundwater. Consequently, the cold end-member for these sampling points comes from circulations at shallow depth in the decompressed zone of the fractured gneiss (Fig. 5.3). In the Lavey-les-Bains area, the decompressed zone probably has a thickness in the range 200-300 metres.

Whereas for the old well which is shallower (28 m) and closer to the Rhone River, correlations show mixing processes with the Rhone groundwater and with cold waters from the slope. The unused well PF2 only crosses the Quaternary deposits, where

higher electrical conductivity values were measured (about 1200 μS/cm, see data in appendix B). They are due to thermal injection in the alluvial deposits of the nearby well P600, creating plumes of highly mineralized water. Before this injection, the electrical conductivity measured in PF2 was around 400 μS/cm.
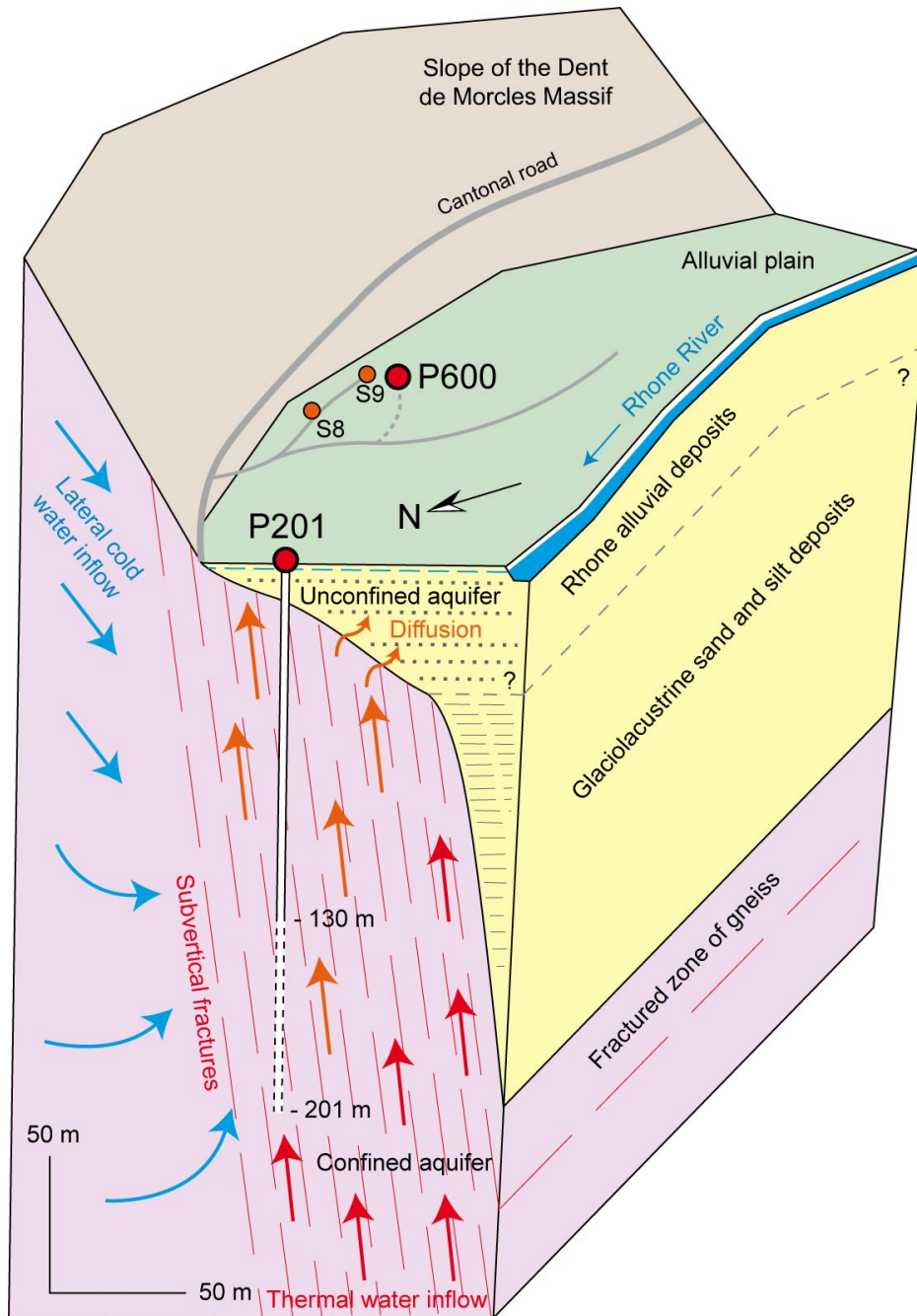
Figure 5.3: Local conceptual model of the Lavey-les-Bains hydrothermal system. The legend for symbols of boreholes is illustrated in Figure 3.2 (Sonney and Vuataz 2009).
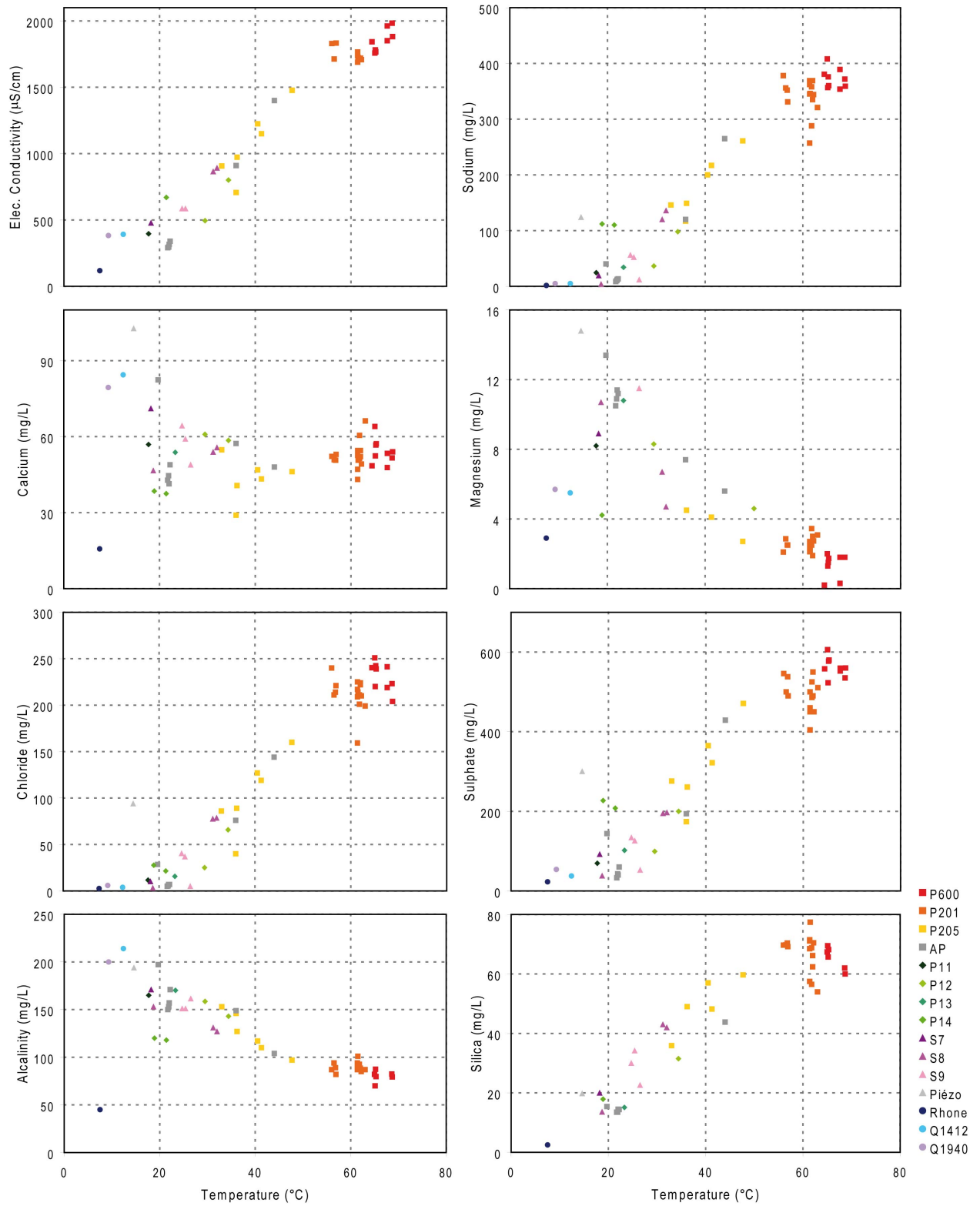
91
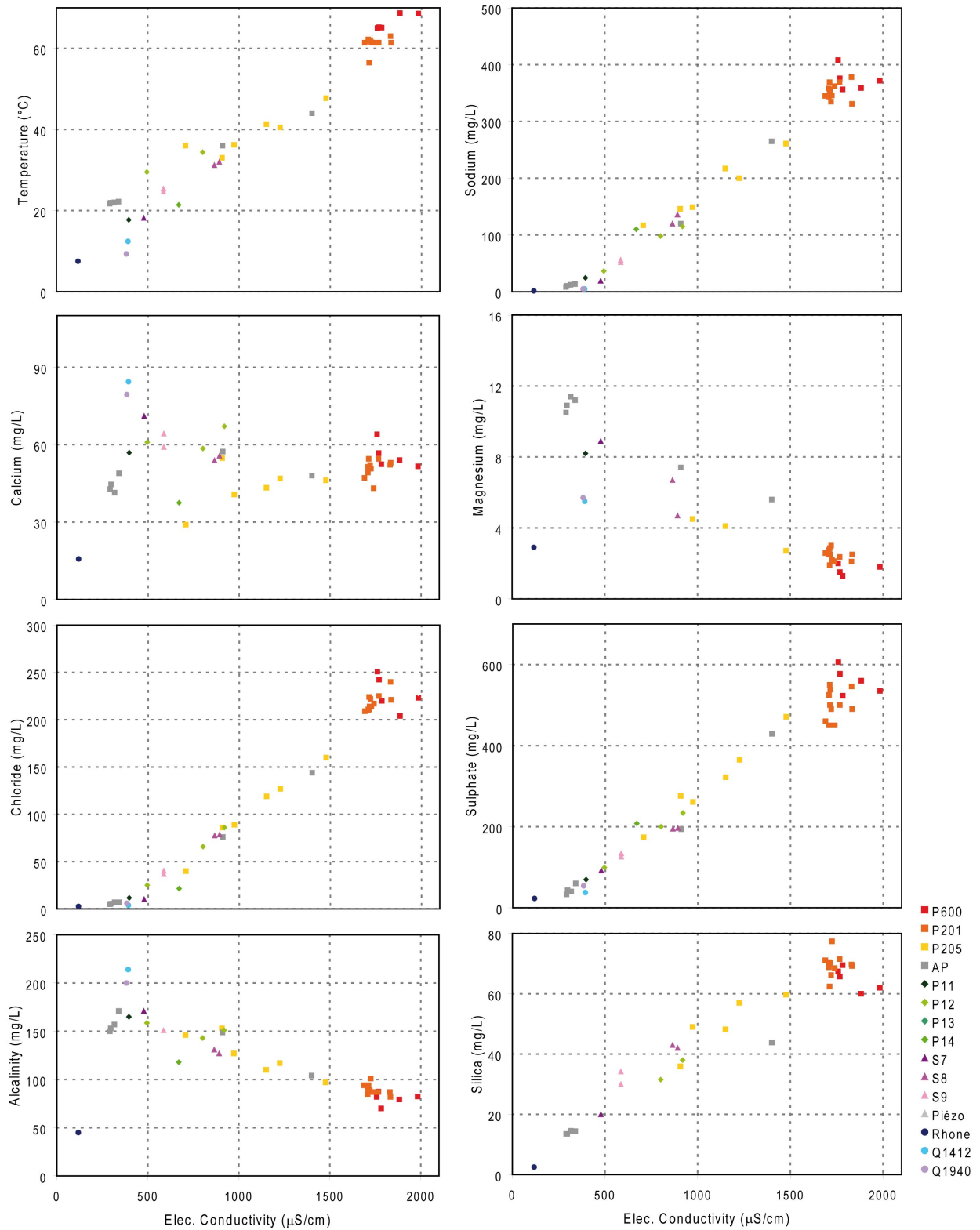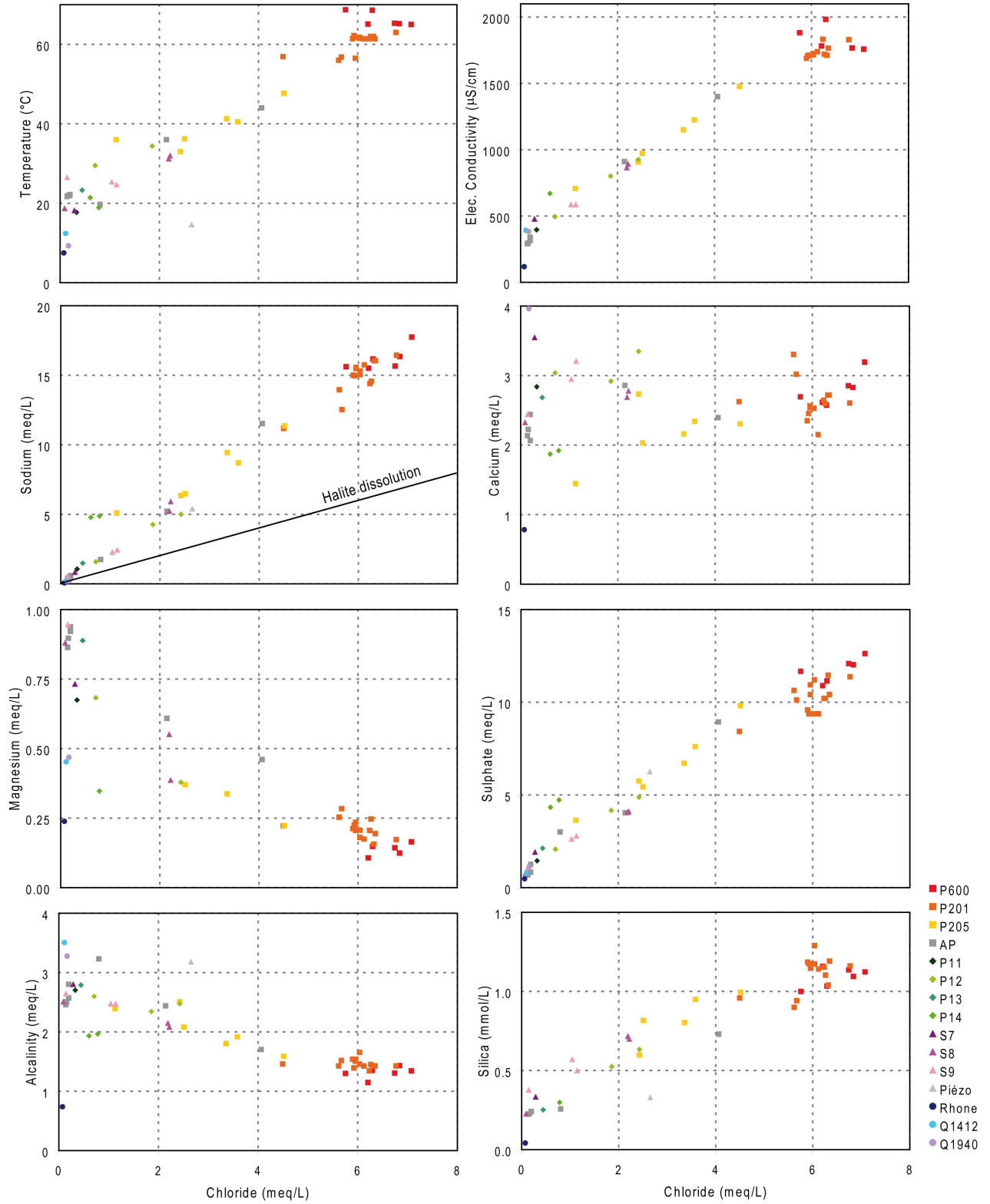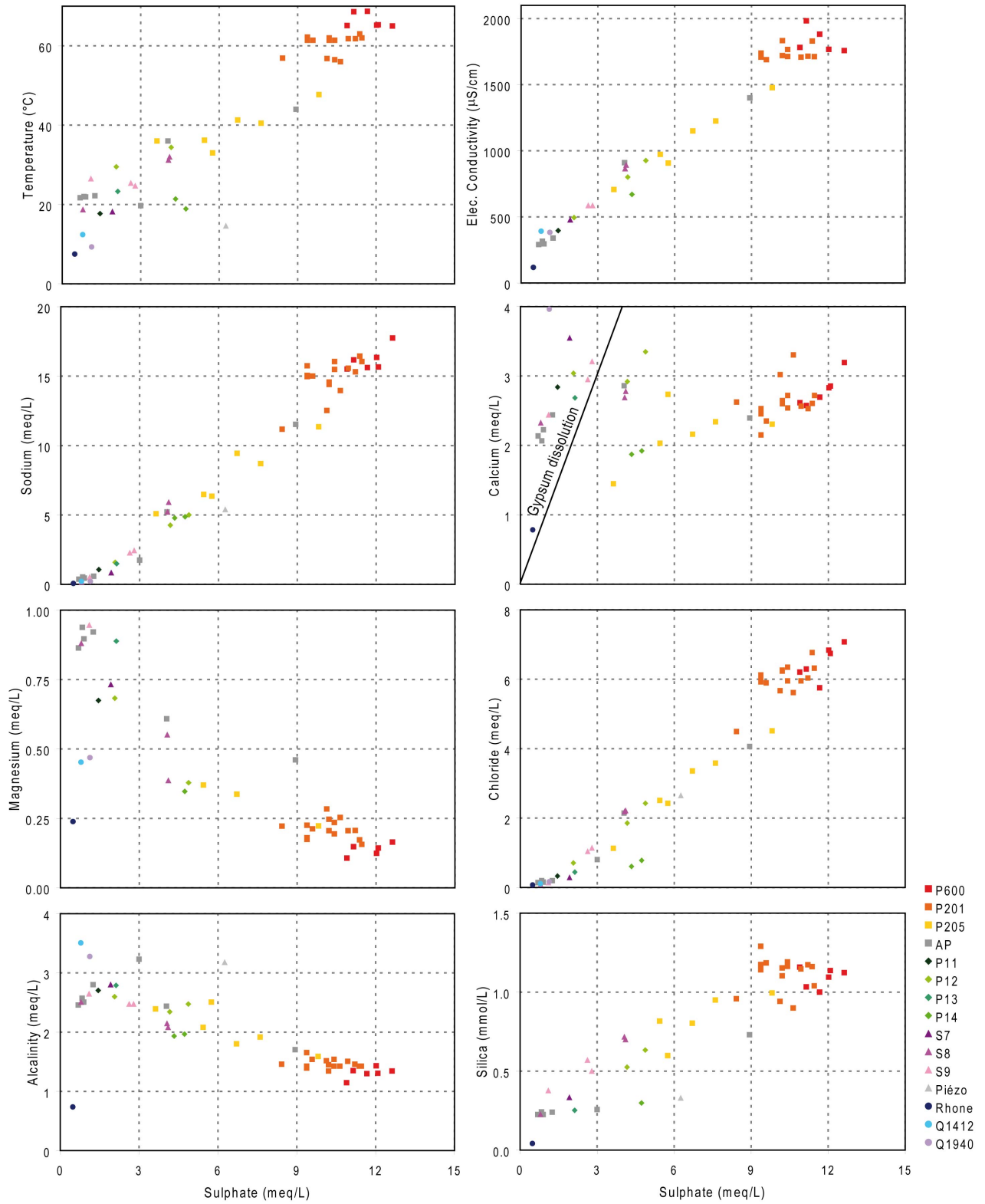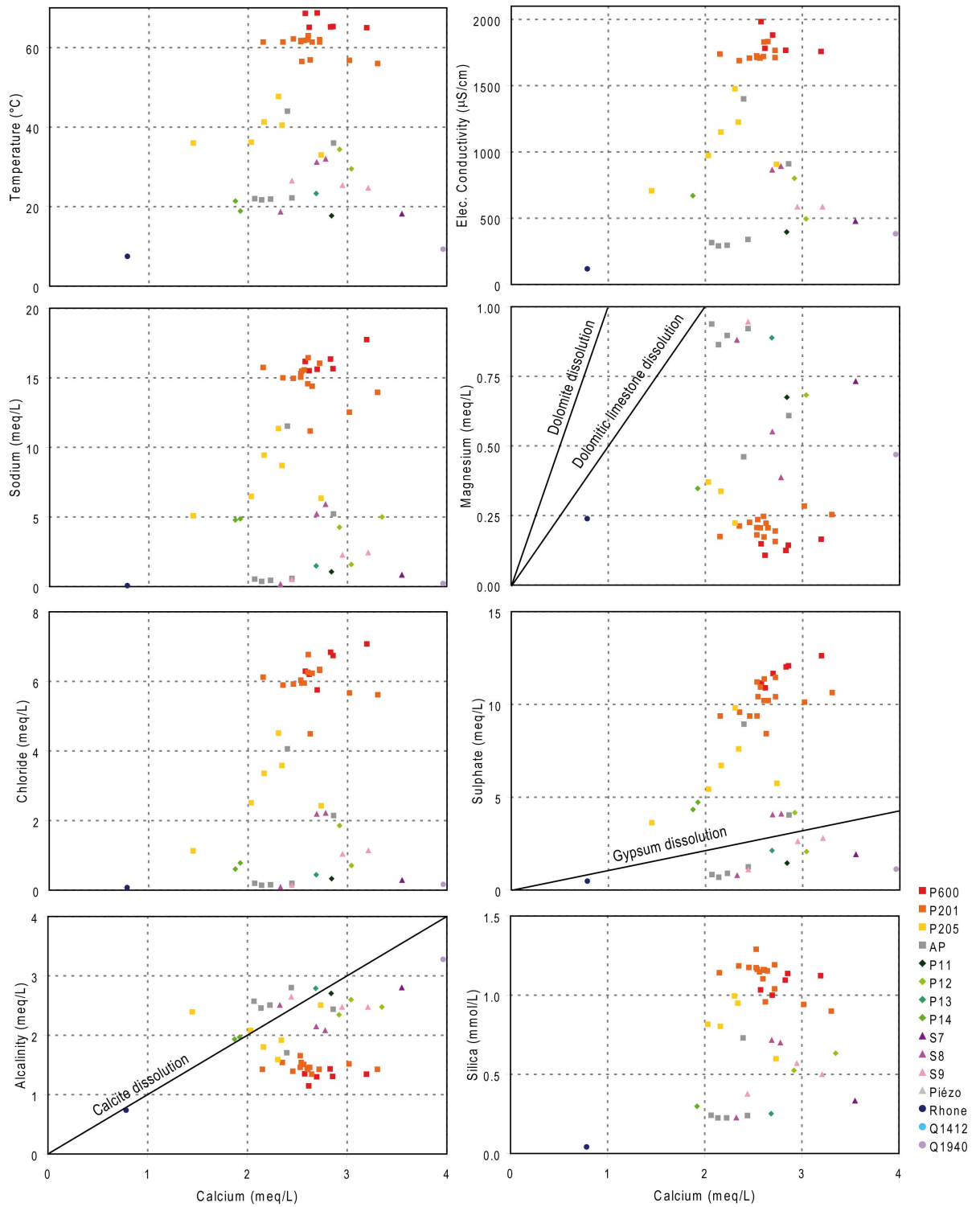
Figure 5.4: Correlations between the physico-chemical parameters in Lavey-les-Bains waters for all existing data (see data in appendix B).

5.1.4 Composition of the end-members

The description of mixing processes revealed the existence of one thermal and two cold components. The thermal end-member circulates in the Aiguilles Rouges basement and is named TC-ARB in Tables 5.1 and 5.2 (Thermal Component of the Aiguilles Rouges Basement). The TC-ARB chemical composition was initially studied by Bianchetti (1993a, 1994 and 2002) and later by Sonney et al. (2007) within the framework of the Alpine Geothermal Power Production project which plans to exploit the deep fluid in a geothermal reservoir close to the thrust fault system putting in contact Aiguilles Rouges and Infra-Aiguilles Rouges basements. Chemical and isotopic data of the sampling points contained in several unpublished reports and publications such as Bianchetti (1993b, 1994 and 2002), Ouedraogo (1989), Sonney (2007), Sonney et al. (2007), Vuataz (1982) and Zahner et al. (1974) were gathered in a database provided in the annexed CD-ROM. Correlations between the physico-chemical parameters illustrated in Figure 5.4 enabled the composition calculation of the end-members (Table 5.1). It was decided to represent the thermal end-member and only the cold component from the slope.

Before the beginning of exploitation of the P600 well in 1997, temperatures of thermal water inflows were measured in the draining zone of the well with an average value of 68°C (Bianchetti 2002). At that time, this temperature reading was probably representative of the TC-ARB before exploitation. In 2007, the annual average temperature of pumped waters in P600 was about 65°C due to the presence in the well of a small proportion of cold and less mineralized water from the decompressed zone. The mixing ratio was estimated by Sonney (2007) and give roughly 5% of cold water and 95% of pure thermal water.

Using correlations between the electrical conductivity, the temperature and the chloride content in water, and assuming that TC-ARB has a temperature about 68°C, the chloride content in TC-ARB which is considered as a conservative element was calculated at about 265 mg/L. With this chloride content, the conductivity at 20°C can be estimated to be about 2070 μS/cm. Moreover, another method using plots with magnesium was tested and gave similar results, assuming that TC-ARB has lower magnesium concentration (< 0.5 mg/L). Using all plots of the physico-chemical parameters versus chloride, it was possible to calculate the other dissolved chemical species and isotope values for TC-ARB and for cold water from the slope (Table 5.1). The composition of cold water was evaluated using the chloride concentration measured in several springs discharging in the gallery of the Lavey hydro power plant (average value of 3 mg/L, CRSFA 1992b).

5.1.5 Variation of the physico-chemical parameters

Since 1997, production rates of the P600 well induced the variation of the physico-chemical parameters in thermal waters. Data collected by the Alpgeo consulting office, and used in this study, showed a significant decrease of temperature and electrical conductivity in thermal waters in the two exploited wells during the period 1997-2005 (Sonney and Vuataz 2009). Orders of magnitude of decline of the temperature and conductivity are about 300 μS/cm - 5°C for the P201 well, and close to 400 μS/cm - 2°C for the P600 well. The origin explaining this decrease is detailed in the next paragraphs and is related to an increase of mixing processes with cold waters from the decompressed zone (Sonney 2007).

Short-term variations induced by the P600 production rates

Production rates imposed to the P600 well depend on the seasonal climatic conditions. As mentioned above, the P600 well mostly pumps thermal water at about 1200 L/min during the coldest periods in winter. On the contrary, periods with production rates about 1200 L/min are less frequent in summer. In summer, the well often functions with a lower mode of 300 L/min because water requirements are less important (no heating of buildings).

Table 5.1: Calculated composition of the end-members from correlations between all the physico-chemical parameters (modified from Sonney et al. 2007). Rhone groundwater was not calculated because its composition is similar to the decompressed zone and can be modified during seasonal conditions.

	Thermal component of the Aiguilles Rouges Basement (TC-ARB)	Decompressed Zone
Temp. (°C)	68	8-12
Elec. Cond. (20°C, μS/cm)	2070	390
pH	7.6	7.9
TDS (mg/L)	1560	335
CATION (mg/L)		
Li	3.9	0.15
Na	430	13.2
K	13.4	2.3
Mg	0.29	12
Ca	≈ 55	≈ 55
Sr	2.3	< 0.7
Ba	0.025	0.025
Rb	0.1	
Cs	0.06	
Al,Cr,Co,Ni,Pb,Ti,V	< 0.01	< 0.01
Cd	< 0.001	< 0.001
U	< 0.0001	< 0.0001
Ge	0.026	0.005
Hg	< 0.00001	< 0.00001
As	< 0.005	0.023
W	0.145	< 0.02
Mn	0.02	0.03
Fe	0.05	0.09
Mo	0.003	0.003
Cu	< 0.005	< 0.005
Zn	0.01	0.01
ANION (mg/L)		
F	8.7	< 1
Cl	265	3
Br	1.3	< 0.2
I	0.4	< 0.05
NO_3	< 0.1	
NO_2	< 0.005	< 0.005
PO_4	< 0.5	< 0.5
SO_4	618	67
HCO_3	70	160
UNDISSOCIATED (mg/L)		
SiO_2	79	< 15
B	2.8	< 2
GAS (mg/L)		
H_2S	3.5	< 0.1
IONIC BALANCE		
Cation (meq/L)	22.45	4.20
Anion (meq/L)	21.98	4.20
Balance (%)	1.05	-0.03
ISOTOPE		
Tritium (TU)	< 0.5	> 10
Deuterium (‰)	-98.5	-87.9
Oxygen-18 H_2O (‰)	-13.4	-12.3

A pumping test of 6 hours was carried out in September 2006 in the P600 well with the assistance of the Alpgeo consulting office. The P201 production rate was not modified during the same test. The objective was to decipher mixing processes occurring with the change of pumping rates. To undertake it, it was decided to follow the evolution of physico-chemical parameters in the pumped water from the P600 well after a sudden increase of the rate from 300 L/min to 1200 L/min, while maintaining the high rate during the 6 hours. Measurements of the parameters were realized with steps in the range 30 seconds - 5 minutes. Samples were taken in precise times for ionic analyses. During the first nine minutes, the rise of the pumping rate caused an increase of the temperature (+0.9°C) whereas the conductivity remained more or less stable (Fig.

5.5). This process is related to an increase of the flow velocities inside the well. Consequently, exchanges of heat due to the conduction process were reduced. After nine minutes, an additional contribution of cold waters was proven and generated a reduction of the temperature (- 0.7°C) and the conductivity (- 25 μS/cm). This dilution was accompanied by a fall of the chloride concentration (- 10 mg/L) and a rise of the magnesium content (+0.3 mg/L). On the basis of these results, it can be assumed that the cold component comes from waters of the decompressed zone because the P600 is cased until 254 metres below the surface, and thus is not subjected to dilution with the Rhone groundwater. At the end of 45 minutes, the mixing processes was attenuated.
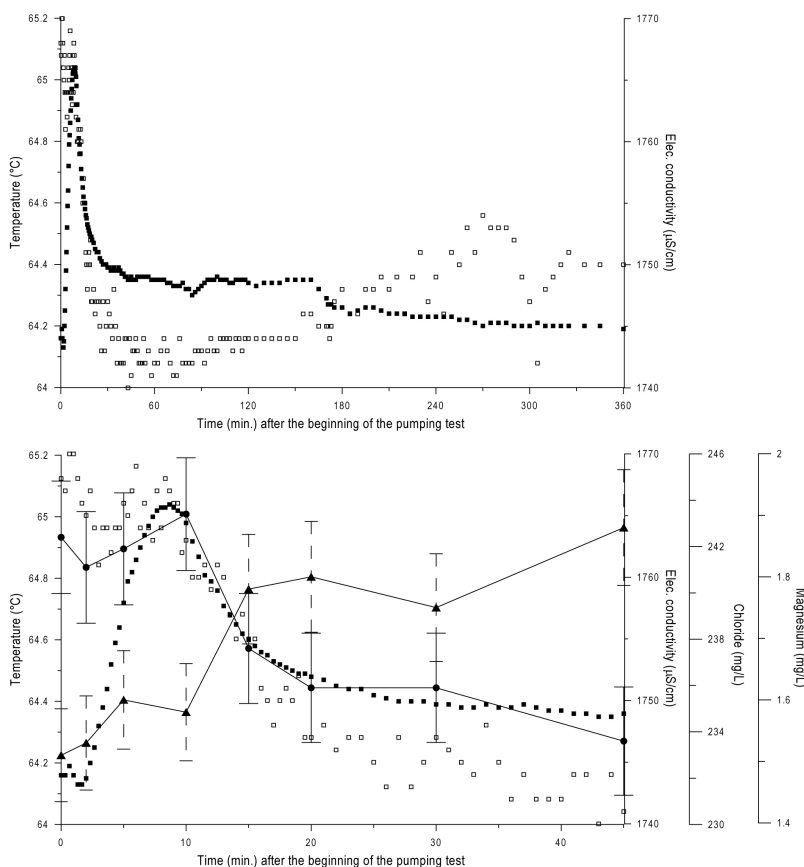
Figure 5.5: Variation of the physico-chemical parameters in the P600 well during a short pumping test with rates from 300 L/min to 1200 L/min (test realized in September 2006). Temperature, electrical conductivity, chloride and magnesium concentrations are symbolized with full squares, empty squares, circles and triangles respectively. These used analyses can be validated with error bars of 1% and 5% respectively for chloride and magnesium contents.

96

Long-term variation since the exploitation of the P201 well

Since 1997, the exploitation of the P600 well generated a significant decrease of temperature and conductivity in the pumped fluid. Data measured in the P201 since the exploitation of this well in 1973 showed a reduction of both these parameters, ranging from 62 to 57°C and from 1800 to 1300 μS/cm between 1997 and 2002. Concerning the P600 well, this diminution is less pronounced during this same time period. Collected data indicated a decrease from 68 to 65°C and from 2000 to 1700 μS/cm during the first two year of production (Fig. 5.6).

This process can be explained by an increase of mixing during the period 1997-2002 between the Na-SO$_4$ thermal end-member and the less mineralized Ca-HCO$_3$ cold water flowing in the decompressed zone of the fractured gneiss. It can be noticed that concentrations of major ions in waters of the P201 are significantly reduced after 1997, with the exception of magnesium and bicarbonate contents considered as natural markers of the cold water (Sonney 2007). Moreover, tritium analyses showed the existence of a recent component younger than nuclear weapons tests in waters of P600 (1 T.U.±0.5) and in waters of P201 (2.3 T.U.±0.4). This difference of tritium contents is related to various mixing rates, the P201 well being more diluted. After 2002, the decrease of temperature and conductivity tends to be attenuated. For the P201, the collected data enabled the seasonal cycles to be defined by relating the exploitation of the thermal aquifer with different production rates during summer and winter periods. For this reason, mixing processes are more important during winter and consequently, measured temperatures as well as conductivities are lower (Fig. 5.6).

These seasonal cycles for temperatures are not easily visible before 2005, but are more marked between 2005 and 2007. The annual average temperature in P600 and P201 wells continued to decrease after 2001 but not as significantly as the first five years of the P600 production (1997-2001). It is difficult to explain why conductivities tend to be stabilized after 2001 whereas temperatures continued to reduce slowly up to 2005. Other processes such as heat exchanges by conduction due to the modification of exfiltration velocities from the deep reservoir the wells can explain this phenomenon. The average water levels in the two wells have stabilized since 2001 (Sonney 2007). Consequently, the thermal aquifer is not overexploited from a quantitative point of view.
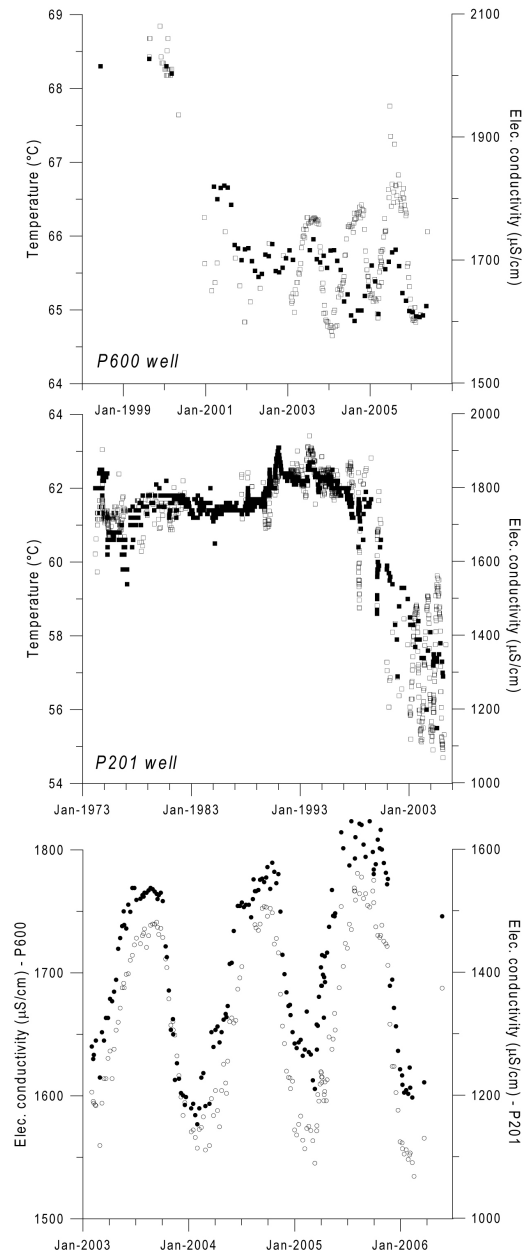
Figure 5.6: Variations of temperatures and conductivities in the two exploitation wells (from Alpgeo data, Sonney and Vuataz 2009). Temperature and electrical conductivity are symbolized with full and empty squares respectively. P600 and P201 data are represented with full and empty circles respectively.

5.1.6 Water-rock interactions

Chemical equilibrium

Thermal waters circulate into fractures of gneiss, and thus minerals in these fractures are subjected to reactions of dissolution/precipitation. To remind the minerals composition of rocks of the Aiguilles Rouges Massif, rocks contain primary minerals such as quartz, albite, anorthite and K-feldspar, and secondary minerals such as biotite, muscovite, garnet, chlorite, etc. Moreover, there are also other minerals present in the fractures forming slip veins. They are millimetre in length or greater, and are mostly sulphide and carbonated minerals which are also subjected to reactions of dissolution and precipitation as well as primary minerals. Gypsum, anhydrite and halite are taken into account in this section due to the high concentrations of sulphate, chloride and sodium measured in thermal waters.

Fluid-mineral equilibria for the thermal end-member and the P600, P201 and AP wells were computed with the PHREEQC code (version 2.12.04) developed by Parkhurst and Appelo (1999). Saturation indices (SI) calculated for alumino-silicates depend on the aluminum contents. Mostly, negative SI values were found for feldspars

and chlorite with aluminum contents lower than 10 $\mu g/L$. The four waters are often over-saturated with respect to the muscovite. The thermal component and P600 are in equilibrium with the kaolinite for aluminum contents reaching 0.01 mg/L (Table 5.2).

Waters are clearly in equilibrium with calcite and aragonite which are controlled by their solubility in relation to temperature. Waters are under-saturated with respect to dolomite, except for AP which has significantly higher magnesium concentrations. They are also under-saturated in gypsum and anhydrite because sulphate contents are not high enough to reach equilibrium. Thus, the presence of Triassic evaporites along the deep flow system is doubtful because waters circulating in evaporites often reach equilibrium with gypsum.

Calculated SIs of quartz are positive about 0.7 whereas SIs of chalcedony for thermal water are closer to equilibrium (0.4). These results could indicate the occurrence of silica precipitation in fractures of gneiss during the uprising. Consequently, calculation of the reservoir temperature using the silica geothermometers can be under-estimated.

Origin of sodium and chloride in waters

Lavey-les-Bains waters were compared with other thermal waters in the Alps range and neighbouring areas to decipher the origin of the sodium and chloride contents. The bromide compound is a good marker to define if the salinity comes from the leaching seawater brines, from fluid inclusions, or from halite and halite-rich gypsum dissolution which often occur in the Triassic formations. For the seawater, the Cl/Br molar ratio is close to 655 whereas it increases (> 1000) for groundwater leaching from halite rich formations (Alcalá and Custodio 2008, Sonney and Vuataz 2010a).

The Cl/Br ratios for Lavey-les-Bains waters belong to the family of hydrothermal sites with waters circulating in crystalline rocks (Fig 5.7). It strongly suggests the presence of deep saline water in the Aiguilles Rouges basement with a composition close to present day seawater. However, the sodium and chloride compounds certainly do not come from the

Aiguilles Rouges Triassic cover because the cover contains little halite (Sonney and Vuataz 2010a). Moreover, low chloride contents (< 5 mg/L) can be measured in thermal waters in the Val d'Illiez resulting from a deep flow system in the Triassic cover (Bianchetti et al. 1992). Consequently, the likely source of Na-Cl in the deep waters is from trapped saline water or fluid inclusions, diluted to various degrees by meteoric waters in the Aiguilles Rouges Massif. However, the hydrolysis of biotite in crystalline rocks (Edmunds et al. 1985) can also explain the occurrence of high chloride concentrations in thermal water.

The Na/Cl ratios in TC-ARB and P600 waters are respectively close to 2.5 and 2.4. In the two cases, the quantity of sodium is higher than chloride. This suggests a second origin of sodium from fluid-rock reactions. For Lavey-les-Bains thermal waters, sodium is certainly related to plagioclase

Table 5.2: Calculated saturation indices of Lavey-les-Bains waters for analyses in August 2007 except for the evaluated thermal end-member (TC-ARB) and the deep fluid in the reservoir. In absence of precise Al analyses, SIs of alumino-silicates are calculated using different Al contents.

Minerals	Formula	TC-ARB	P600	P201	AP	Deep Fluid
Albite	$NaAlSi_3O_8$					
	Al = 0.001 mg/L	-1.8	-1.9	-1.8	-2.1	*with Al = 0.006 mg/L*
	Al = 0.005 mg/L	-1.1	-1.2	-1.1	-1.4	-1.7
	Al = 0.01 mg/L	-0.75	-0.88	-0.77	-1.1	
Anorthite	$CaAl_2Si_2O_8$					
	Al = 0.001 mg/L	-5.0	-5.1	-5.0	-4.8	
	Al = 0.005 mg/L	-3.6	-3.7	-3.6	-3.4	-2.9
	Al = 0.01 mg/L	-3.0	-3.1	-3.0	-2.8	
K-feldspar	$KAlSi_3O_8$					
	Al = 0.001 mg/L	-1.4	-1.5	-1.3	-0.82	
	Al = 0.005 mg/L	-0.69	-0.79	-0.57	-0.12	-1.6
	Al = 0.01 mg/L	-0.39	-0.49	-0.27	0.18	
Muscovite	$KAl_3Si_3O_{10}(OH)_2$					
	Al = 0.001 mg/L	-0.10	0.05	1.1	4.0	
	Al = 0.005 mg/L	2.0	2.2	3.2	6.1	1.3
	Al = 0.01 mg/L	2.9	3.1	4.1	7.0	
Chlorite	$Mg_5Al_2Si_3O_{10}(OH)_8$					
	Al = 0.001 mg/L	-6.6	-3.4	-4.1	-5.0	
	Al = 0.005 mg/L	-5.2	-1.9	-2.7	-3.6	-2.9
	Al = 0.01 mg/L	-4.6	-1.4	-2.1	-3.0	
Kaolinite	$Al_2Si_2O_5(OH)_4$					
	Al = 0.001 mg/L	-2.1	-1.9	-1.0	1.4	
	Al = 0.005 mg/L	-0.73	-0.53	0.41	2.8	-1.2
	Al = 0.01 mg/L	-0.13	0.07	1.0	3.4	
Quartz	SiO_2	0.70	0.67	0.69	0.65	0.42
Chalcedony	SiO_2	0.43	0.39	0.39	0.22	0.22
Amorphous silica	SiO_2	-0.28	-0.33	-0.35	-0.63	-0.40
Aragonite	$CaCO_3$	-0.20	-0.16	-0.27	0.15	-0.21
Calcite	$CaCO_3$	-0.08	-0.05	-0.15	0.30	-0.11
Dolomite	$MgCa(CO_3)_2$	-2.1	-1.2	-1.1	0.09	-2.6
Fluorite	CaF_2	0.11	-0.14	-0.28	-1.1	0.00
Pyrite	FeS_2	22	22	23	24	20
Goethite	$FeOOH$	6.5	6.5	6.7	7.5	5.9
H_2S(gas)	H_2S	-3.7	-3.8	-3.6	-5.3	-3.1
Gypsum	$CaSO_4:H_2O$	-1.2	-1.2	-1.2	-1.4	-0.96
Anhydrite	$CaSO_4$	-1.1	-1.1	-1.2	-1.7	-0.42
Halite	$NaCl$	-5.7	-5.8	-5.9	-7.5	-5.6

weathering from albite with long-time flow within the basement (Henley et al. 1984). The importance and significance of plagioclase dissolution to the evolution of groundwater in crystalline rocks has been demonstrated by field studies from other basement complexes (Gascoyne and Kamineni 1994 in Stober and Bucher 1999).

Arthaud and Dazy (1989) studied the high chloride concentrations in thermal waters along the major thrust faults of the external crystalline massifs in the Western Alps (Fig. 5.8). They assumed that the high chloride contents in thermal waters would probably come from the migration of old marine waters. These waters were expelled from tectonically compacted rocks towards fractured deep reservoirs in the foot-wall of major thrust sheets.

In the Lavey-les-Bains case study, the concerned thrust fault is located at depth between the Aiguilles Rouges and Infra-Aiguilles Rouges Massifs with deep circulations taking place in vertical fractures of gneiss before reaching the thrust fault system. Other hydrothermal sites along the external crystalline massifs are also concerned by this process such as Saint-Gervais-les-Bains. Other examples were illustrated in the Argentera Massif, the most southerly external crystalline massif in France and Italy (Fig. 5.8), where the leaching of seawater brines or fluid inclusions was demonstrated in thermal waters at Terme di Valdieri (Baietto et al. 2008), Bagni di Vinadio and Berthemont-les-Bains (Perrelo et al. 2001). In these three cases, the presence of chloride ions in thermal waters is clearly not related to the leaching of Triassic evaporites.
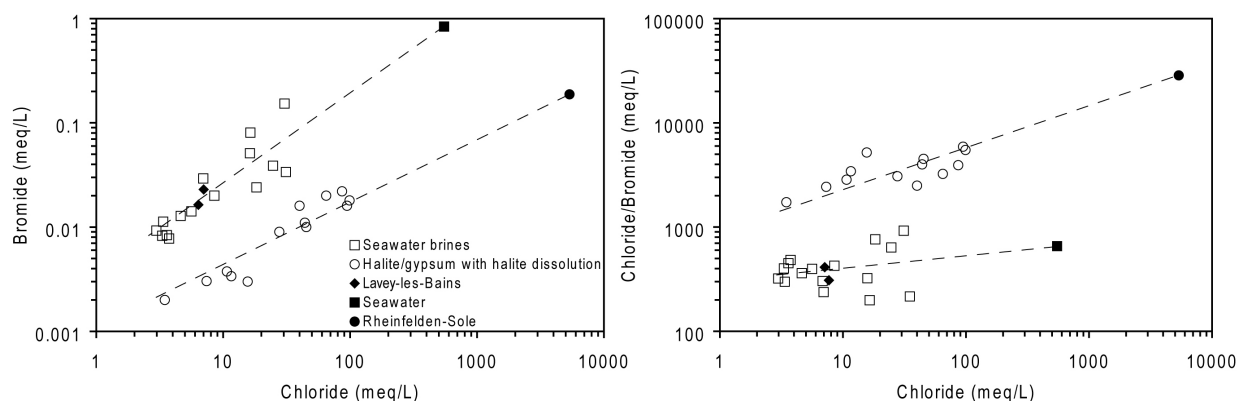
Figure 5.7: Plots of chloride content versus bromide and chloride/bromide ratio in thermal waters for the Alps range and neighbouring zones. All selected waters have a chloride content higher than 100 mg/L. The chloride origin is function of the reservoir geology: basement with seawater brines (squares) or Mesozoic sedimentary rocks rich in halite or gypsum containing halite (circles). The Rheinfelden brine is a subthermal spring in the north of the Molasse Basin, along the Rhine River in Switzerland (location given in Sonney and Vuataz 2008), which dissolves Triassic halite formations.

Origin of sulphate in waters

The origin of sulphate contents in Lavey-les-Bains waters was initially studied by Bianchetti (1994) using the sulphur-34 and oxygen-18 isotopes in sulphate measured in P201 and P205 waters in 1990. These values were compared to other thermal waters in the Alps from data available in Bianchetti (1993b). The sulphur-34 content gives information about the sulphur cycle in groundwater, especially

with respect to the dissolved species SO_4^{2-}, H_2S and HS^-. The oxygen-18 content in sulphate is related to the origin of sulphate and is also an indicator of oxidation-reduction processes. Globally, the interpretation of these stable isotopes in groundwaters enables the origin of dissolved sulphate to be defined: Triassic evaporites dissolution, oxidation of sedimentary sulphides in rocks, leach-

ing of residual seawater brines, etc. (Fouillac et al. 1990). Difficulties in interpretation can be met because the sulphur-34 and oxygen-18 values of marine evaporite sulphate minerals vary with their geologic age due to changes in the isotopic composition of oceanic sulphate (Pearson et al. 1991).
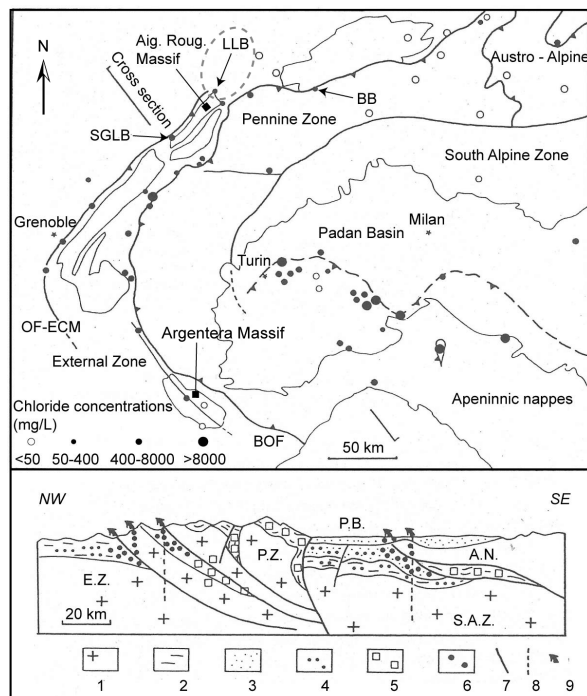
Figure 5.8: Simplified map and cross section of the Alps range with location of the main thrusts and chloride springs (modified after Arthaud and Dazy 1989).

Lavey-les-Bains = Lavey-les-Bains, BB = Brigerbad, Saint-Gervais-les-Bains = Saint-Gervais-les-Bains, BOF = Briançonnais Overthrust Fault, OF-ECM = Overthrust Fault of the External Crystalline Massifs. 1: crystalline basement, 2: sediments, 3: Po Basin, 4: non migrated brines, 5: id. fixed by metamorphism, 6: id. migrated and/or concentrated, 7: major faults, 8: seismic fault, 9: spring.

For thermal waters in the Alps leaching Triassic evaporites, oxygen-18 values are higher and sulphur-34 are lower compared to thermal waters flowing in a crystalline domain (Fig. 5.9). Data in both P201 and P205 waters coincide with values of a crystalline domain and are also close to the present day seawater. Therefore, sulphates in thermal waters at Lavey-les-Bains would come from the leaching of seawater brines or fluid inclusions, probably

coupled to the oxidation of sulphides such as pyrite in rocks of the Aiguilles Rouges basement. Finally, correlations between sulphate contents versus stable isotopes are not good because high sulphate contents can be measured in waters flowing in the crystalline domain as well as in the Triassic formations. Moreover, in the area of Bex 5 kilometres downstream from Lavey-les-Bains, isotopic values in waters in Triassic formations are close to $+16‰$ and $+14‰$ for ^{34}S and ^{18}O respectively (Balderer 1990, Claypool et al. 1980 in Muralt 1999), that is to say strongly different to Lavey-les-Bains waters.

Even if concentrations exceed several hundreds of mg/L in sulphate, the presence of sulphate in Lavey-les-Bains waters can be assumed by the combination between the leaching of seawater brines or fluid inclusions and the oxidation of sulphides contained in fractures of gneiss. Chemical reactions leading to sulphate from sulphide was described by Stumm and Morgan (1981) and reminded in Bianchetti (1994):

$$FeS_{2\ (S)} + 7/2\ O_2 + H_2O \rightleftharpoons Fe^{2+} + 2SO_4^{2-} + 2H^+$$

$$Fe^{2+} + 1/4\ O_2 + H^+ \rightleftharpoons Fe^{3+} + 1/2\ H_2O$$

$$Fe^{3+} + 3H_2O \rightleftharpoons Fe(OH)_{3\ (S)} + 3H^+$$

$$FeS_{2\ (S)} + 14Fe^{3+} + 8H_2O \rightleftharpoons 15Fe^{2+} + 2SO_4^{2-} + 16H^+$$
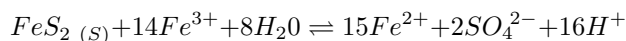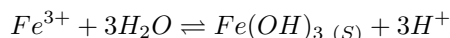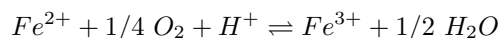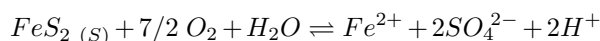
The origin of the hydrogen sulphide in thermal waters (3 mg/L in the P600 well) can be explained by the following chemical reaction, showing the transformation of sulphate to dissolved H_2S with the presence of Desulfovibrio Desulfuricans bacteria (Lloyd and Heathcote 1985 in Bianchetti 1994):

$$SO_4^{2-} + 10H^+ + 8e^- \rightleftharpoons H_2S + 4H_2O$$
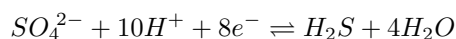
The plot between calcium and sulphate molar concentrations in Alpine thermal waters (Fig. 14.6) also indicates mineral-chemical processes occurring in a crystalline domain to explain the origin of sulphate in Lavey-les-Bains waters. Alpine thermal waters dissolved Triassic evaporites have Ca/SO_4 ratio close to 1 if waters are not subjected to other chemical processes changing the calcium content. Lavey-les-Bains waters have a strong excess of sulphate compared to calcium and the assumption of massive clay exchanges between sodium and calcium cannot be assumed in this context.
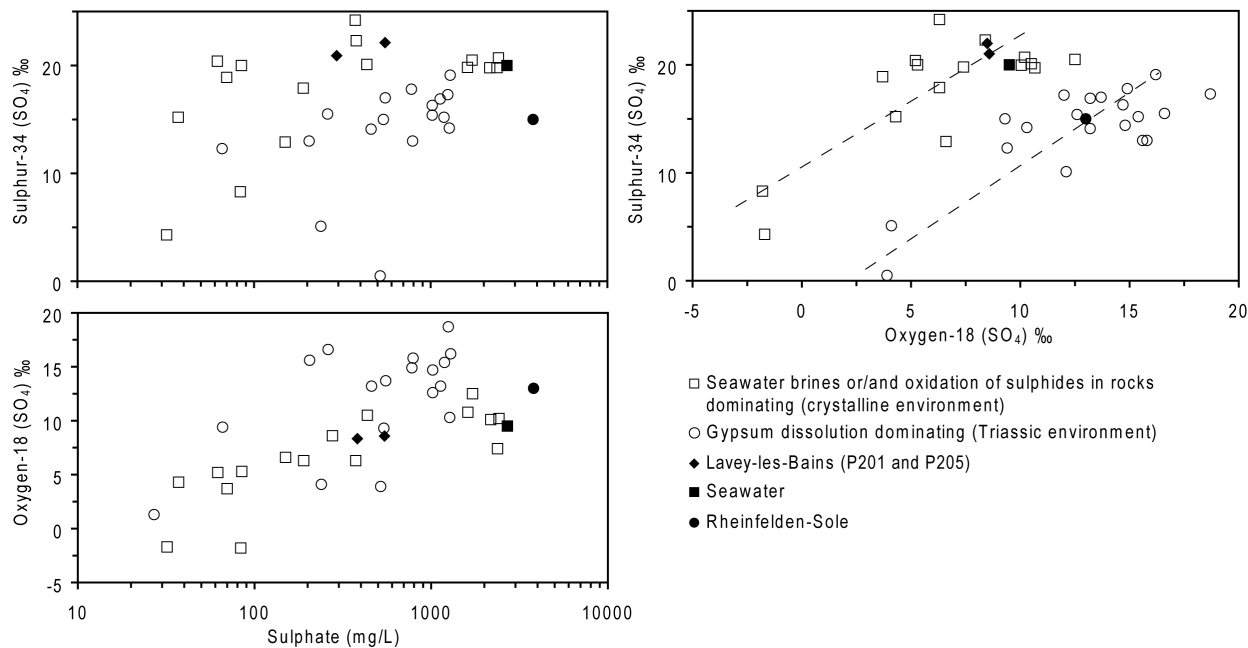
Figure 5.9: Plots of sulphate contents and sulphate isotopes in thermal waters for the Alps range. The sulphate origin is function of the reservoir geology: basement with seawater brines or/and oxidation of sulphides in rocks (squares) or Mesozoic sedimentary rocks containing gypsum formations (circles). There is no direct data for Rheinfelden-Sole but representative data of waters in Keuper located close to this brine (black circle) showed values of 13‰ and 15‰ respectively for oxygen-18 and sulphur-34 (Pearson et al. 1991). Data for Lavey-les-Bains (diamonds) are positioned in the square zone, coming from Bianchetti (1993b).

5.1.7 Chemical and isotopic composition of the deep fluid

The chemical composition of the deep fluid was computed with the PHREEQC code (version 2.12.04) developed by Parkhurst and Appelo (1999) for the AGEPP project (Sonney et al. 2007). To realize the simulation, the TC-ARB composition was employed, and an increase of temperature from 68 to 105°C was imposed to the model. The value of 105°C was selected according to the study of mineral-chemical equilibria occurring in the reservoir (see section 5.2.3).

The simulation requires formulating assumptions based on hydrogeological, hydrodynamical, and geochemical properties of the deep confined aquifer. Firstly, the crystalline aquifer is considered geologically homogeneous in its width and height until 2-3 kilometres depth. For simplification reasons, this assumption excludes the presence of other rocks at depth such as sedimentary rocks. In re-

ality, a sedimentary aquifer pinched in the thrust fault system is assumed based on the interpretation of the seismic profile realized in the Rhone Valley. Secondly, the cooling of the uprising thermal end-member before mixing with cold water from the decompressed zone is only due to heat loss due to the conduction process. Thirdly, a mineral-chemical equilibrium occurs between the deep fluid and the rocks forming the reservoir. This condition implies a long residence time to reach equilibrium. In reality, this assumption cannot be validated in the Lavey-les-Bains case because equilibrium with feldspars requires having a higher reservoir temperature (> 150°C, Fournier 1981).

Results of the simulation are illustrated in the Table 5.3. The calculated TDS of the deep fluid is close to 1900 mg/L, therefore higher than the TDS of the TC-ARB (1560 mg/L). The geochemi-

cal type of the deep fluid remains similar compared to the thermal water with an acceptable ionic balance. This calculated composition was accepted for the AGEPP project what allowed assuming interesting chemical properties for the deep fluid. For this kind of fluid, potential problems with corrosion and precipitation are limited with the exploitation of water.

Concerning trace elements, computed concentrations in the deep fluid vary slightly from the TC-ARB composition, except for the aluminum content which increases from 2 μg/L (selected value for the simulation) to 6 μg/L.

The simulated pH was at 7.2 whereas in reality it was around 7.6 for TC-ARB. It can be explained by a decrease in $CO_{2\ (gas)}$ partial pressure during the uprising of the deep fluid from the reservoir.

Fluid-mineral equilibria for the simulated deep fluid were calculated with the PHREEQC code (Table 5.2). Saturation indices (SI) calculated for alumino-silicates with aluminum content equal to 6 μg/L gave negative values with respect to feldspars, chlorite and kaolinite. On the contrary, the fluid is equilibrated with calcite and aragonite, also controlled by their solubility in relation to temperature. The deep fluid is under-saturated with respect to dolomite because it has significantly lower magnesium content, and is also under-saturated in gypsum and anhydrite because the computed sulphate content is not enough high to reach equilibrium. Finally, calculated SI of quartz is positive about 0.4 whereas SI of chalcedony is closer to equilibrium (0.22).

Table 5.3: Computed composition of the deep fluid at 105°C using the PHREEQC code.

	Deep fluid
Temp. (°C)	105
Elec. Cond. (20°C, μS/cm)	2500
pH	7.2
TDS (mg/L)	1890
CATION (mg/L)	
Li	4.8
Na	525
K	16.4
Mg	0.34
Ca	61
Sr	2.8
Ba	0.03
Rb	0.1
Al	0.06
Ge	0.026
As	< 0.005
W	0.15
Mn	0.024
Fe	0.061
Mo	0.003
Zn	0.012
ANION (mg/L)	
F	9.3
Cl	315
Br	3.3
I	0.4
SO_4	768
HCO_3	72
UNDISSOCIATED (mg/L)	
SiO_2	96
B	3.4
GAS (mg/L)	
H_2S	7.2
IONIC BALANCE	
Cation (meq/L)	27.09
Anion (meq/L)	26.59
Balance (%)	0.94
ISOTOPE	
Tritium (TU)	< 0.5
Deuterium (‰)	-98.5
Oxygen-18 H_2O (‰)	-13.4

5.2 Regional hydrogeological and geochemical investigations

5.2.1 Regional deep flow system

Investigations based on geological, hydrogeological and geochemical methods made possible the building of a regional conceptual model of the deep flow system. The hydrothermal sites of Saint-Gervais-les-Bains and Val d'Illiez were added to the model for comparison in their geological and geochemical settings (Fig. 5.10). As described previously, Lavey-les-Bains and Saint-Gervais-les-Bains hydrothermal sites are both low-elevation points in the Aiguilles Rouges Massif. Pumped waters at Lavey-les-Bains have chemical and isotopic characteristics similar to Saint-Gervais-les-Bains thermal waters, Na-SO$_4$ waters rich in chloride (Sonney and Vuataz 2010d). Lavey-les-Bains waters are hotter than Saint-Gervais-les-Bains waters (65°C against 40°C) but less mineralized (1.5 g/L against 4.8 g/L). This difference in temperature probably results from deeper circulations for the Lavey-les-Bains thermal regime. It could be related to a deepening of the thrust fault system between Aiguilles Rouges and Infra-Aiguilles Rouges Massifs towards the north-east. Various mineral-chemical processes implying rock alterations and leaching of seawater brines or fluid inclusions can explain the difference in mineralization.

An example of a deep flow system in the autochthonous cover is represented by the hydrothermal system in the Val d'Illiez in Switzerland. Thermal waters in the Val d'Illiez at 30°C result in a flow path in the autochthonous cover from the Salanfe Lake area (Bianchetti et al. 1992), and have a different geochemical type (Ca-SO$_4$ poor in chloride). Therefore, a flow path in this autochthonous cover explains why the occurrences of Lavey-les-Bains thermal waters can be excluded.

Infiltration and circulation of surface water leading to the Lavey-les-Bains thermal water should take place mainly in Variscan and Alpine NNE to NE structures in the Aiguilles Rouges basement (Lhomme et al. 1996, Von Raumer and Bussy 2004). In the southern part of the Aiguilles Rouges Massif, groundwaters follow another direction. They flow towards the second lowest elevation point of the Aiguilles Rouges Massif where the Saint-Gervais-les-Bains hydrothermal site is located, with emergence temperatures of water close to 40°C.

Hydraulic conductivities of crystalline rocks in the Aiguilles Rouges Massif certainly decrease with the depth due to the increase of the pressure causing the tightening of fractures. Without major vertical faults, groundwaters remain in the first hectometres of depth in the decompressed zone, and would generate only to cold springs at the foot of slopes. With the presence of major vertical faults which have higher hydraulic conductivities, groundwaters can reach greater depth until thrust faults. The uprising of the deep fluid is often facilitated by the presence of several major directions of fracture. For the Lavey-les-Bains case, extension cracks of NNW-SSE direction parallel to the Rhone Valley, NE-SW brecciated faults and low dip thrust faults are met and certainly drain the uprising thermal water towards the surface.

The Lavey-les-Bains hydrothermal site is located on the right bank of the Rhone Valley, whereas the infiltration area is assumed to be on the other side of the valley. Therefore, Lavey-les-Bains waters have to circulate at depth below the Quaternary filling reaching 600 metres depth. Mixing processes in the Quaternary filling take place where the uprising of thermal water occurs, in the most permeable layers such as the recent alluvial deposits.

5.2.2 Mean elevation of the recharge zone

The elevation of the infiltration area is estimated with data of water stable isotopes and with the relation from Kullin and Schmassmann (1991) for the Bernese Alps (Table 5.4). The location of Lavey-les-Bains in the Western Alps implies that this relation is more appropriate than those given in Blavoux (1978), Bortolami et al. (1979) and Vuataz (1982). Isotope values for Lavey-les-Bains waters are aligned along the World Meteoric Water Line of Craig (1961), as well as Saint-Gervais-les-
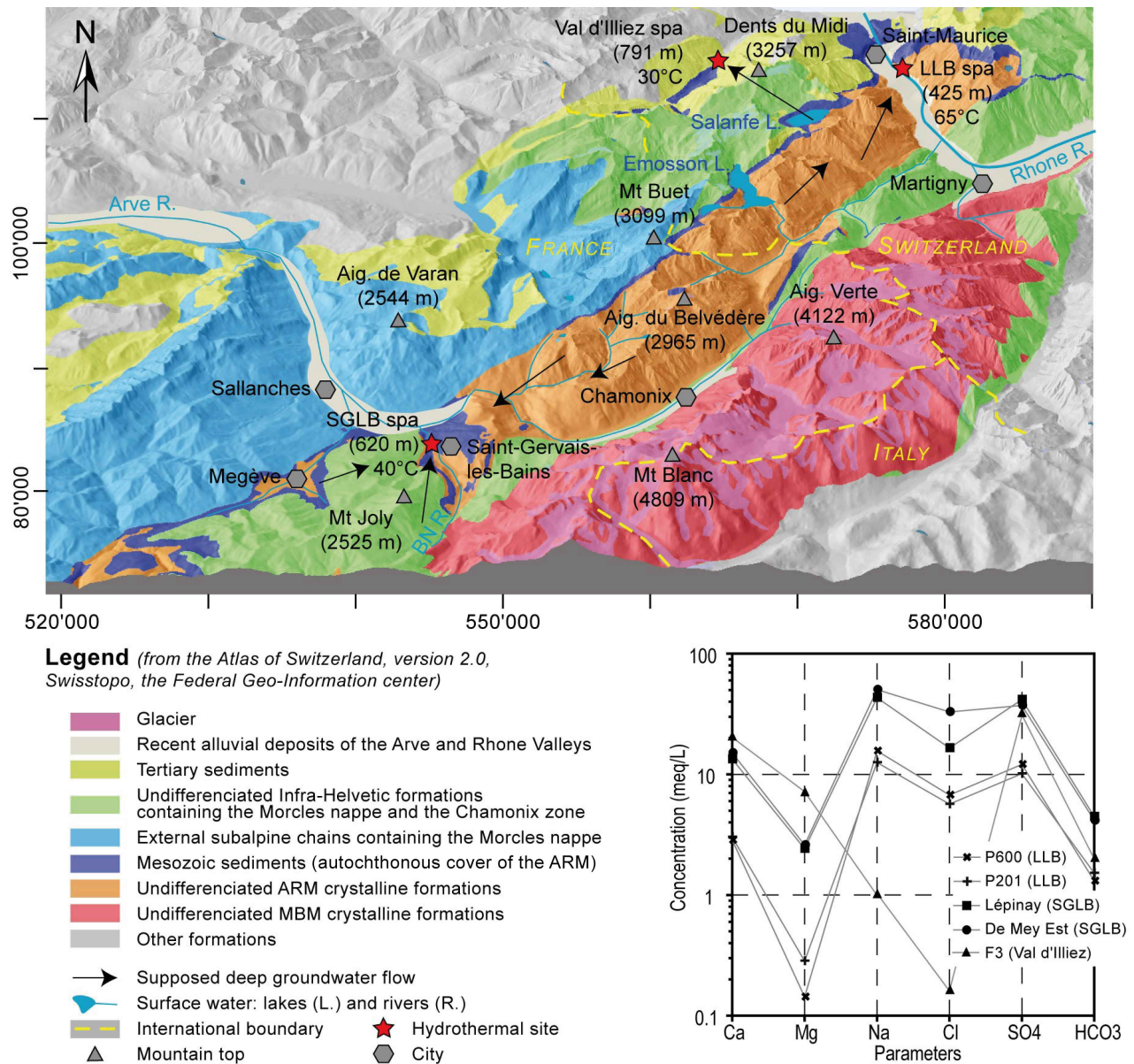
Figure 5.10: Regional conceptual model of the different flow paths ending to the hydrothermal systems of Lavey-les-Bains (LLB), Saint-Gervais-les-Bains (SGLB) and Val d'Illiez. Major element concentration plot (modified Shoeller diagram) for P600 and P201 waters is compared to waters of the two production deep boreholes in Saint-Gervais-les-Bains (Lépinay and De Mey Est) and of the well F3 in the Val d'Illiez. Location refers to the Swiss kilometric coordinates in projection, in standard CH1903. ARM: Aiguilles Rouges Massif, MBM: Mont-Blanc Massif.

Bains, Val d'Illiez and other Alpine thermal waters (Fig. 5.11). Therefore, there is no enrichment in oxygen-18 in spite of the relative high temperature of the reservoir estimated around 100-110°C (chapter 5.2.3).

For Lavey-les-Bains waters, the average elevation of the recharge zone is about 1800-1900 metres using the relation for the Bernese Alps. Results given by other formulas are slightly lower. Considering the recharge zone located in the Aiguilles Rouges Massif has an average elevation of 1800-2200 metres, it can be assumed that the estimation is consistent.

Waters in E1 and E2 boreholes at Epinassey located on the left bank of the Rhone Valley, opposite to Lavey-les-Bains, are strongly mixed with relatively cold waters compared to Lavey-les-Bains waters (respectively 9.8 and 21.5°C in Bianchetti 1994). Calculated elevations for both sampling points are significantly lower, in the range 800-900 and 1200-1400 metres for E1 and E2 respectively. This observation indicates that the cold component should circulate in the Epinassey fan delta and in the gneiss of the Dent de Salantin slope (see location in Figure 6.1).

The study of mixing processes occurring at Lavey-les-Bains showed that the deepest boreholes are not diluted by the Rhone groundwater but with cold water from the decompressed zone. This process is also demonstrated by water stable isotopes. Indeed, isotope values in the Rhone River are much lower than in P600 water and for the thermal end-member. If mixing processes occur with the Rhone

groundwater, the isotope values should be much higher as showed before in the Epinassey case.

With the absence of new investigations establishing other relations between water stable isotopes and the elevation of the infiltration area, the evaluation initially made by Bianchetti (1994) around 1700-2100 metres can be validated. Moreover, isotope values in Lavey-les-Bains waters are close to those in Val d'Illiez waters (Fig. 5.11). The deep flow system of Val d'Illiez starts from infiltration in the autochthonous cover in the Salanfe Lake area, around 1900 metres in elevation (Bianchetti et al. 1992, see Figure 5.10).
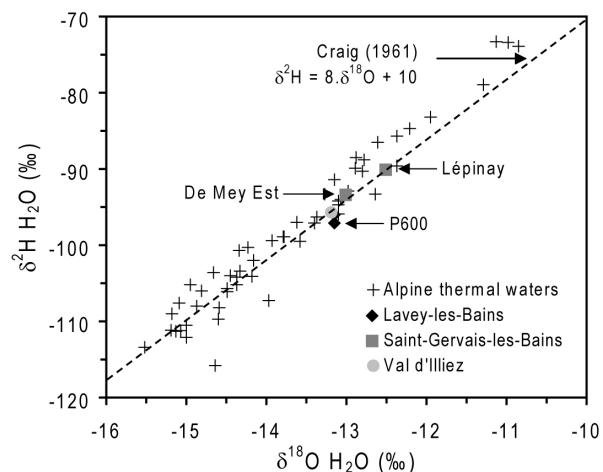
Figure 5.11: Water stable isotopes plot for Alpine thermal waters.

5.2.3 Reservoir temperature

Evaluation with geothermometers

Traditional and multi-component geothermometers were applied to estimate the reservoir temperature. Assumptions formulated to use this method consist of assuming fluid-mineral equilibria, equilibration between mineral assemblages in the reservoir, and stabilization of dissolved chemical elements during uprising before mixing. First geothermal assessments of the reservoir temperature at Lavey-les-Bains are around 100°C based on chemical geothermometers (Bianchetti 1994, Vuataz 1982). Based on the total dissolved silica, cal-

culated temperatures for TC-ARB indicate 96°C with the chalcedony geothermometers from relations of Fournier (1977) and Arnórsson et al. (1983) (Table 5.5). Theoretically, for reservoir temperatures in the range of 120-160°C, the chalcedony geothermometer is usually more adapted than the quartz geothermometer (Arnórsson 1983), due to aqueous phase equilibrium depending on reservoir temperature (Arnórsson 1975). Results using quartz from relations of Fournier (1977) and Truesdell (1976) are not presented in this study. The sil-

Table 5.4: Calculated elevation of the infiltration area with the water stable isotopes for waters of Lavey-les-Bains and Epinassey and for the Rhone River. E1 and E2 in Epinassey are two boreholes with subthermal waters crossing the gneiss. They are located on the left bank of the Rhone Valley opposite Lavey-les-Bains. Isotope-elevation equations in Switzerland and neighbouring areas are given in the chapter 2.2.9 and in Pearson et al. (1991). Some of these equations were not selected for this hydrothermal system.

Sampling date, reference	Well. Riv	$\delta^{18}O$ (H_2O) ‰	δ^2H (H_2O) ‰
12.09.2006 (Sonney 2007)	P600	-13.15	-97.1
12.09.2006 (Sonney 2007)	P201	-13.15	-96
09.12.1991 (Bianchetti 1993b)	E1	-10.73	-77.6
21.02.1992 (Bianchetti 1993b)	E2	-11.86	-86
16.08.1990 (Bianchetti 1993b)	Rhone	-14.61	-103.1
Domain, reference		Calculated elevation (m)	
Bernese Alps	P600	1794	1931
	P201	1794	1846
	E1	371	431
Kullin and Schmassmann 1991	E2	1035	1077
	Rhone	2653	2392
Jura, Northern Alps	P600	1726	1807
	P201	1726	1756
	E1	838	912
Vuataz 1982	E2	1253	1297
	Rhone	2262	2082
Lemanic Prealps	P600	1683	1680
	P201	1683	1636
	E1	877	900
Blavoux 1978	E2	1253	1236
	Rhone	2170	1920
Maritime Alps	P600	1641	1847
	P201	1641	1803
	E1	865	1064
Bortolami et al. 1978	E2	1228	1402
	Rhone	2109	2088

ica geothermometers are strongly affected by mixing processes with cold waters containing low silica concentrations. Consequently, the calculation using the thermal end-member is more appropriate than using the pumped waters. Moreover, silica precipitation certainly occurs during the rise of the deep fluid and thus the calculation can be underestimated.

Cationic geothermometers using ratios between sodium, potassium, lithium and magnesium were tested in the Lavey-les-Bains case and obtained re-

sults largely overestimate the reservoir temperature. Application of these geothermometers is more suitable for high-enthalpy systems (> 150°C), containing waters reaching equilibrium with feldspars (Fournier 1981). All the Alpine hydrothermal systems have a relatively low reservoir temperature (< 150°C) compared to high-enthalpy geothermal systems. They are subjected to various mineral-chemical processes, and thus results using geothermometers of Arnórsson (1983), Fournier (1977), Fournier and Truesdell (1973), Giggenbach (1988), Kharaka et al. (1982), Kharaka and Mariner (1989),

Truesdell (1976) and Verma and Santoyo (1997) were not considered in this study.

However, the Na-K-Ca geothermometer (Fournier and Truesdell 1973) using the Mg-correction (Fournier and Potter 1979) was used because it can be applied in a crystalline environment. The thermal end-member is poor in magnesium (0.34 mg/L) and consequently, the correction is limited compared to the Na-K-Ca geothermometer. The result gave a reservoir temperature of 126°C. Chemical processes with magnesium acquisition do not allow specifying temperature circulation compared to silica and cationic ratios. Finally, the K^2/Mg geothermometer gives similar results of 121°C and 122°C respectively with Fournier (1977) and Giggenbach (1988) relations. This geothermometer was first applied to waters from low-enthalpy reservoirs which had not attained equilibrium with alkali feldspars, but were in equilibrium with K- and Mg bearing clay minerals (Nicholson 1993). The calculation of the reservoir temperature with cationic geothermometers is higher compared to the chalcedony method.

The isotope geothermometer using the fractionation of oxygen-18 in water and sulphate showed 73°C for Lloyd (1968) and 63°C for Mizutani and Rafter (1969). There is no direct measurement in TC-ARB for oxygen-18. Used data come from analyses in P600 water for oxygen-18 in water and in P201 water for oxygen-18 in sulphate assuming that they are representative to TC-ARB.

The evaluation of the reservoir temperature can be based on results using the chalcedony geothermometer (96°C). However, it was shown that chalcedony is slightly over-saturated in the deep fluid ($SI = 0.22$). Therefore, silica precipitation could take place in fractures of gneiss during the uprising of the deep fluid, and thus the calculation is probably underestimated. For this reason and assuming the occurrence of silica precipitation, the reservoir temperature can be evaluated around 100-110°C.

Table 5.5: Calculated reservoir temperatures using a selection of chemical geothermometers for Lavey-les-Bains hydrothermal system illustrated in chapter 2.2.10 and in Arnórsson 2000. The used chemical data come from the calculated thermal end-member from Table 5.1.

Reference	Calculated temperature using the thermal end-member (°C)
Fournier (1977)	$T_{SiO2,chalcedony} = 96$
Arnórsson et al. (1983)	$T_{SiO2,chalcedony} = 96$
Fournier and Potter (1979)	$T_{Na-K-Ca-(Mg-correction)} = 126$
Fournier (1977)	$T_{K^2/Mg} = 121$
Giggenbach (1988)	$T_{K^2/Mg} = 122$
Lloyd (1968)	$T_{\delta^{18}O} = 73$
Mizutani and Rafter (1969)	$T_{\delta^{18}O} = 63$

Evaluation with saturation indices

The variation of SI values with an increase of temperature from 68°C to 120°C was simulated with the PHREEQC code to evaluate the reservoir temperature. The chemical composition of the thermal end-member was used and it was assumed that the reservoir temperature does not reach 120°C. The SI curves of calcite, aragonite, fluorite and dissolved silica curves intersect the chemical equi-

librium state (SI=0) roughly in the range 100-120°C. It coincides with previous results using chalcedony and K^2/Mg geothermometers, but not with geothermometer using oxygen-18 isotopes.

The anhydrite curve is close to SI=0 for temperatures superior to 120°C, whereas the gypsum curve remains around -1 of SI. For alumino-silicates such as feldspars, kaolinite and muscovite the increase of temperature generates a great decrease of SI values. The selected concentration of aluminum in the thermal-end-member for the simulation was 3 μg/L.

The reservoir temperature calculated with the two methods tends to give the same range of values: 100-110°C with geothermometers and 100-120°C with saturation indices. Compared to the TC-ARB temperature (68°C), these results indicate a cooling by conduction of the deep fluid close to 30-40°C from the reservoir to the bottom of the decompressed zone where mixing processes begin to occur. This heat loss can be associated with a relative long time of uprising of the deep fluid through

fractures with high hydraulic conductivities, which probably cross the basement until the thrust fault system at the bottom of the Aiguilles Rouges Massif.

Figure 5.12: Simulation mineral saturation indices versus temperature plots for the thermal end-member.

5.2.4 Depth evaluation of the reservoir

The deep flow system leading to the Lavey-les-Bains thermal waters is certainly related to the presence of a great thrust fault system at 2-3 kilometres below the surface putting in contact two external crystalline massifs: Aiguilles Rouges and Infra-Aiguilles Rouges. The thrust fault should collect waters circulating in vertical permeable faults in the basement. However, it remains difficult to locate exactly where the thrust fault drains the deep fluid, and moreover it dips to the south-east what brings difficulties in evaluating the depth of the reservoir.

The depth of the geothermal reservoir can be also evaluated by a simplified approach considering an average geothermal gradient around 20°C/km in the infiltrated area and a reservoir temperature around 100-110°C. Considering a recharge zone is close to 2000 meters of elevation with water at 0°C and circulation at a depth of roughly 5 kilometers can be calculated from the infiltration area to the reservoir which is be located at 3 kilometers below the sea level.

5.2.5 Groundwater residence time

The information which enables the study of the groundwater residence time for the Lavey-les-Bains deep flow system are the tritium values in waters measured by Vuataz (1982), Bianchetti (1993b) and Sonney (2007), and one carbon-14 analysis measured in 1990 in the P201 well (Bianchetti 1993b). The present day tritium content in precipitation is several orders of magnitude lower than the peak reached during the period of atmospheric nuclear

weapons testing (Person et al. 1991), and for the last 10 years tritium content in precipitation has stabilized around 10 T.U. For Alpine hydrothermal systems in crystalline rocks which have mostly high residence times (older than nuclear weapons tests), the method using tritium data in waters makes possible the detection of younger waters (Fontes 1980).

Between 1990 and 1991, Bianchetti (1993b) measured tritium in waters from six sampling points

(Fig. 5.13). The plot of tritium values versus chloride shows a good correlation and mixing processes between the thermal end-member, devoid of tritium, and cold waters having tritium contents close to 25 T.U. (Bianchetti 1994). In the late 70's, cold waters had higher tritium contents around 120 T.U. giving a greater slope to the mixing line (Vuataz 1982). On the contrary, the slope of the mixing line obtained in July 2006 by Sonney (2007) is more attenuated because cold waters were impoverished in tritium (about 10 T.U.). These different results illustrate a recent residence time for the cold waters, infiltrated after nuclear weapons tests, and a residence time for the thermal end-member older than tests ($<$ 1953). The prolongation of the mixing line obtained in 1990-1991 towards a tritium value close to 0 T.U. give a chloride concentration of 265 mg/L i.e. close to the value found previously the in thermal end-member.

Investigations with tritium data cannot give a residence time for the thermal end-member. The only carbon-14 data measured in the P201 well allowed the estimation of the residence time of the pumped thermal waters (^{14}C = 23.5$\pm$3.0 pmc with $\delta^{13}C$ = 12.3 ‰ in Bianchetti 1993b). The dating method using the carbon-14 has to consider chemical processes which can influence the initial content Ai. In water, the carbon element is dissolved (CO_2, H_2CO_3, HCO_3^-, CO_3^{2-}, organic materials) and it can take part in reactions of dissolution, precipitation, adsorption, isotopic exchange with gas, min-

erals or organic materials in decomposition. Therefore, a correction factor has to be brought using the $\delta^{13}C$ value according to the equations highlighted in the section 2.2.11. At the time of the analysis in 1990, P201 waters were slightly diluted with recent cold waters. Assuming values of -20 and -25 ‰ and 110 pmc for $\delta^{13}C$ and ^{14}C respectively in cold waters, the thermal end-member should have contents around 11 ‰ and 15 pmc (Sonney 2007). Taking into account these values, the average residence time should be higher than 8000 years (table 5.6).
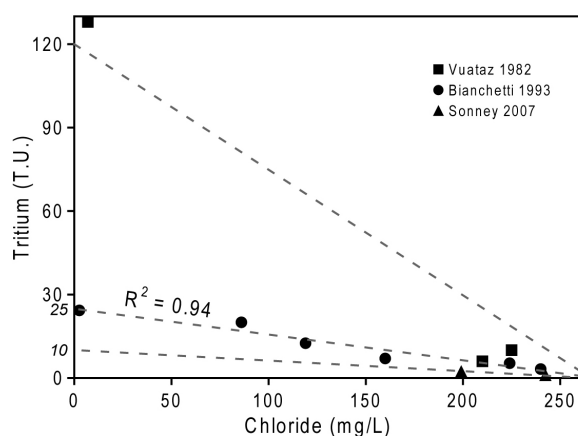
Figure 5.13: Chloride-tritium plot for Lavey-les-Bains waters.

Table 5.6: Calculation of the average residence time for the thermal end-member.

Ao	At (pmc)	$\ln(Ao/At)$	$t_{1/2}$ (years)	$t_{1/2}/\ln(2)$	Residence time (years)
44	15	1.076	5730	8267	8900
55	15	1.299	5730	8267	10800

110

6

Two-dimensional vertical modelling of groundwater flow and heat transport

6.1 Objectives

Until now, no numerical models of flow, heat and mass transport have been constructed for the Lavey-les-Bains hydrothermal system aiming to represent the deep flow system. Firstly, a simplified two-dimensional model of flow and heat transport was built through the Aiguilles Rouges Massif based on a NNE-SSW geological cross section (Fig. 6.1). Briefly, the desired objectives are:

- to represent the deep flow system from the infiltration area to the Rhone Valley imposing water inflows on the tops of the cross section and assigning various hydraulic conductivities to the geological domains.

- to simulate the Lavey-les-Bains hydrothermal anomaly below the Quaternary filling with a constant heat flux imposed at the bottom of the model and with temperatures set in the recharge zone.

- to compare the simulated results with observed data. These observed data are temperatures in wells, temperature in the geothermal reservoir, geothermal gradient, thermal water inflows from the reservoir, groundwater residence time, etc. which come from measurements in wells, data in literature and results obtained with the geochemical investigation.

- to represent the long-term effects of production rates on temperatures in wells for an optimal management scenario of the geothermal resource.

6.2 Construction of the model and assigned parameters

6.2.1 Geological boundary conditions

The two-dimensional model integrates all the geological domains until 3 kilometres depth below the Rhone Valley, assumed as the deepest flow system reaching the geological limit between the two external crystalline massifs (Pfiffner et al. 1997). The thrust fault system has a dip towards the south-east

and thus the NE-SW cross section, perpendicular to the dip direction, should follow the thrust fault roughly at the same elevation. Therefore, it was decided to keep the depth of around 3 kilometres at the bottom of the two-dimensional model and to assume the thrust fault as a geological boundary condition (Fig. 6.1).

The cross section extends from Grande Dent de Morcles to the area of Finhaut and crosses Dent de Salantin and Dent d'Emaney Massifs. Three important valleys are cut by the model including the Rhone Valley being the lowest elevation point of the topographic profile (425 m, average elevation of the hydrothermal area). The two other valleys, Vallon de Van and Le Triège, are located between the Dent de Salantin and the Dent d'Emaney Massifs and they are cut by the model at an elevation close to 1400 metres.

The numerical model is precisely ended in its north-eastern part at the Grande Dent de Morcles top. According to Bianchetti (1994), Vuataz et al. (1993) and Zahner et al. (1974), waters circulating in the sedimentary part of Grande Dent de Morcles probably do not reach in the hydrothermal area at Lavey-les-Bains. Towards the south-western part, the limit of the model is fixed after the Vallorcine shear zone and its intruded granite. The shear zone is considered as a low-permeability limit because the rocks forming the shear zone are highly compacted and fractures are completely shut.

Below the Quaternary filling, the two-dimensional model takes into account the existence of a large fractured zone which has been encountered during drilling (Fig. 6.1). This zone allows the upflow of the deep fluid towards the surface and thus it was highlighted into the model. The Quaternary filling was subdivided into three parts in the model: the permeable Rhone alluvial deposits, the glaciolacustrine deposits (aquiclude) and the Epinassey fan delta. Lateral moraines on the edges of the filling and subglacial deposits at the bottom of the filling are not represented in the model because they are too small compared to the scale of the model.

The infiltration and circulation of waters in the basement are more important in the decompressed zone and locally occur deeply in vertical faults. A contrast of permeability exists in the basement from the surface to depths. It remains difficult to quantify waters which circulate deeply compared to waters flowing in the decompressed zone. In this case, the decompressed zone has to be represented in the model because it drains a large amount of cold waters towards the feet of the slopes (Lhomme et al. 1996). The thickness of the decompressed zone varies between 500 and 600 metres on tops of the Aiguilles Rouges Massif (Cruchet 1985, Maréchal 1998 and 1999b) but there is no strict limit to represent the bottom of this zone. For facilitation reasons, a strict limit was assigned in the model.

6.2.2 Discretization of the geological cross section

The two-dimensional model consists of eleven sub-domains having various sizes. Each sub-domain differentiates the geological domains having contrasted hydraulic conductivities such as the Aiguilles Rouges basement, the decompressed zone, the Quaternary filling, etc. (Fig. 6.2). In details, two sub-domains were created in the first 300-500 hectometres below the surface on tops of the Aiguilles Rouges Massif. They define the decompressed zone of which hydraulic conductivities are higher due to recent tectonic events opening fractures increasing its aquifer capacity (Cruchet 1985, Maréchal 1998 and 1999b). In the studied area, this zone supplies infiltration, circulation and storage of waters. If vertical faults are present in the basement, waters can infiltrate deeply reaching the thrust fault system.

Two other sub-domains were built in the basement below the Quaternary filling. The first sub-domain represents the assumed fault zone draining the deep fluid to the surface, and the second was created beside to extend the fractured zone if necessary to calibrate the model.

The Quaternary filling of the Rhone Valley was divided into three sub-domains. A first sub-domain represents the recent Rhone alluvial deposits with a thickness of around 50 metres. Then, a second area symbolizes the glaciolacustrine Quaternary deposits which is thicker (400-500 m) and is considered as an aquiclude. Finally, the third area is the Epinassey
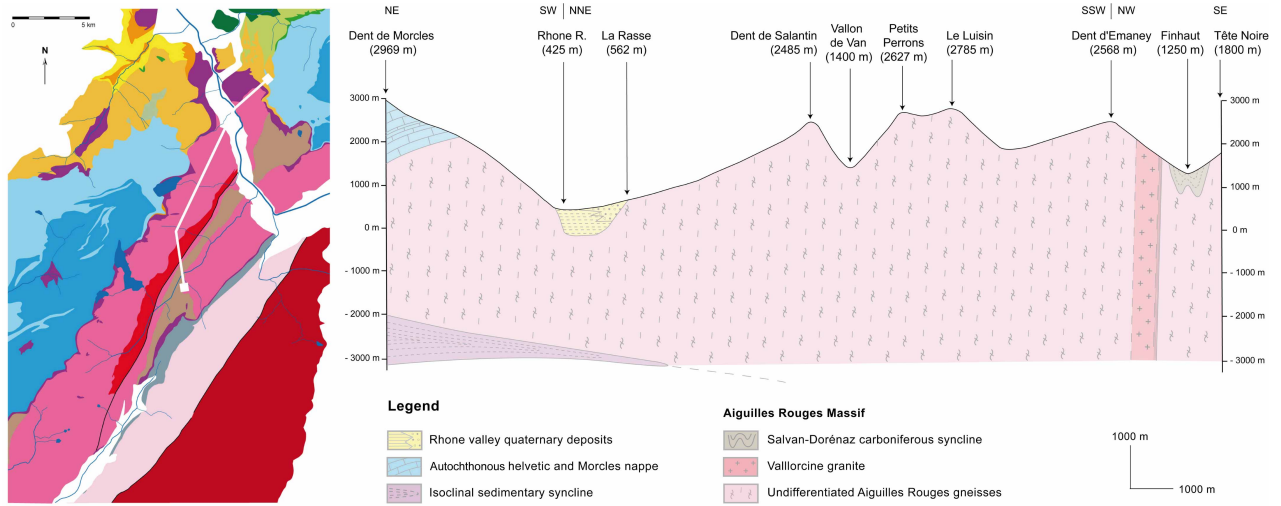
Figure 6.1: Geological cross section of the two-dimensional model for flow and heat transport in the Aiguilles Rouges crystalline Massif. This cross section has two small changes of directions for reason of convenience and to cross the Vallorcine granite (shear zone) which has the same general orientation as the gneiss. The geological map and its legend are visible in Figure 4.1.
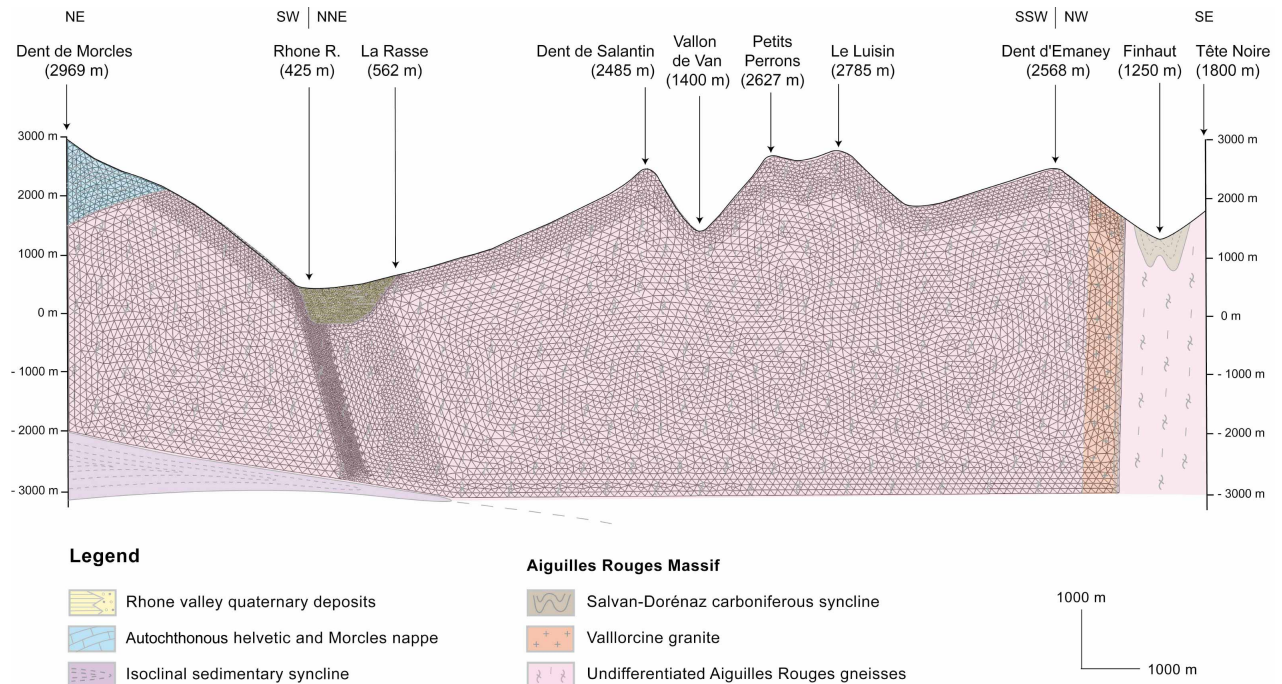
Figure 6.2: Finite element mesh geometry of the two-dimensional vertical model.

fan delta. It was differentiated from the two other units because the lithologies are clearly different.

Finally, the basement below the decompressed zone, on each side of the Rhone Valley, was considered into two large sub-domains. The autochthonous cover of the Aiguilles Rouges Massif, Helvetic formations and the Morcles nappe forming Grande Dent de Morcles were gathered into one sub-domain. This unit does not present a great interest for modelling because groundwaters do not reach the hydrothermal area. It can be assumed as an impermeable limit in the model.

A precise number of meshes was given to each sub-domain aiming to refine selected areas such as the area close to the hydrothermal site, the fractured zones and the Quaternary filling. The fractured zone below the Rhone Valley was particularly refined until 600 metres depth to obtain precise calculated results, and to implement production rates. The size of the triangular meshes varies from roughly 200 metres in the basement to some metres near the hydrothermal site.

6.2.3 Assigned parameters in the model

The assigned parameters in the two-dimensional model of groundwater flow and heat transport are summarized in Table 6.1. The imposed data were documented in literature, from the Swiss Federal Office of Meteorology and Climatology and from collected data in the field. In areas where there is no documented data, imposed values were extrapolated. This section describes the assigned parameters in the two-dimensional model starting with flow conditions, then properties of materials and finally heat conditions.

Flow parameters

The flow parameters correspond to the recharge of water in the model from the infiltration on tops of the Aiguilles Rouges Massif. They also refer to the hydraulic heads being able to characterize inflow or outflow points in the model. In the model, values of hydraulic heads were imposed on the three Rhone, Vallon de Van and Triège Valleys.

The infiltration of water on tops was estimated from precipitations removing the effective evapotranspiration, the surface runoff and the variation of storage. In high mountain domains such as the Aiguilles Rouges Massif, infiltrations within the basement are heterogeneous because they depend on the presence of major fractures and faults. Moreover, the infiltration of water mainly takes place in the decompressed zone where a large amount of water is stored. Therefore, the simulated flow patterns will be mostly affect this domain. The estimation of waters which really infiltrate deeply will be given by the simulation and depends on the contrast of permeability in the basement.

The recharge of water in high mountain areas varies with the seasonal climatic conditions. The infiltration of water is strongly limited in winter because precipitations are stored on the surface as snow. The most important recharge of waters occurs during the period of the snow melt in summer. For simplicity, the seasonal climatic conditions were not considered in the model. An average recharge of water has been assigned to 10% of the total annual precipitation. This value seems to be low but surface runoff strongly occurs in high mountain areas due to the topography. The presence of a lot of torrents proves it as well as the hydraulic properties of rivers which are marked by strong discharge variations.

The geographical distribution of the recharge concerns the Petits Perrons and the Dent d'Emaney domains. The values fluctuate with the elevation from 10% of 1500 mm/yr, average value for the Vallon de Van Valley, to 10% of 2000 mm/yr, average value for the highest areas. These values of precipitation were documented from the Swiss Meteorology and Climatology Federal Office and are illustrated in the Atlas de la Suisse (version 2.0, Fig. 6.3). Areas located in the Rhone Valley have the lowest values of precipitation ($\approx$ 1000 mm/year), but were not considered as zones of recharge.

A recharge zone was also created on the other side of the Rhone Valley, in the basement forming

the slope of Grand Dent de Morcles. Hydrogeologically, this zone should represent the cold water inflows partially pumped in the exploited wells, that is to say the same cold waters emerging in the divergence tunnel of the Lavey hydro power plant.

Finally, no recharge was assigned in the sector of the Dent de Salantin because waters circulate towards the Epinassey fan delta on the other side of the valley, and thus are not included in the deep flow system. For simplicity, flows from the Dent de Salantin slope were not taken into account in the model.
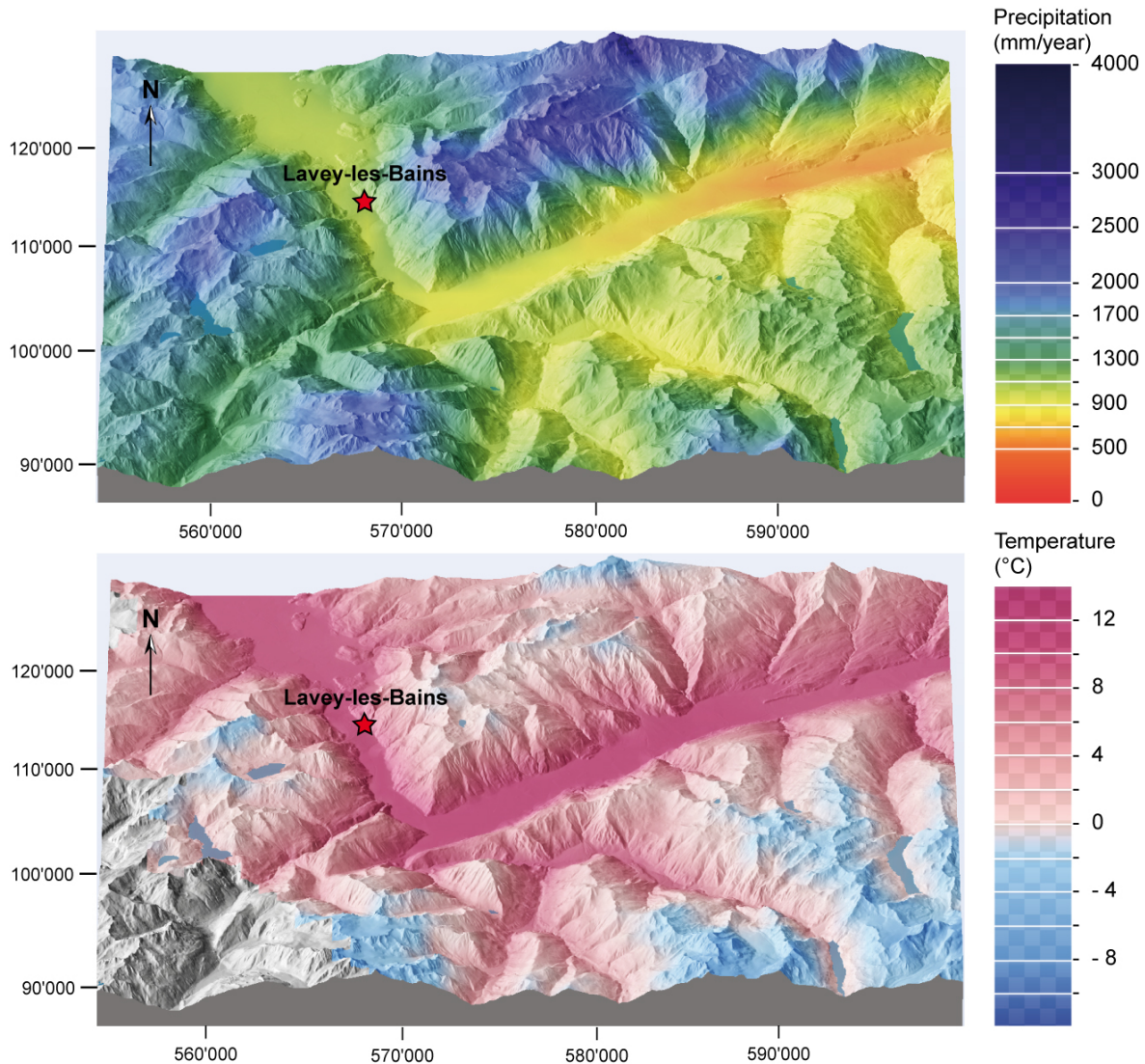
Figure 6.3: Precipitation and temperature maps for the regional area of Lavey-les-Bains (Atlas de la Suisse, version 2.0). Temperature ranges are equivalent to the average annual temperature. Location refers to the Swiss kilometric coordinates in projection, in standard CH1903.

Hydraulic parameters

The hydraulic parameters imposed to the model are the physical properties of the geological domains. In details, different values of hydraulic conductivities with anisotropy factors and porosities were assigned (Table 6.1). The anisotropy factors in the model allow representing the local fractured properties of rocks which strongly influence the deep flow system.

Values of imposed hydraulic conductivities were documented in literature. This physical parameter directly controls flow patterns in the model and the groundwater balance. The calibration of hydraulic conductivities required much time for the construction of the model. In the two-dimensional model seven zones including the Quaternary filling were created with different values of hydraulic conductivities.

Concerning the Quaternary filling of the Rhone Valley, three sub-domains were created with different conductivities. The recent alluvial deposits composed of sandy gravels were represented with a relative high conductivity (10^{-3} m/s). A lower conductivity (10^{-6} m/s) was imposed to the glacio-lacustrine deposits (400-500 metres) due to their lithologies (laminated clay and sandy clay). These formations have a subhorizontal lamination and thus it was necessary to define an anisotropy factor $K_{horizontal}/K_{vertical} = 10$. The Epinassey fan delta was assigned with a median conductivity (10^{-5} m/s) because it consists of coarse rock-falls with clay.

In the crystalline massif, the decompressed zone and the fractured zone below Lavey-les-Bains were differentiated. The calibration of the two-dimensional vertical model required a contrast of conductivities of twenty between the decompressed zone (2.10^{-7} m/s) and the deep gneiss (10^{-8} m/s). These values seem to be suitable even if the contrast of permeability is certainly progressive with the depth. The fractured zone below the Quaternary filling was assigned with a high permeability (10^{-3} m/s) because it drains the deep fluid towards the surface. It was impossible to reproduce the geothermal anomalies at Lavey-les-Bains without its presence. Moreover, an anisotropy factor $K_{horizontal}/K_{vertical} = 10$ with a anti-clockwise angle from the horizontal axis of 110° was imposed in the fractured zone to reproduce the natural fracturing conditions. For the deep gneiss, a low conductivity of 10^{-8} m/s was imposed in the model. This value seems to overestimate the reality compared to measured conductivities in crystalline rocks in tunnels and galleries where values of conductivity are often lower 10^{-10} m/s (Maréchal 1998 and 1999a). However, the model was created parallel to the regional fracturing of the Aiguilles Rouges Massif, in the NE-SW direction. Consequently, the permeability along this direction is certainly higher than the permeability in other directions.

An arbitrary low hydraulic conductivity of 10^{-10} m/s was assigned to the sedimentary formations in the Grand Dent de Morcles area. This domain could be excluded from the model because groundwaters do not reach the hydrothermal site. Finally, values of porosity were assigned in the model. For the Quaternary filling, a porosity of 10% was selected to the glaciolacustrine deposits and the fan delta, 15% for the recent alluvial deposits which have a higher permeability. Porosities were much lower in the crystalline rocks.

Thermal parameters

Surface temperatures were assigned on tops of the model with data documented from the Swiss Federal Office of Meteorology and Climatology, and represented in Atlas de la Suisse (version 2.0, Fig. 6.3). Surface temperatures depend on the elevation. An annual average temperature of 0°C was imposed on tops of the model having an elevation of roughly 2500 m. At Lavey-les-Bains, an annual average temperature of around 10°C can be assumed because data of the Swiss Federal Office of Meteorology and Climatology indicate an annual average temperature of 9.75°C at Sion (Wallis) calculated between 1967 and 2007. For the Vallon de Van and Le Triège Valleys, surface temperatures were extrapolated from Figure 6.1.

Heat fluxes in Switzerland were studied by Chapman and Rybach (1985), Clark and Niblett (1955), Jaboyedoff and Pastorelli (2003), Medici and Rybach (1995), Rybach (1982), Rybach et al.

(1987) and Vollmayr (1983 and 1985). The studied areas are mostly located in the northern part of Switzerland near the Rhine Valley because this sector has the strongest geothermal anomalies ($>$ 150 mW/m^2 in Rybach et al. 1987). In the region around Lavey-les-Bains, the heat flux was evaluated between 80 and 90 mW/m^2 (Medici and Rybach 1995). For the calibration, a value of 87 mW/m^2 was assigned at the bottom of the model and thus is concordant with data found in the literature.

The rock thermal conductivity is also an important parameter for the simulation, because a variation of this parameter modifies the simulated temperatures in the whole of the model. Values of rock thermal conductivity vary from 0.6 to 5.8 W/m/K at ambient temperature (Rybach 1973). Highest values correspond to compacted rocks poor in water (for example: ultrabasic rocks) whereas porous formations containing waters have the lowest value ($<$ 1.5 W/m/K). Clark and Niblett (1956) studied the terrestrial heat flow in Swiss Alps and thermal conductivities of crystalline rocks. They calculate an average value of the thermal conductivity of 2.65 W/m/K from 23 samples of gneiss in the Western Alps. For the calibration of the model, a thermal conductivity value of 2.5 W/m/K was imposed to the Aiguilles Rouges gneiss. For the Quaternary deposits, an average thermal conductivity of 2 W/m/K was assigned (VDI-Richtlinien 2000).

6.3 Comparison with the natural state of the hydrothermal system

6.3.1 Computed temperatures in steady state

The calibration of the model in steady state enabled the heat anomaly at Lavey-les-Bains induced by the deep flow system to be reproduced (Fig. 6.4). The simulation was carried out excluding the assumption that successive glaciations entirely stopped advection processes in the massif. In a general point of view, the simulation showed a large cold plume below the tops of the domain. It corresponds to infiltrations having for impact to cool the whole of the massif. Computed temperatures in the massif depend on the capacity of waters to flow deeply in the model, controlled by hydraulic conductivities and quantity of infiltrated water. The simulation also showed a vertical heat plume from the bottom of the model to the Rhone Valley, due to the high permeability assigned in the fractured zone below the Quaternary filling.

Computed temperatures are close to the observed measurements in the P600 well before its exploitation (68°C) and are similar to the current annual average temperature for the P201 well (57°C) (Table 6.2). It would have been better to obtain the temperature before exploitation (62°C) for the P201. The difference in temperature is due to more cold water inflow towards the P201 well from the decompressed zone of the Grande Dent de Morcles area. In reality, this process is correct but less important than computed because the temperature of the P201 well before its exploitation probably was higher than 62°C. Moreover, computed temperatures at 10 metres below the Quaternary deposits are close to 40°C. It agrees with measurements made in November 1970 in the old well AP (44°C in Högl 1980) before the exploitation of the P201 well.

Moreover, it was not possible to reproduce the observed temperature in the Epinassey borehole (22°C, CRSFA 1992c). The computed temperature is 13.7°C due to the absence of fractured zone on the other side of the Rhone Valley in the model which allows the uprising of the deep fluid. In reality, the presence of thermal water nearby Epinassey supposes that there certainly exist a fractured zone at depth, connected to the major fault system below Lavey-les-Bains.

The simulated geothermal gradient varies along the cross section: the lowest value of gradient (16°C/km) is found below the recharge zone and the highest value corresponds to the Rhone Valley discharge zone due to the uprising of the deep fluid. The geothermal gradient in the Aiguilles Massif was calculated from tops to the bottom of the model (thrust fault). This value is similar to other estimations in crystalline massifs met in the Loetschberg and Furka tunnels, respectively 20°C/km and 16°C/km (CRSFA 1992a, Vuataz et al. 1993). In the fractured zone below the decompressed zone a geothermal gradient higher

than 24°C/km was calculated. It strongly increases in the geothermal field at shallow depth ($\approx$ 120°C/km). Finally, computed temperatures of the inferred deep reservoir give 110-130°C and are close to the value calculated with chemical equilibrium of minerals and with geothermometers (100-110°C). Therefore, this result was considered as acceptable.

Table 6.1: Comparison of observed/evaluated and imposed/simulated values for geological and hydrothermal boundary conditions for the two-dimensional model of Lavey-les-Bains. hor.: horizontal, vert.: vertical, calc.: calculated, resid.: residence and wat.: water.

Boundary conditions	Obs./Eval. values	Imposed values
Water recharge (mountain condition)	1 to 20% of precip.	10% of precip.
Imposed hydraulic head (m)		Elevation of rivers
Surface temperature (°C)	0-10	0-10
Hydraulic conductivity (m/s)		
Gneiss decompressed zone	$> 10^{-7}$	2.10^{-7}
Deep gneiss	10^{-6} to 10^{-12}	10^{-8}
Fractured zone of gneiss (fault)	10^{-2} to 10^{-5}	10^{-3}
Glaciolacustrine deposits	10^{-5} to 10^{-8}	10^{-6}
Epinassey fan delta	10^{-4} to 10^{-6}	10^{-5}
Recent alluvial deposits	10^{-2} to 10^{-5}	10^{-3}
Conductivity anisotropy factor		
Deep gneiss	K(hor.)/K(vert.) = 2 and 75°	
Fractured zone of gneiss (fault)	K(hor.)/K(vert.) = 10 and 110°	
Glaciolacustrine deposits	K(hor.)/K(vert.) = 10 and 0°	
Rock thermal conductivity (W/m/K)		
Aiguilles Rouges gneiss	2.65	2.5
Quaternary deposits	2	2
Heat flux (mW/m^{-2})	80-90	87
Porosity (%)		
Aiguilles Rouges gneiss	< 10	< 10
Quaternary deposits	1 to 20	5 to 15
Pumping discharge (L/min)	Annual average discharge	
P600	800	
P201	350	
Temperature in wells (°C)		Sim. initial conditions
P600 (before exploitation)	68	68.4
P201 (before P600 exploitation)	62	56.4
AP (before P201 exploitation)	44	40
Calc. temperature at depth (°C)	110-110	110-130
Geothermal gradient (°C/km)	15-20	16
Mean resid. time of deep wat.(years)	> 8000 (^{14}C)	> 30000
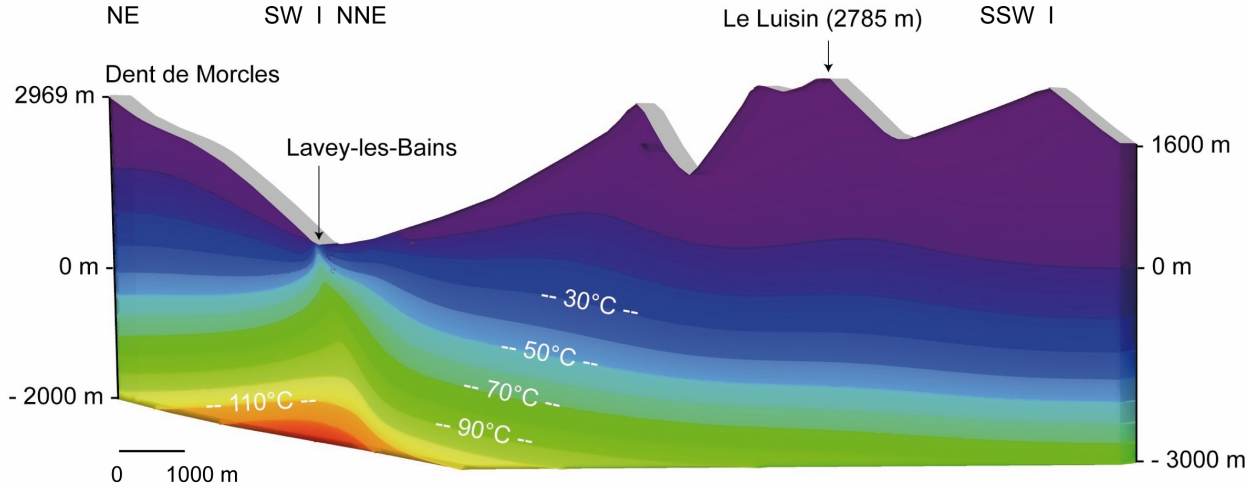
Figure 6.4: Cross section of the Lavey-les-Bains hydrothermal system showing the computed temperatures in the Aiguilles Rouges crystalline Massif.

Table 6.2: Comparison of computed and measured temperatures in three Lavey-les-Bains wells and in one borehole located in Epinassey (other side of the Rhone Valley). Temp.: temperature.

Well/	Observed temp. (°C)		Simulated
Borehole	Temp. before exploitation	Annual average temp. (in 2007)	Temp. (°C)
P600	68	65	68.4
P201	62	57	56.4
AP	44	18 (unused well)	40
E2		22 (unused borehole)	13.7

6.3.2 Computed groundwater for steady state flow

The two-dimensional model in steady state makes it possible to obtain a reasonable picture of hydraulic heads of the thermal aquifer (Fig. 6.5). The top of the groundwater corresponds to the water table of which a simulated pressure equivalent to the atmospheric pressure was calculated. With the simulation, it was shown that the groundwater level has a rather low elevation below the Grande Dent de Morcles because it was decided to limit flows inside the Morcles gneiss. For this reason, the simulated water table has a weak slope and therefore, the geothermal gradient appears stronger compared to the gradient of the Aiguilles Rouges Massif.

Subsurface circulations of the Petits Perrons and the Dent d'Emaney Massifs supply, on one hand, the groundwater of the highest valleys inside the decompressed zone and, on the other hand, the Lavey-les-Bains hydrothermal system from the deepest flows. Infiltrations on the Dent d'Emaney area generate the deepest circulations in the model.

Contrasts of permeability between the decompressed zone and the deep aquifer are responsible for high values of calculated exfiltration on the highest valleys (60% of the total infiltration). In this model, the Rhone Valley discharge is consequently equal to 40% of the total groundwater recharge (1.8 $m^3/d/m$). For the simulation, values of infiltration equal to 10% of total precipitations were selected. Thus, 4% of precipitations supplying the total groundwater recharge is obtained. This value

119
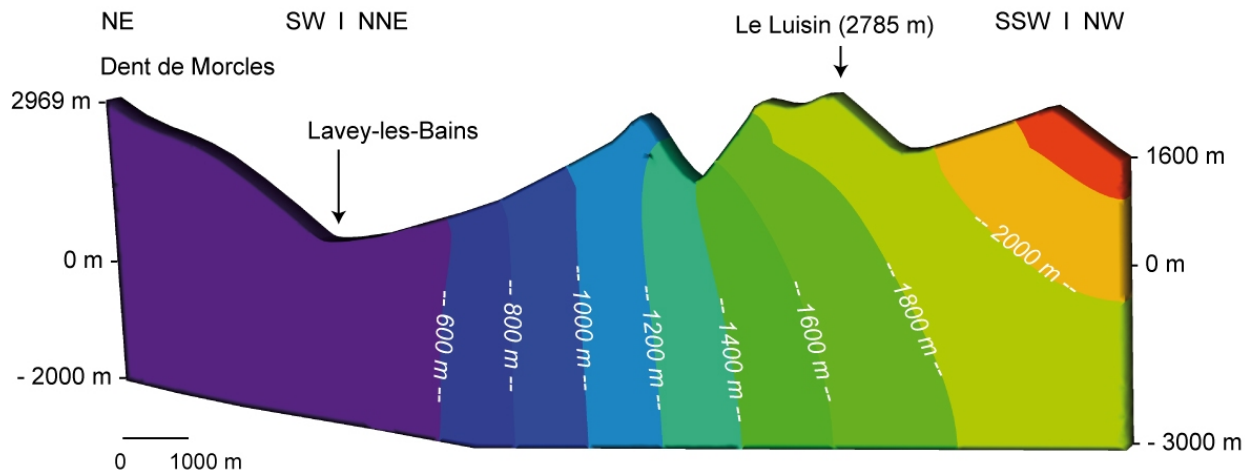
Figure 6.5: Computed hydraulic heads for the Lavey-les-Bains hydrothermal system.

seems to be acceptable for high mountain domains, but appears to be low compared to production rates in Lavey-les-Bains, respectively 1200 L/min and 450 L/min in the two P600 and P201 wells. But this result has to be multiplied by the width of the supposed watershed (approximately 3000-5000 m), meaning that a discharge of about 5400-9000 m^3/d is obtained, 2 to 4 times higher than the maximum rate, which can be pumped (2400 m^3/d). However, it was possible to augment the Rhone Valley exfiltration by prolonging the cross section in the Aiguilles Rouges Massif and thus increasing the infiltration area. An extension of the recharge zone of the Lavey-les-Bains hydrothermal system can be imagined until the sector of the Emosson Lake and the hydrological limit in the surface between France and Switzerland towards l'Aiguille du Belvédère (see location in Figure 4.1).

The water flux through the fractured zone below the Quaternary deposits has an important linear variation with depth. The flux at the bottom of the model is 50 times more important than at shallow depth.

Using the particle tracking option, the model gives an average residence time of the deepest fluid in the order of 30000 years, higher than the carbon-14 evaluation (> 8000 years). The carbon-14 evaluation is most probably influenced by a certain amount of mixing with recent and shallow groundwater. This computed value is dependent on the chosen permeability and porosity values of the deep gneiss unit (10^{-8} m/s).

6.4 Long-term effects of production rates on temperatures

Additional pumping wells put into the two-dimensional model allowed forecasting the long-term effects of reservoir development on the temperature field. An unsteady state model was constructed from the annual average discharge of the two exploited wells: 800 L/min for P600 and 350 L/min for P201. These pumping rates were corrected in the model from the evaluated width of the cone of influence of each well, because it is not appropriate to impose the real pumping rates of exploitation in a two-dimensional model due to the radial flow components out of the cross-section. The computed temperature decreases in the two boreholes due to additional contributions of cold waters from the Morcles gneiss (Fig. 6.6).

The model shows a total loss of temperature of 2°C in P600 and of 10°C in P201, with stabilization after 100 years of exploitation. Nevertheless,

observed values seem to indicate a stabilization of temperature after 2005, less than 10 years of production by the P600 well, and a final decrease of 5°C in the P201 well and 3°C for the P600 well. Consequently, the influence of cold water inflows is more pronounced in the model than in reality. The local calibration of the unsteady state model is difficult because the two-dimensional model represent the regional flow system. Therefore, it is not appropriate to reproduce the local mixing processes.
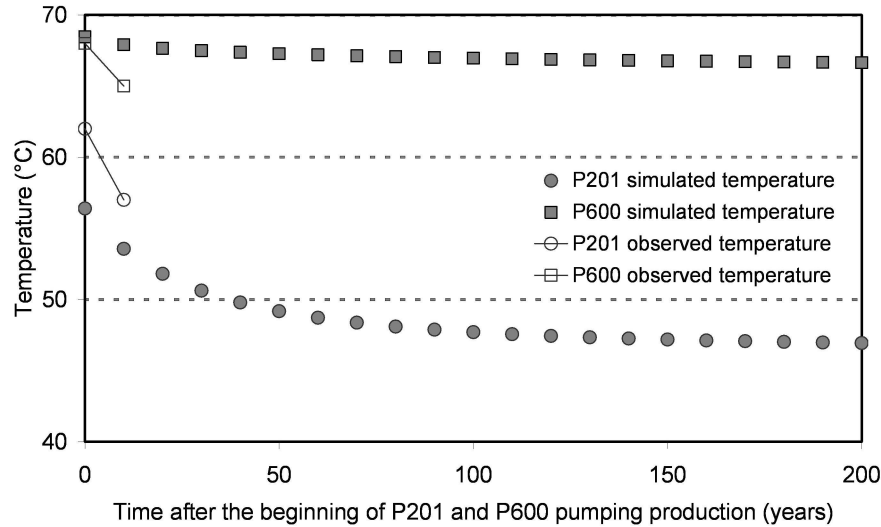
Figure 6.6: Long-term simulated production temperature in the two wells compared with measured temperatures.

6.5   Conclusion

The conception of a simplified two-dimensional numerical model from a regional NNE-SSW cross section through the Aiguilles Rouges crystalline Massif allowed for representation of the initial conditions of the Lavey-les-Bains deep flow system, such as the temperature field below the Quaternary deposits and temperatures of the deep inferred reservoir. Nevertheless, the approximation of the uprising water flux is made difficult because the third dimension can not be taken into account due to the complexity of geological and topographical structures. The width of the watershed and its extension in the NNE-SSW direction, and the quantification of infiltration in the model, also are important parameters that are difficult to evaluate and have a significant influence on the estimation of the uprising water flux. Selected pumping rates gave computed temperatures, which overestimate additional contributions of cold waters from the Morcles gneiss.

Long-term temperature prediction for optimal management of the geothermal resource does not seem fully comparable to the reality. Even if the two-dimensional model correctly represents initial conditions, it is not suitable when new pumping rates are added. For this reason, a three-dimensional model in the boreholes zone has to be considered.

7

Three-dimensional local modelling of groundwater flow, heat and mass transport

7.1 Objectives

Mixing processes at shallow depth between cold waters from the slope and uprising thermal water were represented with the construction of a local three-dimensional model of groundwater flow, heat and mass transport. Compared with the two-dimensional model, conservative chemical elements of various mixing end-members are used as natural tracers in addition to the temperature. In the simulation, each chemical parameter was directly calculated at the nodes where the flow rates are imposed. Water-rock interactions in the mixing zone were not taken into account in the three-dimensional model because faster circulations occur in the mixing zone limiting water-rock interactions. In this zone, variations of the concentrations in waters are mainly due to the mixing processes.

Although the regional deep flow system is not illustrated with the three-dimensional model, it was possible to simulate effects of production rates in the mixing area. Initial conditions of groundwater flow, heat and mass transport were simulated using temporal data in waters of the wells and results obtained with the two-dimensional model. Desired aims are firstly to represent mixing processes before and during the exploitation of wells. Secondly, the objective was to forecast variations of the physico-chemical parameters which have been observed in the P201 well. Finally, the potential long-term effects of a new deep borehole (AGEPP project) on the geothermal resource were highlighted with the simulation.

7.2 Construction of the model and assigned parameters

7.2.1 Geological boundary conditions

The structure of the three-dimensional model consists to a coarse rectangle about 100 x 600 metres size with 600 metres depth, that is to say ap-

proximately 80 metres below the bottom of the P600 well. The model extends 200 metres downstream from the P201 well and 200 metres upstream

from P600. The grid used to simulate groundwater flow, heat and mass transport consists of 62100 cells distributed over 54 layers (Fig. 7.1). The first three layers of cells correspond to the Quaternary filling of the Rhone Valley including the recent Rhone alluvial deposits (coarse sandy gravels) and the glacio-lacustrine sand and silt (see lithologies in Figure 4.5). The other layers are assumed to be the fractured zone of gneiss and are considered equivalent to a porous domain for the simulation. In the model, the geological limit between the basement and the filling was defined from logs of boreholes. A depth of 200 metres was fixed towards the Rhone River to define the geological limit, because in the middle of the valley, the Quaternary filling reaches a thickness of about 500 metres (Besson et al. 1993). Further from the river, at the hillside representing the edge of the model, the interface slope reaches an arbitrary depth of only 5 metres (Fig. 7.1).

The six boundaries are represented by the top, the bottom and the four lateral sides of the three-dimensional model, assuming that they are appropriate and justified. In detail, the description of each boundary is given below:

- The top of the domain represents the totality of the alluvial plain of the geothermal zone from the hillside to the Rhone River. The surface topography was constructed with the kriging option from acquired data, and varies between 441 and 420 m.a.s.l. (Fig. 7.2).

- The bottom of the model is regarded as a plane surface with an elevation equal to 180 metres below the sea level, with an imposed thermal water flux. From the bottom, waters rise towards the surface.

- The northern and southern lateral sides are narrow (approximately 50 m) and support the Rhone phreatic groundwater in the Quaternary filling flowing from the south to the north.

- The eastern side corresponds to the vertical limit between the slope and the alluvial plain. It supports the gradual cold water inflows from Morcles gneiss on all the high parts of its surface.

- The western side consists of the vertical prolongation of the Rhone River, which can be assumed as a hydrogeological barrier with no flow.

Finally, the grid was refined in the vicinity of the two production wells to limit the potential numerical errors during the simulation. The size of the cells where the production rates are imposed is close to the diameter of the wells (approximately 30 cm).

7.2.2 Assigned parameters in the model

Assigned water fluxes are illustrated in Figure 7.1. For the calibration of the model, the necessary total flux of the upflowing thermal water is $5454 \ \mathrm{m^3/d}$ and is homogeneously distributed on the totality of surface, that is to say 2.3 times more than the maximum production rate of the two exploited wells ($2380 \ \mathrm{m^3/d}$). It also corresponds to 79% of the total inflows in the model ($6860 \ \mathrm{m^3/d}$), knowing that the cold components coming from the slope and from the alluvial groundwater are approximately five times less important than the thermal component. However, the calculated water balance is slightly underestimated compared to the two-dimensional model simulation ($5400\text{-}9000 \ \mathrm{m^3/d}$).

Concerning the thermal inflow, a temperature of 68°C was imposed which corresponds to the pure thermal end-member, as measured in the P600 well before production (Bianchetti 2002). A geochemical study carried out within the framework of the AGEPP project indicated that the pure thermal end-member at a depth of 600 metres contains Cl, SO_4 and Mg at respectively 265, 618 and 0.3 mg/L (Sonney et al. 2007).

In addition to the temperature, these three ions, which have certainly limited precipitation/dissolution reactions in the mixing zone due to fast circulations, are used as natural tracers to represent these mixing processes. For the cold inflows, a temperature of 9°C was imposed for the alluvial aquifer and a range of 9 to 20°C for the slope groundwater. Chloride, sulphate and magnesium imposed concentrations are respectively 3,
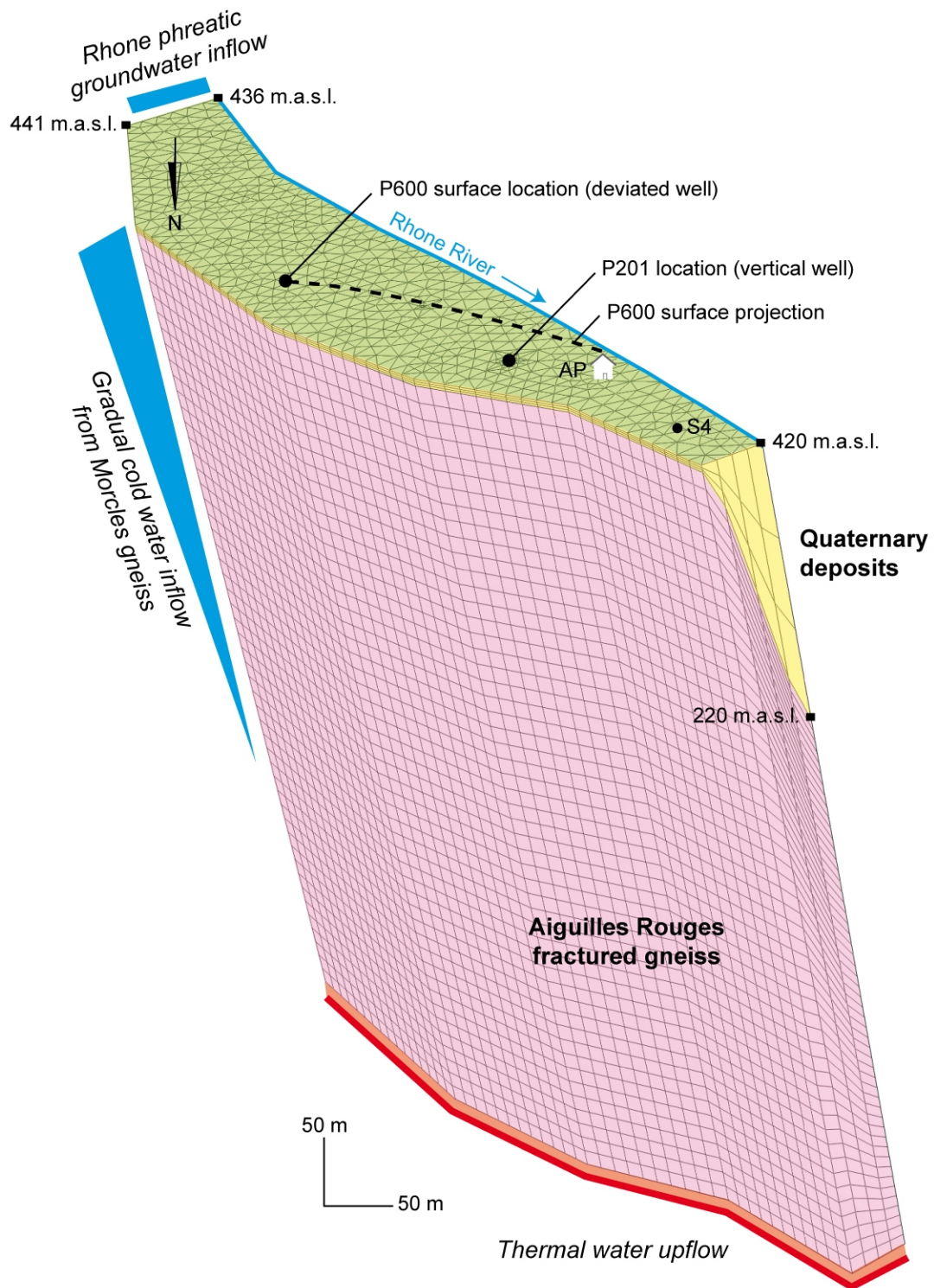
Figure 7.1: Conceptual three-dimensional model of the Lavey-les-Bains geothermal system, showing the finite element mesh geometry used for the simulation and the initial boundary conditions (thermal upflowing and cold water recharge).

Figure 7.2: Constructed top surface topography for the three-dimensional model of the geothermal zone.

67 and 12 mg/L according to extrapolation from chemical analyses of all sampling points (Sonney et al. 2007).

Finally, imposed conditions for rock permeability, anisotropy factors and thermal conductivities remained similar to the conditions of the two-dimensional model. Concerning the fractured zone in gneiss, which was considered equivalent to a porous environment, high hydraulic conductivities in particular on the vertical axis Z were assigned

(use of hydraulic conductivity anisotropy factor option in the FEFLOW code).

Values of hydraulic conductivities on horizontal directions X and Y are equivalent (10^{-4} m/s) and 100 times higher on Z (10^{-2} m/s) due to the presence of permeable vertical fractures. For the Rhone alluvial deposits, imposed conductivities were 10^{-3} m/s on X and Y, and 10^{-4} m/s on Z according to interpretation of pumping tests.

7.3   Discussion of four scenarios

Four scenarios were investigated with steady state and transient models. They present the exploitation history since the installation of the first deep P201 well in 1972. Firstly, the background temperature field and initial mixing conditions were established in the absence of production rates (before P201). In a second scenario, the temperature distribution and the chemical con-

tents are computed with the exploitation of the P201 well (before P600). Then, long-term effects of the P600 well on the P201 production were predicted (before AGEPP project). Finally, the future deep AGEPP borehole was added into the three-dimensional model to show its possible impact on production of the P201 and P600 wells.

7.3.1   First scenario: historical background temperature field (< 1972)

The steady state three-dimensional model without production rates made it possible to approximate the initial background temperature field by a cross section between P201 and P600 wells (Fig. 7.3), and represents the initial aquifer concentrations for the next simulations with production rates. At a given depth (for example 50 m), the temperature below the Quaternary filling increases from the

hillside to the river and then slightly decreases with the sediments due to a permeability contrast. Computed temperatures are acceptable compared to the measurements made before 1972 in the old well and during the drilling of the P201 well before its exploitation (Fig. 7.4). The simulated temperature for the P600 well is equivalent to the imposed temperature of the upflowing fluid in the model (68°C),

and thus it was not influenced by waters of the decompressed zone. Therefore, the dilution zone with cold waters from the decompressed zone has higher elevation at the time preceding the P201 exploitation (< 1972). The computed temperature was 65.8°C for the bottom of the P201 well (Table 7.1).

Compared to measured data during the drilling of the well (63-65°C), this result can be considered as acceptable. Finally, the simulated temperature for the old well (43°C) agrees with measurements made by Högl (1980).
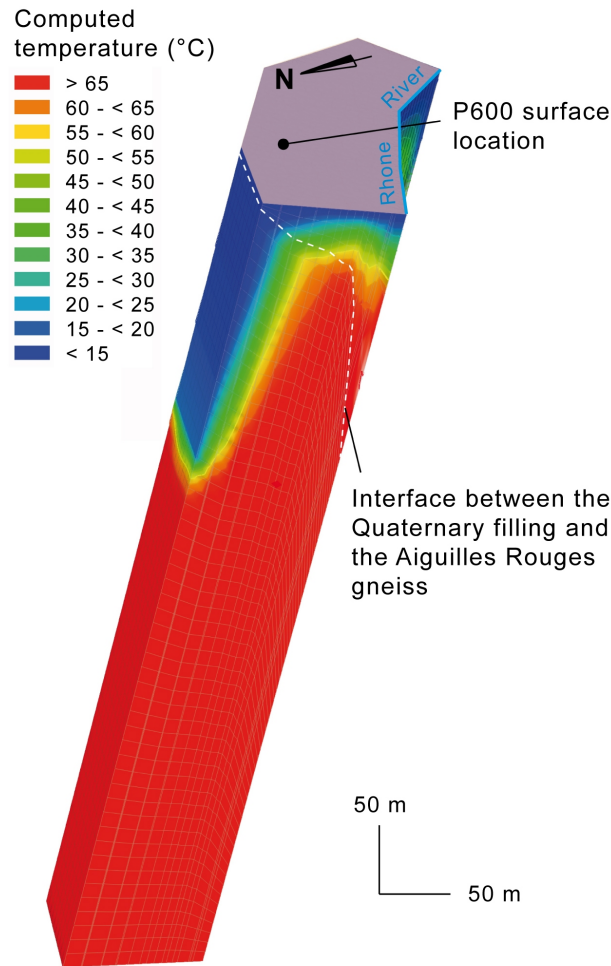
Figure 7.3: Three-dimensional simulation of the initial background temperature field before production (three-dimensional view from a cross section between P201 and P600 wells).

Table 7.1: Comparison of computed and measured temperatures in Lavey-les-Bains wells according to four simulation scenarios. MT: Measured Temperature (°C), CT: Computed Temperature (°C), nd: not defined.

Well	Background field temperature (< 1972) MT	CT	P201 Exploitation (1972-1997) MT	CT	P600 Exploitation added (> 1997) MT	CT	AGEPP production added (probably > 2010) MT	CT
P600	nd	68	nd	68	65	67.5	nd	66-67
P201	63-65	65.8	62	61.5	57	55.7	nd	39-41
AP	44	43	22-36	42	18-22	39	nd	nd

7.3.2 Second scenario: during P201 exploitation only (1972-1997)

The second scenario highlights the effects on the geothermal field due to the production rate of P201 only, with an annual average discharge at 300 L/min. During this time interval, P600 is not yet present and the exploitation of the thermal aquifer is supplied by P201 only, and beyond 1997, P201 exploitation continues with P600.

The decrease of simulated temperatures from 65.8 to 61.5°C is satisfactory compared to the recorded data (Fig. 7.4 and Table 7.1). The measured temperatures with the depth in P201 well in 1989 (unknown discharge condition) represent the aquifer hydrogeological and thermal conditions where a complex fracture network allows thermal water to be arrived in the well in various depths. The three-dimensional model is not able to reproduce these conditions and thus it remains difficult to obtain better results in Figure 7.4.

In the model, the decline of temperature when P201 pumps water is associated with an increase of the mixing ratio as shown by computed concentrations of chemical tracers: Cl = 238 mg/L, SO_4 = 564 mg/L and Mg = 1.5 mg/L. These values represent at the P201 well the initial aquifer concentrations before the simulation with the P600 production rate (first concentration points in Figure 7.5).

Using imposed concentrations, the mixing ratio during the P201 exploitation is estimated at 10%

for cold waters and 90% for the thermal component. Finally, simulated temperatures in the old well do not correspond to observed data (42°C simulated instead of 22-36°C measured). In the three-dimensional model, the Rhone alluvial groundwater circulates mainly in Quaternary deposits whereas characteristics of this shallow well (28 metres including 18 metres inside sediments) support alluvial groundwater inflows inside the well due to a drawdown of the thermal water hydraulic head.

○ Measured temperature in 1989 (unknown discharge condition)
■ Computed temperature before P201 exploitation (<1972)
▲ Computed temperature during P201 exploitation only (1972-1997)
◆ Computed temperature with P201 and P600 exploitation (>1997)
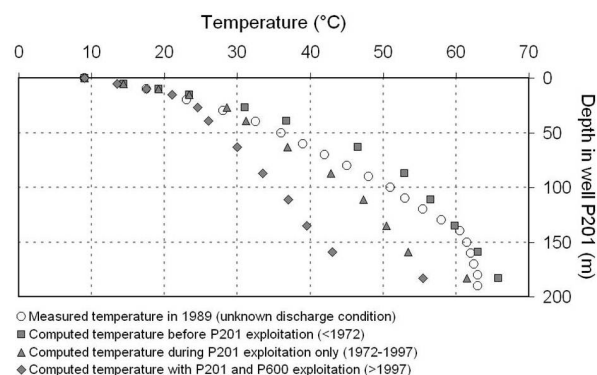
Figure 7.4: Comparison of computed and measured temperature profiles in the P201 well.

7.3.3 Third scenario: effects of P600 exploitation on P201 (after 1997)

In a third scenario, the P600 deeper well is added to the system with an annual average production rate of 800 L/min. Its position close to the bottom section of P201 causes a decrease of the hydraulic head of the upflowing thermal water and favours additional cold water inflows (Fig. 7.5).

Electrical conductivity and temperature measurements taken in P201 since the exploitation of P600 clearly showed a dilution of P201 thermal water and modelled results reproduce these observations. The calibration of the model made it possible to validate the first estimation of the long-term temperature behaviour: time necessary to stabilize the temperature in P201 from 61.5°C in 1997 to 56°C takes 10 to 15 years.

With regard to the variation of the chemical tracers computed by the model (Fig. 7.5), the

pumping rate in P600 induces a reduction in chloride and sulphate concentrations (respectively 204 and 494 mg/L) and an increase of magnesium concentration (3 mg/L). As a reminder, the initial conditions is represented by results obtained with the second scenario during P201 exploitation only (1972-1997). Consequently, the mixing ratio between cold and thermal waters evolves from 10/90% to 23/77%.

Finally, due to the structure of the three-dimensional model and to the position of the deep P600 well close to the thermal inflow, it was not possible to reproduce the temperature decrease in P600 (67.5°C computed instead of 65°C observed in 2007).
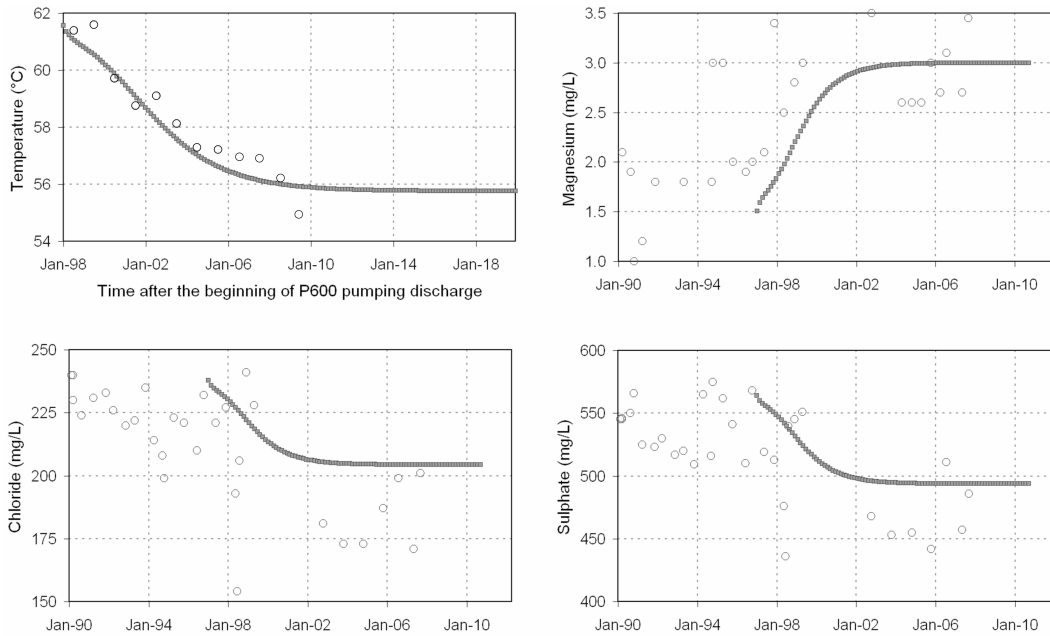
Figure 7.5: Comparison of computed (squares) and measured (circles) physico-chemical parameters in the P201 well after production in the P600 well started in 1997. The initial conditions is represented by results obtained with the second scenario during P201 exploitation only (1972-1997).

7.3.4 Fourth scenario: production simulation of the deep AGEPP borehole (probably > 2010)

In a last scenario, it was decided to simulate the possible impact of the future deep AGEPP borehole on the existing production wells. Inferring that the AGEPP borehole will reach at least 2000 metres below the three-dimensional model, the employed method decreases fluxes uprising at the bottom of the model. Initially, the total imposed value of fluxes at the bottom of the model was 5454 m^3/d or 63 L/s. It appears insufficient for the objectives of the AGEPP project (50-75 L/s). It is impossible to simulate an exploitation rate higher than 63 L/s because the thermal upflowing will be absent in the model. For this reason, a flow rate of 25 L/s was selected for the simulation and is more appropriate for this model than a flow rate of 50 L/s which would generate stronger cold water inflows in wells. It is difficult to appreciate if the AGEPP project overestimates the geothermal potential, or if the calculated total flow at the bottom of the model is underestimated.
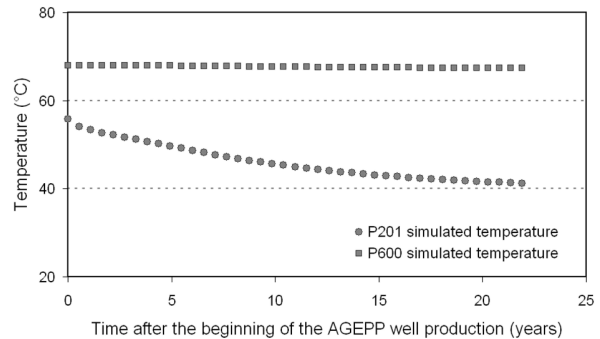
Figure 7.6: Temperature simulation of the two existing production wells during the exploitation of the future deep well AGEPP at a rate of 25 L/s.

The temperature variation shows a major reduction in P201 (more than 15°C), with a stabilization at 40°C after 20-25 years of exploitation (Fig. 7.6). Concerning P600, a decrease of the production yield may be possible but probably less important than for P201, because of a lower variability of the physico-chemical parameters in P600, being less subject to the mixing process by cold water inflow. In case of a significant decrease of the production rates in the P600 and P201 wells, it could be envisaged that water pumped by the AGEPP borehole could be used for thermal spa after extraction of the energy.

7.4 Outline of the two and three-dimensional models

Numerical local modelling of groundwater flow, heat and mass transport were elaborated for the Lavey-les-Bains deep flow system with objectives to represent initial hydrogeological conditions and to manage the long-term exploitation of the geothermal resource. It was considered the same assigned parameters as the two-dimensional model. The exploitation of the P600 well generated additional dilution of pumped waters by cold waters from the decompressed zone. It was thus important to represent these mixing processes using a three-dimensional model and to forecast the long-term behaviour of the physico-chemical parameters.

Continuous measurements of the physico-chemical parameters in P201 and P600 waters, and punctual measurements in all sampling points allowed highlighting mixing processes between the thermal end-member and cold waters at shallow depth. Initially, a two-dimensional model of groundwater flow and heat transport from a regional geological cross section in the Aiguilles Rouges Massif recomposed partly the observed geothermal anomaly below the Rhone Valley (68.4°C, 56.4°C and 40°C respectively for P600, P201 and AP) with a computed reservoir temperature in the range 100-130°C. The calculated thermal flux (5400-9000 m^3/d) in the two-dimensional model corresponded to 2.3-3.8 times the maximum discharge which can be pumped in Lavey-les-Bains (2380 m^3/d) and seemed to be underestimated, with the assumption of an extension of the infiltration area towards the Emosson Lake. Based on these results, a three-dimensional local model was realized in a perimeter including the whole of Lavey-les-Bains sampling points by taking again imposed parameters in the previous model. The thermal upflowing necessary for the calibration is comparable to the evaluation made on the two-dimensional model (5454 m^3/d).

Different simulation scenarios using the average annual discharges of P600 and P201 wells and some natural chemical tracers, made it possible to calculate mixing ratios comparable with those estimated in the P201 well (10/90% before the P600 well and 23/77% with the P600 exploitation). Moreover, long-term effects on P201 could be defined with the three-dimensional model. Computed and measured temperatures are concordant and illustrate a stabilization of the temperature at 56°C after 10 to 15 years of production at the P600 well. According to the model, a future exploitation of the deep inferred reservoir with pumping rates of 25 to 75 L/s may induce a significant decline of thermal output in the two existing wells in Lavey-les-Bains.

Part IV

Saint-Gervais-les-Bains

8

General description of the study area

8.1 Geographical setting of Saint-Gervais-les-Bains

THE hydrothermal zone of Saint-Gervais-les-Bains is located at the end of the narrow gorges of the Bon Nant mountain stream between the cities of Saint-Gervais-les-Bains and Le Fayet. One kilometre downstream from the hydrothermal zone, this torrent returns to the large Arve Valley before recovering the river (Fig. 8.1).

On a regional level, the studied area is located in the Haute-Savoie department in the Western Alps of France. Its geographical position is at the foot of the Mont Blanc Massif, the highest summit of Europe (4808.7 m.a.s.l. according to the French National Geographical Institute), and the recognized therapeutic qualities of the thermal waters make the reputation of this well-known site.

On the right bank of the Bon Nant stream, a spa continuously pumps the upflowing thermal waters through 3 wells: De Mey Est and De Mey Ouest (respectively depth of 196 and 207 m) and the new one Lépinay (101.5 m).

Currently, Lépinay and De Mey Est are used as production wells, respectively for swimming pools and cosmetics, whereas De Mey Ouest is unused but guarantees a stable exploitation of the De Mey Est well (Vigouroux and Kay 2005). On the site, unused waters are rejected 500 metres downstream from the spa into the Bon Nant river and do not take part in mixing processes between the different end-members.
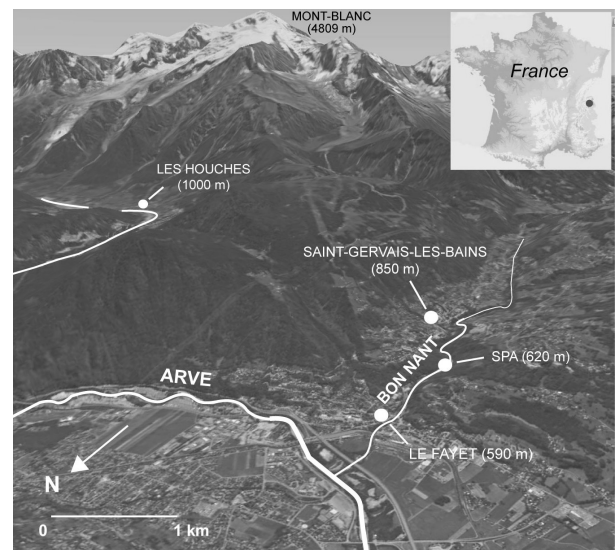
Figure 8.1: Geographical location of Saint-Gervais-les-Bains in France.

8.2 History of Saint-Gervais-les-Bains thermal baths

In 1806, M Gontard discovered thermal springs at Saint-Gervais emerging from the right bank of the Bon Nant bed. At that time, four thermal and mineral springs were counted: Milieu or Gontard spring, De Mey or De La Boisson spring, Du Torrent or Sulfureuse spring and Ferrugineuse spring. The first records authorizing the exploitation of springs were found in archives (September 1842, ANTEA 2004). The first official text is the decree of March 28th, 1884 which authorizes the exploitation of the springs by the General Company of Mineral Water and Sea Baths.

Due to the rupture of a natural water reservoir in the Mont Blanc region in July 1892, a strong mud-flow of around 200'000 m³ was triggered resulting in the accumulation of mud and rocks below the glacier, destroying buildings, and causing 200 casualties (Fig. 8.2). After this natural disaster, a new reservoir was built and the De Mey and Gontard springs were grouped together by a single well called Gontard or Gontard 1 or Gontard-De Mey (Lépinay 1969). At that time, the Torrent (or Sulfureuse) and Ferrugineuse springs were given up and their authorization to exploit was revoked (ANTEA 2004). The Gontard well, single point supplying the mineral and thermal water, was renovated in 1934 and deepened in 1966 until 7.45 metres depth to protect the well from cold water inflows. In 1958, the management of the spa was entrusted to the Thermal Society of Saint-Gervais-Les-Bains. Then in the 1980's, the commune of Saint-Gervais-les-Bains decided to exploit the thermal waters via deep boreholes because the health protection was insufficient in the shallow boreholes. Hydrogeological investigations were undertaken at the same time by FD Vuataz in order to understand the deep flow system and highlight the existence of various types of water: alluvial groundwater, Triassic and crystalline aquifers. Later, another hydrogeological study undertaken by the BRGM consulting office enabled the location points of the future boreholes to be defined (Iundt et al. 1987). The first data acquisitions on the boreholes were carried out by A Barat and P Jerphanion (1989) and G Bianchetti (1993b). Since 1989, works have been continued and are summarized below (ANTEA 2004):

15.01.1989 - 05.04.1989: drilling of the De Mey Est and De Mey Ouest wells.

11.05.1989 - 10.06.1989: first pumping tests on the two wells.

1990: construction of the pumping stations and the transport fittings (pipes).

1992: building of a new establishment, provisional authorizations to exploit the production wells.

18.04.1996: final authorizations (ministerial decree) to exploit the De Mey Est (6.5 m³/h) and De Mey Ouest (7 m³/h) wells.

September 1996: video inspection in wells due to the decrease of production rates observed.

1997: the management of the spa is ensured by the company Les Thermes de Saint-Gervais, subsidiary company of the Rivadis pharmaceutical group.

23.01.1997 - 05.02.1997: deepening works in wells to increase their productivity, supervised by the SOGREAH consulting office. De Mey Est was not deepened due to the presence of a metal object at the bottom of the well. De Mey Ouest was deepened from 166 to 207 metres but the production rates were not improved.

April 1998: recommendation by SOGREAH to exploit the geothermal resource with a rate smaller than 9 m³/h for the two De Mey wells. The submerged pumps of De Mey Est and De Mey Ouest were set more deeply (respectively from -50 to -80 m and -50 to -74 m).

18.03.1999 - 27.05.1999: drilling of the F99 and Lépinay (or La Chapelle) boreholes.

23 and 24.10.1999: acidification and disinfection actions with pressure in the two De Mey wells. Since the completion of the F99 and Lépinay wells, a decrease in temperature (2°C) and in electrical conductivity (from 5900 to 5200 μS/cm) was observed in the De Mey Ouest waters.

10.03.2000 - 31.12.2001: realization of a long pumping test in Lépinay with various production rates.

01.04.2003 - 04.08.2003: a complementary pumping test in Lépinay was carried out with an authorized exploitation production rate of the geothermal resources close to 13 m³/h.

2008: security works for the exploitation of thermal waters: video inspections on the wells, change of the well heads, control of pipes, measurements and recordings, etc.
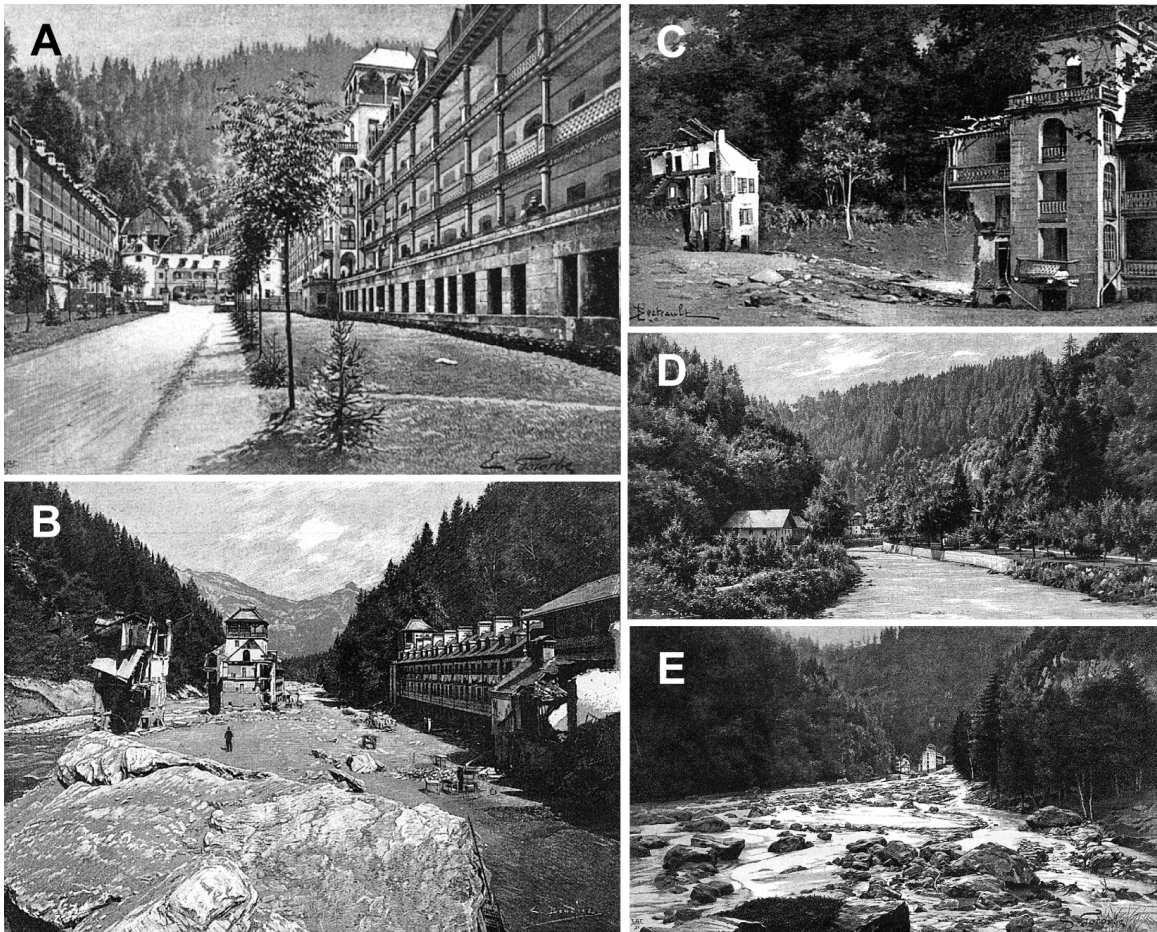
Figure 8.2: Views of the Saint-Gervais-les-Bains hydrothermal zone before (A and D) and after (B, C and E) the disaster of 1892. Drawings of the buildings (A to C) and the park (D and E) by Gotorbe (A and E) and Boudier (B, C and D), made from photographs by Rusché (A, C and D) and Tairraz (B and E).

Source: http://collin.francois.free.fr/Le_tour_du_monde/textes/Durier/Duriergravure.htm.

8.3   Boreholes realized at Saint-Gervais-les-Bains

Four vertical boreholes from 99 to 207 metres depth and another old well (Gontard) of 7.45 metres depth met thermal waters at Saint-Gervais-les-Bains. Four of them are equipped with a pump and are currently used. The Lépinay (101.5 m) and De Mey Est (196 m) wells exploit thermal waters, respectively for swimming pools and cosmetics, whereas De Mey Ouest (207 m) guarantees a stable exploitation of De Mey Est preventing a significant decrease of the temperature. The old Gontard well is also equipped with a pump but there is no wa-

ter production. The F99 borehole (99 m and realized in 1999) was an explanatory well drilled before the Lépinay well, and it was never been really used other than to observe the water table because of its hydrogeological relations with Gontard and Lépinay waters. All of the wells crossed the Quaternary deposits and returned more or less deeply in the fissured Permian and Triassic formations belonging to the autochthonous cover of the Aiguilles Rouges crystalline Massif (Fig. 8.8).

8.3.1 Production well Lépinay

The Lépinay production well was drilled between March and May 1999 downstream from the Gontard and De Mey wells (Fig. 8.3). Lépinay has a depth of 101.5 metres from the surface and its coordinates are 938.941/2108.951/607.586. The borehole is equipped with stainless full tubes with a diameter of 340 millimetres and a submersible pump positioned at 15 metres depth allows the exploitation of water. Beyond 18.6 metres, the hole is open.

The productive formations are located between 27 and 74 metres depth and correspond to the fractured Triassic sandstones and dolomites also called zone of imbricated structures (see section 9.3). The authorized production rate is 13 m^3/h, but Lépinay has natural artesian flow with a rate close to 10.8 m^3/h which was measured in 1999 at the end of drilling (ANTEA 2004). Currently, annual average values of temperature and electric conductivity (measured at 25ºC) of pumped waters are respectively of around 38ºC and 5.7 mS/cm.

Figure 8.3: View of the Lépinay well head (February 2009).

8.3.2 Production well De Mey Est

The De Mey Est production well was drilled between December 1988 and February 1989 (Fig. 8.4). At the beginning, a hole of 196 metres depth was drilled before the construction of the surface station. Its coordinates are 938.932/2108.913/613.903 and the well is equipped with stainless full tubes to a depth of 29.1 metres depth. A submersible pump is positioned at 38 metres, changed in 2006, allowing the exploitation of water.

The productive fractured zone in the Permian rocks is located between 29-36, 82-108.5 and 163-178 metres depth. From the bottom of the well to the surface, cold water inflows dilute the thermal water and decrease the physico-chemical parameters (Iundt 2008).

The authorized production rate is 5.5 m^3/h, and as for Lépinay, the well has natural artesian flow with a rate close to 1 m^3/h which was measured in 1990 before the implementation of Lépinay (ANTEA 2004). Currently, annual average values of temperature and electric conductivity (measured at 25ºC) of the pumped waters are respectively close to 34ºC and 6.1 mS/cm.

Figure 8.4: View of the De Mey Est well head (February 2008).

8.3.3 Production well De Mey Ouest

The De Mey Ouest borehole was drilled between March and April 1989 and is located a few meters away from De Mey Est (Fig. 8.5). At the beginning, a hole of 23 metres depth was bored with the installation of a stainless full tube. Then, the hole was firstly drilled down to 168 metres depth with the percussion drilling method of diameter 162 millimetres (Barat and Jerphanion 1989), then down to 207 metres. Its coordinates are 938.955/2108.912/610 and the well is equipped with a submersible pump set at 74 metres depth.

The first productive fractured zone in the Permian rocks is located below the Quaternary deposits at 21 metres depth. As mentioned for De Mey Est, cold water inflows in the zone 147-153 metres dilute thermal waters and decrease the physico-chemical parameters (Iundt 2008). The authorized production rate is 3.5 m^3/h and the well has natural artesian flow with a rate close to 2.7 m^3/h, measured in 2008 without the De Mey Est production. A flow rate of 3.5 m^3/h is continuously maintained to limit cold water inflows in De Mey Est. Waters of De Mey Ouest are ejected into the river 200 meters downstream from the spa. Currently, annual average values of temperature and electric conductivity (measured at 25ºC) are respectively close to 28ºC and 4.5 mS/cm. Before Lépinay started pro-

ducing water, temperature and conductivity values were higher and therefore the initial authorization to exploit De Mey Ouest water has not been respected.

Figure 8.5: View of the De Mey Ouest well head (February 2009).

8.3.4 Unused well F99

The F99 well is an exploratory borehole drilled before Lépinay in March 1999 close to the Gontard well (Fig. 8.6). The F99 well has a depth of 99 metres and its coordinates are 938.934/2108.942/611. It is equipped with a steel casing between 0-25.5 metres depth and a stainless full tube until 19.65 metres with a diameter of 13" $^3/_8$. Beyond 25.5 metres, the hole is open and currently the F99 is not equipped with a pump. The well is used as piezometer to control hydraulic heads of the aquifer.

The productive Triassic formations correspond, as mentioned for Lépinay, to the zone of imbricated structures. Physico-chemical parameters of waters are influenced by the Lépinay production rates. When Lépinay functions, temperature and conductivity do not exceed 20ºC and 2 mS/cm. The maximum measured temperature of the water was 40ºC at the time of the realization of the well with a conductivity of 5.15 mS/cm.

Figure 8.6: View of the F99 well head (February 2008).

8.3.5 Old well Gontard

The old Gontard well had been exploiting the thermal resource before the drilling of the other deep wells (Fig. 8.7). At the beginning, the natural overflow was only exploited to avoid the disruption of hydrodynamical equilibria of the resource due to the occurrence of mixing processes with shallow groundwaters. The well was deepened between 1892 and 1996 with successive enlarging phases leading to the depth of 7.45 metres. Gontard is equipped with a cemented wall (2.6 m depth and 2.4 m of diameter) and with an unused submersible pump. The pump still functions and can be employed. Its coordinates are 938.936/2108.935/611.5. Currently, the Gontard well is not exploited, but is used to control hydraulic heads. The maintenance of the natural artesian flow avoids the overexploitation of the geothermal resource and guarantees that the pressure of the thermal aquifer will be higher than the pressure of shallower groundwaters.

Waters in Gontard are rejected downstream from the spa. Currently, annual average values of temperature and conductivity (at 25°C) are close

to 20°C and 2 mS/cm. Physico-chemical parameters are influenced by the Lépinay production rates. The maximum measured temperature and conductivity were 41°C and 6.1 mS/cm before the drilling of Lépinay.

Figure 8.7: View of the Gontard well head (July 2008).

8.4 Transport and exploitation of thermal waters

The spa of Saint-Gervais-les-Bains continuously exploits thermal waters below the Bon Nant alluvial deposits via three boreholes. The Lépinay well, which is only devoted to the medical care, makes it possible to exploit thermal waters of around 13 m^3/h and 38°C, and waters are drained towards two storage reservoirs via one pipe (20 m in length). The two reservoirs each have a storage capacity of 70 m^3, and are located in the subsoil of the spa. The quality of drained waters from pipes is controlled with chemical and bacteriological analyses to prove the absence of bacteria and the modification of the water chemistry (Vigouroux and Kay 2005).

The exploitation of the De Mey Est well is devoted to the cosmetics, and the production rate is exceeding the amount requested for cosmetics (5.5 m^3/h at 34°C). Pipes ensuring the transport of thermal waters to the storage reservoirs are insulated in the first 60 metres and then are buried in the last 90 metres (Vigouroux and Kay 2005). The distribution network of waters is entirely computerized, and is cleaned every two weeks to guarantee an irreproachable medical quality. Currently, the exploitation of thermal waters by the spa is mostly continuous with stable production rates in winter as well as in summer.
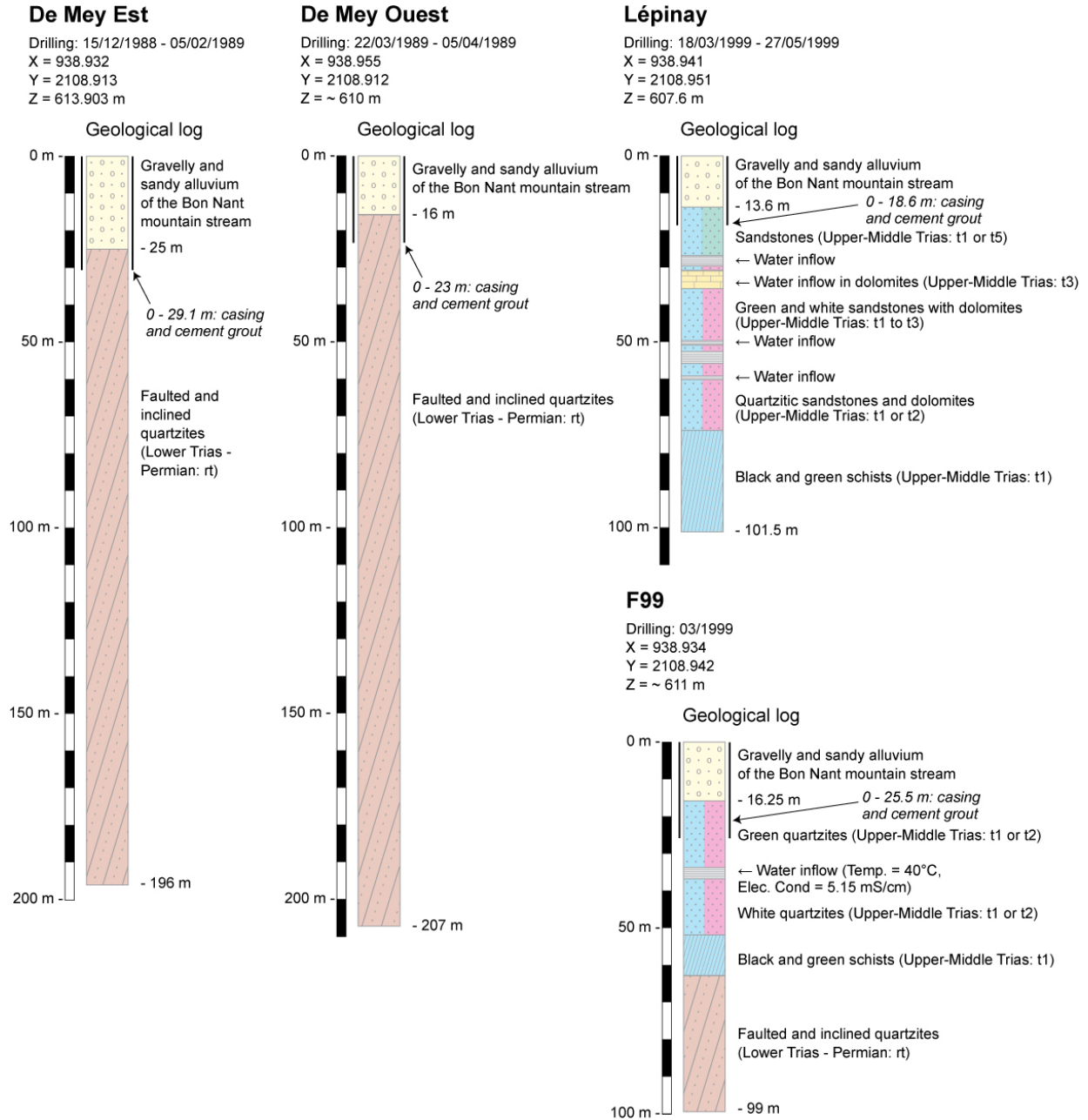
Figure 8.8: Geological descriptions of De Mey Est, De Mey Ouest, Lépinay and F99 boreholes modified from Barat and Jerphanion (1989) and ANTEA (2004). All the deep wells remained in the autochthonous cover of the Aiguilles Rouges Massif without reaching the basement.

9

Geological investigations at Saint-Gervais-les-Bains

9.1 Regional geological investigations

THE hydrothermal site of Saint-Gervais-les-Bains is located at the south-western low-elevation point of the Aiguilles Rouges Massif belonging to the external crystalline massifs of the Mont-Blanc Massif (Fig. 9.1). The Aiguilles Rouges basement consists of different types of crystalline rocks formed during the Hercynian (granite, rhyolite, conglomerate, sandstone) or before (gneiss) and highly deformed by the Hercynian and Alpine tectonic events.

The Aiguilles Rouges basement does not directly outcrop in the hydrothermal area in the Bon Nant Valley. It is certainly present at shallow depth, roughly at 300-500 metres below its autochthonous sedimentary cover (Permian-Triassic) which is overlapped by the Morcles nappe formations, which constitute the Mont d'Arbois and Mont Joly Massifs. The rocks forming the Morcles nappe mainly consist of limestones and marls (Epard 1989) drawing visible recumbent folds (Paréjas 1925). In the Megève area, the Mesozoic cover was eroded during the Quaternary glaciations and some outcrops of the Aiguilles Rouges basement are visible. This area and other zones located at the south of Les Contamines-Montjoie were considered as the recharge zone of the thermal regime with circulations only in the autochthonous cover (Iundt et al. 1987).

The observed major faults in the Saint-Gervais-les-Bains region are mainly vertical strike-slip systems or subvertical reverse faults of N-S to WSW-ENE directions, and are low dip thrusts related to the Morcles nappe movements. In the Bon Nant Valley, a major N-S faulted zone crosses the surroundings of Saint-Gervais-les-Bains inside the Aiguilles Rouges formations including its autochthonous cover. This faulted zone is extended to the limit between Aiguilles Rouges and Mont Blanc Massifs at the south of Les Contamines-Montjoie, and towards the north, the faulted zone seems to divide into several faults within the Aiguilles Rouges formations. One of these subvertical faults intersects the Bon Nant River in the hydrothermal area (named Springs Fault, Fig. 9.2) and certainly allows the upflowing of the deep fluid from the basement.

The deep geological structures are illustrated with three cross sections (Fig. 9.1). The geological history of this zone is highly complicated because it returns to the Hercynian and Alpine tectonic events. The basement had undergone both tectonic events (Von Raumer 1987, Von Raumer and Bussy 2004) whereas the Helvetic unit was only subjected to Alpine tectonic events. The description of the deep geological structures of the external crystalline massifs, given in the section 4.2 for the study of the Lavey-les-Bains hydrothermal system, according to

the seismic profile NRP 20 (Pfiffner et al. 1997), proposes the existence of two major thrust faults with a regional dip towards the south-east. These thrust faults were represented in the geological cross sections in Figure 9.1, and their depths were set according to the seismic profile.

The first thrust fault system is located in the southern part of the studied area, and puts in contact the Mont Blanc Massif over the Aiguilles Rouges Massif. A complex sedimentary syncline is intercalated between these two massifs, called Chamonix-Martigny zone, and disappears below the Quaternary formations in the sector of Les Houches - Chamonix. The Chamonix-Martigny zone is also considered as the root of the reversed limb of the Morcles nappe (Von Raumer and Bussy 2004). Towards the south-west in the area of Les Houches - Les Contamines-Montjoie, this geological

domain is difficult to follow due to the covering of the Liassic formations, named the complex zone in Figure 9.1.

The second thrust fault system corresponds to the limit between the Aiguilles Rouges the called the Infra-Rouges Massifs (Figs. 4.4 and 9.1). The Infra-Aiguilles Rouges basement is not outcropping but probably exists at a depth of roughly 3-4 kilometres below the Arve Valley. The thrust fault system certainly has a lateral extension in the NE-SW direction below the Aiguilles Rouges Massif from the area of Lavey-les-Bains to the area of Saint-Gervais-les-Bains. Inside the contact between the basements, the presence of sedimentary formations was assumed in the sector of Lavey-les-Bains (Bianchetti et al. 2006 for the AGEPP project), but it remains impossible to know if this presence occurs in the region of Saint-Gervais-les-Bains.

9.2 Geological setting of the south-western part of the Aiguilles Rouges basement

The geological history of the Aiguilles Rouges basement was described in the section 4.2 during the study of the Lavey-les-Bains hydrothermal system. As a reminder, the basement registered multiple geological evolutions.

Firstly, Neoproterozoic to Cambrian sediments were deposited with the emplacement of granitoid and metabasic to ultramafic magmatic rocks of Early Palaeozoic age (Von Raumer and Bussy 2004). After rifting and drifting (formation of Palaeotethys) all rocks underwent polyphase metamorphic and structural transformations during the Variscan orogeny, and were intruded by late Variscan granitoids. The resulting polymetamorphic basement was eroded during the formation of Upper Carboniferous sedimentary troughs (Von Raumer and Bussy 2004) receiving molasse-type detrital sediments (Von Raumer et al. 2003). The deformation of Aiguilles Rouges Massif continued on a smaller scale during the Alpine tectonic events. Indeed, Alpine metamorphism reached only the lowermost greenschist facies in the Aiguilles Rouges Massif (Von Raumer et al. 2003).

The rocks in the south-western part of the Aiguilles Rouges Massif are mainly similar to the northeastern area. Paragneiss and their injected veins,

and orthogneiss injection zones are also present in the area of Aiguilles du Belvédère - Lake Cornu - Le Brévent (see location in Figure 4.1).

In the southern part of the Aiguilles Rouges Massif, in the Servoz - Les Houches sector, other crystalline rocks are met in addition to gneiss (Pairis et al. 1992). Similar Carboniferous formations than in the Salvan-Dorénaz syncline outcrop and surround the Variscan granitoids, and especially the Visean sediments and volcanics of low grade metamorphism (Figs. 1.7 and 4.3). In this area, an important depression in the gneiss probably supported successive detrital and volcanic deposits before the Variscan and Alpine tectonic events. Indeed, the gneiss certainly exists at depth below these rocks.

The schistosity in the southern part of the crystalline massif has a preferential N-S direction (Fig. 4.3), different compared to the northern area (NE-SW). This N-S schistosity is prolonged in the basement to the area of Saint-Gervais-les-Bains city - Les Contamines-Montjoie, and is parallel to the complex fault system of the Bon Nant Valley where one of these faults crosses the hydrothermal area. Von Raumer and Bussy (2004) specified that this

LEGEND

Quaternary

- Glacier
- Not differentiated Quaternary deposits (moraine, river deposits)

Aiguilles Rouges massif

- Marl and sandstone (parautochthonous flysch): Lower Oligocene
- Quartzite, dolomite, limestone and marl: Trias - Eocene
- Conglomerate (Vallorcine pudding stone), sandstone, pelite and rhyolite: Carboniferous - Permian
- Vallorcine granite: Upper Carboniferous
- Gneiss and migmatite: Proterozoic - Paleozoic

Morcles nappe

- Limestone, marl and sandstone (including flysch): Cretaceous - Lower Oligocene
- Limestone and marl: Dogger - Malm
- Marl and limestone: Lias

Chamonix zone *(root of reversed limb of the Morcles nappe)*

- Limestone, dolomite, marl and sandstone: Trias - Eocene

Mont Blanc external crystalline massif

- Montenvers granitic gneiss: Carboniferous
- Gneiss: Proterozoic - Paleozoic, lenticular banded gneiss

Mont Blanc internal crystalline massif

- Leucogranite: Carboniferous - Permian
- Mont Blanc granite: Upper Carboniferous
- Rhyolite: Upper Carboniferous
- Gneiss: Proterozoic - Paleozoic

Ultrahelvetic nappes

- Wildflysch: Oligocene

Penninic nappe

- Dolomite, evaporite, limestone, marl and sandstone (including flysch): Trias - Eocene

- Fault
- Surface water: lakes (L.) and rivers (R.)
- International boundary
- Geological cross section
- Numerical cross section
- Mountain top
- Saint-Gervais-les-Bains spa
- City
- Village

Figure 9.1: Geological map and cross sections of the Saint-Gervais-les-Bains regional area according to the tectonic map of the Western Switzerland Alps (modified from Steck et al. 2001).

N-S schistosity often plunges towards the west direction. In the Aiguilles Rouges Massif, groundwater flows are certainly controlled by the presence of this N-S schistosity.

Moreover, a study about faults met in the sector of Aiguille du Belvédère was realized by Payraud (1991). Obtained results showed the presence of three major families of faults. The two most important families have NNE-SSW and NE-SW directions. The first family has a great dip towards the south and the second is subvertical. The third family is less frequent and has a NW-SE direction.

The same families of fractures were highlighted in the northern part of the Aiguilles Rouges Massif.

Moreover, Payraud (1991) also showed the existence of mylonitic zones of NNE-SSW direction such as the Remuaz mylonitic zone which extends towards the Vallorcine granite (see location in Figure 4.1). The crushed aspect of rocks near mylonitic zones was described by Payraud (1991). These rocks with high hydraulic conductivities certainly drain a large amount of water and form aquifers. The erosion processes of these rocks along mylonitic zones generate depressions with lakes. The absence of outlet for these lakes can be explained by a large amount of water infiltrating deeper into the system.

9.3 Local geological setting

The local geological setting concerns the autochthonous sedimentary cover of the Aiguilles Rouges Massif which was intensely affected by the Alpine tectonic events. Before the drilling of deep wells at Saint-Gervais-les-Bains, the geological setting was not completely well-known. Only the Springs Fault was mentioned to explain the presence of thermal waters (Vuataz 1982). Later, geological works carried out by the BRGM consulting office during the 1980's and as well as after drilling of Lépinay and F99 boreholes in 1999 highlighted the presence of a thrust fault system below the Bon Nant deposits. This thrust fault puts in contact a normal series of upper-middle Trias with black and green schists at the bottom of the series (t1) over the lower Triassic-Permian quartzite (Fig. 9.2).

The Permian formations are visible on the right bank of the Bon Nant River and consist of fine grained conglomerates, pelitic schists and quartzite. Their thickness was estimated of around 80 metres (Iundt et al. 1987). The Permian series is thrusted by the upper-middle Triassic series, and the thrust fault is visible in the Bon Nant narrow gorge upstream from the spa, but invisible near the spa where the valley widens. The upper-middle Triassic formations contain various rocks such as dolomites, limestones, gypsum, cellular dolomites, schists, quartzite and sandstones (Figs. 9.2 and 9.3).

Movements of the thrust fault near the contact generated a complex zone of imbricated structures with alternations of quartzite, dolomites and schists

which was observed in Lépinay and F99 wells during drilling (Fig. 8.8). Many uncertainties still exist about the stratigraphy of the log established in Lépinay and F99 wells. Two assumptions can be formulated: 1) Quartzite inside the imbricated structures belong to the lower Triassic-Permian formations and would be rock scaling, because the geological investigations made in the field before drilling does not mention the presence of quartzite in the upper-middle Triassic formations (t1 to t5-L). 2) the geological investigations forgot to specify the presence of quartzite t1 and t2 formations (absence of quartzite).

In the De Mey Est and De Mey Ouest boreholes, only the lower Triassic-Permian quartzite was encountered below the Quaternary filling with the presence of thermal water inflows deeper than 150 metres depth. Therefore, De Mey boreholes are located on the other side of the thrust fault system. Between De Mey wells and Lépinay-F99 wells, the Gontard and Sulfureuse springs occur and thus it can be assumed that springs emerge along the thrust fault and not along the Springs Fault as it was assumed previously. The Springs Fault is a dextral strike-slip and reverse fault shifting the thrust fault system. It has a great dip towards the east and was probably intersected by the two De Mey boreholes.

Downstream from the spa, the Ferrugineuse and Magnésienne springs emerge in the Bon Nant bed at the foot of dolomitic and gypseous outcrops (Figs. 9.2 and 9.3). They are two cold springs with iron oxide deposits, with stable temperature, electrical

conductivity and discharge in summer as well as in winter.

In the hydrothermal area, the thickness of the Quaternary filling varies between 10 and 25 metres. The rooftop of the autochthonous cover appears undulating on short distances.

A fracturing study highlighted the presence of three families of fractures (Iundt et al. 1987). The first family of fractures is sub-meridian with strong dips towards the west and is more frequent in the right bank of the Bon Nant Valley. The second family has E-W to ESE-WNW directions with various dips towards north and south. Fractures of this family are mostly open or sometimes filled with quartz. Finally, the last family has NW-SE to NNW-SSE directions with strong dips towards the east. Fractures of this family intersect the thalweg and the Bon Nant Valley as they are related to the Springs Fault.
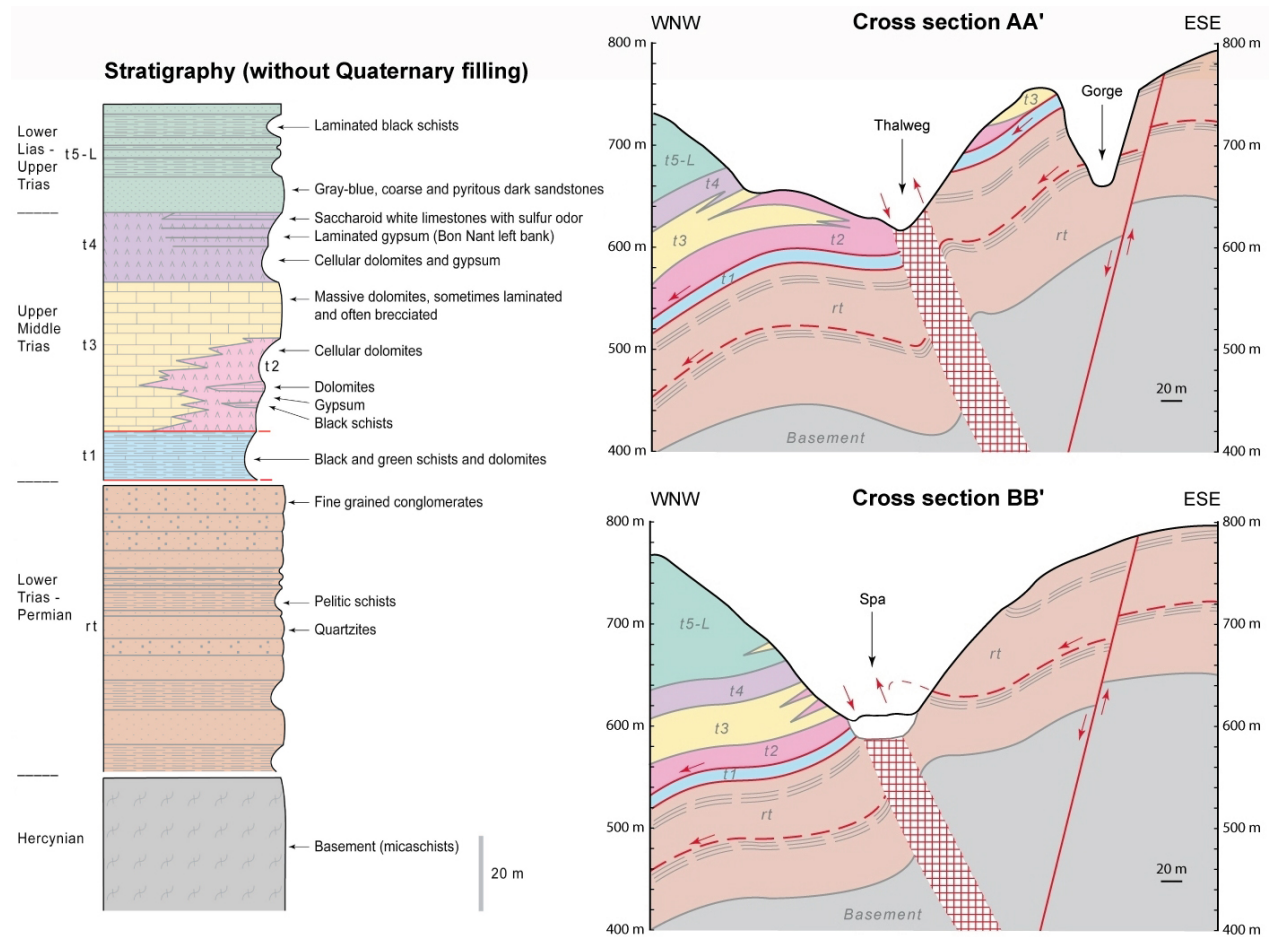
Figure 9.2: Geological cross sections and stratigraphy of the autochthonous cover of the Aiguilles Rouges Massif in the Saint-Gervais-les-Bains hydrothermal area (modified from Iundt et al. 1987). The section lines are illustrated in Figure 9.3.
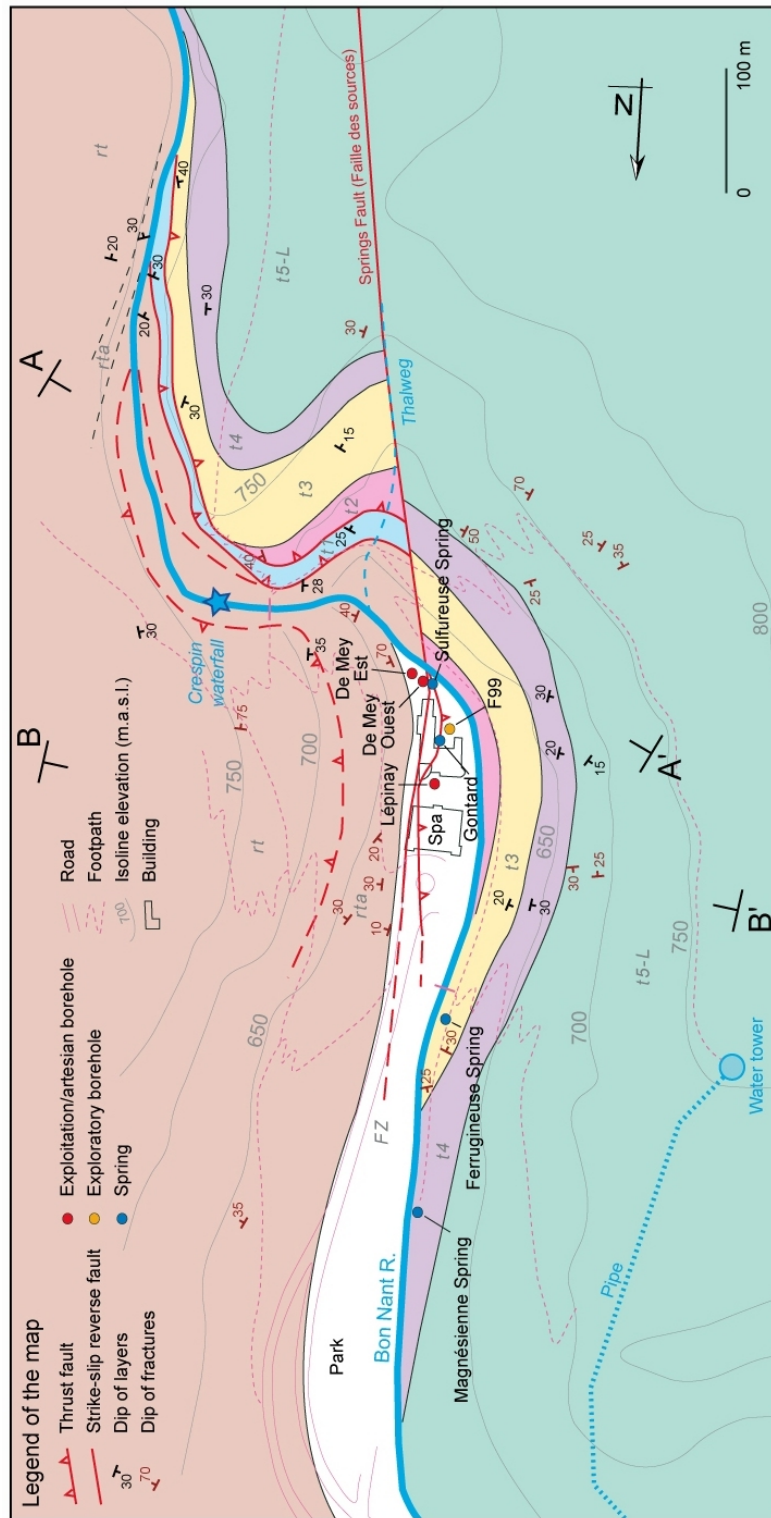
Figure 9.3: Geological map of the Aiguilles Rouges Massif in the Saint-Gervais-les-Bains hydrothermal area (modified from Iundt et al. 1987). The legend of the formations is given in Figure 9.2.

10

Hydrogeological and geochemical investigations at Saint-Gervais-les-Bains

10.1 Local hydrogeological and geochemical investigations

10.1.1 Hydrogeological knowledge before this study

Firstly, a complete hydrogeological study of the Saint-Gervais-les-Bains hydrothermal system was carried out by FD Vuataz between 1977 and 1978 (Vuataz 1982). In the 1970's, boreholes did not exist and his hydrogeological investigations were based on the study of the Gontard well, Sulfureuse and Piscine thermal springs (Piscine was not found during the sampling campaign), the Magnésienne cold spring and the Bon Nant River.

FD Vuataz analysed waters of these sampling points showing that the Gontard well had the highest temperature (40.7ºC) and a mineralization of around 4880 mg/L. He also measured high temperatures for the two thermal springs in the range of 30-35ºC, but various mineralizations, between 4100-4400 mg/L in Piscine and 4800-5000 mg/L in Sulfureuse. Looking at these first results, the temperature and the mineralization do not seem to be well correlated.

FD Vuataz (1982) classified the waters according to their chemical compositions and grouped them into three families based on 20% of the total dissolved solids. Gontard and Sulfureuse are

Na-SO_4>Cl waters whereas Piscine has Na>Ca-SO_4>Cl geochemical type. The Magnésienne spring is frankly a Ca-SO_4 water with high magnesium contents of around 75 mg/L. Based on these observations, properties of the deep groundwater flows were described with the assumption that the two following aquifers were present. 1) For the Magnésienne cold spring which has stable physico-chemical parameters, a flow system was assumed in Triassic formations from the Mont d'Arbois Massif with gypsum and dolomite dissolutions to explain the chemistry of the water. This flow system gives low chloride contents in water (< 20 mg/L), and thus halite is certainly absent in Triassic rocks as it was already mentioned by Arthaud and Dazy (1989). 2) The second flow system concerns thermal waters having high Na-Cl concentrations and a residence time higher than 25 years. To explain the chemistry of the water, FD Vuataz proposes that there are circulations in the Triassic formations from the area of Megève and then deeper circulations in the basement reaching the geothermal reservoir. The relatively high concentration of sodium and sulphate compared to chloride and calcium is probably re-

147

lated to cationic exchanges in the micaschists basement. The Springs Fault ensures the uprising of the deep fluid before mixing with the Bon Nant groundwater, however the water does not seem to mix with the Magnésienne Ca-SO$_4$ waters. Finally, FD Vuataz evaluated the reservoir temperature using the chalcedony geothermometers, and he found 70-75°C and 60-65°C respectively for Gontard/Sulfureuse and Piscine thermal waters.

Later, a second complete hydrogeological study was carried out by the BRGM consulting office (Iundt et al. 1987). The objectives were to evaluate the geothermal potential and to understand the deep flow system with a final aim to suggest drilling areas. Firstly, a local geological investigation with a map and several cross sections was carried out improving the geological knowledge. This investigation defined the stratigraphy of the Triassic and Permian autochthonous cover with the presence of faults. In detail, the middle-upper Triassic formations consist of various rocks including schists at the bottom, cellular dolomite, dolomite, gypsum, limestone and quartzite at the top. To explain the origin of thermal waters at Saint-Gervais-les-Bains, the BRGM consulting office supposed a deep flow system from the Mont Joly Massif where the Triassic formations outcrop in the sector of Les Contamines-Montjoie, with the dissolution of the Triassic rocks at depth. Iundt et al. (1987) analysed thermal waters and obtained results that were concordant with previous analyses made by Vuataz (1982) and Grimaud (1987).

The production rate of the Gontard well is close to 4 m^3/h with a drawdown of 6 metres, which is 1.45 metres higher than the bottom of the well. The artesian rate of the overflow was measured at around 1.5 m^3/h. The Gontard production rate was sufficient for requirements of the spa but it was not possible to increase the rate beyond 4 m^3/h. Therefore, it was necessary to increase the geothermal resource. Moreover, strong mixing processes occur in Gontard and thus it was also necessary to protect the resource from cold water inflows. In 1989, the De Mey Est and De Mey Ouest wells were drilled.

The BRGM consulting office was charged to supervise drilling works (Barat and Jerphanion 1989). Hydrogeological observations during the drilling of De Mey Est showed a strong geothermal anomaly at the bottom of the Quaternary filling with a temperature and an electrical conductivity of around 26°C and 3-4 mS/cm. During drilling, the discharge

of the Sulfureuse spring was disrupted confirming the presence of thermal waters in the filling. After that the drilling continued and thermal inflows at different depths were observed in the De Mey Est well. In detail, two main zones were highlighted between 99-107 and 165-175 metres depth. Globally, the rate, the temperature and the conductivity increased gradually with the depth. At the bottom of the borehole, the temperature reached 32.2°C in the quartzite with a dip of around 60-65°.

Firstly, a pumping test was carried out in February 1989 with the aim to determine the production capacity of the De Mey Est well. The imposed rate was 16 m^3/h over 23 hours. During the first 20 hours, the water table remained relatively stable but tended to decrease slightly after. Measurements made at the end of the test gave a drawdown of 20 metres with a temperature of 28.9°C and a conductivity of around 4 mS/cm. During this test, the Gontard well was not disrupted: 1.5 m^3/h, 41.5°C and 5.75 mS/cm. Finally, an artesian flow rate in De Mey Est was measured at around 9 m^3/h.

Based on the results of the pumping test, it was decided to drill another deep well called De Mey Ouest between De Mey Est and the Sulfureuse Spring. Drilling works occurred in March and April 1989 and a strong geothermal anomaly was also observed at the bottom of the filling (26°C). The Sulfureuse flow rate was also disrupted during drilling. With the deepening of De Mey Ouest, thermal water inflows were encountered from large fractured zones. At the end of the drilling, an artesian flow rate of 10.5 m^3/h was measured with a temperature at 28.9°C and a conductivity of 4.1 mS/cm.

Table 10.1: Temperature and conductivity measurements in De Mey Est, De Mey Ouest and Gontard after the short pumping test in De Mey Ouest in April 05th 1989 (Barat and Jerphanion 1989). Temp.: temperature, Cond.: conductivity., DME: De Mey Est, DMO: De Mey Ouest.

Sampling point	Temp. (°C)	Cond. (mS/cm)	% of Cond. from Gontard
DME	29.2	4.95	85
DMO	29.2	4.35	75
Gontard	41.4	5.80	100

A pumping test was carried out in De Mey Ouest in April 05th 1989 with two different production rates. Firstly, a rate of 8 m^3/h was imposed during one hour. Results showed a drawdown of 7.5 metres in De Mey Ouest and an artesian flow of 5 m^3/h in De Mey Est. A second rate of 15 m^3/h in De Mey Ouest gave 15.5 metres of drawdown and an artesian flow of 3.6 m^3/h in De Mey Est. At the end of the pumping test, temperature and conductivity were measured in the two De Mey and in Gontard wells (Table 10.1). Compared to De Mey Est, the pumping test in De Mey Ouest generated an increase of the physico-chemical parameters in waters in the two De Mey wells, whereas parameters of waters in Gontard remained stable.

To increase the hydrogeological knowledge, longer pumping tests were carried out in the two De Mey wells in 1989. The description of the different pumping phases is given in Table 10.2.

Table 10.2: Description of the pumping phases in the two De Mey boreholes between May and June 1989 (Barat and Jerphanion 1989). nat.: natural.

Period (day/month)	De Mey Est (m^3/h)	De Mey Ouest (m^3/h)
11/05 to 15/05	nat. flow	13
22/05 to 02/06	nat. flow	13.5 to 11.5
02/06 to 10/06	8 to 7.5	11.5 to 10.5

In the period 22/05 to 02/06 and during the first hour of pumping, the water level in the wells remained stable and the transmissivity of the aquifer was evaluated at around 10^{-3} m^2/s. After one day of pumping, a bending in the curve showing the variation of the drawdown was observed. This suggests that the exploited aquifer presents hydraulic properties less favourable. Then, the water level tends to stabilization after 10 days of pumping. For this period, the transmissivity was calculated around 2.10^{-4} m^2/s with an average production rate of 12 m^3/h and a drawdown of 18.6 metres. During the test in De Mey Ouest, the artesian flow rate in De Mey Est decreased up to 1 m^3/h after the first hours of pumping, then it tended towards zero and finally the water table was maintained close to the level of the well head.

At the beginning of the production rate of 8 m^3/h in De Mey Est (June 02nd 1989) generated an increase of the water level in De Mey Ouest (+1 m) due to the opening of fractures in the bedrock (Barat and Jerphanion 1989). Then the water tables in the two boreholes decrease simultaneously and after 10 days of pumping and the slopes of the curves showing the drawdown evolution in the two wells remained constant. Towards the end of the pumping, 3 minutes proved sufficient to obtain the natural artesian flow rate in wells. In summary, with an average production rate of 7.5 m^3/h in De Mey Est and of 10.5 m^3/h in De Mey Ouest, the induced drawdown can be evaluated at around 19 and 22 metres respectively.

In a qualitative overview, the production rate imposed in De Mey Ouest (De Mey Est maintained with its natural rate) generated an increase of the parameters during the first 24 hours of pumping, which is correlated with the observed variation of drawdown. Then, the temperature and the conductivity remained stable until the end of pumping (Table 10.3). In the period 02/06 to 10/06 during the first hours of pumping, the imposed rates in the two De Mey wells produced a slight readjustment of the parameters of waters in the wells, then remained stable. Results also indicated a difference in temperature and conductivity between De Mey Est and De Mey Ouest due to various degrees of mixing processes.

Measurements in the old Gontard well during the first 20 days of these tests showed an unexpected small decrease of the temperature (40.1 to 39.6°C).

Thermal waters were sampled for chemical analyses during pumping tests. Obtained results indicated a Na-SO$_4$>Cl geochemical type for waters in the two De Mey wells, that is to say the same type as in Gontard and Sulfureuse (Barat and Jerphanion 1989). Only the dissolution of the Triassic rocks was used to explain the origin of the compounds in the water.

Later, Bianchetti (1993b) supposed circulations in the basement to explain the chemistry of thermal waters. Bianchetti (1993b) studied thermal waters with high chloride contents in the Western Alps and neighbouring regions. The comparison of the chemistry of thermal waters determined that the Saint-Gervais-les-Bains thermal waters come from circulations in the basement where seawater brines or fluid inclusions are probably leached. Moreover, Grimaud (1987) had already mentioned possible circulations in the basement because the Saint-Gervais-les-Bains thermal waters have ratio of the strontium isotopes (^{87}Sr/^{86}Sr = 0.715).

In 1996, the SOGREAH consulting office was charged to understand the origin of decreasing of the production rates in the De Mey wells, from 13.5 m³/h (authorized rate) to 10.5 m³/h. A video inspection and pumping tests were carried out. September 18th 1996, the video inspection showed that the observed decrease of rate was not related to the filling of fractures from precipitation processes (SOGREAH 1996). The process of sandy deposit in the two wells was proposed to explain it, but not validated. Temperature and conductivity data acquisition in the period 1993-1994 highlighted an increase respectively from 31 to 33°C and from 2.5 to 2.75 mS/cm. Moreover, maintaining a constant pressure in De Mey well heads, flow rates regularly decreased since 1993. During the period September 1989 to February 1990, flow rates in De Mey wells had been decreased from 1.8 to 1.3 m³/h and from 2 to 1.2 m³/h respectively, that is to say significantly lower than artesian rates measured after the drilling in 1989.

Table 10.3: Temperature, conductivity and flow rates measurements in De Mey Est, De Mey Ouest during and after long pumping tests between May and June 1989 (Barat and Jerphanion 1989). Temp.: temperature, Cond.: conductivity, nat.: natural.

Sampling point	Temp. (°C)	Cond. (mS/cm)	% of Cond. from Gontard	Flow rate (m³/h)
First long pumping test (11/05 to 15/05)				
De Mey Ouest (first 24 hours)	29.7	4.35	75	14
De Mey Ouest (end of pumping)	29.9	4.75	82	12
De Mey Est	function of the flow	5.35	93	variable
Third long pumping test (02/06 to 10/06)				
De Mey Ouest (first hours)	29.7	4.75	82	10.5
De Mey Est (first hours)	29.7	5.15	90	7.5
De Mey Ouest (end of pumping)	29.0	4.60	80	nat. flow
De Mey Est (end of pumping)	29.6	5.44	94	nat. flow

A longer pumping test was supervised by SOGREAH between September 17th and October 27th 1990. Obtained results showed that the critical production rate is 8-9 m³/h, adding each rate of the De Mey wells. Therefore, the initial authorized rate of 13.5 m³/h was not at all suitable for the long-term exploitation of the geothermal resource.

In 1999, Lépinay and F99 boreholes were drilled and met thermal waters in the zone of imbricated structures. After the installation of equipment in Lépinay, a long pumping test was carried out between March 2000 and January 2002 with flow rates varying between 8 and 23 m³/h. During the test, production rates in De Mey wells were maintained in their natural rates. The comparison of data acquired in Lépinay, Gontard, F99, Sulfureuse and De Mey sampling points highlighted an immediate hydrogeological relationship between Lépinay, Gontard, F99 and Sulfureuse (Fig. 10.1). The relation with the Sulfureuse Spring was proven with water table measurements, but not with temperatures which are continuously influenced by the seasonal climatic conditions. The Lépinay production rate did not generate a decrease of the parameters of waters in De Mey wells and conversely. This can be explained by their different geological settings, and consequently by the presence of two aquifers below the Quaternary filling separated by the thrust fault.

Thermal waters in Lépinay were sampled for chemical analyses during the long pumping test in 2001. Obtained results from ANTEA (2002) also indicated a Na-SO$_4$>Cl geochemical type for waters in Lépinay, appearing to be similar to types of Gontard, De Mey Est and De Mey Ouest waters. In detail, the chemical composition of waters in Lépinay showed some differences. Sodium, chloride and sulphate contents are lower compared to Gontard values measured in 1994, -30%, -42% and -17% respectively (ANTEA 2002).

The chemical composition of waters in Lépinay was clearly defined to obtain the authorization for the exploitation of the geothermal resource (ANTEA 2004). Later, a long pumping test in 2003 was supervised by the ANTEA consulting office with the objective to define the authorized production rates. Initially, the Lépinay rate was stopped during one month during which time De Mey Est and De Mey Ouest rates remained stable at 5.5 and 3.5 m^3/h respectively. Then, a rate of 13 m^3/h was imposed on Lépinay during three months. Continuous measurements permitted the evolution of the physico-chemical parameters of waters in Lépinay, De Mey, Gontard, Sulfureuse and F99 sampling points to be followed.
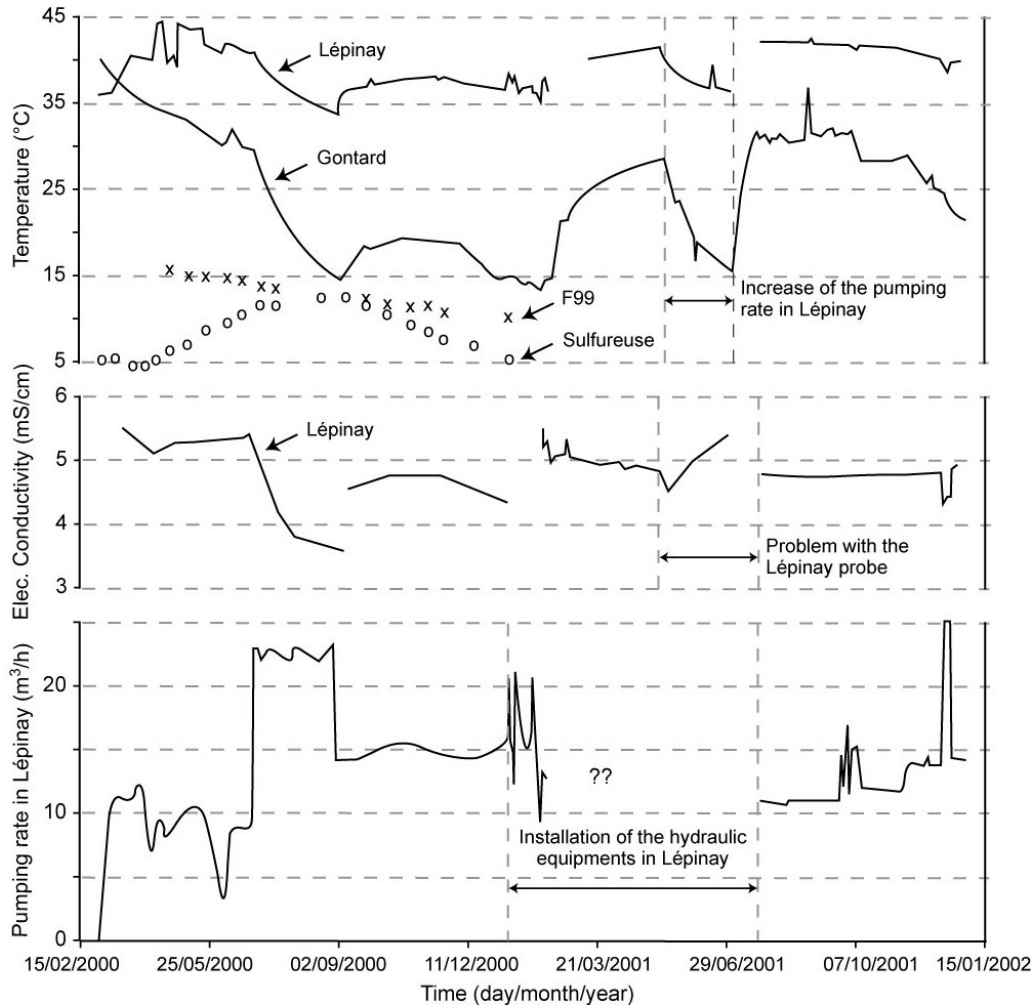
Figure 10.1: Results of the long pumping test on Lépinay well and its impact on Gontard old well, F99 borehole and Sulfureuse spring (ANTEA 2004).

Measurements in Lépinay showed stabilization of the water table and other parameters with a rate of 13 m^3/h. The final drawdown did not exceed 3.3 metres. It was proved an immediate interference between Lépinay and F99 and to a lesser extent with Gontard. For F99, drawdown characteristics are the same as those observed in Lépinay but the amplitude is less important (2 m only). With a rate of 13 m^3/h, the drawdown is stabilized at 3 centimetres above the overflow in Gontard, maintaining its artesian flow. However, the conductivity strongly decreased in Gontard during the test, 2.7 against 6.1

151

mS/cm (ANTEA 2004). Its temperature was also affected (21ºC) and proves a dilution with cold waters. Moreover, the conductivity gradually reduced for the Sulfureuse Spring reaching 0.4 mS/cm. The temperature of Sulfureuse is influenced by seasonal climatic conditions. Finally, the parameters of the two De Mey wells reacted with their own production rates, but were not modified when the production started in Lépinay.

Recently, the spa decided to undertake video inspections and geophysical logging in the two De Mey wells with the aim to optimize their production rates (Iundt 2008). Results for De Mey Est showed three main fissured zones, with the most important zone between 82-108.5 metres depth (Fig. 10.2). Temperature and electrical conductivity measurements at different flow rates raised cold water inflows from these three zones and a thermal water

production below 167 metres depth. A pumping rate of 3.8 m³/h is necessary to obtain a homogeneous mineralization on the full length of the borehole. The low temperature losses seem dependent on the heat exchanges with the surrounding rocks. Concerning De Mey Ouest, results are concordant with the De Mey Est investigation. The current production rates, respectively 5.5 and 3.5 m³/h in De Mey Est and De Mey Ouest, allow attenuating the dilution processes. Their hydraulic connectivity was also proven during these investigations. With the current production rates, the drawdown is close to 50 metres in De Mey Est. While stopping De Mey Ouest, a drawdown of 50 metres can be obtained with a rate of 10 m³/h imposed in De Mey Est. Discussions about the exploitation of the wells were recently raised.
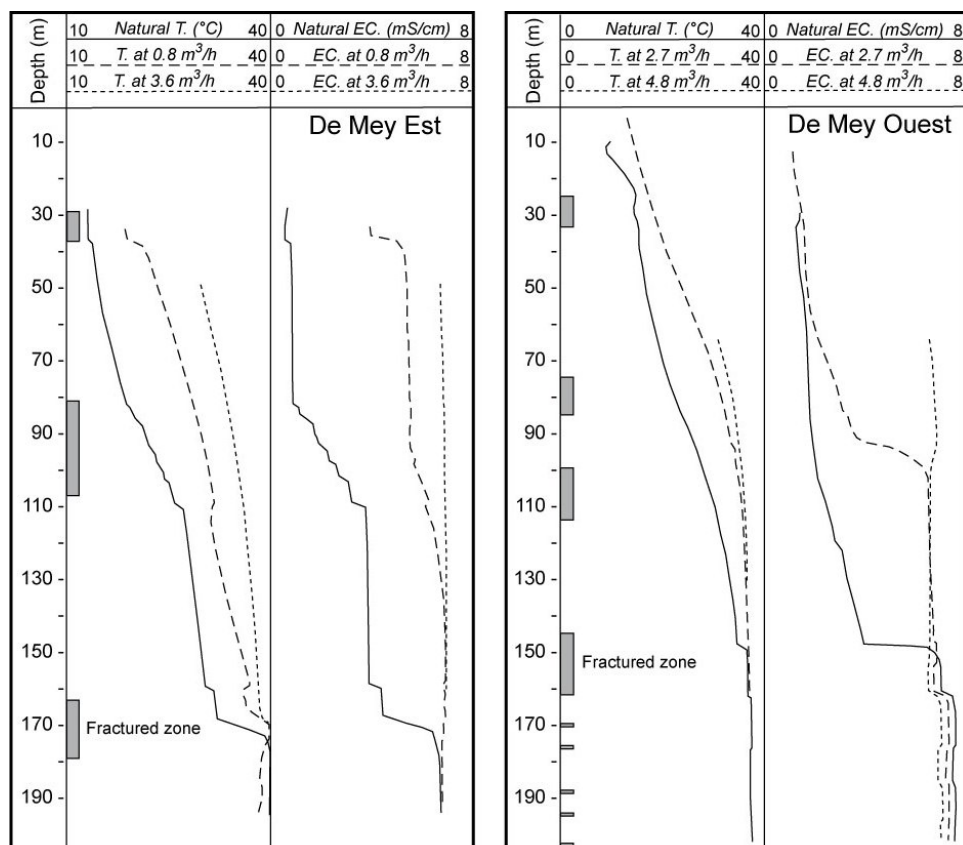
Figure 10.2: Temperature and electrical conductivity profiles in De Mey Est and De Mey Ouest wells realized between 2006 and 2008 (Iundt 2008). T.:Temperature, EC.: Electrical Conductivity.

10.1.2 Water chemistry

On the basis on the chemical and isotopic analyses, the sampled waters can be subdivided into three groups (Fig. 10.3). The first group includes Na-SO$_4$ waters rich in chloride, of around 1.2 g/L, with a high electrical conductivity (above 5 mS/cm) and temperatures (above 35°C). This group represents the deep thermal end-member from the basement. In detail, waters of Lépinay are slightly different, with less chloride, of around 0.6 g/L, and a little more sulphate compared to De Mey Est (2 g/L against 1.8 g/L). Lépinay was closer to the diluted waters of Gontard when the Gontard was not disrupted by Lépinay. The second group refers to Ca-SO$_4$ waters with medium salinity ($\approx$ 2.5 mS/cm)

and low temperature (8-12°C), represented by the cold springs Ferrugineuse and Magnésienne located downstream from the spa. This group with low chloride contents, of around 20 mg/L, is representative of waters circulating inside gypseous formations. The last group is characterized by the superficial groundwaters of the Bon Nant Quaternary filling, including the Sulfureuse spring which has had low physico-chemical values since the exploitation of the thermal aquifer. Concerning the Bon Nant River, temperatures vary in function of the seasons (4-12°C) and the salinity oscillates between values lower than 0.5 mS/cm depending on the season.
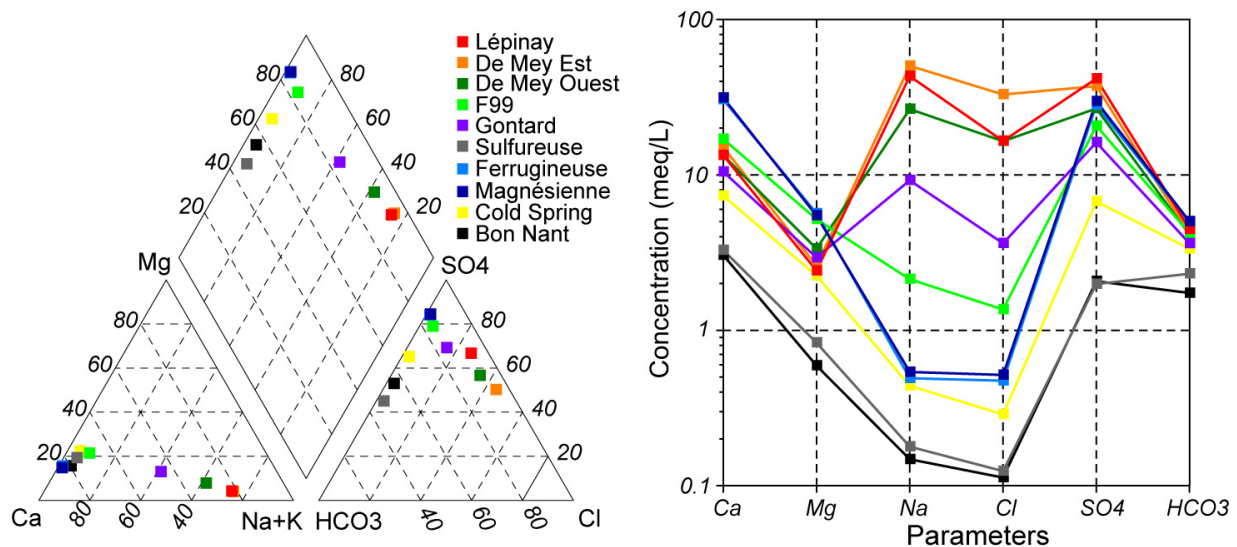
Figure 10.3: Major elements concentration plots (Piper and modified Shoeller diagrams) for groundwaters of the Saint-Gervais-les-Bains area with data collected during the new sampling campaign (see data in appendix C). Locations of the samples are shown in Figure 9.2 except for the Cold Spring which is located close to the Gontard well.

10.1.3 Mixing processes

Mixing processes were described in this section interpreting the correlations between physico-chemical parameters. Previous data were compiled from unpublished reports and from the PhD thesis of Vuataz (1982), and data of the sampling campaign in 2008 were added. Unfortunately, some

old sampling points could not be found on the hydrothermal site in 2008 (Piscine/Salle des Machines sampling), but historical data were taken into account for the geochemical interpretations. The interpretation of correlations between physico-chemical parameters versus temperature, TDS (to-

tal dissolved solids), chloride, sulphate and calcium contents (Fig. 10.5) allowed the presence of different end-member components to be identified. Two assumptions are possible: 1. the thermal end-member from the basement dissolves the rocks of autochthonous cover before mixing with two cold shallow groundwaters (three components); 2. two different thermal end-members from the basement and the Triassic cover having the same temperature are mixed with two cold shallow groundwaters (four components). According to Sonney and Vuataz (2010d), the first formulated assumption seems to be more realistic because it implies a single thermal component. At this stage of the investigation it is difficult to decide what the best hypothesis is to explain the chemical processes occurring at Saint-Gervais-les-Bains.

Mixing processes are different for the two aquifers at depth. For the Permian aquifer crossed by De Mey wells, thermal waters are slightly diluted by the Bon Nant groundwater but considerably by a $Ca-SO_4$ and low-Cl water circulating in the Permian quartzite which is chemically similar to the Ferrugineuse and Magnésienne springs (named PTCW in Table 10.4: Permian-Triassic Cold Water). The Ca/SO_4 molar ratio of this cold water is aligned along the gypsum dissolution line. For this mixing system, the dilution of the saline thermal end-member is accompanied by a significant decrease of temperature, mineralization, alkaline ions and chloride (Fig. 10.5). On the contrary, calcium and magnesium considerably increase whereas sulphate slightly decreases because these two components have high sulphate concentrations. Thereby, this process indicates mixing between a $Na-SO_4$ and high-Cl thermal component from the Aiguilles Rouges basement, also called TC-ARB in Table 10.4, with a cold $Ca-SO_4$ and low-Cl water circulating in the Permian-Triassic autochthonous cover.

Concerning the aquifer in the zone of imbricated structures (upper-middle Trias) crossed by Lépinay and partially by F99 (Fig. 10.6), chemical processes seem to be more complicated because pumped waters are half as concentrated in chloride with temperature of around 39°C. Plots versus chloride show that Lépinay seems to be a mixture between Gontard and a low-Cl water which would have a temperature of around 35-40°C. This assumption calls upon a supplementary other thermal end-member rich in sulphate and poor in chloride resembling to a Triassic water type, this was however not assumed by Sonney and Vuataz (2010d). Lépinay and Gontard waters are also diluted with

154

the Bon Nant groundwater with various degrees. Currently, the Lépinay production rate generates a decrease of the ascending thermal pressure in Gontard, supporting Bon Nant groundwater inflows in the Gontard well (20°C and 1.6 g/L). The only analysis available from the unused borehole F99 shows a mixing between the Bon Nant groundwater, the $Ca-SO_4$ and low-Cl cold water with an almost negligible proportion of thermal water.

Correlations between water stable isotopes versus chloride and temperature were represented in Figure 10.4. Deuterium and oxygen-18 stable isotopes show lower values for the thermal end-member indicating a higher recharge elevation. In detail, results also highlighted the impact of seasonal climatic variations in the Bon Nant groundwater. In summer, the snow melt brings surface waters from a higher elevation whereas in winter, precipitations higher than 1500 metres are mostly stored.
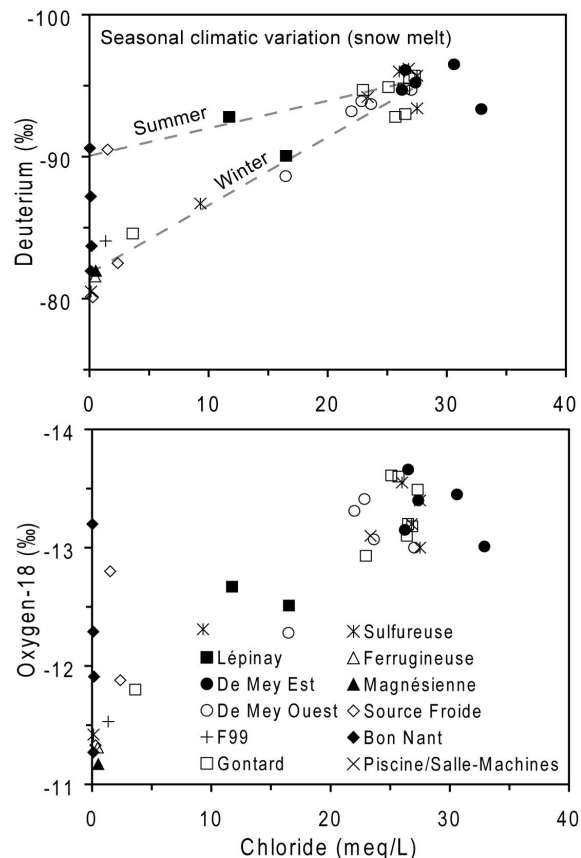
Figure 10.4: Plots of water stable isotopes versus chloride content in waters for all existing data showing seasonal climatic variations (see data in appendix C).
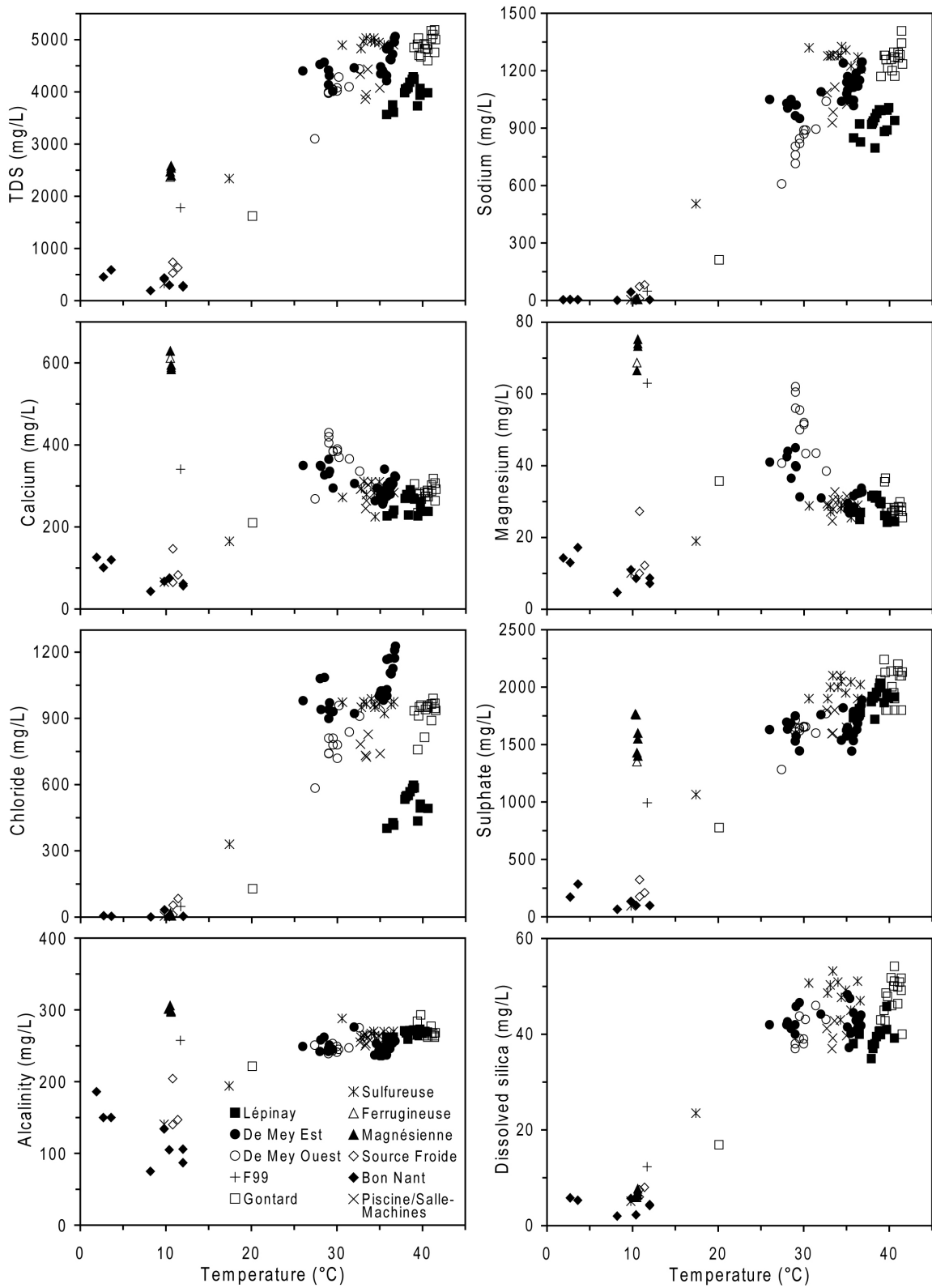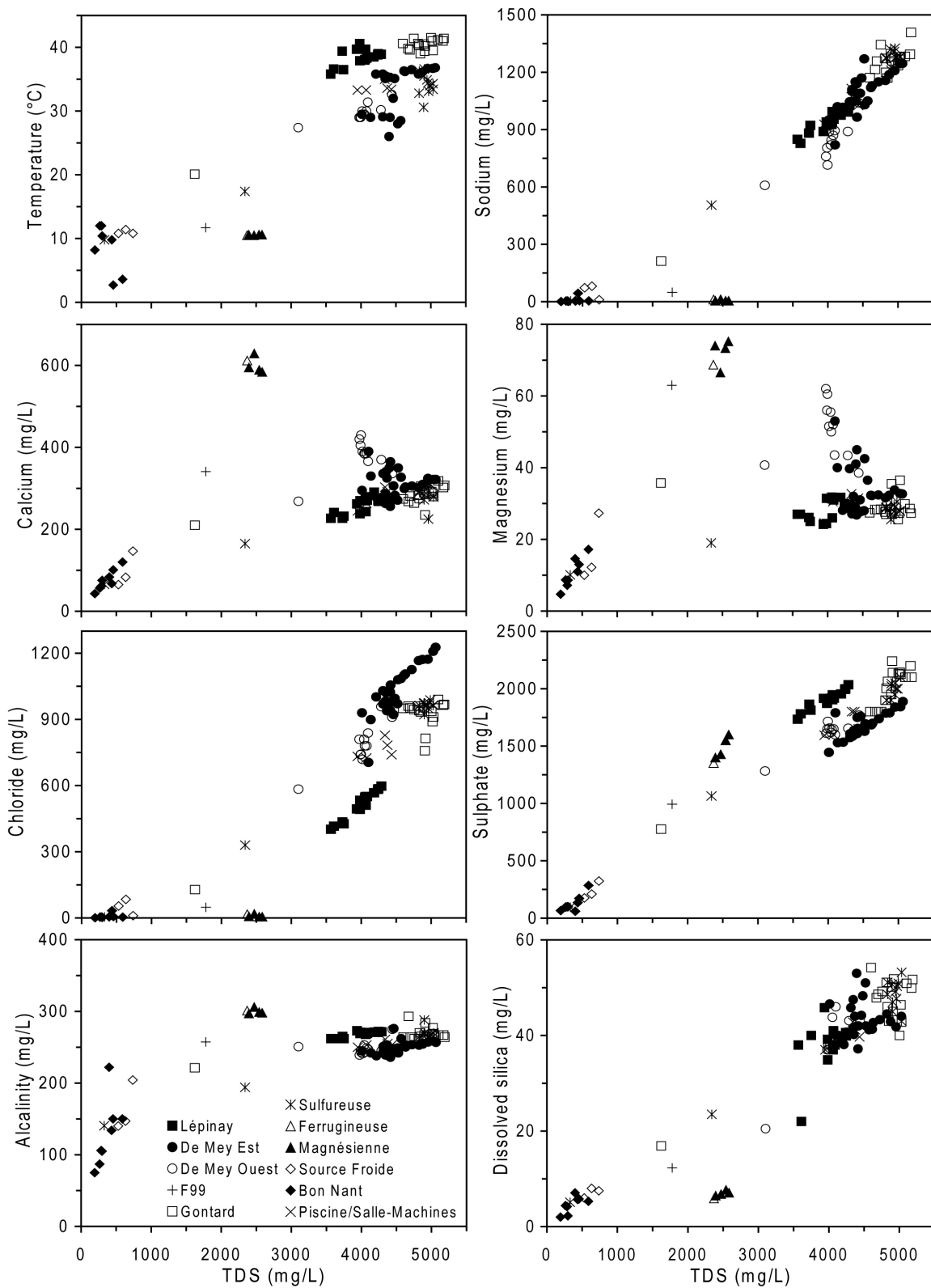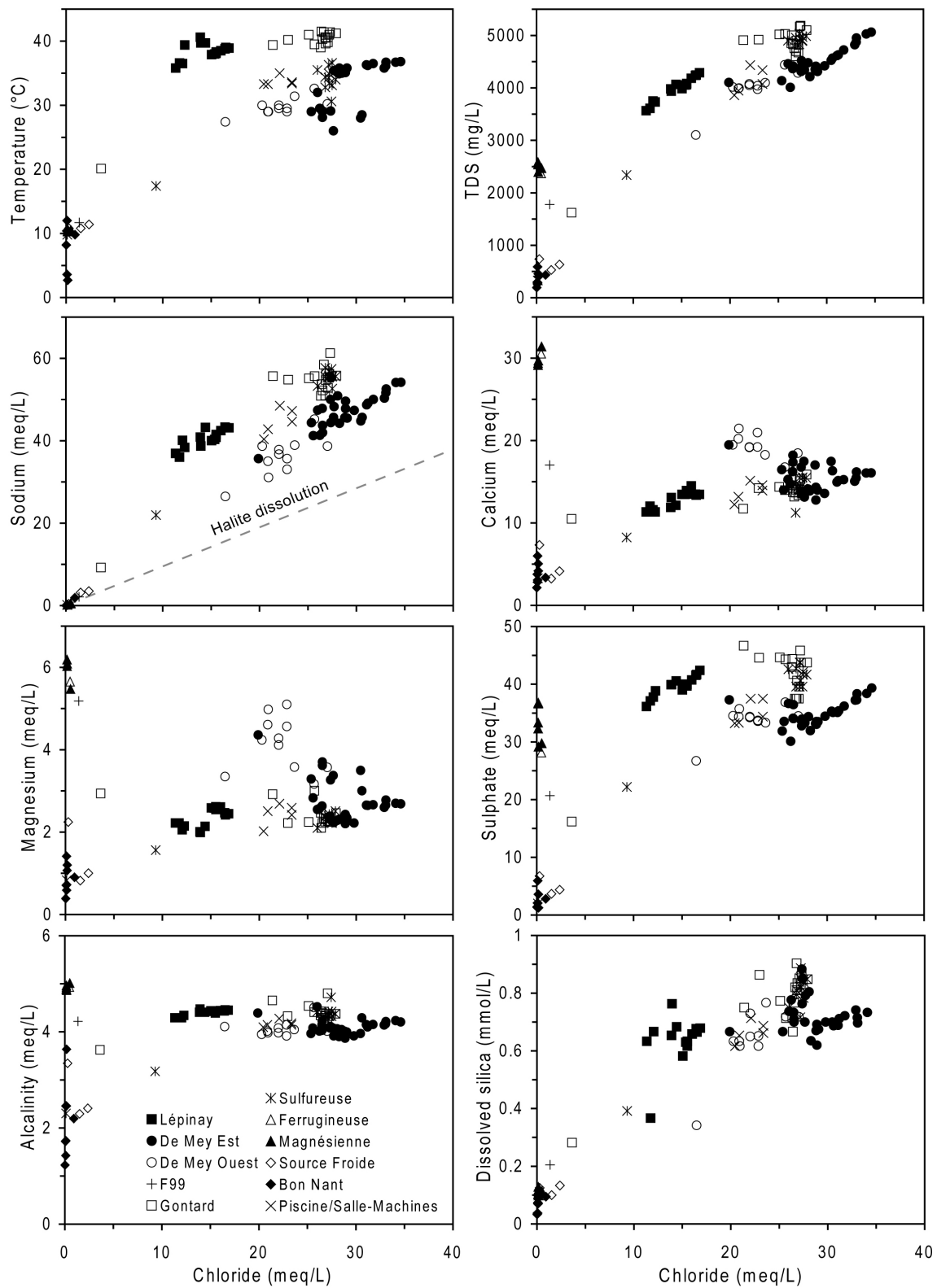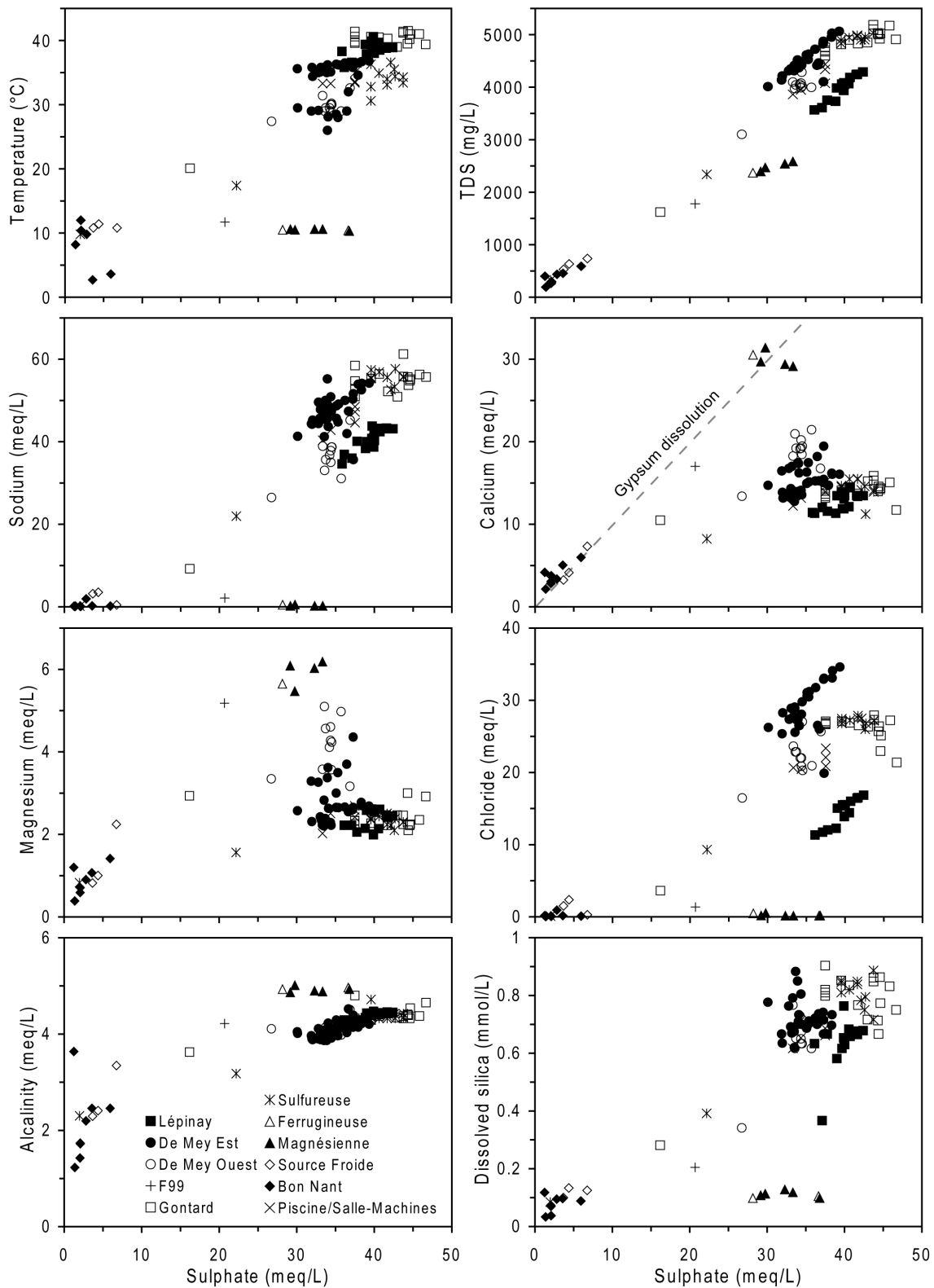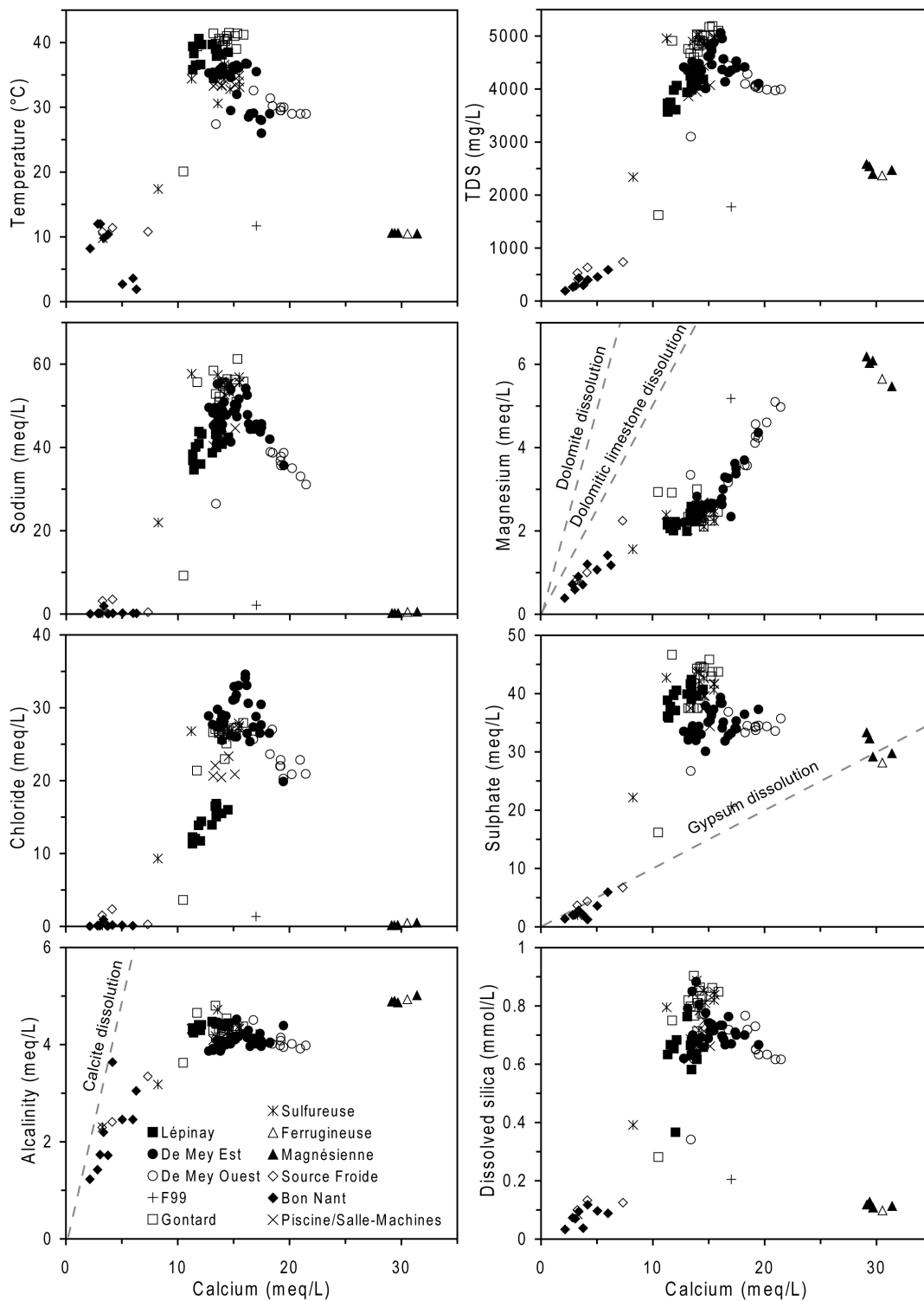
Figure 10.5: Correlations between the physico-chemical parameters in Saint-Gervais-les-Bains waters for all existing data (see data in appendix C).
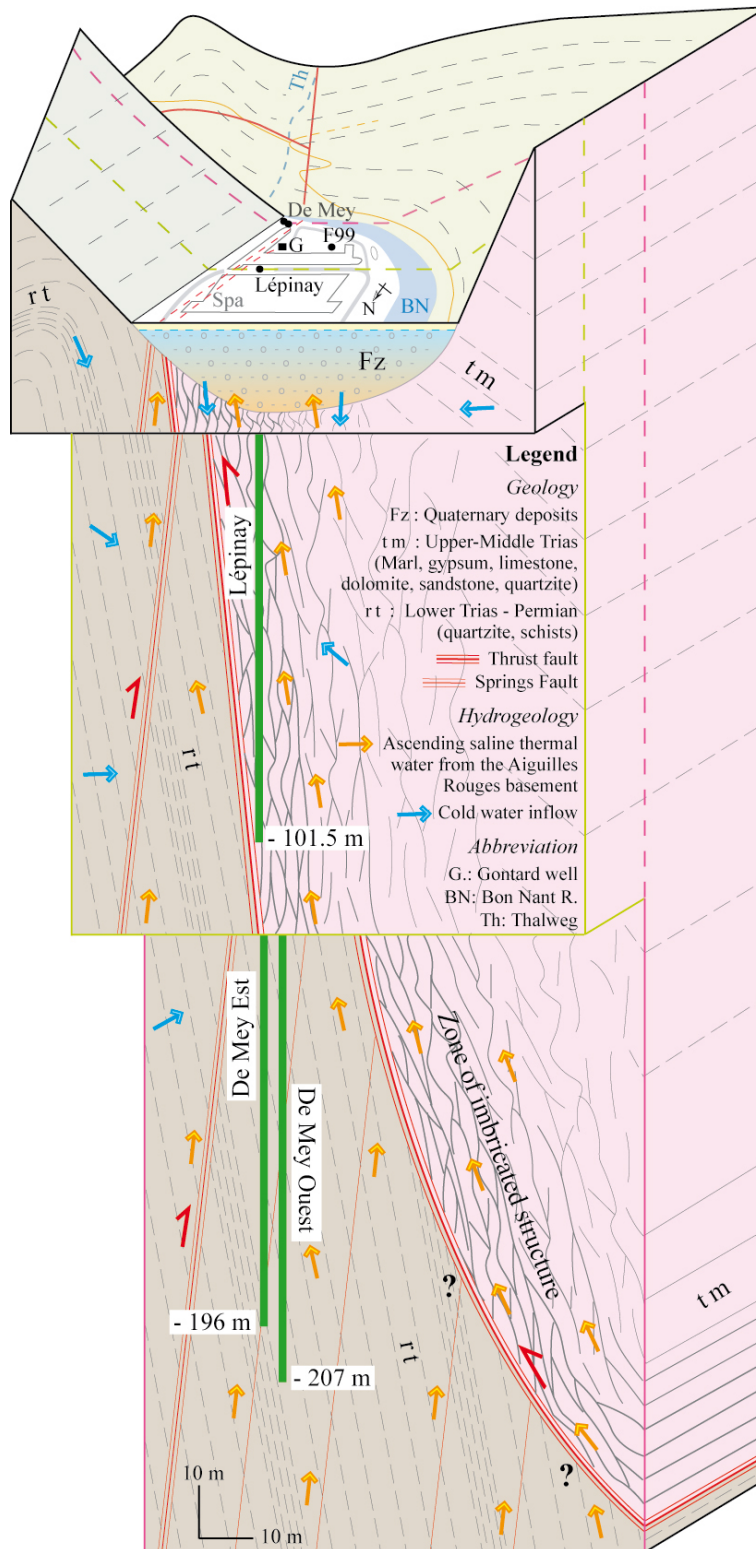
Figure 10.6: Conceptual model of the Saint-Gervais-les-Bains hydrothermal system.

Table 10.4: Calculated chemical composition of the end-members at the origin of mixing processes observed for waters in the Saint-Gervais-les-Bains area. Values were calculated using correlations between all physico-chemical parameters. Bon Nant groundwater was not calculated because its composition can be modified during seasonal conditions. TC-ARB: Thermal Component of the Aiguilles Rouges Basement, PTCW: Permian-Triassic Cold Water, temp.: temperature, EC.: Electrical Conductivity, TDS: Total Dissolved Solids.

Component	TC-ARB	PTCW
Geology	Hercynian	Permian-Trias
Inferred rocks	Gneiss/micaschist	Quartzite/evaporite
Water temp. (^{o}C)	42-45	8-12
EC. (25°C, mS/cm)	7.5	2.6
pH	6.9	7
Oxygen (mg/L)	< 1	> 3
TDS (mg/L)	5500	2550
CATION (mg/L)		
Ca	250	630
Mg	27	66
Na	1500	12
K	42	2
Li	11	0.02
Sr	16	9
ANION (mg/L)		
F	4	0.3
Cl	1400	18
Br	18	< 0.1
SO$_4$	1900	1500
HCO$_3$	250	300
UNDISSOCIATED (mg/L)		
SiO$_2$	53	7
GAS (mg/L)		
H$_2$S	> 2	< 1
IONIC BALANCE		
Cation (meq/L)	82.87	37.65
Anion (meq/L)	83.58	36.67
Balance (%)	-0.4	1.3
ISOTOPE		
Tritium (TU)	< 1	> 5
Deuterium (‰)	-96.5	-82.0
Oxygen-18 H$_2$O (‰)	-13.5	-11.2

10.1.4 Composition of the end-members

Parameter correlations in addition to Figure 10.5 were used to calculate the chemical and isotopic composition for the end-members (Table 10.4). The extrapolation of temperature data before mixing gave the same interval of values for the deep crystalline component (42-45°C). The total mineralization of the thermal end-member seems to reach 5.5 g/L with a calculated dissolved silica concentration of around 53 mg/L excluding silica precipitation in the mixing zone. The calculated values of the water stable isotopes are concordant with the assumption that the thermal component is related to a deep flow system from the summits of the Aiguilles Rouges crystalline Massif.

The estimated composition for the Permian-Triassic cold end-member gave a Ca-SO$_4$ and low-Cl water type which is strongly similar to the water type of Ferrugineuse and Magnésienne springs. The Ca/SO$_4$ ratio is aligned along the gypsum dissolution line which means that the water circulates in the Triassic formations. The high magnesium concentration calculated at 66 mg/L also implies that dolomite dissolution occurs in the Triassic formations. Moreover, this water is relatively poor in Na-Cl concentrations and thus, it can be assumed that the upper-middle Triassic formations are poor in halite. This observation really confirms that the high chloride concentrations in thermal waters have another origin with respect to the Triassic flow system. Finally, the water stable isotopes for the Permian-Triassic cold end-member is higher than those of the thermal component and thus, the assumption of a flow system from the Mont d'Arbois and Mont Joly Massifs having lower elevations compared to Aiguilles Rouges is quite realistic.

10.1.5 Variation of the physical and chemical parameters

Short-term variations caused by the Lépinay and De Mey Est production rates

Production rates in the three exploited wells are stable throughout the year, and thus do not depend on the seasonal climatic conditions contrary to the exploitation mode at Lavey-les-Bains. The spa continuously pumps thermal waters with production rates of 13, 5.5 and 3.5 m^3/h respectively in Lépinay, De Mey Est and De Mey Ouest wells.

Two short pumping tests were carried out in July 2008 in Lépinay and De Mey Est wells aiming to follow the evolution of the physico-chemical parameters with a sudden increase of the rates. The time of pumping when the rise occurs for each test could not exceed one hour because the storage capacity to collect thermal waters is limited. Firstly, the Lépinay production rate was suddenly increased up to 18-20 m^3/h during 45 minutes. Unfortunately, it was not possible to estimate precisely the rate during this test because the device in-situ was unusable. After 45 minutes of pumping test, the production in Lépinay was put back to its normal exploitation rate of 13 m^3/h.

Temperature and conductivity were regularly measured during the pumping tests, and samples were taken in selected times for ionic analyses. Results are illustrated in Figure 10.7. The increase of the production rate in Lépinay immediately generated the decrease of temperature and conductivity. These two parameters varied in the same way and therefore are correlated. This decrease tends to be stabilized beyond 45 minutes of pumping test, but the total decrease of temperature and conductivity reached is around 1°C and 300 μS/cm. For a pumping period of 45 minutes, this would be important.

In details, all the analysed parameters decreased during the test in Lépinay in the same way as variations of the temperature and the conductivity. The magnesium concentrations were the only ones to increase up to +2 mg/L. All these observations highlighted an increase of the mixing processes during the test between the thermal end-member and the colder water, which is less mineralized and has a higher magnesium concentration. Assuming mixing processes with a colder water circulating in the Triassic formations, the observed reduction in sulphate in water (-160 mg/L) should have been less important because the Triassic cold waters also have high sulphate concentrations ($\approx$ 1500 mg/L). Therefore, it remained difficult to decipher precisely the origin of the dilution process occurring.

After 45 minutes of pumping test, the authorized production rate in Lépinay was suddenly put back

causing the decrease of the mixing processes and the rise of temperature and conductivity towards their previous values. In terms of the quality of the water, a production rate of 18-20 m^3/h in Lépinay is certainly not suitable for the long-term exploitation of the geothermal resource because it generates more mixing.
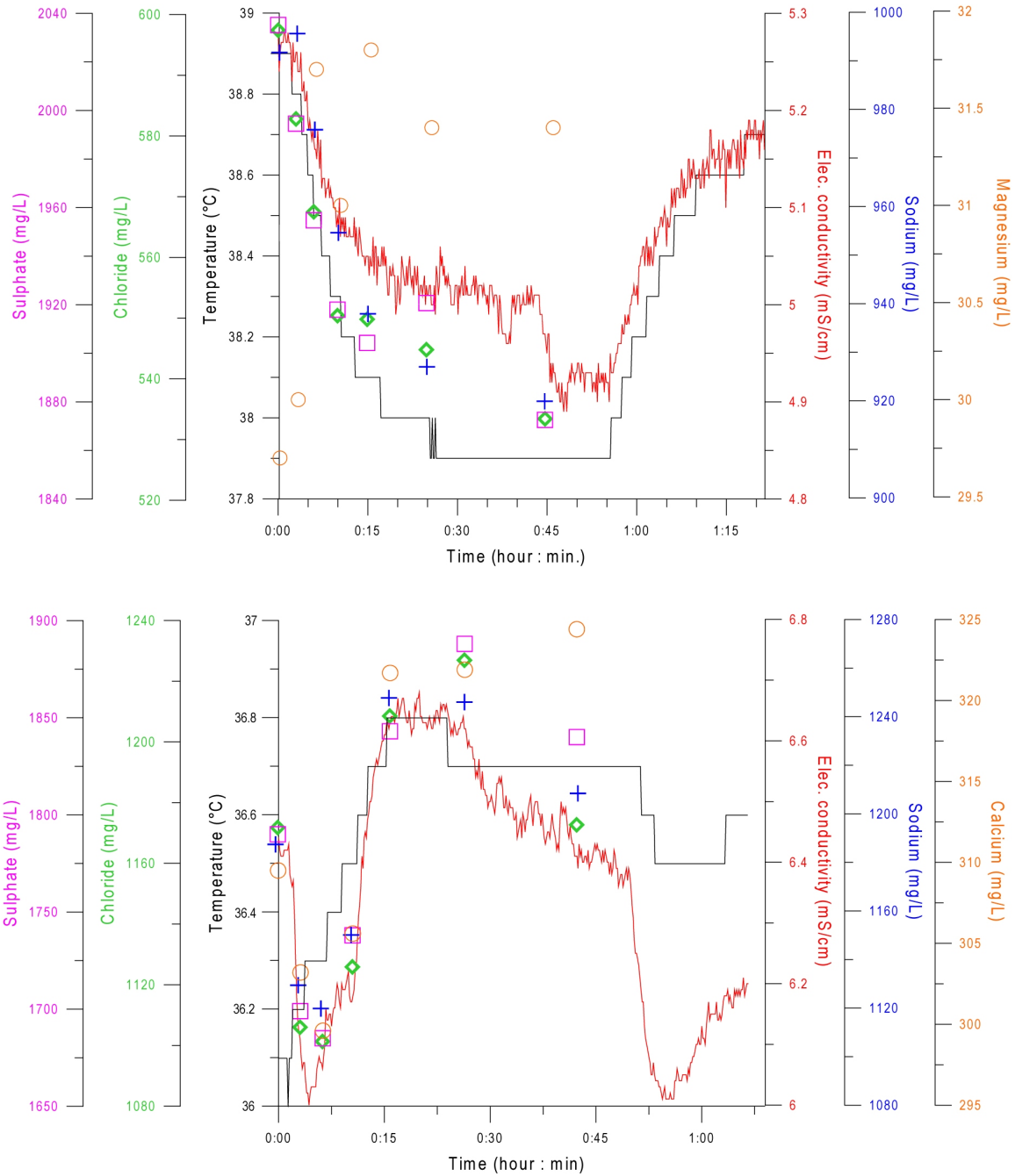
Figure 10.7: Variation of the physico-chemical parameters of thermal waters in Lépinay and De Mey Est wells during two short pumping tests in July 2008 with variation of rates.

163

A second pumping test was carried out in De Mey Est well with the same method as the previous test. The production rate suddenly rose from 5.5 m^3/h to a rate of around 7-9 m^3/h while maintaining the authorized rate in Lépinay. For the same reasons described before, it was not possible to measure precisely the changed flow rate for the test. After 50 minutes of pumping test, the flow rate was put back to its initial value.

Globally, all the physico-chemical parameters varied in the same way and therefore are correlated (Fig. 10.7). In detail, the rise of the production rate caused a decrease of the mineralization during the first 5 minutes (-400 μS/cm). After 5 minutes all parameters increased, reaching the peak at 20 minutes (+0.6°C and +650 μS/cm), and then the parameters decreased gradually as observed in Lépinay (-0.1°C and -300 μS/cm). The rise of temperature and conductivity is accompanied by an increase of all analysed elements and vice versa. With a short pumping test the dilution is characterized by an additional inflow of the Bon Nant groundwater in the De Mey Est well, whereas the long-term exploitation of the resource with De Mey Est produces mixing processes with a cold Ca-SO$_4$ water circulating in the autochthonous cover.

Obtained results with the two short pumping tests seem to contradict assumptions of mixing processes formulated from the interpretation of plots in Figure 10.5, and prove the complexity of these mixing processes occurring at shallow depth. Long-term variations of the physico-chemical parameters seem to be a better method to understand the existing local phenomena.

Long-term variations since the exploitation of boreholes

The exploitation of the Lépinay well since 2000 generated a strong decrease of temperature and conductivity in waters in Gontard well and in Sulfureuse spring. Before Lépinay production, these parameters were measured at around 40°C and 5 mS/cm in Gontard, 35°C and 5 mS/cm in Sulfureuse. In 2008, after eight years of exploitation, the temperature and the conductivity were measured at around 20°C and 2 mS/cm in Gontard, 10°C and 0.4 mS/cm in Sulfureuse. Moreover, their artesian flow rates were considerably affected but this decrease seems to be reversible because it is dependent on the current exploitation of the deeper wells. This process can be easily explained because the Lépinay well pumps the thermal circulations which should normally reach Gontard and Sulfureuse. Therefore, the thermal pressure below the Quaternary filling decreased allowing additional cold water inflows in Gontard. The Sulfureuse spring is the most affected sampling point because this spring is also influenced by the exploitation of the two De Mey wells. Currently, the Sulfureuse spring is a cold spring with a low flow ($<$ 1 L/min in July 2008) where seasonal climatic variations of the Bon Nant groundwater occur (Fig. 10.1).

The variation of the physico-chemical parameters in the water of the wells has remained relatively stable since their exploitation (Fig. 10.8). The temperature has increased slightly for De Mey Est without any change in the mineralization. For De Mey Ouest, measured values in 2008 showed a decrease of the parameters related to the observed decrease of its natural rate. Concerning Lépinay, low values measured between 2000 and 2002 are due to the effect of a long pumping test with rates reaching 23 m^3/h.

Plots between temperature and conductivity for Lépinay and De Mey Est give low correlations. This can be explained by the occurrence of mixing processes with several end-members having various chemical properties. This process seems to be accentuated for Lépinay waters where chemical processes are more complicated to understand.
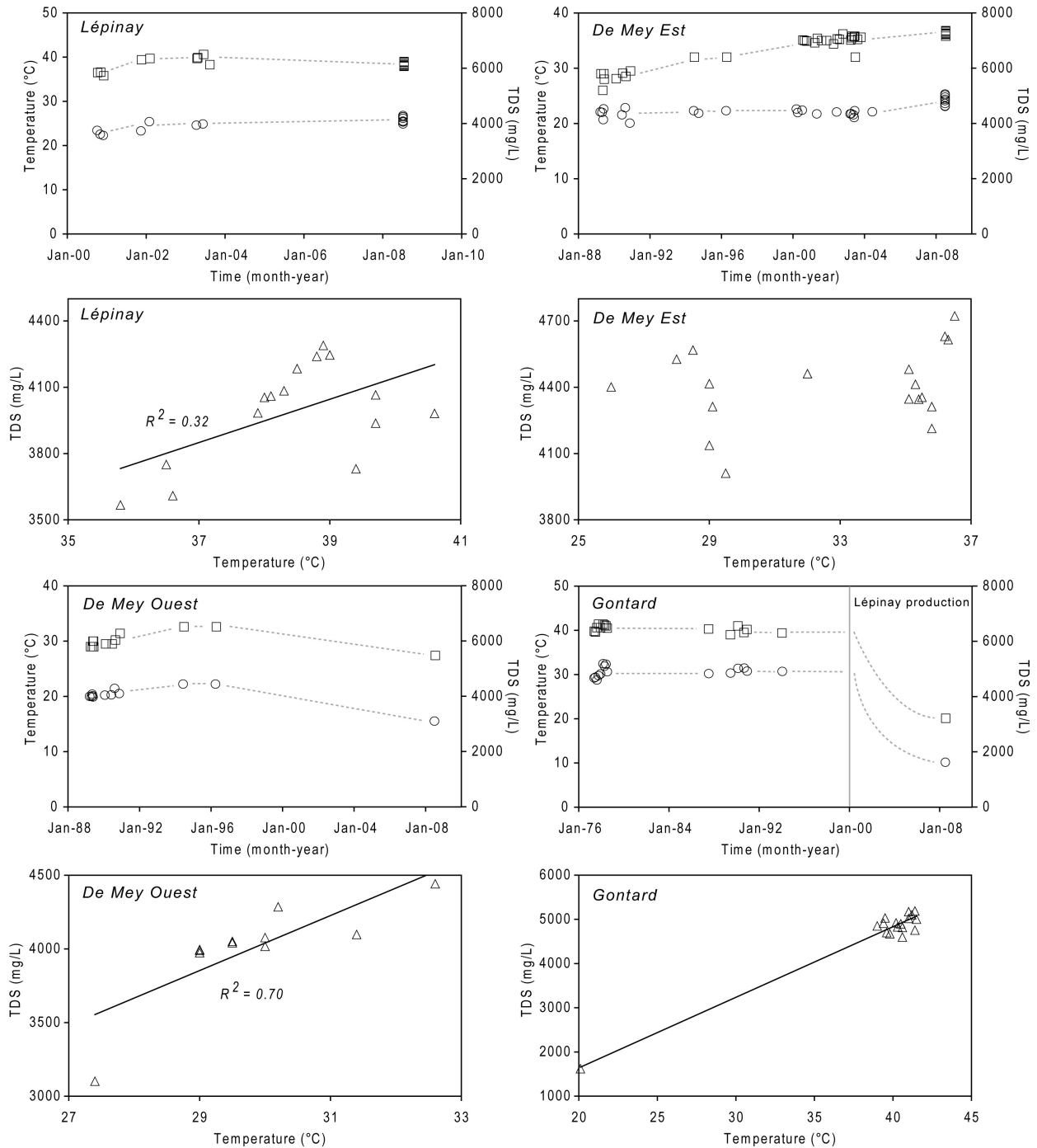
Figure 10.8: Variation of temperature and conductivity in Lépinay, De Mey and Gontard since the exploitation of th wells (except for Gontard). Used data figure in appendix C.

10.1.6 Water-rock interactions

Chemical equilibrium

The deep flow system takes place in the Aiguilles Rouges basement and partially in its autochthonous cover where reactions of dissolution and precipitation occur. Crystalline rocks of the Aiguilles Rouges Massif contain primary minerals such as quartz, albite, anorthite and K-feldspar, and secondary minerals as biotite, muscovite, garnet, chlorite, etc. (Von Raumer and Bussy 2004). Moreover, there still exist other minerals present in fractures of rocks forming slip veins. These minerals are mostly quartz, sulphide and carbonated minerals, and are also subjected to chemical processes as well as primary minerals. Gypsum, anhydrite and dolomite were also selected for the simulation due to their presence in the autochthonous cover and due to high sulphate and magnesium concentrations measured in waters flowing in the cover.

To study the chemical equilibria, saturation indices (SI) were simulated for Lépinay, De Mey Est waters and for the two calculated thermal components (Table 10.5). For alumino-silicates, three aluminum contents were selected. Globally, negative SI values were found for feldspars and chlorite with aluminum contents lower than 10 μg/L. These four waters are strongly over-saturated with respect to muscovite and kaolinite. Waters are clearly in equilibrium with calcite and aragonite which are controlled by their solubility in relation to temperature, and slightly under-saturated with respect to dolomite. They are also under-saturated in gypsum and anhydrite, excepted for the Ca-SO$_4$ cold water from the autochthonous cover which is close to equilibrium. Calculated SIs of quartz are positive between 0.2 and 0.7 for waters whereas SIs of chalcedony for the thermal component are closer to equilibrium. These results show that precipitation of silica could take place in fractures in gneiss during the uprising of the deep fluid. Consequently, calculation of the reservoir temperature can be under-estimated using the silica geothermometers.

Origin of sodium and chloride in waters

Saint-Gervais-les-Bains thermal waters were compared to other thermal waters in the Western Alps range and neighbouring zones to study the origin of the salinity in waters (Fig. 10.9). Bromide concentrations in waters are useful indicators to define if the salinity comes from the leaching of seawater brines or fluid inclusions, or from the dissolution of halite and gypsum rich in halite. In the seawater, the Cl/Br molar ratio is close to 655 whereas it increases beyond 1000 in groundwaters dissolving halite rich formations (Alcalá and Custodio 2008, Sonney and Vuataz 2010a).

Chloride contents in Saint-Gervais-les-Bains thermal waters are in the family of thermal waters circulating in crystalline rocks (Fig. 10.9). This strongly suggests the presence of Na-Cl deep seawater brines or fluid inclusions in the Aiguilles Rouges basement with a composition close to present day seawater. However, Na-Cl elements do not originate from the Aiguilles Rouges Triassic cover because rocks forming the cover are poor in halite (see water chemistry section previously). According to Stober and Bucher (1999), the likely source of Na-Cl in the deep waters from the basements is certainly fossil seawater, diluted to various degrees by meteoric water. However, the hydrolysis of biotite (Edmunds et al. 1985) may also explain the presence of high chloride concentrations in thermal waters at Saint-Gervais-les-Bains. This assumption has to be considered especially as the deep flow system occurs in a crystalline environment.

The Na/Cl molar ratios for Lépinay and De Mey are respectively close to 2.6 and 1.6. In the two cases, the quantity of sodium is higher than chloride. This suggests however a second origin of sodium from fluid-rock reactions. Concerning part of the sodium in the thermal waters at Saint-Gervais-les-Bains, it probably comes from cationic clay exchanges (Lloyd and Heathcote 1985) with schists of the upper-middle Trias or with micaschists of the basement which was already assumed by Vuataz (1982). Indeed for Lépinay, the calcium coming from the dissolution of gypsum in the Triassic formations is probably exchanged for the sodium. For De Mey and the thermal end-member, a part of sodium is certainly related to plagioclase

weathering from albite with long-time flow within the basement (Henley et al. 1984), combined with ion exchange process in micaschists. The importance and significance of plagioclase dissolution to the evolution of groundwater in crystalline rocks has been demonstrated by field studies from other basement complexes (Gascoyne and Kamineni 1994 in Stober and Bucher 1999).

Table 10.5: Calculated saturation indices of Saint-Gervais-les-Bains waters for analyses in July 2008 except for the evaluated thermal end-member called TC-ARB and the cold water end-member from the Permian-Triassic formations named PTCW. In absence of precise Al analyses, SIs of alumino-silicates are calculated using different Al concentrations.

Minerals	Formula	TC-ARB	PTCW	Lépinay	De Mey Est
Albite	$NaAlSi_3O_8$				
	Al = 0.001 mg/L	-1.1	-3.8	-1.4	-1.1
	Al = 0.005 mg/L	-0.45	-3.1	-0.71	-0.36
	Al = 0.01 mg/L	-0.15	-2.8	-0.41	-0.06
Anorthite	$CaAl_2Si_2O_8$				
	Al = 0.001 mg/L	-4.8	-5.3	-4.9	-4.8
	Al = 0.005 mg/L	-3.4	-3.9	-3.5	-3.4
	Al = 0.01 mg/L	-2.8	-3.3	-2.9	-2.8
K-feldspar	$KAlSi_3O_8$				
	Al = 0.001 mg/L	-0.59	-2.1	-0.77	-0.40
	Al = 0.005 mg/L	0.1	-1.4	-0.07	0.30
	Al = 0.01 mg/L	0.41	-1.1	0.23	0.60
Muscovite	$KAl_3Si_3O_{10}(OH)_2$				
	Al = 0.001 mg/L	3.6	4.8	3.7	4.2
	Al = 0.005 mg/L	5.7	6.9	5.8	6.4
	Al = 0.01 mg/L	6.6	7.8	6.7	7.3
Chlorite	$Mg_5Al_2Si_3O_{10}(OH)_8$				
	Al = 0.001 mg/L	-7.3	-12	-7.9	-7.9
	Al = 0.005 mg/L	-5.7	-10	-6.5	-6.5
	Al = 0.01 mg/L	-5.3	-9.8	-5.9	-5.9
Kaolinite	$Al_2Si_2O_5(OH)_4$				
	Al = 0.001 mg/L	0.71	2.7	0.93	1.27
	Al = 0.005 mg/L	2.1	4.1	2.3	2.7
	Al = 0.01 mg/L	2.7	4.7	2.9	3.3
Quartz	SiO_2	0.64	0.28	0.58	0.68
Chalcedony	SiO_2	0.30	-0.19	0.23	0.31
Amorphous silica	SiO_2	-0.48	-1.1	-0.57	-0.49
Aragonite	$CaCO_3$	-0.14	0.08	-0.09	-0.09
Calcite	$CaCO_3$	-0.01	0.23	0.04	0.04
Dolomite	$MgCa(CO_3)_2$	-0.54	-0.37	-0.47	-0.48
Fluorite	CaF_2	-0.03	-1.32	-0.17	0.07
Goethite	$FeOOH$	6.7	6.9	6.9	6.8
Gypsum	$CaSO_4{:}H_2O$	-0.45	0.01	-0.36	-0.36
Anhydrite	$CaSO_4$	-0.56	-0.25	-0.50	-0.53
Halite	$NaCl$	-4.4	-8.3	-5.0	-4.6
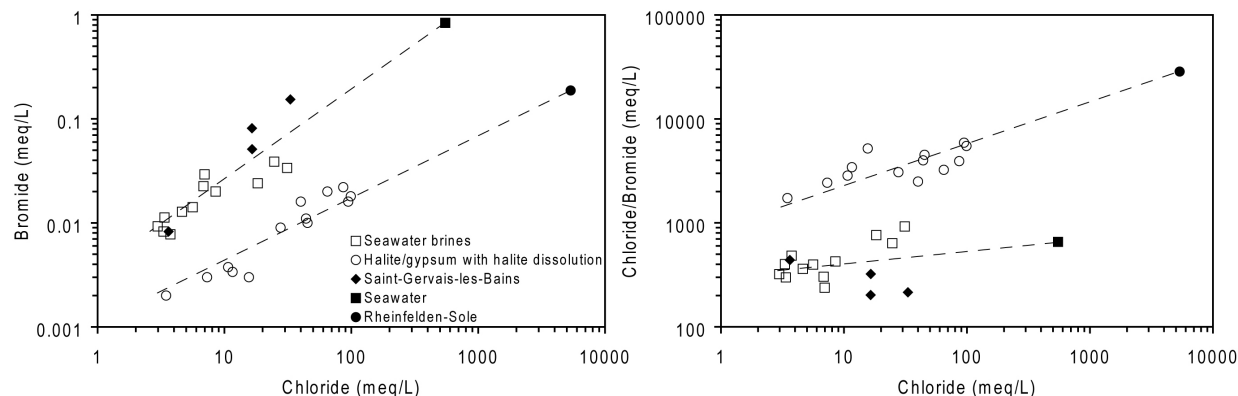
Figure 10.9: Plots of chloride content versus bromide and chloride/bromide ratio in thermal waters for the Alps range and neighbouring zones. All selected waters have a chloride content higher than 100 mg/L. The chloride origin is function of the reservoir geology: basement with seawater brines (squares) or Mesozoic sedimentary rocks rich in halite or gypsum containing halite (circles). The Rheinfelden brine is a subthermal spring in the north of the Molasse Basin, along the Rhine River in Switzerland (location given in Sonney and Vuataz 2008), which dissolves Triassic halite formations.
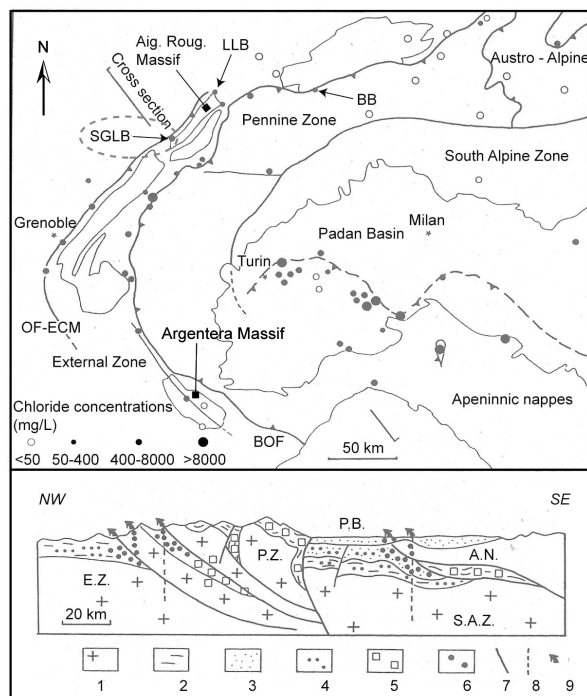
Figure 10.10: Simplified map and cross section of the Alps range with the location of the main thrust faults and springs with their chloride concentrations (modified from Arthaud and Dazy 1989).

Lavey-les-Bains = Lavey-les-Bains, BB = Brigerbad, Saint-Gervais-les-Bains = Saint-Gervais-les-Bains, BOF = Briançonnais Overthrust Fault, OF-ECM = Overthrust Fault of the External Crystalline Massifs. 1: crystalline basement, 2: sediments, 3: Po Basin, 4: non migrated brines, 5: id. fixed by metamorphism, 6: id. migrated and/or concentrated, 7: major faults, 8: seismic fault, 9: spring.

Arthaud and Dazy (1989) studied high chloride concentrations in thermal waters along the main thrust fault systems of the Western Alps (Fig. 10.10). They assumed that the occurrence of high chloride concentrations in thermal waters would probably be due to the leaching of old marine waters inside thrust fault systems from deep flow systems with meteoric waters. According to the same authors, these old marine waters were expelled from tectonically compacted rocks into the pores of the fractured deep reservoirs in the foot-wall of major thrust sheets. In the case of Saint-Gervais-les-Bains, the thrust fault system is the contact between the Aiguilles Rouges and Infra-Aiguilles Rouges Massifs, where residual brines are certainly present. Other hydrothermal sites along the thrust faults of the external crystalline massifs in the Western Alps are also probably concerned by this process such as Brigerbad in Switzerland or Uriage-les-Bains in France. Other examples were illustrated

in the Argentera crystalline Massif between France and Italy (see Fig. 10.10) where the presence of seawater brines in thermal waters in Terme di Valdieri (Baietto et al. 2008), in Bagni di Vinadio and in Berthemont-les-Bains (Perrelo et al. 2001) was assumed. In these three cases, the presence of chloride ions in thermal waters is not related to the leaching of Triassic evaporites.

Origin of sulphate in waters

The origin of sulphate in thermal waters at Saint-Gervais-les-Bains was studied using the sulphur-34 and oxygen-18 (in sulphate) data of Gontard and De Mey Ouest (Bianchetti 1993b), and comparing it to other thermal waters in Western Alps. The sulphur-34 value gives information about the sulphur cycle in groundwater, especially with respect to the dissolved species SO_4^{2-}, H_2S and HS^-. The oxygen-18 value in sulphate is related to the origin of sulphate and is also an indicator of oxidation-reduction processes. According to Fouillac et al. (1990), this origin would be related to the dissolution of Triassic evaporites containing gypsum and anhydrite, the oxidation of sedimentary sulphides in rocks and the leaching of residual seawater brines. Difficulties in interpretation can be met because the sulphur-34 and oxygen-18 values of marine evaporite sulphate minerals vary with their geologic age due to changes in the isotopic composition of oceanic sulphate with time (Pearson et al. 1991).
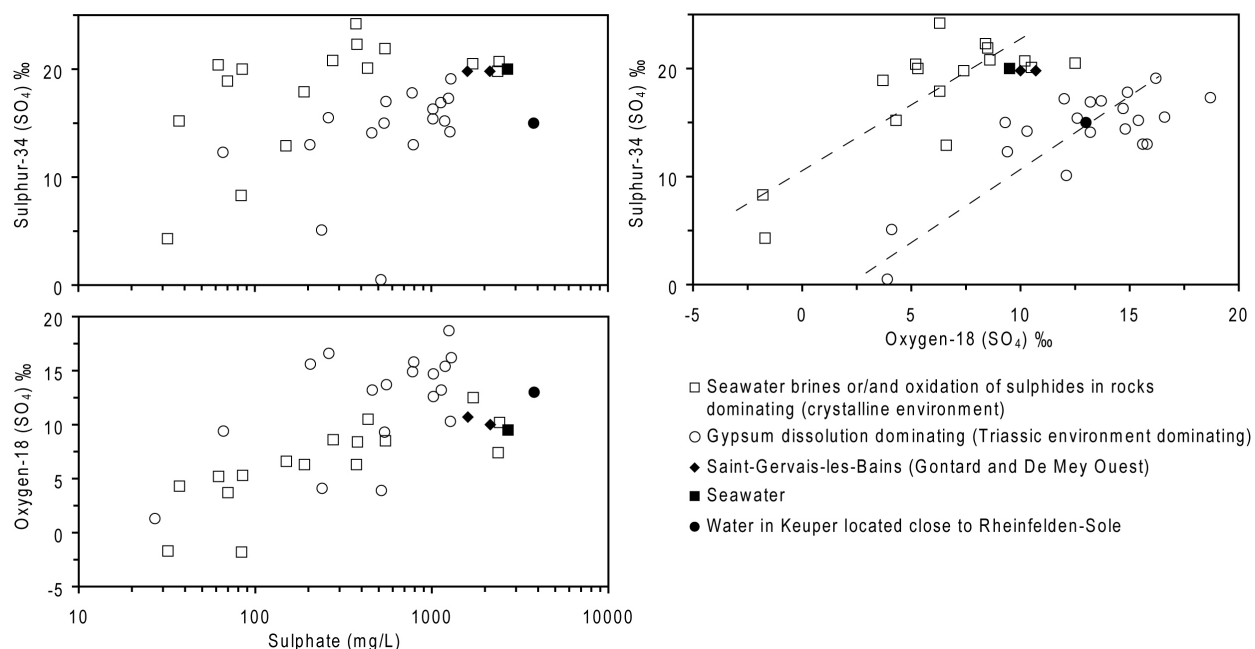
Figure 10.11: Plots of sulphate contents and sulphate isotopes in thermal waters for the Alps range. The sulphate origin is function of the reservoir geology: basement with seawater brines or/and oxidation of sulphides in rocks (squares) or Mesozoic sedimentary rocks containing gypsum formations (circles). There is no direct data for Rheinfelden-Sole but representative data of waters in Keuper located close to this brine (black circle) showed values of 13‰ and 15‰ respectively for oxygen-18 and sulphur-34 (Pearson et al. 1991). Data for Saint-Gervais-les-Bains (diamonds) are positioned in the square zone, coming from Bianchetti (1993b).

In the case of Saint-Gervais-les-Bains, the interpretation of these stable isotope values in thermal waters allowed determining the origin of dissolved sulphate. For thermal waters dissolving Triassic evaporites in the Alps, values are higher for oxygen-18 and lower for sulphur-34 than waters flowing in the crystalline domain (Fig. 10.11). Obtained values in waters of Gontard and De Mey Ouest, measured in 1990, coincide with other values of the crystalline domain and are also close to the present day seawater. In detail, these values tend to approach points of the Triassic domain. Consequently, it can be assumed that the main part of sulphate in waters of Gontard and De Mey Ouest comes from the

leaching of seawater brines coupled to the oxidation of sulphide minerals in rocks of the Aiguilles Rouges basement. Moreover, this suggests a smaller part of sulphate coming from the dissolution of evaporites in the autochthonous cover. This leads to the hypothesis that if chemical processes strongly occur in the imbricated structure zone, Lépinay waters would have isotope values closer to the Triassic domain in Figure 10.11. Finally, correlations between sulphate concentrations versus isotopes are less significant because high sulphate contents thermal waters can be found in crystalline environment as well as in Triassic formations.

10.2   Regional hydrogeological and geochemical investigations

From a regional view, three types of aquifer co-exist in the studied area: aquifers with interstitial and fracture porosities, as well as fissured to karstified aquifers. The aquifers with interstitial porosity such as alluvial groundwaters of the Arve and Bon Nant Valleys, and as glacial groundwaters are globally widespread on the studied area. For this category of aquifer, groundwater flows strongly occur in the upper part of the Arve River Quaternary filling. They are less important but also present for the torrential deposits of the Bon Nant River taking part into mixing processes with thermal waters at Saint-Gervais-les-Bains. Aquifers with fracture porosities concern waters circulating in fissured zones of the Aiguilles Rouges crystalline rocks. Infiltration and

shallow to deep circulation in the south-western part of the Aiguilles Rouges Massif take place in Variscan and Alpine fractures and faults oriented N-S to WNW-ESE (Lhomme et al. 1996, Payraud 1991, Von Raumer and Bussy 2004). Groundwater flows at shallower depth in the decompressed zone of the basement leading to the cold springs at the feet of slopes, whereas deeper flows in highly permeable faults in the basement supply the hydrothermal regime of Saint-Gervais-les-Bains. Finally, fissured to karstified aquifers occur in the carbonated and evaporitic formations of the autochthonous cover and in the Morcles nappe. For the regional studied area, these aquifers are present in the Mont Joly and Mont d'Arbois Massifs (Fig. 9.1).

10.2.1   Regional deep flow system

Investigations based on geological, hydrogeological and geochemical methods have enabled a regional conceptual model of the different flow paths to be built (Fig. 10.13). The hydrothermal sites of Lavey-les-Bains and Val d'Illiez were added to the conceptual model for comparison of their geochemical water type. As described previously, Lavey-les-Bains and Saint-Gervais-les-Bains hydrothermal sites are the lowest elevation points of the Aiguilles Rouges Massif. Pumped waters at Lavey-les-Bains have similar chemical properties to Saint-Gervais-les-Bains waters, Na-SO$_4$ waters rich in chloride (Bianchetti 1994, Sonney and Vuataz 2009, Zahner et al. 1974). Lavey-les-Bains waters are hotter than Saint-Gervais-les-Bains waters (65ºC against 40ºC)

but less mineralized (1.5 g/L against 4.8 g/L). This difference probably results in deeper circulations for the Lavey-les-Bains hydrothermal system with due to a deepening of the thrust fault of the Aiguilles Rouges Massif on Infra-Aiguilles Rouges towards the north-east. In the Aiguilles Rouges Massif, various chemical processes and groundwater residence times can explain the difference in mineralization.

Other observations prove the chemical and isotopic similarities of thermal waters from these two hydrothermal systems such as the presence of the gas H$_2$S in waters, the high silica and lithium concentrations, the significant contents of several trace elements that are markers of crystalline rocks (tungsten, rubidium, bromine, boron, cesium, germa-

nium and vanadium), the same values of the water stable isotopes indicating a recharge zone roughly at the same elevation, and the lack of presence of tritium showing a recharge time before the first atmospheric nuclear weapons testing in 1953. These similar chemical and isotopic properties suggest the occurrence of a regional deep flow systems in the Aiguilles Rouges Massif towards the two low-elevation points, north-east for Lavey-Les-Bains and south-west for Saint-Gervais-Les-Bains. The Arve narrow gorges between Servoz and les Houches cannot be an area with thermal resurgences because this zone has higher elevation than the Bon Nant Valley nearby Le Fayet (see location in Figure 9.1). Moreover, rocks outcropping along the Arve narrow gorges are Visean sediments and volcanics which are being considered as formations of low permeability.

The cold Ca-SO$_4$ end-member at Saint-Gervais-les-Bains certainly has a recharge zone from the Mont d'Arbois and Mont Joly Massifs, more precisely from Triassic outcrops in the sectors of Les Contamines-Montjoie and Megève (Figs. 9.1 and 10.13) belonging to the autochthonous cover of the basement. The gypsum dissolution in the Triassic formations takes place at the bottom of these massifs where the flow system occurs. Another example of groundwater in the autochthonous cover is represented by the hydrothermal system of Val d'Illiez in Switzerland. Thermal waters in the Val d'Illiez (30°C) has the same geochemical water type (Ca-SO$_4$ poor in chloride) and circulates in the autochthonous cover from the north-western edge of the Aiguilles Rouges Massif (see part V).

The hydrothermal site of Saint-Gervais-les-Bains also has geological, hydrogeological and geochemical similarities with the hydrothermal site of Uriage-les-Bains (Fig. 10.12). Sarrot-Reynauld (1987) described the Uriage-les-Bains, Allevard and Challes-les-eaux hydrothermal systems assuming that they are related to deep flow systems in the Belledonne crystalline Massif, which also belongs to the external crystalline massifs. In detail, thermal waters at Uriage-les-Bains have a geochemical type similar to Saint-Gervais-les-Bains waters, but are more influenced by cold mixing processes with waters flowing in the sedimentary cover. Sarrot-Reynauld (1987) explained that groundwater flows are controlled by fractures crossing the basement and its sedimentary cover with a recharge zone in Belledonne and a deep flow system towards the topographic low-elevation points while flowing in deep crystalline thrust faults.
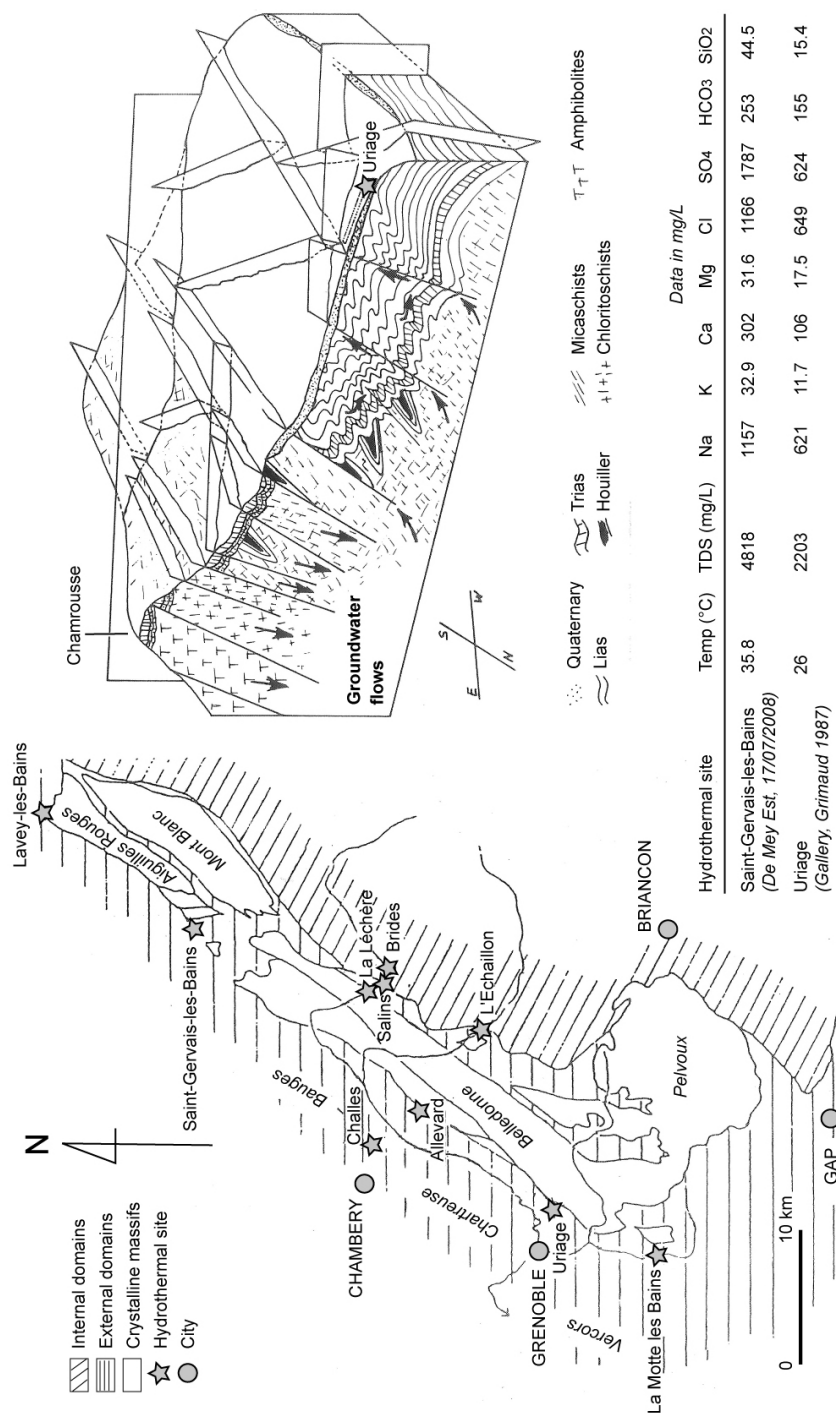
Figure 10.12: Location map of hydrothermal systems close to the external crystalline massifs, and conceptual model of the Uriage-les-Bains hydrothermal system (modified from Sarrot-Reynauld 1987). Chemistry comparison of thermal waters for Saint-Gervais-les-Bains and Uriage-les-Bains. Uriage-les-Bains is located at the front of the Belledonne crystalline massif and thermal waters in this site have a geochemical type similar to Saint-Gervais-les-Bains waters. Names of massifs are given in italic format.
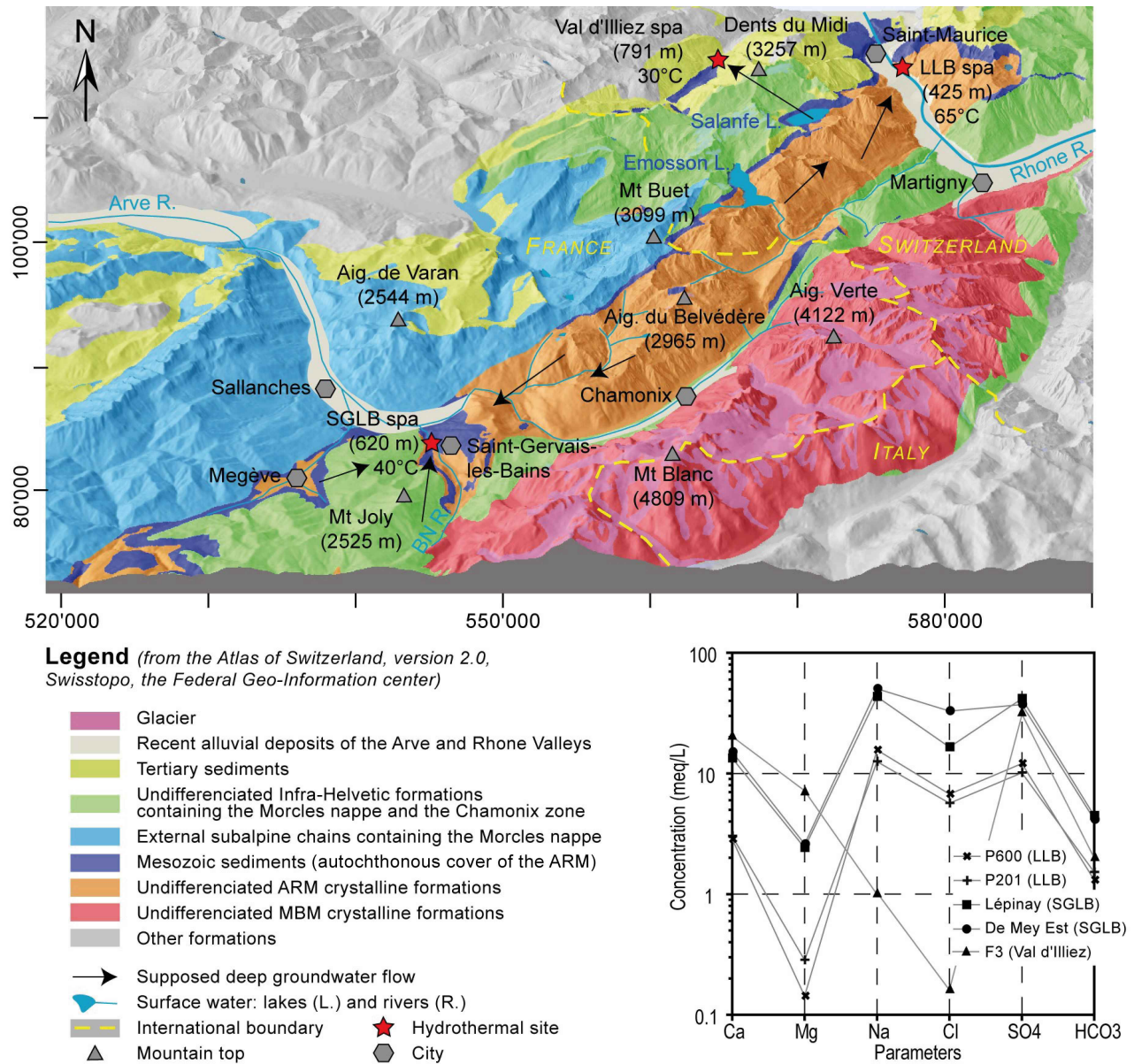
Figure 10.13: Regional conceptual model of the different flow paths ending to the hydrothermal systems of Saint-Gervais-les-Bains (SGLB), Lavey-les-Bains (LLB) and Val d'Illiez. Major element concentration plot (modified Shoeller diagram) for Lépinay and De Mey Est waters is compared to waters of the two production deep boreholes in Lavey-les-Bains (P600 and P201) and of the well F3 in the Val d'Illiez. Location refers to the Swiss kilometric coordinates in projection, in standard CH1903. ARM: Aiguilles Rouges Massif, MBM: Mont-Blanc Massif.

10.2.2 Mean elevation of the recharge zone

The elevation of the infiltration area has been estimated from the data of water stable isotopes and with the equation of Kullin and Schmassmann (1991) for the Bernese Alps. The location of Saint-Gervais-les-Bains in the Western Alps implies that this relation is more appropriate than those given in Blavoux (1978), Bortolami et al. (1979) and Vuataz (1982) but they are also taken into account in Table 10.6. Isotope values for Lépinay and De Mey Est waters and for the end-members are aligned along the World Meteoric Water Line of Craig (1961), as well as the other Alpine thermal waters (Fig. 10.14). The calculation with the thermal end-member leads to the average elevation of the Aiguilles Rouges Massif (1700-2100 m), whereas results for the Cold component indicate a lower elevation from Mont d'Arbois and Mont Joly Massifs of around 1100-1300 metres. The estimation with the thermal end-member is close to that calculated with P600 waters at Lavey-les-Bains.

Isotope values for Lépinay indicate a lower recharge zone because Lépinay water is mixed, but results with De Mey Est resemble the results with the thermal end-member. Concerning the Ferrugineuse and Magnésienne springs, the calculation give a recharge zone between 700 and 1200 metres. This roughly corresponds to the mean elevation of

Triassic formations outcropping in the sector of the Mont d'Arbois Massif where the recharge zone of these springs was assumed (Fig. 10.13).
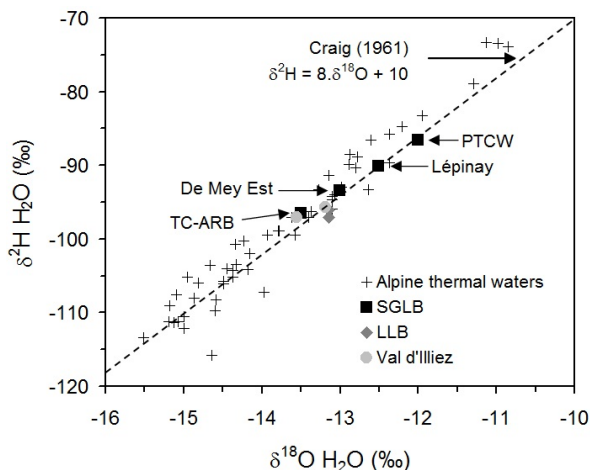
Figure 10.14: Water stable isotopes plot for Alpine thermal waters. LLB: Lavey-les-Bains, SGLB: Saint-Gervais-les-Bains, TC-ARB: Thermal Component of the Aiguilles Rouges Basement, PTCW: Permian-Triassic Cold Water.

10.2.3 Reservoir temperature

Evaluation with geothermometers

Traditional and multi-component geothermometers have been applied to estimate the reservoir temperature for the Saint-Gervais-les-Bains hydrothermal system. First geothermal assessments of the reservoir temperature at Saint-Gervais-les-Bains gave values of 70 to 100°C also based on chemical geothermometers (Vuataz 1982, Bianchetti 1993b). The isotope geothermometer using the fractionation of oxygen-18 in water and sulphate (Lloyd 1968, Mizutani and Rafter 1969) showed a reservoir temperature at around 60°C for Gontard and De Mey Ouest (Bianchetti 1993b). Based on the total dissolved silica, calculated temperatures for the thermal end-member, Lépinay and De Mey Est are in the range 45-80°C with the chalcedony geothermometers (Table 10.7). For reservoir temperatures

in the range of 120-160°C, the chalcedony geothermometer is usually more adapted than the quartz geothermometer (Arnórsson 1983), due to aqueous phase equilibrium which depends on the reservoirs temperature (Arnórsson 1975). Results using quartz from relations by Fournier (1977) and Truesdell (1976) are not presented in this study. Moreover, the silica geothermometers are strongly affected by mixing processes with cold waters containing low silica concentrations. Consequently, the calculation made with the thermal component is more appropriate and gives a reservoir temperature of 75°C.

Cationic geothermometers using ratios between sodium, potassium, lithium and magnesium were

Table 10.6: Calculated elevation of the infiltration area with the water stable isotopes for waters of Saint-Gervais-les-Bains. Location of sampling points are given in Figure 9.2. Isotope-elevation equations in Switzerland and neighbouring areas are given in the chapter 2.2.9 and in Pearson et al. (1991). Some of these equations were not selected for this hydrothermal system.

Sampling date	Sampling points	$\delta^{18}O$ (H_2O) ‰	δ^2H (H_2O) ‰
16.07.2008	Lépinay	-12.51	-90.1
17.07.2008	De Mey Est	-13.01	-93.4
"	De Mey Ouest	-12.28	-88.6
"	F99	-11.53	-84.1
"	Gontard	-11.80	-84.6
"	Sulf. Spring	-11.42	-80.5
16.07.2008	Ferr. Spring	-11.31	-81.6
"	Magn. Spring	-11.17	-82.0
17.07.2008	Cold Spring	-11.33	-80.1
"	Bon Nant	-11.27	-82.0

Domain, reference		Calculated elevation (m)	
	Lépinay	1418	1392
	De Mey Est	1712	1646
	De Mey Ouest	1282	1277
Bernese Alps	F99	841	931
	Gontard	1000	969
Kullin and Schmassmann 1991	Sulf. Spring	776	654
	Ferr. Spring	712	738
	Magn. Spring	629	769
	Cold. Spring	712	623
	Bon Nant	688	769
	Lépinay	1491	1486
	De Mey Est	1675	1637
	De Mey Ouest	1404	1417
Jura, Northern Alps	F99	1132	1210
	Gontard	1231	1233
Vuataz 1982	Sulf. Spring	1091	1045
	Ferr. Spring	1051	1095
	Magn. Spring	999	1114
	Cold. Spring	1051	1027
	Bon Nant	1036	1114
	Lépinay	1470	1400
	De Mey Est	1637	1532
	De Mey Ouest	1393	1340
Lemanic Prealps	F99	1143	1160
	Gontard	1233	1180
Blavoux 1978	Sulf. Spring	1107	1016
	Ferr. Spring	1070	1060
	Magn. Spring	1023	1076
	Cold. Spring	1070	1000
	Bon Nant	1057	1076
	Lépinay	1436	1566
	De Mey Est	1596	1699
	De Mey Ouest	1362	1506
Maritime Prealps	F99	1122	1325
	Gontard	1208	1345
Bortolami et al. 1978	Sulf. Spring	1087	1181
	Ferr. Spring	1051	1225
	Magn. Spring	1006	1241
	Cold. Spring	1051	1165
	Bon Nant	1038	1241

Table 10.7: Calculated reservoir temperatures using a selection of chemical geothermometers for Saint-Gervais-les-Bains hydrothermal system illustrated in chapter 2.2.10 and in Arnórsson 2000. For Lépinay and De Mey Est, the used chemical data come from appendix C.

Reference	Equation	Calculated temperature (°C)		
		Thermal component	Lépinay	De Mey Est
Fournier (1977)	$T_{SiO2,chalcedony}$	75	61	66
Arnórsson et al. (1983)	$T_{SiO2,chalcedony}$	76	63	68
Fournier and Potter (1979)	$T_{Na-K-Ca-(Mg-correction)}$	105	102	104
Fournier (1977)	$T_{K^2/Mg}$	78	63	65
Giggenbach (1988)	$T_{K^2/Mg}$	90	81	82
Lloyd (1968)	$T_{\delta^{18}O}$	59 for De Mey Ouest and 60 for Gontard (a)		
Mizutani and Rafter (1969)	$T_{\delta^{18}O}$	48 for De Mey Ouest and 49 for Gontard (a)		

(a): results from Bianchetti 1993b.

also tested at Saint-Gervais-les-Bains but the obtained results largely overestimated the reservoir temperature. Application of these geothermometers is more suitable for high-enthalpy systems ($> 150°C$), containing waters reaching equilibrium with feldspars (Fournier 1981). Alpine hydrothermal systems such as Saint-Gervais-les-Bains have relative low reservoir temperatures ($< 150°C$) compared to high temperature geothermal fields. They are subjected to mixing processes with shallow groundwaters, to cationic exchange with clay, they are influenced by the contribution of Na-Cl from seawater brines or fluid inclusions, and often do not reach equilibrium with feldspars due to rather short residence times. Consequently, results using these geothermometers from Arnórsson (1983), Fournier (1977), Fournier and Truesdell (1973), Giggenbach (1988), Kharaka et al. (1982), Kharaka and Mariner

(1989), Truesdell (1976) and Verma and Santoyo (1997) were not considered in this study. However, the Na-K-Ca geothermometer (Fournier and Truesdell 1973) using the Mg-correction (Fournier and Potter 1979) was used because the deep waters in Saint-Gervais-les-Bains are diluted with shallow waters rich in calcium and magnesium. Results are close to 100°C for the selected waters. Processes due to magnesium acquisition do not allow temperature circulations to be compared with silica and cationic ratios. Finally, the K^2/Mg geothermometer gives similar and elevated results respectively for Fournier (1977) and Giggenbach (1988) compared to the chalcedony. This geothermometer was first applied to waters from low-enthalpy reservoirs which had not attained equilibrium with alkali feldspars, but were in equilibrium with K- and Mg bearing clay minerals (Nicholson 1993).

Evaluation with saturation indices

The behaviour of saturation indices (SI) of main minerals with an increase of temperature imposed from 40°C to 120°C was simulated with the PHREEQC code. The chemical composition of the thermal end-member and of waters in Lépinay and De Mey Est was used (Fig. 10.15). For this simulation, it can be assumed that the deep reservoir has a temperature lower than 120°C. Intersection of

SI's lines with the chemical equilibrium (SI=0) for all minerals occurs at different temperatures. For all waters, lines tend to reach equilibrium in the range of temperatures coinciding with previous results of chalcedony and K^2/Mg geothermometers, but not with geothermometer using oxygen-18 and Na-K-Ca with Mg correction.

For the thermal component, the calculated reservoir temperature using this method seems to be in the range of 70-100°C. Computed reservoir temperatures for Lépinay and De Mey Est seem to be lower because Lépinay and De Mey Est waters are mixed with cold groundwaters.

Anhydrite lines for all selected waters are close to SI=0 for higher temperatures in the range 85-100°C, whereas gypsum lines remain between -0.5 and -0.1 for the SIs. Concerning alumino-silicates such as feldspars, kaolinite and muscovite the increase of temperature generates a great decrease in SIs. Important uncertainties on aluminum analyses do not make it possible to ensure these results, but the selected aluminum value of 5 μg/L allowed the SIs to be simulated. These minerals are certainly not in equilibrium with the deep fluid because the sub-saturation is accentuated with the increase in temperature.

The reservoir temperature calculated with the two methods converges towards the same range of values: 70-100°C for the thermal end-member. These results indicate a cooling by conduction of the deep fluid with the uprising to the mixing zone. This loss of heat can be associated with a relatively fast uprising time of the deep fluid through fractures in the basement which have high hydraulic conductivities, and also probably cross the basement down to the thrust fault.

Figure 10.15: Simulation of mineral saturation indices versus temperature plots for the thermal end-member and for Lépinay and De Mey Est waters.

10.2.4   Depth evaluation of the reservoir

The study of the Lavey-les-Bains hydrothermal system enabled the thrust fault between Aiguilles Rouges and Infra-Aiguilles Rouges Massifs to be assumed. This fault certainly drains the deep fluid towards the hydrothermal area. This assumption was based on the geological, hydrogeological, geochemical and numerical investigations, that is to say the mineral-chemical equilibria and the interpretation of the seismic profile NRP 20 going through Lavey-les-Bains (Pfiffner et al. 1997). In this case, the depth of the reservoir was evaluated at around 3

kilometres below the surface i.e. close to 2.5 kilometres below the sea level with an average geothermal gradient of around 20°C/km from the recharge zone to the reservoir.

Concerning the hydrothermal system of Saint-Gervais-les-Bains, it would seem that the reservoir is shallower than Lavey-les-Bains because the calculated reservoir temperature is lower for Saint-Gervais-les-Bains. Assuming that the reservoir temperature is roughly 20°C/km lower than Lavey-les-Bains and assuming the same geothermal gradient

from the recharge zone to the reservoir, there would be a difference in depth of roughly of 1 kilometre. Therefore, the geothermal reservoir at Saint-Gervais-les-Bains would be localized at around 2 kilometres depth i.e. close to 1.5 kilometres below the sea level, which would be unrealistic because it would probably be deeper according to the regional geological cross sections. This interpretation raised the question of the presence of a thrust fault system

at the bottom of the Aiguilles Rouges basement and its depth at Saint-Gervais-les-Bains. According to the geological and geochemical studies of Arthaud and Dazy (1989) and of Sarrot-Raynauld (1987), it would seem that the origin of thermal waters at the front of the external crystalline massifs is related to the existence of major thrust faults putting in contact these massifs and extending far into the Western Alps at various depths.

10.2.5   Groundwater residence time

The only information allowing the residence time in Saint-Gervais-les-Bains to be studied is tritium data from Vuataz (1982) and several unpublished reports during the 1980's and 1990's. The present tritium concentration in precipitation is several orders of magnitude lower than the peak reached during the period of atmospheric nuclear weapons testing (Person et al. 1991), and since the early 2000 it has been stabilized around 10 T.U. For Alpine hydrothermal systems in crystalline rocks, with relatively longer residence times (older than nuclear weapons tests), tritium can be used to identify mixing processes with recent waters.

Bianchetti (1993b) measured tritium in several sampling points in 1990 (Fig. 10.16). For De Mey wells (28-32°C) and Gontard (39-41°C), tritium data are in the range 0-5.3. The cold component for Gontard is represented by the Bon Nant groundwater according to the line going through Sulfureuse, Cold spring and Bon Nant. It is different for De Mey wells because data in 1990 indicated mixing with a cold Ca-SO$_4$ water from the autochthonous cover and not or little with Bon Nant groundwater. Consequently, it can be assumed that the cold end-member from Mont d'Arbois and Mont Joly Massifs had low tritium contents in 1990, its underground residence time is certainly higher than 25-30 years.

This tritium data cannot give residence time estimations for the thermal component. Its tritium content could be lower than 0.5 T.U. according to the correlation with the temperature. Residence

time for the thermal component can be compared to the hydrothermal system of Lavey-les-Bains due to their chemical and isotopic similarities and the thermal regime in the Aiguilles Rouges Massif. Sonney and Vuataz (2009) indicate a residence time older than 8000 years for Lavey-les-Bains waters using the carbon-14 method corrected from δ^{13}C measurements. Indeed, it is possible to obtain the same order of magnitude for the residence time of the thermal component at Saint-Gervais-les-Bains.
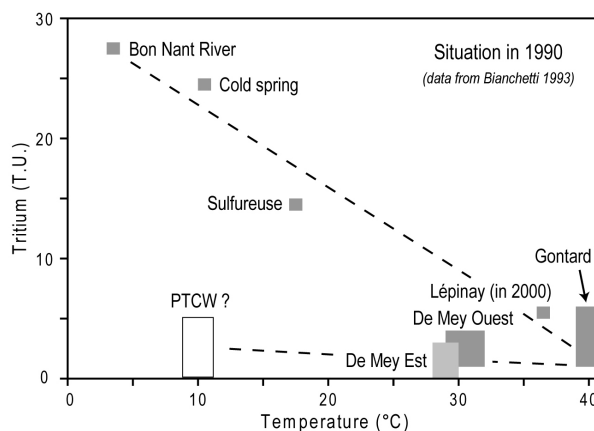
Figure 10.16: Temperature-tritium plot for Saint-Gervais-les-Bains waters in 1990. For Lépinay, the value comes from a technical report of the ANTEA consulting office (2004). PTCW: Permian-Triassic Cold Water.

11

Two-dimensional vertical modelling of groundwater flow and heat transport

11.1 Objectives

As opposed to the Lavey-les-Bains hydrothermal system, no numerical model has been constructed for Saint-Gervais-les-Bains to represent the thermal regime and the temperature field induced by the deep flow system. This is due to the highly complicated geological structures hindering the reproduction of the groundwater flows through a three-dimensional flow and heat transport model. Indeed, this local geological setting is characterized by the presence of two deep aquifers in the autochthonous cover with different thermal flow paths and chemical processes, and by the presence of alternation of horizons with different permeabilities in the zone of imbricated structures. In addition to that, mixing processes occur with two cold and one thermal end-members, and thus locally an inversion of the temperature with the depth is possible. For these reasons, it is not currently possible to represent groundwater flows with a three-dimensional model. Therefore, a simplified two-dimensional numerical model was built through the Aiguilles Rouges and the Mont Joly Massifs based on a regional NNE-SSW geological cross section (Fig. 11.1). In the same way as Lavey-les-Bains, initial conditions of groundwater flow and heat transport were calibrated using data from literature and well measurements. On the contrary, production rates were not added to the two-dimensional model because of geological complexity.

The main objective consists of representing the thermal regime and the induced temperature field from the assumed recharge area to the Bon Nant Valley, using the specific hydrogeological conditions described in the following section. The simulation of the geothermal anomaly in the area of Saint-Gervais-les-Bains was carried out using a heat flux at the bottom of the model in the same way as Lavey-les-Bains. Finally, the computed results will be compared with observed data in the field such as temperature of waters in wells, geothermal gradient, temperature in the geothermal reservoir, groundwater balance and residence time of the thermal component.

11.2 Construction of the model and assigned parameters

11.2.1 Geological boundary conditions

The two-dimensional numerical model integrates all geological horizons down to a thickness of 2500 metres below the sea level, considered as the bottom of the deep flow system along the thrust fault. This selected depth was assumed in the two-dimensional model for Lavey-les-Bains according to the interpretation of the seismic profile NRP20 (Pfiffner et al. 1997). The extension of this thrust fault towards the south-western direction and towards Saint-Gervais-les-Bains is difficult to evaluate. Therefore it was decided to keep this depth value in the case of Saint-Gervais-les-Bains and to assume the thrust fault as a geological limit for the model (Fig. 11.1).

The geological cross section used in the model extends from Aiguille de Belvédère to Aiguille de Roselette, and goes through the hydrothermal zone of Saint-Gervais-les-Bains and the Mont Joly Massif. Three main valleys are cut by the cross section such as Bon Nant Valley which has the lowest elevation (620 m, average elevation of the hydrothermal area). Other valleys are La Diosaz and Arve Rivers, are located in the north-eastern part of the model in the Aiguilles Rouges Massif, and their elevations are higher than the Bon Nant Valley respectively 1500 and 850 metres.

In the Aiguilles Rouges Massif, the two-dimensional model ends in the summit of the Aiguille de Belvédère where a small klippe of autochthonous cover is present. Aiguille de Belvédère is the highest summit of the Aiguilles Rouges sector (2965 m). This summit also represents the hydraulic surface boundary between the watershed of Arve River in France and the watershed of Eau Noire River in Switzerland (see location in Figures 4.1 and 9.1).

Looking towards the south-western direction of the cross section, the Carboniferous formations of the Servoz - Les Houches area are cut by the Arve River and form a narrow gorge. These formations are similar to rocks of the Salvan-Dorénaz syncline in the north-eastern part of the Aiguilles Rouges Massif. In detail, this zone with Visean sediments and volcanics, and surrounded of Variscan granitoids, was taken into account for the model because it represents a permeability contrast with the basement. The depth of this geological domain could be precisely evaluated. However, this old depression in the basement is probably limited by old normal faults which are moved again during Variscan and Alpine tectonic events.

The hydrothermal area of Saint-Gervais-les-Bains is located in the middle part of the cross section. The autochthonous cover was added below the Bon Nant filling with a depth of around 300-500 metres, but it was not possible to detail the highly complicated structures of the cover from a regional scale. Below the cover, the two-dimensional model takes into account the existence of a large fractured zone in the basement down to the thrust fault. The fractured zone would represent the sub-vertical fault system of Les Contamines-Montjoie including the Springs Fault. It certainly allows a fast uprising of the deep fluid up to the autochthonous cover where mixing processes occur. The Quaternary filling was not represented in the model because it is relatively thin compared to the scale of the cross section.

The geological structure of the Mont Joly Massif was simplified for the model, this massif mainly consists of limestones and marls (Epard 1989) drawing recumbent folds (Paréjas 1925) belonging to the Morcles nappe. Vertical infiltrations towards the bottom of the massif were limited by the presence of these recumbent folds, and thus the recharge zone is assumed on the edges of the massif where the Triassic rocks outcrop. The formations with the highest permeabilities are located at the bottom of this sedimentary massif in Triassic rocks. For the model, groundwater infiltrates this horizon. The bottom of the sedimentary cover would plunge towards the north from an elevation close to 1500 metres in the Aiguille de Roselette and Mont Joly area to an elevation of roughly 100-300 metres below the Bon Nant Valley. Therefore, groundwater flows in the Triassic domain will remain cold because they cannot reach deeper zones. In the model, infiltration in the basement below the Mont Joly Massif will be possible but limited compared to flows in the Aiguilles Rouges basement on the other side of the model. Finally, Aiguilles de Roselette represents the second limit of the model with no lateral inflows. It consists of a crystalline domain covering the autochthonous cover via a thrust fault. It is assumed that groundwater flows in this massif follow another direction.

11.2.2 Discretization of the geological cross section

The two-dimensional model consists of twenty one sub-domains of various sizes. Each sub-domain allows differentiating the geological units such as the Aiguilles Rouges basement, the Servoz - Les Houches zone, the Mont Joly sedimentary massif, etc. (Fig. 11.1). Moreover, sub-domains were created to separate zones within the same geological unit showing different hydraulic conductivities.

Sub-domains were created roughly in the first 500 hectometres depth from the surface in the Aiguilles Rouges Massif and in the basement below Mont Joly. In the Aiguilles Rouges Massif, these sub-domains define the decompressed zone where hydraulic conductivities are higher due to recent tectonic processes (Cruchet 1985, Lhomme et al. 1996, Maréchal 1998 and 1999b). As illustrated for Lavey-les-Bains, it remains difficult to precise the thickness of the decompressed zone because the decrease of permeabilities with the depth is not a strict limit but is progressive. The decompressed zone drains a large amount of water towards the feet of the slopes, and therefore important groundwater flows in this unit were simulated reflecting this. The presence of vertical fractures or faults in the basement promotes deeper infiltrations reaching the bottom of the model.

Other sub-domains were created in the Aiguilles Rouges basement, and in the basement below the Mont Joly Massif, with the aim to represent the Carboniferous formations. The largest sub-domain is located in the Arve Valley (Servoz - Les Houches zone) and was assumed in the model with a different permeability compared to the basement.

For the sedimentary domain of Mont Joly, one sub-domain was created with a large extension and symbolizes the Triassic horizon at the bottom of the Mont Joly Massif. It extends from Aiguilles de Roselette to the fractured zone at Saint-Gervais-les-Bains with a low dip towards the north. Below the Bon Nant Valley, one refined sub-domain was created with a thickness of around 300-500 metres including the Quaternary deposits. The regional scale used for the simulation is not appropriate for the reproduction of the local geological setting, which is highly complicated. Other formations of the Mont Joly were gathered to a single sub-domain.

Finally, the deep gneiss below the decompressed zone of the Aiguilles Rouges Massif and below Mont Joly was divided into two large extended sub-domains. The Aiguilles de Roselette crystalline unit was not taken into account for the simulation. Indeed, this unit does not present a great interest for our case study because groundwater flows do not seem to circulate in that direction. It will be simulated as a limit without flow.

Concerning the mesh geometry, the triangulation method was selected and each sub-domain was affected by a precise number of meshes reaching a total of about 24'500 cells. Sub-domains close to the hydrothermal area, such as the fractured zone and the autochthonous cover, were refined to obtain a greater precision in the calculation. The size of the mesh varies from roughly 200 metres in the deep gneiss to several metres in the hydrothermal area.

11.2.3 Assigned parameters in the model

Assigned parameters in the two-dimensional model of groundwater flow and heat transport are summarized in Table 11.1. Imposed values come from data in literature and wells measurements. They were also documented from the Swiss Federal Office of Meteorology and Climatology, but only for regional precipitations because surface temperatures are not given in the French territory. For zones with little data, imposed values were extrapolated. Finally, this section describes types and values of the assigned parameters in the two-dimensional model, starting with flow conditions, then properties of materials and finally heat conditions.
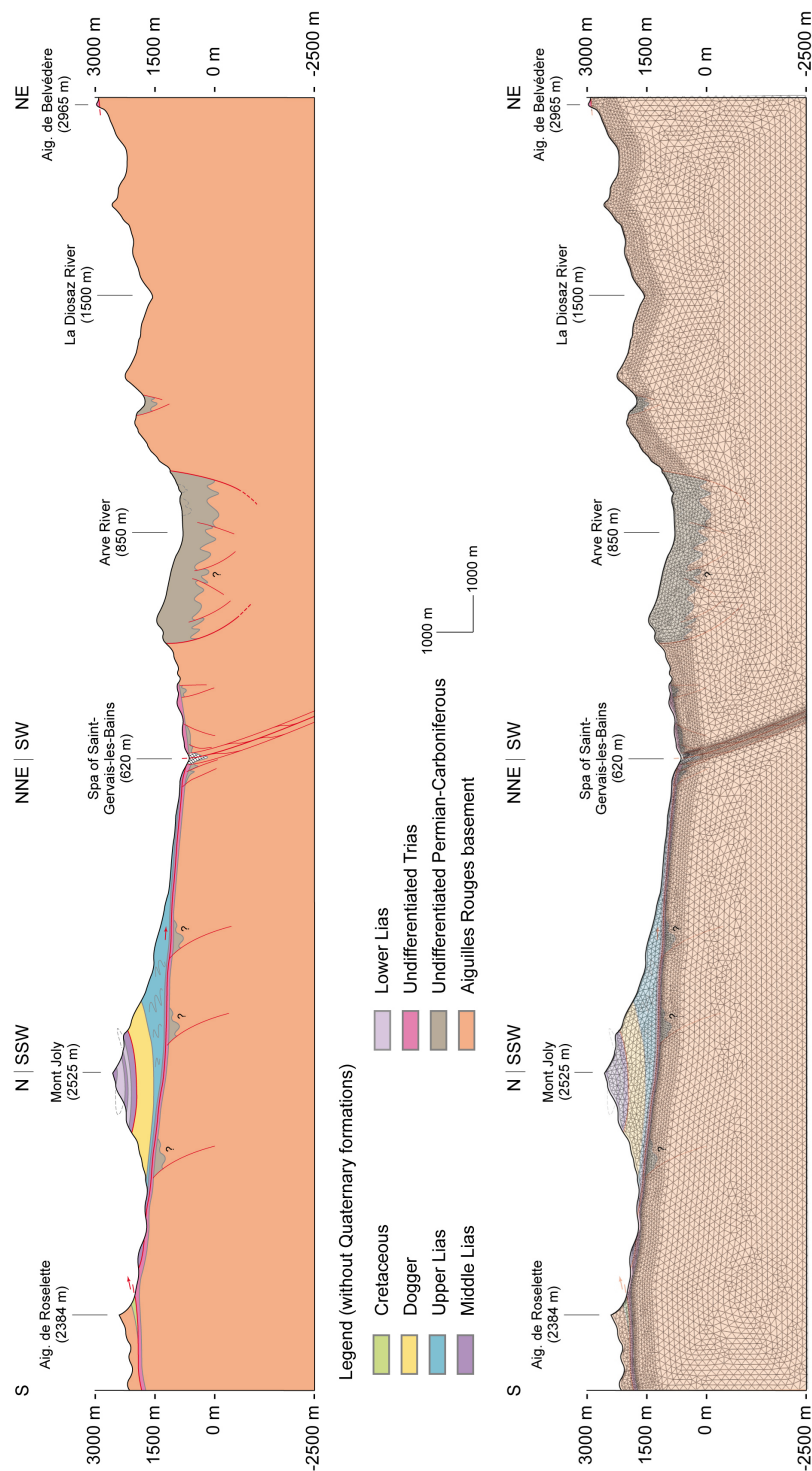
Figure 11.1: Geological cross section of the two-dimensional model for flow and heat transport in the Aiguilles Rouges crystalline Massif and finite element mesh geometry of the two-dimensional vertical model. This cross section has two small changes of directions for reason of convenience and to cross the Mont Joly Massif (autochthonous cover). The cross section line is visible in Figure 9.1.

Flow parameters

The flow parameters correspond to the recharge of water in the model from the infiltration at the tops of the Aiguilles Rouges Massif. They also refer to the hydraulic heads being able to characterize inflow or outflow points in the model. In the model, hydraulic head values were imposed on the three valleys (Bon Nant, Arve and La Diosaz).

The infiltration of water at the top of the Aiguilles Rouges Massif was estimated from precipitations, minus the effective evapotranspiration, the surface runoff and the variation of storage. In high mountain domains such as the Aiguilles Rouges Massif, infiltrations within the basement are heterogeneous because they depend on the presence of major fractures and faults. Moreover, the infiltration of water mainly takes place in the decompressed zone where a large amount of water is stored. Therefore, the simulated flow patterns will be mostly carried out in this domain. The estimation of waters which really infiltrate deeply will be given by the simulation and depends on the contrast of permeability in the basement.

The recharge of water in high mountain areas varies with the seasonal climatic conditions. The infiltration of water is strongly limited in winter because precipitations are stored on the surface as snow. The most important recharge of waters occurs during the period of the snow melt in summer. For facilitation reasons, the seasonal climatic conditions were not considered in the model. An average recharge of water has been assigned to 10% of the total annual precipitation. This value seems to be low but the surface runoff strongly occurs in high mountain areas due to the accentuated topography which limits infiltrations. The presence of a lot of torrents proves it as well as the hydraulic properties of rivers which are marked by strong discharge variations (example of the Arve River in Payraud 1991).

The geographical distribution of the recharge zone mainly concerns the areas surrounding La Diosaz River and extends as far as the summit of the Aiguille de Belvédère. Imposed values fluctuate between 10% of 1500 mm/yr, median value for the La Diosaz Valley, to 10% of 1800 mm/yr, median

value for the area of Aiguille de Belvédère. These precipitations were estimated from data of the Swiss Meteorology and Climatology Federal Office which are illustrated in the Atlas de la Suisse (version 2.0, Fig. 11.2).

Areas located close to the Bon Nant Valley and extending into the city of Saint-Gervais-les-Bains, have the lowest values of precipitation ($\approx$ 1200 mm/year) and were not considered as recharge zones. Groundwaters in this sector will represent cold water inflows in the limit between the basement and its autochthonous cover. In reality, thermal waters in the two De Mey wells are diluted with a Triassic end-member and thus it is possible that the cold end-member comes from shallower circulations in the sector of the city of Saint-Gervais-les-Bains.

Two other sectors were considered as recharge zones and are located between Mont Joly and Aiguille de Roselette Massifs where the Triassic formations outcrop. According to data in Figure 11.1 and precipitation measurements in the city of Les Contamines-Montjoie (1427 mm/yr between 1994-2004 in Vigouroux and Kay 2005), it was decided to assign an average value of 10% of 1600 mm/yr. In the model, recharge conditions in these two domains generated in the model a flow system in the Triassic formations at the bottom of the Mont-Joly Massif.

Finally, it was not decided to impose infiltrations between Mont Joly and the hydrothermal area because the Triassic permeable formations are covered by the Lower Jurassic rocks which mainly consist of marl layers (Epard 1989). Due to the marl layers, the surface runoff is strong in this sector limiting vertical infiltrations down to the Triassic formations.

Hydraulic heads were imposed in the model on three points corresponding to La Diosaz, Arve and Bon Nant Valleys. In this case, they define outflows in the model because the recharge zones have higher elevations. Consequently, the computed water table in the model will go through these three points and it will be possible to calculate the discharge for each outflow point.
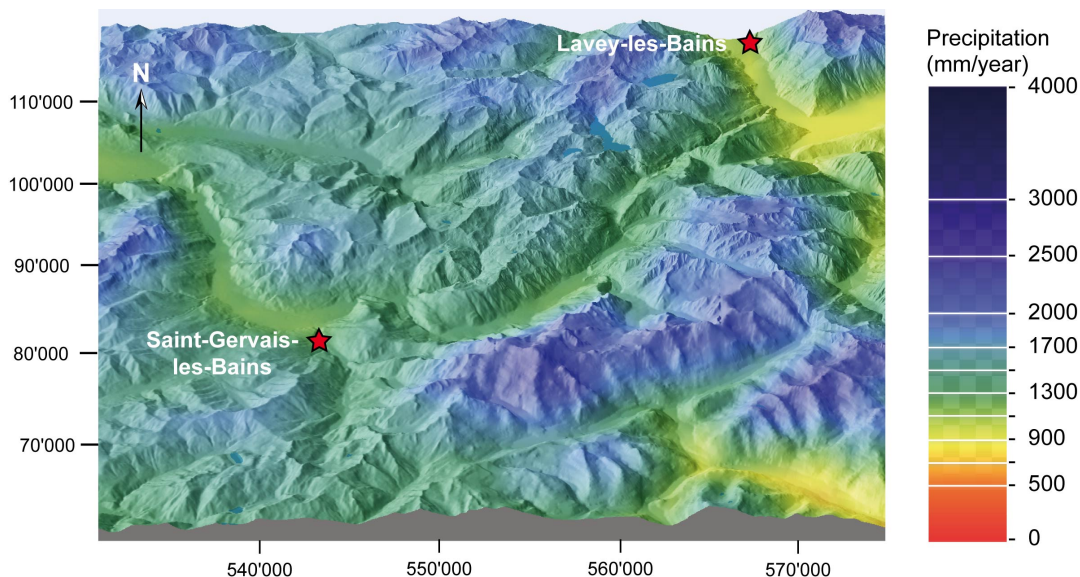
Figure 11.2: Precipitation map for the regional area of Saint-Gervais-les-Bains (Atlas de la Suisse, version 2.0). The temperature map could not be illustrated because there is no temperature data for the French territory. Location refers to the Swiss kilometric coordinates in projection, in standard CH1903.

Hydraulic parameters

The hydraulic parameters imposed in the model are the physical properties of the geological domains. In details, different values of hydraulic conductivities with anisotropy factors and porosities were assigned (Table 11.1). The anisotropy factors in the model enable the local fractured properties of rocks, which strongly influence the deep flow system, to be represented.

Values of imposed hydraulic conductivities were documented in literature, and results of previous pumping tests were also documented for the autochthonous cover. This physical parameter directly controls flow patterns in the model and the groundwater balance. The calibration of hydraulic conductivities required much time for the construction of the model. In the two-dimensional model several zones including the basement and the sedimentary horizons were created with varying hydraulic conductivity values.

A zone including the Quaternary filling and the autochthonous cover was present at shallow depth below the hydrothermal area. This zone showed a relatively high hydraulic conductivity of 10^{-4} m/s,

and the pumping tests showed that this layer was affected. In this sub-domain, an anisotropy factor $K_{horizontal}/K_{vertical} = 10$ with an anti-clockwise angle from the horizontal axis of 110° was imposed to reproduce the local fracture conditions at the origin of the natural upflowing. At a greater depth, the fractured zone in the basement representing the fault system of Les Contamines-Montjoie seems to drain the deep fluid towards the surface. This zone has a permeability of 10^{-5} m/s and an anti-clockwise angle from the horizontal axis of 110°. The model was calibrated so that the variation of permeability values in this sub-domain would not generate strong effects on the computed temperatures in the hydrothermal area.

In regards the Aiguilles Rouges crystalline Massif, the hydraulic conductivity was differentiated between the decompressed zone (2.10^{-7} m/s) and the deeper gneiss (8.10^{-9} m/s). The calibration of the model required a conductivity factor of twenty five between the two. Even though the contrast increases with depth, the value is still adequate. For the deep gneiss, this value seems to be overesti-

mated compared to measured hydraulic conductivities in crystalline rocks from tunnels and galleries where conductivities can reach lower values of 10^{-10} m/s (Maréchal 1998 and 1999a). However, the model was created in the same direction as the main fractures and faults in the Aiguilles Rouges Massif. Therefore the high permeability values in this direction are justified, as they would be comparatively higher than in the other directions. Moreover, anisotropy factors of $K_{horizontal}/K_{vertical} = 2$ and $K_{horizontal}/K_{vertical} = 4$ with an anti-clockwise angle from the horizontal axis of 90º were assigned respectively for the decompressed zone and the deep gneiss aiming to reproduce fracture conditions at the origin of infiltration of waters into the basement. Concerning the basement below the Mont Joly sedimentary Massif, the same values were imposed compared to the Aiguilles Rouges Massif. For the calibration of the model, this domain is of little interest because groundwater flows are mainly drained by the more permeable Triassic formations located above the basement.

The Carboniferous formations are pinched in the basement by schistous layers of relatively low permeabilities. The largest area located in the Arve Valley in the sector of Servoz - Les Houches was

assigned with a value of 10^{-8} m/s whereas a permeability of 10^{-7} m/s was imposed on other much smaller zones. Finally, an arbitrary low hydraulic conductivity of 10^{-9} m/s was placed on the subdomain of crystalline rocks forming the Aiguille de Roselette.

For the other sub-domains characterizing the sedimentary horizons such as the Triassic formations at the bottom of Mont Joly and close to the city of Saint-Gervais-les-Bains, a hydraulic conductivity of 5.10^{-4} m/s was assigned. This high value can be justified by the presence of limestone, cellular dolomite and gypsum in the layers, which are strongly fractured by Alpine tectonic events and probably locally karstified. For the Jurassic formations of Mont Joly which were gathered into a single sub-domain, an arbitrary low hydraulic conductivity of 10^{-9} m/s was assigned. In this unit, vertical infiltrations can be excluded due to the presence of subhorizontal marly layers drawing recumbent folds. Finally, porosity values of around 1-3% were assigned in the model. The highest values were placed on the fractured sub-domain close to the hydrothermal area, whereas the lowest values were placed on the crystalline sub-domains.

Thermal parameters

Surface temperature data from the Swiss Federal Office of Meteorology and Climatology are not documented in the French territory, whereas precipitation data are illustrated. Therefore, surface temperatures in the model were assigned with an extrapolation of data in Switzerland. Indeed, it can be assumed that there is no strong difference in temperature on each side of the Aiguilles Rouges Massif and in neighbouring regions. In the two-dimensional model, imposed values of temperature are in the range of 0-8ºC and depend on the elevation. An annual average temperature of 0ºC was imposed on the summits that have an elevation of around 2500 metres in the model. In Saint-Gervais-les-Bains, an annual average temperature of around 8ºC can be assumed due to its elevation (620 m) and its close proximity to the Arve Valley. In the sectors of Mont Joly and Aiguille de Roselette in the southern part of the model, surface temperatures were extrapolated from their elevations.

Concerning heat fluxes, data were not found in this studied area. For the two-dimensional model,

the assigned heat flux at the bottom was extrapolated from data in the Swiss Alps recorded on the map of Medici and Rybach (1995). The imposed value for the calibration is 85 mW/m^2, that is to say in agreement with data found in the literature, between 80 and 90 mW/m^2 for the Central Alps Massifs.

The rock thermal conductivity is also an important parameter to be considered in the simulation, because a variation of this parameter will strongly modify the simulated temperatures. The thermal conductivity of the rocks varies from 0.6 to 5.8 W/m/K at ambient temperature (Rybach 1973). High values correspond to compact rocks poor in water, for example in ultrabasic rocks, whereas porous formations containing waters have the lowest values < 1.5 W/m/K. Clark and Niblett (1956) studied the terrestrial heat flow in Swiss Alps and thermal conductivities of crystalline rocks. They showed that among 23 gneiss samples the thermal conductivity average value is 2.65 W/m/K. This study can be extrapolated to the French territory in

the Aiguilles Rouges Massif. For the model calibration, a thermal conductivity value for the Aiguilles Rouges gneiss of 2.5 W/m/K was imposed. For the sedimentary formations, which mainly consist of limestone, dolomite, cellular dolomite, gypsum, quartzite and marl, an average thermal conductivity of 2.5 W/m/K was also assigned.

Table 11.1: Comparison of observed/evaluated and imposed/simulated values for geological and hydrothermal boundary conditions for the two-dimensional model of Saint-Gervais-les-Bains. hor.: horizontal, vert.: vertical, obs.: observed, comp.: computed, calc.: calculated, resid.: residence and wat.: water.

Boundary conditions	Obs./Eval. values	Imposed values
Water recharge (mountain condition)	1 to 20% of precip.	10% of precip.
Imposed hydraulic head (m)		Elevation of rivers
Surface temperature (°C)	0-8	0-8
Hydraulic conductivity (m/s)		
Gneiss decompressed zone	$> 10^{-7}$	2.10^{-7}
Deep gneiss	10^{-6} to 10^{-12}	8.10^{-9}
Fractured zone of gneiss (fault)	10^{-2} to 10^{-5}	10^{-5}
Fractured zone below the spa	10^{-3} to 10^{-5}	10^{-4}
Fractured Triassic formations	10^{-3} to 10^{-6}	5.10^{-4}
Mont-Joly Massif	10^{-6} to 10^{-10}	10^{-9}
Conductivity anisotropy factor		
Gneiss decompressed zone	K(hor.)/K(vert.) = 2 and 90°	
Deep gneiss	K(hor.)/K(vert.) = 4 and 90°	
Fractured zone of gneiss (fault)	K(hor.)/K(vert.) = 10 and 110°	
Fractured zone below the spa	K(hor.)/K(vert.) = 10 and 110°	
Rock thermal conductivity (W/m/K)		
Aiguilles Rouges gneiss	2.65	2.5
Sedimentary formations	2-3	2.5
Heat flux (mW/m^{-2})	80-90	85
Porosity (%)		
Aiguilles Rouges gneiss	< 10	< 3
Sedimentary formations	< 10	< 3
Location of obs./comp. temperature	Obs. T (°C)	Comp. T (°C)
Close to the surface	< 42	22
200 m below the surface	43-45	48
400 m below the surface	> 45	51.5
Calc. temperature at depth	70-100	60-75
Geothermal gradient (°C/km)	15-20	13
Mean resid. time of deep wat.(years)	> 8000 (^{14}C)	≈ 3000

11.3 Comparison with the natural state of the hydrothermal system

11.3.1 Computed temperatures in steady state

The calibration of the two-dimensional model in steady state reproduced the geothermal anomaly at Saint-Gervais-les-Bains induced by the deep flow system (Fig. 11.3). The simulation was carried out excluding the assumption that successive glaciations entirely stopped circulation processes in the massif. In a global view, the simulation showed a large cold plume below the summits of the domain. It corresponds to infiltration of cold waters cooling the whole of the massif. Computed temperatures in the massif depend on the capacity of waters to flow deeply in the model, controlled by hydraulic conductivities and quantity of infiltrated water. The simulation also showed a vertical heat plume from the bottom of the model to the Bon Nant Valley, due to the higher permeability assigned in the fractured zone below the autochthonous cover.

Computed temperatures in the sedimentary cover at shallower depth vary from the surface to the limit which is at the basement. This numerical result is controlled by the presence of lateral cold inflows from the Triassic formations on each side of the hydrothermal zone. Indeed, the computed temperature at the surface is 22°C due to mixing processes in the model. The result is really lower than the previous temperatures of the springs before the exploitation of boreholes ($\approx$ 41°C for Gontard) which were almost not influenced by mixing processes with cold waters ($<$ 5 TU in Vuataz 1982). But this simulated temperature approaches the current values for the water at Gontard ($\approx$ 20°C). In reality, the local hydraulic network of flow paths of end-members is complex and there can therefore exist large side variations of temperature at shallow depths. Unfortunately, it was not possible to represent the local geometry of the groundwater flows in the autochthonous cover in the two-dimensional model with a regional scale.

Down to 200 metres below the surface, the simulated temperature is 48°C which corresponds to the limit zone where mixing processes occur in the model. In reality, the influence of the two cold end-members diluting thermal waters can be observed down to this order of magnitude of depth. The geochemical investigations showed that the temperature of the thermal end-member was in the range 43-45°C, that is to say slightly smaller than the computed value. Towards 400 metres depth in the model at the top of the basement, the calculated temperature is close to 51°C. Currently, it is not possible to justify this computed value because the exact depth of the basement is not yet known. However, a temperature close to 50°C can be assumed in the first metres of the top of the basement. About the inferred deep reservoir, the calibration of the model gives computed temperatures roughly of 60-75°C. These values seem to be lower compared to the calculated values with the method using mineral-chemical equilibria which gave 70-100°C.

Concerning the sector of Mont Joly, simulated temperatures in the Triassic formations are always lower than 15°C. The long residence time of the flow system in this unit generates a stabilization of the temperature with time in the model. This simulated flow system can be representative of the natural flow of the Ferrugineuse and Magnésienne springs. Indeed, these two springs have stable discharges, temperatures ($\approx$ 10°C) and conductivities (2.5 mS/cm) in summer as well as in winter. In the model, the subhorizontal groundwater flows in the Triassic formations limit deeper vertical infiltrations in the basement which has a lower permeability. Consequently, the deep massif below Mont Joly cannot be cooled by water infiltration and thus a dominant geothermal gradient occurs in this domain. This seems to be unrealistic in reality.

In the model, the simulated geothermal gradient varies along the cross section. The lowest value of gradient (13°C/km) is found below the recharge zone in the Aiguilles Rouges Massif and the highest value corresponds to the basement below Mont Joly where infiltrations are limited in the model. The fractured zone also has a high geothermal gradient due to the uprising of the deep fluid (22°C/km). The geothermal gradient in the Aiguilles Rouges Massif was calculated from the top to the bottom of the model (thrust fault). This value found in the recharge zone seems to be in agreement with estimations made on other crystalline massifs met in the Central Alps ($<$ 20°C/km in Vuataz et al. 1993).
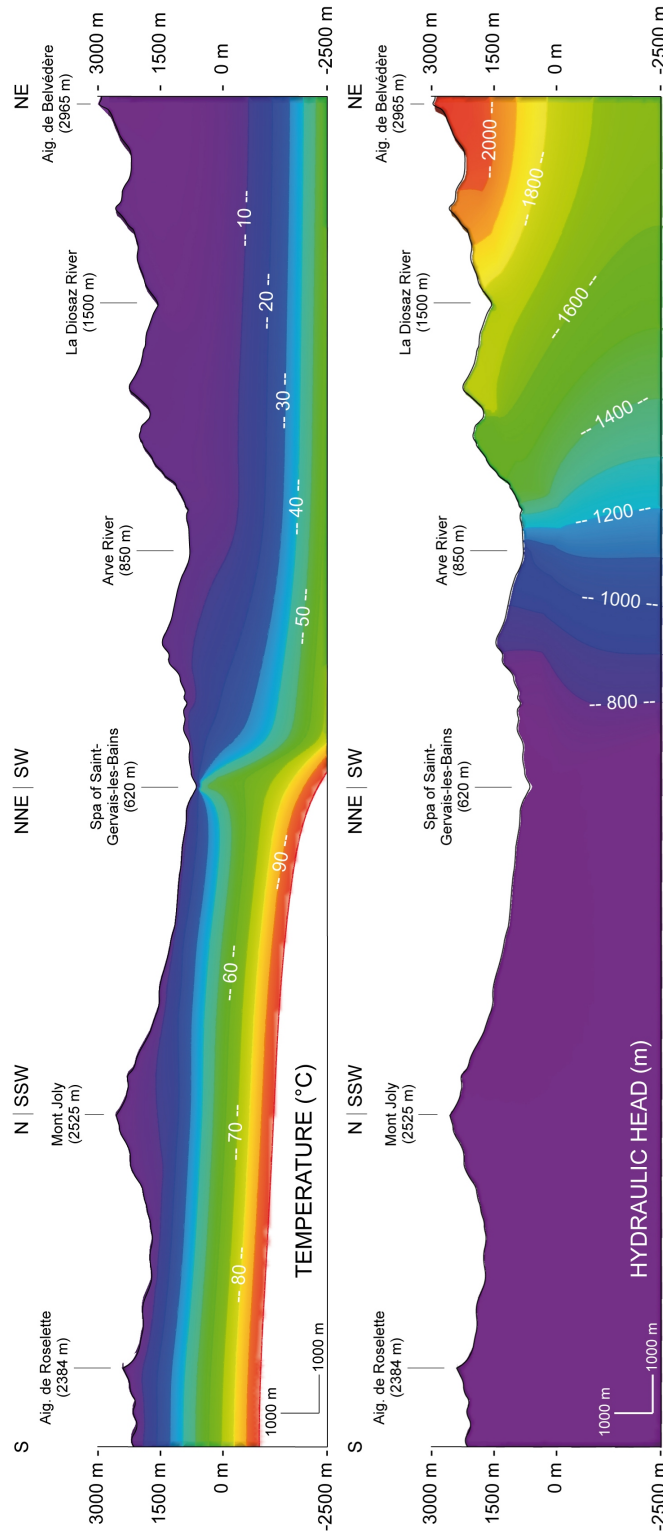
Figure 11.3: Cross section of the Saint-Gervais-les-Bains hydrothermal system showing the computed temperatures and hydraulic heads in the Aiguilles Rouges crystalline Massif.

11.3.2 Computed groundwater for steady state flow

The two-dimensional model in steady state makes it possible to obtain an adequate view of hydraulic heads with values decreasing from the recharge zone to the hydrothermal area (Fig. 11.3). The top of the groundwater corresponds to the water table in the model where a simulated pressure equivalent to the atmospheric pressure was calculated. With the simulation, it was shown that the computed water table has a realistic form in the eastern part of the cross section including the Aiguilles Rouges Massif. It was also shown that the groundwater level has a rather low elevation below Mont Joly because the recharge zone was limited to the Triassic formations. For this reason, the simulated water table in this sector has a slight slope.

In the model, water circulations in the decompressed zone of the Aiguilles Rouges Massif mainly supply the flow system at a shallow depth down to the La Diosaz and Arve Valleys. Moreover these circulations also supply to a lesser extend the Saint-Gervais-les-Bains hydrothermal system with deeper flow paths. Infiltrations on the further massif (Aiguille de Belvédère area) generate the deepest circulations in the model.

Contrasts of permeabilities between the decompressed zone and the deeper gneisses are responsible for high values of calculated exfiltration on the highest valleys (56% of the total infiltration). There is a strong difference between the exfiltration computed in the Arve River (0.15 m^3/d/m) and in La Diosaz River (2.54 m^3/d/m) because the Carboniferous zone of Servoz - Les Houches has a low permeability where the Arve River is located in the model. This gological unit prevents the rise of waters. In the model, the Bon Nant Valley discharge is consequently equal to 44% of the total groundwater recharge (2.14 m^3/d/m) which can be subdivided into three flow rates: 0.5 m^3/d/m from the Triassic formations of Mont Joly, 0.86 m^3/d/m from the Triassic layers on the other side of the valley close to the city of Saint-Gervais-les-Bains, and 0.78 m^3/d/m from the deep thermal aquifer. This calculated value for the deep thermal aquifer corresponds to 22% of the total recharge located in the Aiguilles Rouges Massif. In other terms, 4/5 of the total infiltrations remain in the decompressed zone and 1/5 supply the deep thermal aquifer. According to values of infiltration equal to 10% of total precipitations, 2.2% of precipitations supply the deep thermal aquifer. This value seems to be realistic in high mountain domains, but appears to be low compared to production rates of thermal waters at Saint-Gervais-les-Bains, respectively 13.5, 5.5 and 3.5 m^3/h in the three Lépinay, De Mey Est and De Mey Ouest wells. But this result has to be multiplied by the width of the assumed watershed (roughly of 3000-5000 m). Thus, a discharge of about 2300-3900 m^3/d or 90-160 m^3/h is obtained, 4 to 7 times higher than the maximum rate, which can be pumped in the existing wells. As compared to the Lavey-les-Bains model, the water flux through the fractured zone below the autochthonous cover has an important linear variation with the depth.

Using the particle tracking option, the model gives an average residence time of the deepest fluid roughly of 3000 years, lower than the residence time computed for Lavey-les-Bains. The geological and geochemical similarities between these two hydrothermal systems seem to indicate that values of carbon-14 should be similar to the thermal end-member flowing in the Aiguilles Rouges basement. The calculated residence time with the carbon-14 method gave a value higher than 8000 years for the thermal end-member in Lavey-les-Bains. Therefore, the computed residence time for Saint-Gervais-les-Bains should be validated with carbon-14 analyses. This computed value depends on the selected permeability and porosity values in the model.

Part V

Val d'Illiez

General description of the study area

12.1 Geographical setting of Val d'Illiez

THE hydrothermal area is located in the Wallis canton in Switzerland, at the precise locality of Buchelieule in the north-east of the village of Val d'Illiez (558.400/117.500, 790 m.a.s.l.). All the springs discharge from the left bank of the Vièze River, the major stream of the valley which flows into the Rhone River at Monthey (Figs. 12.1 and 12.2).
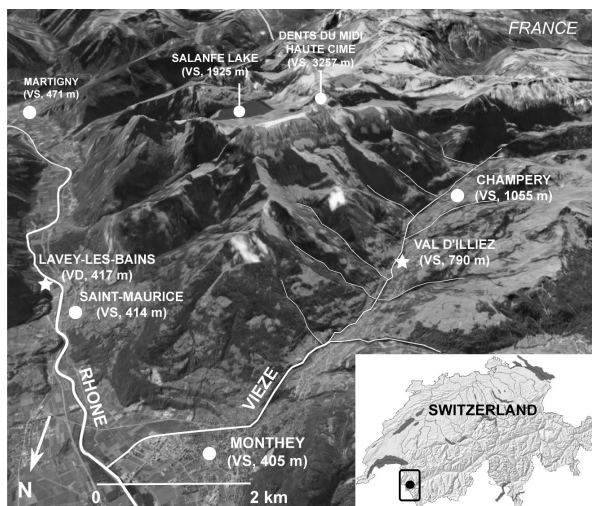
Figure 12.1: Geographical location of Val d'Illiez in Switzerland. Star symbols show hydrothermal sites.

On a regional level, the studied area is located in the Western Alps of Switzerland close to France, precisely at the foot of the Dents du Midi Massif (3257 m.a.s.l.). The spa continuously exploits the artesian uprising thermal waters for swimming pools through the F3 well (F3, 120 m inclined borehole) and one thermal spring. Another group of thermal springs (Cascade) and two other inclined boreholes F1 and F2 (respectively 37 and 60 m) also exist but are not used for swimming pools, and several old thermal springs were present before the F3 production. On the site, thermal seepages occur in the alluvial deposits indicating that this zone has a significant amount of thermal discharge. One kilometre upstream from the spa, two springs in the bed of the Vièze River and trenches dug to 5 metres depth in the alluvial plain in a private property at Play met subthermal waters at 16°C. Between Buchelieule and Play, three vertical borehole heat exchangers for a private residence (Jossi VBE) also met subthermal waters inside rocks below the Quaternary deposits (Alpgeo 2008). Finally, some other subthermal springs are present at Les Fayots situated 1 kilometre downstream from Buchelieule, which is just a few metres downstream from the Cascade spring, with temperatures of around 16°C (see location of Buchelieule, Play, Jossi VBE and Les Fayots in Fig. 12.3).

12.2 History of Val d'Illiez thermal baths

The historical background of the Val d'Illiez hydrothermal site was described many times, and to avoid repetitions and confusions, it was decided to highlight what was written by Bianchetti et al. (1992) which is the only published to date. The occurrence of thermal springs seems to be recent as there is no recorded activity to be found in the literature before 1953, although geologic studies in the Val d'Illiez region were carried out in the 1920's. At the most Mariétan (1953) says that a spring with a temperature of 18°C had been known for a long time. The same author is the first to describe the circumstances under which the present thermal springs appear for the first time: "In September 1953, warm springs gushed forth below the village of Val d'Illiez... near the bridge on the Vièze River (780 m.a.s.l.)... Since last year, one could hear underground noises and one could feel weak earth tremors. But during the summer, these noises became louder. From October 26 to November 2, nine earth tremors were recorded; the one from November 2 shook doors and windows in the village of Val d'Illiez...". These seismic events were also recorded in the annual report of the Swiss Meteorological Office (Wanner 1954). Mariétan (1953) also gives a description of the springs: "...the thermal springs are spread out 70-80 metres, emit a hydrogen sulfide smell and their temperature reaches 28°C...". The total flow rate was estimated around 1300 L/min (Wanner 1954) and the first chemical analysis (Schroeder and Ducloz 1955) carried out in October 1953 mainly revealed a Ca-SO$_4$ composition.

The hydroelectric Salanfe dam was completed in 1952 at the elevation of 1900 metres, at about 9 kilometres south-east of the village of Val d'Illiez. The reservoir lake is rather large compared to other Swiss reservoirs (40.10^6 m^3), but the height of the dam is moderate (52 m). The first partial filling of the lake was carried out during the same year and, in September 1953, the maximum level of 1917.33 metres was reached. Rather quickly major water losses (> 1 m^3/s) through the lake basin were mentioned by the dam supervisors. Several tracer tests were carried out by N Oullianoff to determine locations of resurgences (Schneider 1989 in Vergain 1991). One first test with 20 kg of fluorescein from the Salanfe Lake allowed one small outlet located at Fontaine à Moïse (564.500/110.175) to

be detected. Later, a second tracer provided controversial results: new analyses of samples three years later detected fluorecein in several samples such as in waters of Buchelieule and Fontaine Froide (564.500/112.900). These results were discussed and contested later by hydrogeologists (Pantet 2004).

Between 1953 and 1962, the thermal springs were used to supply warm water basins for the local inhabitants. In 1980, the Société des Bains de Val d'Illiez drilled subhorizontal drainage boreholes and built a swimming-pool (Fig. 12.2). This corresponds to draining zones of Captage A (6 pipes), Captage B (4 pipes) and Cascade springs (11 pipes).

Figure 12.2: View of the Val d'Illiez spa (photo : H Rickenbacher, 1998)

In 1988, the Centre de Recherches Scientifiques Fondamentales et Appliquées de Sion (CRSFA today CREALP) carried out a geothermal and hydrogeological study of the hydrothermal area, within the framework of a research project aiming to study thermal waters in Wallis, sponsored by the Swiss National Science Foundation and the GEOTHERMOVAL program (CRSFA 1992a). At the same time, Bianchetti (1993b) and Vergain (1991) measured physico-chemical and isotopic parameters in thermal and cold waters in the Val d'Illiez. Mandia (1991) also investigated the geochemistry of the Val d'Illiez thermal waters with the aim of studying the Triassic aquifers in the Alpine environment. Temperatures, electrical conductivities and production rates measured between 1988 and 1993; for Captage A they were about 29-30°C, 1670-1850 μS/cm

and 13-24 m^3/h, for Captage B 28-30°C, 1650-1800 μS/cm and 1.2-5.9 m^3/h, for Cascade spring 25-26°C, 850-1430 μS/cm and 21-23 m^3/h (Bianchetti 1996).

Between 1992 and 1994, the management of the hydroelectric dam in Salanfe ordered waterproofing works on the water reservoir to be carried out in order to reduce water losses through infiltration in the fractured and karstified Triassic rocks. They injected concrete inside fractures on the left bank of the lake, via a horizontal gallery of 630 metres length (Pantet, 2004).

In October 1994, the level of the lake reached firstly the elevation of 1923 metres. During this period, the seismic activity increased (Bianchetti and Rouiller 1998) and low earthquakes were felt in the Val d'Illiez in autumn 1994 and later in winter (Bianchetti 1996). In autumn 1994, the owner of the spa reported an increase of flow rates of thermal springs, with the appearance of new thermal springs flooding the site and the alluvial plain. Measurements made on exploited thermal springs showed a slight increase of temperature and conductivity, and this was also visualized for Cascade spring which reached its highest conductivity value since the recording of the parameters (1600 μS/cm). In February 1995, measurements made on thermal springs and thermal seepages showed temperatures in the range 19-27°C. Flow rates of exploited springs increased significantly (33 m^3/h in Captage A) and they doubled for Cascade. To restore the normal situation in the spa, an additional drainage of thermal waters was implemented. Two inclined wells named F1, 37 metres length, and F2, 60 metres length, were drilled in March 1996 on each side of the Cascade spring. The implementation of these wells met technical difficulties related to particular geological and hydrogeological conditions: moraine with low permeability, highly fissured rocks falling into the well and strong water inflows with high pressures (Bianchetti 1996). Temperatures, electrical conductivities and artesian flow rates measured in 1996 were at about 29°C, 1790 μS/cm and 4500 L/min for F1, 30°C, 1830 μS/cm and 300 L/min for F2. Thermal springs appeared in 1994 were drained through wells (925 L/min before and 22 L/min after drilling, Bianchetti 1996).

A third inclined well called F3, 120 metres length, was also drilled in 1996 aiming to collect thermal waters below Captage A and Captage B at higher temperatures expected (33-35°C) and production rates. This objective was not reached because the desired temperature in F3 was lower than the prediction (30°C). However, the production rate in F3 was almost tripled (2000 L/min), and 7000 L/min of thermal water was extracted through the three wells (Bianchetti 1996). Later, a complete technical report on the F3 borehole including two chemical analyses was written by Alpgeo (2006a and 2006b) with the aim to obtain the designation "natural mineral water".

Two tracer tests were carried out in 2000 and 2001 by Sesiano (2003) due to the discovery of water losses located in the south bank of the Salanfe Lake. In the two cases, injected uranine was found in thermal waters at Buchelieule with the fluorometer. Residence times were calculated in the range of 1 to 3 months, but the reliability of the data is debatable there not used by hydrgeologists (Gainon 2008).

Between 2003 and 2005, a project with a geothermal well was proposed in a private property located 1 kilometre upstream from the spa, precisely in Play (see location in Fig. 12.3). In this area along the left bank of the Vièze River, 5 trenches were dug in 1995 in the alluvial plain down to 4-5 metres depth, and a well of 20 metres depth was drilled in 1996 reaching the bedrock. Collected subthermal waters in the Quaternary deposits showed anomalies in electrical conductivity and temperature (1345 μS/cm and 16.5°C) because the rise of thermal waters occurs below the filling (Bureau Tissières 2003, 1996a and 1996b, Vuataz 2005). Due to a law conflict with the spa, the project of the geothermal well had to be abandoned.

In 2003-2004, a specialized diploma in geological engineering at the University of Lausanne (Switzerland) was undertaken by Pantet (2004). This diploma was mainly focused on the structural geology of the Dents du Midi Massif and the area around Salanfe Lake, with a part devoted to the study of hydrogeology and water chemistry of the waters near Val d'Illiez. Samples were collected in the hydrothermal area, and new chemical and isotopic data in thermal waters could be provided. Moreover, Pantet (2004) also investigated subthermal and cold springs around Val d'Illiez which were sampled again for this study. Finally, Gainon (2008) analysed thermal waters in the Val d'Illiez in 2005-2006 during his PhD thesis at the University of Neuchâtel (Switzerland), with the objective of measuring four radio-isotopes of the series ^{222}Rn, ^{226}Ra, ^{238}U and ^{234}U in thermal waters in Switzerland.

195
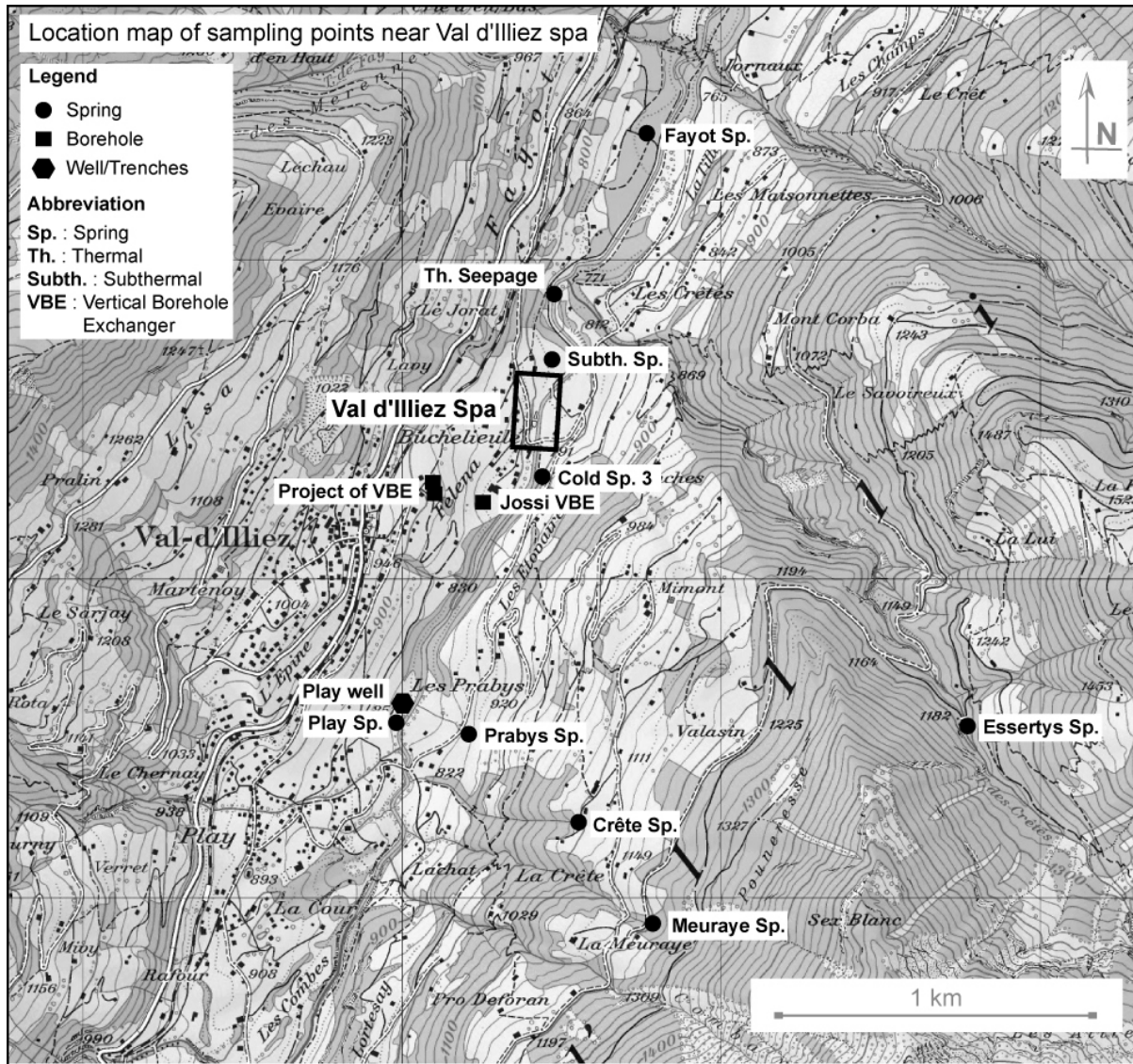
Figure 12.3: Location map of the sampling points around the spa.
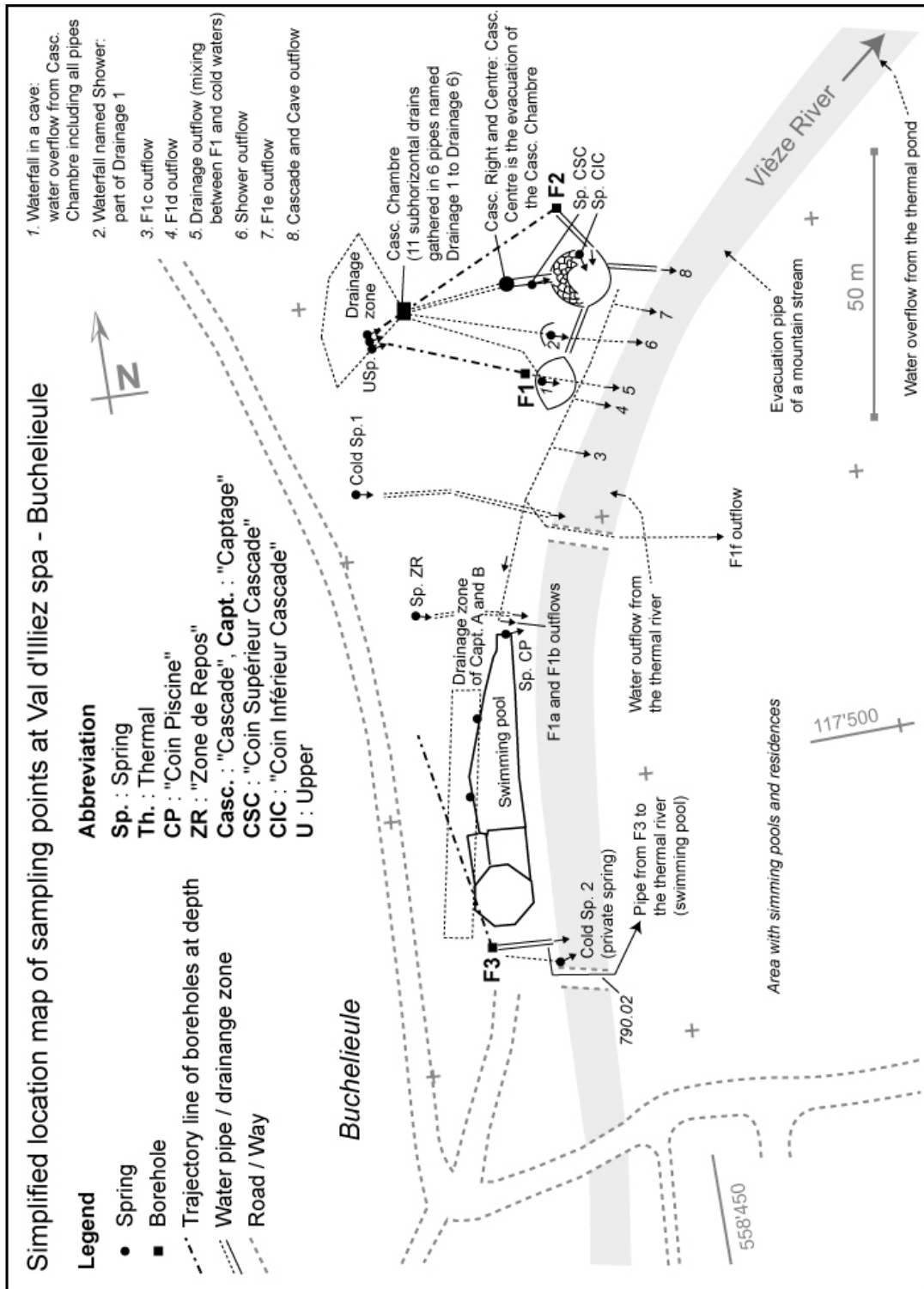
Figure 12.4: Location map of the sampling points in the spa area. Location refers to the Swiss kilometric coordinates in projection, in standard CH1903.

12.3 Sampling points in the Val d'Illiez

Three deviated boreholes carried out in 1996 and several thermal and subthermal springs from horizontal drainage are present in the Val d'Illiez. All the sampling points have a natural artesian flow rate and thus, they are not equipped with pump. The deepest well (F3) is used to fill swimming pools on the two sides of the valley, and thermal waters in both other wells F1 and F2 are discharged into the Vièze River. A part of F1 waters is used to heat paving stones. Moreover, bottled drinking waters are produced in the site with the exceeding F3 thermal water. Subhorizontal drainages inside the slope, downstream from F3, gather thermal waters into a small gallery named the "Chambre de Captage". This feeds with several pipes the waterfall outside the gallery named the "Cascade", the waterfall in a dug grotto called the "Cave" and the waterfall between the Cascade and the Cave named the "Shower" (Fig. 12.4).

12.3.1 Production wells F1 and F2

The F1 and F2 wells were implemented between March and April 1996, 100 metres downstream from the spa on each side of the Cascade waterfall (see location in Figs. 12.4 and 12.6). These wells were drilled aiming to drain thermal seepages from the slope which appeared in autumn 1994 after water-proofing works on the water reservoir at Salanfe Lake to reduce water losses (Bianchetti 1996). Currently, F2 is unused. The F1 well is employed to heat paving stones along the pathway between the swimming pool and the Cascade (10-12 L/min, 28.2°C and 1920 μS/cm in June 2009). Depth, length, inclination and coordinates of F1 and F2 are given in Fig. 12.5. Both wells are equipped with a steel casing of diameter 194 millimetres penetrating in the bedrock. In addition to this, the F2 well is equipped with a full tube in polyethylene of diameter 110 millimetres and cement reaching 18 metres in length. Below the steel casing, the hole is open with a diameter of around 165 millimetres.

Geologically, wells first of all crossed the silty clay moraine down to 7 and 9.5 metres respectively for F1 and F2. Then, roughly of 2 metres of alluvial deposits were drilled before reaching the bedrock composed of tertiary formations (schists and sandstones). The productive formations are located beyond 11.5 and 24 metres in length respectively for F1 and F2 and correspond to the fractured sandstones. The total artesian flow rate in 1996 was significantly higher for F1 than for F2 (4500 L/min against 300 L/min). In 2009 it was not possible to know if the F1 flow rates and discharges measured at seven different outflows in the river corresponded to the total flow rate. Contrary to the waterfalls, the rate in the largest pipe draining mixed F1 water

was not modified by the emptying of the Chambre de Captage in June 2009.
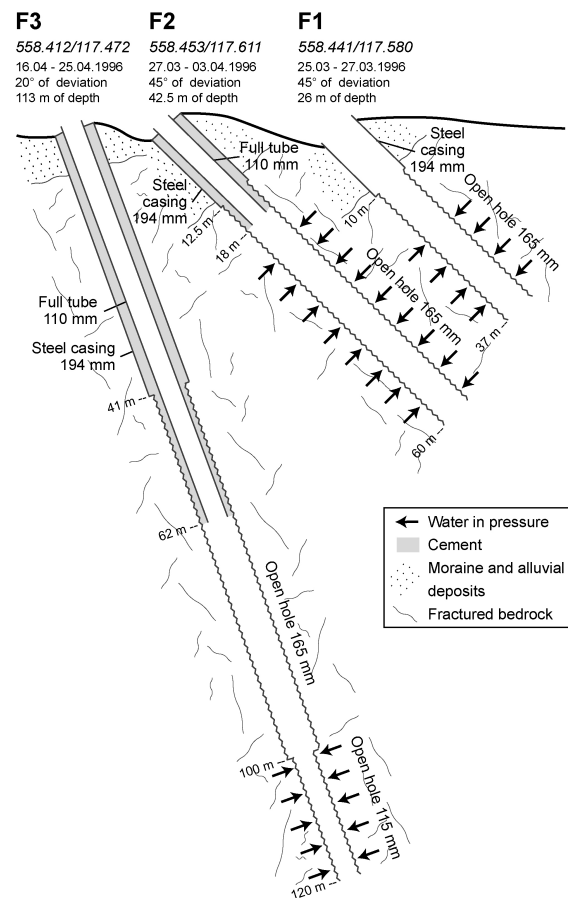
Figure 12.5: Characteristics of the three boreholes in the Val d'Illiez modified from Bianchetti (1996). Locations of wells are given in Fig. 12.4.

Concerning the F2 well, an artesian flow rate of around 200 L/min was measured in June 2009, and thermal waters are continuously discharged at the bottom of the Cascade waterfall before being rejected into the river. Just after the drilling operations in 1996, temperatures and electrical conductivities at 20°C were measured: 28.9°C/1790 μS/cm and 29.9°C/1830 μS/cm respectively for F1

and F2 wells (Bianchetti 1996). In June 2009, new measurements were carried out and showed the stability of the parameters: of around 29 °C and 1935 μS/cm at 25°C for F1, 27.9°C and 1960 μS/cm at 25°C for F2. Differences in electrical conductivity are due to various devices and corrections of measurements.
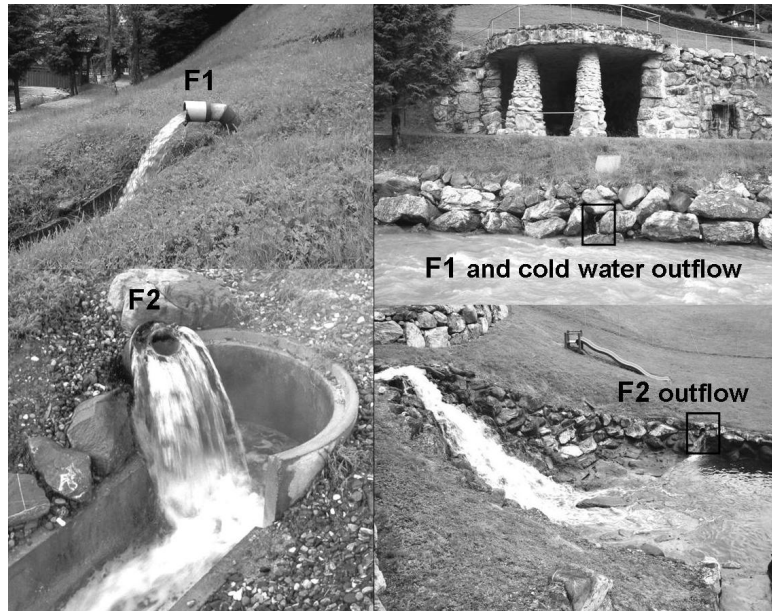
Figure 12.6: View of the F1 and F2 well heads at the end of the new drilling works in 1996 (from Alpgeo). View of discharges of the two wells in June 2009 of which samples were collected. At the time of this study, well heads are covered by the soil.

12.3.2   Production well F3

The F3 exploited well was drilled in April 1996, some metres upstream from the spa on the left bank of the river (see location in Fig. 12.4). This well was carried out with the initial objective to collect thermal waters below the old Captage A and Captage B with a temperature of up to 33-35°C. Unfortunately, this objective was not reached because thermal waters were cooler than expected (30°C) at the end of drilling. However, the artesian flow rate in F3 had almost tripled compared to Captage A and Captage B reaching 2000 L/min against 600 L/min (Bianchetti 1996) and thus, waters are continuously used to fill swimming pools located on both sides of the river.

Technically, the well is inclined with a dip of 20°, a depth of 113 metres and a length of 120 metres (Fig. 12.5). As for F2, the F3 well is equipped with a steel casing of diameter 194 millimetres down to 41 metres in length, and with a cemented full polyethylene tube of diameter 110 millimetres reaching 62 metres in length. Beyond 62 metres, the hole is open with a diameter around 165 millimetres which becomes smaller beyond 100 metres in length (115 mm). A measuring cell set on pipes allows the variation of the production rate and water temperature in F3 to be recorded (Fig. 12.7).

Geologically, the F3 well crossed firstly the silty clay moraine down to 5 metres, but below there was no alluvial deposits as opposed to the other wells. The reached bedrock is also composed of Tertiary formations (schists and sandstones). The productive formations are located beyond 100 metres in length. At that time, the F3 production rate caused a long-term decrease of the flow rate in Captage A and Captage B (320 L/min). Between July 2004 and January 2006, the Alpgeo consulting office measured the production rate in F3 at around 1200-1470 L/min with temperatures and electrical conductivities remaining stable compared to values in 1996, of around 30°C and 1800 μS/cm at 20°C (Alpgeo 2006a and 2006b). In June 2009, these parameters were 1170 L/min, 28°C and 2040 μS/cm at 25°C. When the thermal water extracted in F3 is not used to fill swimming pools, it is directly discharged into the river. Downstream from the spa, the swimming pool filled with the F3 thermal water is discharged into the river.
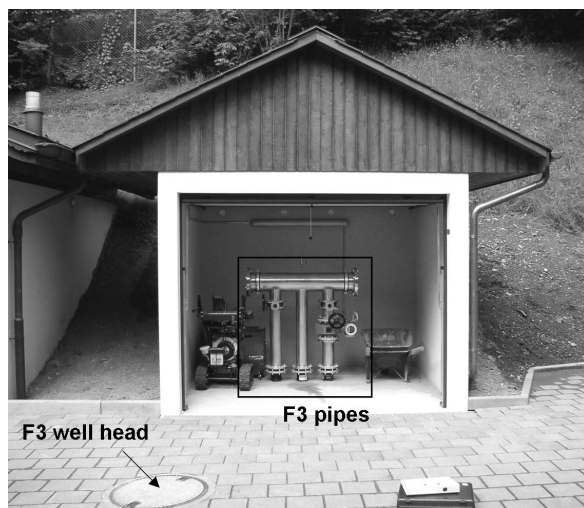
Figure 12.7: View of the F3 water pipes in June 2007 (from Alpgeo).

12.3.3 Sampling points from the "Chambre de Captage"

The called Chambre de Captage was built in 1980 supervised by the Société des Bains de Val d'Illiez (Fig. 12.8). It consists of 11 subhorizontal drainages going through the bedrock in the slope. During the drilling, the geological description of logs was not carried out. The absence of outcrop does not allow the lithology of rocks met below the moraine deposits to be defined. However, according to Vergain (1991) the bedrock would be a sandstone named the "Grès des Carrières" close to a N-S thrust fault.

Currently, 6 pipes are collecting thermal waters in Chambre de Captage with various flow rates, temperatures and conductivities. These waters mix together inside the Chambre de Captage before flowing in two other pipes. One pipe is located at the bottom of the Chambre de Captage and allows thermal waters to be discharged into the Cascade Centre spring supplying the Cascade waterfall. The flow rate of this pipe can be controlled via a hatch. When this hatch is opened, the water level in the Chambre de Captage increases up to a second overflow draining thermal waters to the waterfall in the cave. Consequently, the closing of this hatch generates the decrease of the water level in the Chambre de Captage, accompanied by the increase of the flow rate of Cascade Centre and the drying of the water-

fall in the cave. During this process, the flow rate of the Shower and F1 remain stable.

All the pipes in Chambre de Captage were sampled in June 2009. Their properties are illustrated in Table 12.1. While positioning in front of the Chambre de Captage and looking at the slope, sampling names were assigned to the 6 pipes. The Drainage 1 corresponds to the pipe located at the entrance and crosses the entire Chambre de Captage. This is divided into two pipes: the first is Drainage 1 and drains thermal waters directly above the valve at the highest rate possible (300 L/min) and the second continues beyond the Chambre de Captage down to the Shower waterfall with another valve. Therefore, waters from Drainage 1 and Shower come from the same subhorizontal drainage. The second pipe named Drainage 2 has the lowest rate (7 L/min) and is located at the right and the front of the Chambre de Captage. The third pipe called Drainage 3 is at the right and the bottom. The fourth and fifth pipes named Drainage 4 and 5 discharge thermal waters at the same place at the left and the bottom. Waters from Drainage 4 and 5 are the hottest (23.3 and 23.9°C) and the most mineralized (1663 and 1675 μS/cm). Finally, the last pipe called Drainage 6 is set at the left side and the front of the Chambre de Captage.

Table 12.1: Parameters measured in the Chambre de Captage for each pipes in June 2009, and their location. Temp.: Temperature, EC: Electrical Conductivity.

Assigned name	Location	Temp. (°C)	EC (μS/cm, 25°C)	Flow rate (L/min)
Drainage 1	Entrance	21.5	1422	300
Drainage 2	Right front	22.6	1639	7
Drainage 3	Right bottom	22.1	1560	15-20
Drainage 4	Left bottom - upper	23.3	1675	60-80
Drainage 5	Left bottom - lower	23.9	1663	80-100
Drainage 6	Left front	23.0	1447	30-40
				Total 490-550
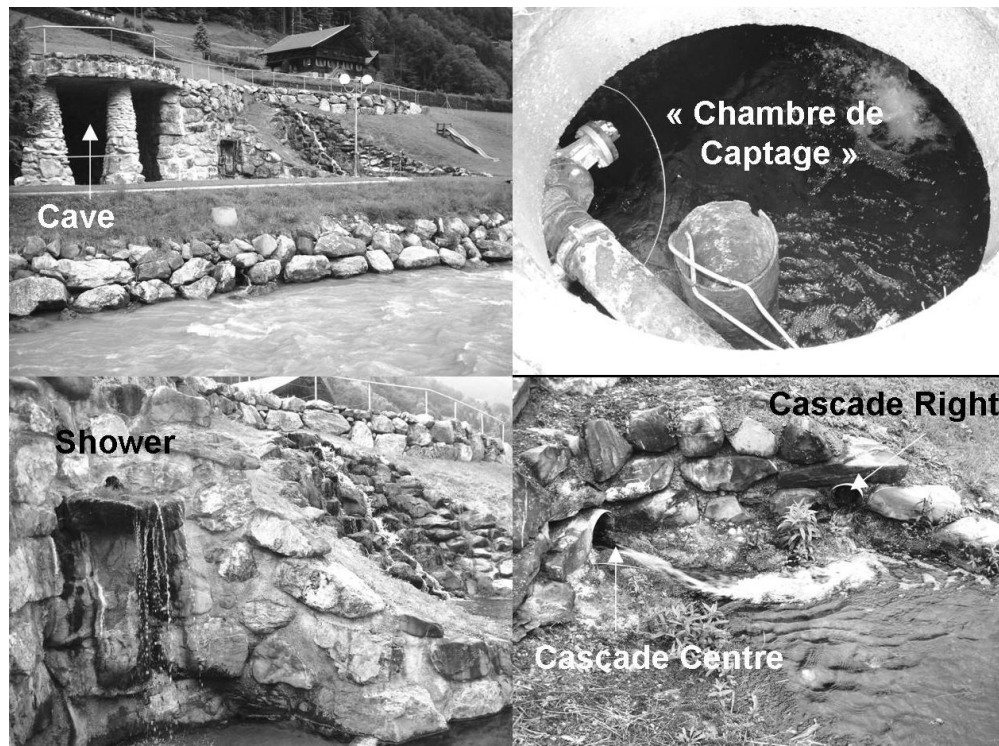
Figure 12.8: View of the sampling points around the Cascade waterfall in June 2009.

The Cascade Centre is one of the outflow point of the Chambre de Captage, and thus thermal waters of Cascade Centre are mixed. The measured rate in June 2009 before the emptying was roughly of 350 L/min because a part of thermal waters in the Chambre de Captage are also drained by the second overflow to the waterfall in the cave (of around 150 L/min). The temperature and conductivity of Cascade Centre were 22.2°C and 1510 μS/cm in June 2009. Close to the Cascade Centre, another subhorizontal drainage called Cascade Right discharges thermal waters at 22.7°C and 1789 μS/cm with a flow rate of around 60-80 L/min (Fig. 12.8). These two sampling points mix together and then are discharged to the Cascade waterfall. Before the sampling campaign in June 2009, measurements were carried out on the Cascade waters without detailed information on the sampling point. However,

this data certainly comes from the Cascade Centre spring because it seems difficult to undertake measurements of flow rates directly in the waterfall. Between July 2004 and January 2006, parameters were at about 22.8-25.7°C, 1340-1640 μS/cm and 300-400 L/min (Alpgeo 2006a and 2006b) whereas they seemed to be higher in 1996 at the time of

12.3.4 Old thermal springs

Even if the majority of the old thermal springs were not found in June 2009 due to drying caused by wells production, their data were used in this study to highlight chemical processes. Therefore, it is necessary to explain the properties of these sampling points (see location in Fig. 12.4).

Two old thermal sampling points called Captage A and Captage B received thermal waters from 6 and 4 subhorizontal drainages respectively. These two springs are located close to the F3 well and have been used to fill the swimming pool on the left bank of the river. The implementation of the F3 well in 1996 caused a long-term decrease of the production rate down to 320 L/min with a temperature and conductivity of around 30°C and 1850 μS/cm. Bianchetti (1996) mentioned that the flow rate of Captage A and Captage B should be roughly the same as before the waterproofing works in the Salanfe Lake in 1994. Between 2004 and 2006, and in June 2009, it was not possible to find and sample these two points because they were almost entirely dried out due to the F3 exploitation.

Moreover, in the area of Captage A and Captage B and close to the swimming pool, Bianchetti (1996) mentioned the presence of a thermal spring called Coin Piscine with parameters at about 100 L/min, 28.4°C and 1850 μS/cm. This spring was totally dried up after drilling in 1996. In the same area and close to both pipes draining waters from F1 well, another thermal spring was detected in June 2009 with parameters at about < 5 L/min,

drilling: 25.4-26.1°C, 1550-1660 μS/cm and 600-800 L/min (Bianchetti 1996). Before the waterproofing works at Salanfe Lake in 1994, the flow rate was roughly the same at 800 L/min, but temperature and conductivity were significantly lower, respectively 21.2-23.1°C and 850-1428 μS/cm (Bianchetti 1996).

22°C and 1907 μS/cm. This spring comes from the slope and is probably the spring named Zone de Repos in 1996 which was partially dried out after drilling. Before drilling, the Zone de Repos spring had a higher flow rate of 150 L/min with a temperature and a conductivity of 28.4°C and 1850 μS/cm respectively.

Two other thermal springs that appeared in 1994 in the area of the Cascade waterfall are dried today. The first called "Cascade Coin Supérieur" was located between the pipes of Cascade Centre and the beginning of the waterfall, 1 metre downstream. This spring had been discharging thermal water at about 60 L/min, 27.8°C and 1780 μS/cm before 1996. After drilling, all parameters decreased till the spring dried out. The second spring was called the "Cascade Coin Inférieur" and was located at the bottom on the Cascade waterfall on its left bank. This spring had been discharging thermal water at about 150 L/min, 28.2°C and 1770 μS/cm before 1996, but it was less affected by the implementation of wells. In June 2009, this spring did not flow and thus it was not possible to sample it.

Finally, three thermal springs in the southern part of the Chambre de Captage also appeared in 1994 (see location in Fig. 12.4) but they practically vanished after drilling. Their properties were similar compared to other thermal springs with a total rate of 925 L/min having temperatures and conductivities in the range of 25.1-26.7°C and 1680-1760 μS/cm respectively.

12.3.5 Subthermal and cold waters

Subthermal and cold springs were also sampled in June 2009 aiming to highlight chemical processes. Moreover, previous chemical and isotopic data on these waters from Bianchetti (1993), CRSFA (1992d), Gainon (2008), Pantet (2004) and

Vergain (1991) were gathered and used in this study. The locations of these sampling points are illustrated in Figures 12.3 and 12.4. Some of them are located in the area of the spa, such as Cold springs 1 and 2. However the majority of them are fur-

ther away but remain within a 2 kilometres radius from the spa: the subthermal spring, Cold spring 3, Play well, Fayot, Prabys, Crête, Meuraye, Essertys, Bètre springs, the Vièze River and three vertical borehole heat exchangers called Jossi VBE.

The subthermal spring is 200 metres downstream from the Cascade waterfall on the left bank of the river. In June 2009, it was not possible to find it because a backfilling had been covered the spring due to the construction of new buildings. This spring was sampled in 1990 within the framework of the GEOTHERMOVAL program (CRSFA 1992d) and the chemical analysis had shown a mixing process between a thermal component and a shallow groundwater. Vergain (1991) specifies that this spring consisted of water from a drain at shallow depth mixed with a thermal seepage at the foot of the slope. A marshy area still exists in the vicinity of the spring.

Several thermal seepages were detected in the bed of the Vièze River from the F3 area to the Fayot spring (Vergain 1991), that is to say within a distance roughly of 1 kilometre. Unfortunately, there is no measurement on these thermal seepages and it was not possible to look for them in the river due to high flow rates present during the sampling campaign in June 2009.

The Fayot spring emerges in a grove on the left bank of the Vièze River, 1 kilometre downstream from the spa. This spring was first sampled and analysed by Pantet (2004) with a temperature and a conductivity of 14.7°C and 1110 μS/cm respectively. It has the same properties as the subthermal spring previously quoted.

Other subthermal springs also exist 1 kilometre upstream from the spa at Play, and were studied for an old geothermal project that was later abandoned (Bureau Tissières 2003, 1996a and 1996b, Vuataz 2005). Five trenches were carried out in 1995 in the alluvial plain down to 4-5 metres depth but were not found in 2009. The other well reaching 20 metres depth was sampled in 2009 (Fig. 12.9). Two other subthermal springs were mentioned in the bed of the river (Bureau Tissières 2003). Collected subthermal waters in Quaternary deposits at the time

of the geothermal project showed anomalies in electrical conductivity and temperature (1345 μS/cm and 16.5°C) related to the rise of thermal fluids up to the filling.

Between Buchelieule and Play, three vertical borehole heat exchangers for a private residence (Jossi VBE) also met subthermal waters (Alpgeo 2008). These boreholes were realized in January-February 2008 and reached a cumulative length of 180 metres in a dark calcareous shale. During drilling, subthermal waters were met with electrical conductivities in the range of 700-1350 μS/cm and with temperature estimated of around 14-18°C. A sample allowed defining the chemical properties of the subthermal water which will be discussed after.

Several cold springs were sampled in the Val d'Illiez area (Fig. 12.4). Three cold spring are located in the zone of the spa. They correspond to the drainage of the slope at the left bank of the river. These waters represent the cold end-member of mixing processes. Outside the spa, the sampled other cold springs in 2009 were already studied by Pantet (2004). Their temperatures and conductivities reached 10°C and 450 μS/cm and they are influenced by seasonal climatic conditions. Finally, the Vièze River was sampled in June 2009 close to the Cascade waterfall during a high flow rate period.

Figure 12.9: View of the Play well in June 2009.

13

Geological investigations in the Val d'Illiez

13.1 Regional geological investigations

THE regional geological setting of the Val d'Illiez hydrothermal system was already described in several publications and unpublished reports. To avoid repetitions and confusions, it was decided to highlight the description from Bianchetti et al. (1992) and to complete it. The Val d'Illiez Valley is located at the limit between the Helvetic domain in the south-east and the Prealps in the north-west (Fig. 13.1). The Helvetic domain, in which the area under study is included, is formed by the following units (Lanterno 1954, Schroeder and Ducloz 1955): the crystalline basement, the autochthonous cover, the parautochthonous cover and the Morcles nappe.

The crystalline basement of the Aiguilles Rouges Massif consists of a Hercynian unit mainly composed of paragneiss, biotite or chlorite hornfels and orthogneiss (Von Raumer and Bussy 2004). In Switzerland, these rocks outcrop from the Salanfe and Emosson areas to the Martigny sedimentary zone (Fig. 13.1), and disappear towards the north-west with a dip of 20 to 30° before forming a complex anticline with a basal thrust fault system.

The autochthonous cover is the sedimentary cover of the crystalline basement, of Triassic to Cretaceous-Tertiary age. The autochthonous cover is distinguished by an unconformity on the Hercynian basement and thrusted by the Mocles nappe

and by the parautochthonous. The Triassic layers are an important unit in this context, because of their petrology (coarse sandstone, quartzite, argilite, dolomitic limestone and gypsiferous cellular dolomite), as well as of their hydrogeologic characteristics. Gypsum dissolution indeed creates preferential pathways for surface water infiltration and deep groundwater circulation. The other layers consist of limestone and marly limestone for the Jurassic, and of limestone, sandstone and marly shale for the Cretaceous series. The history, stratigraphy and structure of this geological unit are detailed in the next section.

The parautochthonous cover, where several sedimentary thrust slices occur, is composed of formations ranging from the Triassic to the Tertiary, with a petrology similar to that of the autochthonous. The most present formation is represented by the lower Oligocene flysch outcrop, forming the slopes of the Vièze Valley.

The Morcles nappe corresponds to a geological unit tectonically thrusted over the parautochthonous. The formations are not quite different from those described for the autochthonous. The Morcles nappe represents the lowest unit of the Helvetic and consists of a great recumbent fold of Jurassic - Cretaceous limestones and marls (Badoux

1971). This unit forms the summits of the Dents du Midi and Dents de Morcles Massifs. Locally, tectonic slices are intercalated below the Morcles nappe and correspond to the outliers of the cover of the Aiguilles Rouges Massif swept along by the crossing of the Morcles nappe (Gagnebin 1934). The base of the Morcles nappe is pinched between the Aiguilles Rouges and Mont Blanc Massifs and forms the Chamonix-Martigny complex syncline.

LEGEND OF GEOLOGICAL MAP OF LAVEY-LES-BAINS AREA

Quaternary

- Not differentiated quaternary deposits

Subalpine molasse

- *Lower Freshwater Molasse*: Sandstone and conglomerate (red molasse, Mont Pelerin pudding stone, coal molasse): Chattien.
- *Lower Marine Molasse*: Marl and sandstone (Vaulruz sandstone): Lower Oligocene.

Aiguilles Rouges massif

- Marl and sandstone (parautochthonous Flysch): Lower Oligocene.
- Marl and sandstone (autochthonous Flysch): Lower Oligocene.
- Quartzite, dolomite, limestone and marl: Trias - Eocene.
- Conglomerate (Vallorcine pudding stone), sandstone, pelite and rhyolite: Carboniferous - Permian.
- Vallorcine granite: Upper Carboniferous (307 ± 2 Ma, Bussy and Hernandez 1997).
- Gneiss and migmatite: Proterozoic - Paleozoic.

Morcles nappe

- Limestone, marl and sandstone (including flysch): Cretaceous - Lower Oligocene.
- Limestone and marl: Dogger - Malm.

Chamonix zone *(root of reversed limb of the Morcles nappe)*

- Limestone, dolomite, marl and sandstone: Trias - Eocene.

Mont Blanc external crystalline massif

- Montenvers granitic gneiss: Carboniferous (307 ± 3 Ma, Bussy and Von Raumer 1993).
- Gneiss: Proterozoic - Paleozoic, lenticular banded gneiss (453 ± 3 Ma, Bussy and Von Raumer 1993).

Mont Blanc internal crystalline massif

- Leucogranite: Carboniferous - Permian.
- Mont Blanc granite: Upper Carboniferous (304 ± 3 Ma, Bussy and Von Raumer 1993).
- Rhyolite: Upper Carboniferous (307 ± 2 Ma, Bussy and Von Raumer 1993).
- Gneiss: Proterozoic - Paleozoic.

Ultrahelvetic nappes

- Sandstone: Eocene (Dent de Valère Flysch).
- Limestone and marl: Malm - Cretaceous (Anzeinde nappe).
- Wildflysch: Oligocene (Plaine Morte nappe).

Penninic nappe

- *Submedian zone*: Dolomite, evaporite, limestone, marl and sandstone (including flysch): Trias - Eocene.

Figure 13.1: Geological map and cross section of the Val d'Illiez regional area according to the tectonic map of the Western Switzerland Alps (modified after Steck et al. 2001).

13.2 Geological setting of the autochthonous cover of the Aiguilles Rouges basement

13.2.1 Abstract of the geological history

The autochthonous cover of the Aiguilles Rouges basement started to be formed during the middle-upper Trias in a low depth basin with erosion of the basement. This period generated the cross-bedding arkose with basement fragments named the Vieux-Emosson formations. Later, during the Mesozoic and the lower Cenozoic, the deposits follow one another under varied conditions of sedimentation leading to the formation of marl, limestone, dolomite, sandstone, quartzite, breccias, evaporite, etc. According to Steck et al. (2001), this sedimentary cover has a low thickness in the exposing part along the limit with the basement. Some great stratigraphic gaps occur that are due to erosion and the absence of sedimentation, especially during the upper Lias - lower Dogger period and Tertiary emergences. Locally, Trümpy (1980) showed the preservation from erosion of the lower-middle Lias (Arbignon sandstone and limestone). In return, formations of Morcles nappe are thicker, in particular the Lias - Dogger series which is continuous.

Tectonically, the autochthonous cover was mainly affected by the Alpine orogen during the Chattian (upper Ologocene). Alpine overfolds of north-east direction in the autochthonous also occur as well as in the parautochthonous and in the Morcles nappe. Bianchetti et al. (1992) and Gagnebin (1934) specified that these folds consist of a succession of anticlines, probably wide, implying that the limbs have low dips. Later, Pantet (2004) assumed that in the Vièze Valley the autochthonous cover ends in a great anticline with a basal thrust fault system plunging towards the south-east, which would be related deeply to the thrust fault system of the external crystalline massifs.

13.2.2 Structure of the autochthonous cover

Stratigraphy

The autochthonous cover is unconformable on the deformed Hercynian basement, essentially composed of paragneiss, orthogneiss and intruded granite with younger detrital deposist forming a Permo-Carboniferous syncline. The first layer consists of a cross-bedding arkose with basement fragments named the Vieux-Emosson formations, of middle-upper Triassic age, which were deposited in a shallow basin (Fig. 13.2). This marks the beginning of the Mesozoic trangression. The discovery of reptile footprints allows the age of this arkose, upper Ladinian or Carnian (Demathieu and Weidmann 1982 in Pantet 2004) to be identified. While going up in the stratigraphy, the Vieux-Emosson formations gradually change into argillic layers (Epard 1990) with a thickness in the range of 0-20 metres. This argillite can have different colours (red, yellow or green) and for this reason, the name "multicoloured argillite" was assigned to it.

The dolomite and cellular dolomite of upper Triassic age overlie the argillite and have a thickness varying from 10 to 100 metres. In this formation, a large amount of groundwaters occur and for this reason, this formation is considered as an aquifer. Significant water losses from the Salanfe Lake were reported from its north to north-east shoreline (about 1 m^3/s for a lake elevation of 1910 m.a.s.l.), and begin as soon as the lake level reaches 1890-1895 m.a.s.l. (Schneider 1982 in Bianchetti et al. 1992). Several sink holes beneath the moraine indicate the presence of dissolution processes in the underlying Triassic cellular dolomite. These sink holes form preferential infiltration zones for the runoff water and for the lake water. The presence of gypsum and anhydrite in the Triassic rocks was not proven studying exposures, but this presence is assumed according to the chemistry of groundwaters. This question will be discussed in the following part.

The top of the Trias is marked by the existence of several metric beds of gray dolo-calcarenite intercalated in dolomite, and finally by the presence of dark pelite and quartzitic sandstone. This layer indicates the beginning of the marine regression which was continued during the Lias. The return to marine conditions corresponds to the Lower Bajocian with the deposit of marly schist and dark limestone.

Stampian, *Red molasse, calcareous schist with coarse limestone, quartzitic sandstone, microconglomerate and limestone with cypris*

Upper Rupelian, *Quartzitic and feldspathic sandstone with radiolarite*

Middle Rupelian, *Marly and micaceous schist*

Lower Rupelian, *Dark schist with globigerine*

Priabonian, *Brecchia with coarse fragments and nummulitic limestone*

Upper Barremian - Lower Aptian (Urgonian), *Reef and massive limestone with oolite, lamellibranchiata and benthonic foraminifera, 100 m*

Lower Barremian, *Bioclastic and spathic limestone with echinoderm and entrochal, 40 - 80 m*

Hauterivian, *Bioclastic, siliceous and brown limestone with echinoderm, rich in glauconite in the upper part, around 100 m*

Valanginian, *Entrochal and brown limestone*

Upper Berriasian, *Bioclastic limestone with organism and thick beds, around 200 m*

Lower Berriasian, *Marly and dark schist with compact beds of limestone containing organism fragments, 50 - 250 m*

Malm, *Massive limestone with dark fractures, > 100 m*

Argovian, *Platy and yellow limestone with dark schistous beds*

Oxfordian, *Sericitic schist with limestone beds rich in ferruginous and dolomitic nodules*

Callovian, *Oolithic and ferruginous limestone*

Bathonian, *Schist with limestone beds*

Upper Bajocian, *Bioclastic and gritty calcarenite with flint nodules in the upper part*

Lower Bajocian, *Marly schist with dark limestone*

Lias, *White quartzite without carbonated cement*

Upper Trias, *Dark pelite and quartzitic sandstone*

Upper Trias
Dolomite and cellular dolomite, 10-100 m

Upper Trias, Vieux Emosson formations
Multicoloured argillite, 0-20 m

Upper - Middle Trias, Vieux Emosson formations
Cross-bedding arkose with basement fragments

Hercynian basement of the Aiguilles Rouges Massif
Paragneiss - Orthogneiss essentially

Figure 13.2: Stratigraphical log of formations forming the autochthonous cover of the Aiguilles Rouges basement (elaborated from Gagnebin 1934, Pantet 2004 and Vergain 1991). The thickness of lithologies is often unknown and can strongly vary.

From the Dogger to the upper part of the lower Cretaceous (Aptian), the stratigraphic series is more or less continuous without major gaps. Deposits alternate between schist and bioclastic limestone and have a total thickness exceeding 500 metres. Two main formations can be considered as the aquifer because they are thicker: the massive Malm limestone (> 100 m) and the bioclastic limestone of lower Cretaceous (> 300 m). These limestones can be affected by karstification processes as shown at Saint-Maurice in the Cretaceous limestone (caves, see location of Saint-Maurice in Figure 13.1).

A great marine regression occurs between the upper Cretaceous and the middle Eocene on a local scale with the erosion of the autochthonous cover. The sedimentation begins again during the upper Eocene up to the upper Oligocene. During this period, the nummulitic limestone was deposited (Priabonian) followed by the dark schist with globigerine (lower Rupelian), the marly and micaceous schist (middle Rupelian), the quartzitic and feldspathic sandstone with radiolarite (upper Rupelian) and red molasse (Stampian). Some of these rocks have been subjected to groundwaters flows. Finally, the Quaternary formations composed of moraine and alluvial deposits locally overlap in discordance the folded autochthonous cover. In the area of Val d'Illiez, it will be demonstrated that groundwaters in Quaternary formations are mixed with the uprising thermal fluid.

Cross section and Champéry window

Initially, the geological cross sections of Alpgeo (2007), Bianchetti et al. (1992), CRSFA (1992d), Ducloz (1944), Gagnebin (1934) and Lanterno (1954) assumed a succession of several wide anticlines to define the structure of the autochthonous cover. According to recent geological investigation in the area of the Dents du Midi, Pantet (2004) refined the previous cross sections and assumed a great recumbent anticline with an axial plane plunging towards the south-east (Fig. 13.3). Moreover, a plunge of axis towards the north-east occurs involving the disappearance of the Champéry window in the zone of Val d'Illiez (Lanterno 1954). This great fold would be limited by a basal thrust fault which is related to the thrust system between the Aiguilles Rouges and Infa-Aiguilles Rouges basements. The assumption of Pantet is quite probable assuming a conceptual deep flow system of the thermal water at the bottom of the autochthonous cover (Bianchetti et al. 1992). The study of the Champéry window could improve the knowledge of the geological structure of this anticline. A geological investigation of the Champéry window is also important for the elaboration of two-dimensional numerical model.

The Champéry window is the area where the autochthonous cover outcrops due to the erosion of the parautochthonous flysch above (Fig. 13.4). The rocks forming the window were initially described by Gagnebin (1934), and detailed later by Lanterno (1954) who made a local geological map. The rocks met at Champéry consist of massive, bioclastic and siliceous limestones of Cretaceous age and form impressive cliffs in the landscape, especially on the south-eastern side of the valley.

To get an idea which of these two assumptions is correct, it was decided to carry out a series of measurements on the dips of the bedding planes in the area of Champéry (Fig. 13.4). This geological investigation was carried out in 2009 with a structural geologist from the University of Neuchâtel and is presented in Figure 13.4. On the south-eastern side of the valley, the dips of the bedding planes are clearly visible and the layers slightly plunge towards the south-east. On the other side of the valley, near Champéry, these dips are difficult to visualize. The main impression is that the layers hang low to the north-west (about 10-15°) up to 35° in contact with the parautochthonous flysch overlapping. In some areas, it seems that the dip becomes vertical, but it could be fracturing planes. Indeed, this area is characterized by intense fracturing composed of two families: 1) a family with a vertical dip perpendicular to the valley, 2) a family with a strong dip to the south-east and parallel to the valley. This observation leads to the assumption of the presence of a complex fault system occurring in this area. Although this study does not clearly indicate the geometry of the anticline as assumed by Pantet (2004), it may nevertheless be assumed that the structure of the anticline proposed by Pantet is adequate in a regional scale due to its relation with the basement (F Negro pers. comm. 2009).
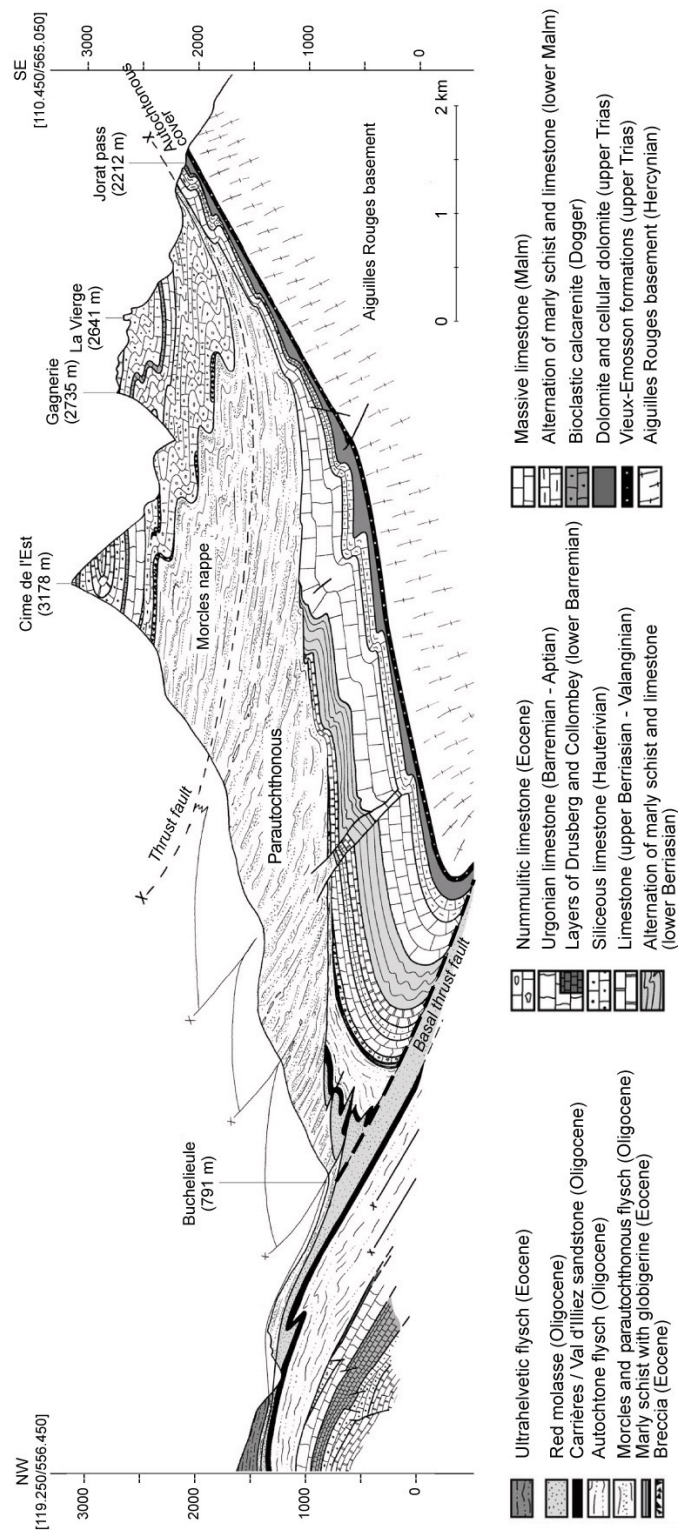
Figure 13.3: Geological cross section of the autochthonous cover in the area of the Dents du Midi (modified from Pantet 2004). The cross section line is shown in Figure 14.8.
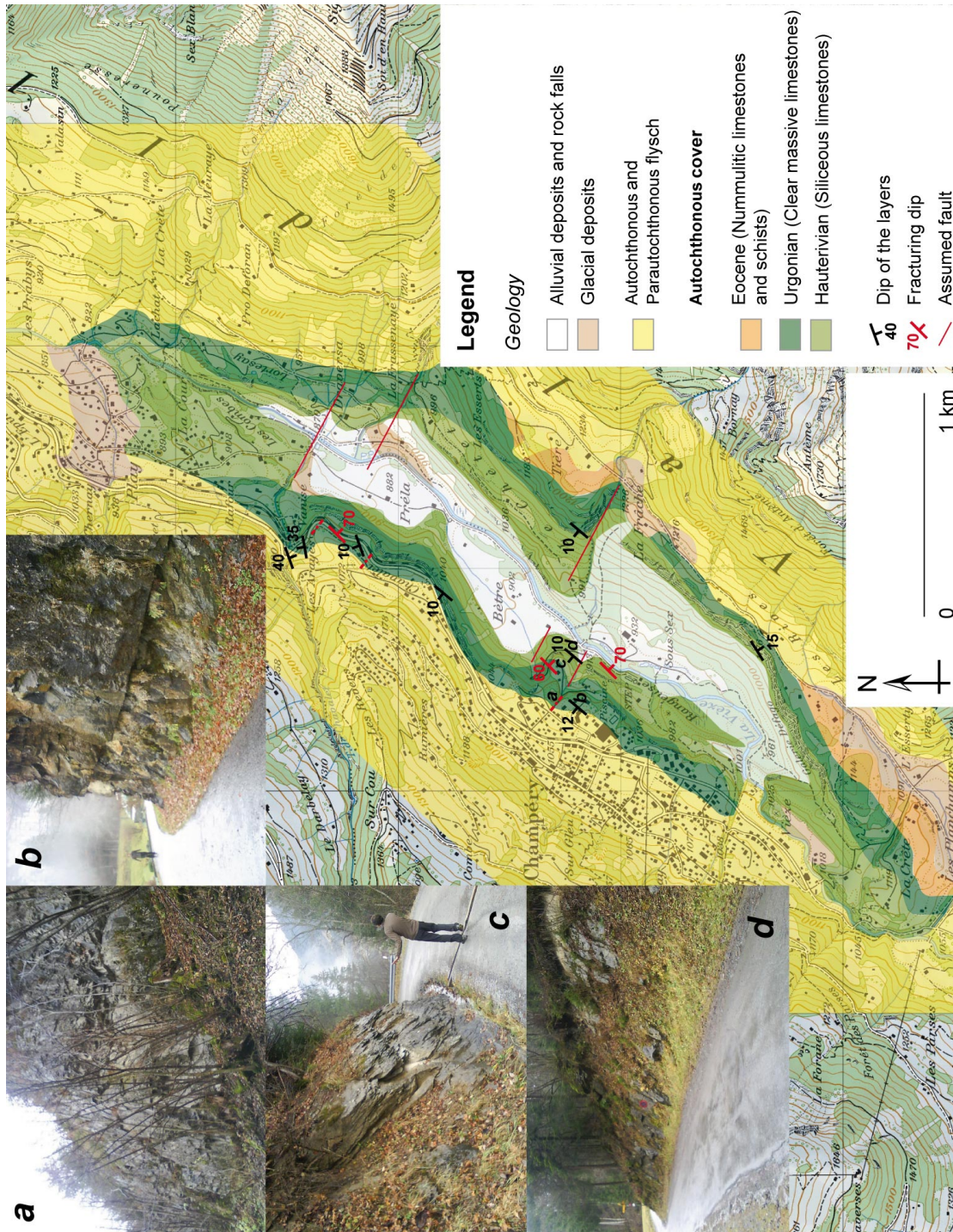
Figure 13.4: Geological map of the Champéry window belonging to the autochthonous cover of the Aiguilles Rouges Massif according to Gagnebin (1934) and Lanterno (1954), and structural study of the outcropping limestones. Pictures a) and d) show a low dip of the layers with a vertical fracturing dip. Pictures b) and c) respectively highlight the dip of the layers and the fracturing dip.

13.2.3 Regional fracturing

The regional fracturing in a sector from the Val d'Illiez to Salanfe lake was detailed by Pantet (2004). This study was carried out for various geological domains including the basement, the autochthonous cover, the parautochthonous and the Morcles nappe. Firstly, Pantet gathered information in the literature (from Amberger 1960, Badoux 1996, Collet et al. 1952, Flamm 1993, Vergain 1991), and then he completed the data with the observation of aerial views in zones where views were available, and with measurements at Salanfe Lake. Pantet reported on a chart the regional directions of faults and fractures (Fig. 13.5). The different families of fractures are:

- **N-S**. This symbolizes large faults in the basement and fractured zones in the sedimentary cover, and was already mentioned by Jamier (1975). According to the diagram of Pantet, this family is not the most represented, but would have a high hydraulic conductivity.

- **NNE-SSW to NE-SW**. This direction is well visible in the Aiguilles Rouges basement, and NE-SW fractures seem to affect the sedimentary cover. It corresponds to Hercynian and Alpine directions draining groundwaters deeply into the basement.

- **E-W**. This direction of fracture seems to affect mainly the sedimentary cover. This is quite visible in the northern part of the cover.

- **ESE-WNW to SE-NW**. This family is widely represented in the whole of the studied area including all geological domains. This

seems to drain groundwaters into the sedimentary cover because several cold springs emerge along this direction of fracture. Moreover, karstified networks are developed along this direction in the Cretaceous limestone at Saint-Maurice.

Finally, Bianchetti et al. (1992) also studied the regional fracturing aiming to define flow paths in the autochthonous cover. From aerial views in the Val d'Illiez region, the presence of a NNW-SSE fracture pattern was shown. Moreover, a secondary hydrological network of the valley is oriented in the same direction. They concluded that regional tectonic structures supply flow systems through the Triassic formations.
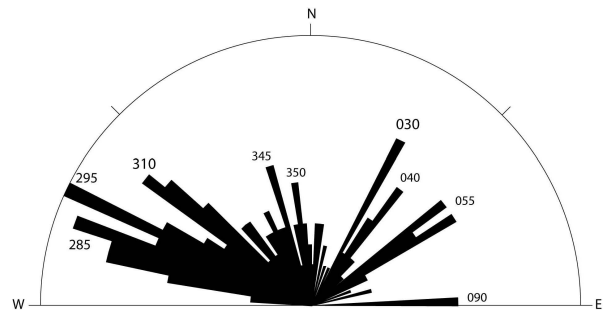
Figure 13.5: Diagram showing regional directions of fracturing (Pantet 2004). The length of bars is proportional to the number of listed faults in a given direction. The longest bar represents 4% of the total of measurements.

13.3 Local geological setting

13.3.1 Geological setting in the Val d'Illiez

The geological setting 1 kilometre around the spa is shown in Figure 13.6 according to the first complete geological investigation of the Val d'Illiez area (Schroeder and Ducloz 1955). The parautochthonous flysch with sandstone layers, outcropping in the old quarry of Val d'Illiez, overlaps the Tertiary autochthonous cover with an angular discordance. In the studied zone, the au-

tochthonous cover is folded and consists of marly and micaceous schist, the Carrières sandstone and the red molasse. Thrust faults are present in these formations as assumed in the Fayot Valley and below the flysch at Léchau. In detail, Schroeder and Ducloz specified that these thrust faults are in reality faulted anticlines with axial planes plunging towards the south-east. This assumption is in agree-

ment with the regional cross section from Pantet (2004).

Quaternary formations overlie the Tertiary bedrock and consist of moraine and alluvial deposits. Lateral mountain streams of ESE-WNW direction follow fractures and form alluvial fans along the Vièze valley. Sometimes, the moraine directly overlies the recent alluvial deposits as in Buchelieule where boreholes crossed the Vièze deposits below the moraine.

The thermal springs at Buchelieule emerge on the left bank of the Vièze Valley from seepages in the moraine. The elevation of these seepages reaches 10 metres from the level of the river. Below the moraine, a layer of recent alluvial deposits of 2 metres thick was crossed by the F1 and F2 boreholes. The bedrock composed of sandstones and arigilites, with a strong dip and with locally crushed zones (Geotechnisches Institut 1980 in Bianchetti et al. 1992), was drilled by the deep wells and by the subhorizontal drainages. According to Vergain (1991), the crossed sandstones would correspond to the called Carrières sandstone (upper Rupelian) which should not be confused with the sandstone of the Val d'Illiez quarry (parautochthonous flysch). At Buchelieule, the Carrières sandstone should be present on the left bank of the valley as illustrated in the cross section in Figure 13.6, and should allow

the rise of thermal waters. Indeed, it can be assumed that the hydraulic conductivity of the Carrières sandstone is higher than the marly and micaceous schist and than the red molasse.

Finally, according to the study of Schroeder and Ducloz (1955), the thermal zone at Buchelieule is located along the thrust fault of the parautochthonous flysch overlapping the Tertiary autochthonous cover (Fig. 13.6). In more detail, the thermal zone in the valley corresponds to the lowest elevation point of the thrust fault (790 m.a.s.l.). The parautochthonous flysch acted as a waterproof roof which prevented the rise of thermal waters up to the surface and focused the rise of thermal waters on the lowest elevation point of the thrust fault. This could be the reason why Vergain had never been able to highlight thermal seepages upstream from the spa. However, the parautochthonous flysch is also subjected to fracturing due to the Alpine tectonic events and thus, subthermal seepages occurs locally inside the flysch. The Jossi vertical borehole heat exchangers are an example of this process. Concerning the Play well, it seems that the flysch was crossed below the Quaternary deposits (Bureau Tissières 1996a), but this had never been proven. It could be Urgonian limestone which outcrops in the river bed just few metres upstream from the well (Fig. 13.7, Bureau Tissières 1996b).

13.3.2   Local fracturing

Due to the absence of outcrops belonging to the autochthonous cover in the thermal area, the local fracturing of rocks cannot be investigated. Indeed, Quaternary formations mask the bedrock everywhere in the thermal zone. Exposures of autochthonous cover are present downstream from the spa, but they were not selected. In the Play area close to the well, at the northern extremity of the Champéry window, the Urgonian limestone outcropping in the bed of the river was selected to investigate the fracturing (Fig. 13.7). Precisely, this exposure of Urgonian limestone had been studied previously during the geothermal project at Play (Bureau Tissières 1996b).

Measurements were carried out on four outcrops of limestone in the bed of the river and another one further on the parautochthonous flysch (Fig 13.7). The average stratification plane of the limestone is subhorizontal whereas for the flysch it has a dip around 30° towards the south. Concerning fractures, they have various directions with dips in the range 50-90°. Several families were highlighted in the limestone but only one for the flysch (070/65). The three most important families are 205/79, 159/76 and 120/66. These families coincide with those observed by Pantet inon a regional scale in particular for the sedimentary formations.
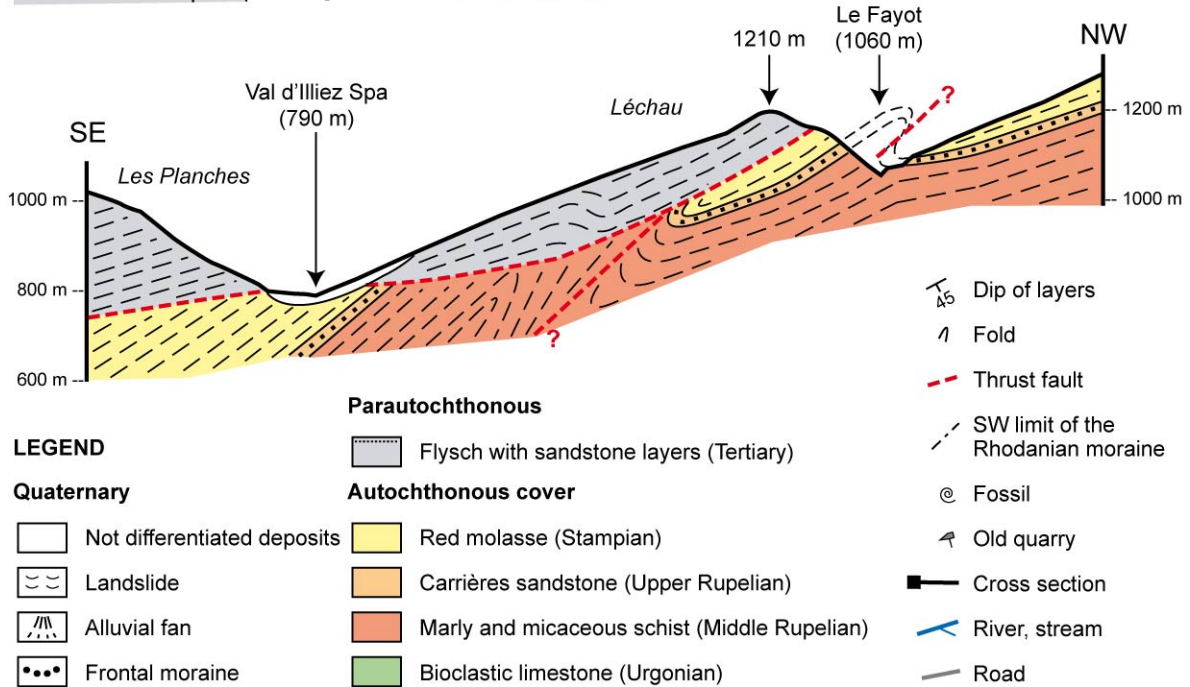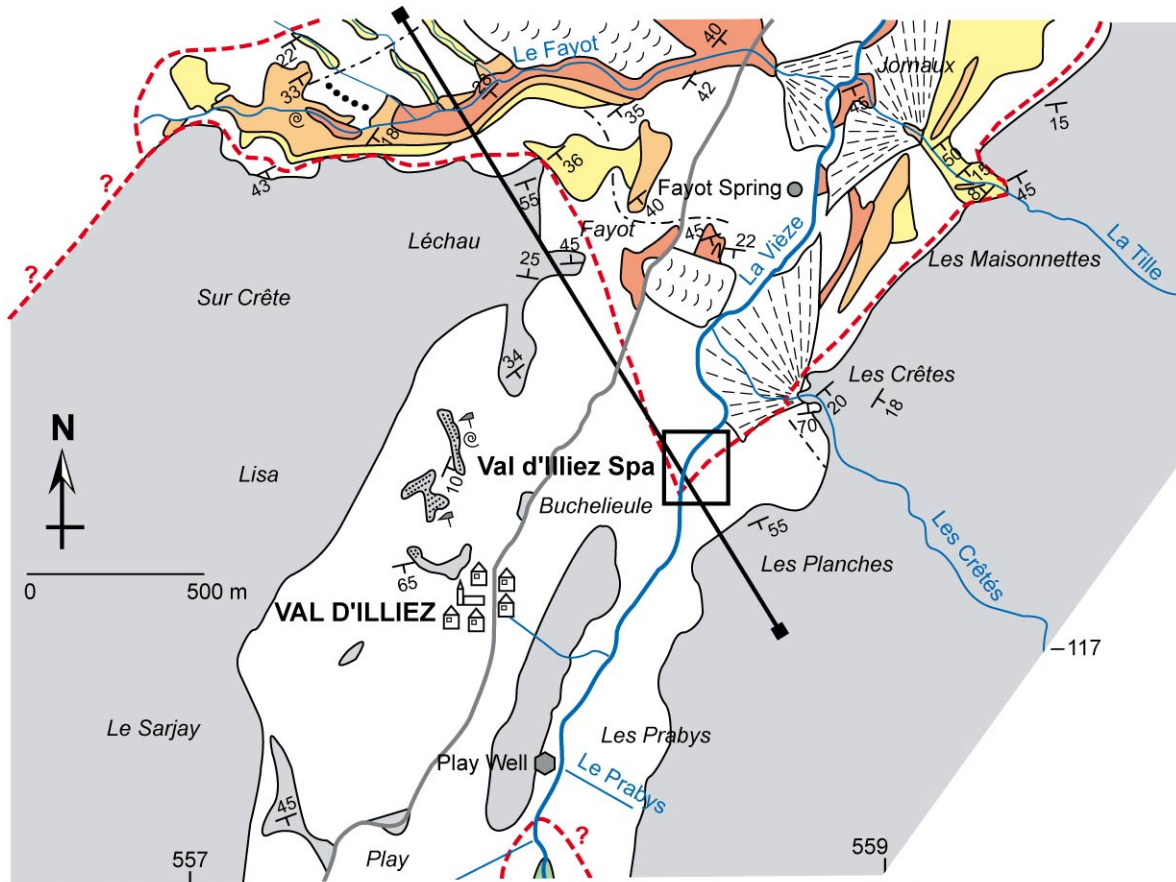
Figure 13.6: Local geological setting of the Val d'Illiez area (modified from Schroeder and Ducloz 1955).
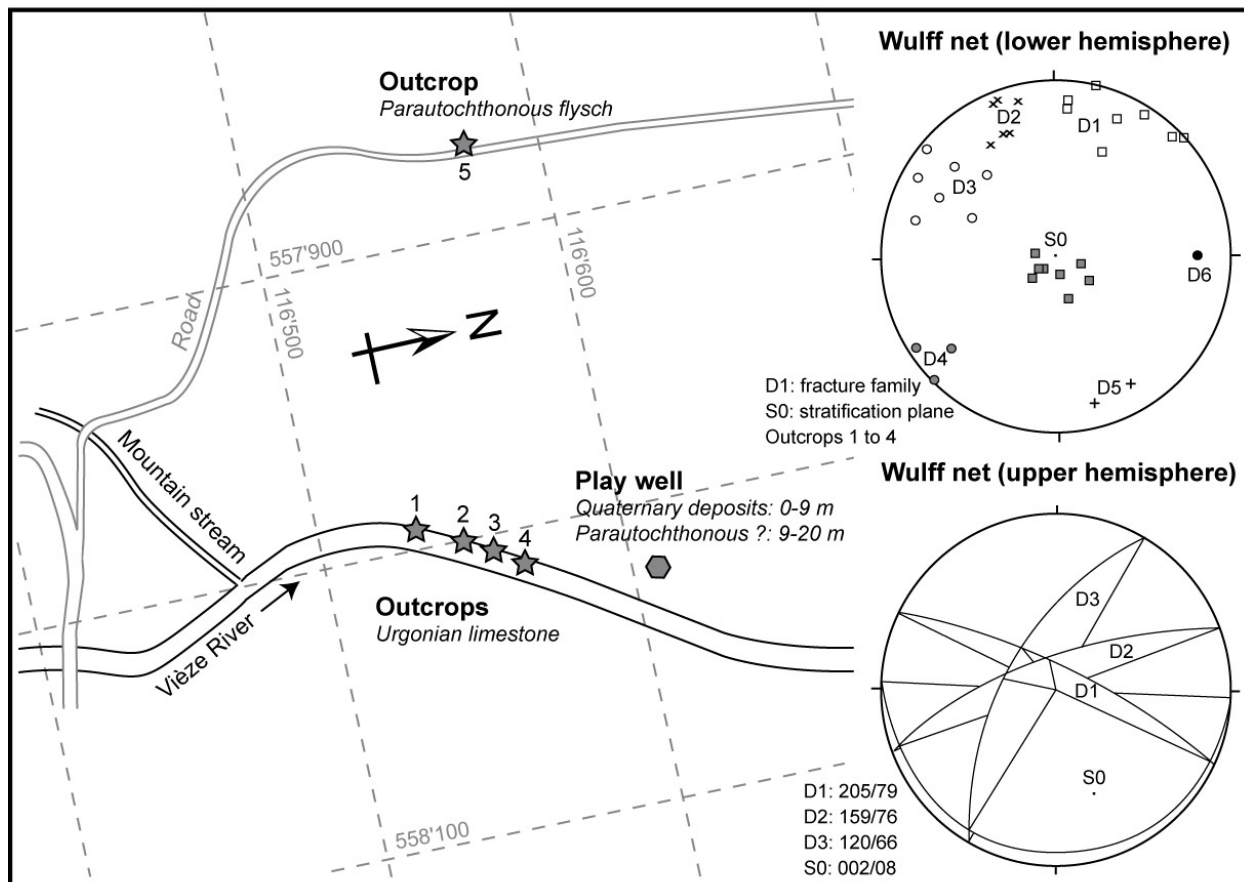
Figure 13.7: Location of exposures at Play used to define the main families of fractures in the Urgonian limestone (modified from Bureau Tissières 1996b). Two directions of fractures were identified in the outcrop number 5 (parautochthonous flysch): the schistosity (360/33) and transverse joints (070/65).

14

Hydrogeological and geochemical investigations in the Val d'Illiez

14.1 Local hydrogeological and geochemical investigations

14.1.1 Hydrogeological knowledge before this study

THE hydrothermal system of Val d'Illiez has been repeatedly investigated since the 1990's (Table 14.1). These studies are mainly unpublished notes and technical reports, but two of them are published papers highlighting the hydraulic connectivity between the Salanfe Lake and the thermal springs (Bianchetti et al. 1992, Sesiano 2003). Several unpublished notes and reports, selected for geothermal investigations, also refer to the geological and hydrogeological properties of the Play and Champéry areas upstream from the spa.

The first hydrogeological approach was carried out by Mariétan (1953) who described the thermal events in the Val d'Illiez in October 1953 related to seismic activities after the filling of the Salanfe Lake with water, which were felt by inhabitants of the Vièze Valley. At that time, two major springs, several small springs and some seepages were detected in the field area in Buchelieule changing it into marshes with a smell of hydrogen sulphide. The first temperature measurements in both major springs were 28 and 27°C. It is also important to specify that before these events a thermal spring

around 18°C had occurred in a marshy area downstream from the new springs, and consequently it can be assumed that the water coming from Salanfe did not directly generate a new deep flow system, but rather added a hydraulic pressure to an existing thermal upflow. This will be discussed further on. A first brief chemical analysis in thermal water showed a total dissolved solids of 2746 mg/L mainly controlled by the calcium and sulphate compounds. Mariétan (1953) suggested a layer of Triassic origin with gypsum dissolution, and he concluded that the gypsum dissolution had been generated large cavities which were then crumbled, causing the seismic events felt.

Later for a Master-thesis diploma, Vergain (1991) carried out the first detailed study of the hydrothermal system with measurements and chemical analyses on several springs including the exploited thermal waters. He also described the presence of thermal seepages along the river in its bed downstream from the spa. According to Vergain, shallower groundwaters close to Buchelieule have electrical conductivities lower than 450 μS/cm with

sulphate, calcium and sodium contents of around 20-68, 67-83 and 1.7-5.6 mg/L respectively. The three exploited thermal springs, the cascade water, one subthermal spring and the Vièze River were sampled several times in 1990 and analysed with respect to the major elements, trace elements and water isotopes. Results are detailed in Bianchetti (1993b), Bianchetti et al. (1992) and CRSFA (1992d). The technical report of CRSFA (1992d) within the GEOTHERMOVAL program really represents the first complete description of the hydrothermal system in a geological, geochemical and geothermal perspective. At that time, the thermal springs reached 30°C, with a total mineralization of 1850 mg/L and a total flow rate of around 1200 L/min. The geochemical type defined as Ca>Mg-SO$_4$ is related to gypsum dissolution in Triassic cellular dolomite with low concentrations with respect to alkaline elements and chloride. Moreover, mixing processes with cold shallower groundwaters were suggested to explain the observed changes in time of the physico-chemical parameters. In detail, it was assumed that the cold component would partially come from a karstified aquifer in the Malm limestone belonging to the upper part of the autochthonous cover.

Table 14.1: Historical studies and their objective about the hydrogeology and hyrochemistry of thermal waters in the Val d'Illiez, Play and Champéry areas.

Reference	General overview of the reference
Mariétan 1953	Thermal and seismic events related to the filling of the Salanfe Lake
Schroeder and Ducloz 1955	First chemical analyses on thermal waters in the Val d'Illiez
Vergain 1991	Hydrogeological study of Val d'Illiez water, Master-thesis diploma, CHYN
CRSFA 1992d	GEOTHERMOVAL program, hydrogeological study
Bianchetti et al. 1992	Published paper about induced seismicity and thermal springs
Bianchetti 1993b	Unpublished report about deep circulations in the Alps
Bianchetti 1996	Thermal events related to the waterproofing works at Safanfe Lake in 1994, and implementation of the F1, F2 and F3 boreholes
Bureau Tissières 1996a	Hydrogeological study of water from the Play well
Bureau Tissières 1996b	Fracturing study on Cretaceous limestones around the Play well
CRSFA 1996	Study of the Léchère spring (Champéry)
Alpgeo 1997	Hydrogeological and geochemical valuation of the exploited water (Thermes-Park project)
CREALP 1998	Analyse of seismical and hydrogeological events beween 1994-1996
Alpgeo 2001	Chemical analysis of the F3 water
Sesiano 2003	Published paper about tracer tests from the Salanfe lake
Bureau Tissières 2003	Valuation related to the implementation of the Play well
Pantet 2004	Geological study around Salanfe Lake and hydrogeological study of cold and thermal waters around Val d'Illiez, Master-thesis diploma, University of Lausanne (Switzerland)
Vuataz 2005	Authorization request for the exploitation of the Play well
Alpgeo 2006a	Protection zone of the F3 borehole, hydrogeological report
Alpgeo 2006b	Borehole F3: draft to obtain the certificate "natural mineral waters"
Alpgeo 2007	Preliminary geological assessment for the realization of the Champéry geothermal borehole
Alpgeo 2008	Implementation of vertical borehole heat exchangers between Play and Val d'Illiez
Gainon 2008	Study of the radio-isotopes in thermal waters from Switzerland including Val d'Illiez, PhD thesis, CHYN

Interpretation of data acquired in the early 1990's shows a hydrogeological relation between Salanfe Lake and the thermal springs. Moreover, the presence of water losses from Salanfe Lake reaching 1 m^3/h into Triassic karstified rocks was reported when the water table of the lake reached the elevation of 1910 metres. Several sink holes beneath the moraine indicate dissolution processes in particular in the cellular dolomite. In addition to this, the geological setting of the Triassic layers with a regional dip to the south-west would promote a flow path of water losses towards Buchelieule. Consequently, the inferred recharge zone of the Val d'Illiez thermal springs was assumed in the Salanfe area from Triassic outcrops bordering the Aiguilles Rouges crystalline massif. The reservoir temperature would be around 35°C according to investigations using geothermometers i.e. at about 1 kilometre depth.

The situation in 1990 concerning the physicochemical properties of thermal springs is given in Table 14.2. These springs were differentiated into two groups: the first group including the warmest and most mineralized waters (Captage A, Captage B and Zone de Repos spring) located in the southern part of the hydrothermal area, and the second group with colder and more diluted springs (Cascade and Subthermal spring) located in the northern part (Bianchetti et al. 1992). Since the first chemical analysis carried out in 1953 (Schroeder and Ducloz 1955), a decrease of the total mineralization as well as of the calcium and sulphate contents had been occurred in Captage A and Captage B (Table 14.3). This process could be explained by an increase of the velocity of the thermal regime, induced by major changes in hydrogeological conditions (Bianchetti et al. 1992).

Compared to Lavey-les-Bains and Saint-Gervais-les-Bains hydrothermal systems, where the thermal end-member comes from the crystalline basement and shows tritium concentrations close to zero, the thermal water in the Val d'Illiez has tritium values close to 40 T.U. measured in 1990 which are larger than the surface water at the same period (20 T.U.). This would indicate that the thermal end-member in the Val d'Illiez probably has a relatively short residence time, typical of a flow system in a Triassic Alpine domain where the hydraulic conductivities are higher than those of the basement. This assumption will be discussed further on interpreting the new tritium data measured in 2009.

Table 14.2: Main physical characteristics of the thermal waters in the Val d'Illiez. The two values represent respectively the minimum and maximum observed in 1990 (Bianchetti et al. 1992). A+B: Captage A and Captage B, ZR: Zone de Repos spring, C: Cascade, ST: Subthermal spring, TDS: total dissolved solids.

Spring	A+B	ZR	C	ST
Temperature (°C)	29.3-29.6	27.3-28.5	22.6-23.1	14.0-22.5
Elec. conductivity (μS/cm, 20°C)	1650-1740	1650-1730	1190-1430	1090-1370
pH	6.7-7.2	7.1-7.4	6.8-7.4	6.7-7.9
TDS (mg/L)	1850-1870	1850-1870	1270-1400	1100-1390
Flow rate (L/min)	400-450	$\approx$ 5-10	$\approx$ 700-750	$\approx$ 10-20

Table 14.3: Time evolution of the mineralization of the main springs A and B in the Val d'Illiez (Bianchetti et al. 1992). 1: dry residue, 2: total dissolved solids.

Year	1953	1963	1980	1990
Sulphate (mg/L)	1642	1387	1270	1240
Calcium (mg/L)	708	414	405	375
Mineralization (mg/L)	2456(1)	2012(2)	1955(1)	1872(2)

To remediate problems of water losses occurring at Salanfe Lake when the water table reaches 1910 metres of elevation, a grout curtain was injected along a drilled gallery. Works were carried out between 1992 and June 1994, and after these works the water level of the lake could reach an elevation of 1923.6 metres in October 1994, that is to say 10 metres higher than the highest elevation measured before (CREALP 1998). At that time flow rates of discharged thermal waters in the Val d'Illiez increased, the appearance of new thermal spring were reported, and new microseismic events were felt (Bianchetti et al. 1992).

Two deep wells in the Cascade area (F1 and F2) and one deep well close to Captage A and Captage B (F3) were drilled in the Val d'Illiez in 1996. Objectives were to drain some new springs that appeared in 1994 close to the Cascade area, and to exploit at depth thermal waters discharging to Captage A and Captage B with higher temperature in the range of 33-35°C (Bianchetti 1996). Objectives were partially reached because temperatures of thermal waters in F3 did not exceed 30.2°C, but the artesian flow rate had almost tripled (2000 L/min against 600 L/min). For each sampling point, temperatures, electrical conductivities and flow rates were measured before and after drilling works in 1996 with the objective to visualize effects caused by the implementation of wells (Table 14.4). According to Bianchetti (1996), the F3 well had no immediate effect on Captage A and Captage B, whereas F1 and F2 wells have significantly changed the physico-chemical parameters of thermal springs excepted for the Cascade Centre. Some of thermal springs appeared in 1994 were totally dried.

With the objective to recognize the curative quality of thermal waters in the Val d'Illiez, a chemical analysis in F3 water was carried out in June 2001 to show if chemical changes in F3 water had been occurred since 1996 (Alpgeo 2001). Values of temperatures and flow rates remained stable whereas a slight decrease of the total dissolved solids was observed (1827 against 1882 mg/L). Later in July 2003 for a Master-thesis diploma (Pantet 2004), a new analysis in F3 water gave a total dissolved solids of 1890 mg/L confirming the chemical stability of thermal waters in time. Moreover, mixing processes were highlighted between a highly mineralized Ca-SO$_4$ thermal end-member and a low concentration Ca-HCO$_3$ cold water according to a sampling campaign in 2003 at several sampling points (Pantet 2004).

The hydrothermal system was again described by the Alpgeo consulting office in 2006 with the aim to obtain the certificate "natural mineral water" as well as to define protection zones around the F3 well (Alpgeo 2006a and 2006b). In these unpublished reports, an inventory of the parameters of the sampling points were undertaken excepting for F1 well and Captage A and Captage B which could not be measured at that time (Table 14.5). Without possible explanations yet, flow rates in the F3 well and Cascade Springs were half the rate they were in 1996. This also occurs in the F2 well where the flow rate was divided by four. Moreover, a decrease of around 10% of the flow rate in F3 well was observed in 2005 caused by the elevation of the pipe draining F3 waters due to works in the bridge crossing the Vièze River. However, temperatures and chemical parameters have slightly decreased since the implementation of boreholes in 1996.

In addition to this requirement, bacteriological tests were carried out in F3 water showing that the F3 water could be consumed as drinking water after removal of hydrogen sulphide, which gives a sulphur smell. The F3 water is almost devoid of nitrate of anthropogenic origin which is found in cold shallower groundwaters (below the detection limit). This analysis agrees with the assumption formulated in 1996 that F3 water is slightly mixed with cold shallower groundwaters and is chemically close to the thermal end-member.

According to Alpgeo (2006a and 2006b), the conceptual hydrogeological model of the hydrothermal system can be summarized as follows: the recharge zone is located in the Salanfe Lake area, infiltration occurs through the sedimentary formations of the Triassic cover of the Aiguilles Rouges basement, dissolution of gypsum and cellular dolomite occurs leading to the mineralization of waters, the reservoir temperature would be in the range 35-40°C at about 1 kilometre depth below the Val d'Illiez, the residence time would be in the range 10-15 years and the upflow of thermal water would occur into permeable faults with potential mixing processes with deep karstified aquifers in the Jurassic-Cretaceous limestones.

Table 14.4: Physico-chemical parameters of thermal waters in the Val d'Illiez before and after the drilling of F1, F2 and F3 wells in 1996 according to Bianchetti (1996). "nd" means not defined.

	Before the drilling of wells (March 1996)			After the drilling of wells (April 1996)		
Sampling point	Flow rate (L/min)	Temp. (°C)	Elec. Cond. (μS/cm, 20°C)	Flow rate (L/min)	Temp. (°C)	Elec. Cond. (μS/cm, 20°C)
Captage A	480	30.0	1861	265	29.8	1857
Captage B	nd	29.9	1864	nd	29.8	1856
Cascade Springs	700	25.8	1663	800	26.0	1637
Coin Supérieur Cascade	60	27.8	1778	6	23.6	1626
Coin Inférieur Cascade	150	28.2	1771	135	28.2	1735
Upper Spring 1	300	26.7	1758	< 1	23.2	1620
Upper Spring 2	100	25.1	1693	20	25.0	1617
Upper Spring 3	525	25.2	1678	< 1	24.5	1677
Coin Piscine Spring	100	28.0	1852	< 1	22.0	1811
Zone de Repos Spring	150	28.4	1850	5	25.2	1764

Measurements in wells between January and May 1996

	Flow rate (L/min)		Temp. (°C)		Elec. Cond. (μS/cm, 20°C)	
Well	Max.	Min.	Max.	Min.	Max.	Min.
F1	4500	nd	29.9	28.8	1841	1738
F2	1000	nd	30.0	29.4	1837	1799
F3	2500	nd	30.2	30.1	1918	1899

Flow rate measurements before and after drilling

Flow rate (L/min)	Wells	Captage A and B	Cascade Springs	Upper Springs	Other Springs	Total (L/min)
Before wells	0	580	800	925	460	2765
After wells	6500	320	900	20	145	7885

Buchelieule was initially considered as the only location where thermal water discharges (Vergain 1991). But in February 1996, a exploration well of 20 metres depth at Play, at about 1 kilometre upstream from Buchelieule, revealed the presence of thermal water below the Quaternary filling inside the Tertiary flysch belonging to the autochthonous cover (Bureau Tissières 1996a and 2003). Just some

metres upstream, the Urgonian limestone outcrops and a few metres downstream from the Play well, there is the thrust fault of the parautochthonous flysch. A chemical analysis of the water from a trench dug around the well in the Quaternary filling showed a Ca-SO_4 water with a temperature of 16.5°C and a total mineralization of 1543 mg/L. This water has chemical properties similar to those

of Val d'Illiez thermal waters (Vuataz 2005). Moreover, it was reported in 2008 the presence of thermal water in the parautochthonous flysch from three vertical borehole heat exchangers, at about 50 metres depth, located 200 metres upstream from the spa (Alpgeo 2008). Temperatures and conductivities of waters discharging in the three wells have values respectively in the range of 14-18°C and 700-

1350 μS/cm with a geochemical type close to the exploited thermal water in the spa. Finally, the presence of another area with uprising thermal water was discovered, 1 kilometre downstream from the spa at Fayot, a Ca-SO$_4$ subthermal spring having a temperature of 14.7°C and a mineralization of 902 mg/L as analysed by Pantet (2004).

Table 14.5: Physico-chemical parameters of thermal waters in the Val d'Illiez during the period July 2004 - January 2006 according to Alpgeo (2006a and 2006b).

Sampling point	Flow rate (L/min)	Temperature (°C)	Elec. Cond (μS/cm, 20°C)
F1	*unknown conditions*		
F2	230-270	28.6-28.9	1685-1741
F3	1200-1470	29.8-30.0	1800-1813
Captage A	*unknown conditions*		
Captage B	*unknown conditions*		
Cascade Springs	300-400	22.8-25.7	1340-1640

14.1.2 Water chemistry

On the basis on the chemical and isotopic analyses, the sampled waters can be subdivided into three groups (Fig. 14.1). The first group includes Ca-SO$_4$ waters with a high total dissolved solids of about 1800 mg/L and temperatures of around 30°C. This group of waters, represented by the three wells, the Zone de Repos spring and the old Captage A and Captage B, is also poor in chloride ($\approx$ 4 mg/L) and in alkaline elements ($\approx$ 20 mg/L), and has high magnesium concentrations reaching 80 mg/L. This water type represents the deep thermal end-member circulating in Triassic formation with the dissolution of gypsum and cellular dolomite (more details in the water-rock interactions section).

The second group refers to Ca-HCO$_3$ waters with low total dissolved solids in the range of 350-420 mg/L and temperatures in the range of 4-12°C depending on seasonal climatic conditions and on air temperatures occurring. This water type is represented by the cold springs located close to Buchelieule and out from the spa. Waters also have

low chloride concentrations in the range of 4-10 mg/L, low alkaline contents of around 5 mg/L, and significant concentrations with respect to magnesium ($\approx$ 16 mg/L) and sulphate ($\approx$ 40 mg/L). But these magnesium and sulphate values are however smaller than the thermal end member. The origin of this water would be linked to groundwater flow at shallower depth in Tertiary formations of the autochthonous and parautochthonous covers (flysch) and in the Quaternary deposits along the mountain slopes (moraine).

The last group is characterized by the superficial groundwater of the Vièze Quaternary filling, including waters of the river. This water has the same geochemical type with respect to the second group but the total dissolved solids is lower, at around 200 mg/L. In the same way, variation of temperatures in the range of 4-12°C are also related to seasonal climatic conditions and to air temperatures occurring.
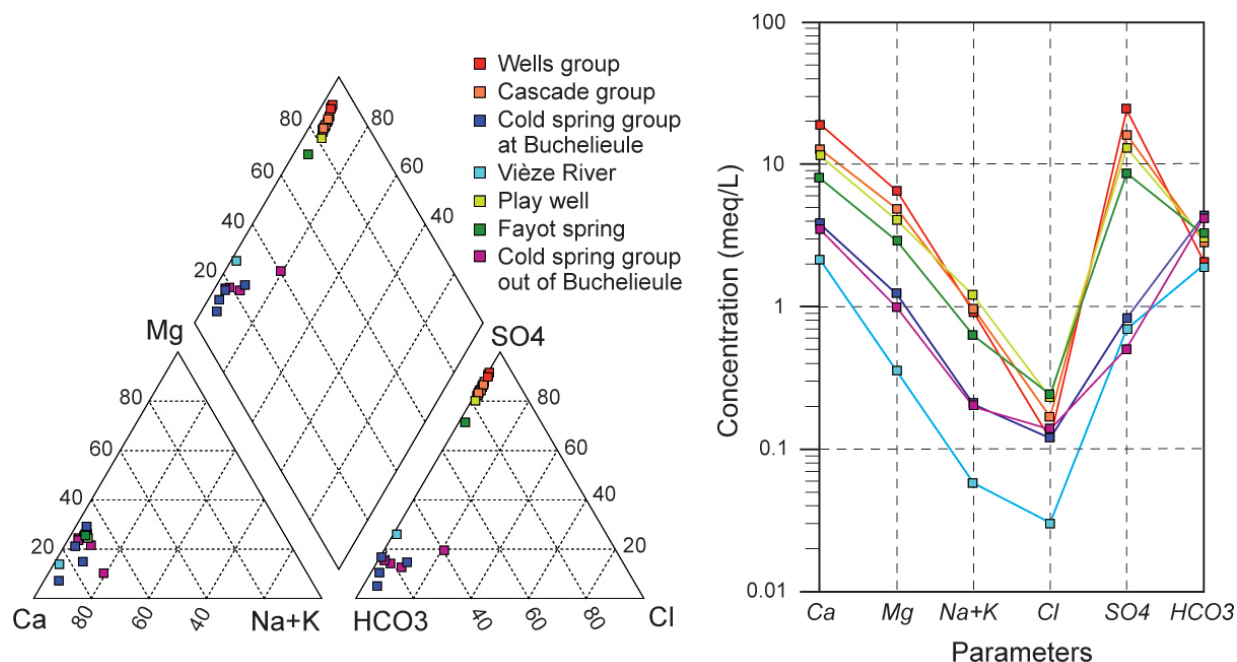
Figure 14.1: Major elements concentration plots (Piper and modified Shoeller diagrams) for groundwaters of the Val d'Illiez area with data collected during the new sampling campaign (see data in appendix D). Locations of the samples are shown in Figure 12.3.

14.1.3 Mixing processes

To highlight mixing processes, previous data were compiled from unpublished reports and from the PhD thesis of Gainon (2008), and data of the sampling campaign in 2009 were added. Unfortunately, some old sampling points could not be found in the hydrothermal site in 2009 (Captage A and Captage B), but historical data were taken into account for geochemical investigations.

The interpretation of correlations between physico-chemical parameters versus temperature, TDS (total dissolved solids), chloride, sulphate and calcium contents (Fig. 14.2) allowed the presence of two end-member components to be identified: a thermal end-member dissolving Triassic formations represented by waters from the wells, old Captage A and Captage B and Zone de Repos spring, and a cold component circulating at shallow depth in the Tertiary and Quaternary formations.

Mixing processes occur in different levels in the Val d'Illiez with these two end-members. The highly mineralized Ca-SO$_4$ thermal water is diluted by a cold Ca-HCO$_3$ water which is 4 to 5 times less mineralized. The dilution of the thermal end-member is accompanied by a significant decrease of temperature, total dissolved solids, calcium, magnesium and sulphate concentrations, and with respect to the dissolved silica to a lesser extend. On the contrary, alkalinity increases with the dilution and also for chloride to a lesser extend, whereas alkaline ions remain stable.

Correlations between parameters versus chloride indicate that the cold end-member certainly has a chloride content higher than the thermal water (8-10 mg/L against 4 mg/L). However, chloride values for all cold waters in the Val d'Illiez region vary greatly in space in the range 1-10 mg/L. This suggests an anthropogenic origin of this dissolved element.

Concerning the Cascade system, all sampling points in 2009 have temperatures and totals dissolved solids respectively in the range 21.5-23.9°C and 1230-1510 mg/L. The Cascade system cannot be considered as a distinct water group because these values are related to the occurrence of mixing processes between the two described components. In correlations in Figure 14.2, points illustrating the Cascade system are quite aligned along all the mixing lines. Due to the location of the cascade sampling points, several metres above the Vièze riverbed, the cold component cannot be Vièze alluvial groundwater but would be related to shallow circulations in the Tertiary and Quaternary deposits from the slope (moraine groundwater).

14.1.4 Composition of the end-members

Correlations in Figure 14.2 coupled with other correlations of the physico-chemical parameters, not illustrated in this study, allow one thermal end-member and one cold component to be defined, explaining the mixing processes occurring. According to geochemical investigations, the thermal end-member surely circulates in the autochthonous cover of the Aiguilles Rouges Massif, in particular in the Triassic formations because the thermal water has high concentrations in calcium, magnesium and sulphate. However, according to the geological cross section of the autochthonous cover (Fig. 13.3), the Triassic formations are probably not the only aquifer existing in the cover. Indeed, the Malm and lower Cretaceous layers which consist of fractured massive limestone are karstified aquifer with groundwaters. Without deep investigations by means of new boreholes, it remains difficult to know if mixing processes occur in these karstified layers with the uprising thermal waters, and if groundwaters in the Malm and lower Cretaceous can also be considered as thermal waters (15-20°C). The geochemical investigation of thermal waters discharging in the Val d'Illiez does not allow this question to be answered.

The evaluation of the chemical and isotopic properties of the unmixed thermal end-member at depth was difficult to define. In 1990, the thermal water in the Val d'Illiez had higher tritium values than cold shallower waters and thus the method using the tritium cannot be used. However, the current discharging thermal waters from deep wells have chemical and isotopic properties that do not necessarily indicate that mixing processes occur due to the absence of nitrate (below the detection limit). Moreover, thermal waters from the Val dŠIlliez and the assumed recharge zone of the deep flow system, the water from the Salanfe Lake, have similar measured values for water stable isotopes. If mixing processes would strongly occur in thermal waters, values of the water stable isotopes would be different and tended towards lower values as those currently measured in the cold waters. Therefore, it can be assumed that thermal waters in the wells are weakly mixed ($< 5\%$), and the composition of the unmixed thermal end-member is probably similar to the current composition of waters discharging in wells (Table 14.6). The thermal component without mixing certainly has temperatures in the range of 30-31°C with a total dissolved solids at about 2 g/L. This water has a Ca-SO$_4$ geochemical type marked by low chloride and alkaline elements concentrations and high magnesium concentrations.

In the same way, the cold waters circulating in the Tertiary and Quaternary formations at a shallower depth have a composition close to that measured in cold springs at Buchelieule. This cold end-member has a different geochemical type, Ca-HCO$_3$, with lower values with respect to magnesium and sulphate. The temperature in groundwaters in the range of 4-10°C depends on the seasonal climatic conditions and the total mineralization is also lower compared to the thermal water, roughly of 400 mg/L.
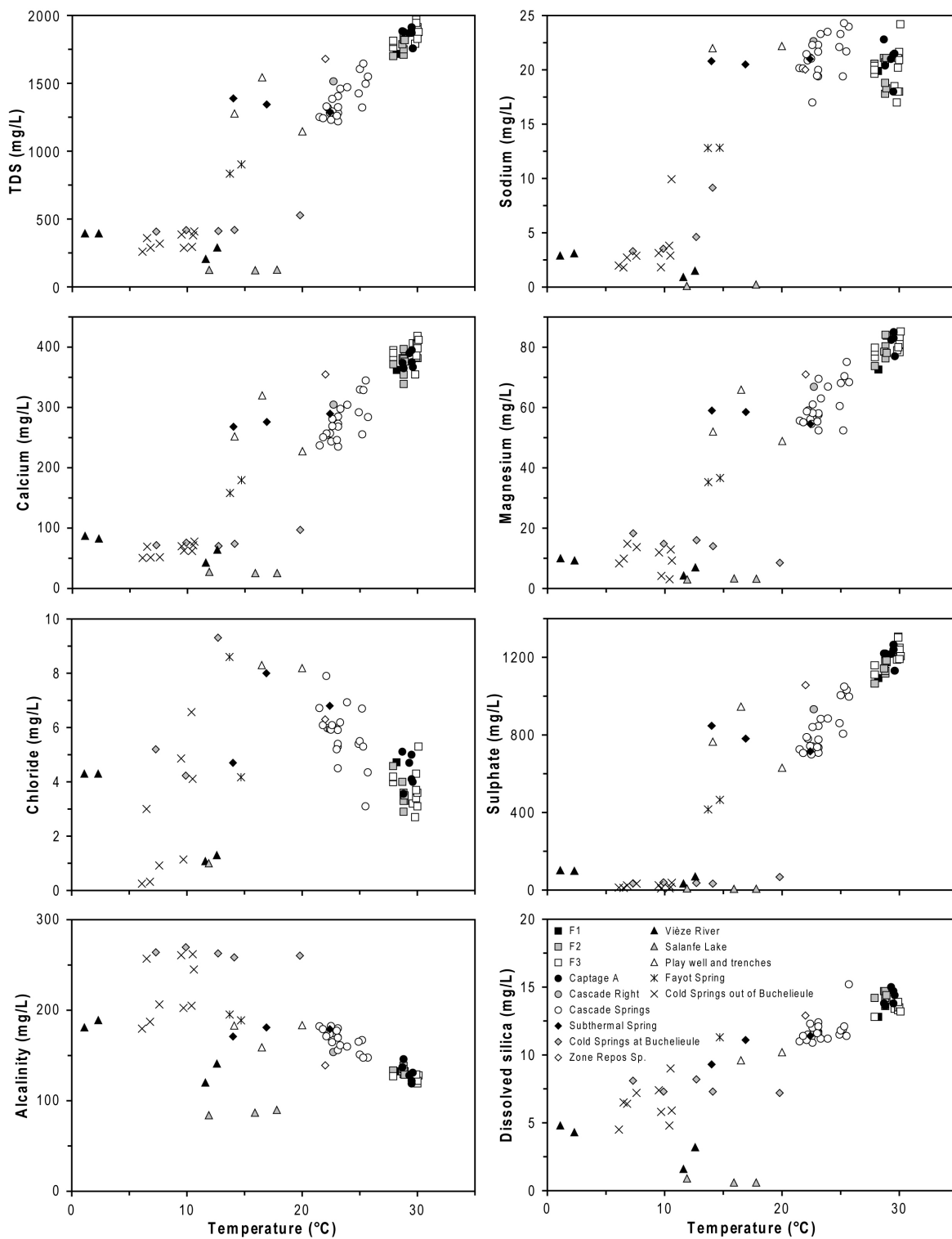
226
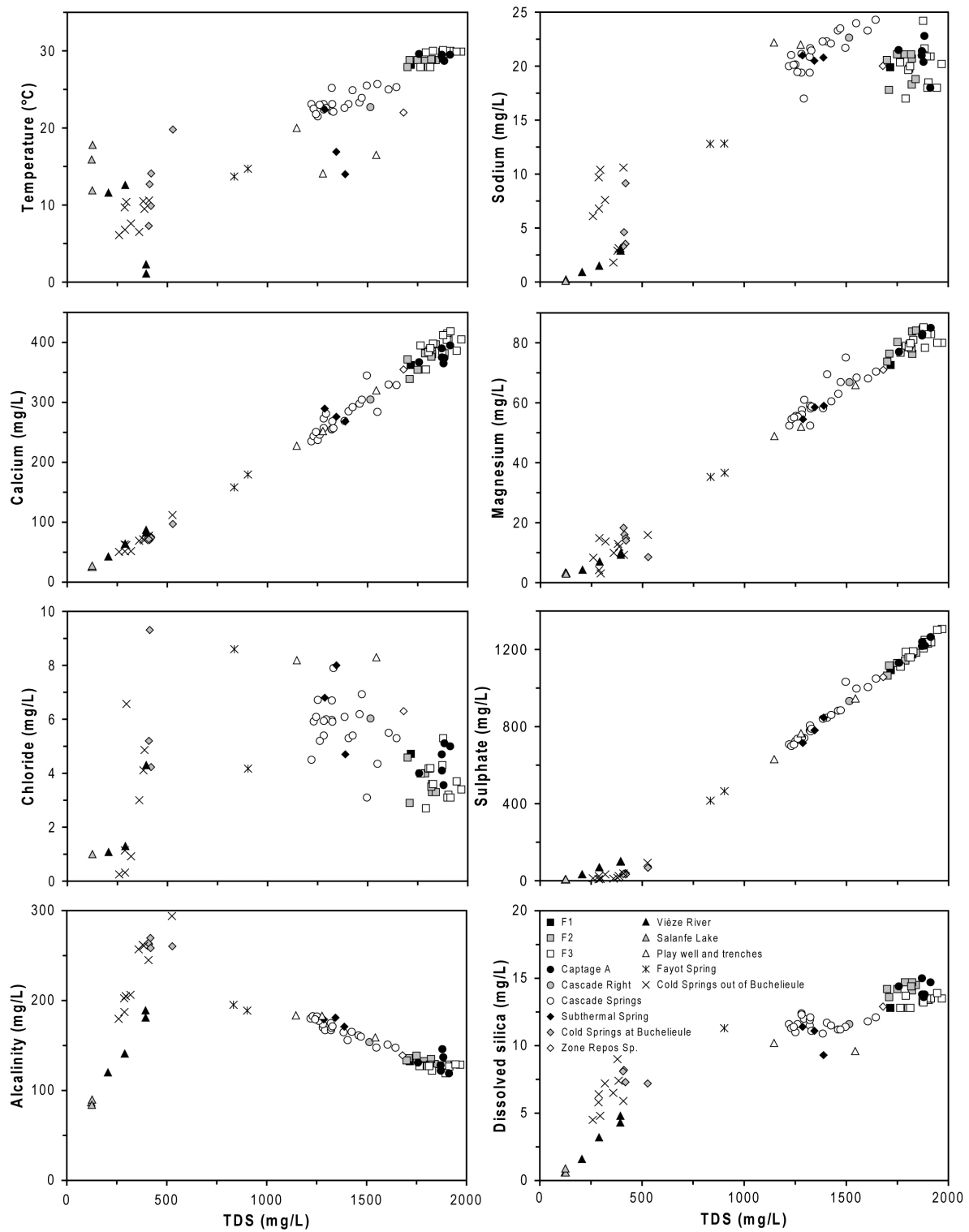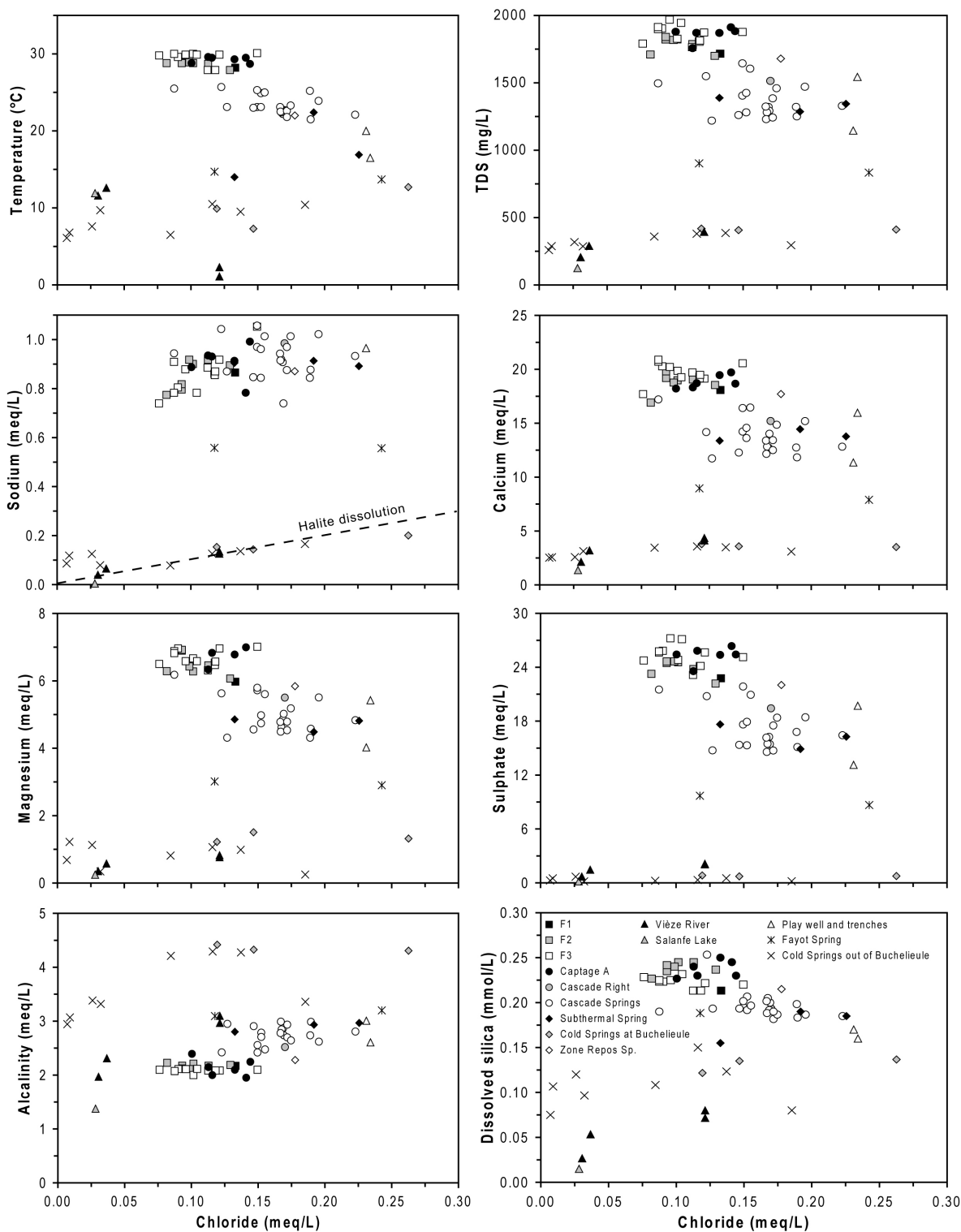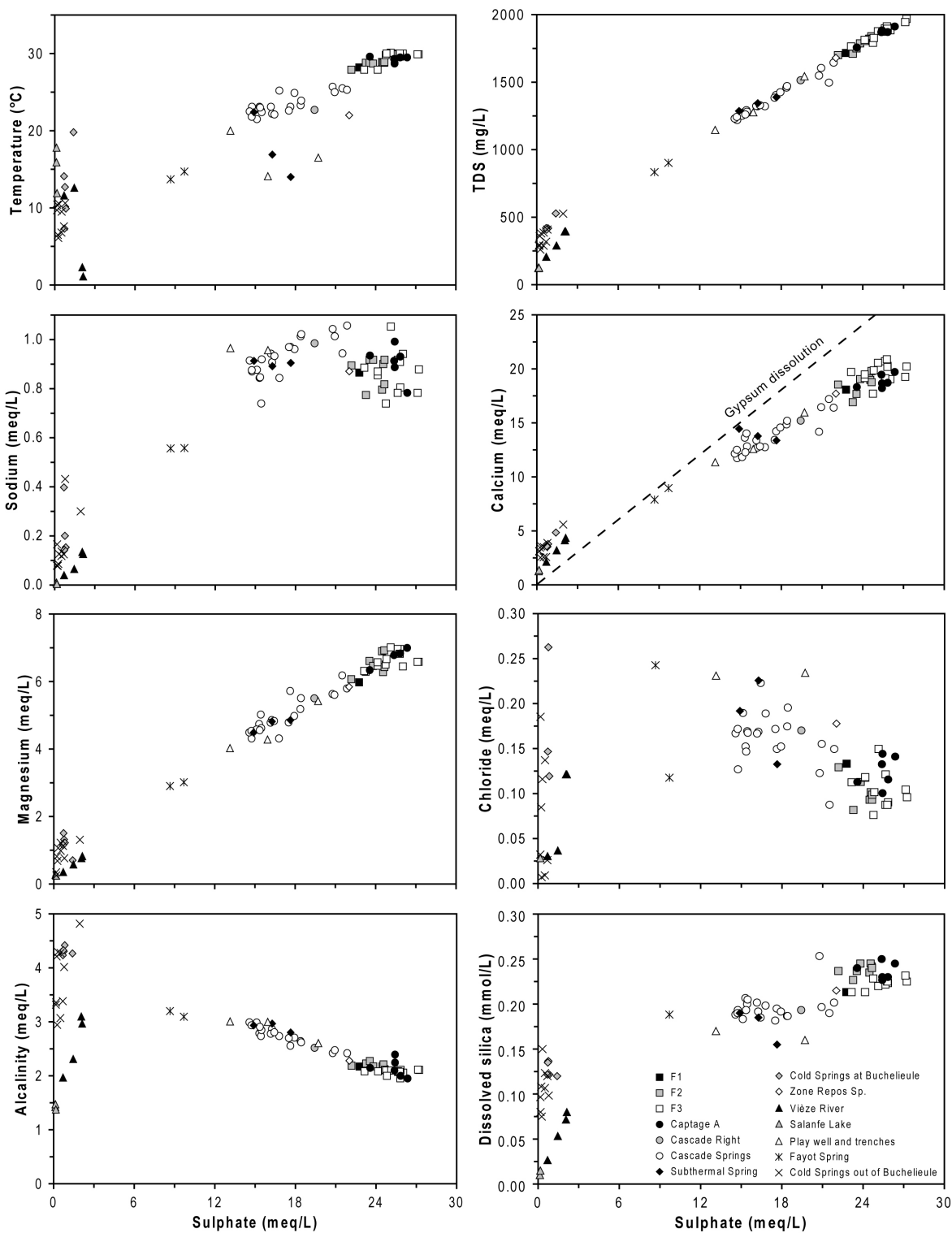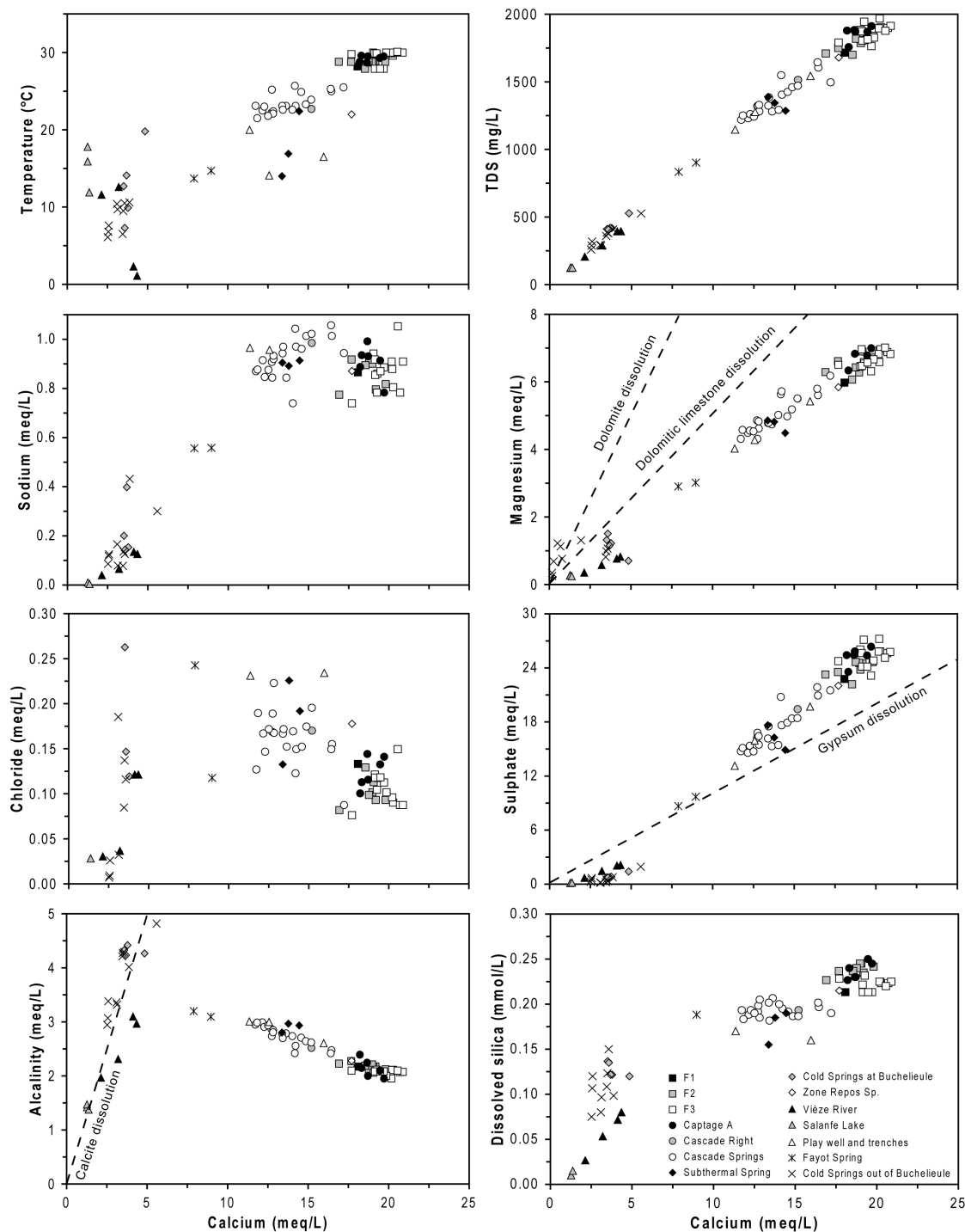
Figure 14.2: Correlations between the physico-chemical parameters in Val d'Illiez waters for all existing data (see data in appendix D).

Table 14.6: Calculated composition of the end-members from correlations between all the physico-chemical parameters.

	Thermal component of the autochthonous cover	Shallow groundwater
Temp. (°C)	30-31	4-10
Elec. Cond. (25°C, μS/cm)	2100	450
pH	7.2	7.8
TDS (mg/L)	1972	411
CATION (mg/L)		
Li	0.1	0.02
Na	21	5
K	1.5	1.8
Mg	85	15
Ca	420	75
Sr	15	1.5
Ba	0.015	0.035
Rb	0.004	0.001
Cs	0.004	< 0.001
Al,As,Cd,Co,Ge,Hg,Mo,Pb,V	< 0.002	< 0.002
Cr	0.006	0.02
U	0.0001	0.0003
Ni	0.004	0.002
Ti	0.7	0.3
Mn	0.3	0.01
Fe	< 0.1	< 0.1
Cu	0.0003	0.002
Zn	0.005	0.02
ANION (mg/L)		
F	1.5	< 0.5
Cl	4	9.5
Br	0.07	< 0.005
I	0.012	< 0.001
NO_3	< 0.1	6
NO_2	< 0.1	< 0.1
PO_4	< 0.5	< 0.5
SO_4	1280	35
HCO_3	130	260
UNDISSOCIATED (mg/L)		
SiO_2	14	8
B	0.12	0.015
GAS (mg/L)		
H_2S	< 3	< 0.1
IONIC BALANCE		
Cation (meq/L)	28.91	5.24
Anion (meq/L)	28.99	5.26
Balance (%)	-0.14	-0.17
ISOTOPE		
Tritium (TU) in 2009	≈ 6	≈ 8
Deuterium (‰)	-96.7	-85.0
Oxygen-18 H_2O (‰)	-13.4	-12.0

14.1.5 Variation of the physical and chemical parameters

Variations of the physico-chemical parameters in the main sampling points were interpreted aiming to understand hydrogeological processes occurring in the Val d'Illiez, in relation with historical events in the region such as the construction of a dam at Salanfe in 1953, waterproofing works in 1994 around the Salanfe Lake and the drilling of the shallow wells. The Figure 14.4 shows the variation of temperatures since 1990 and sulphate concentrations since the appearance of thermal springs in the 1950's. Three analyses in sulphate before 1990 seemed to indicate a strongly decrease in the total mineralization whereas historical temperature measurements remained in the range 27-28°C (these values are not illustrated in Figure 14.4). This process is difficult to explain due to the lack of data before 1990, it would not resemble to a single mixing process with water from lake because because the temperature remains stable whereas the min-

eralization decreases. This will be discussed with the study of the groundwater flow and heat transport via a two-dimensional numerical model (chapter 15). Values measured in the period 1990-1997 clearly illustrate the impact of historical events at Salanfe on the thermal regime. Firstly, the rise of the water level up to 1915 metres of elevation at Salanfe after 1994 generated seismic events (Fig. 14.3) and the increase of the physico-chemical parameters in the thermal springs (Figs. 14.4, 14.5 and 14.6). The drilling of wells in 1996 draining part of thermal waters uprising towards springs, has radically changed theses parameters of the springs with a partial drying of the old Captage A and Captage B. For the last 6-7 years, temperatures and conductivities seem to remain stable in wells and in Cascade waters, however artesian flow rates tend to decline continuously in F3 well (G Bianchetti pers. comm. 2009).
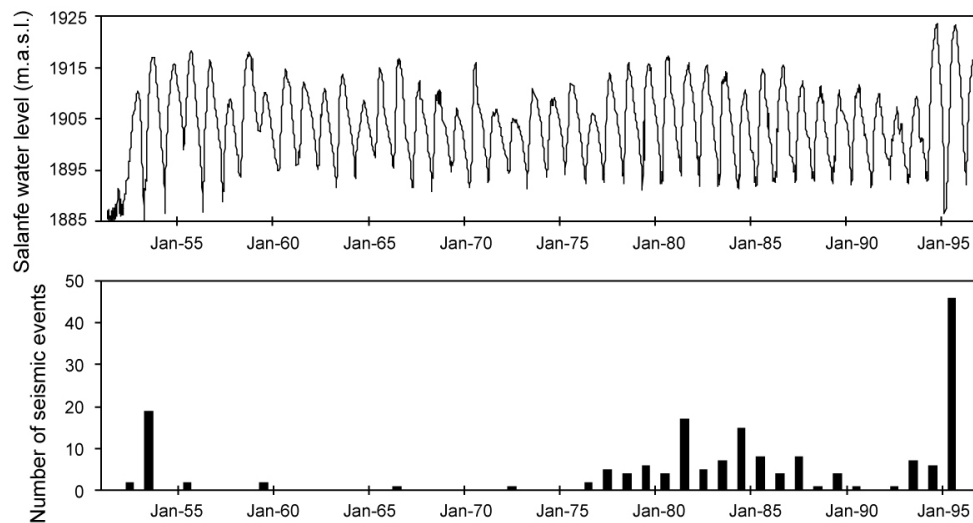
Figure 14.3: Seasonal variation of the water level at Salanfe Lake since 1953 and seismic events related to the history of the lake, according to data from Alpgeo consulting office and CREALP (1998).

Tentative correlations have been tried between the Salanfe water level and the artesian flow rate of thermal springs. Graphics related to this study are not illustrated but are explained in Bianchetti et al. (1992) and CRSFA (1992d). The flow rates of thermal waters in Captage A and Captage B in the Val d'Illiez have been monitored on a daily basis since May 1988 with a precision of 5% indicating

discharge variations at about 30%. Low discharge values occur in summer, whereas high values are prevailing in winter, out of phase with the majority of the Alpine springs with a nival or glacio-nival regime. The water level of the Salanfe Lake has also been monitored daily since 1952 (Fig. 14.3). In accordance with the exploitation schedule of the dam, it rises during the spring and summer and

starts to decrease around the beginning of the fall. For the observation period, the maximum variation of range between the highest and the lowest water level equals 19 metres. In the case of Val d'Illiez, for the period of observation 1988-1992 according to Bianchetti et al. (1992) and CRSFA (1992d), the best-fit of the curves of flow rates in Captage A and Captage B and of water levels at Salanfe seems to give a time-lag of around 140 days. This evaluation was interpreted by Bianchetti et al. (1992) to a reasonable period of time for the diffusion of pore pressure vartaitions from Salanfe to the springs, and

re-interpreted later by G Bianchetti assuming that the time-lag should be the residence time of groundwater in the unsaturated zone.

Finally and contrary to Lavey-les-Bains and Saint-Gervais-les-Bains, it was not possible to assign short sudden changes in the flow rates in wells aiming to observe variations of the physico-chemical parameters in waters. Indeed, there is no pump in the wells as the thermal waters are naturally discharged into the spa due to an artesian pressure at depth without any control on the rates.
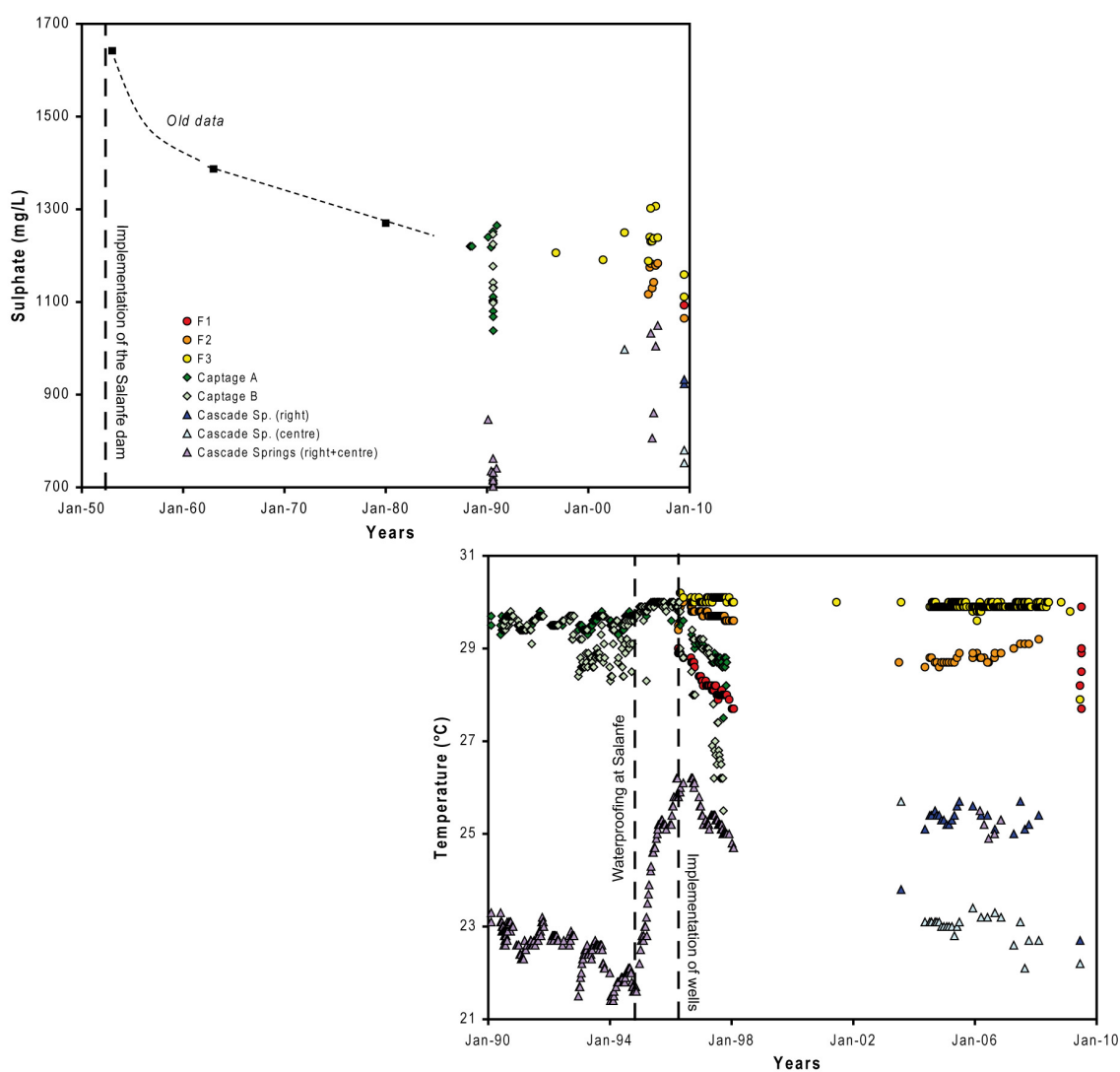
Figure 14.4: Variation of temperature and sulphate for the main sampling points in the Val d'Illiez, according to data from Alpgeo consulting office.
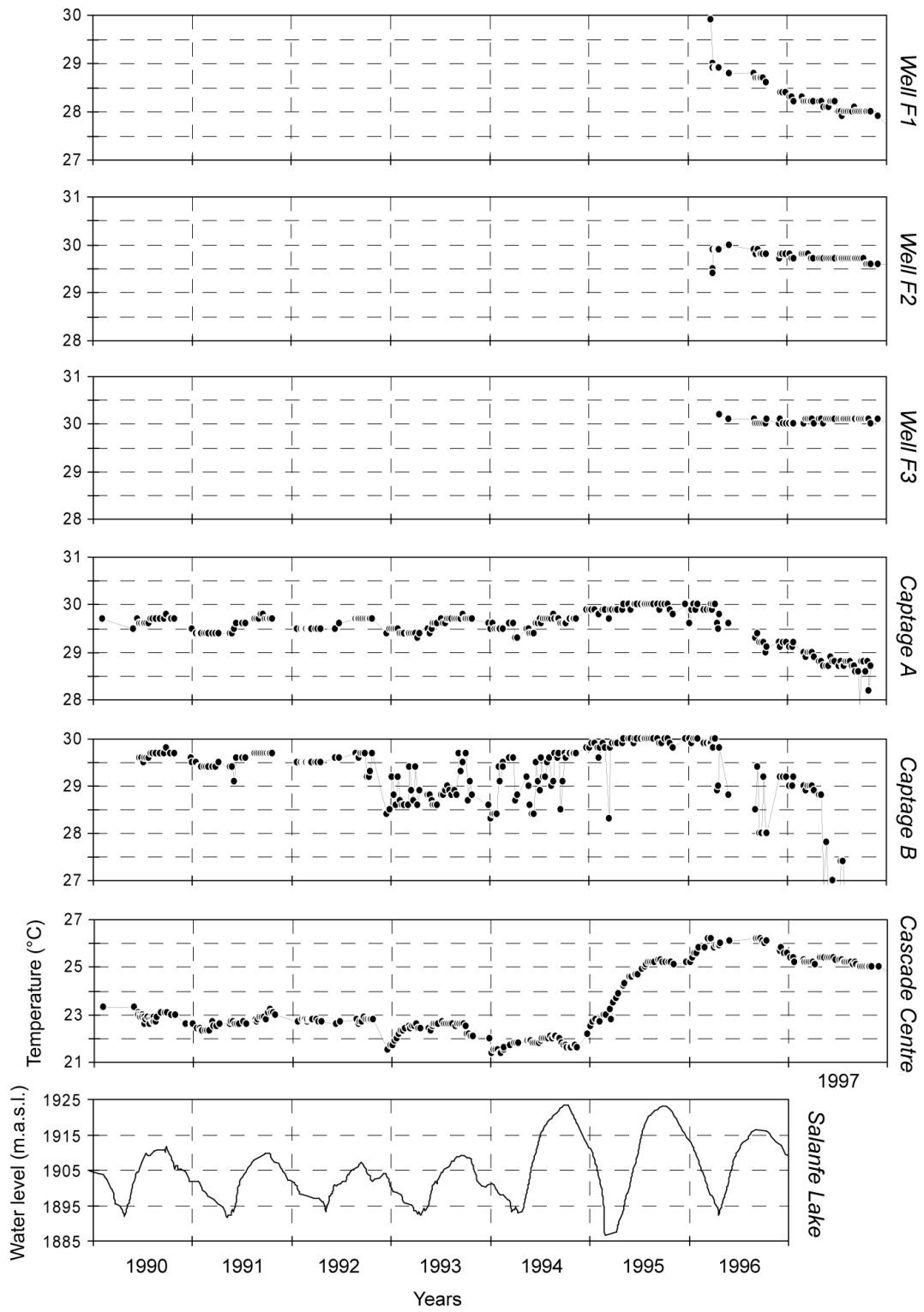
Figure 14.5: Variation of temperatures for the main sampling points between 1990 and 1997 related to the variation of the water level at Salanfe Lake, according to data from Alpgeo consulting office and CREALP (1998).
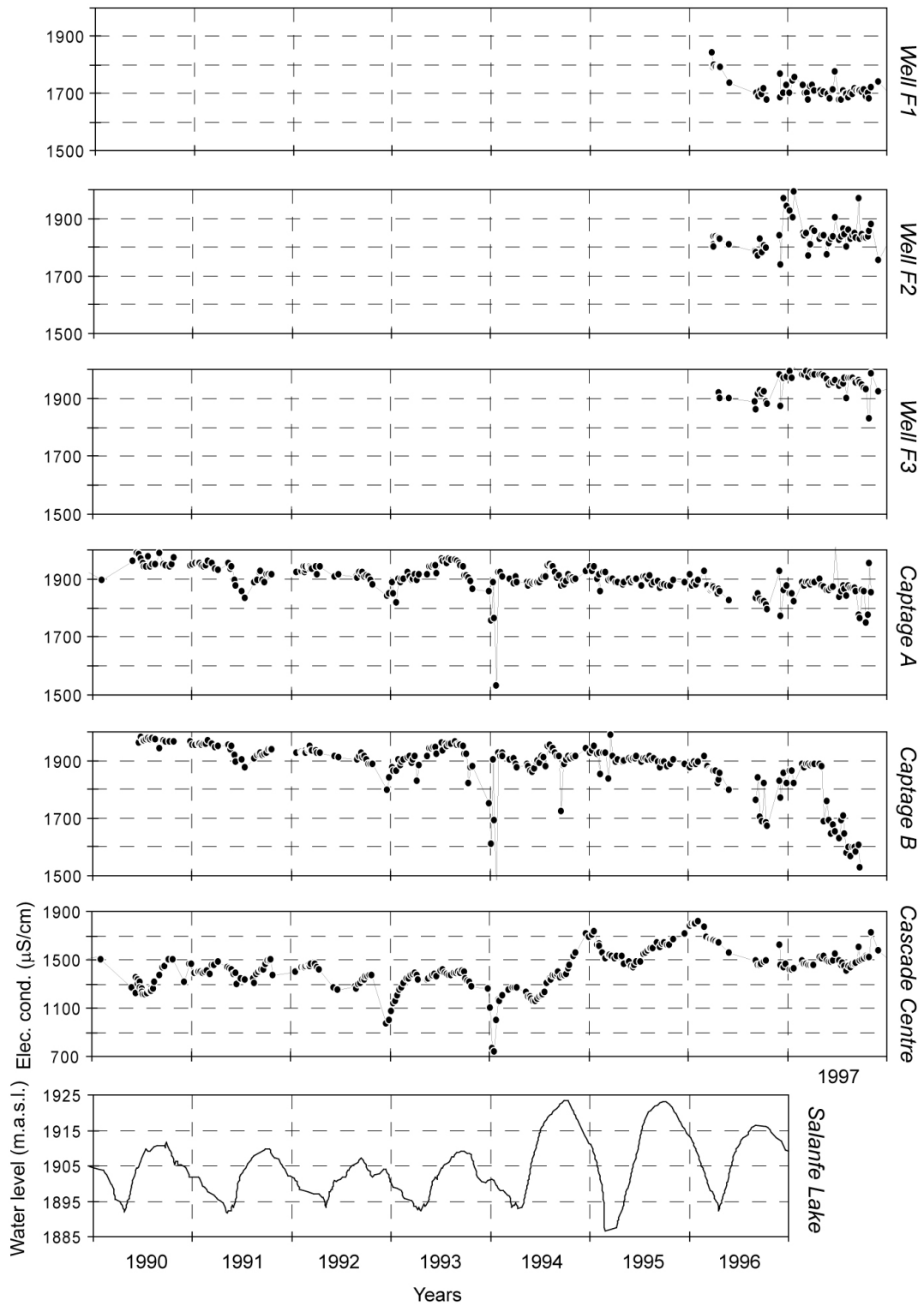
Figure 14.6: Variation of electrical conductivities for the main sampling points between 1990 and 1997 related to the variation of the water level at Salanfe Lake, according to data from Alpgeo consulting office and CREALP (1998).

14.1.6 Water-rock interactions

Chemical equilibrium

Thermal water circulates into Triassic formations of the autochthonous cover of the Aiguilles Rouges basement, and thus reactions of dissolution/precipitation occur with the host rocks leading to the chemical composition of the discharged thermal waters. Therefore, rocks and minerals forming these rocks, such as calcite, gypsum, anhydrite and dolomite were taken into account for the study of water-rock interactions using the PHREEQC code, due to high contents in sulphate and calcium measured in thermal waters. Moreover, other minerals present in the Triassic formations in the fractures forming slip veins may also exist. These minerals are millimetres in length or of greater importance and are mostly sulphide and carbonate minerals which can also be subjected to dissolution/precipitation reactions as well as primary minerals in the Triassic rocks. Finally, quartz, chalcedony, albite, anorthite and K-feldspar, K-mica and chlorite forming crystalline rocks of the Aiguilles Rouges Massif below the Triassic layers were also considered in this study of chemical equilibria.

Saturation indices (SI) for the thermal and cold components were calculated (Table 14.7), and for alumino-silicates an aluminum content of 1 μg/L was selected. Globally, strong negative SI values were found for feldspars and chlorite. Other higher aluminum concentrations upper than 1 μg/L were tested, but not represented in Table 14.7, and SIs results with respect to feldspars and chlorite are strongly negative. This observation is clearly consistent with the geological context of the hydrothermal system, as thermal waters do not circulate in a crystalline domain. The thermal end-member is clearly in equilibrium with carbonate minerals which are controlled by their solubility in relation to temperature. The cold end-member is slightly over-saturated with respect to carbonate minerals implying that carbonate precipitations can occur at the surface. The Ca-SO$_4$ thermal component is slightly under-saturated with respect to gypsum and anhydrite whereas the cold component is strongly under-saturated due to low sulphate and calcium concentrations in cold waters. Calculated SIs of quartz are slightly over-saturated for the two components and SIs of chalcedony are close to zero, showing that weak precipitation of chalcedony can occur in the host rocks during the rise of the deep fluid.

Table 14.7: Calculated saturation indices of Val d'Illiez waters for the evaluated thermal and cold end-members. In absence of precise Al analyses, SIs of alumino-silicates are calculated using a Al content of 1μg/L.

Minerals	Formula	Thermal component	Cold component
Albite	$NaAlSi_3O_8$	-3.2	-3.2
Anorthite	$CaAl_2Si_2O_8$	-4.8	-5.0
K-feldspar	$KAlSi_3O_8$	-2.2	-1.1
Muscovite	$KAl_3Si_3O_{10}(OH)_2$	2.7	4.5
Chlorite	$Mg_5Al_2Si_3O_{10}(OH)_8$	-4.6	-6.1
Kaolinite	$Al_2Si_2O_5(OH)_4$	0.94	1.9
Quartz	SiO_2	0.45	0.53
Chalcedony	SiO_2	0.06	0.06
Amorphous silica	SiO_2	-0.76	-0.83
Aragonite	$CaCO_3$	0.06	0.24
Calcite	$CaCO_3$	0.20	0.40
Dolomite	$MgCa(CO_3)_2$	0.09	0.22
Fluorite	CaF_2	-0.37	-4.8
Goethite	$FeOOH$	7.0	6.9
Gypsum	$CaSO_4{:}H_2O$	-0.22	-2.0
Anhydrite	$CaSO_4$	-0.42	-2.2
Halite	$NaCl$	-8.8	-8.9

Origin of calcium and sulphate in waters

The origin of the sulphate content in thermal waters in the Val d'Illiez was studied using the sulphur-34 and oxygen-18 (in sulphate) values in waters of Captage A measured in 1990 by Bianchetti (1993b), which were compared to other values in the Alpine thermal waters (Fig. 14.7). The sulphur-34 value gives information about the sulphur cycle in groundwater, especially with respect to the dissolved species $SO_4{}^{2-}$, H_2S and HS^-. The oxygen-18 content of sulphate in water is related to the origin of sulphate and is also an indicator of oxidation-reduction processes. The origin of sulphate in water can be related to the dissolution of gypsum from Triassic evaporite, to the oxidation of sedimentary sulphides in rocks and the leaching of residual seawater brines (Fouillac et al. 1990). Moreover, difficulties in interpretation can be met because the sulphur-34 and oxygen-18 values of marine evaporite sulphate minerals vary with their geologic age due to changes in the isotopic composition of oceanic sulphate with time (Pearson et al. 1991). In the case study of the Val d'Illiez the values in plots in Figure 14.7, when compared to other Alpine thermal waters, clearly indicate that the origin of sulphate in thermal water in the Val d'Illiez comes from the dissolution of Triassic evaporites containing gypsum and anhydrite. Compared to thermal waters in crystalline domain such as observed for Lavey-les-Bains and partially for Saint-Gervais-les-Bains, values are higher for oxygen-18 and lower for sulphur-34.

Looking at sulphate and calcium concentrations (meq/L) in the thermal end-member, in comparison to other Alpine thermal waters in Figure 14.7, an excess of sulphate in relation to calcium was highlighted (at about 21 meq/L against 26.7 meq/L). Assuming that sulphate concentrations come entirely from the dissolution of gypsum ($Ca-SO_4$), there ought to be as much calcium as sulphate. Clay exchanges between calcium and sodium may not be the cause of this calcium deficit because sodium concentration represents only 0.9 meq/L. This calcium deficit is probably related to calcite precipitation occurring at depth. Indeed, part of calcium concentration in the thermal end-member from the dissolution of gypsum should interact with bicarbonate because SIs with respect to carbonate minerals are slightly positive. Looking at the typology of Triassic evaporitic aquifers from the Western Alps in Switzerland (Wallis) according to chemical analyses made over 100 springs, including cold and thermal waters, Mandia (1991) shows that Triassic groundwaters have mostly high sulphate concentrations with an average of 1040 mg/L (Fig. 14.8). Val d'Illiez thermal waters are thus slightly above the average (1280 mg/L), and according to the interpretation of Mandia, the most mineralized groundwaters would circulate in a special way in gypseous karstified environments. From a geological point of view, high sulphate contents in groundwaters were measured in Triassic domains from the Prealps, the Helvetic and Ultrahelvetic domains, and from the Penninic zone at the south of the Rhone Valley. For these aquifers, Mandia also indicates that 90% of the molar chemical composition is represented by calcium and sulphate elements.

Origin of other elements in thermal waters

The presence of high magnesium concentrations in thermal waters in the Val d'Illiez (85 mg/L) is related to the dissolution of dolomite ($Mg-Ca-(HCO_3)_2$), dolomitic limestone and cellular dolomite occurring at low temperature (35-40°C) in the reservoir forming by Triassic rocks. This process is also confirmed by Mandia (1991) who showed that the average magnesium concentration in Alpine thermal waters is of around 67 mg/L for Triassic groundwaters. As a reminder, the Ferrugineuse and Magnésienne springs at Saint-Gervais-les-Bains flowing in the Triassic cover (Mont d'Arbois and Mont Joly Massifs) have also high magnesium contents at about 66 mg/L. Similarly, thermal waters in the Val d'Illiez have high strontium contents of around 15 mg/L also found in other Triassic groundwaters from Western Alps, especially in thermal waters (Combioula, etc.). The dissolution of celestite ($Sr-SO_4$) is proposed to explain the presence of strontium in waters. Finally, low chloride concentrations in thermal waters in the Val d'Illiez (4 mg/L) are similar with other Triassic groundwaters from Western Alps, mostly lower than 20 mg/L, and with the cold Triassic springs at Saint-Gervais-les-Bains (Ferrugineuse and Magnésienne). This observation clearly indicates that Triassic formations in the studied area contain very little halite.
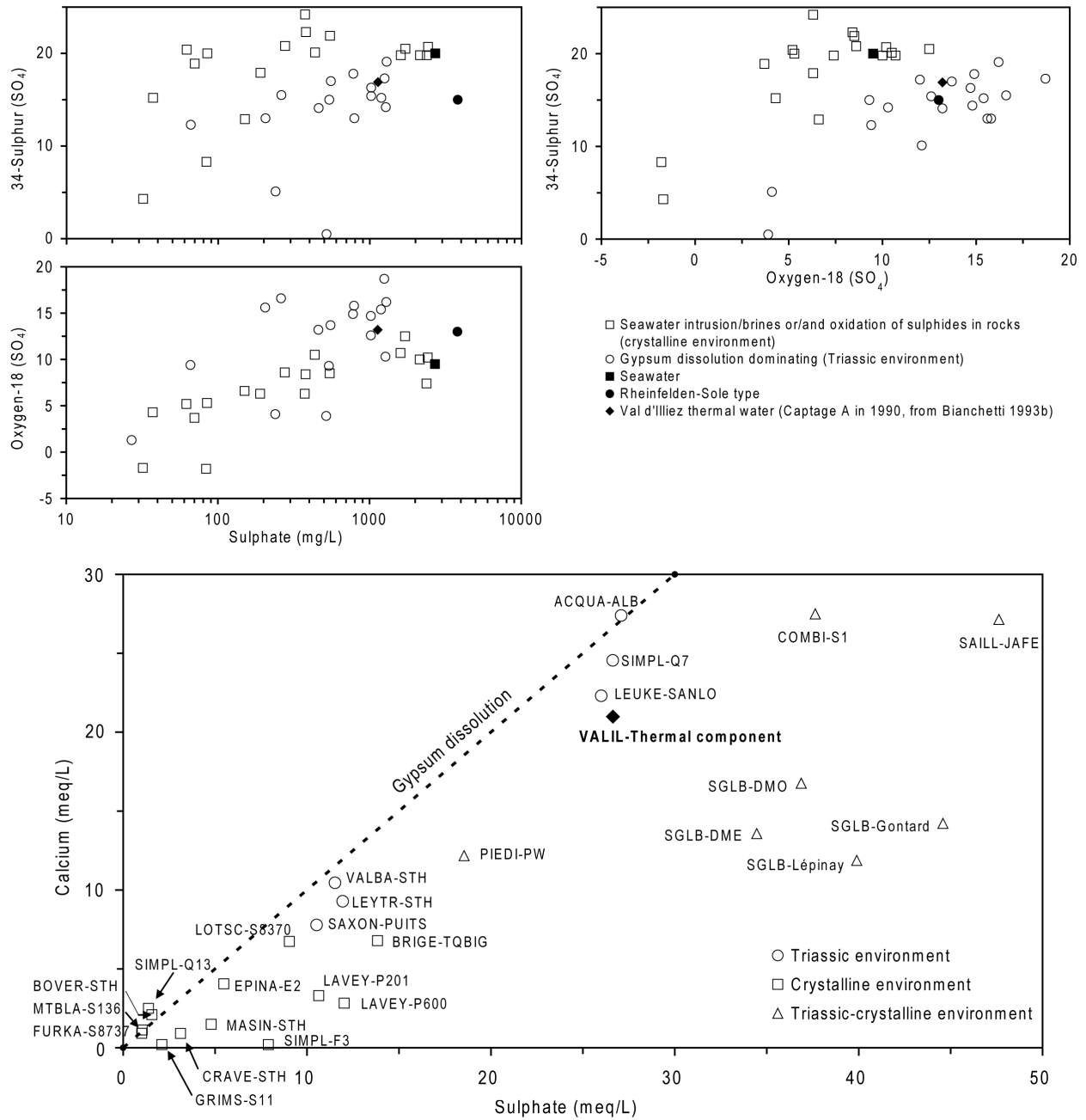
Figure 14.7: Plots of calcium-sulphate contents and sulphate isotopes in thermal waters for the Alps range. The sulphate origin is function of the reservoir geology: basement with seawater brines or/and oxidation of sulphides in rocks (squares) or Mesozoic sedimentary rocks containing gypsum formations (circles). There is no direct data for Rheinfelden-Sole but representative data of waters in Keuper located close to this brine (black circle) showed values of 13‰ and 15‰ respectively for oxygen-18 and sulphur-34 (Pearson et al. 1991). Data for Val d'Illiez (diamond) are positioned in the circle zone, coming from Bianchetti (1993b). Names of Alpine thermal water in the calcium-sulphate plot are illustrated for each point ("Abbreviated site name - Sampling point").
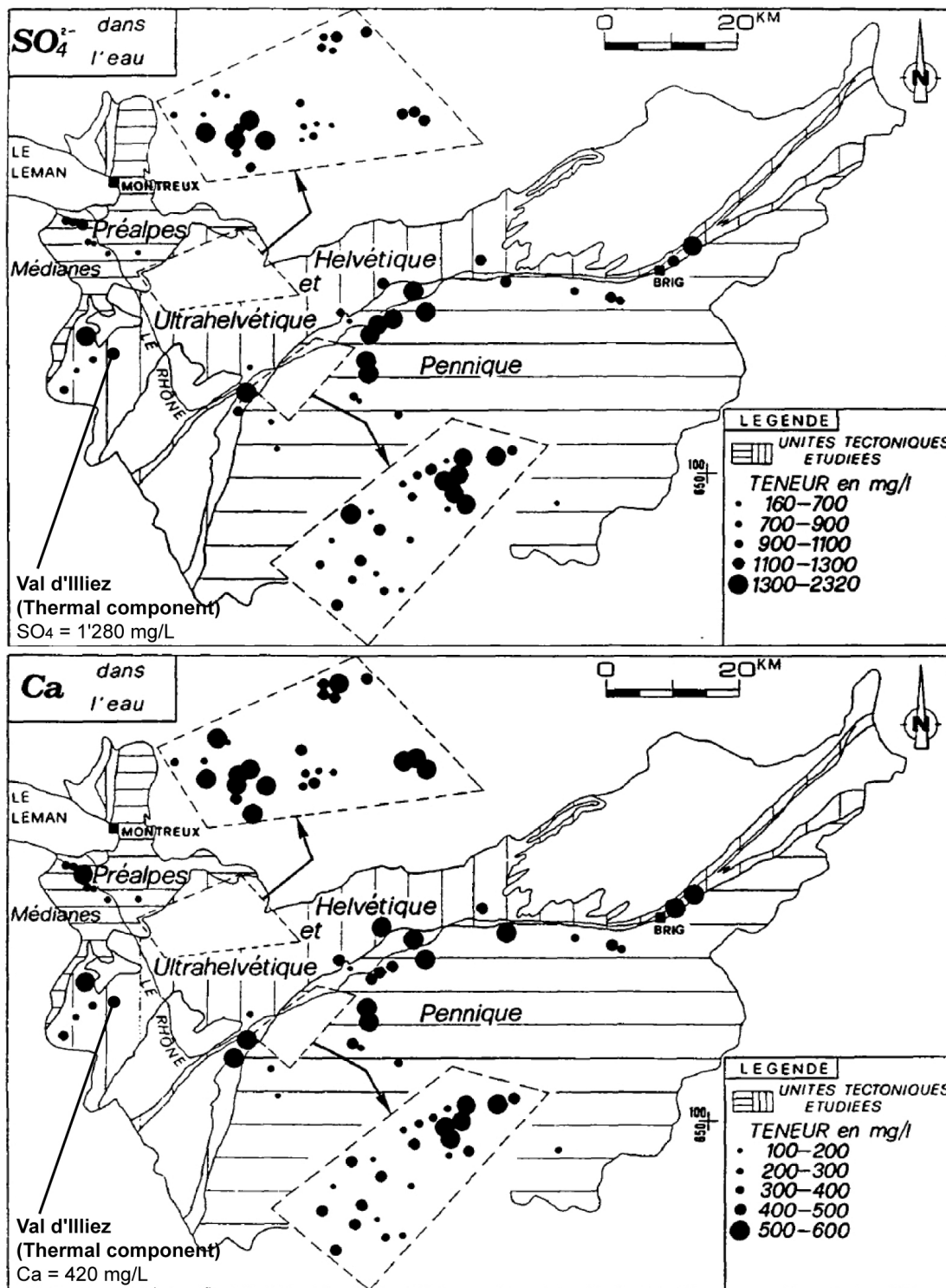
Figure 14.8: Spacial distribution of sulphate and calcium contents in cold and thermal groundwaters from Western Alps (Wallis, Switzerland) according to Mandia (1991).

14.2 Regional hydrogeological and geochemical investigations

14.2.1 Regional deep flow system

Investigations based on geological, hydrogeological and geochemical methods enable a regional conceptual model of the different flow paths to be built. The two hydrothermal sites of Lavey-les-Bains and Saint-Gervais-les-Bains were added into the conceptual model for comparison of their geochemical type in relation to host rocks met during the flow system (Figs. 14.9 and 14.10). As described previously, the Lavey-les-Bains and Saint-Gervais-les-Bains hydrothermal sites are the two lowest elevation points of the Aiguilles Rouges crystalline Massif and their pumped waters have similarities in their chemical and isotopic properties, that is to say Na-SO$_4$ waters rich in chloride (Sonney and Vuataz 2010d). Infiltration and circulation within summits of the Aiguilles Rouges crystalline Massif take place in a NE-SW direction via Variscan and Alpine fractures and faults leading to Lavey-les-Bains thermal waters (65°C) and to Saint-Gervais-les-Bains thermal waters (40°C).

Concerning the hydrothermal system of Val d'Illiez, thermal groundwaters occur in the autochthonous cover of the crystalline massif, in particular in Triassic formations as made evident by its chemical and isotopic composition, Ca-SO$_4$ water poor in chloride, which differs from Lavey-les-Bains and Saint-Gervais-les-Bains thermal waters. During the deep flow system in the autochthonous cover, illustrated in Figures 14.9 and 14.10 according to the geological cross section from Pantet (2004), it remains difficult to know if the deep flow system only occurs in the Triassic formations at the bottom of the cover, or if the deep flow system partially occurs in the Malm and lower Cretaceous massive limestones above. Until now, the geochemical investigation in Val d'Illiez waters does not allow this assumption to be specified. The Malm and lower Cretaceous formations are certainly karstified with groundwaters suggesting that they contribute to the deep flow system with mixing processes.

The recharge zone is certainly located in the Salanfe area due to the hydrogeological relation between the lake and the thermal flow regime. Bordering the lake, major water losses occur in the high permeable Triassic formations, in particular into the cellular dolomite. The possibility about a recharge zone along a band of few hundred metres wide of Triassic outcrops can be evoked, from the Salanfe lake to the Emosson lake and further on the French territory (Figs. 14.9 and 14.10). From a geological view, this assumption is plausible because groundwaters are certainly present in the Triassic formations in more remote areas of the Salanfe Lake. Another question can be raised about groundwaters in the decompressed zone of the Aiguilles Rouges crystalline rocks. The geological contact between the basement and the autochthonous cover having high hydraulic conductivities could be the place where part of groundwaters from the decompressed zone discharge into the cover. Without drilling wells into these formations, it remains difficult to prove this process.

According to the geological investigation of Pantet (2004), the rise of the deep fluid would occur along a major thrust fault system bordering the autochthonous cover. Close to the surface, thermal waters rise in the permeable Carrières sandstone below the Quaternary deposits on the left bank of the valley.

Finally, aquifers with interstitial porosity are present in the Val d'Illiez such as alluvial groundwaters of the Vièze Valleys and the moraine groundwaters globally quite widespread along mountain slopes in the zone studied. Groundwaters take an important place in the upper part of the Vièze Quaternary filling, but they contribute weakly to mixing processes with the thermal end-member. Cold groundwaters from the mountain slopes in moraine deposits would dilute the thermal component at different degrees as highlighted previously for thermal springs in the Cascade system.
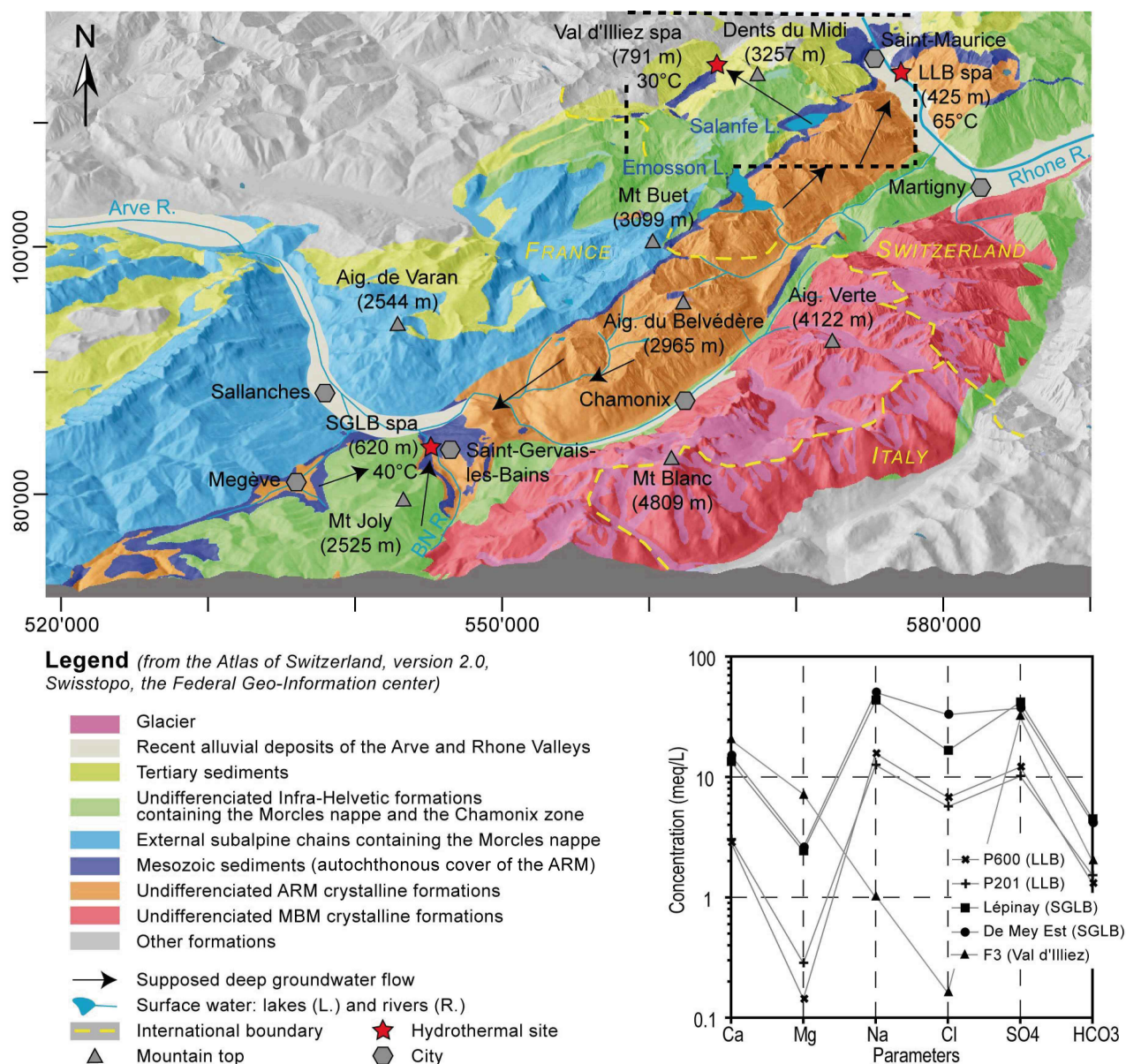
Figure 14.9: Regional conceptual model of the different flow paths ending to the hydrothermal systems of val d'Illiez, Lavey-les-bains (LLB) and Saint-Gervais-les-Bains (SGLB). Major element concentration plot (modified Shoeller diagram) for the well F3 in the Val d'Illiez is compared to waters of the two production deep boreholes in Lavey-les-Bains (P600 and P201) and in Saint-Gervais-les-Bains (Lépinay and De Mey Est). Location refers to the Swiss kilometric coordinates in projection, in standard CH1903. ARM: Aiguilles Rouges Massif, MBM: Mont-Blanc Massif.
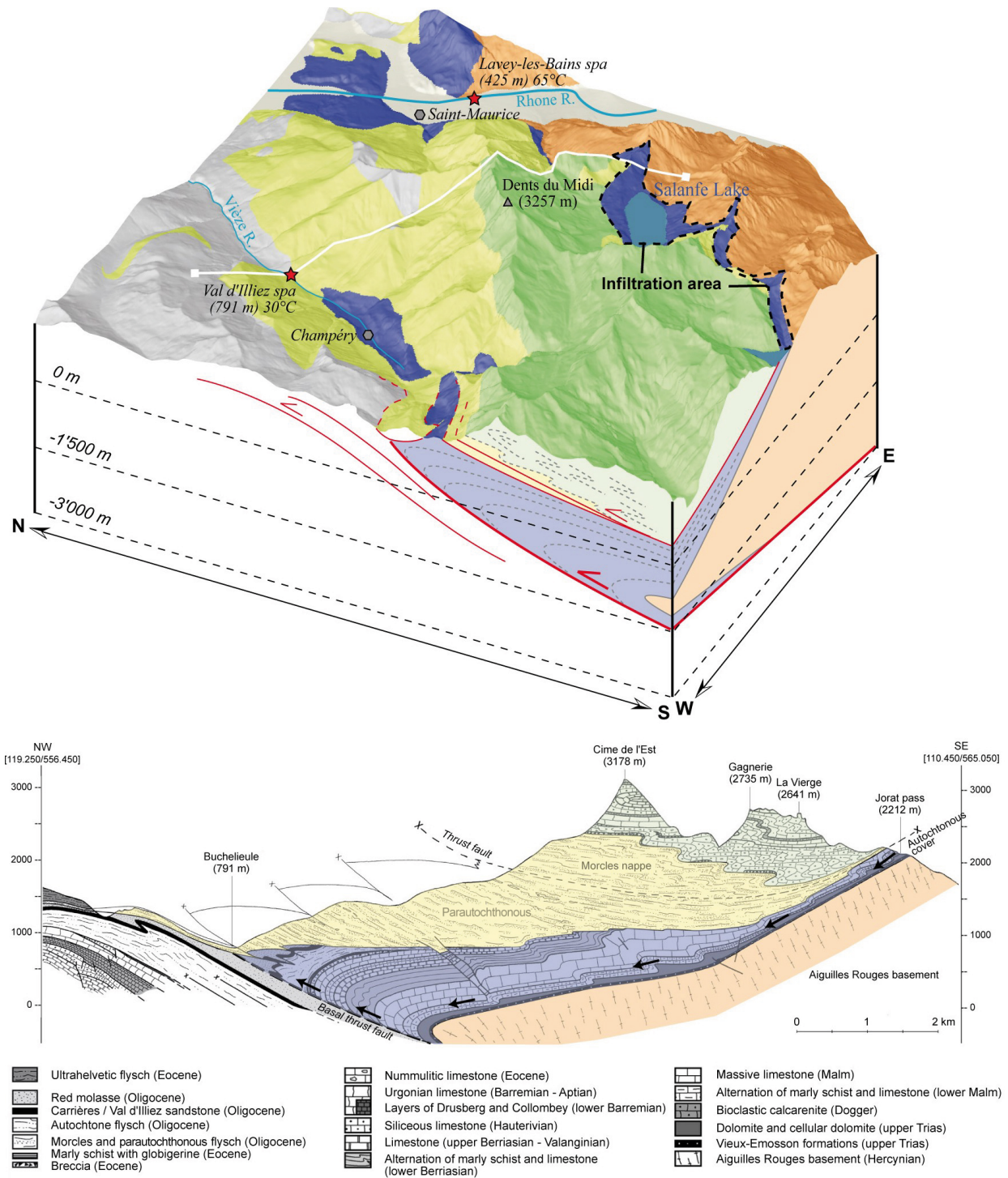
Figure 14.10: Regional conceptual model of the Val d'Illiez hydrothermal system. The cross section showing the sedimentary formation of the autochthonous cover (Pantet 2004) goes through the Val d'Illiez spa and the Salanfe Lake region (line white in the 3D feature).

14.2.2 Mean elevation of the recharge zone

The mean elevation of the recharge zone was studied with data of water stable isotopes and with equations from Kullin and Schmassmann (1991) for the Bernese Alps, Blavoux (1978) for the Lemanic Prealps, Bortolami et al. (1979) for the Maritime Alps and Vuataz (1982) for the Northern Alps. Results illustrated in Table 14.8 and Figure 14.11 are concordant with assumptions formulated in the study of the regional deep flow system and mixing processes. Firstly, isotope values for Val d'Illiez thermal waters in F1, F2 and F3 wells indicate a recharge zone close to the elevation of Salanfe Lake (roughly of 1900 m), which would tend to confirm that thermal waters are slightly diluted with waters infiltrated at lower elevation. Moreover, these isotope values in waters for the Val d'Illiez wells are similar to those measured in thermal waters at Lavey-les-Bains and Saint-Gervais-les-Bains, where the previous calculations gave an elevation of the recharge area in the range of 1700-2100 metres that is to say the mean elevation of the Aiguilles Rouges Massif.

Measurements of water stable isotopes in thermal and cold waters in the Val d'Illiez also highlight the occurrences of mixing processes between a thermal end-member recharged at higher elevation and a cold component flowing at lower elevations. Indeed, the well waters have the lowest isotope values whereas the cold springs have the highest, and between, Cascade diluted waters have intermediate values. But looking at calculations made on the cold springs, some of the results are unrealistic us-

ing equations in Table 14.8, that is to say lower than the elevation of the sampling point. This could result in error analysis or in evaporation effects of cold waters caused by air temperature during the sampling campaign in June 2009. Thus isotopes values for cold springs 1 and 3 have to be considered with caution because they give unrealistic results with equations in Table 14.8. Finally, Val d'Illiez, Lavey-les-Bains and Saint-Gervais-les-Bains isotope values are aligned along the World Meteoric Water Line of Craig (1961), as are the Alpine thermal waters (Fig. 14.11).
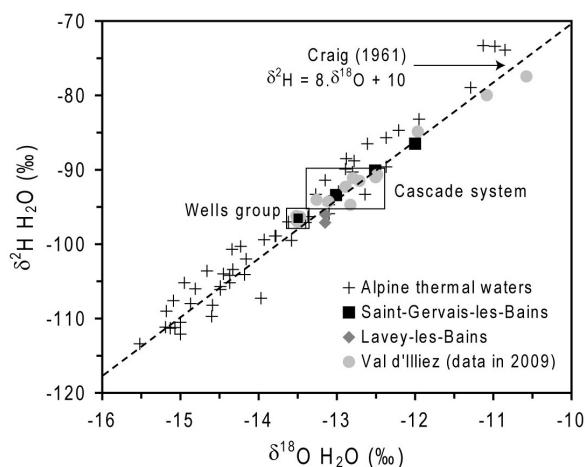
Figure 14.11: Water stable isotopes plot for Alpine thermal waters.

14.2.3 Reservoir temperature

Evaluation with geothermometers

Traditional and multi-component geothermometers have been applied to estimate the reservoir temperature for the Val d'Illiez hydrothermal system. First geothermal assessments of the reservoir temperature in the Val d'Illiez from Bianchetti et al. (1992) indicated that the reservoir temperature should probably not exceed 35-40°C. Looking at chalcedony geothermometers based on the total dissolved silica calculated in the thermal end-member (Table 14.9), obtained results are significantly lower

than emergence temperatures of thermal waters including the wells and Cascade springs (1 to 12°C of difference). This low calculated reservoir temperature can be explained by different manners. Firstly, the deep hydrothermal fluid is most probably never in contact with crystalline rocks and consequently cannot dissolve enough silicate minerals on which the main geothermometers are based (Bianchetti et al. 1996). The origin of the dissolved silica in thermal waters in the Val d'Illiez is explained by Mandia

242

Table 14.8: Calculated elevation of the infiltration area with the water stable isotopes for waters of Val d'Illiez. Location of sampling points are given in Figures 12.3 and 12.4. Isotope-elevation equations in Switzerland and neighbouring areas are given in the chapter 2.2.9 and in Pearson et al. (1991). Some of these equations were not selected for this hydrothermal system.

Sampling date	Sampling points	$\delta^{18}O$ (H_2O) ‰	δ^2H (H_2O) ‰
15.06.2009	F1a+b	-13.52	-96.2
16.06.2009	F2	-12.83	-94.7
15.06.2009	F3	-13.50	-97.0
16.06.2009	Cascade Right	-13.26	-94.0
-	Cascade Centre	-12.89	-92.3
-	Zone de Repos Sp.	-13.47	-96.33
15.06.2009	Cold Spring 1	-9.51	-72.7
-	Cold Spring 2	-11.08	-80.0
-	Cold Spring 3	-10.58	-77.5
16.06.2009	Vièze River	-11.97	-84.6

Domain, reference		Calculated elevation (m)	
	F1a+b	2010	1863
	F2	1604	1747
	F3	2000	1923
Bernese Alps	Cascade Right	1858	1695
	Cascade Centre	1640	1561
Kullin and Schmassmann 1991	Zone de Repos Sp.	1981	1871
	Cold Spring 1	-	50
	Cold Spring 2	578	614
	Cold Spring 3	280	419
	Vièze River	1097	989
	F1a+b	1861	1766
	F2	1608	1697
	F3	1855	1802
Jura, Northern Alps	Cascade Right	1766	1666
	Cascade Centre	1630	1586
Vuataz 1982	Zone de Repos Sp.	1843	1771
	Cold Spring 1	392	685
	Cold Spring 2	968	1021
	Cold Spring 3	782	905
	Vièze River	1291	1245
	F1a+b	1806	1645
	F2	1576	1584
	F3	1800	1676
Lemanic Prealps	Cascade Right	1720	1558
	Cascade Centre	1596	1487
Blavoux 1978	Zone de Repos Sp.	1789	1649
	Cold Spring 1	472	702
	Cold Spring 2	994	995
	Cold Spring 3	826	894
	Vièze Rivert	1288	1191
	F1a+b	1759	1812
	F2	1538	1751
	F3	1753	1843
Maritime Prealps	Cascade Right	1676	1725
	Cascade Centre	1557	1654
Bortolami et al. 1978	Zone de Repos Sp.	1743	1816
	Cold Spring 1	476	865
	Cold Spring 2	979	1160
	Cold Spring 3	816	1058
	Vièze River	1261	1356

(1991) based on leaching tests with Triassic rocks. Mandia specifies that groundwaters dissolving gypsum have low silica contents, whereas groundwaters in detrital rocks such as cellular dolomite, argillite and quartzite have higher silica values, reaching 10-15 mg/L, because these rocks contain quartz grains derived from erosion of crystalline rocks. But generally, the silica geothermometer cannot be used in the case of hydrothermal systems in Alpine Triassic formations because they systematically underestimate the reservoir temperature.

The isotope geothermometer using the fractionation of oxygen-18 of sulphate showed a reservoir temperature of 45°C and 33°C respectively with equations of Lloyd (1968) and Mizutani and Rafter (1969). Results are certainly at the origin of the first geothermal assessment, but conditions of application (beyond 100°C in geothermal fields) described by Fournier (1981) do not relate to the hydrothermal system of the Val d'Illiez having a different geothermal setting. Based on the assumption that the reservoir temperature is effectively close to 35-40°C according to the deep flow system highlighted in Figures 14.9 and 14.10, calculated temperatures using isotope geothermometers would be a mathematical coincidence. The cationic geothermometer of Fournier and Potter (1979) using the magnesium correction was also tested in the case of Val d'Illiez and the obtained result largely overestimated the reservoir temperature (155°C). Application of this geothermometer derived from the Na-K-Ca geothermometer, is more suitable for high-enthalpy geothermal systems (> 150°C), containing waters reaching equilibrium with feldspars (Fournier 1981), thus different conditions compared to Val d'Illiez. Moreover, results using other cationic geothermometers from Arnórsson (1983), Fournier (1977), Fournier and Truesdell (1973), Giggenbach (1988), Kharaka et al. (1982), Kharaka and Mariner (1989), Truesdell (1976) and Verma and Santoyo (1997) were not considered in this study. Finally, the K^2/Mg geothermometer gives unrealistic results with Fournier (1977) and Giggenbach (1988) equations.

The hydrothermal regime of Val d'Illiez occurs in Triassic formations and thus the Ca/Mg geothermometer of Marini et al. (1986) was also tested. This had been developed in the evaporitic environment in the Italian Alps. But the calculated value of 93°C is not in agreement with the conceptual hydrogeological model proposed in Figures 14.9 and 14.10. Furthermore, flow rates of thermal waters in the Val d'Illiez are relatively high: at about 1400 L/min for the warmest waters in wells and up to 600 L/min for Cascade springs. This should prevent any major conductive cooling processes during the rise of the deep fluid, and therefore the reservoir temperature should not be much higher than the emergence temperature (Bianchetti et al. 1992).

Table 14.9: Calculated reservoir temperatures using a selection of chemical geothermometers for Val d'Illiez hydrothermal system illustrated in chapter 2.2.10 and in Arnórsson 2000. For Lépinay and De Mey Est, the used chemical data come from the calculated thermal end-member from Table 14.6.

Reference	Equation	Calculated temperature using the thermal end-member (°C)
Fournier (1977)	$T_{SiO2,chalcedony}$	18
Arnórsson et al. (1983)	$T_{SiO2,chalcedony}$	22
Fournier and Potter (1979)	$T_{Na-K-Ca-(Mg-correction)}$	155
Fournier (1977)	$T_{K^2/Mg}$	-59
Giggenbach (1988)	$T_{K^2/Mg}$	11
Marini et al. (1986)	$T_{Ca/Mg}$	93
Lloyd (1968)	$T_{\delta^{18}O}$	45 (a)
Mizutani and Rafter (1969)	$T_{\delta^{18}O}$	33 (a)

(a): oxygen-18 isotope values from Bianchetti 1993b, measured in Captage A.

Evaluation with saturation indices

The variation of saturation indices of main minerals forming the host rocks with an increase of temperature from 30°C to 100°C was simulated with the PHREEQC code. The composition of the calculated thermal end-member was used to calculate saturation indices (Fig. 14.12). In this geochemical simulation, it can be supposed that the deep reservoir does not have a temperature higher than 100°C as assumed by the conceptual deep flow system in Figures 14.9 and 14.10.

Intersection of lines with the chemical equilibrium (SI=0) for all minerals remains dispersed along the selected interval of temperatures, and therefore this method of investigation gives no relevant results to evaluate the reservoir temperature (Fig. 14.12). However it should be mentioned that the variation of saturation indices with an increase of temperature does not suggest that reservoir temperatures are significantly warmer than the emergence temperatures.
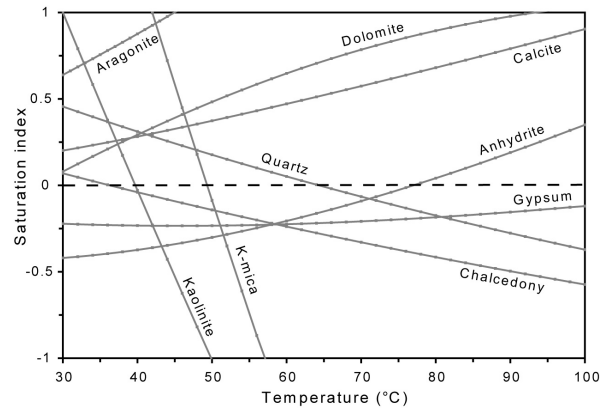
Figure 14.12: Simulation of mineral saturation indices versus temperature plot using the calculated thermal end-member in the Val d'Illiez.

14.2.4 Depth evaluation of the reservoir

The depth evaluation of the reservoir was initially described by Bianchetti et al. (1992), and this section takes into account their comments. The Triassic rocks outcropping at Salanfe are dipping at about 30° towards the north-west (Figs. 14.9 and 14.10). Due to the presence of fractured zones and sink holes, these sediments represent the ideal pathway for the infiltration of surface water. Assuming that these layers are homogeneous at depth, the Triassic reservoir should be deeper than 1500 metres below the Val d'Illiez thermal area. However, the presence of Cretaceous limestones in the Champéry region (Lanterno 1954), belonging to the upper part of the autochthonous cover, requires the existence of an anticline at depth having a fold axis more or less parallel to the valley axis. This anticline would raise the Triassic rocks less than 1000 metres below the Val d'Illiez spring zone. According to the geological cross section of Pantet (2004), this anticline should thrust younger formations with a fault system probably related deeply to the thrust fault putting in contact the Aiguilles Rouges and Infra-Aiguilles Rouges Massifs.

This depth evaluation of the reservoir at about 1 kilometre below Val d'Illiez according to the geological investigation is in agreement with a reservoir temperature of around 35°C, assuming a mean regional geothermal gradient of 15°C/km from the recharge zone in Salanfe area (roughly of 1900 m).

14.2.5 Groundwater residence time

Assuming that the groundwater residence time of the hydrothermal system of Val d'Illiez is relatively short (several months or years), according to the high tritium values and the hydraulic relations between Salanfe Lake and Val d'Illiez thermal springs previously described, several tracer tests were carried out with dyes (Pantet 2004, Schneider 1982 in Bianchetti et al. 1992, Sesiano 2003). Hydrogeological investigations with tracer tests failed to assess the residence time because results of these tests have long been discussed and sometimes disapproved. Bianchetti et al. (1992), indicating that even though the investigations of the present study indicate that the water infiltrates through

245

the Salanfe basin and percolates through a shallower pathway than the one proposed by Schneider (1982), the groundwater residence time needed to reach the Val d'Illiez area would be too long to be successfully evaluated by means of a tracer test with dyes. Therefore, Bianchetti et al. (1992) proposed a groundwater residence time of the deep thermal fluid in the range of 10-15 years according to tritium isotope measurements in Val d'Illiez thermal and cold waters in 1990. Indeed, at that time the thermal end-member had an average tritium content of around 40 T.U. quite different from that of the cold groundwaters of around 24 T.U. (Table 14.10).

Later, a new tritium analysis was carried out in thermal water from the well F3 in May 2005, this water being the most representative of the thermal end-member. Aiming to evaluate the residence time using the piston flow model described in the section 2.2.11., a new sampling campaign was undertaken in June 2009 on cold and thermal waters. Results are illustrated in appendix D. To use the piston flow model, average values of tritium isotope data in surface waters from Switzerland were used (Table 14.10).

Firstly, all tritium data were plotted with the electrical conductivity (Fig. 14.13). The first sampling campaign in 1990 showed that the thermal end-member was richer in tritium compared to cold surface and shallower groundwaters, with a good correlation with the electrical conductivity involving occurrences of mixing processes. This first observation in 1990 indicated that the thermal end-member is younger than the first atmospheric weapon testing with a residence time higher than cold groundwaters. This is different from the situation in the deep flow systems of Lavey-les-Bains and Saint-Gervais-les-Bains in crystalline domain, where the thermal end-member has a low tritium contents close to zero (older than atmospheric weapon testing). Later in 2009, this trend is reversed because the thermal end-member in the Val d'Illiez contains slightly less tritium than cold waters mixing (6 T.U. against 8 T.U.), with a correlation coefficient of 0.78. This can be explained assuming that the thermal end-member had been infiltrated with tritium values between 8 and at about 15 T.U., that is to say early 2000's.

The piston-flow model was used to calculate the residence time (Fig. 14.14). This method takes into account the simplest case study of pathway assuming that water infiltrates in a well defined area and flows like in a pipe towards the spring without mixing process. This simplified case is certainly not representative of the deep flow system of Val d'Illiez. But considering the piston-flow model, the tritium concentration in the thermal end-member is only modified by the radioactive decay process (equation in section 2.2.11.). In the case study of the Val d'Illiez, the piston-flow model allowed an average residence time for the thermal end-member to be estimated at around 5 years, that is to say slightly lower than the initial evaluation in Bianchetti et al. (1992) which was in the range of 10-15 years.
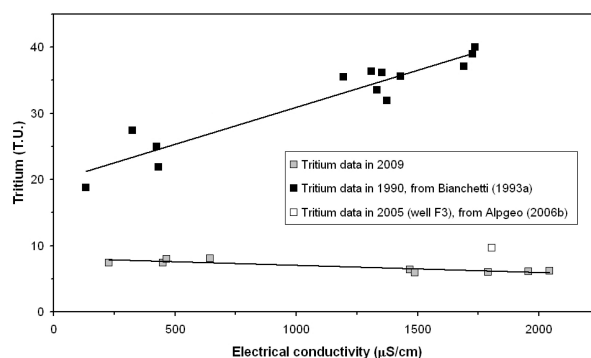
Figure 14.13: Correlation between electrical conductivity and tritium in cold and thermal waters in the Val d'Illiez. Conductivity measurements were carried out at 20°C by Bianchetti (1993b and 2006b) and at 25°C for this study. Used data are described in Table 14-10.
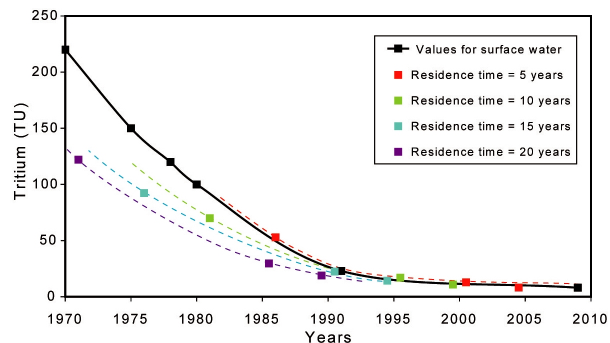
Figure 14.14: Evaluation of the groundwater residence time for the thermal end-member in the Val d'Illiez using tritium isotope data in the Val d'Illiez, average tritium values in surface waters from Switzerland since the seventies and the piston flow model described in section 2.2.11.

Table 14.10: Tritium isotope data in cold and thermal groundwaters in Val d'Illiez. Average values of tritium isotope data in surface waters from Switzerland since the seventies.

Reference	Sampling point	Date	Temp. (°C)	Elec. Cond. (μS/cm, 20°C)	Tritium (T.U.)
This study	Mixed F1	16.06.2009	21.8	1467 (a)	6.4 ± 0.4
-	Well F2	16.06.2009	27.9	1956 (a)	6.1 ± 0.7
-	Well F3	15.06.2009	27.9	2042 (a)	6.2 ± 0.4
Alpgeo (2006b)	-	30.05.2005	30	1804	9.7 ± 0.9
Bianchetti (1993b)	Captage A	05.02.1990	29.5	1727	39
-	-	16.08.1990	29.6	1691	37.1
-	-	20.12.1990	29.5	1735	40
This study	Cascade Right	16.06.2009	22.7	1789 (a)	6 ± 0.5
Bianchetti (1993b)	Cascade Centre	05.02.1990	23.1	1430	35.6
-	-	16.08.1990	23.1	1195	35.5
-	-	06.12.1990	22.6	1310	36.4
This study	Cave	15.06.2009	22.4	1489 (a)	5.9 ± 0.7
Bianchetti (1993b)	Subthermal Sp.	05.02.1990	14	1374	31.9
-	-	16.08.1990	22.4	1332	33.5
-	-	06.12.1990	16.9	1353	36.2
This study	Cold Spring 1	15.06.2009	19.8	645 (a)	8.1 ± 0.6
-	Cold Spring 2	15.06.2009	12.7	451 (a)	7.4 ± 0.5
-	Cold Spring 3	15.06.2009	9.9	466 (a)	8 ± 0.8
Bianchetti (1993b)	Vièze River	05.02.1990	2.3	432	21.9
-	-	16.08.1990	12.6	324	27.4
-	-	06.12.1990	1.1	424	25
This study	-	16.06.2009	11.6	228 (a)	7.4 ± 0.4
Bianchetti (1993b)	Salanfe Lake	12.09.1990	11.9	134	18.8

Range of values of tritium isotope data in surface waters from Switzerland.

Reference	Date	Tritium (T.U.)
Pearson et al. (1991)	1970	250 ± 20
-	1975	150 ± 15
Vuataz (1982)	1977-1978	120 ± 10
-	1980	100 ± 10
Bianchetti (1993b)	1990	23 ± 5
Schotterer et al. (2000)	1993-1999	15 ± 5
This study	2009	8 ± 1

(a): electrical conductivity at 25°C

15

Two-dimensional vertical modelling of groundwater flow and heat transport

15.1   Objectives

THE hydrothermal system of Val d'Illiez has never been represented with a numerical model of groundwater flow and heat transport as well as Lavey-les-Bains and Saint-Gervais-les-Bains. A first numerical approach with a two-dimensional model was thus carried out in this study aiming to represent the deep flow system occurring in the autochthonous cover of the Aiguilles Rouges Massif. Moreover, other objectives were:

- To represent the temperature field in the autochthonous cover from the recharge zone to the Val d'Illiez using assigned parameters in the model (water fluxes, hydraulic conductivities of rocks, geothermal heat flux, etc.).

- To evaluate the reservoir temperature and to simulate the heat losses from conduction processes up to the surface.

- To understand the role of Salanfe Lake in the thermal regime, that is to say to know if the lake can be considered as a imposed hydraulic head in the model, or should be considered as a single increase of infiltration in the deep flow system.

- To evaluate the approximate width of the recharge zone using the water balance in the model and the flow rates of the springs in the Val d'Illiez, that is to say to know if the recharge zone is limited only to the Salanfe basin or if it extends there along Triassic formations outcropping on the edge of the Aiguilles Rouges crystalline Massif.

- To understand the role of the crystalline basement below the autochthonous cover in heat processes, that is to say if the basement acts as a natural heat exchanger assuming that the basement is less influenced by cooling process from infiltrated water (lower permeabilities compared to Triassic rocks).

- To validate the groundwater residence time calculated with tritium data analysed at different time and the piston flow model.

A simplified two-dimensional model was thus built in the Dents du Midi Massif based on a regional NE-SW geological cross section going through the Val d'Illiez and Salanfe and adapted

from Pantet (2004) (Fig. 15.1). As for Lavey-les-Bains and Saint-Gervais-les-Bains, initial conditions of groundwater flow and heat transport were calibrated using data from literature and spring/well measurements. Natural springs and wells flow were added to the model but none is under pumping.

The complicated geological structure in the hydrothermal area does not allow groundwater flows to be reproduced with a three-dimensional model of flow and heat transport. Indeed, this local geological setting is characterized by the presence of a thrust fault putting in contact parautochthonous and autochthonous flysch. Moreover, the autochthonous flysch where thermal waters upflow is also affected by thrust faults, and inside this flysch, an alternation of thin folded layers with various hydraulic conductivities occurs. For these reasons and with the data available, it is hardly possible to undertake a local three-dimensional model. Concerning a regional three-dimensional model, it is also difficult to carry out a good representative model because it was not possible to clearly demonstrate the flow path of the thermal water inside the autochthonous cover, i.e. if groundwater occurs in Malm and Cretaceous limestones.

15.2 Construction of the model and assigned parameters

15.2.1 Geological boundary conditions

Geographically, the cross section extends from an area located at about 2 kilometres north-west of the Val d'Illiez to the Petits Perrons Massif where the basement outcrops. This cross section goes through the hydrothermal zone of Buchelieule, then the La Cathédrale top belonging to the Dents du midi Massif, and Salanfe Lake after. The Vièze River is the main valley cut by the cross section and represents the lowest elevation point in the two-dimensional model (791 m, average elevation of the flood plain).

The two-dimensional model integrates all the geological horizons of the Aiguilles Rouges basement and its autochthonous cover down to a thickness of 500 metres below the sea level (Fig. 15.1), considered as the base of deep circulations according to Bianchetti et al. (1992) and Pantet (2004) and linked to the presence of a major thrust fault which extends at depth between the Aiguilles Rouges and Infra-Aiguilles Rouges basements (Pfiffner et al. 1997). The prolongation of this major fault towards the south-western and north-eastern directions along the Vièze Valley was assumed but difficult to see in the field because it is hidden by overlapping geological units.

In detail, the autochthonous cover was divided into five main geological units for the modelling: 1) the Triassic formations composed of quartzite, cellular dolomite, dolomite and gypsum were gathered into one main unit, 2) the Malm which was subdivided into two horizons differentiating the marly part (lower Malm) and massive limestone (upper Malm), 3) the lower Berriasian mainly consisting of marl, 4) the Cretaceous massive limestone, 5) and finally the Tertiary rocks including the autochthonous flysch (Fig. 15.1). The geological structure of these horizons was simplified for the model to avoid complicated calculation. Small folds were represented in the series, and to ensure continuity of layers in the model, no fault has been added.

The parautochthonous flysch and the Morcles nappe forming the Dents du Midi Massif were not taken into account for the simulation. Indeed, it can be assumed that the hydrothermal regime leading to the Val d'Illiez springs only occurs in the Aiguilles Rouges horizons. Groundwaters in the parautochthonous flysch and Morcles nappe probably do not participate in the hydrothermal system, but supply cold springs having emergence elevations significantly higher than the Val d'Illiez springs. In the north-western part of the cross section, a small zone with parautochthonous flysch was considered with the aim to represent the cold end-member diluting the uprising thermal fluid.

Finally, the hydrothermal zone of Val d'Illiez is located on Quaternary formations having low thickness (< 50 m) including the recent Vièze deposits and the moraine which is visible on the slopes. The Quaternary cover was not added in the numerical model because it has a low thickness compared to the scale of the cross section, up to 15 kilometres in length. The thrust fault system highlighted at the front of the autochthonous cover was differentiated for the simulation. It certainly allows a fast uprising of the deep thermal fluid to the surface.

Jurassic-Cretaceous - Morcles nappe

Oligocene - Morcles and parautochthonous flysch

Eocene-Oligocene - Autochthonous flysch, Val d'Illiez
sanstone and red molasse

Cretaceous - limestone (upper Berriasian to Urgonian)

Lower Berriasian - marly schist and limestone

Jurassic - calcarenite (Dogger), marly schist and
limestone (lower Malm), massive limestone (Malm)

Triassic - Vieux-Emosson formations, dolomite
and cellular dolomite

Hercynian - Aiguilles Rouges basement
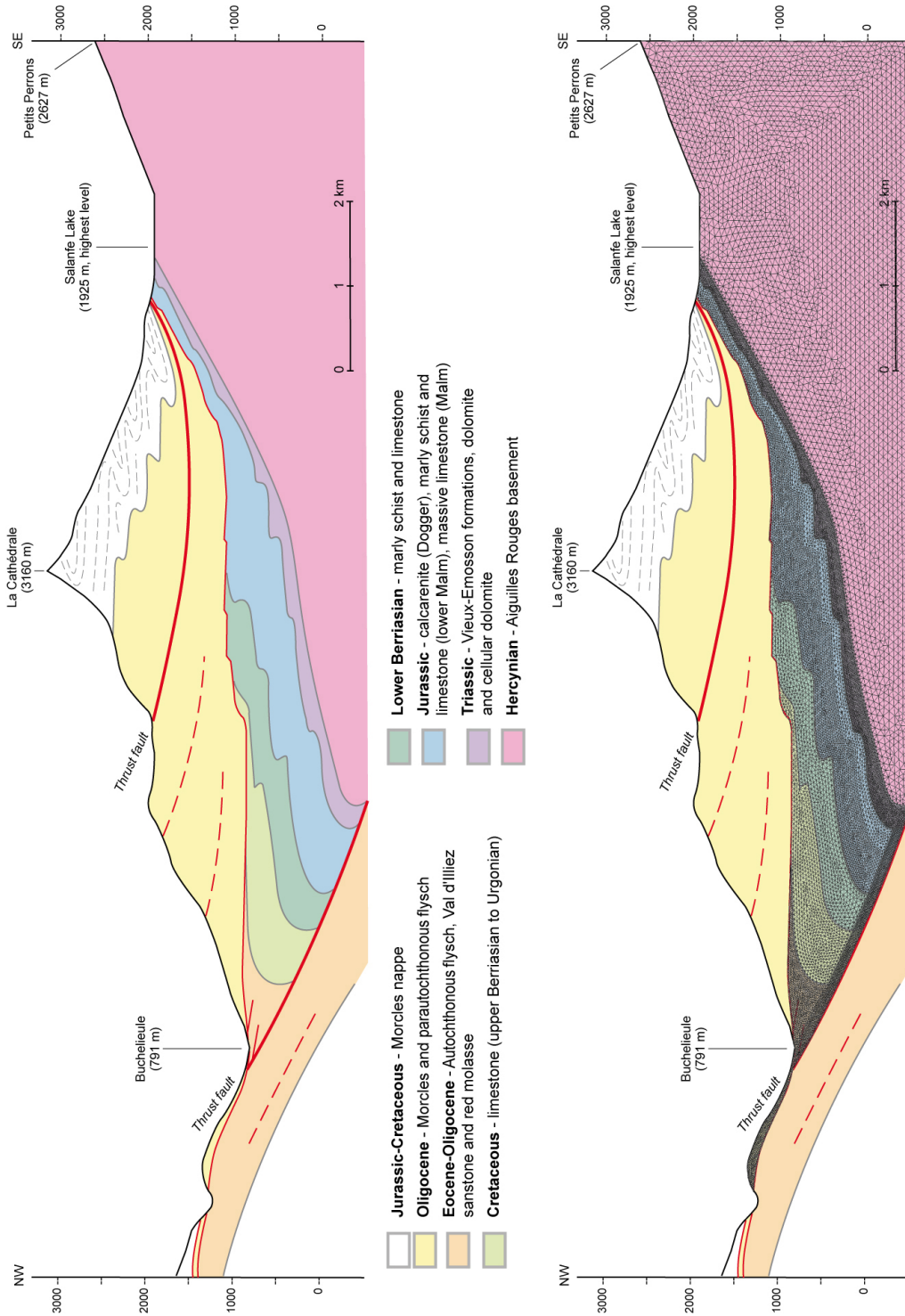
Figure 15.1: Geological cross section of the two-dimensional model for flow and heat transport in the Aiguilles Rouges crystalline Massif and its autochthonous cover, and finite element mesh geometry of the two-dimensional vertical model. This cross section of Pantet (2004) in Figures 13.3 and 14.8 was used and slightly adjusted in the Salanfe area.

251

15.2.2 Discretization of the geological cross section

The two-dimensional model consists of nine sub-domains having various sizes. Each sub-domain allow differentiating geological horizons with different physical properties such as the Aiguilles Rouges basement, Triassic formations, lower Malm, upper Malm, lower Berriasian, upper Berriasian to Urgonian, Tertiary autochthonous flysch, parautochthonous flysch and thrust fault zone.

Through this, it will be possible for the simulation to assign refined meshes in sub-domains where groundwater mainly occurs. Therefore, a selected number of cells were assigned to each sub-domain, of three-nodded triangle type. In total, the two-dimensional model contains about 31'000 mesh elements in an area close to 2.10^7 square metres.

15.2.3 Assigned parameters in the model

Assigned parameters in the two-dimensional model of groundwater flow and heat transport are summarized in Table 15.1. Imposed values come from data in literature, spring/well measurements, and were documented in the Swiss Federal Office of Meteorology and Climatology for regional precipi-

tations and surface temperatures. In several zones with a lack of data, imposed values were extrapolated. Finally, this section describes types and values of the assigned parameters while starting from flow conditions, then properties of materials and finally heat conditions.

Flow parameters

Looking at the two-dimensional model of the Val d'Illiez, flow parameters refer to water fluxes defining recharge zones from precipitations through the Aiguilles Rouges sedimentary cover. They also refer to hydraulic heads being able to characterize inflow or outflow points in the model. Concerning water fluxes or infiltration, they were estimated from precipitations removing the effective evapotranspiration, the surface runoff and the variation of storage. In the Aiguilles Rouges area, infiltrations through the sedimentary formations are certainly different compared to those occurring in the crystalline basement. As a reminder, infiltrations within the basement are heterogeneous with the depth and depend on the presence of major fractures in the so-called decompressed zone which supports the storage of cold waters (Lhomme et al. 1996). Concerning the sedimentary cover of the Aiguilles Rouges, infiltrations do not depend on the presence of faults but mainly occur in areas where highly permeable rocks outcrop which can be subjected to karstic processes. For example, it had been observed that the presence of sinkholes in the Triassic cellular dolomite which allow the infiltration of water from the Salanfe Lake. The amount of water which really infiltrates at depth in the autochthonous cover and takes part in the thermal regime is difficult to evaluate in this context be-

cause some of these sinkholes supply cold springs in the Salanfe area. For the simulation, the effective average groundwater recharge has been evaluated as roughly of 10% of precipitation. This relatively low value is also related to the importance of surface runoff, developed in high mountain areas due to the accentuated topography limiting the infiltration, as assumed for other numerical investigations. Moreover, the covering of glacial deposits on the Triassic formations often occurs and can prevent water from infiltrating. Finally, the recharge of groundwater in high mountain domains also depends on the seasonal climatic conditions. The winter is associated to the lowest infiltration values due to the storage of snow. The most important recharge of water in the autochthonous cover probably occurs during the period of the snow melt in summer.

The geographical distribution of water fluxes in the two-dimensional model concerns two areas. The first area is located in the Salanfe area is where the autochthonous cover outcrops. According to data of the Swiss Meteorology and Climatology Federal Office, the assigned infiltration corresponds to 10% of the 2000 mm/yr average annual precipitation occurring at Salanfe which is illustrated in the Atlas de la Suisse (version 2.0, Fig. 15.2). Areas located towards the south-east of the Salanfe Lake, where crystalline rocks are present, were not considered as

recharge zones in the model. It is difficult to determine if part of groundwaters in the decompressed zone discharges into the sedimentary formations. The second area with infiltration in the model is located along the parautochthonous cover forming the north-western mountain slope from the Val d'Illiez. For the simulation, it was decided to assign an infiltration value of 10% of the 1500 mm/yr according to data visible in Figure 15.2. This zone with groundwater corresponds to the cold end-member diluting the uprising thermal water in the Val d'Illiez.

A hydraulic head equal to its elevation was imposed in the Vièze Valley. The Vièze Valley is the lowest elevation point in the model, and this represents the discharged point out of the model. Consequently, the computed water table in the model will go through this point, and it will be possible to calculate the value of discharged water in the Val d'Illiez which is also the sum of infiltrated water from both areas. Later in the model, a hydraulic head will be imposed in the Salanfe area equal to the mean elevation of the lake with the aim of understanding the relation between Salanfe and the Val d'Illiez springs, and to view the impact on the simulated temperatures in the autochthonous cover.

Hydraulic parameters

This section describes hydraulic parameters imposed to the two-dimensional model and illustrated in Table 15.1. They concern the hydraulic conductivities with anisotropy factors and the porosities of the rocks. Anisotropy factors were assigned in two sub-domains to represent the fractured conditions at the origin of the deep flow system.

The values of hydraulic conductivities in rocks were assigned according to data documented in the literature. This parameter directly controls groundwater flows in the model and thus the simulated temperature field. The calibration of the conductivities required much time during the construction of the model. In this case study, the change of the geological unit is related to a change in the imposed hydraulic conductivity.

Concerning the Aiguilles Rouges basement, the calibration of the model required a hydraulic conductivity of 10^{-9} m/s to be imposed without defining the presence of the decompressed zone. This imposed value seems to be overestimated compared to conductivities measured in crystalline rocks in tunnels and galleries where values can be lower than 10^{-10} m/s (Maréchal 1998 and 1999a). Lower conductivities in the basement were tested for the simulation, and beyond 10^{-9} m/s the simulated temperature field does not vary. The conductivity along this NW-SE direction in the model is certainly lower than the conductivity in the SW-NE direction because the basement is affected by SW-NE to SSW-NNE fracturing. Moreover, an anisotropy factor in the conductivity of $K_{horizontal}/K_{vertical} = 5$ with anti-clockwise angle from the horizontal axis of 90° was assigned in the basement aiming to reproduce fracturing conditions at the origin of water infiltration in the massif. For the calibration of the model,

this geological unit has a great interest because it allows a heat transfer to other horizons above.

Higher hydraulic conductivities were imposed to horizons of the sedimentary formations including the autochthonous cover and the parautochthonous flysch (Table 15.1). Firstly, the highest value of conductivity (10^{-4} m/s) was assigned to thrust fault zone at the front of the model, with an anisotropy factor of $K_{horizontal}/K_{vertical} = 10$ reproducing the physical conditions in the thrust fault at the origin of the natural uprising. The consideration of a thrust zone for the simulation with a high value of conductivity allows heat losses by conduction process with host rocks to be limited in the model. For the other sedimentary sub-domains, a hydraulic conductivity of 5.10^{-6} m/s was selected for the Triassic formations at the bottom of the autochthonous cover where the deep flow system mainly occurs. This value represents the second highest value and can be justified by the presence of fractured cellular dolomite, dolomite, limestone and gypsum which can be subjected locally to karstic processes. For the same reasons, both geological units with massive limestone (Malm and lower Cretaceous) were considered with a conductivity close to that of the Triassic formations (3.10^{-6} m/s). Then, both sub-domains symbolizing marl and marly limestone of the Lower Malm and Lower Berriasian were described as low-permeable layer in the model with a conductivity of 10^{-7} m/s, that is to say 30 times lower than the massive limestone. Finally for the parautochthonous and autochthonous flysch composed of various detrital deposits, a conductivity value of 10^{-6} m/s was assigned. Because of the heterogeneity of layers in the flysch with various permeabilities, it is difficult to allocate a representative average value of conductivity.

253
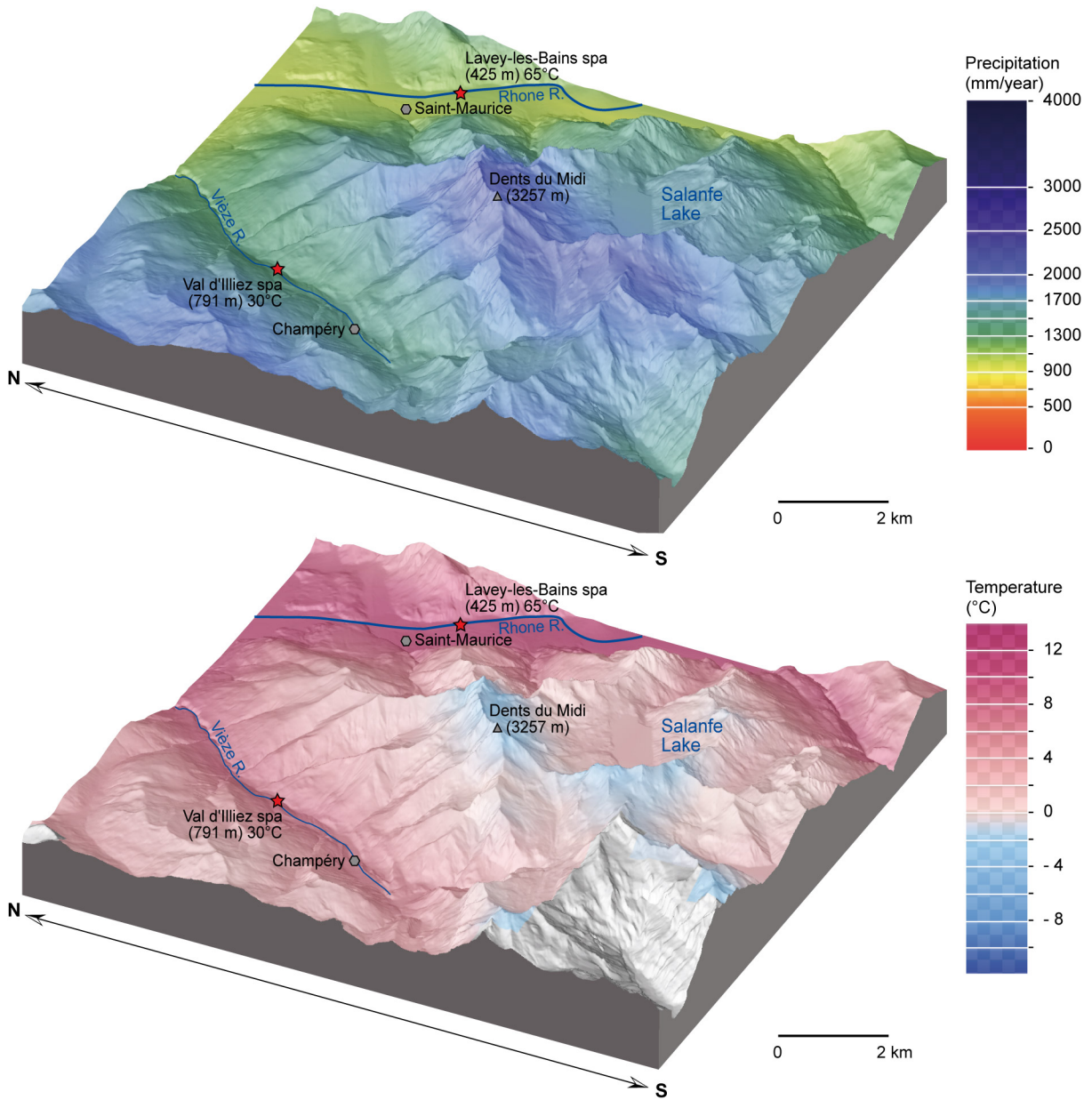
Figure 15.2: Precipitation and temperature maps for the regional area of Val d'Illiez (Atlas de la Suisse, version 2.0). Temperature ranges are equivalent to the average annual temperature.

Table 15.1: Comparison of observed/evaluated and imposed/simulated values for geological and geothermal boundary conditions for the two-dimensional model of Val d'Illiez. hor.: horizontal, vert.: vertical, obs.: observed, comp.: computed, calc.: calculated, resid.: residence and wat.: water.

Boundary conditions	Obs./Eval. values	Imposed values
Water recharge (mountain condition)	1 to 20% of precip.	10% of precip.
Imposed hydraulic head (m)		Elevation of Vièze R.
Surface temperature (°C)	0-8	0-8
Hydraulic conductivity (m/s)		
Decompressed zone of the Aiguilles Rouges	Not considered in this model	
Aiguilles Rouges basement	10^{-6} to 10^{-12}	1.10^{-9}
Thrust fault below Val d'Illiez	10^{-2} to 10^{-5}	10^{-4}
Parautochthonous flysch	10^{-5} to 10^{-7}	10^{-6}
autochthonous flysch	10^{-5} to 10^{-7}	10^{-6}
Upper Berriasian to Urgonian limestone	10^{-5} to 10^{-7}	3.10^{-6}
Lower Berriasian marl	10^{-6} to 10^{-8}	10^{-7}
Upper Malm limestone	10^{-5} to 10^{-7}	3.10^{-6}
Lower Malm marl and limestone	10^{-5} to 10^{-8}	10^{-7}
Triassic formations	10^{-5} to 10^{-7}	5.10^{-6}
Conductivity anisotropy factor		
Aiguilles Rouges basement	K(hor.)/K(vert.) = 5 and 90°	
Thrust fault below Val d'Illiez	K(hor.)/K(vert.) = 10 and 150°	
Rock thermal conductivity (W/m/K)		
Aiguilles Rouges gneiss	2.65	2.5
Triassic formations	2-4	2.5
Other sedimentary horizons	2-3	2
Heat flux (mW/m^{-2})	80-90	85
Porosity (%)		
Aiguilles Rouges gneiss	< 10	1
Sedimentary formations	< 10	3
Location of obs./comp. temperature	Obs. T (°C)	Comp. T (°C)
Close to the surface	30	26
200 m below the surface	30-31	31
500 m below the surface	> 31	35
Calc. temperature at depth	35-45	36-40
Geothermal gradient (°C/km)	Obs. T (°C)	Comp. T (°C)
For the basement with low infiltration	20-30	32
For the autochthonous cover	15-20	20
Mean resid. time of deeper wat.(years)	5 (tritium piston flow model)	750-800

Thermal parameters

For the simulation of groundwater flow and heat transport, the surface temperatures were locally assigned in the model with data documented from the Swiss Federal Office of Meteorology and Climatology and illustrated in Figure 15.2. In detail, three areas are concerned in the model with imposed temperatures depending on their elevations. The first zone corresponds to the Salanfe area and the Petits Perrons Massif where surface temperatures were set between 0 and 2°C. In the Aiguilles Rouges Massif, an annual average temperature of 0°C can be measured at an elevation of about 2500 metres. The second zone is located between the Salanfe Lake and the Vièze Valley where temperatures were assigned along the geological limit between the parautochthonous and autochthonous flysch. In this case, it can be assumed that temperatures along this limit should be close to the annual average temperature at the elevation of the limit. This means that the temperature at the interface parautochthonous and autochthonous flysch should gradually increase between 2 and 8°C from the Salanfe Lake (1925 m) to the Vièze Valley (791 m). Finally, surface temperatures between 6 and 8°C were imposed along the parautochthonous cover in the north-western side of the model aiming to represent the shallow cold groundwater.

For the calibration of the two-dimensional model, a heat flux of 85 mW/m^2 was assigned at the bottom of the model, that is to say along the basement and along the thrust fault at the front of the model. This value is in agreement with data in the Swiss Alps according to the map of Medici and Rybach (1995) with a heat flux between 80 and 90 mW/m^2 in the central Alps domain. During the simulation, different tests carried out to compute a representative temperature field in the model have shown that it was not necessary to set a heat flux along the thrust fault.

The rock thermal conductivity is also an important parameter to be selected for the simulation, because a variation of this parameter will notably modify computed temperatures. Values of rock thermal conductivity vary from 0.6 to 5.8 W/m/K at ambient temperature (Rybach 1973). High values correspond to compact rocks poor in water (for example: ultrabasic rocks) whereas porous formations containing waters have values lesser than 1.5 W/m/K. Clark and Niblett (1956) studied the terrestrial heat flow in Swiss Alps and thermal conductivities of crystalline rocks. They showed that among 23 gneiss samples the thermal conductivity average value is 2.65 W/m/K. For the model calibration, a thermal conductivity value of 2.5 W/m/K was imposed for the dominantly gneissic Aiguilles Rouges basement. For the Triassic formations, which mainly consist of cellular dolomite, dolomite, limestone, gypsum and quartzite, an average thermal conductivity of 2.5 W/m/K was also assigned. Finally, the other sedimentary horizons composed of limestone, marl and flysch, were represented in the model with a value of 2 W/m/K.

15.3 Comparison with the natural state of the hydrothermal system (before the implementation of the Salanfe Lake)

15.3.1 Computed temperatures in steady state

The calibration of the two-dimensional model in steady state enabled the heat anomaly in the Val d'Illiez induced by the deep flow system to be reproduced (Fig. 15.3). The simulation was carried out excluding the assumption that successive glaciations entirely stopped advection processes in the massif. From a global view, the simulation showed a large cold plume below the top of the domain. It corresponds to infiltrations having for impact to cool the whole of the massif, especially in the autochthonous cover where hydraulic conductivities are higher. Computed temperatures in the massif depend on the capacity of waters to flow deeply in the model, controlled by hydraulic conductivities and the quantity of infiltrated water. The simulation also showed a heat plume from the bottom of the model to the Vièze Valley along the main thrust fault, due to the higher permeability assigned in the fractured zone along the thrust fault.

Figure 15.3: Cross section of the Val d'Illiez hydrothermal system showing the computed temperatures and hydraulic heads in the Aiguilles Rouges basement and its autochthonous cover.

Computed temperatures in the autochthonous flysch in the hydrothermal area vary from the surface to the thrust fault. This numerical result is controlled by the presence of lateral cold inflows from the parautochthonous flysch at the northwestern side of the Val d'Illiez area. Indeed, the computed temperature at the surface is 25.5°C due to mixing processes in the model with a cold groundwater. The result is slightly lower than the current temperatures of the wells close to the surface ($\approx$ 28-30°C) which are almost not influenced by mixing processes with a cold groundwater. But this simulated temperature is close to the values for all the Captage springs ($\approx$ 21-24°C) which are mixed at various degrees. In reality, the local hydraulic network of flow paths of end-members is complex and therefore, large lateral variations of temperature are possible at shallow depth. Unfortunately, it was not possible to represent the local geometry of the groundwater flows in the autochthonous flysch with a two-dimensional model in a regional scale. Moreover, the local geological setting inside the flysch in the Val d'Illiez is too complicated to be represented with a numerical model.

Down to 200 metres below the surface and along the thrust fault, the simulated temperature reaches 31°C and corresponds to the limit zone of mixing processes in the model. In reality, the influence of the cold end-member diluting the uprising thermal water can be observed to this depth, and according to the geochemical investigation, the temperature of the thermal end-member is certainly close to 30-31°C. At 500 metres depth in the model and along the thrust fault, the calculated temperature is at about 35°C. Without deep drilling investigation, it is not possible to determine if this value is in agreement with the reality. For the inferred deep reservoir, the calibration of the model gives computed temperatures of 36-40°C, assuming that they are in agreement with the previous geochemical investigations using fluid-mineral equilibrium in the reservoir. Consequently, the heat loss caused by conduction processes is relatively limited in the uprising zone along the thrust fault as assumed by Bianchetti et al. (1992).

Due to its assigned low hydraulic conductivity (10^{-9} m/s), the simulated temperature in the basement tends to increase more strongly than in the cover, because the deep flow system and its thermal impact mainly occurs in the cover. Consequently, the temperature in the basement cannot be buffered by groundwater and thus the geothermal gradient in this domain is more important ($\approx$ 32°C/km). On the contrary, the geothermal gradient in the autochthonous cover is lower ($\approx$ 20°C/km) because the deep flow system occurs with a thermal impact on the host rocks. These values seem to be in agreement with observations in massifs where the infiltration of water occurs to various degrees.

15.3.2   Computed groundwater for steady state flow

The two-dimensional model in a steady state makes it possible to obtain a reasonable picture of the hydraulic heads of the hydrothermal aquifer with decreasing values from the recharge zones to the outflow point of the model (Fig. 15.3). The top of the groundwater corresponds to the water table of which a simulated pressure equivalent to the atmospheric pressure was calculated. With the simulation, it was shown that the picture of the computed water table has a realistic form in the geological cross section including the autochthonous cover and the basement. It was also shown that the simulated water table in the model has a weak slope in the Aiguilles Rouges formations because the calculated hydraulic heads slightly vary between 800 and 816 metres from the thermal springs to the Salanfe area (Fig. 15.3). This process is simple to define because the calculated hydraulic heads depend on infiltrations assigned to the model. In this case, the infiltration in the Aiguilles Rouges cover appears weak i.e. 10% of the average annual precipitation on a limited area, that is to say 0.24 m^3/d/m, compared to the flow rate discharging in the Val d'Illiez ($>$ 1000 m^3/d). But the two-dimensional model evaluates the assigned infiltration with a third dimension of 1 metre. Consequently, the width of the watershed has to be considered for the calculation.

Assuming a watershed limited to the area of Salanfe, of which the width is close to 4 kilometres, the groundwater recharge reproducing the hydrothermal system in the model is at about 960 m^3/d (667 L/min). This result seems to underestimate the initial conditions of the system before the implementation of the Salanfe Lake, but this is

difficult to evaluate. Considering a wider recharge zone along the stripe of Triassic formations outcropping at the front of the Aiguilles Rouges crystalline rocks, of which the length can be evaluated of around 20 kilometres (Fig. 14.8), the groundwater recharge to reproduce the system in the model becomes 4800 m^3/d (3330 L/min). According to the geological structure of the autochthonous cover along the Aiguilles Rouges Massif, it is quite conceivable to have a natural flow system from infiltration zones much further away than the Salanfe area. This result could represent the natural state of the hydrothermal system before the implementation of the Salanfe Lake.

The shallower circulation in the parautochthonous flysch in the north-western side of the Val d'Illiez supplies in the model the mixing process in the final part of the uprising zone, with a flow rate at about 0.026 m^3/d/m. Consequently, the total discharged flow rate in the model is at about 0.27 m^3/d/m.

Using the particle tracking option in the model, an average residence time of the hydrothermal regime was evaluated in the range 750-800 years according to the imposed values of porosity in Table 15.1. Indeed, the computed residence time in the model depends on conductivities and porosities assigned. This result is not in agreement with the evaluation of the residence time from the piston flow model using the tritium data (about 5 years). This relatively short residence time provided a change of porosities can be reproduced in the model, but in this case these values should be lower than 0.03%, and are thus unrealistic.

15.4 Impact of the Salanfe Lake in the hydrothermal system

15.4.1 Objectives and used strategy for the simulation

After reproducing the natural state of the hydrothermal system of the Val d'Illiez before the implementation of the Salanfe Lake, it was decided to introduce this lake in the same two-dimensional model. Indeed, an increase of the infiltrated water in the model has to be considered because the water losses from the lake have a strong influence on the thermal regime such as the increase of the discharged thermal water in the Val d'Illiez, observed in 1953 and 1996. Firstly, the objective is to show the long-term thermal impact of the water losses in the hydrothermal system (steady state), because it can be assumed that an increase of the infiltrated cold water will generate a long-term cooling of the host rocks. Secondly, the same process will be viewed as a function of time (transient state) to assess the velocity of the cold plume in the two-dimensional model related to the quantity of infiltrated cold water. From a hydrogeological point of view, this study should allow the role of the lake on the thermal regime to be discussed. That is whether the lake can be considered as a single intake into the system.

In order to simulate the thermal impact on the hydrothermal system, four scenarios are proposed and are illustrated in Figure 15.4. Three of them represent a water flux in the model to show the influence of the cold water infiltrated from the lake,

with three different values proposed (1, 2 and 5 mm/d of water losses). To assign these values in the model, a calculation taking into account the surface of the lake and the thickness of the two-dimensional model is necessary (1 metre in the used software). The Figure 15.4 highlights the used method to assign in the model a value of water infiltration representing water losses from the lake. For example, taking into account a value of water losses equal to 1 mm/d, the volume of infiltrated water is 1 mm/d multiplied by the surface of the lake, that is about 2000 m^3/d assuming that the lake surface is a rectangle of about 1x2 kilometres. With a two-dimensional model crossing the lake more or less perpendicularly to the largest side of the lake (at about 2 kilometres), the value to assign in the model has to be 1 m^3/d. Then, the fourth scenario tested is the simplest to implement because it consists of replacing the water flux by a hydraulic head roughly equal to the main elevation of the lake. In this case, it generates a greater amount of water circulating in the model, by a factor 10. Finally, it was not decided to impose a fluctuating hydraulic head to represent the natural variation of the elevation of the lake because it is not necessarily useful to visualize effects of this scenario on the hydrothermal system.
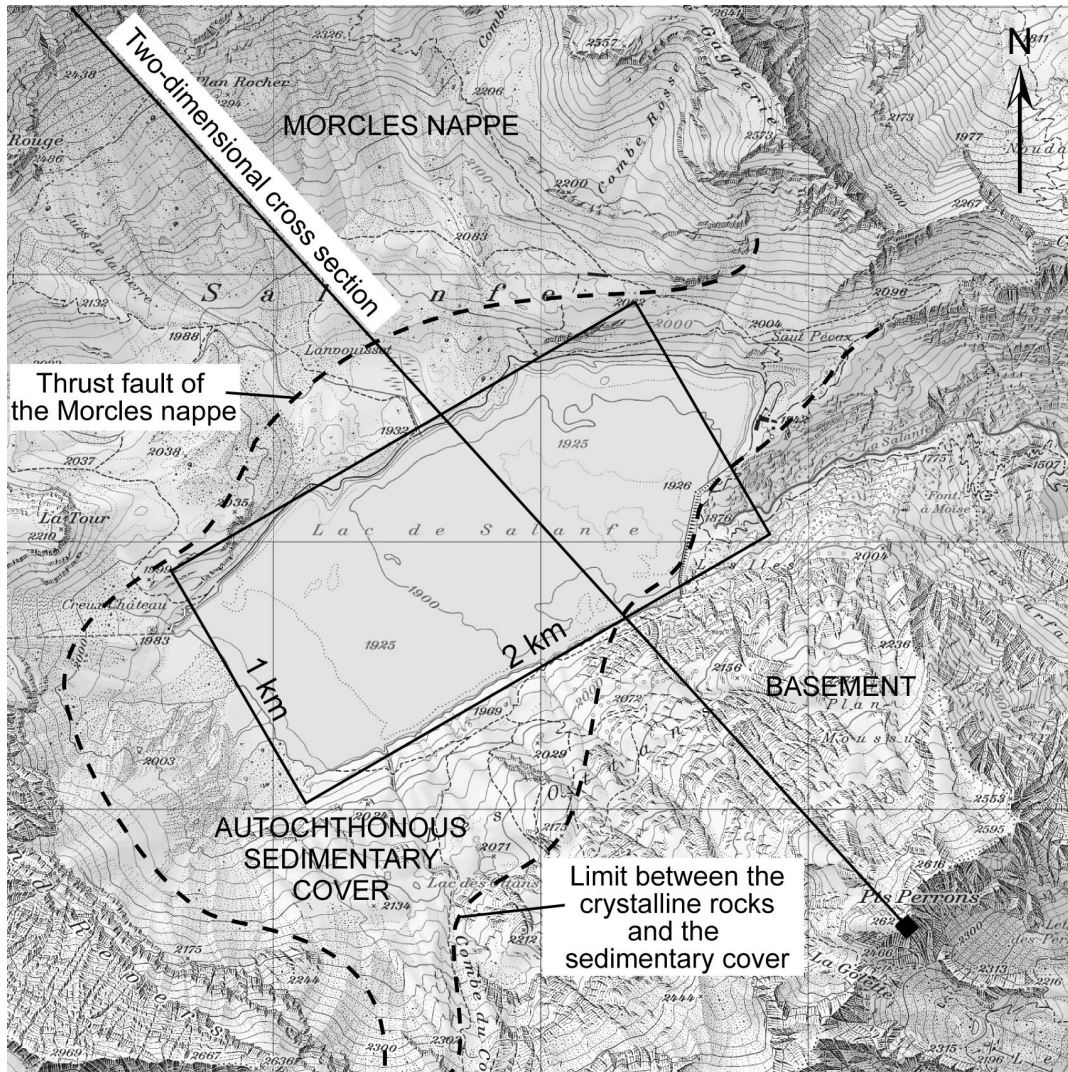
Water losses (WL) occurring at the Salanfe Lake	Total flow rate (TFR) of infiltrated water through the cover (surface of the lake about 2 km^2)	Infiltrated water (IW) imposed to the two-dimensional model
Selected value	TFR = WL * lake surface	IW = TFR / lake length
1 mm / day	2'000 m^3/ day	1 m^3/ day / m
2 mm / day	4'000 m^3/ day	2 m^3/ day / m
5 mm / day	10'000 m^3/ day	5 m^3/ day / m

Figure 15.4: Calculation of the imposed water flux into the two-dimensional model to reproduce three selected water losses from the Salanfe Lake.

15.4.2 Discussion of the results in steady state

Firstly, the four proposed scenarios were modelled in steady state to show their long-term effects on the temperature field in the host rocks (Fig. 15.5) and on the hydraulic heads (Fig. 15.6). For all the scenarios, the two-dimensional model representing the natural state of the hydrothermal system before the implementation of the lake was used keeping the same physical properties of the geological formations (hydraulic conductivity, porosity and rock thermal conductivity), the same heat flux at the bottom of the model and the same surface temperature. Only the infiltrated water was modified for each scenario.

The Figure 15.5 illustrates the change of the temperature field in the formations due to the increase of the infiltrated cold water in the model. Initially, the natural state of the hydrothermal system before the implementation of the lake was modelled with a value of the infiltrated water equal to 0.24 m^3/d representing at about 10% of the total precipitation. In this case, the simulated temperature of the discharged water was 25.5°C with a reservoir temperature in the range of 36-40°C. Taking into account the lake and selecting a value for the infiltrated water equal to 1 m^3/d (first scenario), representing 1 mm/d of water losses from the lake, the simulated temperature of the discharged water in steady state becomes 16.8°C with a reservoir temperature of around 18-21°C (Table 15.2). This process clearly indicates that the increase of the infiltrated water in the hydrothermal system generates a long-term cooling of the host rocks, while maintaining the same thermal regime.

The second and third scenarios represent two case studies with water losses from the lake equal to 2 and 5 mm/d. The induced long-term cooling of the model is more pronounced because the simulated temperatures of the discharged water, and in the reservoir, are lower than 15°C and 9°C respectively with water losses of 2 and 5 mm/d (Fig. 15.5 and Table 15.2). Finally, the fourth scenario involving an imposed hydraulic head equal to the elevation of the lake instead of water losses generated in the model a significant decrease of the computed temperatures at about 5°C because this condition implies larger amounts of water in the model. In the same way, all scenarios also lead to an increase of the computed hydraulic heads in the model (Fig. 15.6).

These four different tests were carried out with a two-dimensional model from a cross section going through the Val d'Illiez and Salanfe Lake, with an extension into the third dimension equal to 1 metre. The results indicate a long-term cooling of the formations in 2-dimensional view but not in the third dimension which is extended to the entire watershed assumed along the Triassic formations outcropping at the front of the Aiguilles Rouges basement. Without the elaboration of a three-dimensional model, it is difficult to know the extension of this cooling process occurring on the third dimension. It is conceivable to have a cooling process only in the area of the Salanfe basin. Moreover, this discussion does not take into account that the water level of the lake varies annually due to snow melt in summer and electricity production in winter. Furthermore, a period promoting more infiltration is occurring because of the melting glaciers. They are also important factors having a thermal effect on massifs.

In terms of the quantity of water, the hydrothermal system of the Val d'Illiez has the peculiarity of discharging a large amount of water compared to other hydrothermal sites in the Alps. The total flow rate in the discharged thermal springs reached 1300 L/min in 1990, 8000 L/min in 1996 after the drilling of the three F1, F2 and F3 wells, and 2200 L/min in June 2009 during the sampling campaign. But it was not possible to quantify thermal inflows before the implementation of the lake in 1953, the flow rate was probably much lower (several hundreds L/min ?). The implementation of the lake is clearly responsible for the increase in flow rate in the Val d'Illiez but it is difficult to assume if the lake acts as a single intake into the system or if the lake only applies a hydraulic pressure on an existing hydrothermal system. The computed groundwater recharge to reproduce the thermal regime before the lake was 4800 m^3/d (3330 L/min) considering a wider recharge zone along the stripe of the Triassic formations outcropping at the front of the Aiguilles Rouges basement. This value is significantly lower than the flow rate measured in 1996 but could well represent the current flow rate. For this reason, it is difficult to assert that the lake acts as a single intake into the system, especially that no temperature drop was measured since 1953, which could have occurred with the cooling of the formations caused by an increase of the infiltrated water.
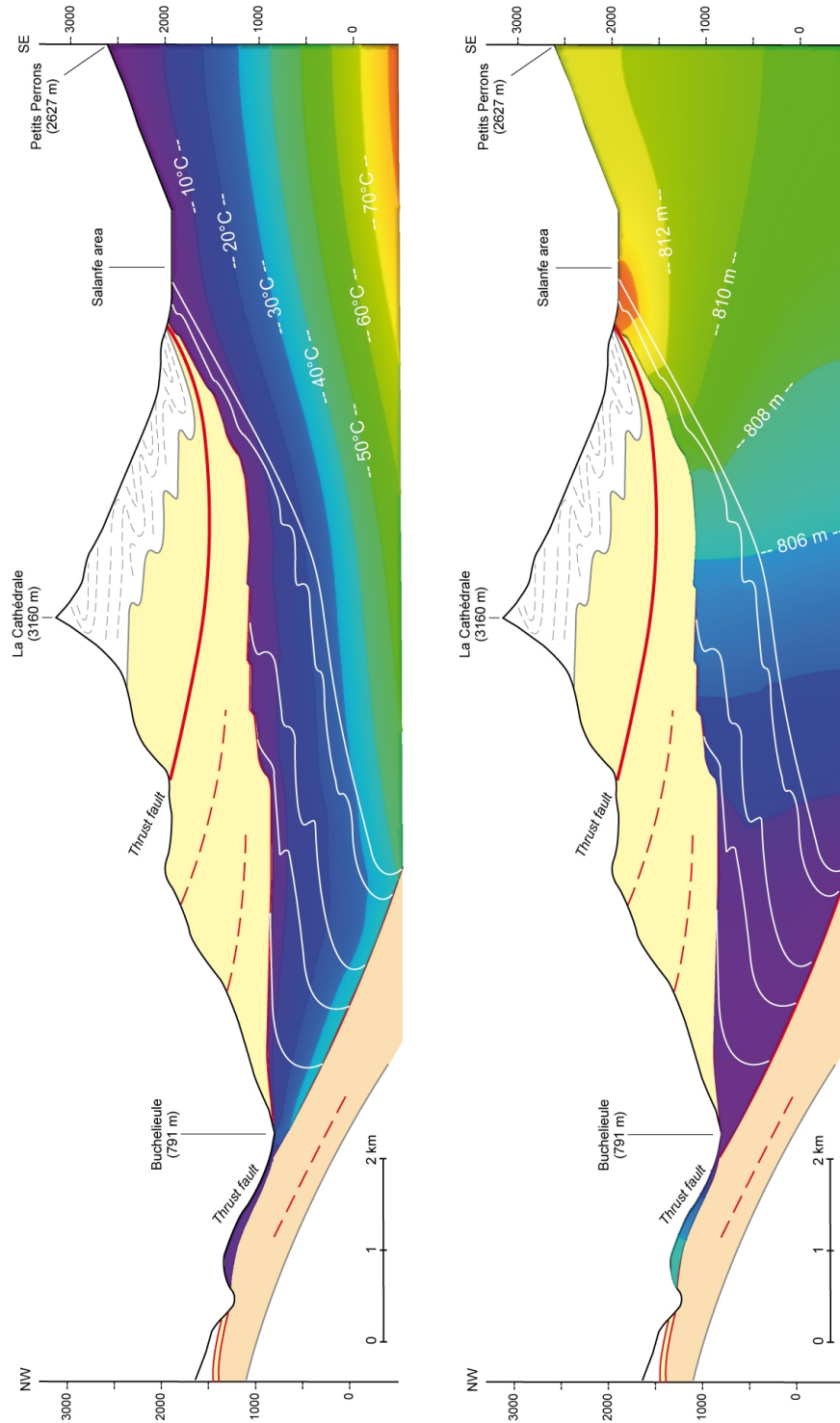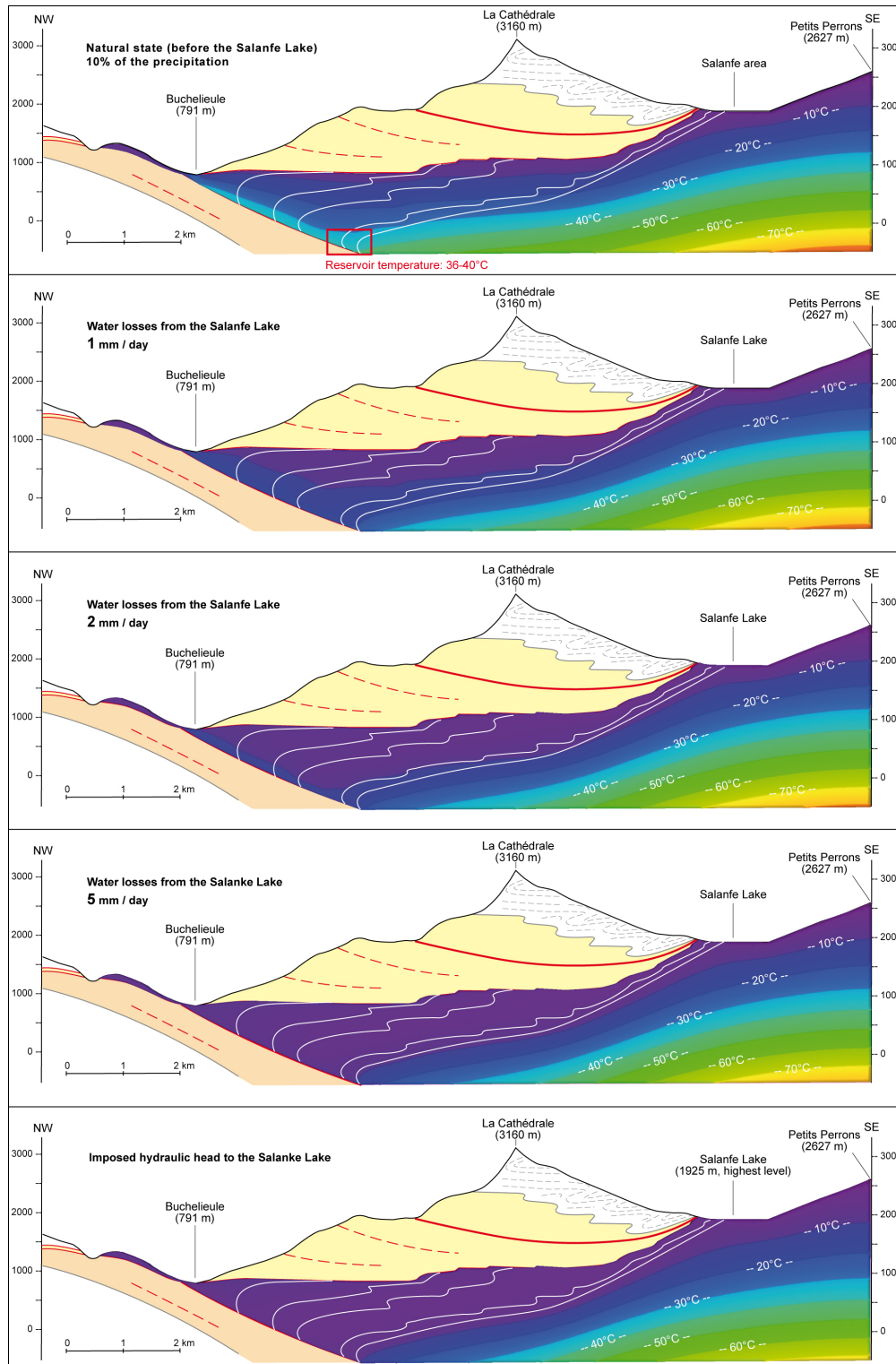
Figure 15.5: Cross section of the Val d'Illiez hydrothermal system showing the computed temperature field in the Aiguilles Rouges basement and its cover for different scenarios related to the Salanfe Lake and area.
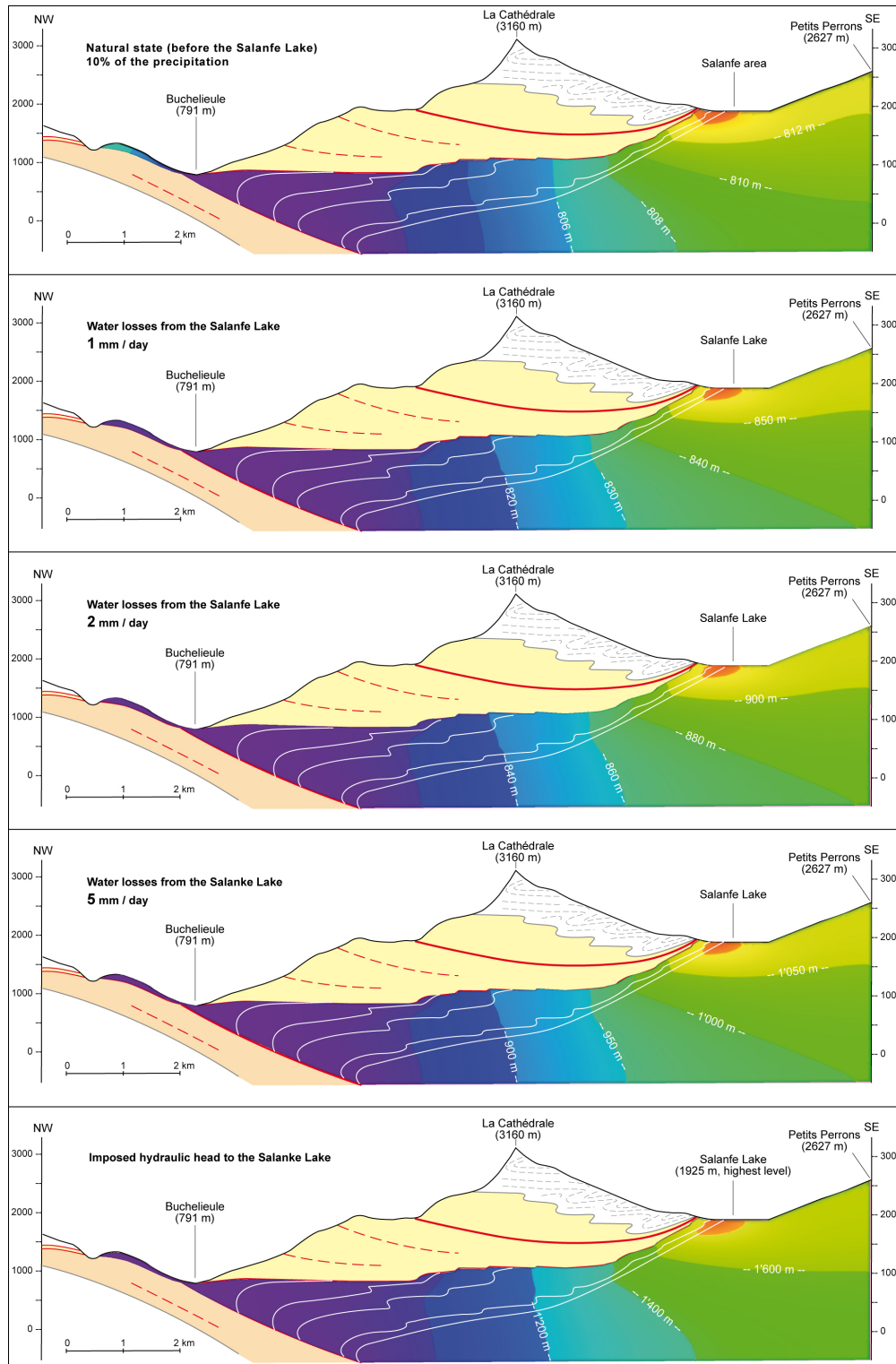
Figure 15.6: Cross section of the Val d'Illiez hydrothermal system showing the computed hydraulic head field in the Aiguilles Rouges basement and its cover for different scenarios related to the Salanfe Lake and area.

The hydrothermal system in the Val d'Illiez seems to have hydrogeological similarities to the Bad Ragaz hydrothermal system located in the canton of St Gallen, eastern part of the Swiss Alps (Fig. 15.7). At Bad Ragaz, a thermal spring named Pfäfers discharges into the Cretaceous rocks belonging to the sedimentary cover of the Aar crystalline Massif. This spring is also characterized by particular hydrogeological conditions. Indeed, the natural flow rate in the hydrothermal area which varies during the seasons by a factor 10 depends on the precipitations and snow melt, whereas temperature and mineralization remain very stable (Vuataz 1982). This behaviour has been interpreted as the effect of an increase of the hydrostatic pressure applied on the aquifer thermal by an overlying aquifer. Therefore, when snow melt occurs, increasing the infiltrated waters, the upper aquifer applies a pressure on the thermal aquifer, without mixing processes, which raises the flow rate of the thermal spring without changing its temperature and chemistry. For the Bad Ragaz system, this process is seasonal because the amount of infiltrated water depends on rainfall and melting snow. But for the Val d'Illiez case, it could be assumed the same process is occurring continuously because water losses from Salanfe Lake are more or less constant in time, and thus the applied pressure on the deep thermal aquifer is permanent.

15.4.3   Discussion of the results in transient state

The main objective of this discussion is to determine if the lake can be considered as a single intake in the thermal regime. To answer this question, a series of numerical simulations in transient state was carried out taking into account the four scenarios and the initial conditions of the model before modelling (natural state). In this case, it will be possible to see variations of temperatures and flow rates in the discharge area of the model, under different conditions of increasing water infiltration. Therefore, the lake will act on the hydrothermal system as a single intake for the simulation.

All scenarios were selected for the simulation in transient state but for each scenario, the amount of water restored to the discharge point is different. Water losses of 1 mm/d from the lake having a surface of about 2 kilometres square will bring an additional quantity of water of 2000 m^3/d or at about 1390 L/min. To restore a total flow rate in the discharged thermal springs of 8000 L/min in 1996, at least 4 mm/d of water losses from the lake have to be added to the computed flow rate of the natural state (3330 L/min). Therefore, it is mainly the result of simulation with losses of 5 mm/d which will interest us.

For each scenario, the variation of temperatures and flow rates in the outflow point of the model was computed and the associated curves are illustrated in Figure 15.8. For these tests in transient state, the lake represents a single intake into the model. An increase of the infiltrated water at the top of the model generates firstly the raise of the computed temperatures and rates at the outflow point, and secondly the decrease of the temperatures whereas the rates remain stable. For each scenario, the gain in temperature progresses to values between 30-32°C, that is to say an increase of about 5°C. Then, these temperature values come down progressively reaching the computed temperatures in steady state (see values in Table 15.2). This process can be explained as follows: firstly, the cold plume at the top of the model pushes the warm waters in the reservoir towards the surface generating the raise of the temperature and the rate (as a piston flow process) and secondly, the cold plume is discharged after the warm waters causing a progressive decrease of the temperature while maintaining the rate. Assuming that the lake acts on the thermal regime as a single intake, these results highlight a progressive change in temperature and rate, which does not seem to be the case in reality. Indeed in 1953 and 1996, the variation of the parameters in the discharged thermal springs in the Val d'Illiez was rather sudden and accompanied by small earthquakes. Moreover, it appears that the temperature and the chemistry of thermal waters in the Val d'Illiez have a current steady evolution, while the flow rate seems to vary with natural variations of the lake level with a time lag of around 140 days (Bianchetti et al. 1992). All these observations coupled with the simulation results seem to indicate that the relation between the lake and the thermal springs is more complicated than it appears. This relation bears some resemblance to the hydrothermal system of Bad Ragaz, illustrated pre-

viously, where an upper aquifer overlies the thermal aquifer, without fluid mixing, applying a pressure which raises the flow rate of the thermal spring without changing its temperature and chemistry.

Table 15.2: Thermal impact of the Salanfe Lake infiltrations in the two-dimensional model with four different scenarios in steady state.

Scenarios	Simulated temperature (°C)			
	At the discharge thermal area	200 metres depth	500 metres depth	In the reservoir
Natural state (before the lake)	25.5	31.2	34.8	36-40
1 mm/day of water loss from the Salanfe lake	16.8	17.3	17.6	18-21
2 mm/day -	11.6	11.6	11.6	12-15
5 mm/day -	7.3	7.3	7.3	7.5-8.5
Imposed hydraulic head (1925 m)	4.8	4.8	4.8	4.8-5
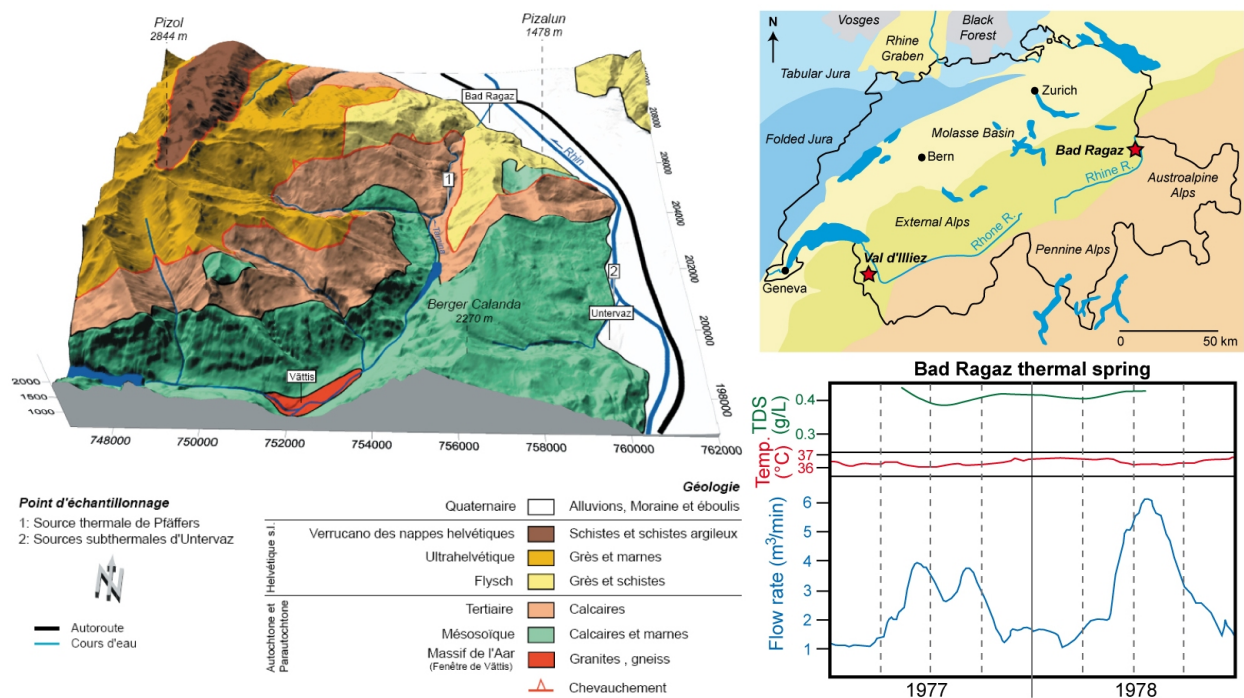
Figure 15.7: Geological and hydrogeological settings of the Bad Ragaz thermal spring (from Gainon 2008 and Vuataz 1982).
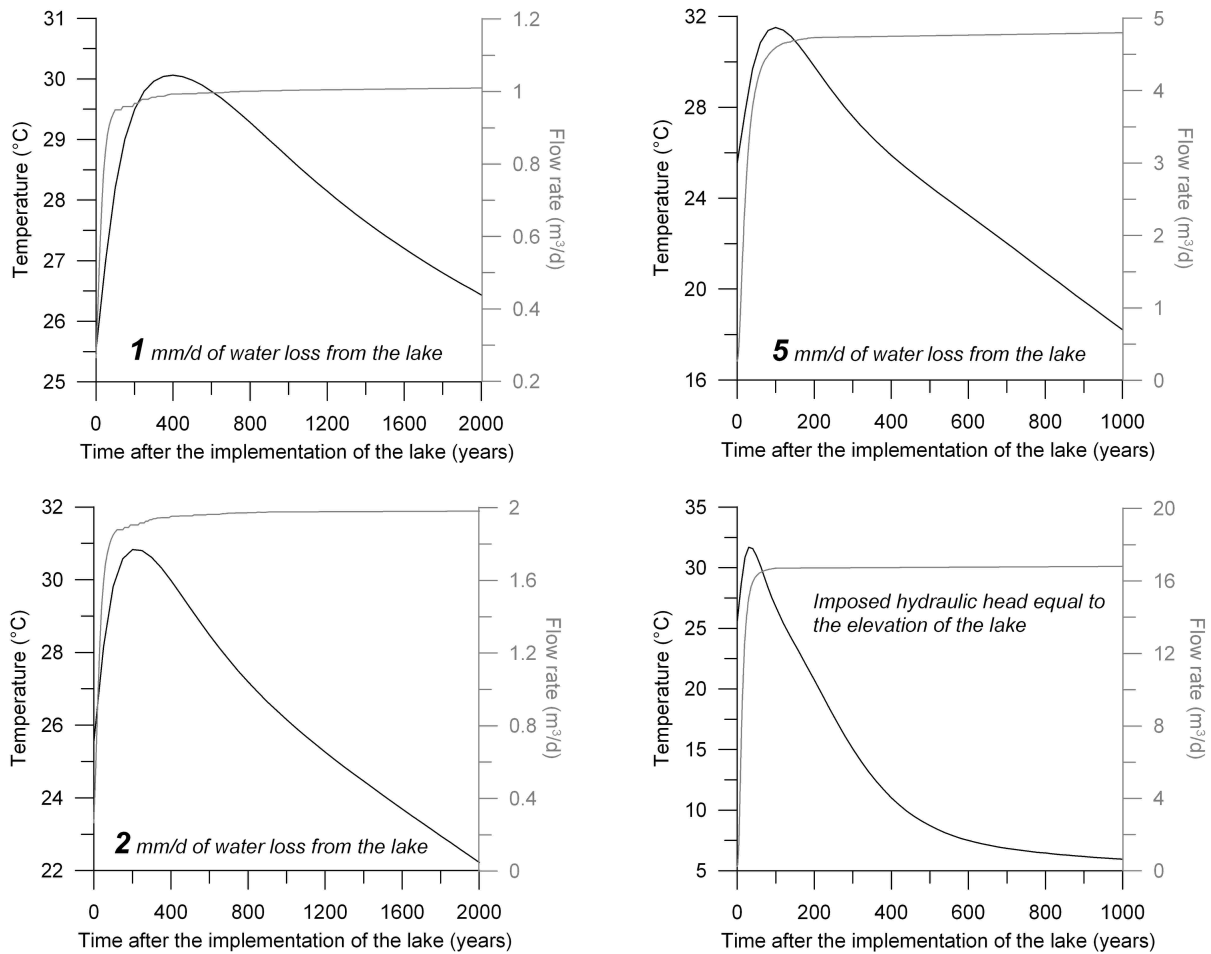
Figure 15.8: Variation of the computed temperatures and flow rates in the discharge zone of the model (Val d'Illiez) related to a change of the infiltration conditions due to the implementation of the Salanfe Lake. For these tests in transient state, the four scenarios were selected assuming that the lake is considered as a single intake into the model.

Part VI

Concluding comments

1. Synthesis of the studied hydrothermal sites

1.1 Lavey-les-Bains

The Lavey-les-Bains hydrothermal site is located along the Rhone Valley in the canton of Vaud, Switzerland (Table 16.1). Firstly, the geological investigations carried out at Lavey-les-Bains are located in the hydrothermal area of the Rhone Valley at the north-eastern low-elevation point of the Aiguilles Rouges Massif, belonging to the pre-Mesozoic basement areas of the Alpine external crystalline massifs. The Aiguilles Rouges basement is affected by NNE-SSW to NE-SW Variscan and Alpine structures (faults and folds) which are considered as potential direction flows of infiltrated waters from the subsurface decompressed zone to a deep geological anomaly considered as a pinched synclinal into a major thrust fault, putting in contact the Aiguilles Rouges Massif on another crystalline massif named the Infra-Aiguilles Rouges.

Continuous measurements of physico-chemical parameters in P201 and P600 waters and discrete measurements on several sampling points made it possible to highlight mixing processes occurring from three types of water. Two cold end-members are slightly mineralized, tritiated, and circulate in the alluvial deposits and in the fissured gneissic massif of the mountain slope (decompressed area). The last one is visible by the springs inside the gallery of the Lavey power plant.

The evolution from the Na-SO$_4$ and high-Cl thermal end-member, represented by the well P600 with a temperature of 65°C and a total dissolved solid content of 1.4 mg/L, to the cold end-members is marked by a reduction in Li, Na, K, Cl, SO$_4$, F and SiO$_2$, compensated by an increase in Ca, Mg, HCO$_3$ and tritium. This evolution is also accompanied by a decrease in the total mineralization and of the temperature. Moreover, the geochemical investigation draws attention to a purely thermal component of around 68°C and 1.5 mg/L circulating in the basement where the dissolution of feldspar, the oxidation of sulphides as pyrite and the leaching of small amount of seawater brine occurs. The hydrolysis of biotite from the crystalline rocks was also assumed to explain the origin of the high chloride concentrations in thermal water. This component is strongly under-saturated with respect to the feldspar, but clearly in equilibrium with calcite and aragonite which are controlled by their solubility in relation to temperature. It is also under-saturated with respect to dolomite, gypsum and anhydrite because sulphate and dolomite contents are not high enough to reach equilibrium, and is slightly over-saturated with respect to the quartz and chalcedony. The precipitation of quartz and chalcedony probably take place in the gneiss fractures during the uprising of the thermal water from the reservoir. Consequently, calculation of the reservoir temperature can be under-estimated using the chalcedony geothermometer. A reservoir temperature of 100-110°C was finally assumed.

The exploitation of the P600 well causes dilution of the thermal water in the P201 well due to infiltration of the shallow cold groundwater from the gneissic Morcles Massif. It was thus important to decipher these mixing processes with chemical investigations and numerical models, and to estimate the long-term behavior of physico-chemical parameters for optimal management of the geothermal resource.

Initially, a two-dimensional model of groundwater flow and heat transport within a regional cross section of the Aiguilles Rouges Massif partly recomposed the observed geothermal anomaly below the Rhone Valley (computed temperatures of 68, 56 and 40°C respectively in the P600, P201 and AP wells), and gave a temperature of the deep inferred reservoir of 100-130°C. The simulated thermal water flux (5400-9000 m^3/d) corresponds to 2 to 4 times the maximum production rate (2380 m^3/d) and still seems to be underestimated. The watershed probably extends towards the south-western part of the Aiguilles Rouges Massif.

Then, a three-dimensional local model on a perimeter including all the Lavey-les-Bains sampling points was realized, using the same assigned parameters as in the two-dimensional model. The used thermal water flux is comparable to the one obtained with the two-dimensional model (5454 m^3/d). Different simulation scenarios using the average annual discharges of P600 and P201 wells and some natural chemical tracers, made it possible to calculate the mixing ratios comparable with those estimated in the P201 well (10% of cold water before

the P600 well and 23% with the P600 exploitation). Moreover, long-term effects on P201 could be defined with the three-dimensional model. Computed and measured temperatures are concordant and illustrate a stabilization of the temperature at 56°C in the P201 well after 10 to 15 years of production at the P600 well. According to the model, a future exploitation of the deep inferred reservoir with pumping rates of 25 to 75 L/s may induce a significant decline of thermal output in the two existing wells in Lavey-les-Bains.

1.2 Saint-Gervais-les-Bains

The hydrothermal site of Saint-Gervais-les-Bains is located in the Bon Nant Valley at the south-western low-elevation point of the Aiguilles Rouges Massif, in a similar regional geological environment as Lavey-les-Bains (Table 16.1). In the southern part of the Aiguilles Rouges basement, NNE-SSW to NE-SW Variscan and Alpine structures (faults and folds) also occur and are assumed as potential direction flows of infiltrated waters from the subsurface decompressed zone to the same deep geological anomaly considered as major thrust fault, putting in contact the Aiguilles Rouges Massif on another crystalline massif named Infra-Aiguilles Rouges.

The local geological setting at Saint-Gervais-les-Bains is highly complicated compared to Lavey-les-Bains because the basement does not outcrop directly in the field. Indeed, its autochthonous sedimentary cover which overlies the basement is intensely affected by Alpine stresses (faults, thrust faults and folds). The implementation of wells in the Bon Nant Valley highlighted the presence of a thrust fault putting in contact a normal series of upper-middle Trias with black and green schists at the bottom on the lower Triassic-Permian quartzite.

The hydrogeological investigation via pumping test showed the presence of two deep aquifers below the Bon Nant Quaternary filling. The combination of the results from pumping tests with the geochemical investigations made it possible to define mixing processes between an ascending Na-Cl thermal water and shallow groundwaters at Saint-Gervais-les-Bains. This Na-Cl component is certainly related to the remobilization of trapped saline water by deep flow systems reaching the thrust fault of the Aiguilles Rouges Massif on the Infra-Aiguilles Rouges Massif. However, the hydrolysis of biotite may also explain the presence of high chloride concentrations in thermal waters at Saint-Gervais-les-Bains. This assumption has to be considered especially as the deep flow system occurs in a crystalline environment. The origin of the deep flow system probably comes from infiltration and circulation within the fractures of the Aiguilles Rouges basement. Concerning the De Mey boreholes (27-36°C), uprising Na-SO$_4$ and high-Cl thermal water in the lower Trias-Permian quartzite from the Aiguilles Rouges basement is mostly diluted by a Ca-SO$_4$ and low-Cl end-member circulation in the autochthonous cover, which is represented by the Ferrugineuse and Magnésienne cold springs. The leaching of residual brines or fluid inclusions is responsible for the Na-Cl fingerprint as it was observed calculating a Cl/Br molar ratios at Saint-Gervais-les-Bains lower than 655. The Na-Cl end-member does not result from halite dissolution in Triassic formations. Moreover, halite is not present in gypseous formations in Saint-Gervais-les-Bains because the Triassic cold water has a low-Cl concentration ($<$ 20 mg/L).

Water-rock interactions occur during the uprising of the thermal water via N-S strike-slip faults in the basement and later on in the autochthonous cover. Data for De Mey Est borehole show that gypsum dissolution is occurring with cationic exchanges involving Na and low-temperature Mg dissolution from dolomite in the Triassic formations. For the imbricated structure zone crossed by the Lépinay well (39°C), gypsum dissolution occurs and thermal waters are strongly mixed with a low-Cl water.

The reservoir temperature for the thermal end-member was estimated up to 65°C but not exceeding 100°C. All groundwater end-members originate through circulation of meteoric waters but from different infiltration areas. The thermal end-member has the same infiltration area range (1700-2100 m) as the hydrothermal systems of Lavey-les-Bains and Val d'Illiez in the Aiguilles Rouges Massif. It is higher than the calculated infiltration area for the Ca-SO$_4$ and low-Cl water at about 1100-1300 metres, corresponding to flow paths from the Mont Joly area.

The conception of a simplified two-dimensional numerical model from a regional NNE-SSW cross

section through the Aiguilles Rouges crystalline Massif and the Mont Joly Massif allowed for representation of the initial conditions of the Saint-Gervais-les-Bains deep flow system, such as the temperature field inside the autochthonous cover and temperatures of the deep inferred reservoir (60-75°C). Nevertheless, the approximation of the uprising water flux is made difficult because the third dimension cannot be taken into account due to the complexity of geological structures and the accentuated topography. Obtained results showed a thermal discharge of about 90-160 m^3/h, that is to say 4 to 7 times higher than the maximum rate, which can be pumped from existing wells (22.5 m^3/h). The width of the watershed and its extension in

the Aiguilles Rouges Massif, and the quantification of infiltration in the model, also are important parameters that are difficult to evaluate and have a significant influence on the estimation of the uprising water rate.

Even if the two-dimensional model correctly represents initial conditions of groundwater flow and heat transport, it is not suitable when one wants to add pumping rates in the model. To carry out a simulation including the pumping rates, a three-dimensional numerical model in the boreholes zone has to be built but the complexity of the geological structures in the autochthonous cover represents an obstacle for its conception.

1.3 Val d'Illiez

The hydrothermal area of Val d'Illiez is situated in the Wallis canton, Switzerland, at the precise locality of Buchelieule (Table 16.1). Thermal springs actually discharge from several inclined artesian wells on the left bank of the Vièze River, the major stream of the valley which flows into the Rhone River at Monthey. In this area, the presence of subthermal springs was detected 1 kilometre downstream from the spa (Les Fayots) and also 1 kilometre upstream from Buchelieule (Play). The history of the Val d'Illiez thermal springs is related to the creation of the Salanfe Lake on the autochthonous cover at the front of the Aiguilles Rouges basement. Important water losses occur at the bottom of the lake generating seismic events and the variation of discharge rates of thermal springs.

The Val d'Illiez area is located at the limit between the Helvetic domain in the south-east and the Prealps in the north-west. The Helvetic domain, in which the area under study is included, is formed by the crystalline basement of the Aiguilles Rouges Massif, the autochthonous and parautochthonous covers and the Morcles nappe. The deep flow system leading to the thermal springs occurs at the bottom of the autochthonous cover, especially inside the Triassic formations consisting of various rocks such as cross-bedding arkose (Vieux-Emosson formations), multicoloured argillite, dolomite and cellular dolomite where sink holes are present at Salanfe, gypsum and anhydrite. An alternation of marl and limestone completes the series for the Jurassic and Cretaceous formations, and a Tertiary detrital series ends the autochthonous cover. The

geological study of the cover highlights the structure which was assumed as a great recumbent anticline with an axial plane plunging towards the south-east. In detail, a plunge of axis towards the north-east occurs involving the disappearance of the Champéry window in the zone of Val d'Illiez. This great fold would be limited by a basal thrust fault which is related to the thrust system between the Aiguilles Rouges and Infra-Aiguilles Rouges basements.

The local geological setting is also highly complicated because the autochthonous flysch is intensively deformed and overlapped by the parautochthonous flysch. From observation in the inclined wells, the Carrières sandstone should be present on the left bank of the valley at Buchelieule and should allow the rise of thermal waters.

The hydrogeological and geochemical investigations highlighted mixing processes occurring between a Ca-HCO$_3$ cold groundwater and a Ca-SO$_4$ and low-Cl thermal end-member, having a temperature and a total dissolved solid content of roughly 30-31°C and 2 g/L respectively. The thermal component acquires its mineral composition from the dissolution of gypsum and dolomite occurring in the Triassic formations of the autochthonous cover during the flow path, whereas the cold water acquires its composition with circulation at shallow depth in the moraine deposits. The thermal end-member is clearly in equilibrium with carbonate minerals and is slightly under-saturated with respect to gypsum and anhydrite. Looking at the sulphate and calcium concentrations in the thermal end-member, an

excess of sulphate in relation to calcium was highlighted (about 26.7 meq/L against 21 meq/L). This was interpreted as the presence of carbonate precipitation occurring at depth. Looking at the typology of Triassic evaporitic aquifers from the Western Alps in Switzerland (Wallis), according to chemical analyses made over 100 springs, the Val d'Illiez water is clearly in the family of waters circulating in a gypseous karstified environment.

According to measurements in water stable isotopes, it was demonstrated that the thermal component has an infiltration area close to the elevation of the Salanfe Lake ($\approx$ 1900 m). These analysed values are similar to those measured in thermal components for Lavey-les-Bains and Saint-Gervais-les-Bains, of which the previous calculations gave an elevation of the recharge area in the range of the mean elevation of the Aiguilles Rouges Massif (1700-2100 m). Using chemical-mineral equilibria, the reservoir temperature of the deep flow system should probably not exceed 35-40°C to a depth around 1 kilometre below the Val d'Illiez spring zone. Based on tritium data, the piston-flow model enabled the calculation of an average residence time for the thermal end-member of around 5 years, that is to say slightly lower than the initial evaluation from Bianchetti et al. (1992) in the range of 10-15 years.

Initially, a two-dimensional model of groundwater flow and heat transport was carried out with a cross section in the autochthonous cover below the Dents du Midi Massif to represent the initial state of the thermal regime before the creation of the Salanfe Lake. This model has partly restored the observed geothermal anomaly below the Viéze Valley (computed temperature of 31°C at 200 metres depth below the valley), and gave a temperature of the deep inferred reservoir of 36-40°C. Considering a wider recharge zone along the stripe Triassic formations outcropping at the front of the Aiguilles Rouges crystalline rocks, of which the length can be evaluated around 20 kilometers, a groundwater recharge of 4800 m^3/d or 3330 L/min is expected to reproduce the system in the model.

After reproducing the natural state of the hydrothermal system before the implementation of the lake, it was decided to introduce the lake into the same two-dimensional model. To undertake it, four scenarios were tested with different values of water loss from the lake. In the model this caused an increase of the infiltrated water and thus a long-term cooling of the host rocks, but with this method it was difficult to assert that the lake acts as a single intake into the thermal system.

To answer this question, a series of numerical modelling in transient state was carried out taking into account the four scenarios, and the initial conditions of the model before the lake. In this case, it was possible to see the time variation of temperature and flow rate at the discharge zone. For each scenario, the gain in temperature is about 5°C. Then, these temperature values come down progressively reaching the same computed temperatures as for the steady state. This process was explained as follows: firstly, the cold plume at the top of the model pushes the warm waters in the reservoir towards the surface generating the raise of the temperature and the rate (as a piston flow process) and secondly, the cold plume is discharged after the warm waters causing a progressive decrease of the temperature while maintaining the rate. Assuming that the lake acts on the thermal regime as a single intake, these results highlight a progressive change in temperature and rate, which does not seem to be the case in reality. Indeed in 1953 and 1996, the variation of the parameters in the discharged thermal springs in the Val d'Illiez was rather sudden and accompanied by small earthquakes. Moreover, it appears that temperature and chemistry of thermal waters in the Val d'Illiez have a current steady evolution, while the flow rate seems to vary with the natural variation of the water level of the lake with a time lag around 140 days. All these observations coupled with the simulation results seem to indicate that the relation between the lake and the thermal springs is more complicated than it appears. This relation bears some resemblance to the hydrothermal system of Bad Ragaz, illustrated previously, where an upper aquifer applies on the thermal aquifer, without mixing processes, a pressure which raises the flow rate of the thermal spring without changing its temperature and chemistry.
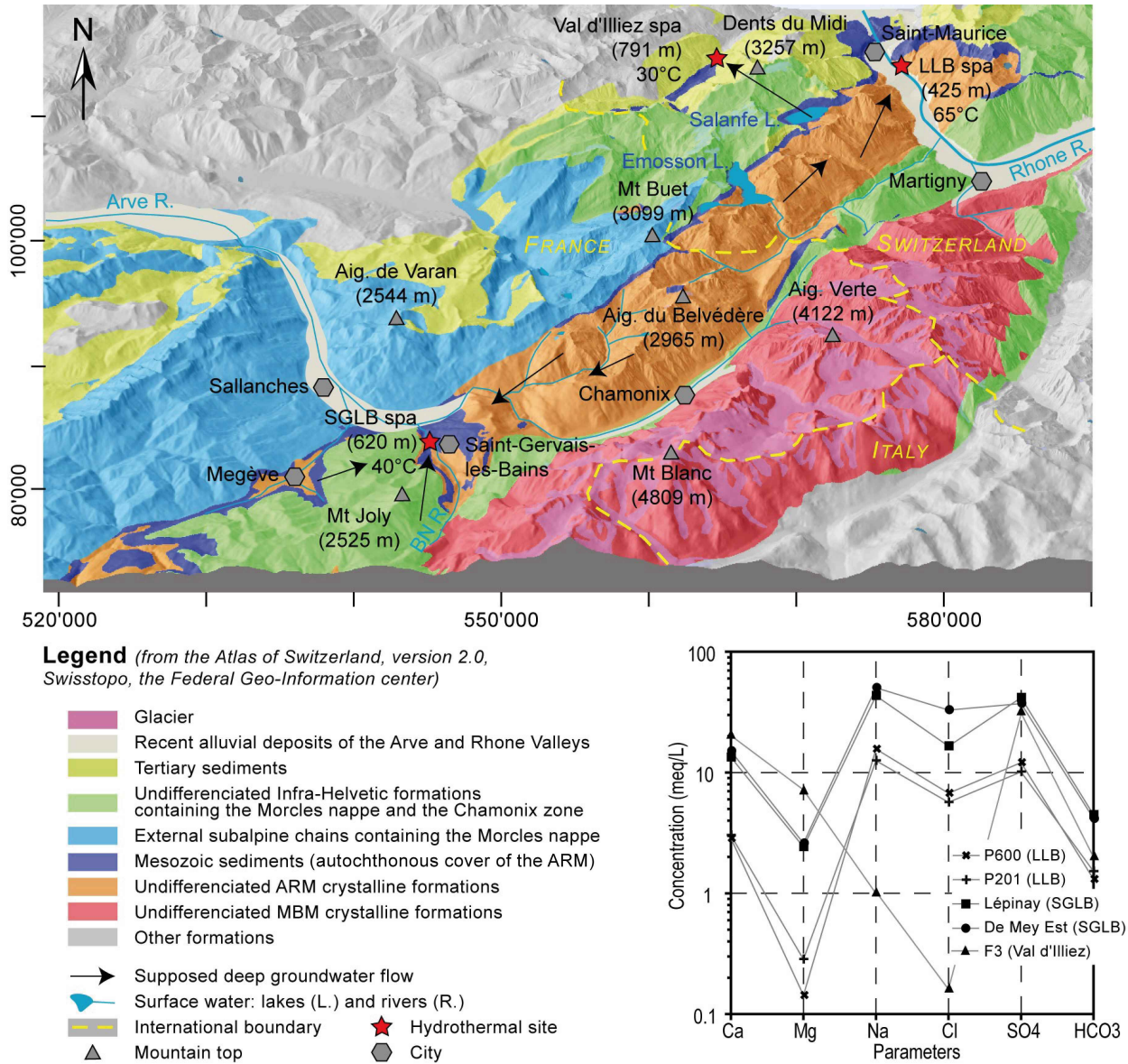
Figure 16.1: Regional conceptual model of the different flow paths ending to the hydrothermal systems of Lavey-les-Bains, Saint-Gervais-les-Bains and Val d'Illiez. Major element concentration plot (modified schoeller diagram) represents thermal waters of Lépinay and De Mey Est at Saint-Gervais-les-Bains, P600 and P201 at Lavey-les-Bains, and F3 in the Val d'Illiez. Location refers to the Swiss kilometric coordinates in projection, in standard CH1903. ARM: Aiguilles Rouges Massif, MBM: Mont-Blanc Massif.

2. Regional view and perspectives

From a regional view, what is brought to mind when we visualize the location of Lavey-les-Bains and Saint-Gervais-les-Bains is that these two sites are positioned at the two low-elevation parts of the Aiguilles Rouges crystalline Massif, on each side (Fig. 16.2). These positions are certainly no coincidence because the geological structure of the Aiguilles Rouges Massif could be considered as a volume having distinct boundaries playing an important role in the circulation of the deep fluids:

- at the front and at the bottom: the thrust fault system of the Aiguilles Rouges Massif overlapping the Infra-Aiguilles Rouges Massif.

- behind: the thrust fault system of the Mont Blanc Massif overlapping the Aiguilles Rouges Massif.

- on the two sides: two NNW-SSE valleys, Rhone and Bon Nant Valleys, where major vertical faults are present.

Considering infiltrations inside this enclosed volume, the generated deep regional flow systems have to exit the massif via the two low-elevation points. This complex geological structure with distinct boundaries could explain the occurrences of the hydrothermal systems of Lavey-les-Bains and Saint-Gervais-les-Bains.

The knowledge gained through this study about the deep flow systems in the Aiguilles Rouges Massif is also useful to improve to understand of the deep flow processes occurring in the other external crystalline massifs. The Figure 16.2 illustrates the location of hydrothermal sites bordering other external crystalline massifs such as the Aar, Mont Blanc, Belledonne and Argentera Massifs, and the Table 16.2 highlights the details about these sites, which are mostly located in low-elevation points (Brigerbad, Uriage-les-Bains, etc.). Only the Pelvoux Massif does not have a hydrothermal site.

Similarly to the Aiguilles Rouges Massif, the Mont Blanc Massif is bound by two major thrust fault systems along both sides, and thus it may also be considered as another example of a closed volume. The lowest elevation point of the Mont Blanc Massif is located along the Rhone Valley at Saxon in Switzerland (Fig. 16.2). At Saxon, there exists a "thermal spring" discharging a water around 24°C from the autochthonous cover which is probably influenced by mixing processes. The fingerprint of the water is complicated because chemical-mineral processes occur in the sedimentary cover but the origin seems to come from circulation in the basement. Also at Saxon, boreholes at shallow depth below the Quaternary filling intersected the basement which also contained thermal water at 26°C. The geochemical investigations could not prove the presence of a large geothermal potential at depth, but there certainly exists an area below the Rhone filling where the Mont Blanc Massif discharges a large amount of warmer thermal water. Further investigations at Saxon are necessary to determine this. In the Mont Blanc Massif, two other hydrothermal sites are present. Bovernier in Switzerland is located in a valley crossing the Mont-Blanc Massif (21°C, 620 m of elevation) and Pré-Saint-Didier is the lowest elevation point of the south-eastern part of the Mont Blanc Massif (36°C, 1100 m of elevation).

We could also cite other examples but generally, the density of hydrothermal sites is often higher in Western Alps where the basement outcrops. Indeed, the vertical faults in the basement allow easier the deep infiltration of water leading to deep flow systems, whereas in sedimentary domain the superposition of nappes tends to generate shallower flow systems. Consequently, it would be interesting to investigate other low-elevation zones bordering the external crystalline massifs where the Quaternary filling could mask areas of uprising thermal waters. To undertake fast and inexpensive preliminary investigations in some selected areas, electrical tomography would be an interesting solution because this method enables the location of anomalies of electrical conductivity at shallow depth. Since deep uprising thermal waters are often more mineralized than cold shallow water in the Quaternary filling, this geophysical method would help to decipher the uprising areas. The use of geophysical tools in our case study could have improved the knowledge about the hydrogeological processes occurring in the discharged thermal areas and even better, these tools could have detected new uprising zones.

Table 16.1: Summary table of the main characteristics of the three studied geothermal sites.

	Lavey-les-Bains		Saint-Gervais-les-Bains			Val d'Illiez		
Canton or Province / Country	Vaud / Switzerland		Haute-Savoie / France			Wallis / Switzerland		
River	Rhone		Bon Nant			Vièze		
Swiss kilometric coordinates (CH1903)	568'000 / 116'600		544'000 / 80'050			558'400 / 117'500		
Elevation of the thermal area (m.a.s.l.)	425		620			791		
Regional geology	North-eastern low elevation point of the Aiguilles Rouges crystalline Massif		South-western low elevation point of the Aiguilles Rouges crystalline Massif			Sedimentary autochthonous cover of the Aiguilles Rouges crystalline Massif Triassic to Tertiary formations		
Local geology	Aiguilles Rouges gneiss		Sedimentary autochthonous cover			Tertiary parautochthonous flysch		
Local tectonic conditions	NE and NNW fracturing		Thrust fault in the autochthonous cover Springs fault (Contamine-Montjoie fault system)			Thrust fault between the autochthonous and parautochthonous flysch		
Rocks outcropping in the thermal area	Gneiss (Hercynian)		Quartzite - Evaporite (Permian - Trias)			Flysch (Tertiary)		
Reservoir rocks at depth	Crystalline rocks (Hercynian)		Gneiss (Hercynian), sedimentary formations ?			Evaporite (Trias)		
Production well	P600	P201	Lépinay	De Mey Est	De Mey Ouest	F1	F2	F3
Year of drilling	1997	1972-1973	1999	1988-1989	1989	1996	1996	1996
Length of the production well (m)	595	201	101.5	196	207	37	60	120
Depth of the production well (m)	517	201	101.5	196	207	26	42.5	113
Geochemical water type	$Na-SO_4>Cl$	$Na-SO_4>Cl$	$Na-SO_4>Cl$	$Na-SO_4>Cl$	$Na-SO_4>Cl$	$Ca-SO_4$	$Ca-SO_4$	$Ca-SO_4$
Average well head temperature (°C)	65	57	39	36	27	28	28	30
Total Dissolved Solids (mg/L)	1450	1215	4245	4820	3100	1715	1700	1805
pH	7.7	7.4	6.9	6.9	7.1	7.3	7.3	7.2
Current production rate (L/min)	300-1200	50-450	225	92	58	>10	200	1170
Geothermal potential (KWth) - 10°C*	1150-4600	165-1475	455	165	70	>15	250	1470
Current use of thermal water	Swimming pools, heating buildings, sanitary hot water		Medical care	Cosmetics	Protection of De Mey Est production	Heating of an outside pathway	Unused	Swimming pool
Observed mixing processes	Weak mixing with a cold $Ca-HCO_3$ water flowing in the gneissic slope (decompressed zone)		Weak to medium mixing with two cold waters: a $Ca-SO_4$ water from the Triassic autochthonous cover and a $Ca-HCO_3$ water from the Quaternary filling			Weak mixing with a cold $Ca-HCO_3$ water flowing in the Tertiary and Quaternary formations		
Elevation of the recharge area (m.a.s.l.)	1700-2100		1700-2100			1700-2100		
Recharge area of the thermal end-member	North-eastern part of the Aiguilles Rouges basement		South-western part of the Aiguilles Rouges basement			Autochthonous cover outcropping along the Aiguilles Rouges basement		
Reservoir temperature (°C)	100-110		70-100			35-40		
Reservoir depth (m.a.s.l.)	About - 3000		About -2500			About -500		

* final temperature after cooling arbitrarily fixed at 10°C

275

Table 16.2: Hydrothermal systems linked to the External Crystalline Massifs (ECM). Lat.: Latitude, Long.: Longitude, Geoch.: Geochemical, Temp.: Temperature, TDS: Total Dissolved Solids, n.d.: not defined. The symbol "*" means that chemical-mineral processes also occur in the autochthonous cover modifying the chemical composition of the thermal waters.

Site name	Country	Lat./Long. (dec.deg.)	ECM	Geoch. type	Temp. (°C)	TDS (mg/L)	Cl/Br (molar)
Gletsch	Switzerland	46.5627/8.3610	Aar	Na-SO$_4$	18.6	184	n.d.
Brigerbad	-	46.3030/7.9310	-	Na-SO$_4$	47	1100	266
Lavey-les-Bains	-	46.1990/7.0251	Aiguilles Rouges	Na-SO$_4$	65.1	1320	207
Saint-Gervais-les-Bains	France	45.8931/6.7111	-	Na-SO$_4$*	29.5	4000	221
Saxon	Switzerland	46.1450/7.1716	Mont Blanc	Ca-SO$_4$*	24.3	1750	293
Bovernier	-	46.0812/7.0987	-	Ca-HCO$_3$	21.1	294	241
Pré-Saint-Didier	Italy	45.7575/6.9867	-	Ca-HCO$_3$*	36	950	n.d.
La Léchère	France	45.5158/6.4836	Belledonne	Ca-SO$_4$*	60.2	2640	250
Allevard	-	45.3939/6.0750	-	Na-SO$_4$*	14.5	1870	425
Uriage-les-Bains	-	45.1372/5.8247	-	Na-Cl*	26	2200	762
Vinadio	Italy	44.2886/7.0767	Argentera	Na-Cl	52.3	1970	n.d.
Valdieri	-	44.2064/7.2689	-	Na-SO$_4$	60.5	260	n.d.
Roquebilière	France	44.0119/7.3064	-	Na-HCO$_3$*	29	280	n.d.

3. Personal views about the use of methods to investigate the hydrothermal systems

3.1 Geological methods

The geological investigations represent the basis of all research programs in the domain of geothermics, and they have to be undertaken systematically for each type of geothermal project regardless of the environment, sedimentary basin or a mountain range. In our case study where the geological structures are complicated to define, the time devoted to understanding these structures can sometimes seems quite long but otherwise we could not formulate assumptions about the deep flow systems in the Alps. The occurrences of thermal water uprising is often related to a change in the geological conditions generating a permeability contrast at depth. The geological investigations at depth via cross sections, seismic profiles, etc., allow the limits of the geological units to be located. The hydrothermal site of Brigerbad, Wallis canton in Switzerland, is a good example where the uprising thermal water is certainly controlled by the geological limit between the Aar fractured gneiss which contains the water, and the Termen calcareous shale and marl considered as impermeable (Fig. 16.3). This permeability contrast which probably extends deeply could be the origin of uprising thermal water and coupled with the hydraulic pressure prevailing in the Aar basement.

In addition, the study of the fracturing and the presence of faults on a regional scale enables the infiltration conditions and thus the groundwater recharge to be determined. For example in our study, it was interesting to use this for the Aiguilles Rouges basement where prevailing NNE-SSW to NE-SW structures were highlighted (schistosity, fracturing, folds, faults, etc.). In the same way, the study of the fracturing at a local scale, limited to the hydrothermal area, allows the uprising conditions of the deep thermal water towards the surface to be specified. Moreover, the local fracturing condition has to be considered for the implementation of futures geothermal drillings, in case the safety of the supply should assured or the temperature and the flow have to be improved. For each studied hydrothermal site in this study, information on the regional and local fracturing has been documented.

The study of the geological structures is also mandatory to build a sound numerical model of the
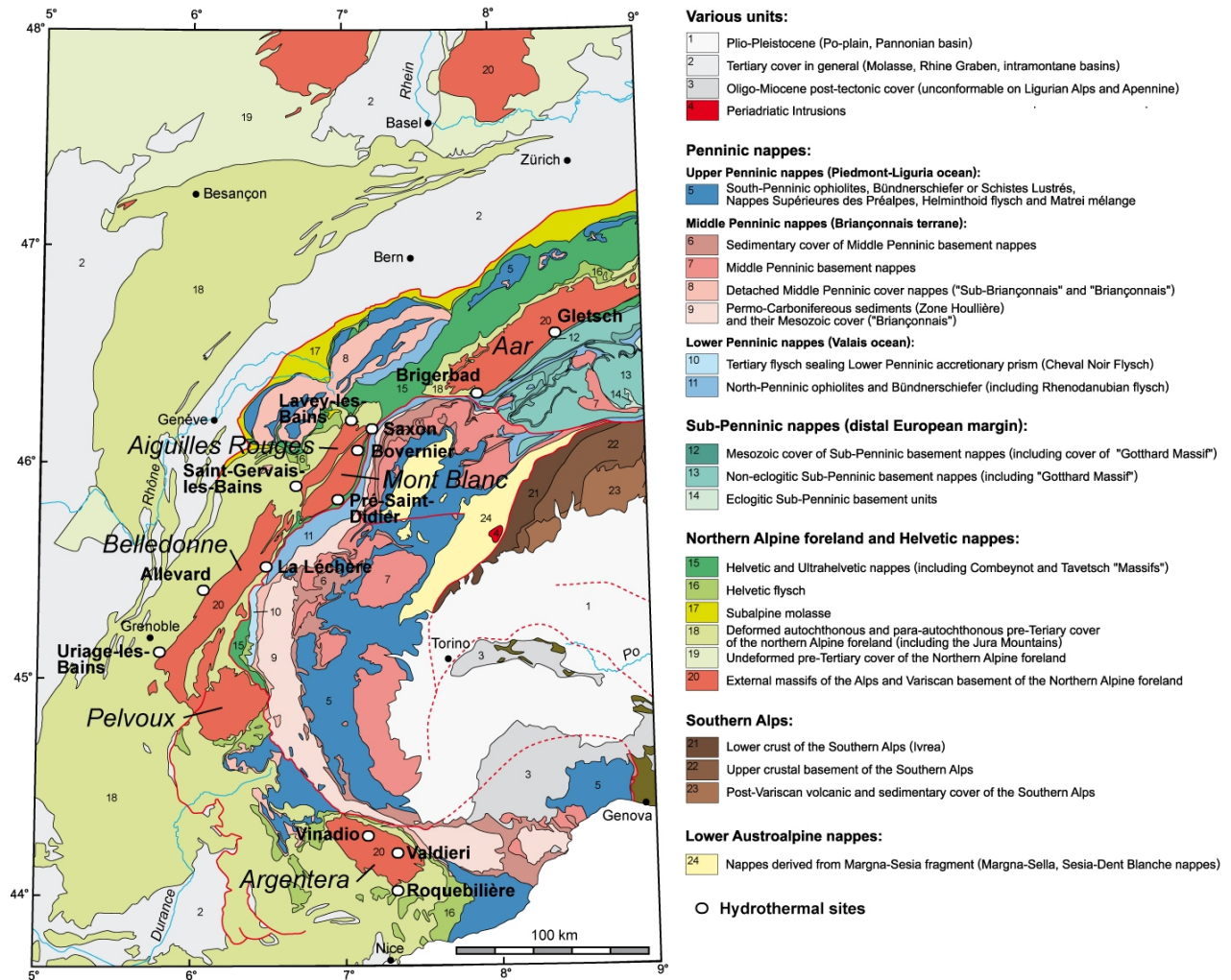
Figure 16.2: Location of the hydrothermal sites on the tectonic map of the Alps (modified from Schmid et al. 2004) related to deep flow systems in the external crystalline massifs.

groundwater flow, heat and mass transport. In addition to this, the study of the mineralogical composition of host rocks through which deep fluids flow are necessary to simulate the water-rock equilibrium, with adapted codes, aiming to calculate the chemical composition of thermal waters at depth in the reservoir before mixing processes take place. This is also very helpful for geothermal projects before and during the drilling phase.

3.2 Geochemical and hydrogeological methods

The chemical analyses carried out for each studied hydrothermal system allow the various types of water met on the field to be defined. Moreover, the chemical processes occurring such as mixing processes and water-rock interactions were detailed to explain the origin of waters. Then, the hydrogeological relationship between the different aquifers could be shown. Finally, these analyses allow the reservoir temperature and the mean elevation of the infiltration area to be evaluated. All the analyses carried out were very inexpensive, such as major and trace elements and water stable isotopes, which can be easily in research laboratories equipped for water analysis. This is the minimum schedule that should be done routinely during the study of a hydrothermal system and especially during the implementation of new wells, with several sampling campaigns before, during and after drilling, as well as during production tests.

Indeed, in this study several production tests with sudden and step rate changes were carried out to understand mixing processes. These sudden and step rate changes immediately generated a variation of the physical and chemical parameters (temperature and electrical conductivity). While taking samples for analysis during the variation pahse, it was possible to visualize in detail the mixing processes. This method is easy to establish with a technician on site and gives interesting and useful results.

However, the formulated assumptions about the deep flow system and the origin of the thermal water should be validated by additional studies, involving isotopic analyses. These ones are more expensive compared to major elements analysis for example. Therefore, it was not possible to realize additional isotopic analyses due to limited funding.

Finally, the long-term measurements of the physico-chemical parameters have to be carried out if possible for each exploited sampling point including springs and wells. This allows a better long-term management of the geothermal resource to be improved. This is also a way for a better understanding of hydrogeological conditions. It is important to have long-term measurements with quality which are often lacking in spas.

3.3 Numerical methods

Engineers and modellers working in hydrogeology and geothermics need to illustrate the physical processes representing groundwater flow, heat and mass transport. The elaboration of these illustrations comes from the modelling of flow, heat and mass transport. In the case study of Alpine deep flow systems, the two and three-dimensional models are difficult to build because the representation of the geological structures in a model have to be oversimplified. Moreover, the areas with thermal water discharging in the Alps are often related to highly complex geological structures and thus it is almost impossible to represent the local variety of geological and tectonic conditions. In addition, the geometry of the formations where the deep flow system occurs sometimes cannot be discretized in a three-dimensional model. To develop an acceptable regional three-dimensional model for the systems of Lavey-les-Bains, Saint-Gervais-les-Bains and Val d'Illiez, a complete PhD thesis would be required on this topic, by having enough information from deep wells.
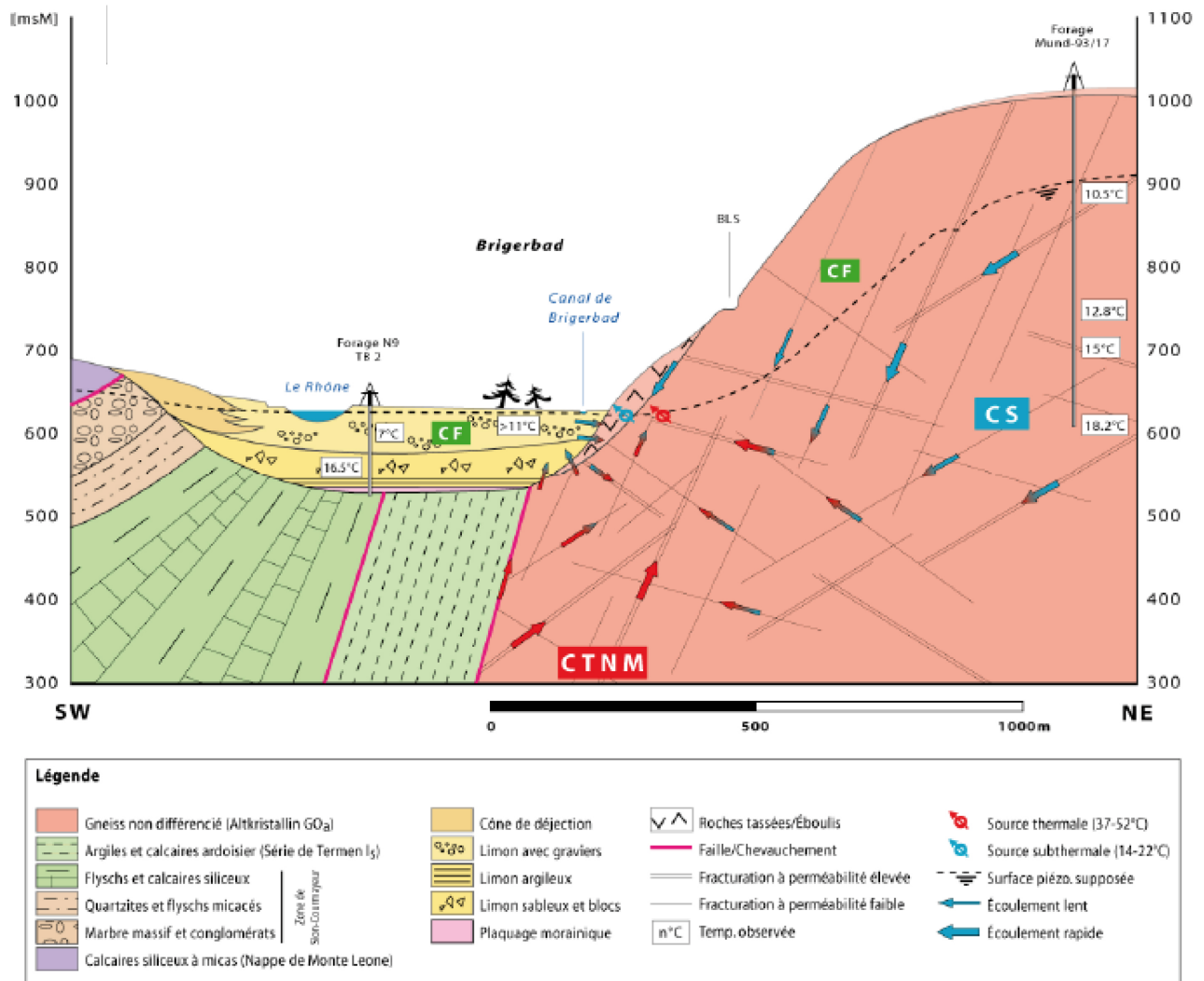
Figure 16.3: Conceptual model of the hydrothermal system of Brigerbad (Alpgeo and Norbert SA 2008). The location of this site is indicated in Figure 16.2. CF means "Cold end-member", CS means "Sub-thermal end-member" and CTNM means "Thermal end-member".

279

Part VII

Bibliography

Bibliography

Aemissegger, B. (1993). Geothermie-Bohrung Pro San Gian, St. Moritz [The geothermal borehole of Pro San Gian, St. Moritz]. *Bull Ver schweiz Petroleum-Geol u -Ing 60*(136), 1–18.

Albu, M., D. Banks, and H. Nash (1997). *Mineral and thermal groundwater resources*. London, England: Chapman & Hall.

Alcalá, F.-J. and E. Custodio (2008). Using Cl/Br ration as a tracer to identify the origin of salinity in aquifers in Spain and Portugal. *Journal of Hydrology 359*, 189–207.

Allegrini, G., F. Luccioli, and A. Trivella (1992). Industrial uses of geothermal fluids at Larderello. *Geothermics 21*(5-6), 623–630.

Alpgeo Sàrl (1997). Expertise hydrogéologique et géochimique des eaux thermales exploitées par les bains de Val d'Illiez [Hydrogeological and geochemical valuation of exploited thermal waters at Val d'Illiez]. Unpublished report for SPIC S.A., Genève.

Alpgeo Sàrl (2001). Analyse chimique du forage F3 [Chemical analysis of the F3 borehole]. Société d'exploitation des eaux thermales et minérales de Val d'Illiez, Unpublished report.

Alpgeo Sàrl (2006a). Zone de protection du forage F3. Rapport hydrogéologique [Protection zone of the F3 borehole. Hydrogeological report]. Société d'exploitation des eaux thermales et minérales de Val d'Illiez, Unpublished report.

Alpgeo Sàrl (2006b). Forage F3. dossier pour l'obtention du certificat "eaux minérales naturelles" [Borehole F3. draft to obtain the certificate "natural mineral waters"]. Société d'exploitation des eaux thermales et minérales de Val d'Illiez, Unpublished report.

Alpgeo Sàrl (2007). Evaluation géologique préliminaire d'un forage profond à Champéry [Preliminary geological assessment of a deep borehole at Champéry]. SA des eaux et d'électricité de Champéry (SEE), Unpublished report.

Alpgeo Sàrl (2008). 3 forages pour l'installation de sondes géothermiques. Note hydrogéologique [3 boreholes for the installation of vertical borehole exchangers. Hydrogeological note]. Unpublished report.

Alpgeo Sàrl and Norbert SA (2008). Campagne de forage de reconnaissance 2008 [Drilling recognition in 2008]. Unpublished report, Hans Kalbermatten Thermalbad AG, Brigerbad (VS) - Projet de géothermie profonde à Brig-Glis - Phase 1.

Amberger, G.-F. (1960). *L'autochtone de la partie nord-ouest du massif des Aiguilles Rouges (Haute-Savoie et Valais) [The autochtonous cover in the north-western part of the Aiguilles Rouges Massif (Haute-Savoie and Wallis)]*. Ph. D. thesis, University of Geneva, Switzerland.

André, L., V. Rabemanana, and F.-D. Vuataz (2006). Influence of water-rock interactions on fracture permeability of the deep reservoir at Soultz-sous-Forêts, France. *Geothermics 35*(5), 507–531.

ANTEA (2000). Saint-Gervais (74). Expertise du potentiel thermal actuel et des systèmes d'exploitation [Saint-Gervais (74). Expertise of the current thermal potential and of the exploitation systems]. Unpublished report Nr 26163/B.

ANTEA (2004). Demande d'autorisation d'exploiter à l'émergence et de transporter l'eau minérale du forage Lépinay [Authorization request to exploit and to transport the mineral water from the Lépinay borehole]. Unpublished report Nr 33153/C.

Appelo, C.-A.-J. and D. Postma (2005). *Geochemistry, groundwater and pollution*. Rotterdam: Balkema.

Arnórsson, S. (1975). Application of the silica geothermometer in low temperature area in Iceland. *American Journal of Science 275*, 763–784.

Arnórsson, S. (1983). Chemical equilibria in icelandic geothermal systems - Implications for chemical geothermometry investigations. *Geothermics 12*, 119–128.

Arnórsson, S. (2000). Isotopic and chemical techniques in geothermal exploration, development and use. Vienna, Austria. International Atomic Energy Agency.

Arnórsson, S., A. Andrésdottir, I. Gunnarsson, and A. Stefánsson (1998). New calibration for the quartz and Na/K geothermometers - valid in the range 0-350ºC. pp. 42–43. Proc. Geoscience Society of Iceland Annual Meeting.

Arnórsson, S., E. Gunnlaugsson, and H. Svavarsson (1983). The chemistry of geothermal waters in Iceland. III. Chemical geothermometry in geothermal investigations. *Geochimica and Cosmochimica Acta 47*, 567–577.

Arthaud, F. and J. Dazy (1989). Migration des saumures au front des chevauchements de l'arc alpin [Migration of brines in front of Alpine thrust faults]. *CR Acad Sci Paris 309*(2), 1425–1430.

Badoux, H. (1971). *Atlas géologique de la Suisse 1/25'000, Feuille 1305: Dents de Morcles. Notice explicative [Geological atlas of Switzerland 1/25'000, Map 1305: Dents de Morcles. Explanatory leaflet]*. Bern, Switzerland: Commission Géologique Suisse, Kümmerly and Frey SA.

Badoux, H. (1996). Le substratum des Préalpes du Chablais [The substratum of the Chablais Alps]. *Bull Soc Vaud Sci Nat 84*(2), 113–124.

Baietto, A., P. Cadoppi, G. Martinotti, P. Perello, P. Perrochet, and F.-D. Vuataz (2008). Assessment of thermal circulations in strike-slip fault systems: the Terme di Valdieri case (Italian western Alps). *Geological Society, London, Special Publications 299*, 317–339.

Balderer, W. (1990). Hydrogeologische Charakterisierung der Grundwasservorkommen innerhalb der Molasse der Nordostschweiz aufgrund von hydrochemischen und isotopenuntersuchungen [Hydrogeological properties of alluvial groundwaters in the northeastern part of the molasse basin from hydrochemical and isotopic methods]. *Steir Beitr zur Hydrogeologie 41*, 35–104.

Barat, A. and P. Jerphanion (1989). Réalisation de deux forages d'eau thermale SG1 et SG2. Compte rendu des travaux et résultats [Realization of the two SG1 and SG2 boreholes for thermal waters. Report of works and results]. BRGM,8SGN496RHA, unpublished report.

Baria, R., J. Baumgärtner, A. Gérard, R. Jung, and J. Garnish (1999). European HDR research programme at Soultz-sous-Forêts (France) 1987-1996. *Geothermics 28*, 655–669.

Bächler, D., T. Kohl, and L. Rybach (2003). Impact of graben-parallel faults on hydrothermal convection - Rhine Graben case study. *Phys Chem Earth 28*, 431–441.

Bear, J. (1972). *Dynamics of fluids in porous media*. New York, United States: American Elsevier.

Bertani, R. (2005). World geothermal power generation in the period 2001-2005. *Geothermics 34*, 651–690.

Besson, O., R. Marchant, A. Pugin, and J.-D. Rouiller (1993). Campagne de sismique réflexion dans la vallée du Rhône entre Sion et Saint-Maurice: perspectives d'exploitation géothermique des dépôts torrentiels sous-glaciaires [Seismic reflexion profile in the Rhone Valley between Sion and Saint-Maurice: prospects for geothermal exploitation in the subglacial torrential deposits]. *Bull Centre d'Hydrogeol Neuchâtel 12*, 39–58.

Besson, O., J.-D. Rouiller, W. Frei, and H. Masson (1992). Campagne de sismique-réflexion dans la vallée du Rhône entre Sion et Martigny [Seismic reflexion profile in the Rhone Valley between Sion and Martigny]. *Bull Murithienne 109*, 45–63.

Bianchetti, G. (1990). Recherche d'eau thermale à Lavey-les-Bains. Forage P205: suivi et interprétation hydrogéologique [Search of thermal water in Lavey-les-Bains. Borehole P205: measurements and hydrogeological interpretation]. Master's thesis, University of Neuchâtel, Switzerland.

Bianchetti, G. (1993a). Etablissement thermal de Lavey-les-Bains. Zones de protection des forages P201 et P205 [Thermal establishment of Lavey-les-Bains. Protection zones of the P201 and P205 boreholes]. Unpublished report, ETBL 92/3.

Bianchetti, G. (1993b). Circulations profondes dans les Alpes: Hydrogéologie, géochimie et géothermie des sources thermales du Valais (Suisse) et régions limitrophes [Deep flow systems in the Alps: Hydrogeology, geochemistry and geothermal properties of thermal waters in Wallis (Switzerland) and neighbouring areas]. Unpublished report.

Bianchetti, G. (1994). Hydrogéologie et géothermie de la région de Lavey-les-Bains (Vallée du Rhône, Suisse) [Hydrogeology and geothermal properties of the Lavey-les-Bains area (Rhone Valley, Switzerland]. *Bull Centre d'Hydrogeol Neuchâtel 13*, 3–32.

Bianchetti, G. (1996). Forages géothermiques F1, F2 et F3. Rapport hydrogéologique [Goethermal boreholes F1, F2 and F3. Hydrogeological report]. Les Bains de Val d'Illiez, Unpublished report.

Bianchetti, G. (2002). Opération géothermique de Lavey-les-Bains (VD). Réalisation du forage géothermique profond P600 et exploitation de la ressource énergétique par pompage dans les puits P600 et P201 (Juin 1997 - Décembre 2002) [Geothermal operation of Lavey-les-Bains (VD). Realization of a deep geothermal borehole named P600 and exploitation of the energy resource by pumping in the P600 and P201 wells (June 1997 - December 2002)]. Unpublished report.

Bianchetti, G., G. Crestin, T. Kohl, and O. Graf (2006). Géothermie du cristallin profond de la vallée du Rhône. Etude préliminaire [Geothermal properties of the deep basement of the Rhone Valley. Preliminary study]. Unpublished report.

Bianchetti, G. and J.-C. Hadorn (1996). Forage géothermique profond de Lavey-les-Bains. Requête pour l'obtention de la garantie du risque de forage [The deep geothermal borehole of Lavey-les-Bains. Request for the obtaining of the guarantee of the drilling risk]. Unpublished report.

Bianchetti, G., P. Roth, F.-D. Vuataz, and J. Vergain (1992). Deep groundwater circulation in the Alps: Relations between water infiltration, induced seismicity and thermal springs. the case of Val d'Illiez, Wallis. *Eclogae geol Helv 85*(2), 291–305.

Bianchetti, G. and J.-C. Rouiller (1998). Relation hydrogéologique Lac de Salanfe - sources thermales de Val d'Illiez, analyses des évènements séismo-hydrogéologiques de la période 1994-1996 [Hydrogeological relationships between the Salanfe Lake and thermal springs at Val d'Illiez, analyses of seismo-hydrogeological events for the period 1994-1996]. Unpublished report, CREALP98.03.

Bianchetti, G., F. Zuber, F.-D. Vuataz, and J.-D. Rouiller (1993). Programm GEOTHERMOVAL. Hydrogeologische und Geothermische Untersuchungen im Simplontunnel [Program GEOTHERMOVAL: Hydrogeological and geothermal studies about groundwaters in the Simplon tunnel]. *Matér Géol Suisse, Sér Géotech 88*, 75.

Bissig, P. (2004). Die CO_2-reichen Mineralquellen von Scuol-Tarasp (Unterengadin, Kt. GR) [The CO_2-rich mineral springs of Scuol-Tarasp (Lower Engadine, Canton GR]. *Bull angew Geol 9*(2), 39–47.

Bissig, P., N. Goldscheider, J. Mayoraz, H. Surbeck, and F.-D. Vuataz (2006). Carbogaseous spring waters, coldwater geysers ans dry CO_2 exhalations in the tectonic window of the Lower Engadine Valley, Switzerland. *Eclogae geol Helv 99*, 143–155.

Blavoux, B. (1978). *Etude du cycle de l'eau au moyen de l'oxygène-18 et du tritium [Study of the water cycle using oxygen-18 and tritium].* Ph. D. thesis, Université P et M Curie, Paris 6, France.

Blavoux, B. and F. Berthier (1985). Les originalités hydrogéologique et technique des eaux minérales [hydrogeological and technical properties of mineral waters]. *Bull Soc géol France 1*(7), 1033–1044.

Blavoux, B., A. Burger, P. Chauve, and J. Mudry (1979). Utilisation des isotopes du milieu à la prospection hydrogéologique de la chaîne karstique du Jura [Use of the isotopes for hydrogeological investigation in the karstic Jura range]. *Revue de géologie dynamique et géographique physique 21*, 295–306.

Bortolami, G.-C., B. Ricci, G.-F. Susella, and G.-M. Zuppi (1979). Isotope Hydrogeology of the Val Corsaglia, Maritime Alps, Piedmont, Italy. In Isotope Hydrogeology. Vienna, Austria. International Atomic Energy Agency.

Bowen, R. (1989). *Geothermal resources.* London and New York: Elsevier Applied Science, Second Edition.

BRGM (2006). *Aquifères et eaux souterraines de France [Aquifers and groundwaters in France].* Orléans, France: BRGM éditions.

Brändlein, P., G. Nollau, Z. Sharp, and J.-F. Von Raumer (1994). Petrography and geochemistry of the Vallorcine granite (Aiguilles Rouges massif, Western Alps). *Schweiz Mineral Petrogr Mitt 74*, 227–243.

Bureau Tissières (1996a). Analyse structurale succincte du massif rocheux à Play, Val d'Illiez [A brief structural analysis of the bedrock at Play, Val d'Illiez]. Unpublished report Nr 3.123-3.

Bureau Tissières (1996b). Etude hydrogéologique des eaux souterraines de Play à Val d'Illiez et forage de reconnaissance sur la parcelle Nr 171 [Hydrogeological study of groundwaters of Play at Val d'Illiez and exploration borehole on the piece Nr 171]. Unpublished report Nr 3.123-2.

Bureau Tissières (2003). Notice d'impact liée à l'exécution d'un forage géothermique sur la parcelle Nr 171 à Play (commune de Val d'Illiez) [Notice of impact related to the implementation of a geothermal borehole on the piece Nr 171 at Play (township of Val d'Illiez)]. Unpublished report Nr 3.123-4.

Bussy, F., J.-F. Von Raumer, and N. Capuzzo (2001, Lausanne). Mont Blanc and Aiguilles Rouges Massifs - (External Massifs). Field-Trip 1. *Mémoires de Géologie 36*, 53–85.

Calmbach, L. (1995). *Etude géochimique et isotopique des émergences thermominérales du Fossé Rhénan supérieur (Alsace et Baden-Württemberg) [Geochemical and isotopic study of thermal and mineral waters in the upper Rhine Graben (Alsace and Baden-Württemberg)].* Ph. D. thesis, University of Lausanne, Switzerland.

Capuzzo, N. and F. Bussy (2000). High-precision dating and origin of synsedimentary volcanism in the late carboniferous Salvan-Dorénaz basin (Aiguilles Rouges Massif, Western Alps). *Schweiz Mineral Petrogr Mitt 80*, 147–167.

Carlé, W. (1975). *Die Mineral- und Thermalwässer von Mitteleurope. Geologie, Chemismus, Genese. 2 vol., Wissenschaftliche [Mineral and thermal waters of central Europe: Geology, Chemistry, Origin, 2 vol., Science].* Stuttgart, Germany: Verlagsgesellschaft mbH.

Castany, G. (1963). *Traité pratique des eaux souterraines [Practical aspect of groundwaters].* Paris, France: Dunod.

Castany, G. and J. Margat (1977). *Dictionnaire français d'hydrogéologie [French dictionary of hydrogeology].* Orléans, France: BRGM éditions.

Cataldi, R. (1999). The year zero of geothermics. In *R Cataldi, SF Hodgson and JW Lund. Stories from a heated Earth, Geothermal Resource Council*, Davis, California, USA, pp. 7–17.

Cavalli, D. (1993). Etablissement thermal de Lavey-les-Bains. Forage de reconnaissance pour la recherche d'eau potable et l'exploration pour l'eau thermale au lieu-dit Gravière du Bras [Thermal establishment of Lavey-les-Bains. Drilling of recognition for the search of drinking water and exploration for thermal water in the site of Gravière du Bras]. Unpublished report.

Chapman, D.-S. and L. Rybach (1985). Heat flow anomalies and their interpretation. *Journal of Geodynamics 4*, 3–37.

Clark, I.-D. and P. Fritz (1997). *Environmental isotopes in hydrogeology.* New York: Lewis Publischers.

Clark, S.-P. and E.-R. Niblett (1956). Terrestrial heat flow in the Alps. *Astr Soc Mon Not 7*, 176–195.

Clauser, C. (2003). *Numerical simulation of reactive flow in hot aquifers.* Berlin, Heidelberg, New York: Springer-Verlag.

Claypool, G.-E., W.-T. Holser, I.-R. Kaplan, H. Sakai, and I. Zai (1980). The Age Curves of Sulfur and Oxygen Isotopes in Marine Sulfate and their Mutual Interpretation. *Chemical Geology 28*, 199–260.

Collet, L.-W., N. Oulianoff, and M. Reinhard (1952). *Atlas géologique de la Suisse 1/25'000, Feuille 525: Finhaut. Notice explicative [Geological atlas of Switzerland 1/25'000, Map 525: Finhaut. Explanatory leaflet].* Bern, Switzerland: Commission Géologique Suisse, Kümmerly and Frey SA.

Collin, J.-J. (2004). *Les eaux souterraines: connaissance et gestion [Groundwaters: knowledge and management].* Orléans, France: BRGM éditions.

Cook, P.-G. and A.-L. Herczeg (2000). *Environmental tracers in subsurface hydrology.* Dortrecht, Netherlands: Kluwer Academic Publishers.

Craig, H. (1961). Standard for reporting concentrations of deuterium and oxygen-18 in natural waters. *Science 133*(3467), 1833–1834.

CREALP (1998). Relation hydrogéologique Lac de Salanfe - Sources thermales de Val d'Illiez. Analyse des évènements séismo-hydrogéologiques [Hydrogeological relation between Salanfe Lake - Val d'Illiez thermal springs. Analysis of seismical and hydrogeological events]. Unpublished report, CREALP/98.03.

CRSFA (1989). Programme GEOTHERMOVAL, Recherche et mise en valeur des ressources géothermiques du Valais: Région Evionnaz - Collonges - Saint-Maurice. Rapport intermédiaire [Program GEOTHERMOVAL, Search and development of the geothermal resources from Wallis: Evionnaz - Collonges - Saint-Maurice area. Intermediate report]. Unpublished report, CRSFA/89.15.

CRSFA (1992a). Programme GEOTHERMOVAL, Recherche et mise en valeur des ressources géothermiques du Valais. Rapport final, phase 1 [Program GEOTHERMOVAL. Prospection and development of the geothermal resources from Wallis: Final report, phase 1]. Unpublished report, CRSFA/92.01.

CRSFA (1992b). Programme GEOTHERMOVAL, Recherche et mise en valeur des ressources géothermiques du Valais. Rapport final, phase 1: Saint-Maurice [Program GEOTHERMOVAL, Prospection and development of the geothermal resources from Wallis. Phase 1, final report: Saint-Maurice]. Unpublished report, CRSFA/92.03.

CRSFA (1992c). Programme GEOTHERMOVAL, Recherche et mise en valeur des ressources géothermiques du Valais. Rapport final, phase 1: Forage de reconnaissance E1 et E2 à Epinassey (Saint-Maurice) [Program GEOTHERMOVAL, Prospection and development of the geothermal resources from Wallis. Phase 1, final report: Drilling of recognition E1 and E2 in Epinassey (Saint-Maurice)]. Unpublished report, CRSFA/92.18.

CRSFA (1992d). Programme GEOTHERMOVAL, Recherche et mise en valeur des ressources géothermiques du Valais. Rapport final, phase 1: Val d'Illiez [Program GEOTHERMOVAL, Prospection and development of the geothermal resources from Wallis. Phase 1, final report: Val d'Illiez]. Unpublished report, CRSFA/92.25.

CRSFA (1996). Avis hydrogéologique sur la source de la Léchère à Champéry [Hydrogeological advice on the Léchère spring at Champéry]. File note.

Cruchet, M. (1985). Influence de la décompression sur le comportement hydrogéologique des massifs cristallins de basse maurienne (Savoie, France) [Role of the decompressed zone on the hydrogeological behavior in the crystalline massifs of the Lower Maurienne (Savoy, France]. *Géologie Alpine 61*, 65–73.

D'Amore, F. and S. Arnórsson (2000). Geothermometry. In S Arnórsson. Isotopic and chemical techniques in geothermal exploration, development and use. Vienna, Austria, pp. 152–199. International Atomic Energy Agency.

Debelmas, J. and C. Kerkhove (1980). Les Alpes Franco-Italiennes [Italian and French Alps]. *Géologie Alpine 56*, 21–58.

De Marsily, G. (1986). *Quantitative hydrology. Groundwater Hydrology for Engineers.* New York, United States: Academic press.

Demathieu, G. and M. Weidmann (1982). Les empreintes de pas de reptiles dans le Trias du Vieux Emosson [The footprints of reptiles in the Vieux Emosson formations (Trias)]. *Eclogae geol Helv 75*(3), 721–757.

Diersch, H.-J. (1996). *Interactive, graphics-based finite element simulation system FEFLOW for modeling groundwater flow, contaminant mass and heat transport processes.* Berlin, Germany: WASY.

Dobson, P.-F., S. Salah, N. Spycher, and E.-L. Sonnental (2004). Simulation of water-rock interaction in the Yellowstone geothermal system using TOUGHREACT. *Geothermics 33*(4), 493–502.

Drever, J.-I. (1997). *The geochemistry of natural waters: surface and groundwater.* Upper Saddle River, New Jersey: Prentice-Hall.

Dubois, J.-D. (1991). *Typologie des aquifères du cristallin: exemples des massifs des Aiguilles Rouges et du Mont-Blanc (France, Italie, Suisse) [Typology of crystalline aquifers: examples of Aiguilles Rouges and Mont-Blanc Massifs (France, Italy, Switzerland].* Ph. D. thesis, EPFL, Lausanne, Switzerland, Nr 950.

Ducloz, C. (1944). *Le flysch des Dents du Midi (Valais) [The flsych of the Dents du Midi (Wallis)].* Ph. D. thesis, University of Geneva, Switzerland.

Durand-Fardel, M. (1857). *Traité thérapeutique des eaux minérales de France et d'étranger et de leur emploi dans les maladies chroniques [Therapeutic aspect of mineral water in France and abroad and their employment in the chronic diseases].* Paris, France: Martinet.

Duriez, A. (2006). *Origine et processus de minéralisation d'eaux thermales en milieu continental méditerranéen: cas du système géothermal des Thermophyles (Grèce) [Origin and process of mineralization in thermal waters from Mediterranean continental environment: the case of Thermophyles hydrothermal system (Greece)]*. Ph. D. thesis, University of Paris Sud 11, Orsay, France.

Dzikowski, M. and D. Lhomme (2004). Hydrogéologie des massifs cristallins alpins [Hydrogeology of the Alpine crystalline massifs]. Unpublished report.

Eaton, A.-D., L.-S. Clesceri, and A.-E. Greenberg (1995). *Standards Methods for the Examination of Water and Wastewater*. 19th edition.

Edmunds, W.-M., R.-L. Kay, and R.-A. McCartney (1985). Origin of saline groundwaters in the Carnmenellis granite (Cornwall, England): natural processes and reaction during hot dry rocks reservoir circulation. *Chemical Geology 49*, 287–301.

Ellis, A.-J. (1979). Chemical geothermometry in geothermal systems. *Chemical Geology 25*, 219–226.

Epard, J.-L. (1989). Stratigraphie du Trias et du Lias dauphinois entre Belledonne, Aiguilles Rouges et Mont-Blanc [Stratigraphy of the helvetic Trias and Lias between Belledonne, Aiguilles Rouges and Mont-Blanc]. *Bull Soc Vaud Sci Nat 79*(4), 310–338.

Epard, J.-L. (1990). La nappe de Morcles au sud-ouest du Mont-Blanc [The Morcles nappe in the southwest of the Mont-Blanc]. *Mémoires de Géologie 8*, 165.

Etcheverry, D. (2002). Valorisation des méthodes isotopiques pour les questions liées aux eaux souterraines. Isotopes de l'oxygène et de l'hydrogène [Valuation of isotopic methods to issues related to groundwaters. Isotopes of oxygen and hydrogen]. Technical report OFEG.

Falconnier, A. (1952). Source thermale de Lavey-les-Bains. Considérations géologiques et hydrogéologiques [Thermal springs of Lavey-les-Bains. Geological and hydrogeological considerations]. *Mém Soc Vaud Sci Nat 65*(280), 245–252.

Fischer, G., P.-A. Schnegg, J. Ma, I. Müller, and M. Burkhard (1987). Etude VLF-R du remplissage quaternaire de la vallée de Gastern (Alpes Bernoises, Suisse) [Study of the Quaternary filling of the Gastern Valley (Bernese Alps, Switzerland)]. *Eclogae geol Helv 80*(3), 773–787.

Flamm, C. (1993). Etude de la fracturation du Massif des Aiguilles Rouges dans la région de Saint-Maurice [Study of the fracturation of the Aiguilles Rouges Massif in the area of Saint-Maurice]. Master's thesis, University of Lausanne, Switzerland.

Flores-Márquez, E.-L., G. Jiménez-Suárez, R.-G. Martínez-Serrano, R.-E. Chávez, and D. Silva-Pérez (2006). Study of geothermal water intrusion due to groundwater exploitation in the Puelba Valley aquifer system, Mexico. *Hydrogeology Journal 14*(7), 1216–1230.

Féneyrou, G. (1989). *La vie des eaux thermominérales [Thermal waters characteristics]*. Toulouse, France: Erès.

Fontes, J.-C. (1976). Les isotopes du milieu dans les eaux naturelles [The water stable isotopes in groundwaters]. *La Houille Blanche 3*(4), 205–221.

Fontes, J.-C. (1980). *Environmental Isotopes in Groundwater Hydrology. In P Fritz and JC Fontes Ed. Handbook of Environmental Isotope Geochemistry, The Terrestrial Environment*, Volume 1, pp. 75–140. Amsterdam, Netherlands: Elsevier.

Foucault, A. and J.-F. Raoult (2001). *Dictionnaire de Géologie [Dictionary of geology]*. Paris, France: Dunod, 5e édition.

Fouillac, C., A.-M. Fouillac, and A. Criaud (1990). Sulphur and oxygen isotopes of dissolved sulphur species in formation waters from the Dogger geothermal aquifer, Paris Basin, France. *Applied Geochemistry 5*(4), 415–427.

Fouillac, C. and S. Michard (1981). Sodium/lithium ratio in water applied to geothermometry of geothermal reservoirs. *Geothermics 10*, 55–70.

Fournier, R.-O. (1977). Chemical geothermometers and mixing models for geothermal systems. *Geothermics 5*, 41–50.

Fournier, R.-O. (1979). A revised equation for the Na/K geothermometer. *Geothermal Resources Council Transactions 3*, 221–224.

Fournier, R.-O. (1981). *Application of water geochemistry to geothermal exploration and reservoir engineering. In L Rybach and LJP Muffler Ed. Geothermal systems: principles and case histories*, pp. 109–143. New York, United States: John Wiley and Sons.

Fournier, R.-O. (1991). Water geothermometers applied to geothermal energy. In F D'Amore. Application of geochemistry in geothermal reservoir development. Rome, Italy, pp. 37–69. United Nations Institute for Training and Research.

Fournier, R.-O. and R.-W. Potter (1979). Magnesium correction to the Na-K-Ca chemical geothermometer. *Geochimica and Cosmochimica Acta 43*, 1543–1550.

Fournier, R.-O. and R.-W. Potter (1982). A revised and expanded silica (quartz) geothermometer. *Geothermal Resourcse Council Bulletin 11*(10), 3–12.

Fournier, R.-O. and A.-H. Truesdell (1973). An empirical Na-K-Ca geothermometers for natural waters. *Geochimica and Cosmochimica Acta 37*, 1255–1275.

Fritz, P. and J.-C. Fontes (1986). *Handbook of Environmental Isotope Geochemistry*, Volume 2: The Terrestrial Environment, B. Amsterdam, Netherlands: Elsevier.

Gagnebin, E. (1934). *Atlas géologique de la Suisse 1/25'000, Feuille 483: St-Maurice. Notice explicative [Geological atlas of Switzerland 1/25'000, Map 483: St-Maurice. Explanatory leaflet].* Bern, Switzerland: Commission Géologique de la Société Helvétique des Sciences Naturelles, A Franke SA.

Gainon, F. (2008). *Les isotopes radioactifs de la série de l'uranium-238 (^{222}Rn, ^{226}Ra, ^{238}U and ^{234}U) dans les eaux thermales de Suisse [Radioactive isotopes in the series of uranium-238 (^{222}Rn, ^{226}Ra, ^{238}U and ^{234}U) in thermal waters from Switzerland].* Ph. D. thesis, University of Neuchâtel, Switzerland.

Gallino, S. (2008). *Hydrogéologie, géochimie et modélisation hydrodynamique-thermique d'un système thermo-minéral associé à un contact structural alpin (Aix-les-Bains - Savoie) [Hydrogeology, chemistry and numerical modelling of groundwater heat and flow transports of a hydrothermal system related to a Alpine fault system (Aix-les-Bains - Savoie)].* Ph. D. thesis, University of Savoie, Chambéry, France.

Gascoyne, M. and D.-C. Kamineni (1994). The hydrogeochemistry of fractured plutonic rocks in the Canadian Shield. *Applied Hydrogeology 2*, 43–49.

Geothechnisches Institut (1980). Sources d'eau thermominérales à Buchelieule, Val d'Illiez: rapport hydrogéologique et géothechnique [Thermal and mineral springs at Buchelieule, Val d'Illiez: hydrogeological and geotechnical report]. Unpublished report, Bern.

GEOWATT AG (2009). Statistik der geothermischen. Nutzung in der Schweiz - Ausgabe 2008 [Statistics of the geothermal energy. Use in Switzerland - Edition 2008]. Unpublished report.

Gevrek, A.-I. (2000). Water/rock interaction in the Kizilcahamam Geothermal Field, Galatian Volcanic Province (Turkey): a modelling study of a geothermal system for reinjection well locations. *Journal of Volcanol and Geotherm Res 96* (3-4), 207–213.

Geyh, M.-A. (2000). An overview of ^{14}C analysis in the study of groundwater. *Radiocarbon 42* (1), 99–114.

Giggenbach, W.-F. (1988). Geothermal solute equilibria. Derivation of Na-K-Mg-Ca geoindicators. *Geochimica and Cosmochimica Acta 52*, 2749–2765.

Gilli, E., C. Mangan, and J. Mudry (2004). *Hydrogéologie: Objectifs, méthodes et applications [Hydrogeology: Objectives, methods and applications]*. Paris, France: Dunod.

Gorhan, H.-L. and J.-C. Griesser (1998). Geothermische Prospektion im Raume Schinznach Bad - Baden [Geothermal prospection in the area of Schinznach Bad - Baden]. *Matér Géol Suisse, Sér Géotech 76.*

Gérard, A., A. Genter, T. Kohl, P. Lutz, P. Rose, and F. Rummel (2006). The deep EGS (Enhanced Geothermal System) project at Soultz-sous-Forêts (Alsace, France) 1987-1996. *Geothermics 35* (5-6), 473–483.

Grimaud, D. (1987). *Etude géochimique et géothermométrique de eaux thermominérales des Alpes Françaises [Geochemical study and use of geothermometers in mineral and thermal waters in the French Alps]*. Ph. D. thesis, University of Paris 7, France.

Hartmann, P. (1998). *Mineralwasservorkommen im nördlichen Bündnerschiefergebeit mit Schwerpunkt Valsertal [Mineral water occurences in the northern Bündner schist zone, with focus on the Valser Valley]*. Ph. D. thesis, ETHZ, Zurich, Switzerland, Nr 12'632.

Hem, J.-D. (1985). *Study and interpretation of the chemical characteristics of natural water*. US Geological Survey, Water-Supply Paper 2254.

Henley, R.-W., A.-H. Truesdell, and P.-B. Barton (1984). *Fluid-mineral equilibria in hydrothermal systems. Chapter 6 Hydrolysis reactions in hydrothermal fluids*, pp. 65–82. Society of Economic Geology Reviews in Economic Geology.

Högl, O. (1980). *Die Mineral- und Heilquellen der Schweiz. [Mineral and wellbeing waters from Switzerland]*. Bern and Stuttgart, Switzerland and Germany: Haupt.

Hunkeler, D. (2006). Hydrochemistry. Introduction. Course note, University of Neuchâtel, Switzerland.

Ingerson, E. and F.-J. Pearson (1964). *Estimation of age and rate of motion of ground-wasser by the ^{14}C-method. In Y Miyake and T Koyama Ed. Recent Researches in the Fields of Hydrosphere Atmosphere and Nuclear Geochemistry*, pp. 263–283. Tokyo, Japan: Maruzen.

Iundt, F. (2008). Interprétation des inspections vidéos et diagraphies des forages De Mey Est et Ouest [Interpretation of video inspections and diagraphies in the De Mey est and De Mey Ouest boreholes]. Unpublished report.

Iundt, F., M. Lopoukhine, and A. Malatrait (1987). Etude du système thermal de Saint-Gervais-les-Bains (Haute-Savoie) [Study of the hydrothermal system of Saint-Gervais-les-Bains (Haute-Savoie)]. BRGM, 88SGN016RHA, unpublished report.

Jaboyedoff, M. and S. Pastorelli (2003). Pertubation of the heat flow by water circulation in a mountainous framework: Example from the Swiss Alps. *Eclogae geol Helv 96*, 37–47.

Jaeckli, H. (1970). Kriterien zur Klassifikation von Grundwasservorkommen [Classification criteria of groundwater resources]. *Eclogae geol Helv 63* (2), 389–434.

Jaffé, F.-C., F. Benoit, and D. Roux (1976). Low enthalpy geothermal energy development in Switzerland: the thermal springs of Lavey and its utilisation. In *Proc Int Congr Thermal Waters, Geothermal Energy and Volcanism Mediterranean Area*, Volume 1, Athens, Greece.

Jamier, D. (1975). *Etude de la fissuration, de l'hydrogéologie et de la géochimie des eaux profondes des massifs de l'Arpille et du Mont-Blanc [Study of the fissuration, hydrogeology and geochemistry in deep waters of the Arpille and Mont-Blanc Massifs]*. Ph. D. thesis, University of Neuchâtel, Switzerland.

Jenny, J., J.-P. Burri, R. Muralt, A. Pugin, R. Schegg, P. Ungemach, F.-D. Vuataz, and R. Wernli (1995). Le forage géothermique de Thônex (canton de Genève): Aspects stratigraphiques, tectoniques, diagénétiques, géophysiques et hydrogéologiques [The Thônex geothermal borehole (canton of Geneva): stratigraphic, tectonic, diagenetic, geophysics and hydrogeological aspects]. *Eclogae geol Helv 88*(2), 365–396.

Kaufman, S. and W.-F. Libby (1954). The natural distribution of tritium. *Phys. Rev. 93*(6), 1337–1344.

Kern, A. (1982). Etude hydrogéologique et géochimique des sources du Chamblon et des autres sources thermales et minérales de la région d'Yverdon-les-Bains (Vaud) [Hydrogeological and geochemical study of the Chamblon springs and other thermal and mineral springs from the Yverdon-les-Bains region (Vaud)]. Master's thesis, University of Geneva, Switzerland.

Kerrich, R., I. Allison, R.-L. Barnett, S. Moss, and J. Starkey (1980). Microstructural and chemical transformations accompanying deformation of granite in a shear zone at Miéville, Switzerland; With implications for stress corrosion craking and superplastic flow. *Contrib Mineral Petrol 73*, 221–242.

Kharaka, Y.-K., M.-S. Lico, and L.-M. Law (1982). Chemical geothermometers applied to formations waters. Gulf of Mexico and California Basin. *Am Assoc Petroleum Geol Bull 66*, 558.

Kharaka, Y.-K. and R.-H. Mariner (1989). *Chemical geothermometers and their application to formation waters from sedimentary basins. In ND Neaser and TH McCulloh Eds. Thermal History of Sedimentary Basins - Methods and Case Histories*, pp. 99–117. New York, United States: Springer-Verlag.

Kharaka, Y.-K., D.-J. Specht, and W.-W. Carothes (1985). Low to intermediate subsurface temperatures calculated by chemical geothermometers. New Orleans. American Association of Petroleum Geologists, Annual meeting.

Kühn, M. (2004). *Reactive flow modeling of hydrothermal systems*. Berlin, Heidelberg, New York: LNES 103, Springer-Verlag.

Kühn, M. and H. Stöfen (2004). A reactive flow model of the geothermal reservoir Waiwera; New Zealand. *Hydrogeology Journal 13*(4), 606–626.

Kohl, T., K.-F. Evans, R.-J. Hopkirk, and L. Rybach (1995). Coupled hydraulic, thermal and mechanical considerations for the simulation of hot dry rock reservoirs. *Geothermics 24*(3), 345–359.

Kolditz, O. and C. Clauser (1998). Numerical simulation of flow and heat transfer in fractured crystalline rocks: Application to the Hot Dry Rock site in Rosemanowes (UK). *Geothermics 27*(1), 1–23.

Krummenacher, P. and G. Bianchetti (1995). Pour une énergie géothermique vraiment concurrentielle: optimisation de la cascade énergétique du centre thermal cantonal de Lavey-les-Bains (VD), sans pompe à chaleur et avec forage géothermique profond. Rapport final [For a really competing geothermal energy: optimization of the energy of the cantonal thermal center of Lavey-les-Bains (VD), without heat pump and with a deep geothermal borehole. Final report]. Unpublished report, Projet Nr 10'630.

Kullin, M. and H. Schmassmann (1991). *Isotopic Composition of Modern Recharge. In FJ Pearson et al. Applied Isotope Hydrogeology. A Case Study in Northern Switzerland*, pp. 65–116. Amsterdam, Netherlands: Studies in Environmental Science 43, Elsevier.

Ladner, F. (2005). Hydrogéologie, hydrochimie et conditions d'exploitation du système hydrothermal de Combioula, Val d'Herens (Valais) [Hydrogeology, hydrochemistry and exploiting conditions of the Combioula hydrothermal system, Herens Valley (Wallis)]. Master's thesis, University of Neuchâtel, Switzerland.

Langmuir, D. (1997). *Aqueous environmental geochemistry*. Upper Saddle River, New Jersey: Prentice-Hall.

Lanterno, E. (1954). *Etude géologique des environs de Champéry (Val d'Illiez, Valais) [Geological study around Champéry (Val d'Illiez, Wallis)]*. Extrait des Archives des Sciences, University of Geneva, Switzerland 6(6), 295-376.

Lebdioui, S. (1985). *Origine des composés du soufre et du carbone dans les eaux d'un massif cristallin fracturé: le Mont-Blanc [Origin of sulfur and carbon components in groundwaters of a fractured crsytalline massif: the Mont-Blanc]*. Ph. D. thesis, Université Paris-sud, France.

Lehner, R. (1990). Reflexionseismische und geothermische Prospektion im Rhonetal (Vaud/Valais) [Seismic reflexion and geothermal prospection in the Rhone Valley (Vaud/Wallis)]. Master's thesis, ETHZ, Zurich, Switzerland.

Le Fanic, R. (2005). *Hydrogéologie d'un système thermal et modélisation couplée hydrodynamique - thermique en vue de la gestion de la ressource. Application au système de Dax - Saint-Paul-les-Dax [Hydrogeology of a deep flow system and numerical modelling of groundwater heat and flow transports for the management of the resource. Application to the system of Dax - Saint-Paul-les-Dax]*. Ph. D. thesis, University of Bordeaux 3, France.

Lhomme, D., M. Dzikowski, G. Nicoud, B. Payraud, S. Fudral, and P. Guillot (1996). Les circulations actives des eaux souterraines des massifs cristallins alpins: exemple des Aiguilles Rouges (Haute-Savoie, France) [Active circulations of groundwaters in the Alpine crystalline massifs: example of the Aiguilles Rouges (Haute-Savoie, France)]. *CR Acad Sci Paris 323*(2a), 681–688.

Lindal, B. (1973). Industrial and other applications of geothermal energy. In *Geothermal Energy: Review of Research and Development, UNESCO*, Paris, France, pp. 135–148.

Lis, G., L.-I. Wassenaar, and M.-J. Hendry (2008). High precision laser spectroscopy D/H and $^{18}O/^{16}O$ measurements of microliter natural water samples. *Analytical Chemistry 80*, 287–293.

Lloyd, J.-W. and J.-A. Heatcoate (1985). *Natural Inorganic Hydrochemistry in Relation to Groundwater. An introduction*. Oxford, England: Clarendon Press.

Lloyd, R.-M. (1968). Oxygen isotope behavior in the sulphate-water system. *Journal Geophys Res 73*, 6099–6110.

Lépinay, E. (1969). *Histoire des bains de Saint-Gervais [History of the baths of Saint-Gervais]*. Saint-Gervais-les-Bains, France: Ed. Lépinay.

Lüttig, G. (1985). The role of geothermal energy in the relation between resources and demand of conventional energies. In *E Romijn et al. Geothermics thermal - mineral waters and hydrogeology, Theophrastus Publications SA*, Athens, Greece, pp. 3–17.

Lugeon, M. and E. Argand (1937). *Atlas géologique de la Suisse 1/25'000, Feuille 485: Saxon-Morcles. Notice explicative [Geological atlas of Switzerland 1/25'000, Map 485: Saxon-Morcles. Explanatory leaflet]*. Bern, Switzerland: Commission Géologique de la Société Helvétique des Sciences Naturelles, A Franke SA.

Mandia, Y. (1991). *Typologie des aquifères évaporitique du Trias dans le bassin lémanique du Rhône (Alpes occientales) [Typology of the Triassic evaporitic aquifers in the Rhone Lemanic Basin (Western Alps)]*. Ph. D. thesis, EPFL, Lausanne, Switzerland, Nr 948.

Maréchal, J.-C. (1998). *Les circulations d'eau dans les massifs cristallins alpins et leurs relations avec les ouvrages souterrains [Water flows in the Alpine crystalline massifs and their relations with underground constructions]*. Ph. D. thesis, EPFL, Lausanne, Switzerland, Nr 1769.

Maréchal, J.-C. (1999a). Observation des massifs cristallins alpins au travers des ouvrages souterrains. 1. Caracérisation de la conductivité hydraulique à l'échelle du massif [Observation of Alpine crystalline massifs via underground constructions. 1. Characterization of the hydraulic conductivity on a massif scale]. *Hydrogéologie 1*, 21–32.

Maréchal, J.-C. (1999b). Observation des massifs cristallins alpins au travers des ouvrages souterrains. 2. Définition du rôle hydrogéologique de la zone décomprimée [Observation of Alpine crystalline massifs via underground constructions. 2. Definition of the hydrogeological role of the decompressed zone]. *Hydrogéologie 1*, 33–42.

Maréchal, J.-C., P. Perrochet, and L. Tacher (1999). Long-term simulation of thermal and hydraulic characteristics in a mountain massif: The Mont Blanc case study, French and Italien Alps. *Hydrogeology Journal 7*, 341–354.

Mariétan, I. (1953). Les sources chaudes à Val d'Illiez [The thermal springs at Val d'Illiez]. *Bulletin Murithienne 70*, 94–96.

Marini, L., G. Chiodini, and R. Cioni (1986). New geothermometers for carbonate-evaporite geothermal reservoirs. *Geothermics 15*(1), 77–86.

Marquer, D., E. Petrucci, and P. Iacumin (1994). Fluid advection in shear zones: evidence from geological and geochemical relationships in the Aiguilles Rouges Massif (Western Alps, Switzerland). *Schweiz Mineral Petrogr Mitt 74*, 137–148.

Mazor, E. (2004). *Chemical and isotopic groundwater hydrology*. New York: Marcel Dekker Publisher, 3rd edition.

McDermott, C.-I., A.-R.-L. Randriamanjatosoa, H. Tenzer, and O. Kolditz (2006). Simulation of heat extraction from crystalline rocks: The influence of coupled processes on differential reservoir cooling. *Geothermics 35*(3), 321–344.

Medici, F. and L. Rybach (1995). Geothermal map of Switzerland 1995 (Heat flow density). *Matér Géol Suisse, Sér Géophy 30*.

Mizutani, Y. and T.-A. Rafter (1969). Oxygen isotopic composition of sulphates - part 3. Oxygen isotopic fractionation in the bisulfate ion-water system. *New Zealand Journal Sci 12*(1), 54–59.

Moret, L. (1946). *Les sources thermominérales: Hydrologie, géochimie et biologie [Mineral and thermal waters: Hydrology, chemistry and biology]*. Masson.

Muralt, R. (1999). Processus hydrogéologiques et hydrochimiques dans les circulations profondes des calcaires du Malm de l'arc jurassien (zones de Delémont, Yverdon-les-Bains, Moiry, Genève et Aix-les-Bains) [Hydrogeological and hydrochemical processes in deep flow systems in the Malm limestones from the Jura range (zones of Delémont, Yverdon-les-Bains, Moiry, Geneva and Aix-les-Bains)]. *Matér Géol Suisse, Sér Géotech 82*.

Muralt, R. and F.-D. Vuataz (1993). Emergence d'eau thermale et mélange avec des eaux souterraines froides dans la gorge de la Dala à Leukerbad (Valais, Suisse) [Thermal springs and mixing processes with cold groundwaters in the gorge of Dala in Leukerbad (Wallis, Switzerland)]. *Bull Centre d'Hydrogeol Neuchâtel 12*, 111–135.

Nicholson, K. (1993). *Geothermal fluids. Chemistry and exploration techniques*. Berlin, Germany: Springer-Verlag.

Nieva, D. and R. Nieva (1987). Developments in geothermal energy in Mexico, Part 12. A cationic geothermometer for prospecting of geothermal resources. Volume 7, pp. 243–258. Heat Recovery Systems & CHP.

Nold, M. (1991). Interprétation des profils sismiques (réflexion) de la région de Saint-Maurice - Epinassey [Interpretation of the seismic profiles in the area of Saint-Maurice - Epinassey]. Unpublished report.

Ouedraogo, K. (1989). Etablissement thermal de Lavey-les-Bains. Exécution du forage P205: suivi des travaux et approche du comportement hydrodynamique de la nappe [Thermal establishment of Lavey-les-Bains. Realization of the P205 borehole: work progress and approach of the hydrodynamic behavior of the groundwater]. Master's thesis, University of Neuchâtel, Switzerland.

Pairis, J.-L., B. Pairis, J. Bellière, J. Rosset, H. Détraz, A. Muller, B. Muller, F. Villars, G. Mennessier, J. Charollais, P. Kindler, X. Pierre, and J.-P. Uselle (1992). *Carte géologique de la France 1/50'000, Feuille Cluses. Notice explicative [Geological map of France 1/50'000, Map Cluses. Explanatory leaflet].* Orléans, France: BRGM.

Pantet, A. (2004). Etude structurale et hydrogéologique de la région de Salanfe et du massif des Dents du Midi (Valais, Suisse) [Hydrogeological and structural study in the Salanfe region and in the Dents du Midi Massif (Wallis, Switzerland)]. Master's thesis, University of Lausanne, Switzerland.

Paréjas, E. (1925). La tectonique du Mont-Joly (Haute-Savoie) [The tectonic of the Mont-Joly (Haute-Savoie)]. *Eclogae geol Helv 19*(2), 419–503.

Parkhurst, D.-L. and C.-A.-J. Appelo (1999). *User's guide to PHREEQC (version 2) - a computer program for speciation, reaction-path, 1D-transport, and inverse geochemical calculations.* US Geological Survey Water-Resources Investigations, Report 99-4259.

Parriaux, A. and G. Nicoud (1993). Les formations glaciaires et l'eau souterraine [Quaternary formations and groundwater]. *Quaternaire 4*(2-3), 61–67.

Pastorelli, S. (1999). *Low enthalpy geothermal resources of the western Alps. Geochemical and isotopic consideration and tectonic constraints. Example from the cantons of Ticino and Bern (Switzerland).* Ph. D. thesis, University of Lausanne, Switzerland.

Pastorelli, S., L. Marini, and J.-C. Hunziker (1999). Water chemistry and isotope composition of the Acquarossa thermal system, Ticino, Switzerland. *Geothermics 28*, 75–99.

Pastorelli, S., L. Marini, and J.-C. Hunziker (2001). Chemistry, isotope value (δD, $\delta^{18}O$, $\delta^{34}S\ SO_4$) and temperatures of the water inflows in two Gotthard tunnels, Swiss Alps. *Applied Geochemistry 16*, 633–649.

Payraud, B. (1991). Etude hydrogéologique. Recherches sur l'origine d'eaux souterraines dans le massif des Aiguilles Rouges (Haute-Savoie) [hydrogeological study. search about the origin of groundwaters in the Aiguilles Rouges Massif (Haute-Savoie)]. Master's thesis, University of Savoie, Chambéry, France.

Pearson, F.-J., W. Balderer, H.-H. Loosli, B.-E. Lehmann, A. Matter, T.-J. Peters, H. Schmassmann, and A. Gautschi (1991). *Applied Isotope Hydrogeology. A case study in northern Switzerland.* Amsterdam, Netherlands: Studies in Environmental Science 43, Elsevier.

Pearson, F.-J., J.-L. Lolcama, and A. Scholtis (1989). Chemistry of waters in the Bottstein, Weiach, Riniken, Schafisheim, Kaisten and Leuggern boreholes: A hydrochemically consistent data set. Unpublished report.

Perello, P., L. Marini, G. Martinotti, and J.-C. Hunziker (2001). The thermal circuit of the Argentera Massif (western Alps, Italy): An example of low-enthalpy geothermal resources controlled by Neogene alpine tectonics. *Eclogae geol Helv 94*, 75–94.

Perrochet, P. (2006). Mathematical modeling of flow and transport processes in hydro-geological media. Course note, University of Neuchâtel, Switzerland.

Pfiffner, O.-A., P. Lehner, P. Heitzmann, S. Mueller, and A. Steck (1997). *Deep structure of the Swiss Alps. Results of NRP 20.* Basel, Switzerland: Birkenhaüser.

Pomerol, C. and J. Ricour (1992). *Terroirs et thermalisme de France [Soils and thermal sites in France].* Orléans, France: BRGM éditions.

Porras, E.-A., T. Tanaka, H. Fujii, and R. Itoi (2007). Numerical modeling of the Momotombo geothermal system, Nicaragua. *Geothermics 36*(4), 304–329.

Portier, S., L. André, F.-D. Vuataz, and T. Kohl (2007). Modelling the impact of forced fluid-rock interactions on reservoir properties at Soultz-sous-Forêts EGS geothermal site. In *Proc. European Geothermal Congress*, Unterhaching, Germany, 30 May - 1 June.

Preisig, G. (2009). Prospection d'eau thermominérale à Acquarossa par les méthodes hydrogéologiques, géochimiques et géophysiques [Thermal and mineral water investigation at Acquarossa from hydrogeological, geochemical and geophysical methods]. Master's thesis, University of Neuchâtel, Switzerland.

Pruess, K. (2002). Mathematical modeling of fluid flow and heat transfer in geothermal systems - an introduction in five lectures. Geothermal Training Programme, Report 3, LBNL-51295.

Pruess, K. (2006). Enhanced geothermal system (EGS) using CO_2 as working fluid - A novel appraoch for generating renewable energy with simultaneous sequestration of carbon. *Geothermics 35*(4), 351–367.

Pugin, A., R. Marchant, and G.-M. Stämpfli (1992). Interprétation des profils sismiques de GEOTHER-MOVAL (vallée du Rhône, de Saint-Maurice à Bramois) [Interprétation of the seismic profiles of GEOTHERMOVAL (Rhone Valley, from Saint-Maurice to Bramois)]. Unpublished report.

Rozanski, K., R. Gonfiantini, and L. Araguas-Araguas (1991). Tritium in the global atmosphere: distribution patterns and recent trends. *J Phys G: Nucl Part Phys 17*, 523–536.

Rybach, L. (1973). Wärmeproduktionsbestimmungen an Gesteinen der Schweizer. Alpen [Properties of heat production in rocks from Switzerland. Alps]. *Beitr Geol Schweiz, Geotech Ser 51*, 43.

Rybach, L. (1982). Die geothermischen Verhältnisse in der Schweiz [Geothermal anomalies in Switzerland]. *Bull Ver schweiz Petroleum-Geol u -Ing 48*(115), 23–34.

Rybach, L. (1992). Geothermal potential of the Swiss Molasse Basin. *Eclogae geol Helv 85*(3), 733–744.

Rybach, L., W. Eugster, and J.-C. Griesser (1987). Die geothermischen Verhältnisse in der Nordschweiz [Geothermal anomalies in the northern part of Switzerland]. *Eclogae geol Helv 80*(2), 531–534.

Rybach, L. and R. Minder (2007). Swiss Country Report. In *Proc. European Geothermal Congress*, Unterhaching, Germany, 30 May - 1 June.

Sarrot-Reynauld, J. (1987). Tectonique et thermalisme. Conditions d'emergence des eaux thermominérales d'Allevard et Uriage (Isère) et de Challes-les-Eaux (Savoie) [Tectonic and thermal conditions of uprising of the mineral and thermal waters at Allevard and Uriage (Isère), and Challes-les-Eaux (Savoy)]. In *Actes 112ᵉ Congrès National des Sociétés Savantes*, Lyon, Section des Sciences 1, Ed. CTHS, Paris, France.

Sartori, M., A. Escher, and M. Escher (2001). Modèle géologique virtuel de Zermatt au Jura [Conceptual geological model from Zermatt to the Jura range]. Musée cantonal de géologie, Lausanne, Switzerland.

Schmassmann, H. (1980). *Geologie und Genese der schweizerischen Mineral- und Thermalwässer. In O Högl: Die Mineral- und Heilquellen der Schweiz [Geology and origin of mineral and thermal waters from Switzerland. In O Högl: The mineral and medicinal springs in Switzerland].* Bern und Stuttgart: Haupt, Verlag.

Schmid, M., B. Fügenschuh, E. Kissling, and R. Schuster (2004). Tectonic map and overall architecture of the Alpine orogen. *Eclogae geol Helv 97*, 93–117.

Schneider, T. (1982). Etude sur les pertes d'eau du bassin d'accumulation de Salanfe [Study of water losses from the Salanfe accumulation Basin]. Rapport Salanfe SA, Unpublished report, Lausanne.

Schneider, T. (1989). Rapport Nr 172: Etanchement du lac - recherches préliminaires [Report Nr 172: Lake sealing - preliminary research]. Rapport Salanfe SA, Unpublished report, Lausanne.

Schotterer, U., T. Stocker, H. Bürki, J. Hunziker, R. Kozel, D.-A. Grasso, and J.-P. Tripet (2000). Das Schweizer Isotopen-Messnetz - Trends 1993-1999 [The Swiss isotope measurements network - Trends 1993-1999]. *Schweizerischer Verein des Gas- und Wasserfaches 10*, 733–741.

Schroeder, J.-W. and C. Ducloz (1955). Géologie de la molasse du Val d'Illiez (Bas-Valais) [Geology of the molasse of Val d'Illiez (Lower-Wallis)]. *Matér Carte Géol Suisse 100*, 43.

Sesiano, J. (2003). Traçage entre le lac du barrage de Salanfe et les sources thermales de Val d'Illiez (Valais, Suisse) [Tracer tests between the dam of the Salanfe Lake and the thermal springs at Val d'Illiez (Wallis, Switzerland)]. *Karstologia 41*, 49–54.

Signorelli, S. (2004). *Geoscientific investigations for the use of shallow low-enthalpy systems*. Ph. D. thesis, ETHZ, Zurich, Switzerland, Nr 15'519.

SOGREAH (1996). Diagnostic relatif à la perte de débit des sources De Mey [Diagnosis relating to the loss of flow rate in the De Mey boreholes]. Unpublished report Nr 100438.

Sommaruga, A. (1997). Geology of the Central Jura and the Molasse Basin. *Mem Soc Neuch Sci Nat 12*.

Sonney, R. (2007). Système hydrothermal de Lavey-les-Bains (Vaud): Evolution des paramètres physiques et chimiques de l'eau thermale avec la production [Hydrothermal system of Lavey-les-Bains (Vaud): Variation of the physico-chemical parameters in waters with the production rate]. Master's thesis, University of Neuchâtel, Switzerland.

Sonney, R., S. Portier, and F.-D. Vuataz (2007). Estimation de la composition chimique de l'eau thermale en profondeur à Lavey-les-Bains (Vaud) [Estimation of the chemical composition of the deep fluid in Lavey-les-Bains (Vaud)]. Unpublished report for the AGEPP project.

Sonney, R. and F.-D. Vuataz (2007). BDFGeotherm: the database of geothermal fluids in Switzerland. In *Proc. European Geothermal Congress*, Unterhaching, Germany, 30 May - 1 June.

Sonney, R. and F.-D. Vuataz (2008). Properties of geothermal fluids in Switzerland: A new interactive database. *Geothermics 37*, 496–509.

Sonney, R. and F.-D. Vuataz (2009). Numerical modelling of Alpine deep flow systems: a manegement and prediction tool for an exploited geothermal reservoir (Lavey-les-Bains, Switzerland). *Hydrogeology Journal 17*(3), 601–616.

Sonney, R. and F.-D. Vuataz (2010a). Use of Cl/Br ratio to decipher the origin of dissolved mineral components in deep fluids from the Alps range and neighbouring areas. Bali, Indonesia, 25-29 April. Accepted for World Geothermal Congress.

Sonney, R. and F.-D. Vuataz (2010b). Validation of chemical and isotopic geothermometers from low temperature deep fluids of northern Switzerland. Bali, Indonesia, 25-29 April. Accepted for World Geothermal Congress.

Sonney, R. and F.-D. Vuataz (2010c). The database of geothermal fluids in Switzerland on Google Earth. Bali, Indonesia, 25-29 April. Accepted for World Geothermal Congress.

Sonney, R. and F.-D. Vuataz (2010d). Remobilisation of deep Na-Cl waters by a regional flow system in the Alps: case study of Saint-Gervais-les-Bains (France). *CR Geoscience 342*, 151–161.

Steck, A., J.-L. Epard, A. Escher, Y. Gouffon, and H. Masson (2001). *Carte tectonique de la Suisse occidentale et des régions avoisinantes 1/100'000. Notice explicative [Tectonic map of the Western Switzerland and neighbouring areas 1/100'000. Explanatory leaflet]*. Office Fédéral des Eaux et de la Géologie.

Steyrer, H.-P. and R. Strum (2002). Stability of zircon in a low-grade ultramylonite and its utility for chemical mass balancing: the shear zone at Miéville, Switzerland. *Chemical Geology 187*, 1–19.

Stober, I. and K. Bucher (1999). Deep groundwater in the crystalline basement of the Black Forest region. *Applied Geochemistry 14*(2), 237–254.

Stober, I. and K. Bucher (2007). Hydraulic properties of the crystalline basement. *Hydrogeology Journal 15*, 213–224.

Stumm, W. and N.-J. Morgan (1981). *Aquatic Chemistry. An introduction emphasizing chemical equilibria in natural waters*. New York, United States: John Wiley and Sons, 2nd edition.

Surbeck, H. (1995). Determination of natural radionuclides in drinking water; a tentative protocol. *The Science of the Total Environment 1*, 173–174.

Surbeck, H. (2000). Alpha spectrometry sample preparation using selectively adsorbing thin films. *Applied Radiation and Isotopes 53*, 97–100.

Suski, B., F. Ladner, L. Baron, F.-D. Vuataz, F. Philippossian, and K. Holliger (2008). Detection and characterization of hydraulically active fractures in a carbonate aquifer: results from self-potential, temperature and fluid electrical conductivity logging in the Combioula hydrothermal system in the southwestern Swiss Alps. *Hydrogeology Journal 16*, 1319–1328.

Teng, Y. and K. Koike (2007). Three-dimensional imaging of a geothermal system using temperature and geological models derived from a well-log dataset. *Geothermics 36*(6), 518–538.

IAEA/WMO (2006). Web site of the Global Network of Isotopes in Precipitation (GNIP) and Isotope Hydrology Information System (isohis). Vienna, Austria. International Atomic Energy Agency.

Thiébaud, E. (2008). *Fonctionnement d'un système hydrothermal associé à un contact tectonique alpin (La Léchère, Savoie) [Functioning of a hydrothermal system related to a Alpine tectonic contact (La Léchère, Savoie)]*. Ph. D. thesis, University of Savoie, Chambéry, France.

Thierrin, J., P. Steffen, S. Cornaz, F.-D. Vuataz, W. Balderer, and M. Looser (2003). Guide Pratique - Echantillonnage des eaux souterraines [Guide Book - Sampling of groundwaters]. Federal Office of the Environment.

Tonani, F.-B. (1980). Some remarks on the application of geochemical techniques in geothermal exploration. Strasbourg, France, pp. 428–443. Proc. Second Symposium Advances in European Geothermal Research.

Trümpy, R. (1980). *An outline of the Geology of Switzerland*. Basel, Switzerland: 1st edition Wepf.

Truesdell, A.-H. (1976). Summary of Section III. Geochemical Techniques in Exploration. In *Proceedings of the Second United Nations Symposium on the Development and Use of Geothermal Resources*, San Francisco, California, United States, 20-29 May.

VDI-Richtlinien (2000). Thermal use of the underground - Fundamentals, approvals and environmental aspects. VDI4640, Part 1.

Vergain, J. (1991). Etude hydrogéologique et géochimique des eaux thermales de Val d'Illiez (Valais, Suisse) [Hydrogeological and geochemical study of the thermal springs at Val d'Illiez (Wallis, Switzerland)]. Master's thesis, University of Neuchâtel, Switzerland.

Verma, S.-P. and E. Santoyo (1997). New improved equations for Na/K, Na/Li and SiO$_2$ geothermometers by outlier detection and rejection. *Journal Volcanol Geoth Res 79*(1-2), 9–23.

Vigouroux, P. and B. Ray (2005). Ressource en eau thermale de la station de Saint-Gervais-les-Bains - Rapport final [Thermal resource of the Saint-Gervais-les-Bains spa - Final report]. BRGM/RP-53842-FR, unpublished report.

Vollmayr, T. (1983). Temperaturmessungen in erdölbohrungen der Schweiz [Geothermometers in deep boreholes in Switzerland]. *Bull Ver schweiz Petroleum-Geol u -Ing 49*(116), 15–27.

Vollmayr, T. (1985). Temperature in the subsurface of the Swiss and German alpine foreland. *Journal of Geodynamics 4*, 305–319.

Von Raumer, J.-F. (1984). The external massifs, relics of variscan basement in the Alps. *Geologische Rundschau 73*, 1–31.

Von Raumer, J.-F. (1987). Les Massifs du Mont-Blanc et des Aiguilles Rouges: témoins de la formation de la croûte varisque dans les Alpes occidentales [Mont-Blanc and Aiguilles Rouges Massifs: sites of the formation of the Variscan crust in the Western Alps]. *Géologie Alpine 63*, 7–24.

Von Raumer, J.-F. and F. Bussy (2004). Mont Blanc and Aiguilles Rouges geology of their polymetamorphic basement (External massifs, Western Alps, France-Switzerland). *Mémoires de G*éologie 42.

Von Raumer, J.-F., G. Galetti, H.-R. Pfeifer, and R. Oberhansli (1990). Amphibolites from lake Emosson/Aiguilles Rouges, Switzerland: Tholeiitic basalts of a paleozoic continental rift zone. *Schweiz Mineral Petrogr Mitt 70*, 419–435.

Von Raumer, J.-F., G.-M. Stämpfli, and F. Bussy (2003). Gondwana-derived microcontinents - the constituents of the Variscan and Alpine collisional orogens. *Tectonophysics 6832*, 1–16.

Vuataz, F.-D. (1982). Hydrogéologie, géochimie et géothermie des eaux thermales de Suisse et des régions limitrophes [Hydrogeological, geochemical and geothermal properties of thermal waters from Switzerland and neighbouring regions]. *Matér Géol Suisse, Sér Hydrol 29*.

Vuataz, F.-D. (1997). Natural variations and human influences on thermal water resources in the Alpine environment. In *33e Conférence de la Société Internationale des Techniques Hydrothermales*, Hakone, Japon, December.

Vuataz, F.-D. (2005). Note sur les relations entre les eaux subthermales de Play et les eaux thermales de Buchelieule, Val d'Illiez [Note on the relations between subthermal waters at Play and thermal waters at Buchelieule, Val d'Illiez]. CREGE, Unpublished report.

Vuataz, F.-D., J.-D. Rouiller, J.-D. Dubois, G. Bianchetti, and O. Besson (1993). Programme GEOTEHRMOVAL: résultats d'une prospection des ressources géothermiques du Valais, Suisse [GEOTHERMOVAL program: prospection results of the geothermal resources in Wallis, Switzerland]. *Bull Centre d'Hydrogeol Neuchâtel 12*, 1–37.

Wanner, E. (1954). Jahresbericht 1953 des Erdbebendienstes der Schweiz [Annual report 1953 of the seismological service]. Annalen der Schweizerischen Meteorologischen Zentralanstalt, Unpublished report.

Welch, A.-H., D.-B. Westjohn, D.-R. Helsel, and R.-B. Wanty (2000). Arsenic in Ground Water of the United States: Occurrence and geochemistry. *Groundwater 38*(4), 589–604.

Wexsteen, P. (1988). *Hydrogéologie et géochimie des eaux minérales riches en* CO$_2$ *de la région de Scuol-Tarasp [Hydrogeology and geochemistry of* CO$_2$-*rich mineral waters in the area of Scuol-Tarasp]*. Ph. D. thesis, University of Geneva, Switzerland, Nr 2299.

Wexsteen, P., F.-C. Jaffé, and E. Mazor (1988). Geochemistry of cold CO_2-rich springs of he Scuol-Tarasp region, Lower Engadine, Swiss Alps. *Journal of Hydrology 104*, 77–92.

Yurtsever, Y. and J.-R. Gat (1981). Atmospheric waters. In: Stable isotope hydrology: Deuterium and oxygen-18 in the water cycle. IAEA, Vienna, Technical report series 210.

Zahner, P., J. Mautner, and H. Badoux (1974). Etude hydrogéologique des sources thermominérales de Lavey, d'Yverdon et de Saxon [Hydrogeological study of the mineral and thermal waters of Lavey, Yverdon and Saxon]. *Mém Soc Vaud Sci Nat 15* (95), 209–234.

Ziegler, H.-J. (1992). Entwicklung einer Trinkwasser bohrung mit Salzsaüre [Development of a drinking water borehole with hydrochloric acid]. *Bull Ver schweiz Petroleum-Geol u -Ing 59* (135), 39–48.

Zienkiewicz, O.-C. (1979). *La méthode des éléments finis [The finite element method]*. Paris, France: Mc Graw-Hill.

Part VIII

Appendixes: Chemical and isotopic analyses of waters

A

Description of analysed and measured parameters

The complete name of the analysed and measured parameters is given in the next table. For each parameter of the studied waters, the in-situ measurement methods and the analytical methods at the laboratory are explained in the section 2.2 "Hydrochemical investigations".

The historical chemical and isotopic data are not printed here because they include hundreds of sample points. However, all data can be viewed in the attached CD-ROM accompanying this manuscript (Site-name_data.xls).

In the attached CD-ROM are also included the manuscript built under the LaTeX code and converted into a .pdf file (PhD_Thesis_Romain_Sonney_2010.pdf), and all the figures in .jpeg or .png formats are given separately.

Finally, for each table showing data of the studied sites, the symbol "-" means the parameter was not analysed or measured.

PARAMETERS	DESCRIPTION
GENERAL INFOS	
Borehole / Spring	Name of the borehole, well or spring sampled
Sampling Date	Date when the sample was taken (day.month.year)
Laboratory or reference	Name of the laboratory which analysed the sample
reference	or the reference where the data are documented
IN SITU MEASUREMENT	
Water Temp. (^{o}C)	Temperature of the water during the sampling
Air Temp. (^{o}C)	Temperature of the air during the sample
Elec. Cond. 25°C (μS/cm)	Electrical conductivity of the water during the sampling
Flow Rate (L/min)	Flow rate of the sampling point when the sample was taken
pH	pH of the water during the sampling
Oxygen at saturation (%)	Oxygen at saturation of the water during the sampling
Oxygen (mg/L)	Oxygen content of the water during the sampling
Pump Depth (m)	Depth of the pump in well if a pump had been used to collect the water
Final Drawdown (m)	Final drawdown in well after stabilization of the water level if a pump had been used
ANALYSES	
Calculated TDS (mg/L)	Sum of the total dissolved solids (TDS) in the analysed water
CATIONS (mg/L)	
Li	Lithium
Na	Sodium
K	Potassium
Mg	Magnesium
Ca	Calcium
Sr	Strontium
ANIONS (mg/L)	
F	Fluoride
Cl	Chloride
Br	Bromide
SO_4	Sulphate
HCO_3	Bicarbonates
UNDISSOCIATED (mg/L)	
SiO_2	Silica
B	Boron
TRACE ELEMENTS (μg/L)	
Rb	Rubidium
Ba	Barium
Al	Aluminum
Cr	Chromium
Co	Cobalt
Ni	Nickel
Cd	Cadmium
U	Uranium
Pb	Lead
Ti	Titanium
As	Arsenic
Mn	Manganese
Fe	Iron
Mo	Molybdenum
Cu	Copper
Zn	Zinc
I	Iodide
IONIC BALANCE	
Cations (meq/L)	Sum of the cations in the analysed water
Anions (meq/L)	Sum of the anions in the analysed water
Difference (%)	Ionic balance calculated from the sums of cations and anions
ISOTOPES	
Deuterium (H_2O, ‰)	Content of the stable isotope of hydrogen (^{2}H) of the water molecule
Oxygen-18 (H_2O, ‰)	Content of the stable isotope of oxygen of the water molecule
Tritium (TU)	Content of the radioactive isotope of hydrogen (^{3}H) in the analysed water
Radon-222 (Bq/L)	Content of the isotope radon-222 in the analysed water
Radium-226 (mBq/L)	Content of the isotope radium-226 in the analysed water
Uranium-238 (mBq/L)	Content of the isotope uranium-238 in the analysed water
Uranium-234 (mBq/L)	Content of the isotope uranium-234 in the analysed water

B

Lavey-les-Bains, Switzerland

GENERAL INFOS						
Borehole / Spring	P600	P600	P201	P201	AP	P13
Sampling Date	03.05.2007	30.08.2007	03.05.2007	30.08.2007	30.08.2007	30.08.2007
Laboratory or	Gainon	Sonney and	Gainon	Sonney and	Sonney and	Sonney and
Reference	2008	Vuataz 2009	2008	Vuataz 2009	Vuataz 2009	Vuataz 2009
IN SITU MEASUREMENT						
Water Temp. (°C)	65.0	65.3	56.8	56.8	19.7	23.3
Air Temp. (°C)	20	18	20	18	18	18
Elec. Cond. 25°C (μS/cm)	1963	1984	1550	1709	676	515
Flow Rate (L/min)	285	300	480	450	17	24
pH	7.71	7.56	7.61	7.41	7.69	7.17
Oxygen at saturation (%)	2	0.3	4.7	1.9	39.3	32.9
Oxygen (mg/L)	0.07	0.01	0.21	0.09	3.25	2.55
Pump Depth (m)	-	93	-	50	12	10
Final Drawdown (m)	-	-	-	29.3	7.12	8.95
ANALYSES						
Calculated TDS (mg/L)	1452	1415	1151	1215	527	407
CATIONS (mg/L)						
Li	3.8	3.2	2.4	2.5	0.3	0.33
Na	380	360	280	288	40	34.2
K	14.3	11.2	13.2	9.5	3.0	2.8
Mg	1.8	1.7	3.9	3.5	13.4	10.8
Ca	55.4	57.2	55.5	60.5	82.4	53.8
Sr	2.5	2.6	1.4	1.4	1.7	0.55
ANIONS (mg/L)						
F	5.7	6.2	5.0	4.6	0.8	1.3
Cl	236	239	171	201	29	16
Br	1.00	1.28	1.20	1.13	< 0.5	< 0.5
SO_4	592	580	457	486	144	102
HCO_3	86.9	79.7	101	92.6	197	170
UNDISSOCIATED (mg/L)						
SiO_2	69.5	68.2	57.5	56.5	15.4	15.1
B	3.2	4.2	2.2	3.0	0.35	-
TRACE ELEMENTS (μg/L)						
Rb	114	127	92	106	18	29
Ba	26	28	20.6	29	59	41
Al	< 10	8.3	< 10	5.2	4.1	3.4
Cr	< 10	2.1	< 10	2.4	25	4.1
Co	< 10	0.1	< 10	0.1	0.2	0.1
Ni	< 10	1.3	< 10	1.5	3.1	2.2
Cd	< 1	< 1	< 1	< 1	0.1	0.1
U	< 0.1	< 1	< 1	3.2	10.3	11
Pb	< 10	2	<10	1	1.4	0.3
Ti	< 10	108	< 10	98	81	58.6
As	1	2.7	6	6.5	9.8	< 1
Mn	30	26	29	33	1.1	0.5
Fe	12	< 10	10	10	< 10	< 10
Mo	< 1	1	< 1	1	4.2	0.1
Cu	< 5	3.5	< 5	2.5	4	0.9
Zn	12	14	< 10	16	174	21
I	-	39	-	28	7.2	1.7
IONIC BALANCE						
Cations (meq/L)	20.40	19.47	15.98	16.47	7.12	5.19
Anions (meq/L)	20.71	20.45	16.26	17.55	7.08	5.42
Difference (%)	-0.7	-2.5	-0.8	-3.2	0.3	-2.2
ISOTOPES						
Deuterium (H_2O, ‰)	-	-	-	-	-	-
Oxygen-18 (H_2O, ‰)	-	-	-	-	-	-
Tritium (TU)	-	-	-	-	-	-
Radon-222 (Bq/L)	70.8±0.6	73.1±0.7	115±0.8	106±0.8	11.2±0.4	
Radium-226 (mBq/L)	120±10	153±11	114±10	102±9	-	54±7
Uranium-238 (mBq/L)	< 5	4±2	33±5	28±5	-	121±10
Uranium-234 (mBq/L)	< 5	6±3	31±5	29±5	-	114±10

GENERAL INFOS					
Borehole / Spring	P14	S8	S9	Piézo	PF2
Sampling Date	31.08.2007	31.08.2007	31.08.2007	30.08.2007	31.08.2007
Laboratory or	Sonney and	Sonney and	Sonney and	Sonney and	Sonney and
Reference	Vuataz 2009	Vuataz 2009	Vuataz 2009	Vuataz 2009	Vuataz 2009
IN SITU MEASUREMENT					
Water Temp. (°C)	18.9	18.7	26.5	14.6	15.1
Air Temp. (°C)	22	20	20	18	22
Elec. Cond. 25°C (μS/cm)	767	328	380	1167	1229
Flow Rate (L/min)	16	7	16	15	15
pH	7.93	7.65	7.22	7.30	7.40
Oxygen at saturation (%)	0.8	38.5	3.4	70.8	57.9
Oxygen (mg/L)	0.07	3.25	0.25	6.35	5.22
Pump Depth (m)	12	15	18	10	15
Final Drawdown (m)	7.5	14	15.34	6.67	11.96
ANALYSES					
Calculated TDS (mg/L)	556	272	321	858	889
CATIONS (mg/L)					
Li	0.68	0.02	0.67	0.85	0.97
Na	112	3.9	11.9	124	139
K	3.5	1.2	2.5	4.6	4.7
Mg	4.2	10.7	11.5	14.8	13.8
Ca	38.5	46.6	48.9	103	100
Sr	1.18	0.63	1.23	< 0.5	< 0.5
ANIONS (mg/L)					
F	2.9	0.9	2.2	1.4	1.5
Cl	28	3	5	94	102
Br	< 0.5	< 0.5	< 0.5	< 0.5	< 0.5
SO_4	227	38	53	300	320
HCO_3	120	153	162	194	185
UNDISSOCIATED (mg/L)					
SiO_2	17.9	13.6	22.6	19.8	21.3
B	-	0.05	-	1.4	1.6
TRACE ELEMENTS (μg/L)					
Rb	9.5	2.7	17	15	16.7
Ba	36	62	70	100	105
Al	4.7	1.6	2.9	2.3	2
Cr	2.8	16	3.5	22	19.3
Co	0.1	0.1	0.1	0.2	0.2
Ni	1.3	1.9	1.6	2.4	2.7
Cd	< 1	0.2	< 1	< 1	0.1
U	0.1	2.6	2.6	10.3	9.9
Pb	0.3	0.2	0.1	0.7	0.1
Ti	54	50	50	106	108
As	< 1	3.2	1.7	3.6	3.5
Mn	33	1.5	37	0.1	0.1
Fe	< 10	< 10	315	< 10	< 10
Mo	0.1	6.4	< 1	6	6.2
Cu	1	0.5	0.5	2.5	2.8
Zn	15	15.2	17.8	18.5	20.9
I	8.4	2.5	1.1	15	23.3
IONIC BALANCE					
Cations (meq/L)	7.35	3.42	4.09	11.97	12.42
Anions (meq/L)	7.63	3.44	4.00	12.15	12.64
Difference (%)	-1.8	-0.3	1.1	-0.7	-0.9
ISOTOPES					
Deuterium (H_2O, ‰)	-	-	-	-	-
Oxygen-18 (H_2O, ‰)	-	-	-	-	-
Tritium (TU)	-	-	-	-	-
Radon-222 (Bq/L)	116±0.8	-	49±0.6	23.1±0.5	-
Radium-226 (mBq/L)	66±8	-	< 5	-	-
Uranium-238 (mBq/L)	< 5	-	31±5	-	-
Uranium-234 (mBq/L)	< 5	-	23±5	-	-

C

Saint-Gervais-les-Bains, France

GENERAL INFOS					
Borehole / Spring	Lépinay	De Mey Est	De Mey Ouest	F99	Gontard
Sampling Date	16.07.2008	17.07.2008	17.07.2008	17.07.2008	17.07.2008
Laboratory or	CHYN	CHYN	CHYN	CHYN	CHYN
Reference	This study	This study	This study	This study	This study
IN SITU MEASUREMENT					
Water Temp. ($^{\circ}$C)	39.0	35.8	27.4	11.7	20.1
Air Temp. ($^{\circ}$C)	25	20	20	20	20
Elec. Cond. 25°C (μS/cm)	5290	6440	4110	1926	2113
Flow Rate (L/min)	217	88	50	20	< 10
pH	6.93	6.94	7.06	7.06	7.12
Oxygen at saturation (%)	-	-	-	-	-
Oxygen (mg/L)	0.37	0.18	1.37	0.04	1.04
Pump Depth (m)	15	74	74	15	-
Final Drawdown (m)	0	0	0	> 5	-
ANALYSES					
Calculated TDS (mg/L)	4245	4821	3101	1778	1621
CATIONS (mg/L)					
Li	6.7	8.7	4.6	0.28	1.4
Na	992	1157	609	49	212
K	29.9	32.9	17.8	3.0	8.6
Mg	29.4	31.6	40.7	63.0	35.7
Ca	268	302	268	341	210
Sr	10.9	13.4	10.4	10.0	7.1
ANIONS (mg/L)					
F	3.02	3.65	2.83	< 0.1	1.14
Cl	585	1167	584	48.2	129
Br	4.1	16.6	6.5	0.102	0.66
SO$_4$	2000	1787	1283	993	776
HCO$_3$	272	253	251	257	221
UNDISSOCIATED (mg/L)					
SiO$_2$	39.9	44.5	20.5	12.3	16.9
B	3.5	4.4	2.6	0.3	1.1
TRACE ELEMENTS (μg/L)					
Rb	188	212	118	23	55
Cs	251	298	177	58	89
Ba	16	16	18	13	16
Al	< 5	< 5	< 5	< 5	< 5
Cr	18	10	14	17	11
Co	1	1	1	3	1
Ni	12	10	9	15	7
Cd	< 1	< 1	< 1	< 1	< 1
U	1	1	3	6	3
Pb	1	< 1	1	1	< 1
Ti	310	319	265	319	204
As	3	4	3	1	2
Mn	242	289	208	96	147
Fe	90	220	260	< 1	110
Mo	< 1	< 1	1	1	2
Cu	10	10	7	1	4
Zn	10	10	10	18	21
I	15	21	12	1	3
IONIC BALANCE					
Cations (meq/L)	60.94	70.41	44.59	24.66	23.24
Anions (meq/L)	62.82	74.66	47.52	26.26	23.49
Difference (%)	-1.5	-2.9	-3.2	-3.1	-0.5
ISOTOPES					
Deuterium (H$_2$O, ‰)	-90.1	-93.4	-88.6	-84.1	-84.6
Oxygen-18 (H$_2$O, ‰)	-12.51	-13.01	-12.28	-11.53	-11.80
Tritium (TU)	-	-	-	-	-
Radon-222 (Bq/L)	120±3	88±3	74±3	29±2	51±2
Radium-226 (mBq/L)	55±7	128±11	59±8	7±4	27±6
Uranium-234+238 (mBq/L)	36±8	23±6	84±9	163±15	65±9

GENERAL INFOS					
Borehole / Spring	Sulf. Spring	Ferr. Spring	Magn. Spring	Cold Spring	Bon Nant
Sampling Date	17.07.2008	16.07.2008	16.07.2008	17.07.2008	17.07.2008
Laboratory or	CHYN	CHYN	CHYN	CHYN	CHYN
Reference	This study	This study	This study	This study	This study

IN SITU MEASUREMENT					
Water Temp. (°C)	9.8	10.5	10.5	10.8	12.0
Air Temp. (°C)	20	25	25	20	20
Elec. Cond. 25°C (μS/cm)	408	2440	2550	907	362
Flow Rate (L/min)	< 1	60	120	< 5	> 5000
pH	7.6	6.91	7.01	7.32	8.03
Oxygen at saturation (%)	-	-	-	-	-
Oxygen (mg/L)	4.03	1.97	4.13	3.34	10.13
Pump Depth (m)	-	-	-	-	-
Final Drawdown (m)	-	-	-	-	-

ANALYSES					
Calculated TDS (mg/L)	329	2369	2470	736	287

CATIONS (mg/L)					
Li	0.01	0.028	0.022	0.046	0.001
Na	4.1	11.3	12.4	10.1	3.4
K	1.9	1.8	1.8	2.1	1.1
Mg	10.1	68.7	66.5	27.3	7.2
Ca	65.7	612	629	147	61
Sr	2.1	< 0.5	< 0.5	4.1	< 0.5

ANIONS (mg/L)					
F	0.10	0.21	0.30	0.20	0.04
Cl	4.4	16.8	18.3	10.2	4.0
Br	< 0.5	< 0.5	< 0.5	< 0.5	< 0.5
SO_4	95.2	1352	1428	324	99.3
HCO_3	141	301	306	204	106

UNDISSOCIATED (mg/L)					
SiO_2	5.1	5.9	6.8	7.5	4.2
B	0.062	0.015	0.013	0.133	0.080

TRACE ELEMENTS (μg/L)					
Rb	6	5	4	10	3
Cs	12	10	8	32	< 1
Ba	20	11	13	22	20
Al	< 5	< 5	< 5	< 5	< 5
Cr	5	24	20	9	4
Co	< 1	3	3	1	< 1
Ni	4	32	32	8	3
Cd	< 1	< 1	< 1	< 1	< 1
U	2	5	6	4	1
Pb	3	< 1	1	1	1
Ti	48	351	371	164	48
As	2	1	1	1	2
Mn	4	2	1	28	2
Fe	50	40	2	150	< 1
Mo	2	3	2	2	1
Cu	1	1	3	1	1
Zn	16	22	27	23	7
I	< 1	< 1	< 1	< 1	< 1

IONIC BALANCE					
Cations (meq/L)	4.38	36.72	37.45	10.17	3.83
Anions (meq/L)	4.42	33.56	35.29	10.38	3.92
Difference (%)	-0.4	4.5	3.0	-1.0	-1.1

ISOTOPES					
Deuterium (H_2O, ‰)	-80.5	-81.6	-82.0	-80.1	-82.0
Oxygen-18 (H_2O, ‰)	-11.42	-11.31	-11.17	-11.33	-11.27
Tritium (TU)	-	-	-	-	-
Radon-222 (Bq/L)	32±2	13±1	4±1	46±2	0.5±0.2
Radium-226 (mBq/L)	< 5	9±4	< 5	< 5	< 5
Uranium-234+238 (mBq/L)	63±9	104±11	103±11	83±12	56±10

D

Val d'Illiez, Switzerland

GENERAL INFOS						
Borehole / Spring	F1a+b	F2	F3	Casc. Right	Casc. Centre	Cave
Sampling Date	15.06.2009	16.06.2009	15.06.2009	16.06.2009	16.06.2009	15.06.2009
Laboratory or	CHYN	CHYN	CHYN	CHYN	CHYN	CHYN
Reference	This study	This study	This study	This study	This study	This study
IN SITU MEASUREMENT						
Water Temp. (^{o}C)	28.2	27.9	27.9	22.7	22.2	22.4
Air Temp. (^{o}C)	25	25	25	25	25	25
Elec. Cond. 25°C (μS/cm)	1922	1956	2042	1789	1511	1489
Flow Rate (L/min)	10	200	1170	70	300	100
pH	7.29	7.28	7.20	7.30	7.68	7.95
Oxygen at saturation (%)	-	-	-	-	-	-
Oxygen (mg/L)	1.8	1.5	1.5	4.6	6.9	7.4
Pump Depth (m)	-	-	-	-	-	-
Final Drawdown (m)	-	-	-	-	-	-
ANALYSES						
Calculated TDS (mg/L)	1716	1700	1805	1514	1321	1281
CATIONS (mg/L)						
Li	0.09	0.10	0.09	0.10	0.09	0.09
Na	19.9	20.6	19.7	22.6	20.9	21.1
K	1.31	1.36	1.41	1.56	1.61	1.44
Mg	72.6	73.7	78.6	66.9	59.0	56.1
Ca	362	372	384	305	255	257
Sr	15.5	13.7	16.3	13.1	10.8	9.2
ANIONS (mg/L)						
F	1.31	1.87	1.69	1.31	1.20	1.13
Cl	4.7	4.6	4.2	6.0	6.0	5.9
Br	< 0.5	0.070	0.056	< 0.5	< 0.5	0.068
SO$_4$	1093	1065	1159	933	780	743
HCO$_3$	132	133	127	154	175	174
UNDISSOCIATED (mg/L)						
SiO$_2$	12.8	14.2	12.8	11.6	11.5	12.3
B	-	0.115	0.106	-	-	0.118
TRACE ELEMENTS (μg/L)						
Rb	-	4.7	4.2	-	-	3.9
Cs	-	2.4	3.7	-	-	1.7
Ba	-	17.5	12.9	-	-	24.5
Al	-	-	-	-	-	-
Cr	-	9.6	6.4	-	-	12.1
Co	-	0.5	0.4	-	-	0.3
Ni	-	4.9	4.3	-	-	3.1
Cd	-	< 0.1	< 0.1	-	-	< 0.1
U	-	< 0.1	< 0.1	-	-	0.1
Pb	-	< 0.1	< 0.1	-	-	< 0.1
Ti	-	< 0.1	< 0.1	-	-	< 0.1
As	-	0.1	< 0.1	-	-	< 0.1
Mn	-	295	15.5	-	-	8.3
Fe	-	-	-	-	-	-
Mo	-	< 0.1	< 0.1	-	-	2.8
Cu	-	0.3	0.3	-	-	0.8
Zn	-	7.9	3.9	-	-	18.8
I	-	13.2	11.7	-	-	10.1
IONIC BALANCE						
Cations (meq/L)	24.95	25.54	26.51	21.73	18.53	18.40
Anions (meq/L)	25.14	24.60	26.44	22.19	19.35	18.55
Difference (%)	-0.39	1.89	0.14	-1.03	-2.2	-0.40
ISOTOPES						
Deuterium (H$_2$O, ‰)	-96.2	-94.7	-97.0	-94.0	-92.3	-91.0
Oxygen-18 (H$_2$O, ‰)	-13.52	-12.83	-13.50	-13.26	-12.89	-12.50
Tritium (TU)	-	6.1±0.7	6.2±0.4	6.0±0.5	-	5.9±0.7
Radon-222 (Bq/L)	-	-	-	-	-	-
Radium-226 (mBq/L)	-	-	-	-	-	-
Uranium-234+238 (mBq/L)	-	-	-	-	-	-

GENERAL INFOS						
Borehole / Spring	Shower	Casc. Waterfall	Mixed-F1	Drainage 1	Drainage 2	Drainage 3
Sampling Date	15.06.2009	15.06.2009	16.06.2009	16.06.2009	16.06.2009	16.06.2009
Laboratory or	CHYN	CHYN	CHYN	CHYN	CHYN	CHYN
Reference	This study	This study	This study	This study	This study	This study
IN SITU MEASUREMENT						
Water Temp. (^{o}C)	22.5	23.1	21.8	21.5	22.6	22.1
Air Temp. (^{o}C)	25	25	25	25	25	25
Elec. Cond. 25°C (μS/cm)	1401	1529	1467	1422	1639	1560
Flow Rate (L/min)	120	400	300	300	7	17
pH	7.90	7.99	7.40	7.40	7.36	7.41
Oxygen at saturation (%)	-	-	-	-	-	-
Oxygen (mg/L)	6.8	7.4	5.1	5.5	3.3	4.5
Pump Depth (m)	-	-	-	-	-	-
Final Drawdown (m)	-	-	-	-	-	-
ANALYSES						
Calculated TDS (mg/L)	1231	1324	1243	1251	1385	1329
CATIONS (mg/L)						
Li	0.09	0.09	0.10	0.09	0.08	0.09
Na	21.0	21.7	20.1	20.2	22.3	21.5
K	1.64	1.48	1.54	1.51	1.55	1.52
Mg	54.6	58.1	55.1	55.6	58.2	58.7
Ca	244	268	251	237	269	257
Sr	8.8	9.6	10.5	9.6	10.2	10.5
ANIONS (mg/L)						
F	1.49	1.13	1.00	1.31	1.25	1.23
Cl	5.9	5.9	6.1	6.7	6.1	7.9
Br	< 0.5	0.086	0.063	< 0.5	< 0.5	< 0.5
SO$_4$	700	776	707	726	841	789
HCO$_3$	183	170	179	182	165	171
UNDISSOCIATED (mg/L)						
SiO$_2$	11.3	12.1	11.4	11.0	10.9	11.1
B	-	0.131	0.114	-	-	-
TRACE ELEMENTS (μg/L)						
Rb	-	4.3	3.5	-	-	-
Cs	-	2.4	1.1	-	-	-
Ba	-	23	23.1	-	-	-
Al	-	-	-	-	-	-
Cr	-	9.9	15.1	-	-	-
Co	-	0.5	0.3	-	-	-
Ni	-	5.1	3.2	-	-	-
Cd	-	< 0.1	< 0.1	-	-	-
U	-	0.1	0.1	-	-	-
Pb	-	< 0.1	< 0.1	-	-	-
Ti	-	< 0.1	< 0.1	-	-	-
As	-	0.1	< 0.1	-	-	-
Mn	-	350	3.4	-	-	-
Fe	-	-	-	-	-	-
Mo	-	2.8	0.3	-	-	-
Cu	-	0.4	0.3	-	-	-
Zn	-	9.6	6.4	-	-	-
I	-	15.1	7.6	-	-	-
IONIC BALANCE						
Cations (meq/L)	17.60	19.15	17.95	17.32	19.22	18.62
Anions (meq/L)	17.81	19.17	17.89	18.36	20.45	19.52
Difference (%)	-0.59	-0.05	0.18	-2.9	-3.1	-2.4
ISOTOPES						
Deuterium (H$_2$O, ‰)	-91.1	-	-90.7	-91.5	-94.3	-
Oxygen-18 (H$_2$O, ‰)	-12.79	-	-12.48	-12.71	-13.11	-
Tritium (TU)	-	-	6.4±0.4	-	-	-
Radon-222 (Bq/L)	-	-	-	-	-	-
Radium-226 (mBq/L)	-	-	-	-	-	-
Uranium-234+238 (mBq/L)	-	-	-	-	-	-

GENERAL INFOS					
Borehole / Spring	Drainage 4	Drainage 5	Drainage 6	Zone Repos Sp.	Cold Spring 1
Sampling Date	16.06.2009	16.06.2009	16.06.2009	16.06.2009	15.06.2009
Laboratory or	CHYN	CHYN	CHYN	CHYN	CHYN
Reference	This study	This study	This study	This study	This study
IN SITU MEASUREMENT					
Water Temp. (^{o}C)	23.3	23.9	23.0	22.0	19.8
Air Temp. (^{o}C)	25	25	25	25	25
Elec. Cond. 25°C (μS/cm)	1675	1663	1447	1907	645
Flow Rate (L/min)	80	100	35	< 5	3
pH	7.24	7.25	7.31	8.18	8.28
Oxygen at saturation (%)	-	-	-	-	-
Oxygen (mg/L)	1.4	1.5	3.7	7.7	7.5
Pump Depth (m)	-	-	-	-	-
Final Drawdown (m)	-	-	-	-	-
ANALYSES					
Calculated TDS (mg/L)	1460	1473	1265	1680	528
CATIONS (mg/L)					
Li	0.09	0.10	0.08	0.09	0.00
Na	23.3	23.5	19.5	20.0	27.3
K	1.45	1.58	1.47	1.56	5.3
Mg	63.0	66.9	55.4	71.0	8.5
Ca	298	305	246	355	97.1
Sr	11.8	12.7	9.9	15.3	1.43
ANIONS (mg/L)					
F	1.16	1.44	1.58	1.80	< 0.5
Cl	6.2	6.9	5.2	6.3	53.1
Br	< 0.5	< 0.5	< 0.5	0.064	0.004
SO_4	883	885	737	1057	67.4
HCO_3	161	160	177	139	260
UNDISSOCIATED (mg/L)					
SiO_2	11.2	11.2	11.6	12.9	7.2
B	-	-	-	0.112	0.032
TRACE ELEMENTS (μg/L)					
Rb	-	-	-	3.7	1.4
Cs	-	-	-	2.1	< 0.1
Ba	-	-	-	21.2	36.5
Al	-	-	-	-	-
Cr	-	-	-	8.1	19.9
Co	-	-	-	0.5	0.2
Ni	-	-	-	5.1	2.1
Cd	-	-	-	< 0.1	< 0.1
U	-	-	-	0.1	0.2
Pb	-	-	-	< 0.1	< 0.1
Ti	-	-	-	< 0.1	< 0.1
As	-	-	-	< 0.1	1.2
Mn	-	-	-	7.2	9.5
Fe	-	-	-	-	-
Mo	-	-	-	< 0.1	1
Cu	-	-	-	0.6	2.1
Zn	-	-	-	7.7	4.6
I	-	-	-	11.4	0.3
IONIC BALANCE					
Cations (meq/L)	21.09	21.76	17.72	24.46	6.87
Anions (meq/L)	21.27	21.32	18.50	24.57	7.17
Difference (%)	-0.42	1.03	-2.2	-0.23	-2.1
ISOTOPES					
Deuterium (H_2O, ‰)	-	-	-	-96.3	-72.7
Oxygen-18 (H_2O, ‰)	-	-	-	-13.47	-9.51
Tritium (TU)	-	-	-	-	8.1±0.6
Radon-222 (Bq/L)	-	-	-	-	-
Radium-226 (mBq/L)	-	-	-	-	-
Uranium-234+238 (mBq/L)	-	-	-	-	-

GENERAL INFOS					
Borehole / Spring	Cold Spring 2	Cold Spring 3	Cold Spring Egout	Vièze River	Play well
Sampling Date	15.06.2009	15.06.2009	15.06.2009	16.06.2009	16.06.2009
Laboratory or	CHYN	CHYN	CHYN	CHYN	CHYN
Reference	This study	This study	This study	This study	This study

IN SITU MEASUREMENT					
Water Temp. (°C)	12.7	9.9	14.1	11.6	20.0
Air Temp. (°C)	25	25	25	25	25
Elec. Cond. 25°C (μS/cm)	451	466	492	228	1305
Flow Rate (L/min)	42	> 10	40	> 10 m^3/s	-
pH	7.83	7.22	7.92	8.13	7.30
Oxygen at saturation (%)	-	-	-	-	-
Oxygen (mg/L)	8.9	8.8	8.7	9.8	3.2
Pump Depth (m)	-	-	-	-	-
Final Drawdown (m)	-	-	-	-	-

ANALYSES					
Calculated TDS (mg/L)	411	418	419	206	1146

CATIONS (mg/L)					
Li	0.02	0.01	0.01	< 0.01	0.08
Na	4.6	3.5	9.2	0.9	22.2
K	1.74	1.22	3.1	0.41	5.1
Mg	16.0	14.8	14.0	4.3	48.9
Ca	70.4	75.8	74.0	42.8	228
Sr	1.57	1.66	1.51	0.84	8.9

ANIONS (mg/L)					
F	< 0.5	< 0.5	< 0.5	0.04	1.02
Cl	9.3	4.2	18.3	1.08	8.2
Br	< 0.005	< 0.005	< 0.5	< 0.005	< 0.5
SO_4	36.6	39.8	33.3	33.7	630
HCO_3	263	270	258	120	183

UNDISSOCIATED (mg/L)					
SiO_2	8.2	7.3	7.3	1.60	10.2
B	0.014	0.013	-	0.001	-

TRACE ELEMENTS (μg/L)					
Rb	1.4	0.9	-	0.4	-
Cs	0.2	0.1	-	< 0.1	-
Ba	34.8	32.1	-	7.8	-
Al	-	-	-	-	-
Cr	21	23.9	-	8.4	-
Co	0.1	0.1	-	0.1	-
Ni	1.5	1.4	-	1.6	-
Cd	< 0.1	< 0.1	-	< 0.1	-
U	0.4	0.3	-	0.1	-
Pb	< 0.1	< 0.1	-	< 0.1	-
Ti	< 0.1	< 0.1	-	< 0.1	-
As	< 0.1	< 0.1	-	< 0.1	-
Mn	< 0.1	< 0.1	-	0.8	-
Fe	-	-	-	-	-
Mo	1.1	0.7	-	0.1	-
Cu	0.7	0.3	-	1.8	-
Zn	29.5	12.7	-	6.3	-
I	0.3	0.2	-	0.2	-

IONIC BALANCE					
Cations (meq/L)	5.08	5.19	5.32	2.54	16.47
Anions (meq/L)	5.33	5.37	5.44	2.70	16.43
Difference (%)	-2.5	-1.69	-1.11	-3.1	0.14

ISOTOPES					
Deuterium (H_2O, ‰)	-80.0	-77.5	-	-84.9	-
Oxygen-18 (H_2O, ‰)	-11.08	-10.58	-	-11.97	-
Tritium (TU)	7.4±0.5	8.0±0.8	-	7.4±0.4	-
Radon-222 (Bq/L)	-	-	-	-	-
Radium-226 (mBq/L)	-	-	-	-	-
Uranium-234+238 (mBq/L)	-	-	-	-	-

GENERAL INFOS					
Borehole / Spring	Fayot Spring	Prabys Spring	Crête Spring	Meuraye Spring	Bètre Spring
Sampling Date	16.06.2009	17.06.2009	17.06.2009	17.06.2009	17.06.2009
Laboratory or	CHYN	CHYN	CHYN	CHYN	CHYN
Reference	This study	This study	This study	This study	This study
IN SITU MEASUREMENT					
Water Temp. (°C)	13.7	9.5	10.4	7.6	10.6
Air Temp. (°C)	25	20	20	20	20
Elec. Cond. 25°C (μS/cm)	1010	437	335	353	477
Flow Rate (L/min)	> 50	20	15	20	10
pH	7.24	7.34	7.83	7.94	8.23
Oxygen at saturation (%)	-	-	-	-	-
Oxygen (mg/L)	5.4	9.5	9.1	9.3	9.3
Pump Depth (m)	-	-	-	-	-
Final Drawdown (m)	-	-	-	-	-
ANALYSES					
Calculated TDS (mg/L)	841	386	295	318	409
CATIONS (mg/L)					
Li	0.04	0.01	< 0.01	0.01	0.01
Na	12.8	3.1	3.8	2.9	9.9
K	1.63	1.41	0.59	0.83	2.3
Mg	35.3	12.0	3.1	13.7	9.3
Ca	158	70.0	62.0	51.8	77.6
Sr	5.7	1.20	0.34	1.57	1.17
ANIONS (mg/L)					
F	0.37	0.03	0.04	0.09	0.07
Cl	8.6	4.9	6.6	0.92	19.8
Br	< 0.5	< 0.5	< 0.5	< 0.5	< 0.5
SO_4	416	24.7	8.8	32.9	38
HCO_3	195	261	205	206	245
UNDISSOCIATED (mg/L)					
SiO_2	6.8	7.4	4.8	7.2	5.9
B	-	-	-	-	-
TRACE ELEMENTS (μg/L)					
Rb	-	-	-	-	-
Cs	-	-	-	-	-
Ba	-	-	-	-	-
Al	-	-	-	-	-
Cr	-	-	-	-	-
Co	-	-	-	-	-
Ni	-	-	-	-	-
Cd	-	-	-	-	-
U	-	-	-	-	-
Pb	-	-	-	-	-
Ti	-	-	-	-	-
As	-	-	-	-	-
Mn	-	-	-	-	-
Fe	-	-	-	-	-
Mo	-	-	-	-	-
Cu	-	-	-	-	-
Zn	-	-	-	-	-
I	-	-	-	-	-
IONIC BALANCE					
Cations (meq/L)	11.39	4.65	3.53	3.86	5.13
Anions (meq/L)	12.13	4.93	3.73	4.10	5.36
Difference (%)	-3.1	-2.9	-2.8	-3.0	-2.2
ISOTOPES					
Deuterium (H_2O, ‰)	-	-	-	-	-
Oxygen-18 (H_2O, ‰)	-	-	-	-	-
Tritium (TU)	-	-	-	-	-
Radon-222 (Bq/L)	-	-	-	-	-
Radium-226 (mBq/L)	-	-	-	-	-
Uranium-234+238 (mBq/L)	-	-	-	-	-

E

CD-R